THE MINERALOGY, PETROLOGY AND GEOCHEMISTRY OF THE SERRES-DRAMA GRANITIC COMPLEX, NORTHERN GREECE

Stergios Theodorikas

A thesis submitted for the degree of Doctor of Philosophy,

University of Keele

1982

ORIGINAL COPY TIGHTLY BOUND

DEDICATION

This thesis is dedicated to my wife Anna

and

my children Dimitrios and Stamoulis

ABSTRACT

The Serres-Drama granitic complex is situated in the Rhodope massif (North Greece). It comprises a broad spectrum of rock-types (gabbro, dioritic xenoliths, monzonite, quartz monzonite, granodiorite, granite, aplite and pegmatite veins).

From petrographical, mineralogical, geochemical and field studies, it can be seen that the granitic complex separates distinctly into two groups of rock-types, termed the "intermediate" group (granite, granodiorite and quartz monzonite) and the "basic" group (gabbro, dioritic xenoliths and monzonite). Aplites and pegmatites have not been classified in this group.

The Serres-Drama granitic complex is a calc-alkaline "I-type" complex, sensu Chappell and White (1974). It is similar to the "magnetite" series complexes described by Ishihara (1977, from Takahashi et al, 1980). Chemical characteristics indicate that it originated in the compressional zone (Petro et al, 1979) of a mature continental arc system (G.C. Brown, 1982).

ACKNOWLEDGEMENTS

The research for this thesis was carried out in the Department of Geology, University of Keele during the period September 1979 to October 1982.

I am grateful to Professor G. Kelling for providing essential facilities in the Geology Department and to Dr G. Rowbotham who supervised the research project and also read and suggested improvements to the draft manuscript.

I am further indebted to Drs. C.S. Exley and P.A. Floyd for many discussions and ideas and also to Drs. R.G. Park, R.A. Roach, J.D. Collinson, B.K. Holdsworth, H.S. Torrens, J.A. Winchester, N.J. Kusznir and P.D. Lane.

My thanks also to Professors J. Zussman and W.S. Mackenzie who allowed use of the microprobe analysis facilities at the Department of Geology, University of Manchester, and to my supervisor Dr G. Rowbotham, who very kindly performed the mineral analyses.

I am grateful to Mr G.J. Lees for many discussions and ideas which he gave me and also for help with technical and programming aspects of the work. Also Mr J. Constable, Miss P. Haselock and Mr P. Gambles have given much assistance.

Thanks are also due to the technical staff of the Department, Mr M. Stead, Mr D. Kelsall, Mr P. Greatbatch, Mr D. Wilde, Mr M. Wright, Miss M. Aikin and Miss

H. Thompson, and especially to Mr D. Emley and Mr A. Lawrence, who improved the language of the text.

Mrs J. Heath is sincerely thanked for her efficient typing of the manuscript and Miss J. Morris for typing the tables.

I am grateful to the Bodosakis Foundation for financial assistance for the final year to enable me to finish the study.

TABLE OF CONTENTS

CHAPTER III continued:

CHAPTER 1 : INTRODUCTION

CHAPTER I

INTRODUCTION

1-1 Statement of purpose

This thesis examines the mineralogy, petrology and geochemistry of the Serres-Drama granitic complex, Northern Greece. The area is situated in the Rhodope massif and is surrounded by Precambrian marbles, gneisses, mica-schists and Neogene sediments. The objectives were achieved by:

a - Determination in the field of the rock-types in the granitic complex, of their amounts, distribution and a laboratory study of their petrography. Modal analysis was performed using a point counter.

b - Determination by means of x-ray diffractometry and electron microprobe analysis, of the variations in the structural state and composition of the potassium feldspars.

c - Determination by means of an electron microprobe, of the chemical composition of the plagioclase feldspars, pyroxenes, amphiboles, biotites, epidotes, chlorites, magnetites and sphene.

d - Determination of both major and trace element chemistry of the whole rocks by X-ray fluorescence spectrometry. Ferrous iron was determined by titrimetric techniques.

An additional objective was to attempt an understanding of the generation and emplacement of the magma which formed the complex.

1-2 A short review of the geology of the Rhodope massif.

1-2a Introduction

Many geologists have considered the Rhodope massif "to be a median mass or zwischengebirge between the Hellenides and the Alpine chains in Bulgaria" (Spencer, 1974).

The Rhodope massif (fig. 1-2a-1) encloses the eastern part of Greek Macedonia (western border has been called the Strimon line), Greek Thrace (western part of Thrace), the islands of the northern Aegean (Thasos, Samothrace, Limnos, Agios Eustratios, Lesvos) and the southern part of Bulgaria. The Strimon line separates the Rhodope massif from the Serbo-Macedonian massif (fig. 1-2e-1).

1-2b Lithostratigraphy of the Rhodope massif

It is difficult to ascertain the precise geological age of the massif, as there is no clear stratigraphic sequence. This area is composed predominantly of crystalline metamorphic rocks and some igneous rocks. Most previous research pertains to the evolution of the crystalline rocks. Many geologists estimate the stratigraphic thickness to be 16 km and others about 20 km (Osswalt 1938; Jaranov 1938, Dimitrov 1959 vide Mountrakis 1977).

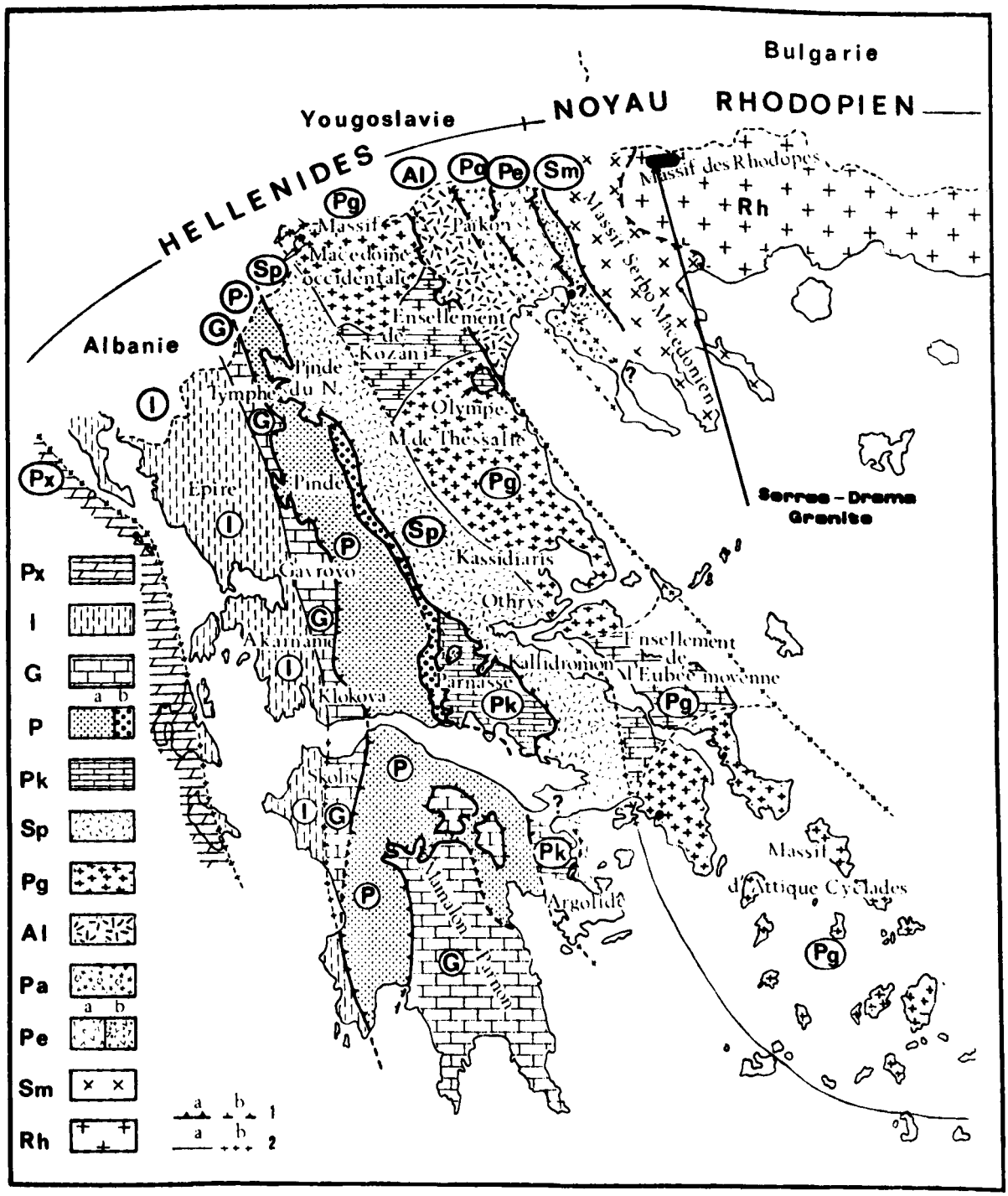

Fig (1-2a-1) Sketch map of the Isopic-tectonic zones in the Hellenides and their structural relationships (Mercier, 1966, fig. 13 — modified). After Aubouin (1958) and Aubouin, Brunn, Celet, Dercourt, Godfriaux and Mercier (1960—1963), simplified where the external zones are concerned. The internal zones are represented after the following: Godfriaux (1965) — Pelagonian zone and its relationships with the Olympus window; Brunn, (1959 and 1960) — Pelagonian and Almopias zones; Mercier — Pelagonian, Almopias and Paikon zones, pre-Peonian subzone, Peonian and Serbo-Macedonian zones; Kockel and Walther (1965) — relationships between the Serbo-Macedonian and Rhodope massifs.

Px = pre-Apulian zone (or Paxos zone); *I* = Ionian zone; *G* = Gavrovo zone; *P* = Pindus zone (*b* = ultra-Pindic subzone); *Pk* = Parnassus zone; *Sp* = sub-Pelagonian zone; *Pg* = Pelagonian zone; *Al* = Almopias zone; *Pa* = Paikon zone; *Pe* = Peonias zone (*a* = pre-Peonian subzone, *b* = eastern Peonian units); *Sm* = Serbo-Macedonian zone and Serbo-Macedonian massif; *Rh* = Rhodope massif. *1* = overthrust (*1a* = known; *1b* = supposed); *2* = limit of zone (*2a* = known; *2b* = supposed).

(R. BLANCHET AND J. MERCIER *1978*)

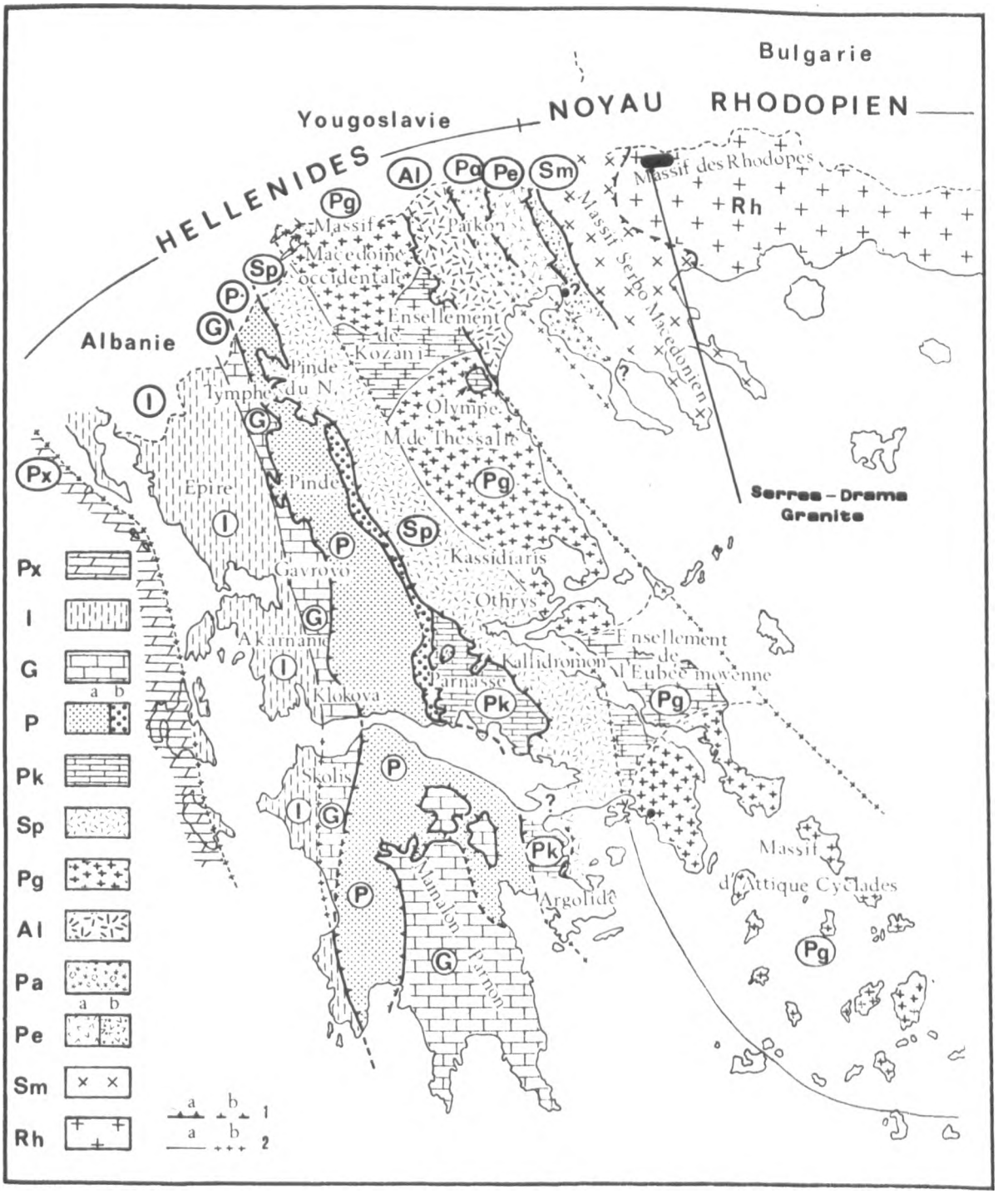

Fig (1–2a–1) Sketch map of the Isopic-tectonic zones in the Hellenides and their structural relationships (Mercier, 1966, fig. 13 – modified). After Aubouin (1958) and Aubouin, Brunn, Celet, Dercourt, Godfriaux and Mercier (1960—1963), simplified where the external zones are concerned. The internal zones are represented after the following: Godfriaux (1965) — Pelagonian zone and its relationships with the Olympus window; Brunn, (1959 and 1960) — Pelagonian and Almopias zones; Mercier — Pelagonian, Almopias and Paikon zones, pre-Peonian subzone, Peonian and Serbo Macedonian zones; Kockel and Walther (1965) — relationships between the Serbo-Macedonian and Rhodope massifs.

Px = pre-Apulian zone (or Paxos zone); *I* = Ionian zone; *G* = Gavrovo zone; *P* = Pindus zone (*b* = ultra Pindic subzone); *Pk* = Parnassus zone; *Sp* = sub-Pelagonian zone; *Pg* = Pelagonian zone; *Al* = Almopias zone; *Pa* = Paikon zone; *Pe* = Peonias zone (*a* = pre-Peonian subzone, *b* = eastern Peonian units); *Sm* = Serbo-Macedonian zone and Serbo-Macedonian massif; *Rh* = Rhodope massif. *1* = overthrust (*1a* = known; *1b* = supposed); *2* = limit of zone (*2a* = known; *2b* = supposed).

(R. BLANCHET AND J. MERCIER 1978)

However, Jaranov (1938, in Mountrakis, 1977) and Dimitrov (1959, in Mountrakis, 1977) separate the crystalline rocks of the Rhodope massif area in Bulgaria into two sequences:

An older sequence made up of gneisses with aplites dykes and pegmatitic intrusions, kyanite-schists, amphibolite-schists and a thick series of marbles. A younger overlying sequence made up biotite-gneisses, muscovite-gneisses and a very thick series of marbles.

The age of the lower sequence is considered to be Precambrian and that of the overlying sequence to be Palaeozoic (Silurian to lower Carboniferous).

Osswalt (1938, in Christofides, 1977) separates the Greek part of the Rhodope massif into four sequences labelled, E, F, G and H by Osswalt (op. cit.).

The sequence of gneisses (E) which occupy the western part of the area, are the oldest rocks. The lower part of this sequence consists of muscovite-gneisses with biotite-gneisses and two-mica-gneisses. In the middle there are mica-schists and in the upper series occur amphibolites. Rare localised thick series of marbles also occur. The thickness of this sequence is not known accurately because the base cannot be seen, but it is at least 7 km (Osswalt op. cit.).

This sequence has been studied by Welter (1919, in Papadakis, 1965) and Kossmat (1924, in Papadakis, 1965) who considered the schists and gneisses to be originally of igneous origin with subsequent metamorphism. According to

Osswalt (ibid.) the sequence of gneisses with mica-schists and marbles is indisputably of a sedimentary origin. In evidence he cites a gradational transition upwards into the overlying series of marbles. He considered the overlying sequences to have likewise a sedimentary origin.

The sequence of marbles (F) which extends into eastern Macedonia as far as the river Nestos, is considered to be conformable with the underlying sequences (E). It consists of mainly white marbles which are replaced in many areas by chestnut - or ash-coloured marbles. A similar situation was found on the island of Thasos by Speidel (1929, in Papadakis, 1965).

The sequence of mica schists (G) overlies and is conformable with that of the marbles. In addition to mica-schists it consists of gneisses and, rarely, amphibolites (Kato Nevrokopi, Leivadaki), but near Leivadaki there are a series of marbles. The sequence extends into the Nestos area and is estimated to be between 5 and 5.5 km thick.

The sequence of schists and marbles (H) extends north-east of the river Nestos. Here it consists of an alternation of amphibolites and mica-schists followed by marbles, the estimated thickness being 3 km.

According to Osswalt (op. cit.) the whole thickness is between 21 km and 24 km, while the age of the first two sequences is Precambrian, the upper sequences date back to the lower Cambrian.

Metamorphism of the original sedimentary rocks must have been prior to the Carboniferous, because cobbles of

these metamorphic rocks have been found in the Permian.

Boreadis (1954) found sequences similar to those described by Osswalt (op. cit.) on the island of Thasos.

1-2c Chronostratigraphy of the Rhodope Massif

None of Osswalt's sequences have yielded any fossil evidence for their age and in the area of Alexandroupolis the high grade metamorphic rocks are overlain by a great thickness of phyllites. Within these phyllites, near the village of Makri, fossil tubiphytes (=Nigriporella) have been found (Maratos, 1972), which, along with other microfossils, have determined the age of the sequence as Triassic. Also, both Kopp (1961, in Maratos, 1972) and Maratos et al (1964, 65) have found in the upper phyllites from the area of Aliki, algae and foraminifera, such as Acicularia, Bacinella irregularis Radoicic, Cuneolina, Textulariella etc., which are of lower Cretaceous age. These sediments were subsequently metamorphosed during the Alpine orogenesis.

Within the post-Alpine sediments, in the area of Alexandroupolis, there is an interesting sequence of clastic rocks consisting of conglomerates, sandstones, marly clay, and marly limestone. The age of this was determined, from fossil evidence, to be Eocene to Oligocene. This sequence has been gently tilted which is thought to be due to the influence of the closing stages of the Alpine folding.

Based on the previous reviews and his own observations, Maratos (1972) gives a brief stratigraphic-lithological account of the evolution, illustrated in fig. (1-2c-1).

RHODOPE MASSIF / *Sedimentary - Metamorphosed*

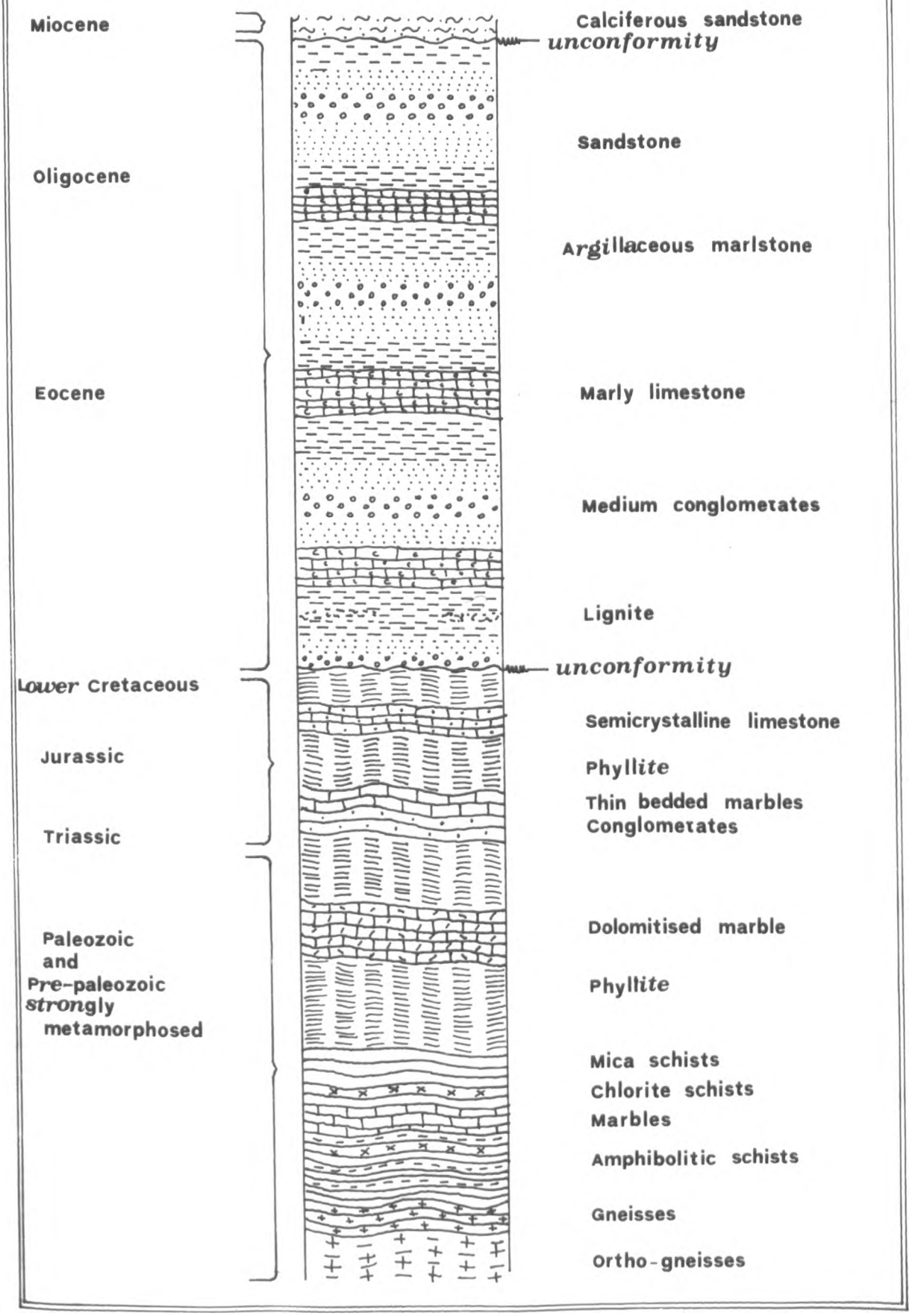

Fig (1-2c-1) Maratos (1972)

1-2d Magmatism of the Rhodope Massif

Both volcanic and plutonic acid igneous rocks make up a significant proportion of the Rhodope massif.

The volcanic rocks have been studied: in Feres-Sapes area (Thrace), Liatsikas (1938), Rentzeperis (1956), Sideris (1973); in Dipotamos-kalotuhos area, Soldatos (1961); in Eastern Xanthi, Soldatos and Papadakis (1971).

The volcanic rocks are essentially tholeiites, dacites and andesites. Papadakis (1972) observes that the chemical composition of these volcanic rocks is similar to the plutonic rocks.

According to Rentzeperis (1956), Soldatos (1961), Kopp (1966) the age of the volcanic rocks is Eocene to Oligocene. Boccaletti et al (1974) considered that all the volcanic centres in western Thrace range in age from Neogene to Quaternary.

The plutonic rocks of the following areas have been studied: in Dipotamos (Soldatos, 1961), the island of Samothraki (Davi, 1963), Kavala (Fischer, 1964; Kronberg et al, 1970; Kokkinakis, 1977), Serres-Drama (Papadakis, 1965), Philippi (Melidonis, 1969a), Aimonion-Kotuli (Melidonis, 1969b), the Pangaion (Schenk, 1970), Falakron - Granite village - Panorama - Potamoi (Kronberg et al, 1970), Menoikion (De Boer, 1970), Xanthi (Christofides, 1977) and Paranesti (Dipotamos) (Sklavounos, 1981).

Osswalt (1938, in Papadakis, 1965) considered that all the granites of the Greek Rhodope massif show a close similarity

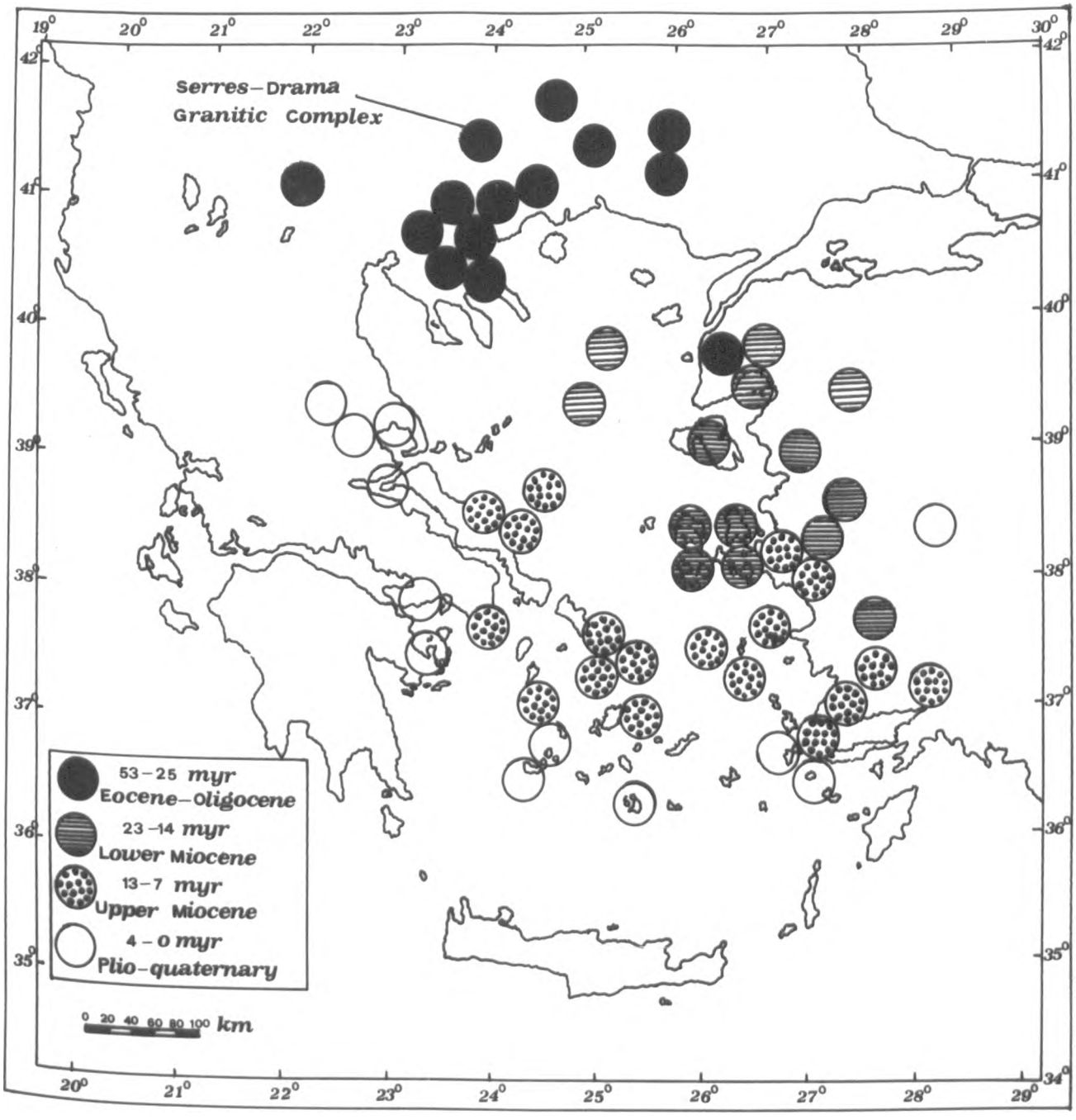

Fig. (1-2d-1) Papadopoulos (1982)

and concludes that the age is indisputably Eocene.

Papadopoulos (1982) has reviewed the geochronological data for one hundred and thirteen plutonic and volcanic rocks in the Aegean region (Greece and West Turkey). Of these only fifty six have been plotted on to figure (1-2d-1). The age of these fifty six have been determined by more accurate physical methods.

It can be noted (fig. 1-2d-1) that there has been virtually continuous magmatism in the area over the last 53 million years.

The magmatism can be divided into the following periods: (Papadopoulos, op. cit.).

Eocene - Oligocene	53-25 myr
Lower Miocene	23-14 myr
Upper Miocene	13-7 myr
Pliocene - Quaternary	4-0 myr

With reference to the above figure (1-2d-1), it can be concluded that the area of Caenozoic magmatic activity of the Aegean region has been moving from north to south.

Petrov (1977) observed a similar change in location for Caenozoic volcanic activity developed between the Balkanic range and the south Aegean arc. Papadopoulos (op. cit.) has also noted this in the Neogene magmatism of the Aegean region.

The magmatic activity in the Greek Rhodope massif is Eocene-Oligocene age (53-25 myr). This is in agreement with the earlier geological observations made by Osswalt (1938).

1-2e Tectonics of Rhodope Massif

According to Osswalt (1938, in Papadakis, 1965) the Rhodope massif was deformed during the Eocene, as recognized from the deformation of the crystalline schists in the areas of Kato Brontou, the river Nestos and west of the Gulf of Orphanou (figure 1-2e-1). After this period of deformation there followed the intrusion of a large volume of mainly acid magma of Eocene to Oligocene age. After this intrusive episode there was a period of vertical movement.

Fischer (1964, in Papadakis, 1965) observed that the granite of Kavala had been subjected to stresses from a NW-SE direction during the Eocene, when it was in a solid state, resulting in the formation of a gneissose texture.

Kronberg et al (1970) examined the structure of the Rhodope massif in the area between the rivers Strimon and Nestos. There are two periods of folding (B_1 and B_2) recognised. The B_1 folds have NE-trending axes and are small scale isoclinal folds. The B_1 axes, however, are dominantly overprinted by the WNW-ESE trending B_2 folds.

1-3a The geological location of the Serres-Drama granitic complex

The Serres-Drama granitic complex (map in end pocket) was emplaced into the upper part of the oldest sequence of gneisses (E) and the overlying sequence of marbles (F). The depth to the base of the granitic complex is unknown.

The northern contact, west of Katafiton village, is

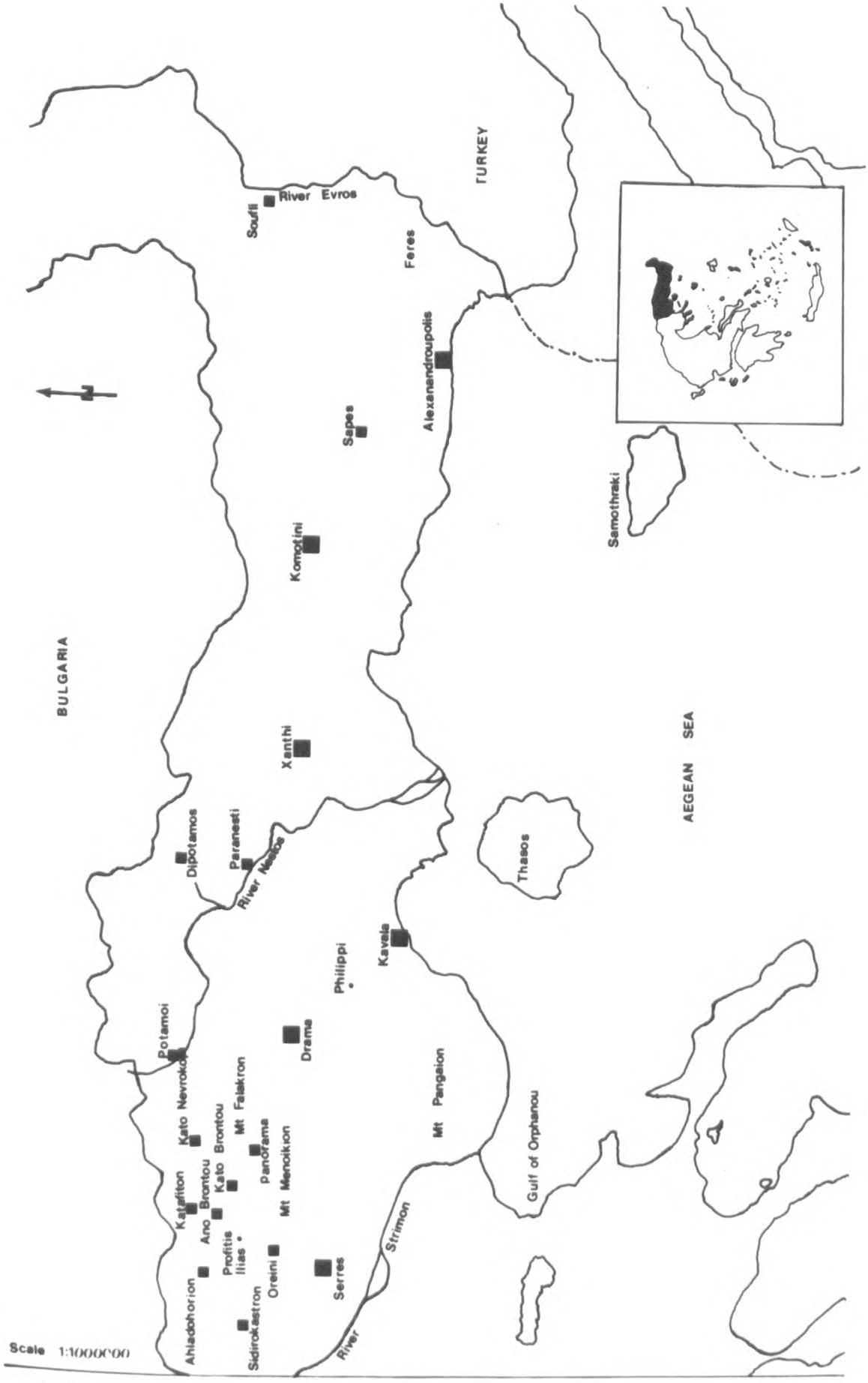

Fig. (1-2e-1) Greek Rhodope massif

with Precambrian marbles. At this contact there is no evidence of deformation during the intrusion of the granite. This marble extends from the contact into Bulgaria. Between the marble and Katafiton there is a small area of Pleistocene conglomerate.

At the contact between Katafiton and Kato Brontou, there are gneisses, mica-schists and some amphibolites. It can easily be seen that there is no evidence of forceful intrusion at this contact. Near Kato Brontou there is a small area of marble. To the southwest of Kato Brontou there is an area of marbles, amphibolites, granites and aplites. There appears to be no relationships between these granites and aplites and the plutonic complex.

At the southern contact, two distinct areas may be seen. The area around the main road between Serres and Ano Brontou is characterized by marbles, while the rest is characterised by gneisses, which also occupy part of the area SW of the granitic complex.

In the SW corner of the granitic complex, north of the village of Oreini, a gneissose texture was observed in the rocks within the intrusion with a gradational change at the contact into country rock gneisses. This may be due to localised shearing after intrusion. The western contact, the area enclosing Kapnofiton and extending as far as Ahladohorion is occupied by Neogene sediments. North of Ahladohorion and west of the intrusion is occupied by Pleistocene conglomerate. In this area the presence of cobbles of material derived from the granitic complex can be observed.

The Serres-Drama granitic complex consists of gabbro, monzonite, quartz monzonite, granodiorite and granite. Sheets of aplite and occasionally pegmatite also occur.

The quartz-monzonite occupies the western, southern and part of the northern area of the intrusion with a gradual transition into granite towards the centre of the complex. The rock-types mentioned above cover about three-quarters of the outcrop. There appears to be a continuous transition also between the granite and the granodiorite which outcrops in the vicinity of Ano Brontou. A narrow strip of quartz monzonite also protrudes from the main mass, this strip runs from south of the 'Diabasis Ag. Paraskevis' to the north of the village of Ano Brontou and surrounds the mass of monzonite to its south-west. Monzonite occupies the area NE of the intrusion.

A small sheet - like body of gabbro is located near the main Serres to Ano Brontou road and the body is elongated in a NE-SW direction. The relationship between this gabbro and the surrounding quartz monzonite is totally obscured.

In all the rock-types, with the exception of the gabbro, the occurrence of numerous xenoliths may be noted. The Xenoliths are all of igneous origin, and appear more basic than the enclosing rock-type, the majority of these are of diorite compositon.

1-3b The age of the complex

The complex is intruded into Precambrian marbles and

the presence of cobbles of the granitic rocks in the Pleistocene conglomerate dates of the complex between Precambrian and Pleistocene. However, from Section (1-2b) the metamorphic rocks have been found in Permian conglomerates, therefore the intrusive is post-Permian and pre-Pleistocene.

Two sets of isotopic ages have been determined using the K/Ar dating technique. Papadakis (1965) determined an age of 53 ± 4.2 myr for rocks of quartz monzonite composition using the whole-rock technique. However, ages obtained from hornblendes and again using the K/Ar technique, Marakis (1968) determined the age of the complex as follows:

TABLE (1-3b-1) (From Marakis, 1968)

Sample No.	area	mineral	K%	$^{40}_{*}$Ar ppm	$^{40}_{*}$Ar%	Age(myr)
24.1	Ano Brontou	hornblende	0.65	0.00136	62.0	29 ± 1
24.2	"	"	0.68	0.00141	61.5	29 ± 1
24.3	"	"	0.66	0.00140	56.8	30 ± 1
24.6	"	"	0.96	0.00205	50.2	30 ± 1
24.4	"	"	0.67	0.00147	58.6	30 ± 1
24.5	"	"	0.70	0.00166	58.7	30 ± 2

Although there is a large discrepancy between the two sets of results from the Serres-Drama granitic complex the ages belong to the group of igneous complexes intruded during the Eocene and Oligocene (Papadopoulos op.cit.).

1-4 Previous work on the Serres-Drama granitic Complex

Wurm (1922, 1925, in Papadakis, 1965) characterized the outcrop as hornblende granite, parts of which were porphyritic and others syenitic in character. In the vicinity of Ano Brontou he found that the periphery of the granite was hornblende syenite with augite.

Papadakis (1965) has made a study of the descriptive mineralogy and petrography of the Serres-Drama granitic complex and the contact-metamorphism of the aureole.

All his observations were made using petrographic techniques, with the exception of two x-ray diffractograms of minerals from the contact-alteration zone of the marble (spinel and chabazite) and four wet chemical analyses of grabbro, monzonite, granodiorite and quartz-monzonite (analyst K. Soldatos).

He made an interesting study of the optical properties of the above minerals. The x-ray diffraction determinations of microcline in the Serres-Drama granitic complex undertaken in the present study support his optical determinations, both indicating maximum microcline.

He classified the types of twinning developed in the plagioclase feldspars and has determined the compositional zoning of these plagioclases. The electron-microprobe analyses, differ slightly from his optical results.

There has been no systematic geological mapping in this area up to the present. In this study, Papadakis' map has been used as a base but modifications have been necessary namely: Oxies, where the rocks are quartz monzonite

rather than syenite, at Papazora where the area of monzonite is larger than mapped out by Papadakis, and a small area to the south of Diabasis Ag. Paraskevis, an area called granodiorite by Papadakis which is in fact quartz monzonite.

CHAPTER II : PETROGRAPHY

CHAPTER II

PETROGRAPHY

2-1-1 Introduction

This study was begun with a field programme to establish:

a - the rock-types that occur in the granitic complex;
b - the area in which each rock-type occurs; and
c - how each rock-type is related to the others.

A subsidiary objective was to make some observations in the field, which might help in the formulation of a preliminary hypothesis of the genesis of the batholith.

The Serres-Drama granitic complex is the largest intrusion (greater than approximately 250 km^2) in the Greek Rhodope massif area, with a broad spectrum of composition ranging from felsic to mafic.

This area is close to the Bulgarian border; consequently there are some difficulties with field work. The relief of the area is high (Profitis Ilias, 1849 m, Mavro Bouno, 1663 m, Siderobouni, 1475 m, Ano Brontou village about 900 m) with abundant steep hill sides. The majority of the area is aforested. The area is accessible by secondary unmade roads and overgrown trails provide further access; many of these are passable only with difficulty. For the above reasons it was not possible

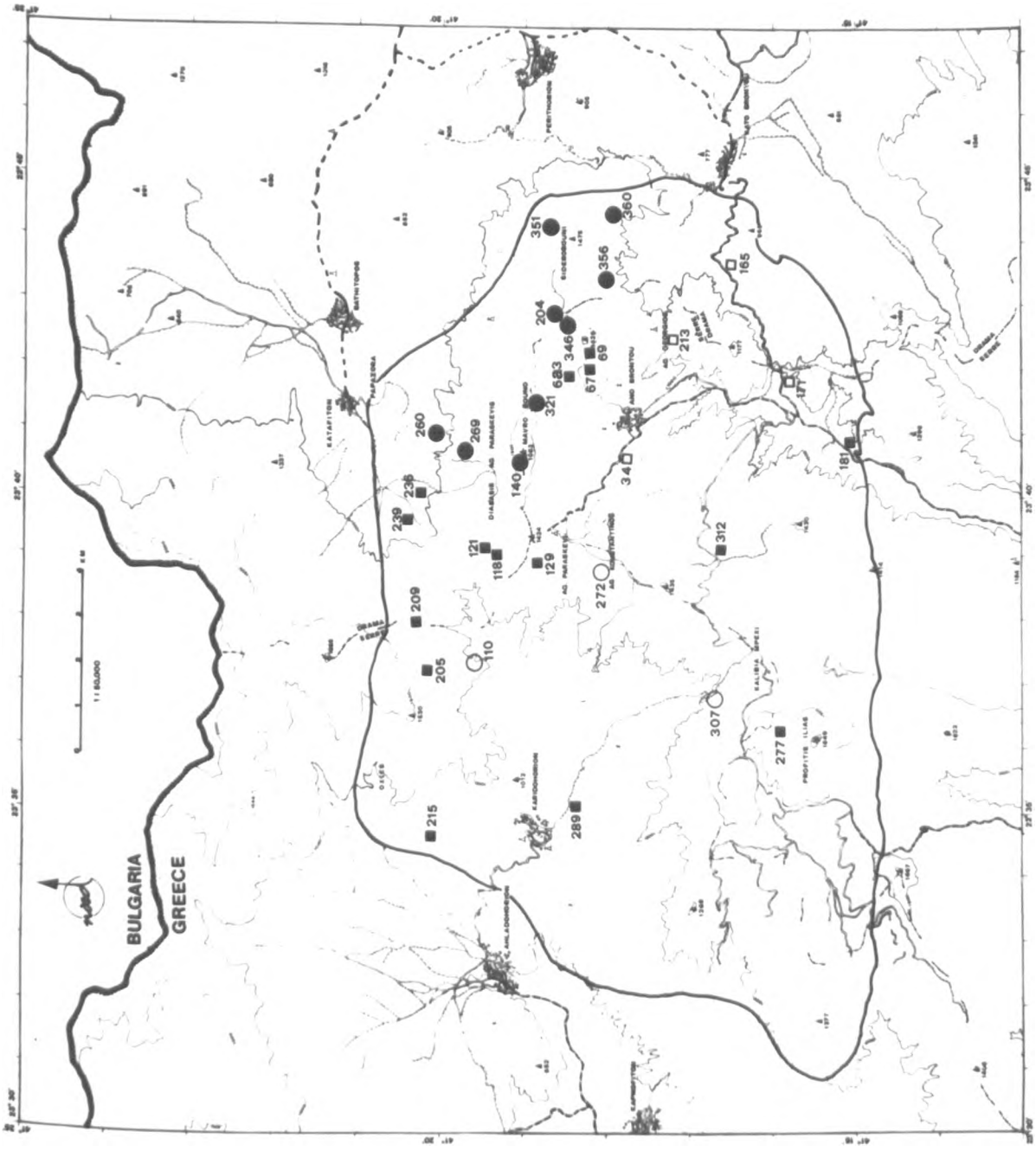

Fig. (2–1–1a)

○ Granite

▪ Quartz monzonite

□ Granodiorite

● Monzonite

to sample the area well, but the author was able to collect over three hundred and fifty samples, so as to include the full range of rock-types present in the granitic complex. No photographs of the area could be taken, as this is a military zone in which it is forbidden. Locations for samples which have been modally analysed are shown in fig. (2-1-1a).

2-1-2 Compositional Classification

Papadakis (1965) has described quartz monzonite, granodiorite, monzonite, xenoliths, gabbro, aplite and pegmatite from this intrusion, but does not describe a small area of syenite near 'Oxies', although it is marked as such on his map.

The quartz monzonite and the comparatively small area of granodiorite cover about three-quarters of the outcrop. Papadakis (op. cit.) used the petrographic scheme of Tröger (1955) to classify the rock-types. His modal analysis of the twenty samples classed as quartz monzonite (see table, 2-1-2b) plotted on the Streckeisen (1976) diagram (see, fig. 2-1-2b), give different results to that of Tröger (1955). On Streckeisen's scheme the above mentioned samples separate into ten granites and ten quartz monzonites. Consequently the area which Papadakis (op.cit.) classified as quartz monzonite, included, according to this recent classification, granite. However, Papadakis (op. cit.) does not include the location of his samples in his text.

The author has replotted on the Streckeisen QAPF double triangle all the modal analyses originally given by Papadakis (op.cit.); no significant differences were observed for the other rock-types.

Field work has not established any textural difference between granite, quartz monzonite and granodiorite. These three rock-types have been seen to be fairly uniform with slight variation in colour and grain-size (coarse) of the same mineralogical composition Two exceptions are the small area of 'Oxies' and one to the north-west of 'Diavasis Ag. Paraskevis', along the border between quartz monzonite and monzonite, in which occur megacrysts of potassium feldspar. The distribution of megacrysts can be seen in fig. (2-1-2c).

An abundance of aplite veins, but only a few pegmatite veins, occurs in the above rock-types. In the field a sharp contact between these intermediate rock-types and the more basic monzonite has not been found. However, the group consisting of monzonite, the dioritic xenoliths, and gabbro has been distinguished by an increase in mafic mineral content and the decrease or absence of quartz. Consequently, it can be seen from field studies, that the Serres-Drama granitic complex separates distinctly into two groups of rock-types:

a) an 'intermediate' group: granite, granodiorite, and quartz monzonite; and

b) a 'basic' group: monzonite, dioritic xenoliths, and gabbro.

From the study of over three hundred thin-sections, the following general observations have been made for separating the above groups:

a) Clinopyroxenes occur only in the 'basic' group; and

b) Microcline is the sole potassium feldspar polymorph to be found in the 'intermediate' group, while orthoclase occurs in the 'basic' group (does not include gabbro).

The distribution of potassium feldspar polymorphs is shown in fig. (2-1-2d).

Thirty-one samples were separated for modal analysis (the samples are identified by station numbers and a symbol to denote rock-type, fig. 2-1-1a) to try to distinguish between quartz monzonite, granite, granodiorite, and monzonite. Each specimen was stained under the supervision of Dr C.S. Exley (details for the procedure for staining thin sections can be found in appendix A).

Modal analysis of single thin sections of different rock-types is not considered to be a very satisfactory method of assessing the mineral variation in coarse-grained rock complexes (cf. Booth, 1966).

Modes obtained for a particular rock-type sample may not be representative of the sample that they illustrate and certainly do not give a true indication of variation within that rock-type. A modal point count can only be relied upon to obtain data for the thin-section upon which it is performed. However, it is considered that in this study

a sufficient number of samples was taken from each rock-type to give a reasonable picture of the range of modal composition to be observed in those types.

The modal variation of the Serres-Drama granitic complex is shown in table (2-1-2a). It can be seen from this table that for plagioclase the range is from 30.71% to 49.08%; for potassium feldspars (including albite) the range is from 18.33% to 56.39%; for quartz the range is from 0.00% to 32.99%; for amphiboles the range is from 0.63% to 9.91%; for biotite the range is from 0.00% to 5.53%; for clinopyroxenes the range is from 2.80% to 9.57% (only in monzonite); for sphene the range is from 0.08% to 1.30%; and for ore (including some small fragments) the range is from 0.39% to 2.31%.

Plutonic rocks are classified and named according to their mineral contents. According to the classification scheme of Streckeisen (1976), rocks with M (mafic and related minerals) less than 90% are classified and named according to their position in the triangle Q (quartz), A (alkali feldspar), P (plagioclase). The data from table (2-1-2a) have been plotted on the above triangle, fifteen samples fell into the composition field of quartz monzonite; three samples fell into the composition field of granite; four samples fell into the composition field of granodiorite; and nine samples fell into the composition field of monzonite.

For general classification of the rock-types, modal analysis, thin-section study and chemical (X-R-F)

TABLE: (2-1-1a) Modal analyses of quartz monzonite, granite, granodiorite and monzonite from the Serres-Drama granitic complex.

	Plag	K-feld	Qz	Amph	Biot	Clinopy	Sphene	Ore	Total	No. of points counted
					Quartz monzonite					
6a3	38.98	40.06	12.49	6.49	0.27	-	0.43	1.27	99.99	4800
67	33.35	42.99	14.34	5.78	1.87	-	0.44	1.32	100.09	4800
69	43.67	35.44	5.20	9.91	2.28	-	1.23	2.12	99.85	4800
118	52.23	31.99	5.81	6.47	0.51	-	0.91	2.08	100.00	4800
121	36.11	49.69	4.51	6.05	0.36	-	1.08	2.16	99.96	4800
129	36.08	47.66	4.43	7.27	1.93	-	1.30	1.30	99.97	4800
181	48.69	31.23	10.54	7.47	0.25	-	0.58	1.24	100.00	4800
205	44.57	27.93	17.58	5.59	2.99	-	0.94	0.39	99.99	4800
209	41.59	25.53	16.64	9.24	3.93	-	1.05	2.01	99.99	4800
215	41.56	34.73	17.26	3.75	0.35	-	0.79	1.57	100.01	4800
236	40.52	29.57	17.51	8.26	2.23	-	0.52	1.38	99.99	4800
239	40.97	28.87	17.20	8.46	2.59	-	0.61	1.30	100.00	4800
277	39.19	46.26	8.23	4.01	0.66	-	0.46	1.19	100.00	4800
289	42.90	29.42	16.92	6.92	1.35	-	0.63	1.86	100.00	4800
312	49.08	32.29	6.85	7.36	1.78	-	0.82	1.80	99.98	4800
					Granite					
110	45.06	25.16	19.16	6.90	2.43	-	0.46	0.83	100.00	4800
272	37.22	35.23	22.38	2.07	1.54	-	0.81	0.75	100.00	4800
307	33.43	22.64	32.99	6.45	1.93	-	1.08	1.48	100.00	4800
					Granodiorite					
34	47.87	22.32	22.05	3.56	2.05	-	0.22	1.96	100.03	4800
165	46.80	25.85	20.44	3.51	1.77	-	0.48	1.15	100.00	4800
171	47.00	18.33	19.23	6.29	5.53	-	1.30	2.31	99.99	4800
213	48.15	23.73	21.11	2.91	2.65	-	0.28	1.19	100.02	4800
					Monzonite					
140	30.71	56.39	0.59	0.83	-	9.50	0.95	1.03	100.00	4800
204	42.35	43.74	-	1.67	0.47	9.57	0.28	1.91	99.99	4800
260	45.97	33.70	4.04	8.23	0.10	4.57	1.16	2.13	99.90	4800
269	49.33	33.65	4.26	7.27	0.10	2.18	1.50	1.71	100.00	4800
321	35.01	50.51	2.24	4.22	0.50	5.54	0.83	1.16	100.01	4800
346	41.51	44.90	4.53	1.78	0.81	4.29	0.65	1.54	100.01	4800
351	47.48	37.23	3.64	5.14	0.59	3.30	1.26	1.35	99.99	4800
356	37.15	46.04	2.88	9.45	0.08	2.80	0.48	1.12	100.00	4800
360	42.11	43.76	3.12	6.24	-	3.62	0.08	1.07	100.00	4800

Fig. (2-1-2a): Streckeisen Q - A - P triangle showing the position of the rocks of the Serres-Drama granitic complex based on modal analysis. The small figure (top right) indicates the compositional fields which are: 1a, quartzolite (silexite); 1b, quartz-rich granidoids; 2, alkali-feldspar granite; 3, granite; 4, granodiorite; 5, tonalite; 6*, quartz alkali-feldspar syenite; 7*, quartz syenite; 8*, quartz monzonite; 9*, quartz monzodiorite/quartz monzogabbro; 10*, quartz diorite/quartz gabbro/quartz anorthosite; 6, alkali-feldspar syenite; 7, syenite; 8, monzonite; 9, monzodiorite/monzogabbro; 10, diorite/gabbro/anorthosite, (after Streckeisen, 1976).

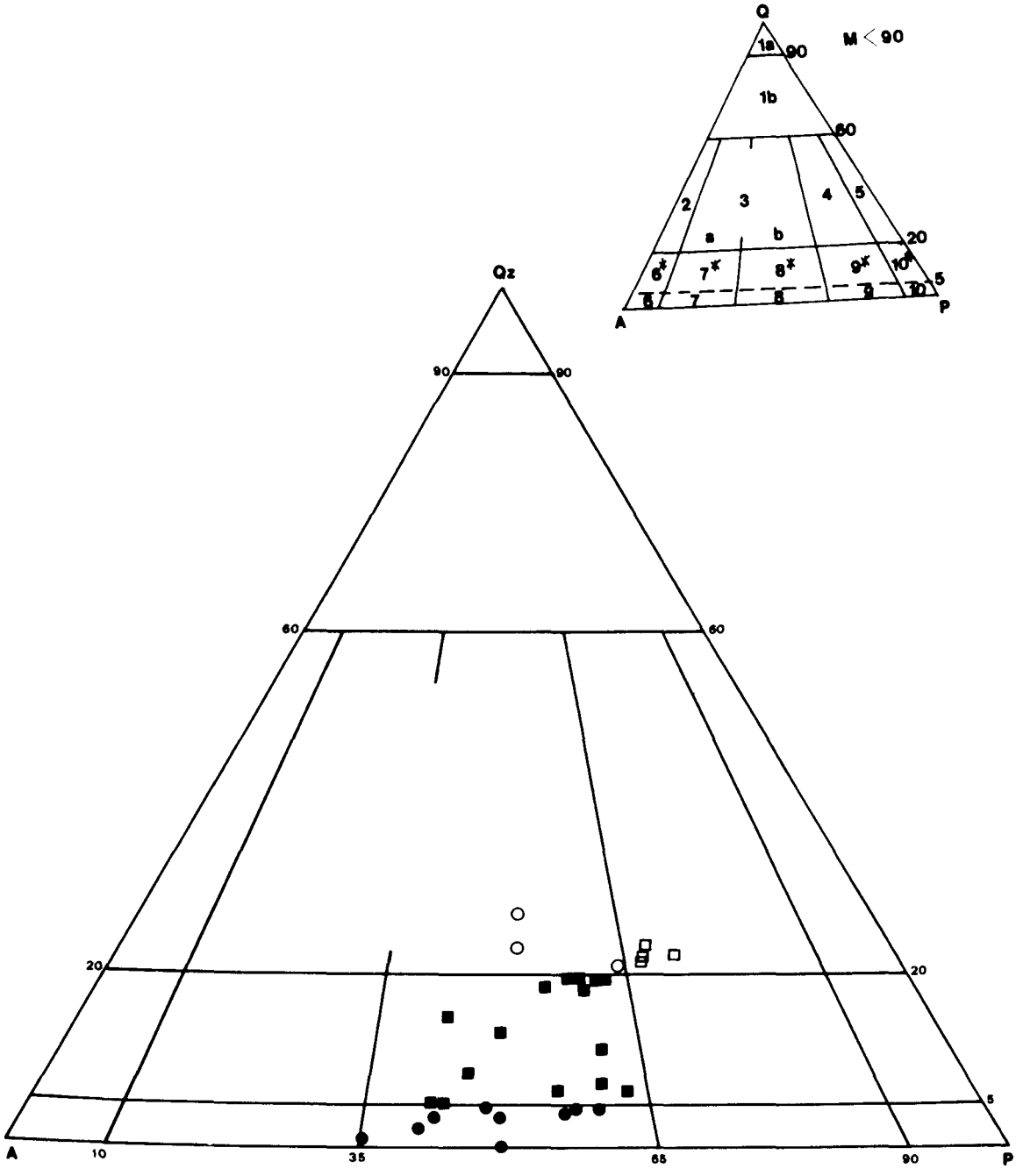

Fig. (2-1-2a) (from Streckeisen, 1976)

○ Granite

■ Quartz monzonite

□ Granodiorite

● Monzonite

TABLE: (2-1-2b) Modal analyses of quartz monzonite from the Serres-Drama pluton. (Papadakis, 1965, table 10,p 60)

	Plag.	K-feld	Qz	horn	biot	all. oth. min.
15	48•18	26•70	13•88	9•85	4•20	2•68
Gr 23	43•90	33•72	12•24	8•20	-	1•94
29'	38•28	42•25	10•86	7•81	-	0•80
43	46•05	30•95	10•80	9•84	-	2•37
46	38•93	31•95	19•17	6•43	-	3•51
46'	42•91	25•23	17•81	12•70	-	1•27
66	35•88	29•31	12•57	5•48	2•82	1•93
103	33•82	33•40	27•43	-	4•28	1•07
106	27•87	33•04	20•61	15•09	-	3•35
109	37•67	25•74	27•72	4•64	2•33	1•90
113	30•62	17•95	18•07	19•32	8•72	5•32
116	34•73	34•15	17•57	10•46	1•24	1•84
118g	32•96	34•01	15•36	13•01	1•50	3•17
121	31•63	27•66	29•12	5•46	4•82	1•32
140	42•34	36•16	10•92	8•30	-	2•22
141a	40•24	27•40	26•90	4•73	-	0•73
158	42•03	37•99	14•17	3•57	-	2•84
181	47•94	29•16	15•23	5•83	-	1•84
28	34•30	45•70	10•76	6•96	-	2•28
11	25•21	43•17	25•09	1•64	3•51	1•35

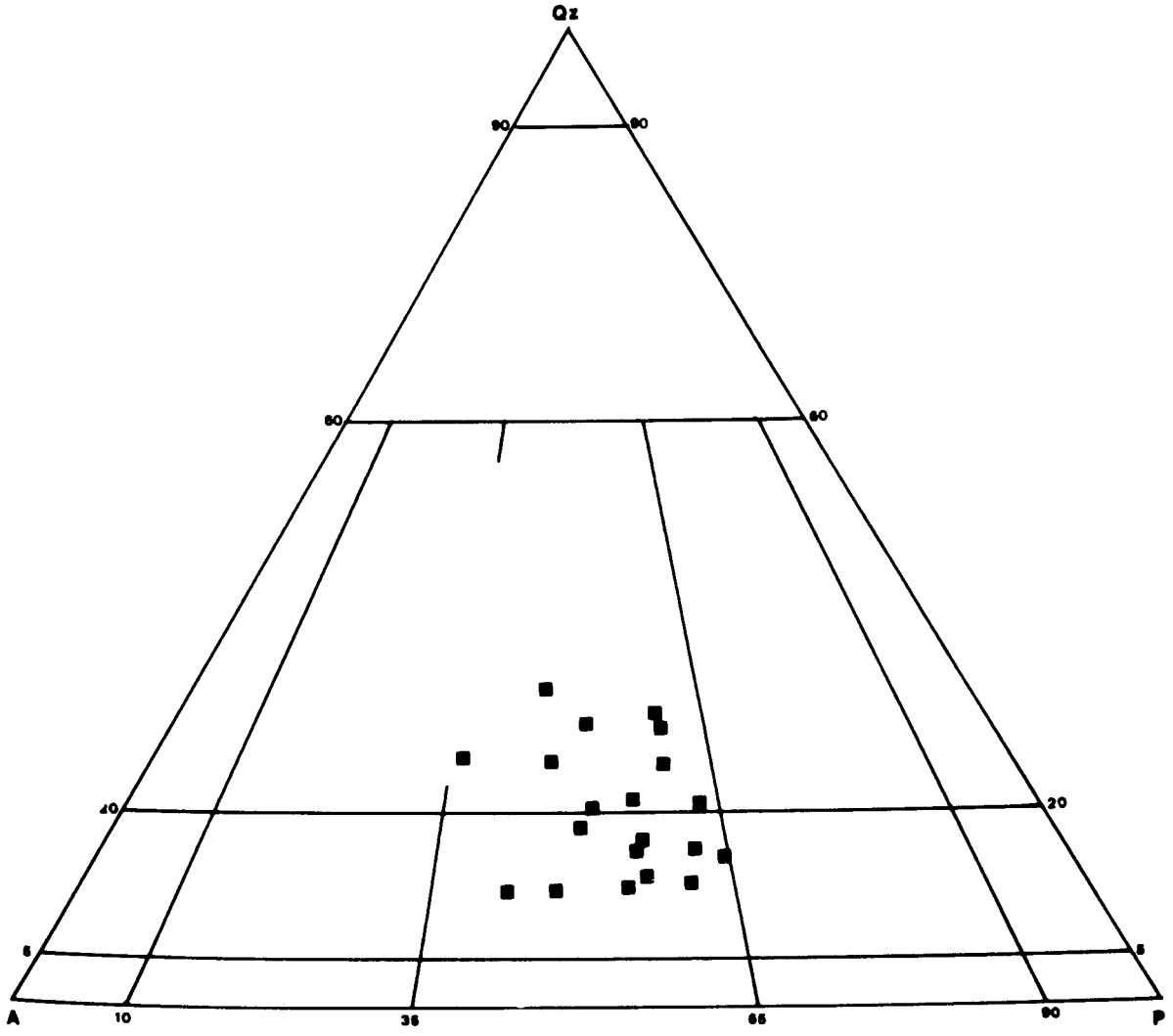

Fig. (2-1-2b)

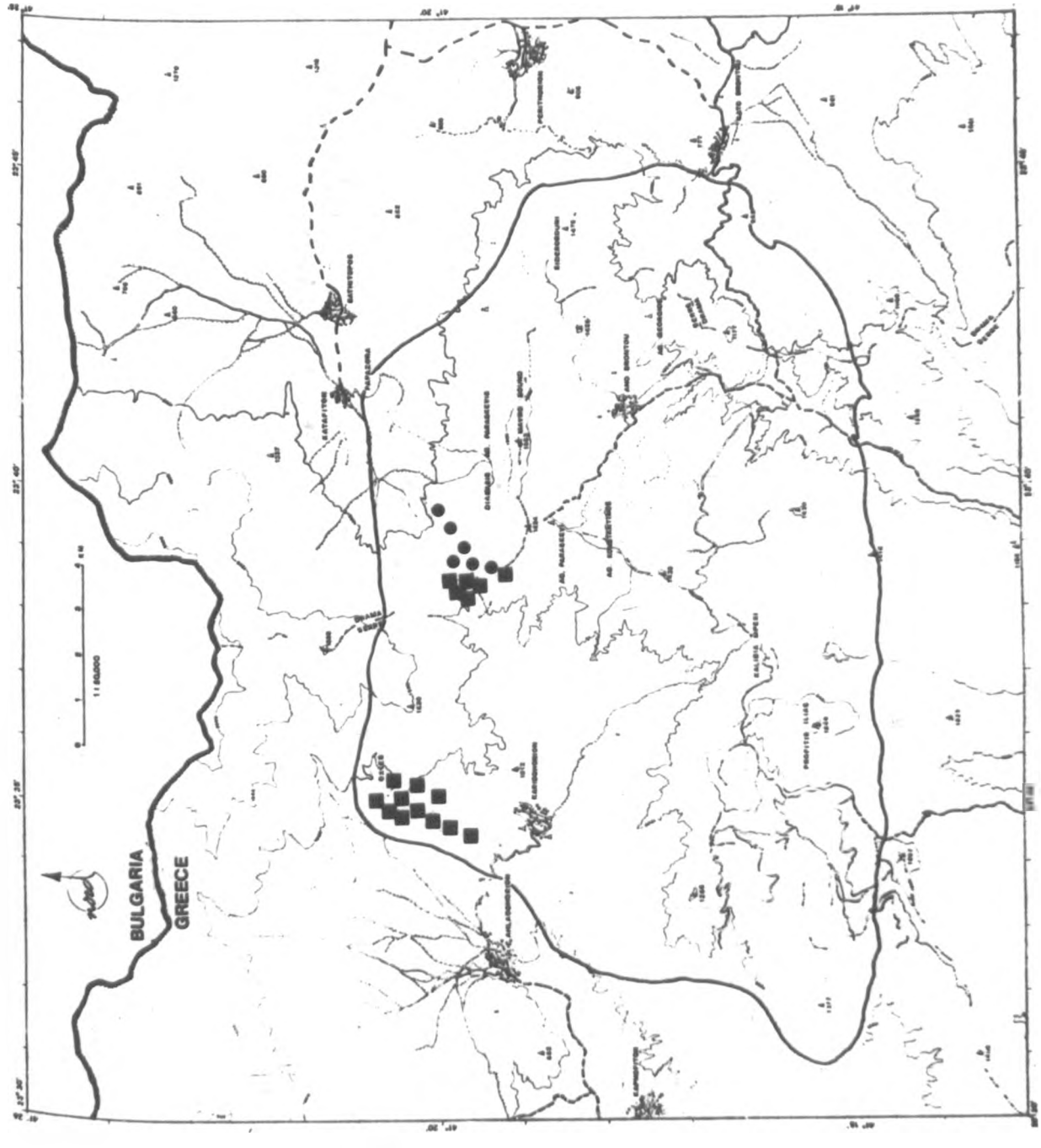

Fig. (2-1-2c)

■ Triclinic K-feldspar megacrysts

● Monoclinic " "

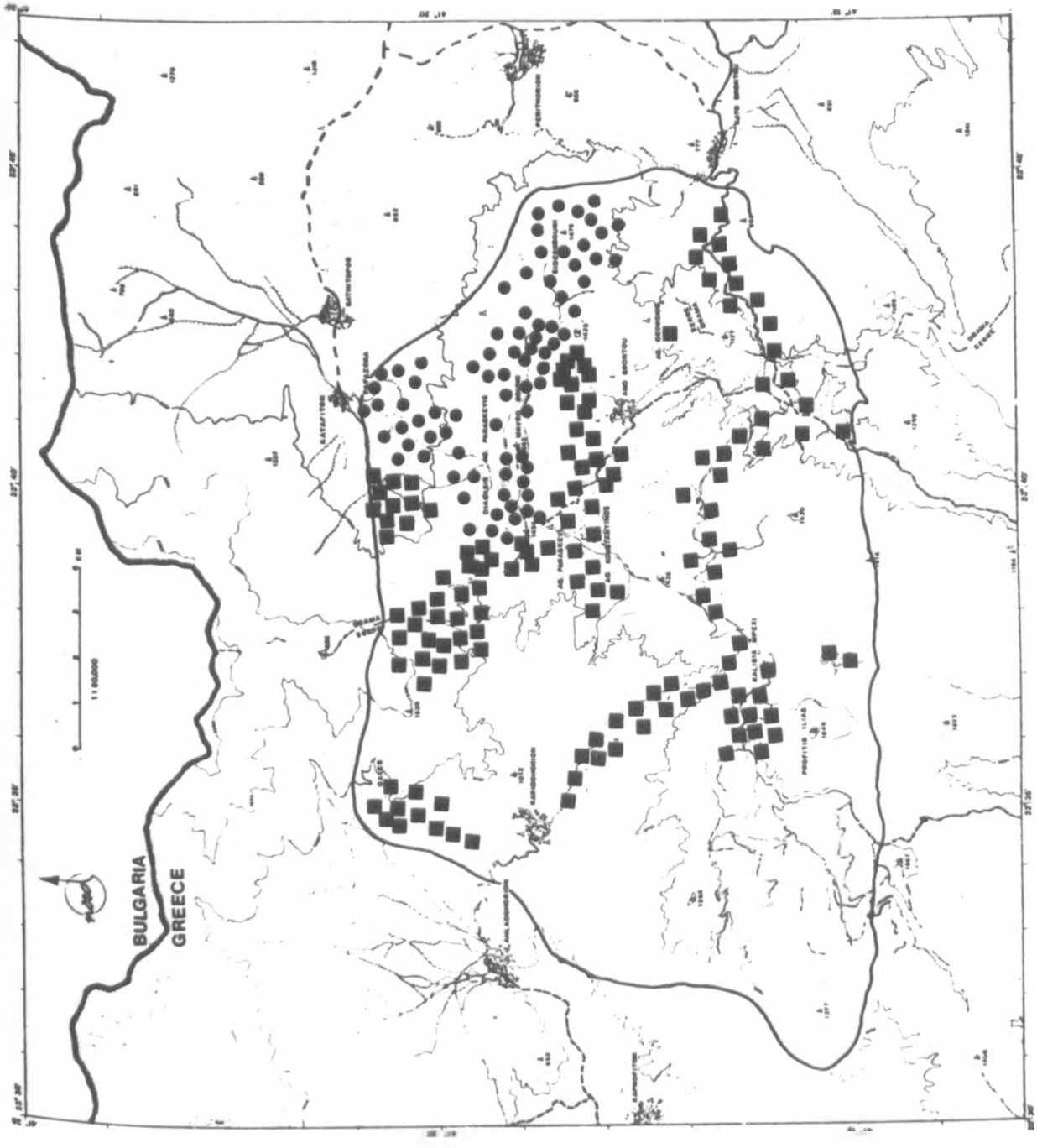

Fig. (2-1-2d)

analysis are used comparatively. Some samples are found to lie close to the boundaries between two rock-types so classification becomes largely a matter of the author's opinion (for general classification of rock-types developed in the area see fig. 4-1-1a).

2-2 PETROGRAPHY OF THE 'INTERMEDIATE' GROUP ROCKS

2-2-1 Quartz monzonite.

Quartz monzonite is the most abundant rock-type in the Serres-Drama granitic complex and occurs over the whole of the south, west and part of the north (west of Katafiton) of the intrusion. A narrow strip of quartz monzonite also protrudes from the main mass, and this small strip runs from south of 'Diavasis Ag. Paraskevis' to the north of the village of Ano Brontou and surrounds the mass of monzonite to its southwest.

The quartz monzonite is coarse-grained but as mentioned above, two small areas with megacrysts of potassium feldspar occur, in the area of 'Oxies' (see fig. 2-2-1a) and along the boundaries with monzonite (see figs. 2-2-1b, 2-2-1c, 2-2-1d). These areas are illustrated in fig. (2-1-2c). In thin-section, shearing was observed in samples collected at the end of the road from 'Kalibia Mpexi' to 'Karidohorion' and in samples collected to the west of 'Kalibia Mpexi'. The presence of shearing is based upon

Fig. (2-2-1a). Euhedral megacryst of alkali feldspar in quartz monzonite (sample No.222) with inclusions of mafic minerals throughout the crystal. 'Oxies' (scale bar is 5 cm long).

Fig. (2-2-1b). Quartz monzonite (sample No.120) with megacrysts of alkali feldspar. West of 'Diabasis Ag. Paraskevis'. (scale bar is 5 cm long).

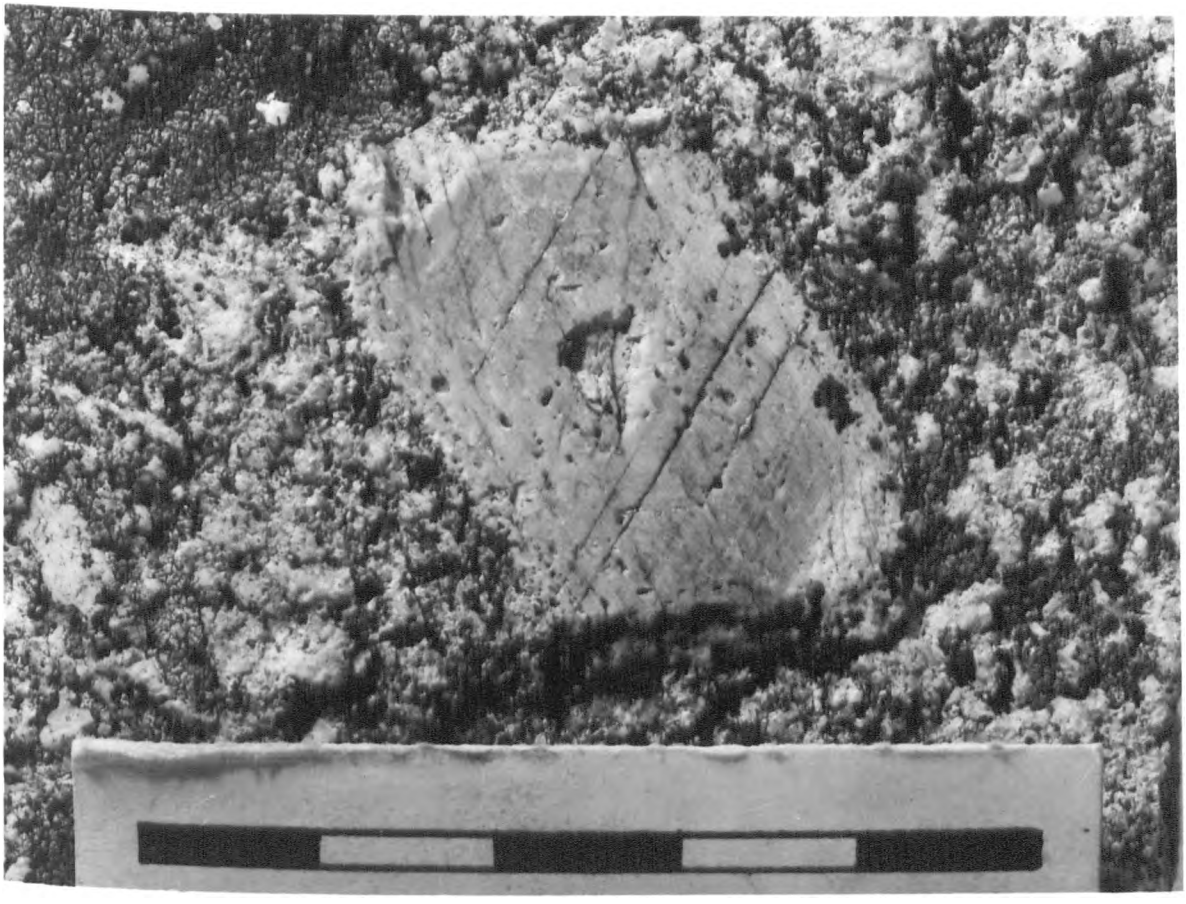

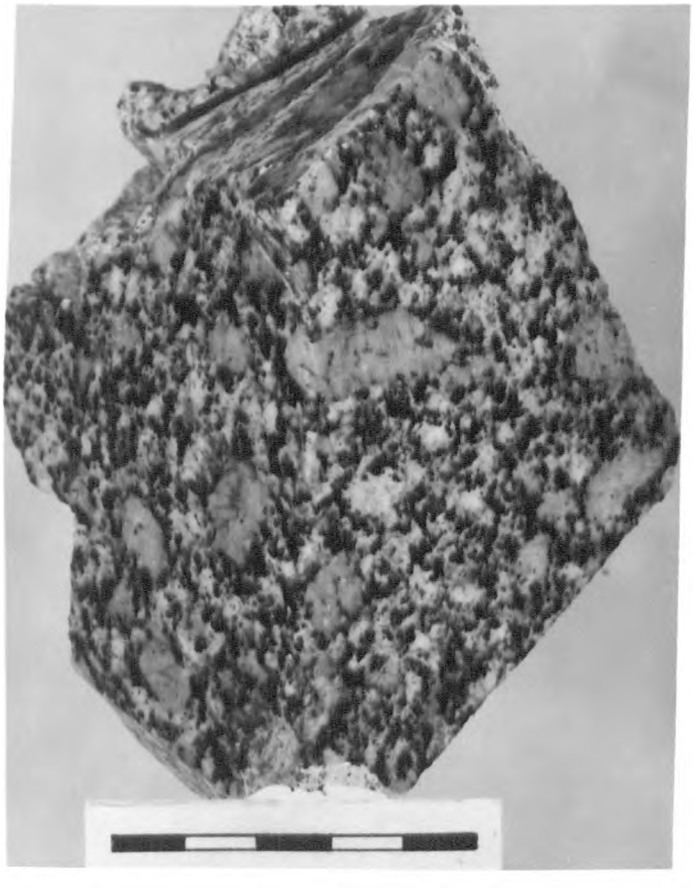

Fig. (2-2-1c). Quartz monzonite (sample 121) with megacrysts of alkali feldspar. West of 'Diabasis Ag. Paraskevis'. (Scale bar is 5 cm long.)

Fig. (2-2-1d). Euhedral megacrysts of alkali feldspar in monzonite (sample No.188). North of 'Diabasis Ag. Paraskevis'. (Scale bar is 5 cm long.)

Fig. (2-2-1e). Photomicrograph of recrystallisation textures of quartz in quartz monzonite (sample No.289). Karidohorion-Kalibia Mpexi road. (Mag. x 156)

Fig. (2-2-1f). Photomicrograph of recrystallization and granulation textures in quartz from quartz monzonite (sample No.275). Profitis Ilias. (Mag.x 319)

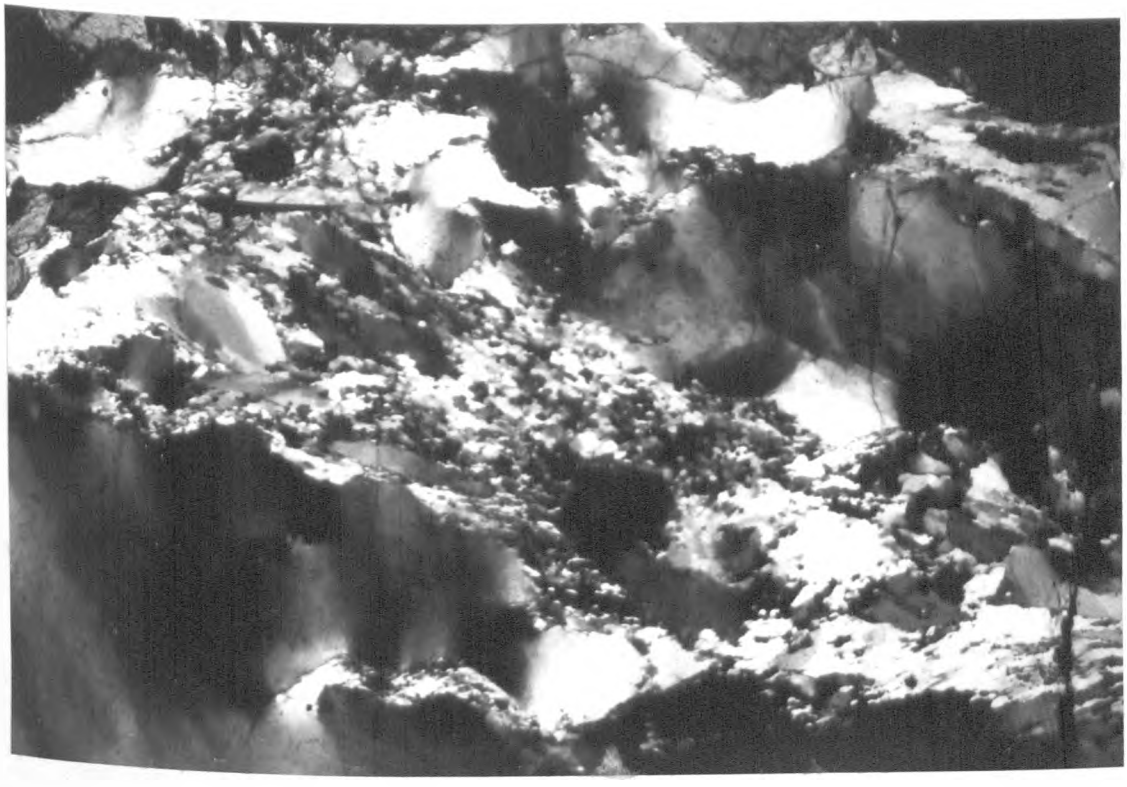

Fig. (2-2-1g). Quartz monzonite (sample No.275) exhibiting deformation lamellae in plagioclase feldspar. (Mag X 312)

Fig. (2-2-2a). Granite (sample No.307) exhibiting the effects of shearing. Cleavage of biotite is bent (centre) and on the right the quartz has been recrystallized. (Mag X 156)

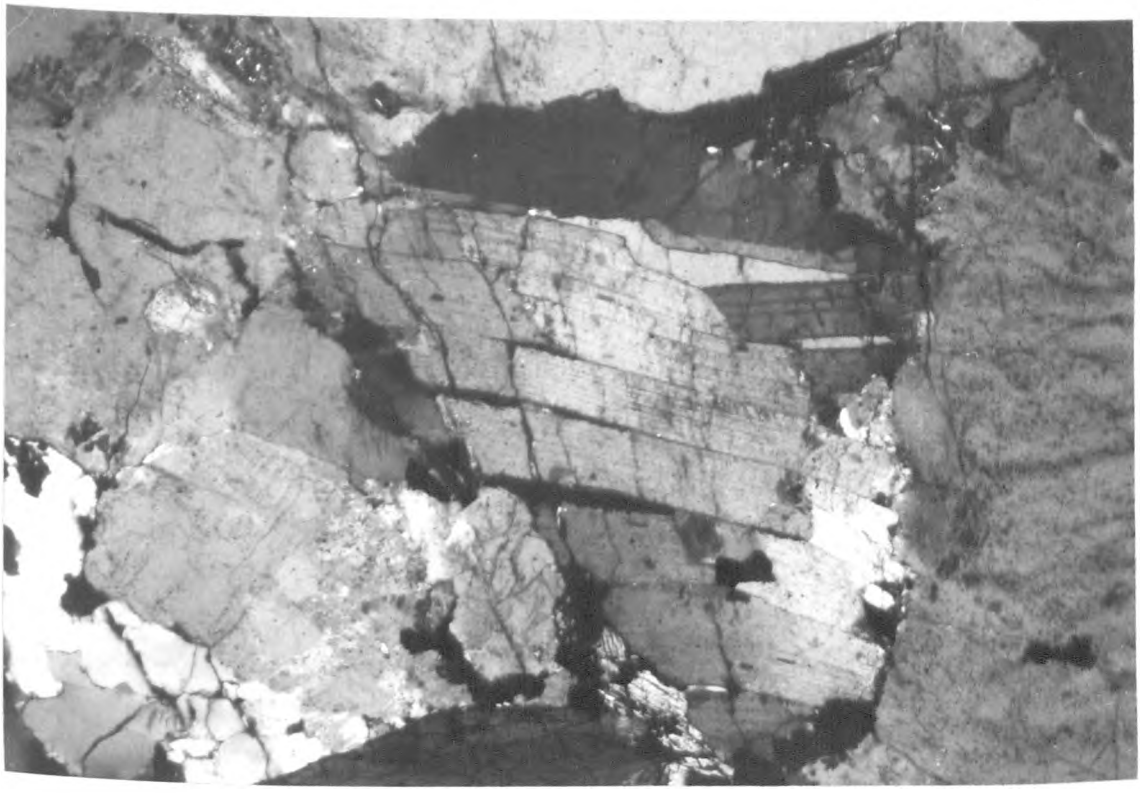

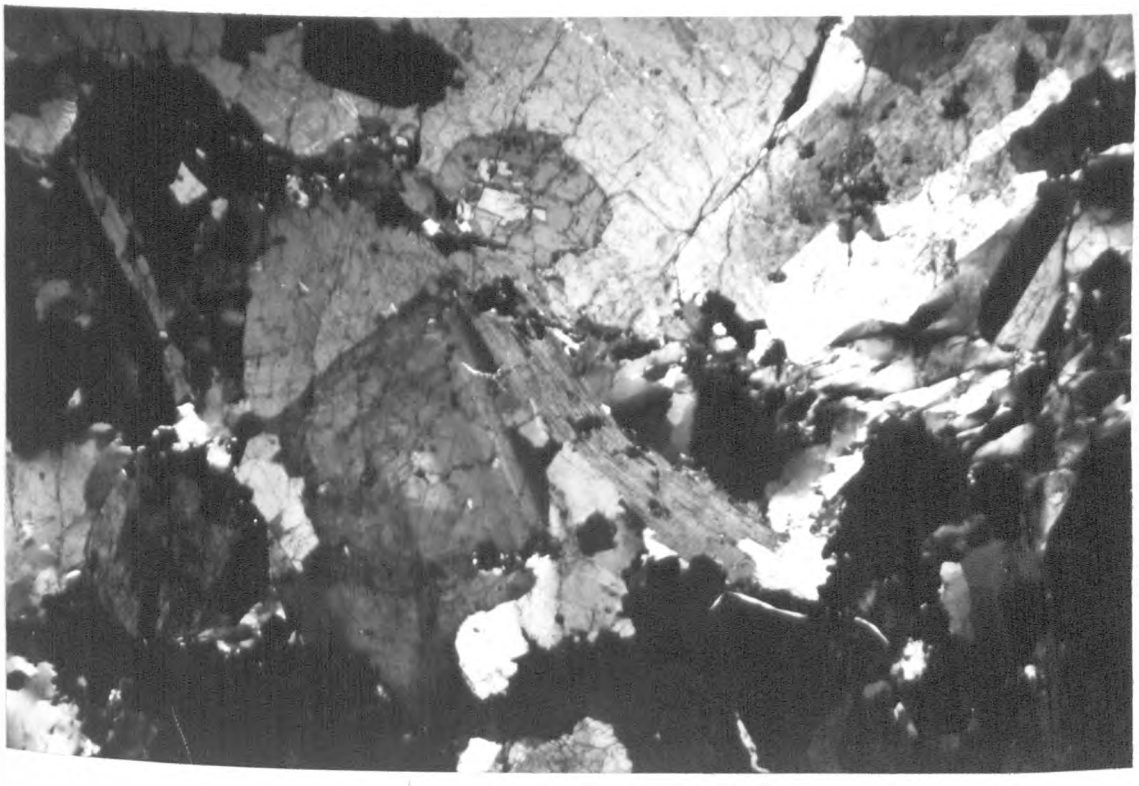

observation of recrystallization of and granulation in quartz (see figs. 2-2-1e and 2-2-1f); deformation of plagioclase twin lamellae (see fig. 2-2-1g); the deformation planes developed in microcline; and deformation of biotite cleavage. Epidote produced as a result of plagioclase alteration is abundant in this area, but there is little chloritization of biotite and amphibole.

2-2-2 Granite

The centre of the 'ring' of quartz monzonite is occupied by an area of granite. The transition from the quartz monzonite to the granite is gradual and no distinct boundary is recognisable, though the expected slow increase in the quartz content is observed in thin section (see modal analysis). The area included within the triangle formed by sample numbers 110, 272, 307 (see location in fig. 2-1-1a) could be the centre of the granite outcrop.

Thin-section study of the granite shows it to be coarse-grained.

In samples collected along the road from 'Kalibia Mpexi' to 'Karidohorion', which is marked by a large valley, there is considerable evidence of shearing. Observations from thin-section study showed deformation of plagioclase twin lamellae; deformation of biotite cleavage (fig. 2-2-2a); microcline fracture patterns (fig. 2-2-2b); and granulation and recrystallization of quartz

Fig. (2-2-2b). Deformation planes developed in microcline microperthite from granite (sample No.301). (Mag X 312)

Fig. (2-2-2c). Photomicrograph showing recrystallization of quartz following an episode of shearing in granite (sample No.307) (Mag X 312)

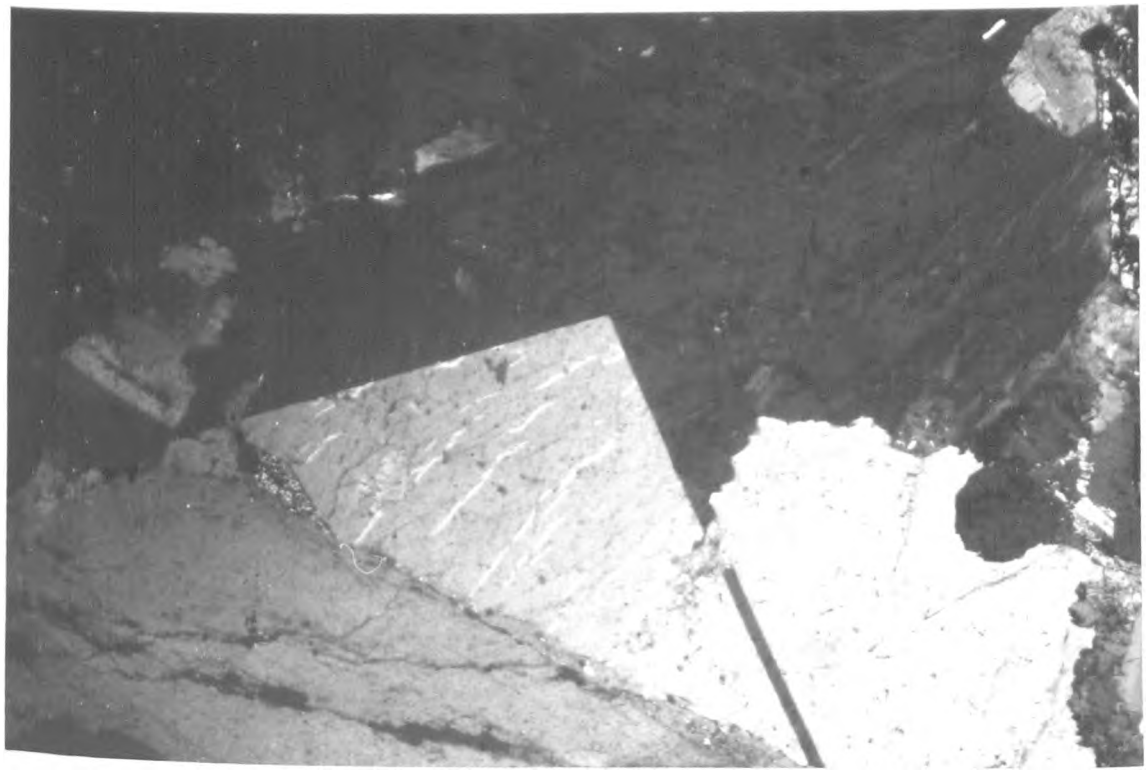

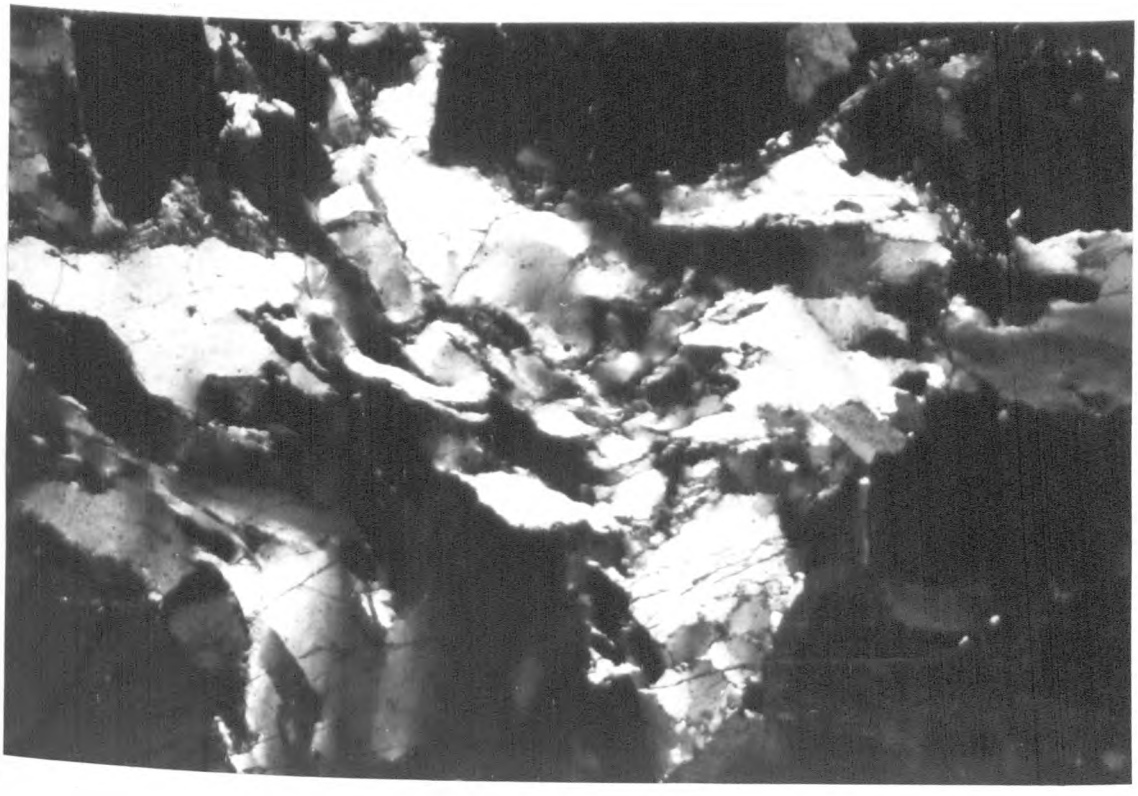

Fig. (2-2-2d). Photomicrograph showing recrystallization of quartz following an episode of shearing in granite (sample No.301). (Mag X 312)

Fig. (2-2-2e). Epidote forming as a result of the alteration of plagioclase feldspar in granite (sample No.307). (Mag X 787)

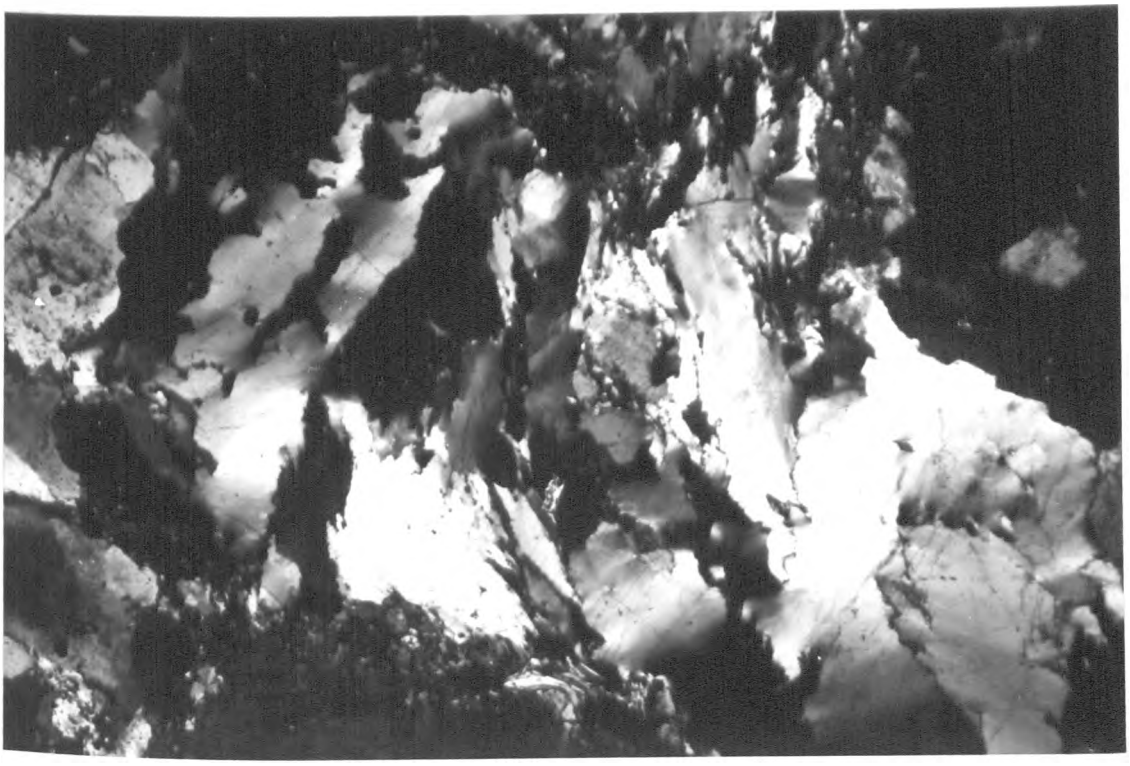

(figs. 2-2-2c and 2-2-2d). Epidote formed as a result of plagioclase alteration is abundant in this area (fig. 2-2-2e). Amphiboles and biotites are occasionally chloritised parallel to the cleavages.

2-2-3 Granodiorite

The granodiorite extends to the east of 'Ag. Konstantinos' (Ag. Konstantinos itself consists of granite) and includes the village of 'Ano Brontou' the area around 'Ag. Georgios', to the Kato Brontou - Ano Brontou, Serres - Ano Brontou road junction and then follows the road to Kato Brontou.

The change from granite to the grandiorite is gradual with a slow increase in plagioclase content. Thin-section study of the granodiorite shows it to be coarse-grained. The mineralogical composition and texture of the granodiorite is similar to quartz monzonite and granite.

2-3-1 DESCRIPTIVE MINERALOGY OF THE 'INTERMEDIATE' GROUP ROCKS

The texture and the mineralogical composition of the quartz monzonite, granite and granodiorite are the same, all being fairly uniform.

Quartz is evenly distributed within each rock type in the whole area; however, the quartz content slowly increases both from the quartz monzonite and the granodiorite to the granite. Often it can be seen with a wavy extinction

and always occurs as an interstitial mineral which indicates that it must be a late crystallizing phase. In the area of shearing quartz granulation and recrystallization is observed. Myrmekitic intergrowth of quartz with plagioclase feldspar occurs over the whole of the area, but occasionally graphic intergrowth of quartz with potassium feldspar occurs.

Potassium feldspars occur throughout the whole area as microcline. Simple Carlsbad twins together with albite-pericline twinning was frequently observed in thin section under crossed nicols. Presumably this is evidence to suggest that the initial potassium feldspar polymorph was monoclinic (orthoclase) and during cooling, exsolution and inversion to the triclinic polymorph (microcline) has taken place (Laves, 1950, 1952b, from J.V. Smith, 1974, vol.2; Laves and Goldsmith, 1954a, b, from J.V. Smith, 1974, vol.2). A 'complete' twinned microcline and 'patchy' twinned microcline (Edmondson, 1970) are illustrated in figs. (2-3-1a) and (2-3-1b). These observations of 'patch' twinning can be interpreted as being due to incomplete inversion from optically monoclinic to triclinic symmetry. The above observations are not confined to any one area.

Perthitic intergrowths, formed as a consequence of falling temperature, characteristically develop with the contact face between the host and the lamellae in a specific crystallographic orientation. According to the size classification of perthites (Laves and Soldatos, 1963),

the albite lamellae of quartz monzonite, granite and granodiorite can be characterised as microperthite. Papadakis (op. cit.) measured the maximum width of albite lamellae as 0.03 mm but usually the width is about 0.008 mm. He observed in (010) sections that the albite lamellae formed an angle of approximately 8^{o} with the (001) cleavage. These microperthites may be described as 'Patch perthite' (Andersen, 1928; from J.V. Smith, 1974, vol.2). Papadakis (op. cit) reports that in addition to lamellae of albite developed almost parallel to (100) he occasionally observed albite lamellae called 'plate perthite' (Laves and Soldatos, 1962a, 1963) parallel to (010). A similar observation was made in the alkali feldspars from the quartz monzonite.

The potassium feldspar megacrysts are commonly euhedral to subhedral, but usually their margins are irregular when examined in detail (see figs. 2-3-1c and 2-3-1d). Similar observations were reported by Exley and Stone (1982). These megacrysts range in size between about 1 cm to 6 cm maximum. They are usually twinned on the Carlsbad Law. Megacrysts frequently enclose other minerals such as plagioclase feldspar, amphibole, biotite, sphene and iron ore (see fig. 2-3-1e).

Plagioclase feldspars are distributed throughout the whole area. They are usually twinned on the combined Carlsbad and albite laws. They are frequently zoned (see figs. 2-3-1f and 2-3-1g) with maximum size of about 3 mm and they are euhedral to subhedral. The plagioclase feldspars range in composition from oligoclase to labradorite (Michel-Levy method). The cores of the plagioclase feldspars

Fig. (2-3-1a). Crystal of microcline in quartz monzonite (sample No.2) showing "complete" twinning on the albite and pericline laws. (Mag. X100.)

Fig. (2-3-1b). Crystal of microcline in granodiorite (sample No.171) showing "patch" twinning, indicating incomplete inversion to optical triclinic symmetry. (Mag. X 100.)

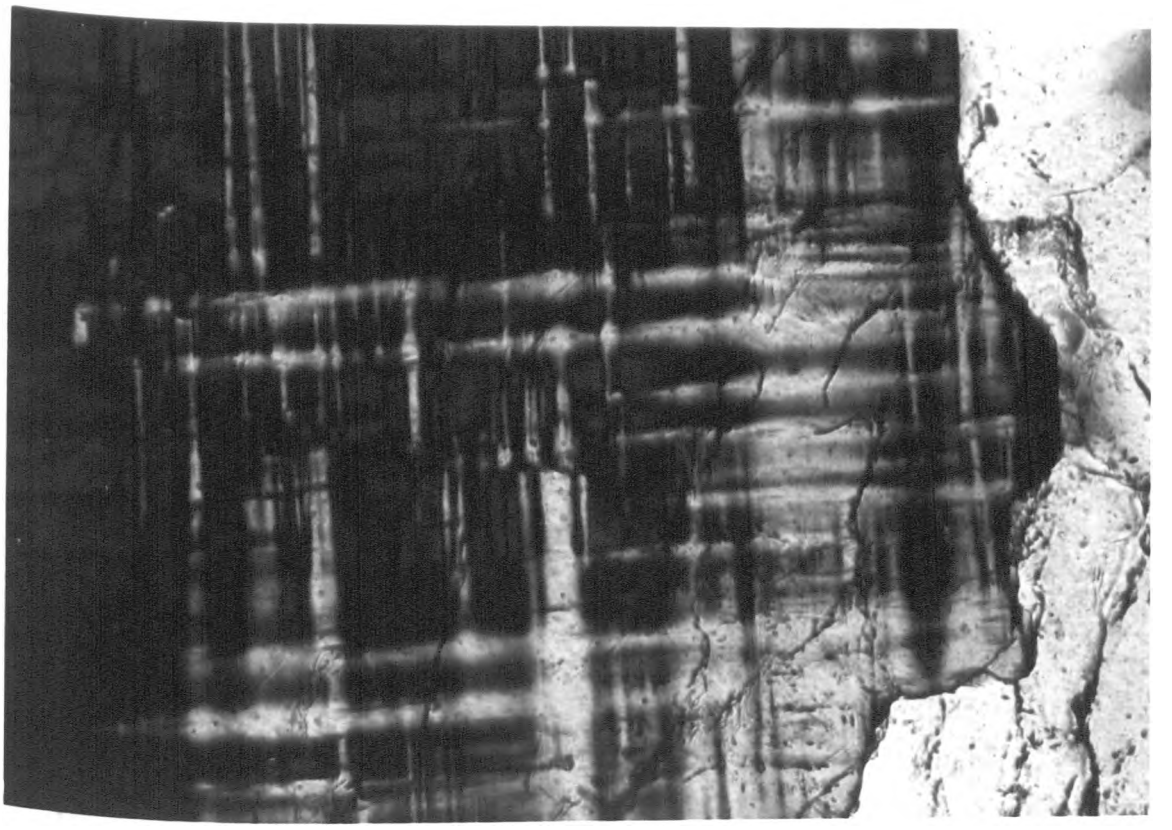

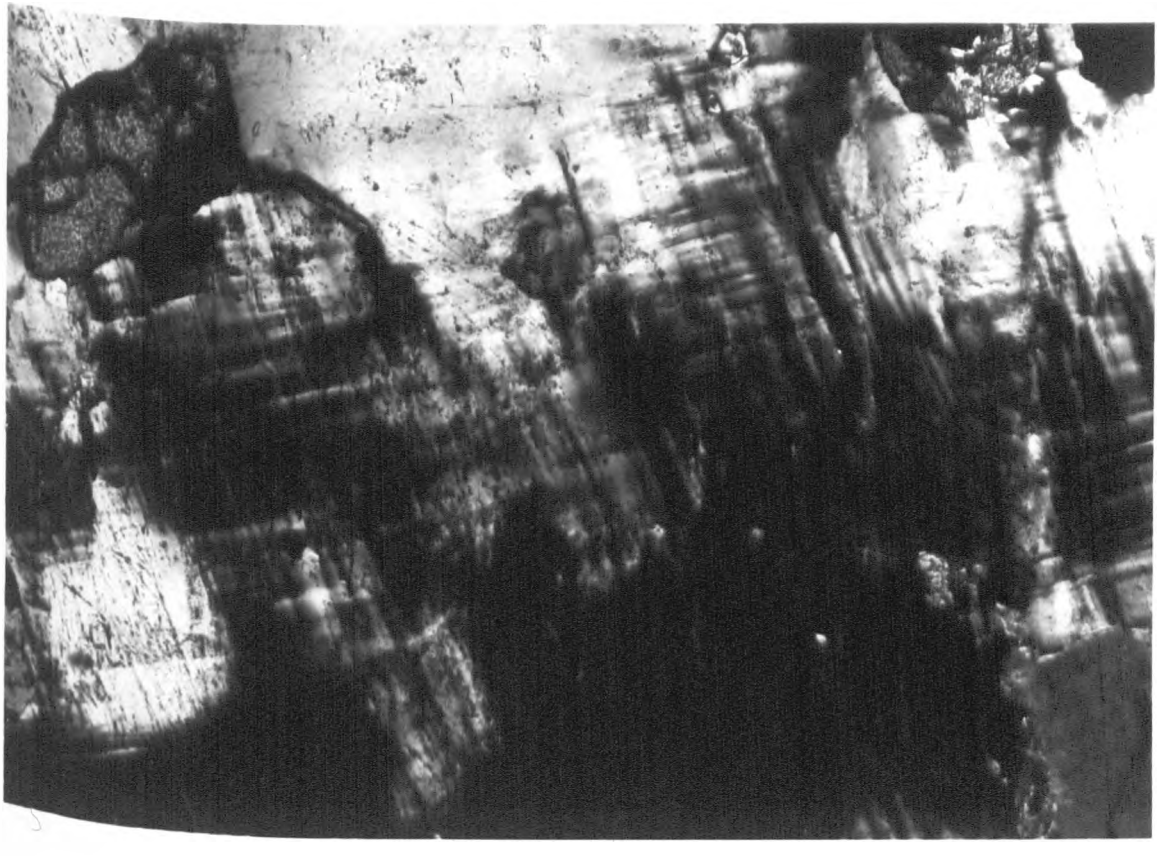

Fig. (2-3-1c). Megacryst of microcline microperthite showing simple Carlsbad twinning and an irregular margin to the crystal. Plagioclase feldspar crystals appear to be in parallel alignment to the alkali feldspar. From quartz monzonite (sample No.222) 'Oxies'. (Mag X 156)

Fig. (2-3-1d). Megacryst of microcline microperthite from quartz monzonite (sample No.119). Note the irregular margin to the megacryst in the bottom left and right of the photomicrograph. (Mag X 156)

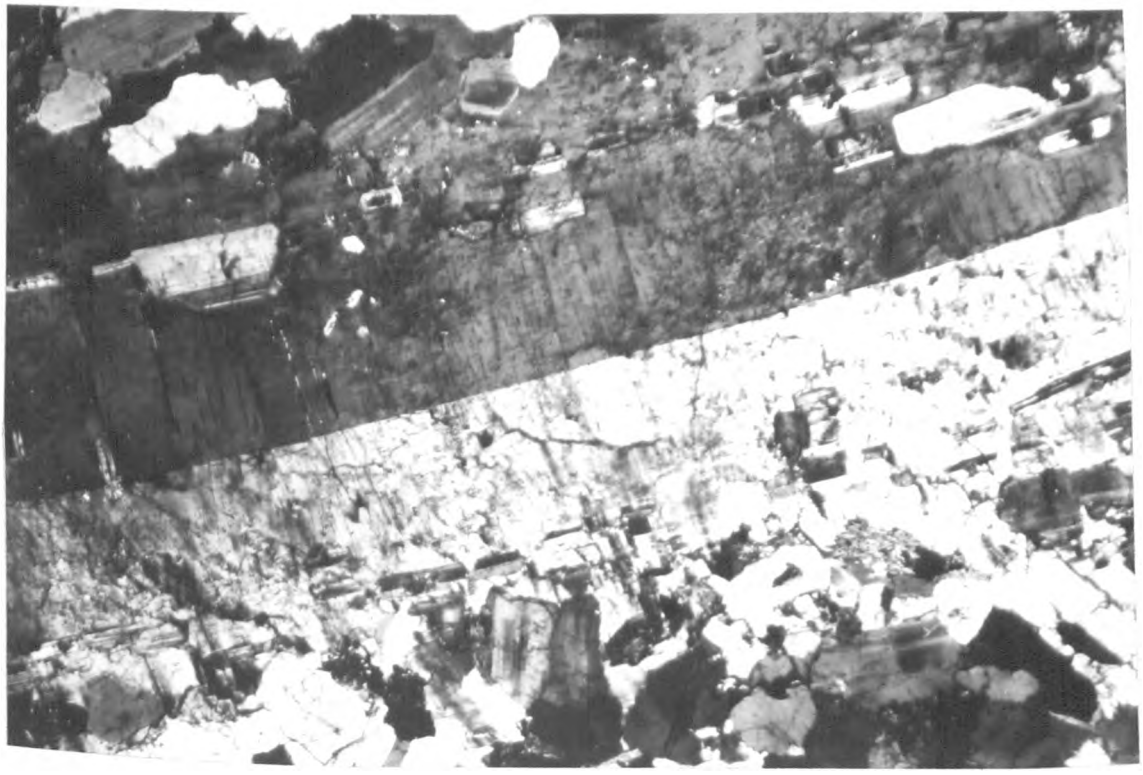

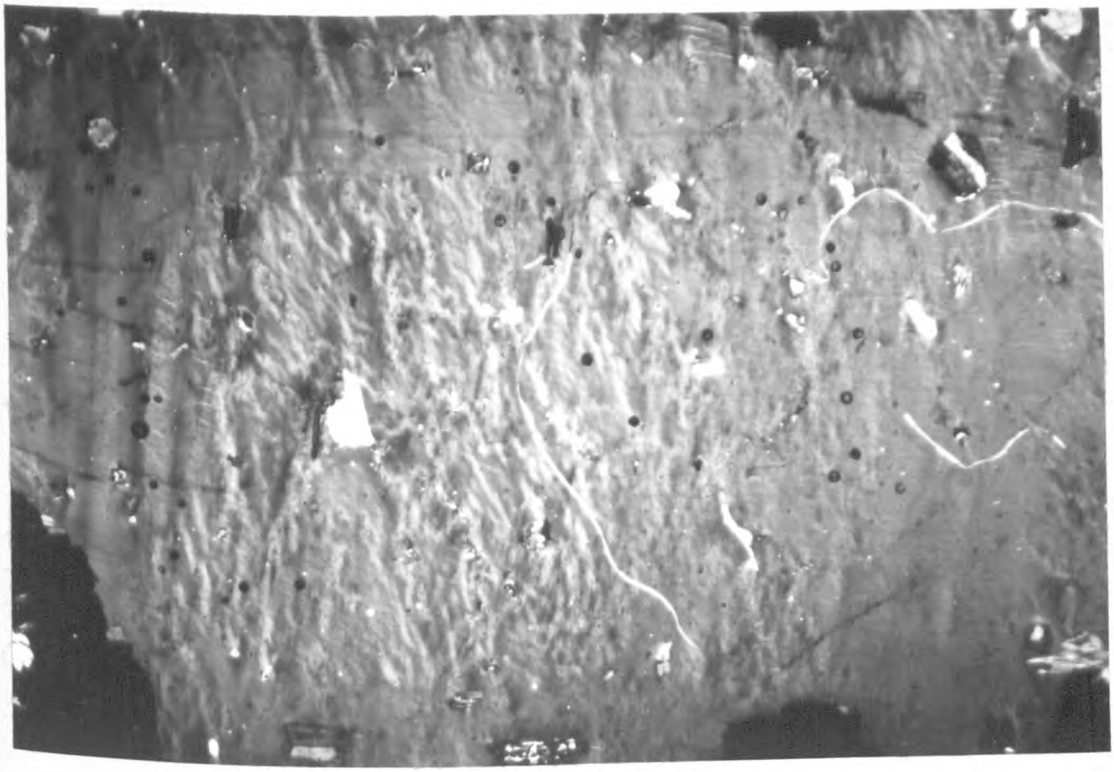

Fig. (2-3-1e). Microcline crystal from granodiorite (sample No.171) which includes simple twinned hornblende (top centre right) and plagioclase feldspar (white area-centre right). (Mag X 312)

Fig. (2-3-1f). Complex plagioclase zoning in quartz monzonite (sample No.236). (Mag X 312)

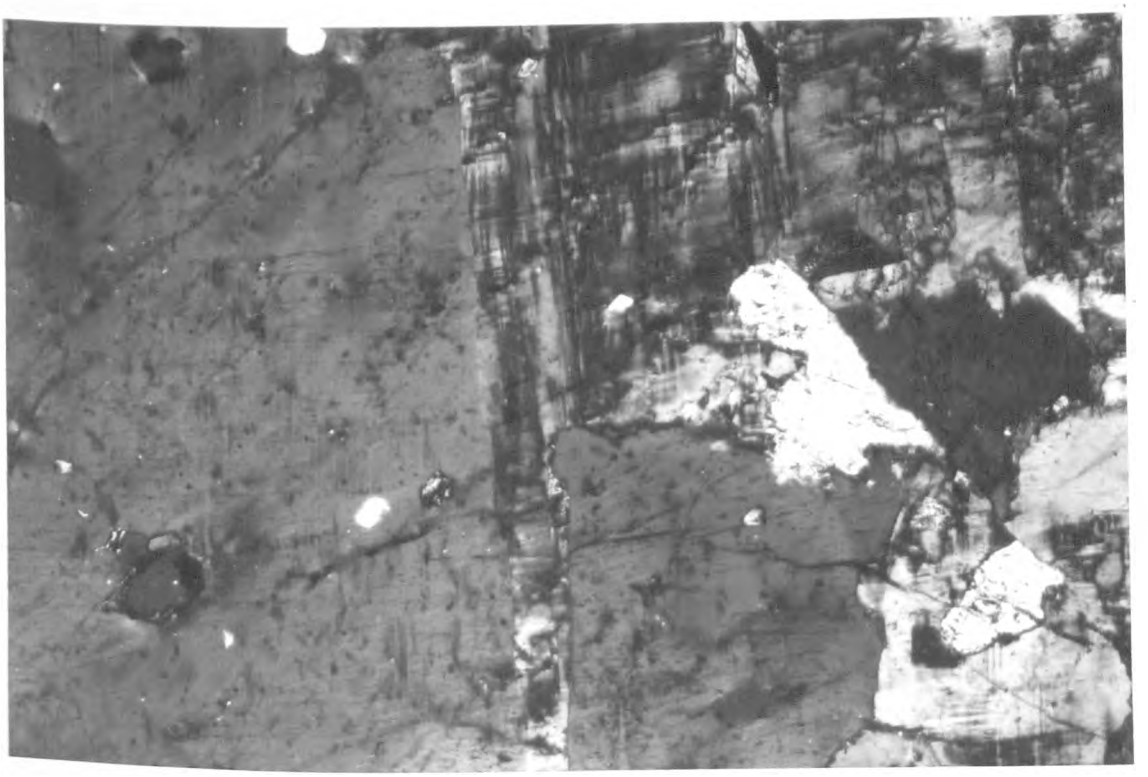

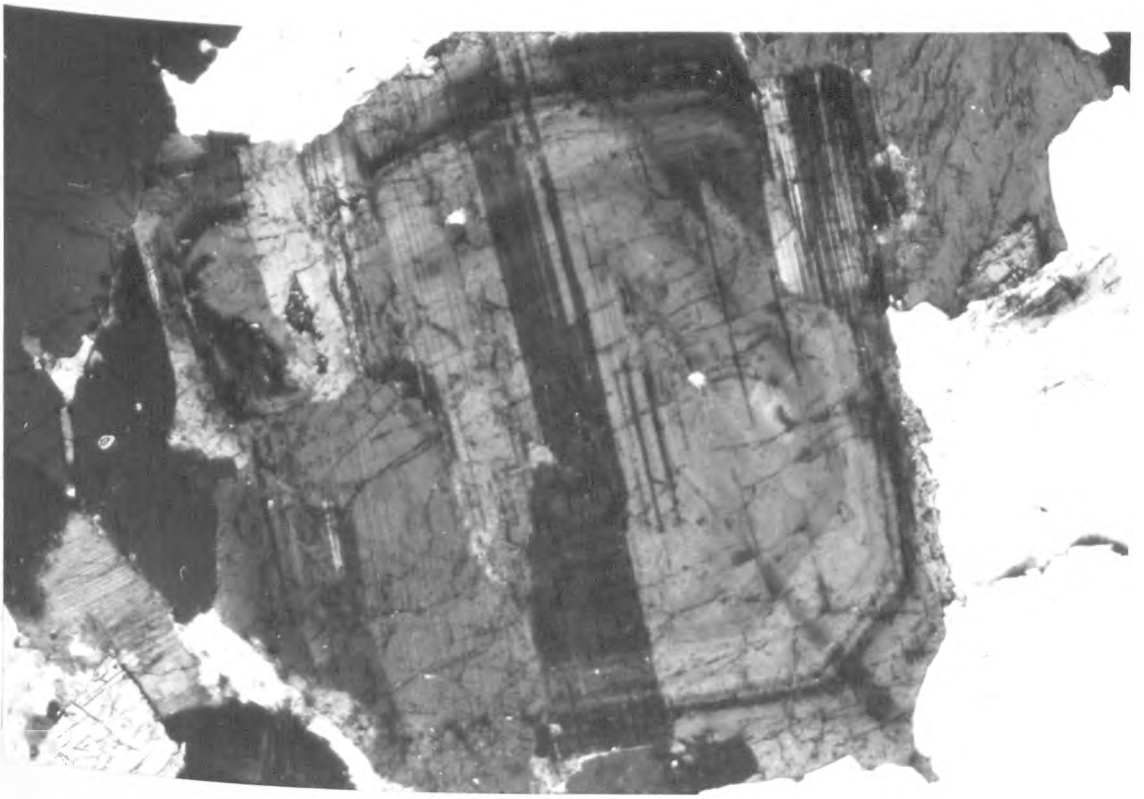

have often compositions of about An_{50}, and rarely some section of feldspars slightly exceed this value (An_{53} maximum). The rims of these crystals are usually in the range An_{25-30}. Plagioclase is usually surrounded by potassium feldspar, but occasionally other smaller, plagioclase crystals, amphibole, biotite and iron ore are included. Plagioclase could have crystallized in two stages; the early one, plagioclase, possibly crystallized together with amphibole because small unzoned crystals are sometimes included in the amphiboles (see fig. 2-3-1h). These unzoned crystals of plagioclase have compositions more anorthitic (An_{48}) than the zoned crystals, referred to above, except for the cores of some of these crystals. Plagioclase feldspars are occasionally altered to epidote, but no kaolinisation nor sericitisation was observed.

Amphiboles are distributed over the whole of the area and are the most abundant mafic mineral. The crystals are commonly euhedral or subhedral and usually show the characteristic cleavage for amphiboles parallel to {110}. The extinction angles ($\gamma \wedge [001]$) range from 15° to 21°. The colour is usually green. The pleochroic scheme is light green (α) to yellow green (β) to greenish brown (γ). The size of the crystals varies up to 2mm and they are commonly twinned parallel to {100}. Sometimes biotite, accessory minerals and small unzoned plagioclase are included in the amphibole, but they are rarely chloritized. The crystal form and texture indicate that the amphiboles are of primary origin.

Fig. (2-3-1g). Oscillatory zoning in plagioclase feldspar from quartz monzonite (sample No.239). (Mag X 787)

Fig. (2-3-1h). Euhedral twinned crystal of hornblende from quartz monzonite (sample No.236) which includes an unzoned crystal of plagioclase feldspar. (Mag X 312)

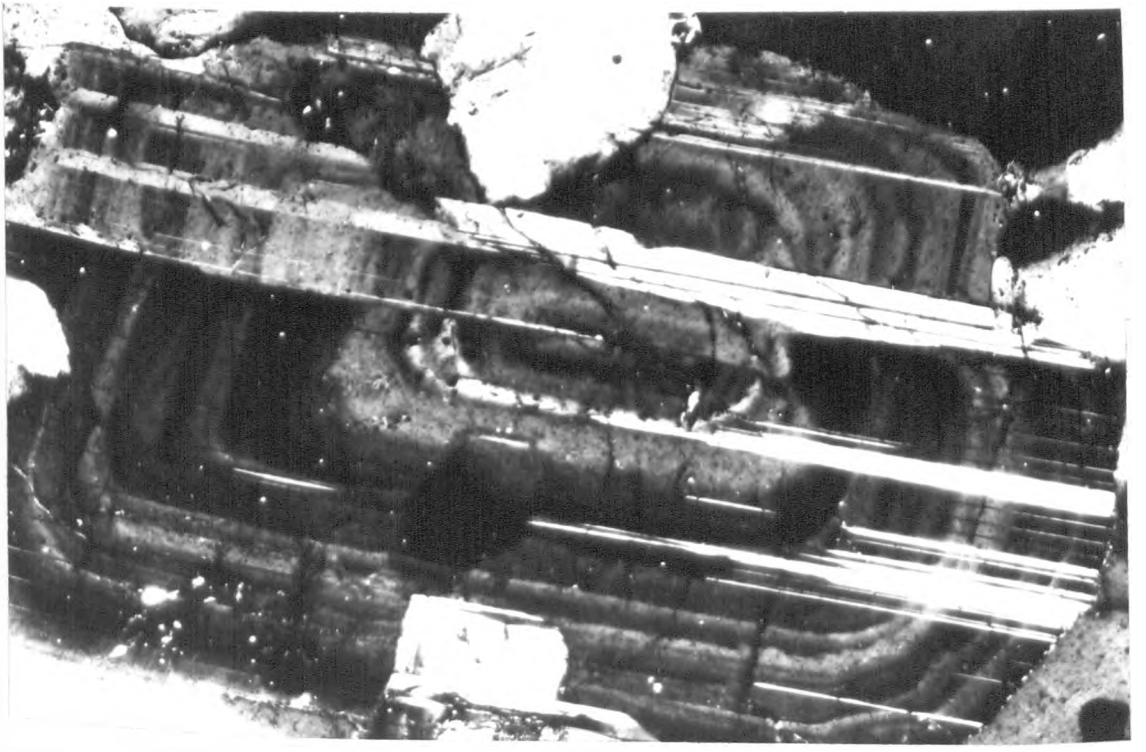

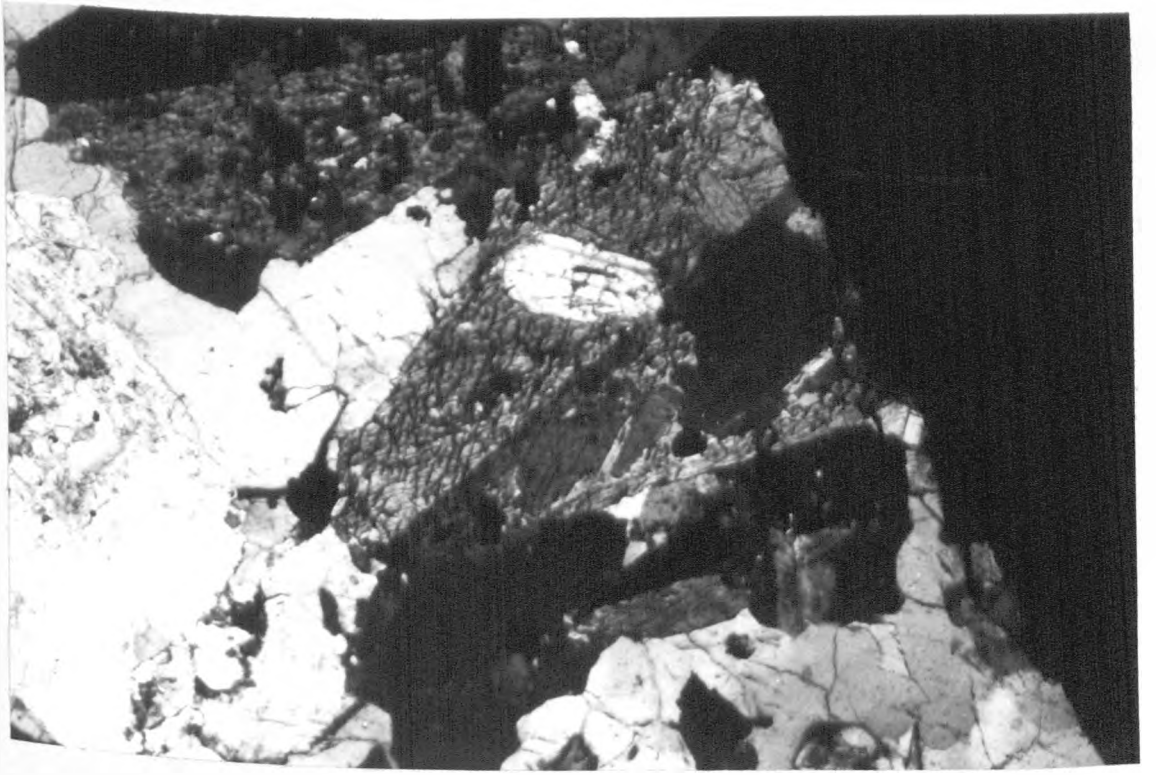

Biotite occurs over the whole area, always in smaller quantities than the amphibole and usually as brown, well formed crystals having a reddish brown maximum absorption colour ($\beta = \gamma$ = reddish brown, α = yellowish brown) which may vary and extinction parallel to the cleavage traces. The biotite is occasionally chloritized parallel to the cleavages, the chlorite showing anomalous grey-blue birefringence. Occasionally some accessory minerals are included. Zircon is often surrounded by pleochroic haloes. The crystal form and texture indicate that the biotites are of primary origin.

Accessory minerals occur in the area and include sphene, iron ore, zircon, apatite, allanite, chlorite and epidote.

Sphene is widely distributed in the whole of the area and ranges in abundance from 0.22% to 1.30% (see modal analyses). Sphene is usually seen as euhedral crystals of rhombic section (fig. 2-3-1i), with a honey-yellow colour and high relief. This indicates that it probably formed as a primary mineral which subsequently became included in amphibole, biotite and plagioclase.

Iron ore is found occasionally with sphene. It rarely forms euhedral crystals. From the modal analysis the concentration ranges from 0.39% to 2.31% (including some small fragments of other minerals). The ore mineral is presumably magnetite due to the ease of extraction during mineral separation.

Apatite occurs as minute prismatic crystals sometimes with a hexagonal outline. Apatite is colourless

Fig. (2-3-1i). Euhedral crystal of sphene surrounded by quartz. From quartz monzonite (sample No.119). (Mag X 787)

Fig. (2-4-2a). Photomicrograph of gabbro (sample No. showing plagioclase feldspar with combined Carlsbad-albite-pericline twinning and replacement of clinopyroxene by amphiboles. (Mag X 156)

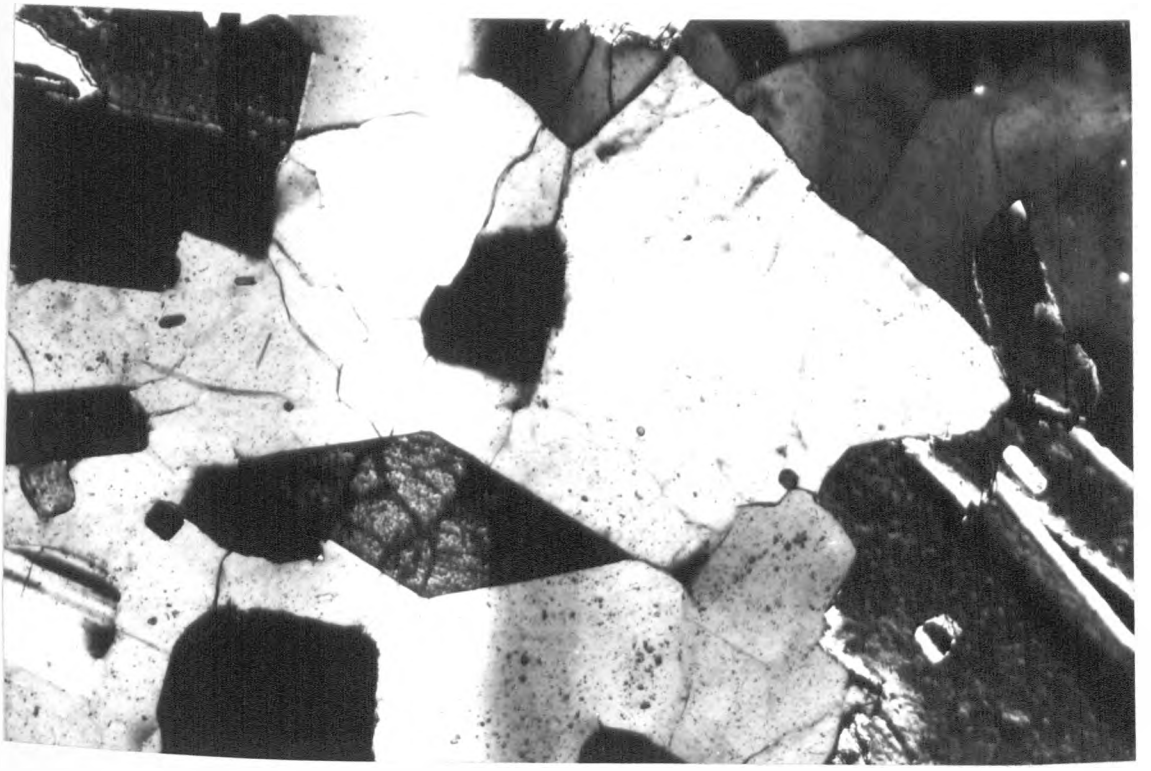

with parallel extinction, moderate relief and is usually found included in amphibole.

Zircon is usually present as short prismatic crystals and often found as inclusions in amphiboles or biotites and often surrounded by pleochroic haloes. They have parallel extinction, high relief and a strong birefringence.

Allanite occurs very rarely in the quartz monzonite. It has high relief, brown colour the pleochroic scheme is dark brown (γ) to brown (β) to light brown (α) and parallel extinction. In granite and granodiorite, allanite was not observed, possibly because the mineral is distributed randomly over the area.

Chlorite occurs as a small part of the alteration of amphiboles and biotites and usually develops along the cleavage.

Epidote occurs as an alteration product of plagioclase feldspar (see fig. 2-2-2e) and is found as granular aggregates. It is colourless to yellowish green with a high relief.

2-4 PETROGRAPHY OF THE 'BASIC' GROUP ROCKS

2-4-1 Monzonite

Monzonite occupies the north-east part of the intrusive complex. As mentioned above megacrysts of potassium feldspar appear only in a small area. The colour of

the potassium feldspar in handspecimens, from 'Mavro Bouno', 'Diabasis Ag. Paraskevis' and the area to the north of these is found to be of a slight pinkish hue, but in the area of 'Siderobouni' the alkali feldspar is white. In this latter area the predominant mafic mineral is amphibole (see modal analyses), which is also the case in the area to the north of 'Diabasis Ag. Paraskevis' near the border with quartz monzonite (modal analyses samples No. 260, 269). However, in the area of 'Mavro Bouno' the predominant mafic mineral is clinopyroxene. No sharp contacts between the monzonite and the surrounding quartz monzonite and granodiorite were observed during field work. However, in the transition zones between the monzonite and the 'intermediate' rock types, variation in the amount of quartz can be seen and also an increase in mafic mineral content.

Thin-section study of the monzonite shows it to be coarse-grained. From modal analysis it can be seen that the quartz ranges from 0.00% to 4.53%. The area with the lowest quartz is 'Mavro Bouno' (sample No. 140, 204) which lies at the centre of the monzonite outcrop. In this area the clinopyroxene content is at its greatest with amphibole and biotite content being at their minimum. Also the potassium feldspar content is greater than that of plagioclase. The majority of the samples for which there is modal analysis have a larger potassium feldspar content than plagioclase.

The striking differences between, the monzonite and the 'intermediate' group rock-types are:

a - the potassium feldspars are monoclinic;

b - the occurrence of clinopyroxene; and

c - the replacement of clinopyroxene by amphibole.

Consequently, in this area both primary and secondary amphibole may be found. This phenomenon is more intense at the centre of the monzonite (Mavro Bouno).

2-4-2 Gabbro

Gabbro crops out near the main Serres to Ano Brontou road, in a small area which is elongated in a NE-SW direction into the quartz monzonite. The relationship between gabbro and the surrounding quartz monzonite is totally obscured. This gabbro possibly represents a marginal section of the main body.

Thin section study of gabbro shows it to be coarse-grained. In this rock-type the phenomenon of high temperature alteration is seen more often, the main feature being the replacement of clinopyroxene by amphibole (see fig. 2-4-2a).

Amphiboles are the most abundant mafic minerals in the gabbro with extinction angles ($\gamma \wedge [001]$) from 14° to 16°. The pleochroic scheme is light green (α) to olive green (β) to nut brown (γ). Twinning is common. Since these amphiboles usually include clinopyroxene remnants, they are interpreted as being of secondary origin. Sometimes amphiboles are included in plagioclase (fig. 2-4-2b).

Fig. (2-4-2b). Photomicrograph of gabbro (sample No.152) showing large plagioclase feldspar which includes crystals of amphiboles. (Mag X 156)

Fig. (2-4-2c). Large plagioclase feldspar with albite-pericline twinning. Epidote veins cut across this crystal (sample No.152) from gabbro. (Mag X 156)

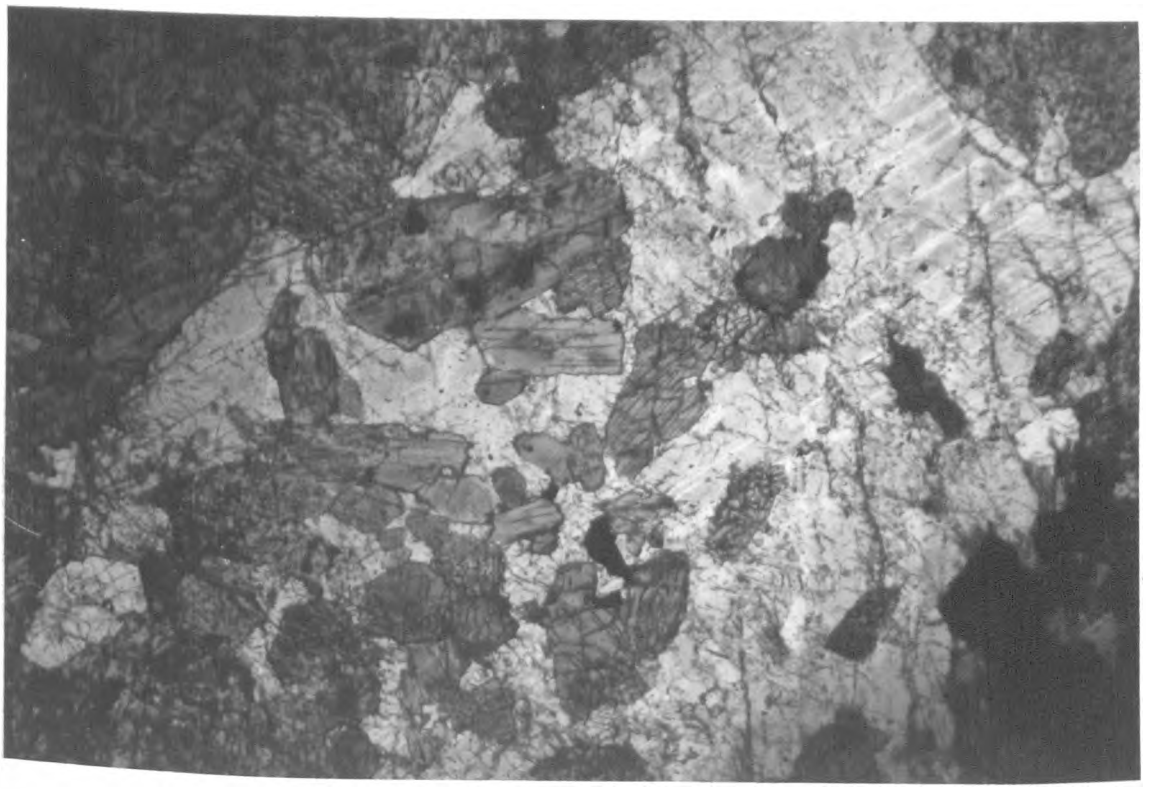

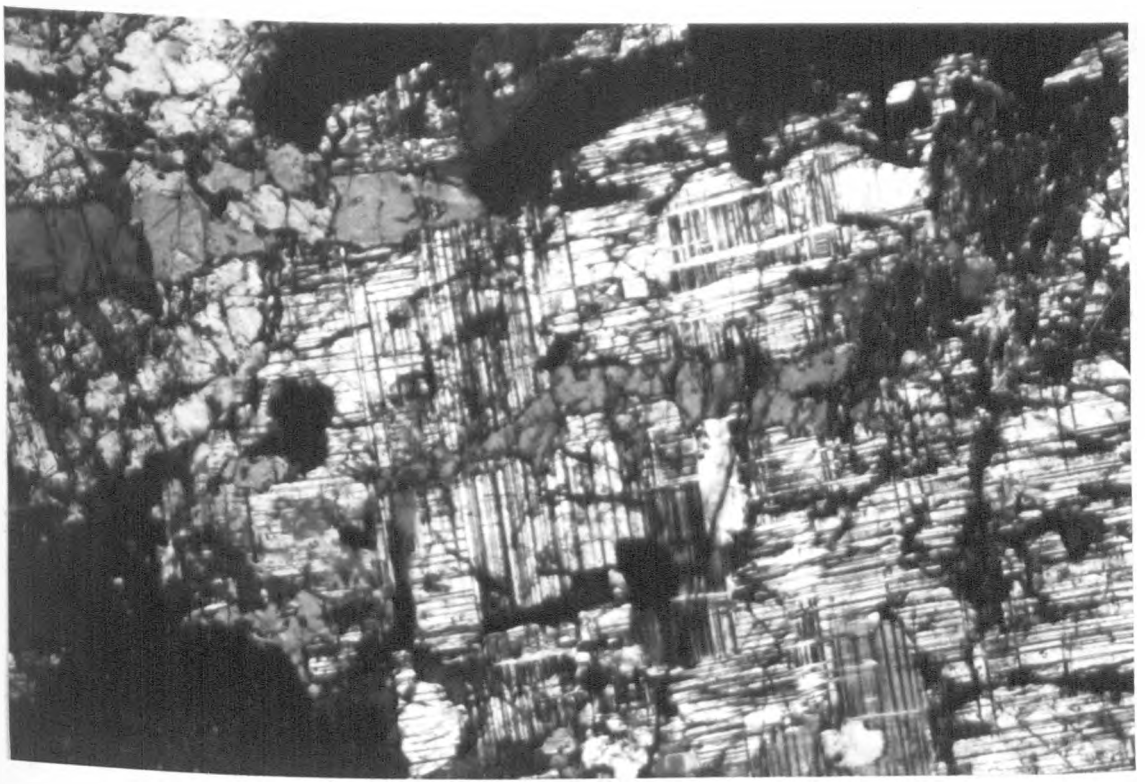

Fig. (2-4-2d). Large plagioclase feldspar with albite-pericline twinning. Epidote veins cut across this crystal (gabbro, sample No.152). (Mag X156)

Fig. (2-4-2e). Gabbro (sample No.153) showing biotite crystals (centre with cleavage) with hornblende. Clino-pyroxene is seen top centre left and lower right of the photomicrograph. (Mag X 312)

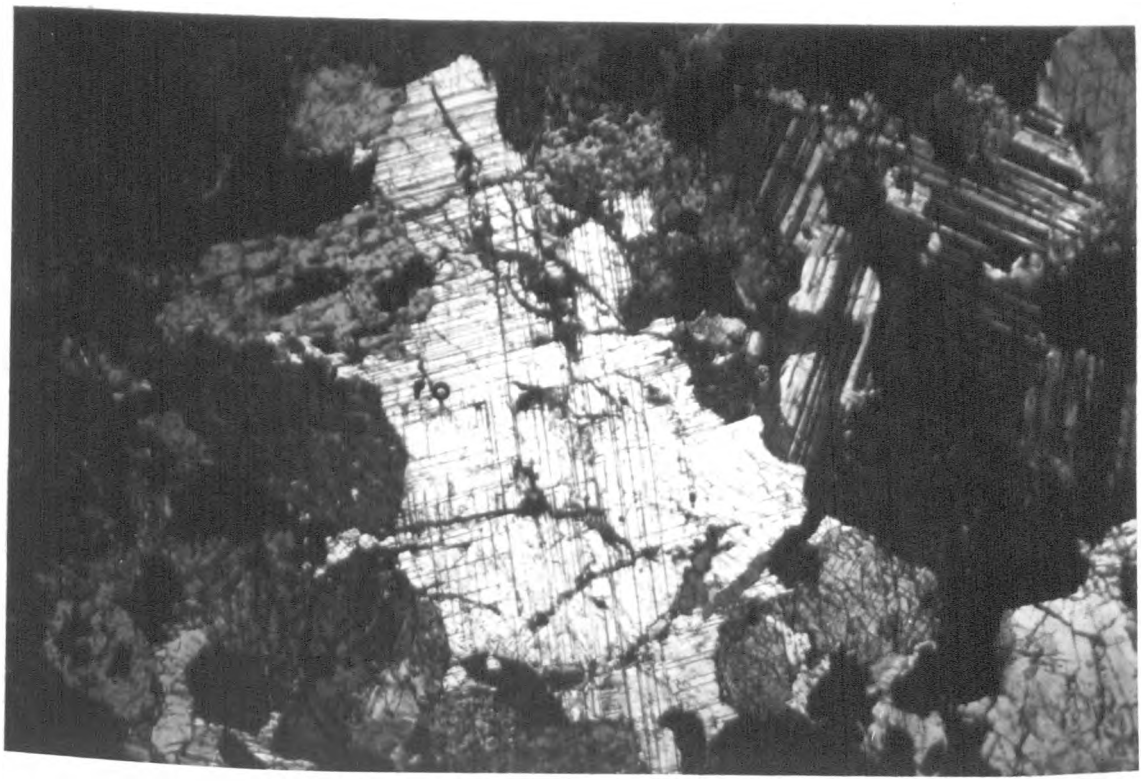

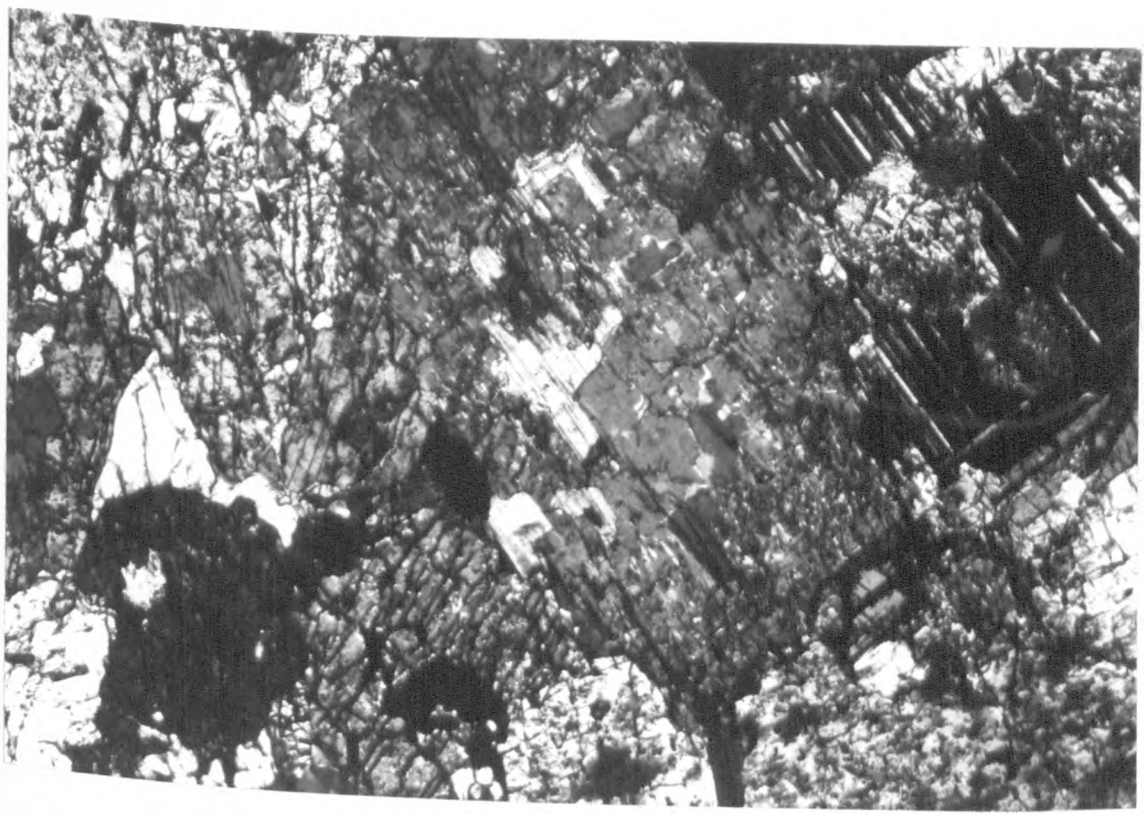

Fresh plagioclase in the gabbro is very An-rich (C. An_{90} using the Michel-Levy optical method). It is however nearly always altered, containing discrete crystals of epidote (see fig. 2-4-2c). Anorthitic plagioclase was suspected in these gabbros because of the high birefringence and relatively high relief. These factors together with a knowledge of the chemical composition from electron microprobe analysis indicate anorthite.

Biotite was observed in only one thin-section (No.153, see fig. 2-4-2e). This is thought to be of late magmatic origin.

Ore minerals (magnetite) are common but are usually found as aggregates associated with alteration products (haematite and sphene). Iron pyrite has been observed in hand specimen.

2-4-3 Diorite Xenoliths

Diorite xenoliths are distributed along and around the boundaries between monzonite and the 'intermediate' group rocks. The size ranges from a few mm (microscope observation) to about 20 cm. Thin-section study shows them to be medium-grained (see, fig. 2-4-3a).

The diorite xenoliths appear to provide a link in composition between the monzonite and the gabbro. The transitional character between these two rock-types is noted by:

a - the plagioclase feldspar is andesine in composition

Fig. (2-4-3a). Contact (A-A') between quartz monzonite on the right and dioritic inclusion on the left (sample No.5a). (Mag X 156)

Fig. (2-6-1a). Texture developed in aplite (sample No.41) between plagioclase feldspar and quartz. (Mag X 312)

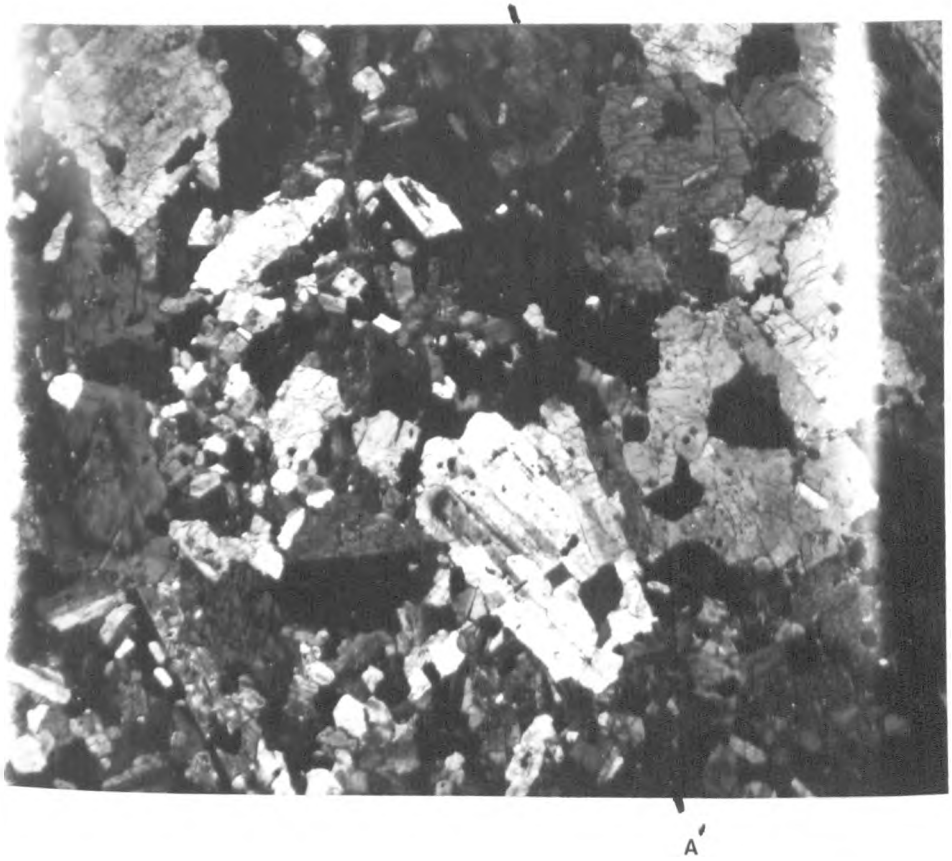
A
A'

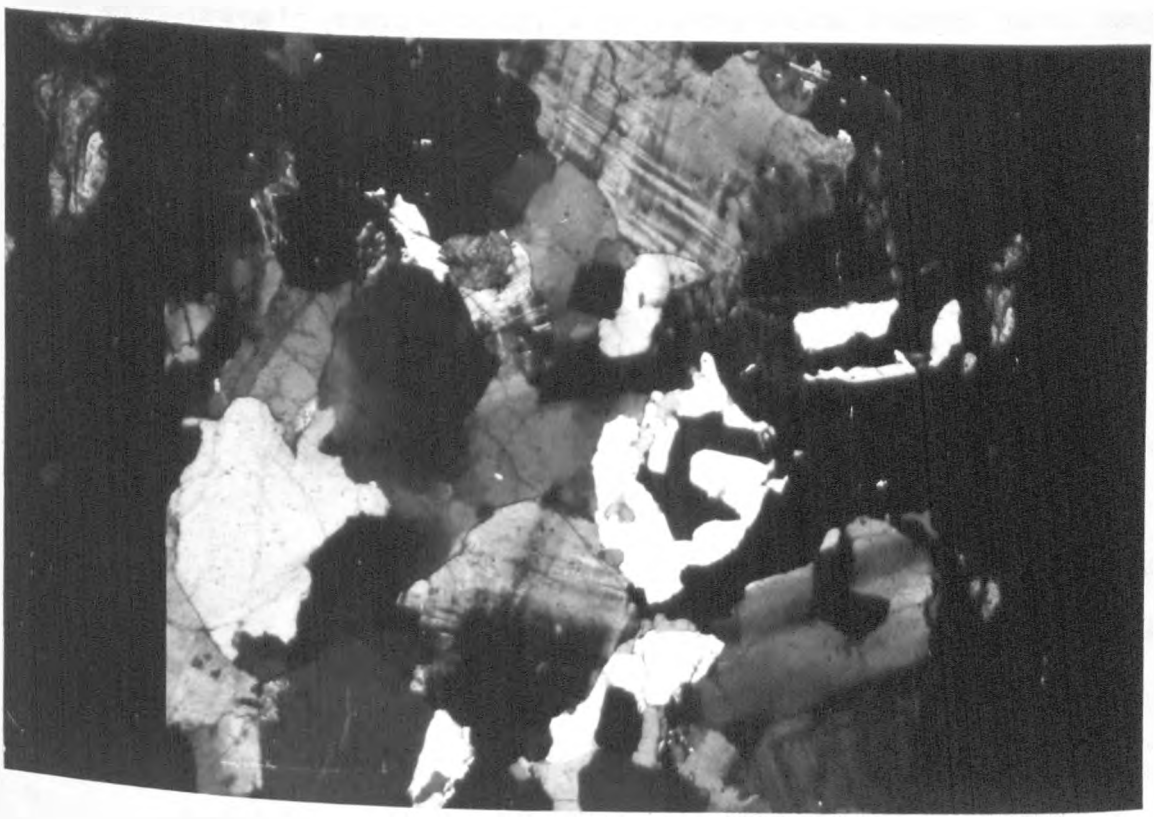

(C. An_{50} max.), being close to that of the monzonite but different from that of the gabbro.

b - Unlike monzonite which is rich in potassium feldspar, the majority of the diorite xenoliths, like the gabbro, show a complete absence of that mineral,

c - as in monzonite, little or no quartz is found in the diorite xenoliths,

d - as in the monzonite, clinopyroxenes are occasionally altered to amphiboles, and amphiboles are sometimes chloritized,

e - as in some areas of monzonite, biotite occurs in a slightly greater abundance than in gabbro,

f - the form taken by sphenes and iron ores are analogous to that of these minerals when found in monzonite.

During the incorporation of the diorite in the 'intermediate' group rocks, zenoliths were formed that may have been influenced by this host rock. Evidence of assimilation may be seen in one or two xenoliths. In a few examples growth of potassium feldspar (both orthoclase and microcline) cutting across the fabric of the xenolith is seen.

2-5-1 DESCRIPTIVE MINERALOGY OF THE 'BASIC' GROUP ROCKS

Quartz is found in monzonite both in the area where potassium feldspar megacrysts are located and around 'Siderobouni' as small interstitial mineral grains; it does not occur at all in the area of 'Mavro Bouno'. Quartz is found in few samples of diorite xenoliths. In the monzonite,

myrmetitic intergrowth of quartz with plagioclase feldspars occurs and also graphic intergrowth of quartz with potassium feldspar.

Potassium feldspar occurs throughout the outcrop area of monzonite as orthoclase and rarely in a few samples of diorite xenoliths as othoclase with one exception in sample No.315 (microcline). The megacryst are easily recognised as microperthitic. These potassium feldspar megacrysts are usually euhedral to subhedral, but their margins are irregular when examined in detail. The maximum size is about 5 cm and they are usually twinned on the Carldsbad law. Sometimes small plagioclase or other minerals are included within this megacrysts. In the area of 'Mavro Bouno' potassium feldspars do not have distinct crystal faces but have an interlocking relationship with the plagioclase feldspar.

Plagioclase feldspars are distributed over the whole area of monzonite, gabbro, and all the diorite xenoliths and are usually twinned on either the combined Carlsbad-albite or albite law. Plagioclase composition in gabbro is distinctly different from those of the monzonite and the diorite xenoliths.

Clinopyroxenes are much more common in the gabbro but less so in the monzonite and the diorite xenoliths. Sometimes they are subhedral with a grain size of about 0.5 mm and are colourless or pale green. The extinction angle ($\gamma \wedge [001]$) is about 46°. They are commonly altered

to amphiboles and this phenomenon occurs most frequently in gabbro.

Amphiboles occur in this group of rocks as both primary and secondary minerals and have an extinction angle ($\gamma \wedge C$) of 14° to 16°. Comparing this with amphiboles of 'intermediate' group rocks the extinction angle is lower.

Biotites rarely occur in this group as mentioned above.

Accessory minerals that occur in this group of rocks are sphene, iron ore, zircon, apatite. Chlorite occurs rarely as a product of alteration of amphiboles and biotites, and epidote as a product of alteration of plagioclase. In gabbro haematite and iron pyrite occur.

2-6-1 Aplite and Pegmatite veins

In the area of 'intermediate' group rocks many aplite veins can be seen, sometimes two parallel veins within a few metres of each other. The majority have a south-north orientation. Pegmatite veins, however, occur very rarely.

The aplite veins are light-coloured and in hand specimen appear to have little mafic mineral content. Thin-section study shows they are medium-grained and small fragments of mafic minerals occur rarely.

Quartz occurs as an interstitial mineral in aplite veins forming 'glassy' patches with a maximum diameter of 2.5 mm. Replacement textures may be seen between plagioclase

Fig. (2-6-1b). Fluid inclusions from the aplite veins (sample No.41). (Mag x 787).

Fig. (2-6-1c). Graphic intergrowth between k-feldspar and quartz in pegmatite (sample No.109). (Mag x 312).

Fig. (2-6-1d). Graphic intergrowth between k-feldspar and quartz in pegmatite (Sample No.109). (Mag. x 312).

Fig. (2-6-1e). Fluid inclusions from the pegmatite vein. (Sample No.109). (Mag x 312).

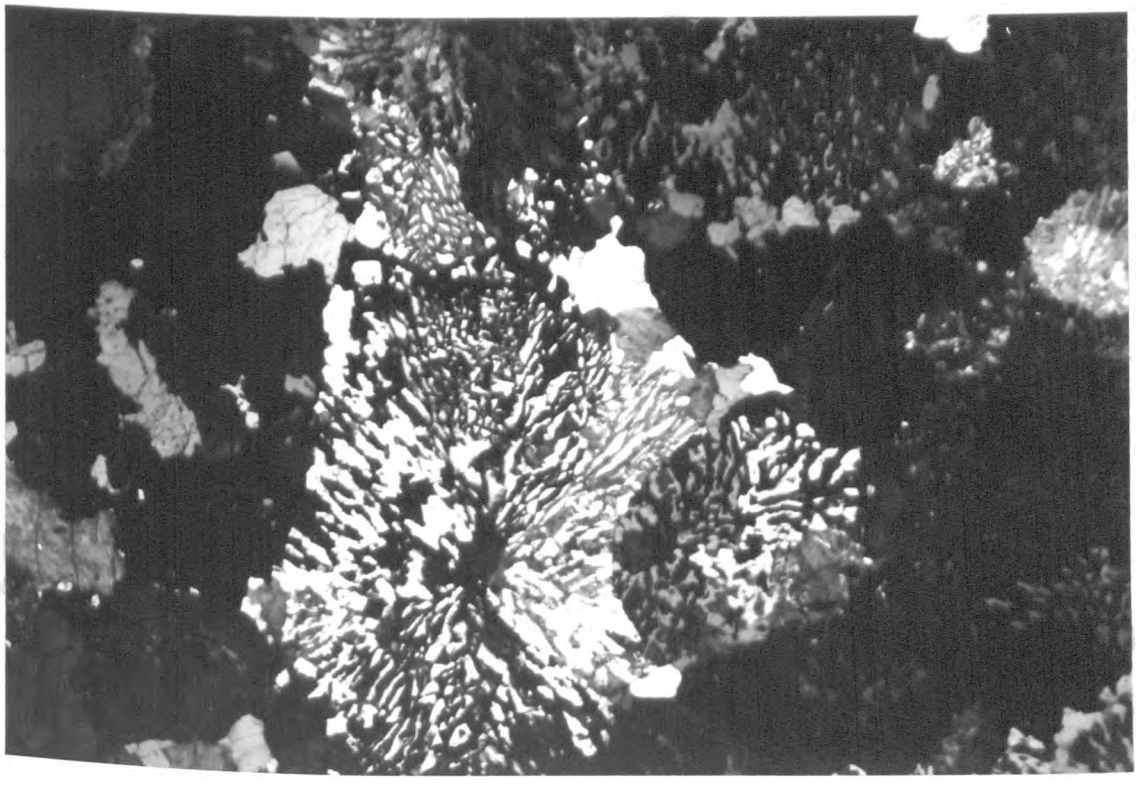

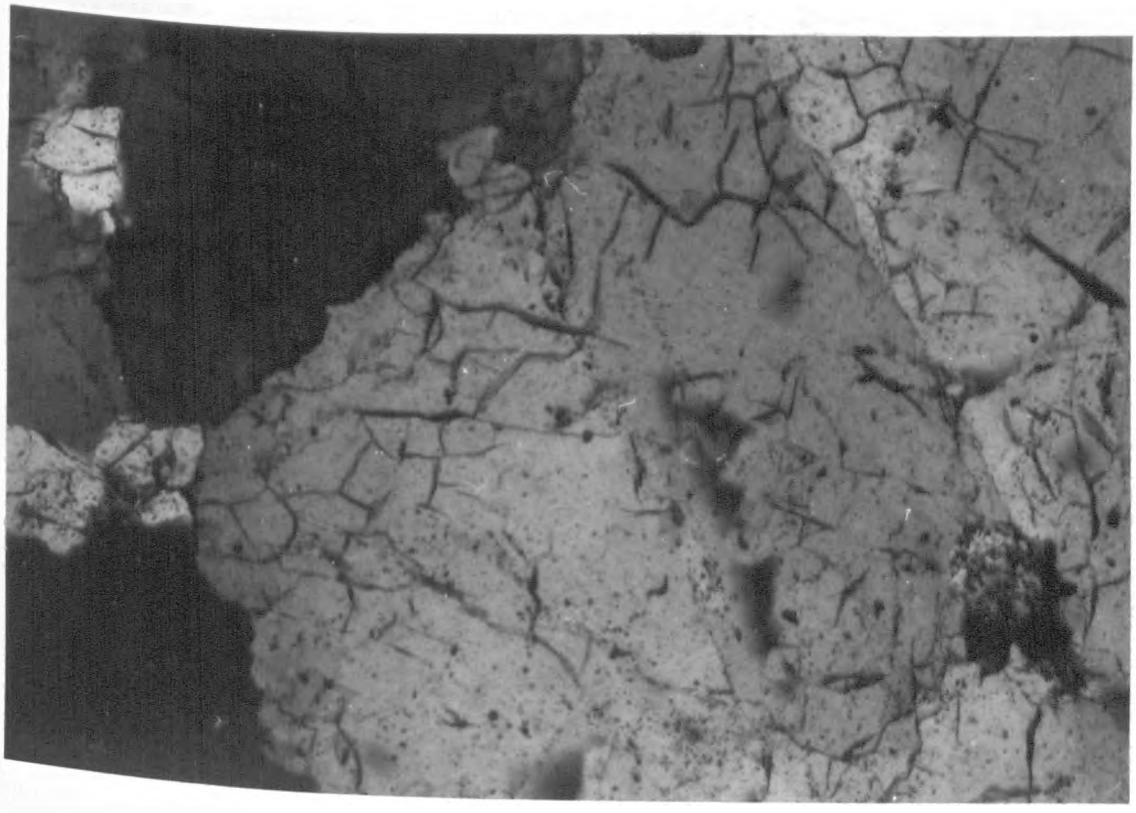

feldspars and quartz, but these could be the result of simultaneous growth (see, fig. 2-6-1a). Fluid inclusions commonly occur in the quartz (see fig. 2-6-1b).

Potassium feldspars occur as microcline. A 'complete' twinned microcline is frequently observed in thin section. Potassium feldspar grains are commonly non-perthitic, although large grains do contain exsolution lamellae. Rare zircon or sphene may be found and very rarely biotite, muscovite, and amphibole grains may be seen.

The plagioclase feldspars in the aplite are usually twinned and the composition of plagioclase is oligoclase ($C.An_{25}$).

The mineralogical composition of pegmatite veins are the same as the aplite, only the grain size is greater. Replacement textures again may be seen between plagioclase and quartz, microcline and quartz (fig. 2-6-1c and fig. 2-6-1d), but as mentioned above these could be the result of simultaneous growth. Fluid inclusions containing solid and liquid phases commonly occur in the quartz crystals (fig. 2-6-1e).

2-7-1 Summary

From mineralogical composition and field studies of the Serres-Drama granitic complex it can be seen that the granitic complex separates distinctly into two groups of rock-types, termed the 'intermediate' group and the 'basic' group. The former are considered to be made up of the rock types quartz-monzonite, granite, and granodiorite while

the latter comprises the gabbro, monzonite and dioritic xenoliths. Aplite and pegmatite have not been classified in this grouping.

CHAPTER III : MINERALOGY

CHAPTER III

MINERALOGY

3-1 Potassium feldspars

3-1-1 Introduction

The potassium feldspars are polymorphic. They consist of the high temperature polymorph sanidine, present in only volcanic rocks and orthoclase and microcline (stable at lower temperatures).

Orthoclase was named by Breithaupt (1823) from the presence of perpendicular cleavages ((010) and (001)) and comes from the Greek (ortho-clase = angle 90^{o} cut).

Microcline was distinguished from orthoclase by Breithaupt (1830) by a small deviation (in Greek, micro-cline) from 90^{o}, of the angle between the (010) and (001) cleavages.

The formula for potassium feldspar is K Al Si_3 O_8. More recent distinctions between orthoclase and microcline polymorphs have been based upon X-ray studies of alkali feldspars (reviewed in Smith, 1974). The large cation in the alkali feldspar structure (Na,K),sits in interstices between the linked aluminosilicate tetrahedra. There is only one type of site in which the large cation is found, hence the alkali feldspar polymorph cannot be distinguished using this criterion. There are however four distinct tetrahedral sites in the feldspars labelled t_{1O}, t_{1m}, t_{2O},

t_{2m} by Megaw (1962) and aluminium in the monoclinic sanidine polymorph is randomly distributed over all these four sites. In orthoclase, aluminium has been partially ordered into the T_1 sites, thus still preserving monoclinic symmetry. In maximum microcline this process has been taken one stage further and almost all the aluminium is found in the $T_{1(O)}$ site. This therefore makes microcline both topochemically and structurally triclinic. There are, however (Goldsmith and Laves, 1954), thought to be a whole series of intermediate stages between orthoclase and microcline and these have been called 'intermediate microclines' which also have triclinic symmetry. This ordering process is particularly well shown by observation of the variation in the interaxial angle α in the lattice parameters.

3-1-2 X-ray diffraction study of the potassium feldspars

The study includes:

I Determination of the cell parameters (a, b, c, α, β, γ) of the potassium feldspars.

II Determination of the structural states of the potassium feldspars.

III Determination of the composition of the potassium phase of the alkali feldspar from the cell volume.

IV Determination of the bulk composition of potassium feldspar by homogenization experiments.

V Determination of the ordering process in potassic feldspars.

Methods:

In order to determine the cell parameters, structural states and the composition of the potassic phase of the alkali feldspar the methods of Wright and Stewart (1968), Wright (1968), Stewart and Wright (1974), Jones et al (1969, in Hutchinson, 1974), Evans et al (1963) were used.

The sample localities are shown in fig. (3-1-2a). The fifty-seven specimens of potassium feldspar for X-ray diffraction study were obtained as single crystals. However, material from the groundmass had to be obtained by crushing the rocks and extracting the potassium feldspars by hand using a microscope.

Before this material was diffracted it was again crushed down to between 125-250 mesh, washed, dried and purified by separation with heavy liquids.

The purified potassium feldspars were mixed with calcium fluoride (CaF_2), which then served as an internal standard (a_o= 5.4620 (A^o) at 25° C), in an agate mortar. Smear mounts were prepared from the mixture and run on a Siemens X-ray diffractometer using $CuKa_1$ radiation (λ = 1.5405 A^o, 35 KV, 20 mA) with a nickel monochromator. Three scans from 10° to 57° degrees were made of each sample. A goniometer speed of 0.5 degree 2θ per minute was used and a chart speed of 1 cm/min.

All peaks were measured as near to the top as possible in order that the $CuKa_1$ peak is used. The three strongest CaF_2 peaks of each diffractogram were measured and compared with the theoretical peaks in the J.C.P.D.S. file for CaF_2.

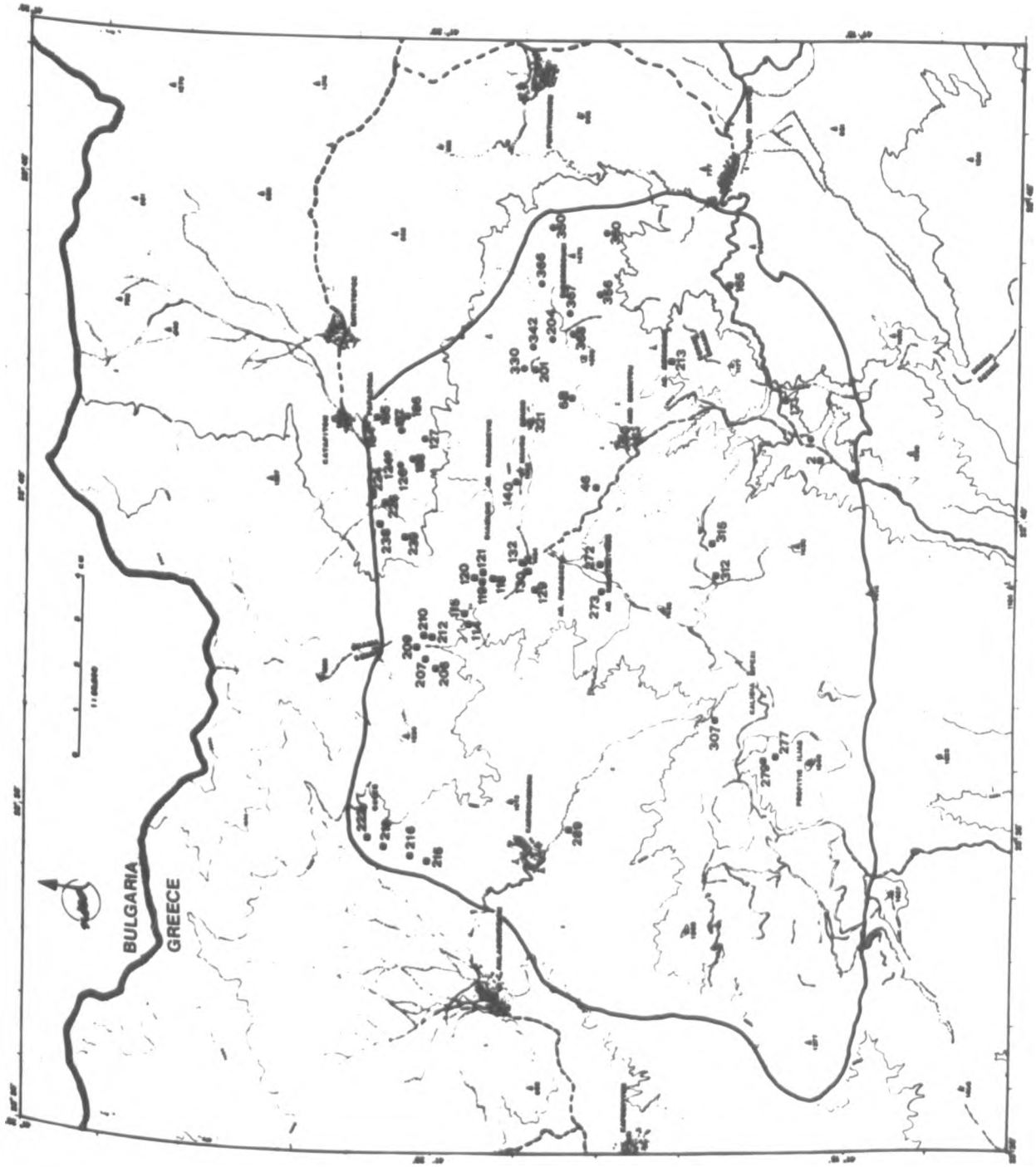

Fig (3-1-2a)

A correction factor was obtained by calculating the differences between the theoretical 2θ values and the measured 2θ values. This factor was then applied to the potassium feldspar peaks.

The mean of the 2θ values from the sample diffraction patterns were used as input data, after consultation of table (10-15) in Wright and Stewart (1968), in a cell refinement programme (Evans et al, 1963) to obtain refined unit cell parameters.

The input data for the first refinements included only the strongest potassium feldspar peaks. More than one refinement of the unit cell parameters was made for many of the samples, whose measured peak positions were again checked. The intensities of these reflections were compared with data of table 11 and 13 in Wright and Stewart (1968), as a further check for final indexing of the individual reflection.

Ratios of acceptance and rejection of the reflections in the refinement program are similar to data given by Wright and Stewart (1968) (tables, 11, 13).

Of the fifty-seven specimens that were diffracted, fifteen were selected for homogenization experiments. These fifteen samples were selected to cover the whole of the area of the complex. The samples were heated to a temperature of 1050^{o} C for forty-eight hours. After cooling, the treated powders were ground in a mortar with an equal volume of potassium bromate ($KBrO_3$) which served as an internal standard.

Smear mounts of the heat treated samples were run on

a Siemens X-ray diffractometer using $CoK\alpha_1$ radiation (λ = 1.7890 A°, 30 KV, 16 mA) and using the iron monochromator. Three scans from 19° to 24° degrees were made of each sample. A goniometer speed 0.5 degree 2θ per minute was used and a chart speed 1cm/min. From the difference in degrees between the $(\bar{2}01)$ feldspar reflection and (101) peak for $KBrO_3$, the corrected value for the $(\bar{2}01)$ feldspar reflection could be calculated and then by using the mean of the $d_{(\bar{2}01)}$ values for each specimen, it is possible to determine the bulk composition of the alkali feldspars.

3-1-3 X-ray diffraction results

The refined unit cell parameters for the potassium feldspars are listed in tables (3-1-3a) for triclinic samples and (3-1-3b) for monoclinic samples.

According to Stewart and Wright (1974, table 1), the cell parameter values of maximum microcline and high sanitine (end members) are respectively: a, 8.597 A° and 8.610 A°; b, 12.964 A° and 13.033 A°; c, 7.222 A° and 7.174 A°; α, 90.637° and 90.000°; β, 115.933° and 116.017°; and γ, 87.683° and 90.000°. In the rocks of the Serres-Drama granitic complex as determined by the present author, the range of cell parameters for the triclinic potassium feldspars is: a, 8.564 to 8.593; b, 12.953 to 12.971; c, 7.207 to 7.218; α, 90.496 to 90.913; β, 115.944 to 116.118; and γ, 87.737 to 87.997. For the monoclinic potassium feldspars the range is: a, 8.545 to 8.583; b, 12.949 to 12.991; c, 7.189 to 7.207; β, 115.929 to

TABLE: (3-1-3.a) X-ray powder diffraction data for triclinic potassium feldspars from Serres-Drama granitic complex.

Sample number	a,A°	b,A°	c,A°	α	β	γ	α*	γ*	V,A°3
2	8.573(1)*	12.953(1)	7.207(0)	90.496	116.049	87.837	90.505	92.165	718.47
6a	8.575(0)	12.961(0)	7.210(0)	90.617	115.971	87.927	90.324	92.005	719.85
46	8.570(0)	12.960(0)	7.208(0)	90.785	116.038	87.739	90.231	92.133	718.74
114	8.575(0)	12.962(0)	7.209(0)	90.860	115.996	87.786	90.123	92.044	719.65
115	8.588(1)	12.971(1)	7.208(0)	90.806	116.035	87.939	90.109	91.900	720.97
118	8.573(1)	12.962(1)	7.209(0)	90.908	116.016	87.744	90.091	92.068	719.36
119	8.567(1)	12.961(0)	7.214(0)	90.754	116.088	87.835	90.220	92.042	718.95
120	8.574(0)	12.959(0)	7.209(0)	90.771	115.954	87.812	90.208	92.059	719.74
121	8.572(0)	12.958(0)	7.209(0)	90.674	116.007	87.895	90.277	92.013	719.17
129	8.582(1)	12.960(0)	7.212(0)	90.582	116.029	87.882	90.387	92.073	720.26
130	8.584(2)	12.962(1)	7.209(0)	90.601	116.028	87.880	90.366	92.065	720.26
132	8.585(0)	12.963(0)	7.213(0)	90.627	116.028	87.871	90.342	92.063	719.96
165	8.587(0)	12.967(0)	7.217(0)	90.739	116.118	87.849	90.232	92.034	721.03
171	8.564(1)	12.965(0)	7.215(0)	90.643	116.008	87.737	90.389	92.205	719.37
206	8.578(0)	12.970(0)	7.210(0)	90.913	116.024	87.833	90.042	91.966	720.38
207	8.576(1)	12.965(0)	7.210(0)	90.901	116.007	87.803	90.070	92.005	719.94
209	8.592(0)	12.969(0)	7.210(0)	90.773	115.976	87.966	90.130	91.885	721.77
210	8.593(1)	12.968(0)	7.209(0)	90.721	116.042	88.074	90.139	91.792	721.33

(1)* Indicates standard error and is relevant to the third figure after decimal point.

TABLE: (3-1-3a) X-ray powder diffraction data for triclinic potassium feldspars from Serres-Drama granitic complex (continued).

Sample number	a,A°	b,A°	c,A°	α	β	γ	α*	γ*	V,A°3
212	8.585(1)*	12.969(1)	7.210(0)	90.864	116.040	87.821	90.103	92.003	720.68
213	8.587(0)	12.954(0)	7.216(0)	90.766	115.944	87.885	90.177	91.979	721.32
215	8.586(0)	12.961(0)	7.213(0)	90.794	116.058	87.864	90.160	91.989	720.57
216	8.576(1)	12.961(0)	7.218(0)	90.716	116.016	87.829	90.263	92.067	720.52
218	8.572(0)	12.961(0)	7.214(0)	90.831	116.051	87.818	90.142	92.023	719.86
222	8.581(2)	12.969(1)	7.220(0)	90.719	116.085	87.849	90.253	92.043	721.09
224	8.582(1)	12.962(1)	7.210(0)	90.770	115.964	87.882	90.176	91.981	720.63
226	8.578(1)	12.964(1)	7.210(0)	90.829	116.010	87.938	90.084	91.890	720.17
238	8.580(1)	12.959(0)	7.212(0)	90.860	116.039	87.786	90.124	92.044	719.88
239	8.578(0)	12.967(0)	7.212(0)	90.496	115.976	87.878	90.483	92.119	720.55
272	8.566(1)	12.960(1)	7.217(0)	90.658	116.040	87.997	90.246	91.908	719.37
273	8.581(1)	12.954(1)	7.213(0)	90.688	115.941	87.888	90.263	92.014	720.48
277	8.586(1)	12.958(0)	7.211(0)	90.610	116.054	87.928	90.334	92.008	720.27
279	8.575(0)	12.957(0)	7.216(0)	90.598	115.958	87.807	90.402	92.147	720.36
289	8.565(0)	12.963(0)	7.210(0)	90.644	116.065	87.836	90.342	92.094	718.62
307	8.572(1)	12.961(1)	7.211(0)	90.583	116.037	87.963	90.346	91.983	719.46
312	8.576(0)	12.958(0)	7.211(0)	90.581	116.073	87.822	90.420	92.141	719.31
315	8.574(0)	12.965(0)	7.212(0)	90.573	116.105	87.880	90.401	92.080	719.39

(1)* Indicates standard error and is relevant to the third figure after decimal point.

TABLE: (3-1-3b) X-ray powder diffraction data for monoclinic potassium feldspars from Serres-Drama granitic complex.

Sample number	a,A°	b.A°	c,A°	α	β	γ	α*	γ*	V,A°3
1	8.566(1)*	12.969(0)	7.198(0)	90.000	115.963	90.000	90.000	90.000	718.94
124	8.556(0)	12.984(0)	7.196(0)	90.000	116.009	90.000	90.000	90.000	718.40
126	8.568(0)	12.963(0)	7.194(0)	90.000	116.003	90.000	90.000	90.000	717.99
127	8.566(0)	12.964(0)	7.194(0)	90.000	115.947	90.000	90.000	90.000	718.44
140	8.563(0)	12.973(0)	7.207(0)	90.000	116.098	90.000	90.000	90.000	719.04
184	8.560(0)	12.978(0)	7.193(0)	90.000	115.995	90.000	90.000	90.000	718.28
185	8.580(0)	12.991(0)	7.204(0)	90.000	115.969	90.000	90.000	90.000	721.94
186	8.575(0)	12.974(1)	7.205(0)	90.000	116.027	90.000	90.000	90.000	720.33
187	8.583(0)	12.977(0)	7.199(0)	90.000	116.007	90.000	90.000	90.000	720.67
188	8.578(1)	12.959(1)	7.189(0)	90.000	115.929	90.000	90.000	90.000	718.77
201	8.575(0)	12.984(0)	7.200(0)	90.000	116.031	90.000	90.000	90.000	720.35
204	8.558(0)	12.968(0)	7.196(0)	90.000	115.967	90.000	90.000	90,000	717.95
321	8.552(1)	12.949(2)	7.186(0)	90.000	115.957	90.000	90.000	90.000	715.77
330	8.545(0)	12.967(0)	7.204(0)	90.000	116.035	90.000	90.000	90.000	717.21
342	8.560(0)	12.979(0)	7.201(0)	90.000	115.998	90.000	90.000	90.000	719.13
350	8.564(0)	12.952(0)	7.194(0)	90.000	116.010	90.000	90.000	90.000	717.14
356	8.570(0)	12.965(0)	7.195(0)	90.000	116.024	90.000	90.000	90.000	718.36
360	8.566(0)	12.965(0)	7.200(0)	90.000	116.129	90.000	90.000	90.000	717.96
366	8.573(0)	12.974(0)	7.201(0)	90.000	115.979	90.000	90.000	90.000	720.05
367	8.567(0)	12.958(0)	7.196(0)	90.000	116.065	90.000	90.000	90.000	717.63
368	8.549(0)	12.967(0)	7.200(0)	90.000	115.992	90.000	90.000	90.000	717.40

(1)* **Indicates standard error and is relevant to the third figure after decimal point.**

116.129; and $\alpha = \gamma = 90.000$.

The X-R-D data confirm the distribution of structural states inferred from the twinning of the potassium feldspar polymorphs in the course of optical studies. The structural states are independent of the texture of the rock-types in which they occur, but appear to be dependant on the chemical composition of the rocks.

Several methods have been used to elucidate the structural state of potassium feldspars, i.e. whether they are monoclinic or triclinic. The first of the methods was introduced by Goldsmith and Laves (1954) who introduced the concept of triclinicity, as defined by the following equation:

$$\text{Triclinicity } \Delta = 12.5\ (d_{131} - d_{1\bar{3}1})$$

From this equation it is possible to obtain an arithmetic expression of Al/Si order in alkali feldspars by measuring the separation of (131) and $(1\bar{3}1)$ reflections. This definition results in values ranging from 0.0 for monoclinic feldspars, where these doublets of reflections merge into one; to 1.0 for fully ordered maximum microcline. The implication from Goldsmith and Laves'(op.cit.) work was that there could be a continuum between orthoclase and maximum microcline i.e. there was a whole range of intermediate states of microcline which were subsequently called 'intermediate microcline'. In the present study the values range from $\Delta = 0.686$ to 0.969 for triclinic samples. The above results have been calculated, using the d- spacing from the refinement program. Fig (3-1-3a) shows some examples

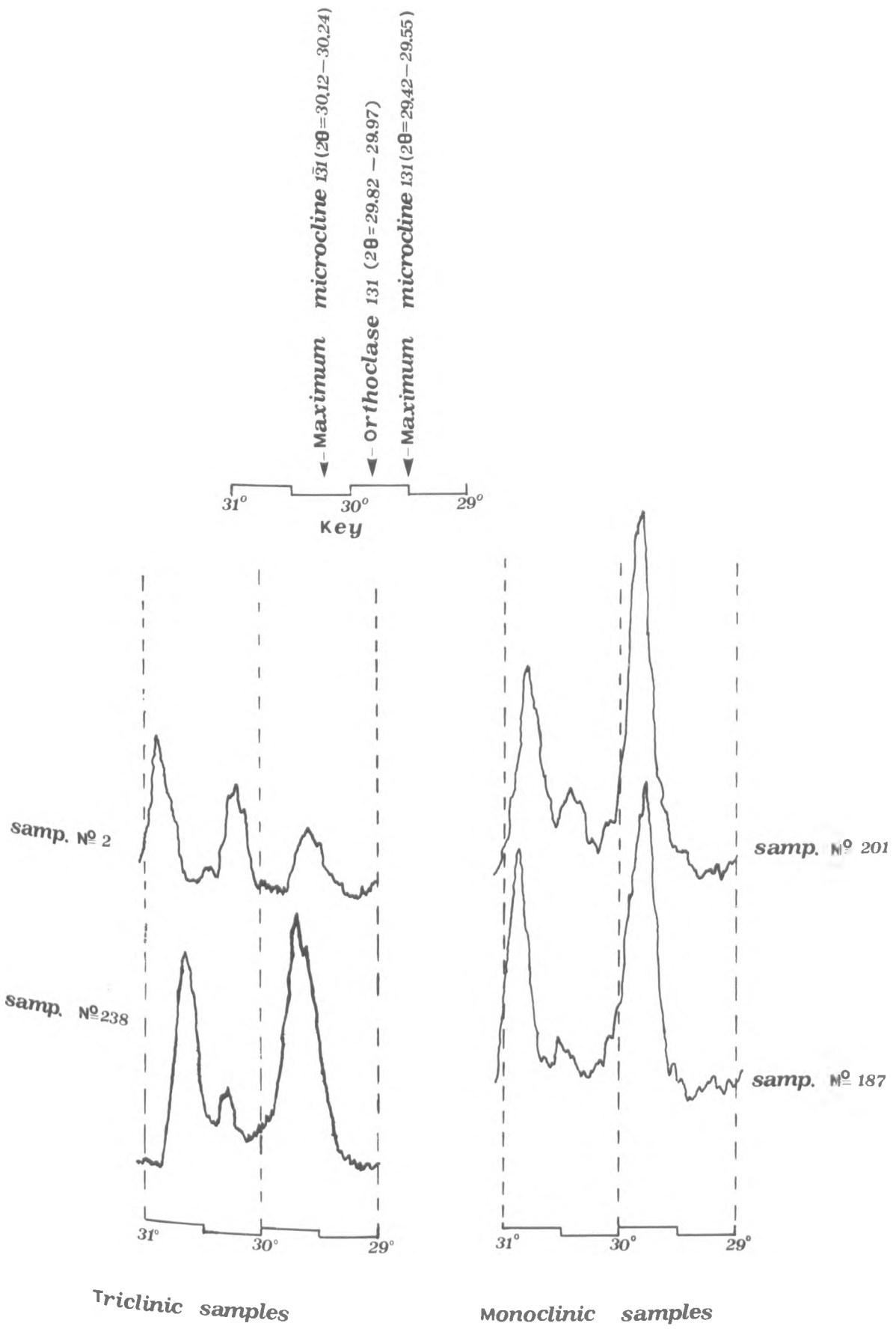

Triclinic samples

Monoclinic samples

Fig (3-1-3a)

of the reflection types with different triclinicities.

Refined unit cell parameters of the natural potassium feldspars from the above tables are plotted onto b-c and $\alpha^* - \gamma^*$ diagrams, as illustrated in fig. (3-1-3b) and fig. (3-1-3c). The initial plots are based upon those of Steward and Wright (1974). In addition to the b and c parameters Stewart and Wright (op.cit.) have contoured the diagram (fig. 3-1-3b) for variations in the a parameter and $t_{1O} + t_{1m}$. From this plot it is possible to see that there are two distinct groups of data points. The triclinic potassium feldspars are tightly grouped on the b-c cell dimension plot with values between 0.89 and 0.98 $(t_{1O} + t_{1m})$. The values quoted of $t_{1O} + t_{1m}$ are calculated from the equations below and are not estimations from the diagram (fig. 3-1-3b). This is for the sake of clarity. This indicates that they are highly ordered and close to maximum microcline. In contrast, the monoclinic potassium feldspars have values of between 0.77 and 0.88 $(t_{1O} + t_{1m})$. There is a continuum in the values of $t_{1O} + t_{1m}$ obtained from the graphic displays of the structural state of the potassium feldspars as shown in fig. (3-1-3b). The distinction between the above groups is more clearly shown in the histograms in fig. (3-1-3e). These results indicate that there is no intermediate microcline present using the refined cell parameter data.

The difference between the triclinicity (Δ) values using the Goldsmith and Laves (op.cit.) method and the

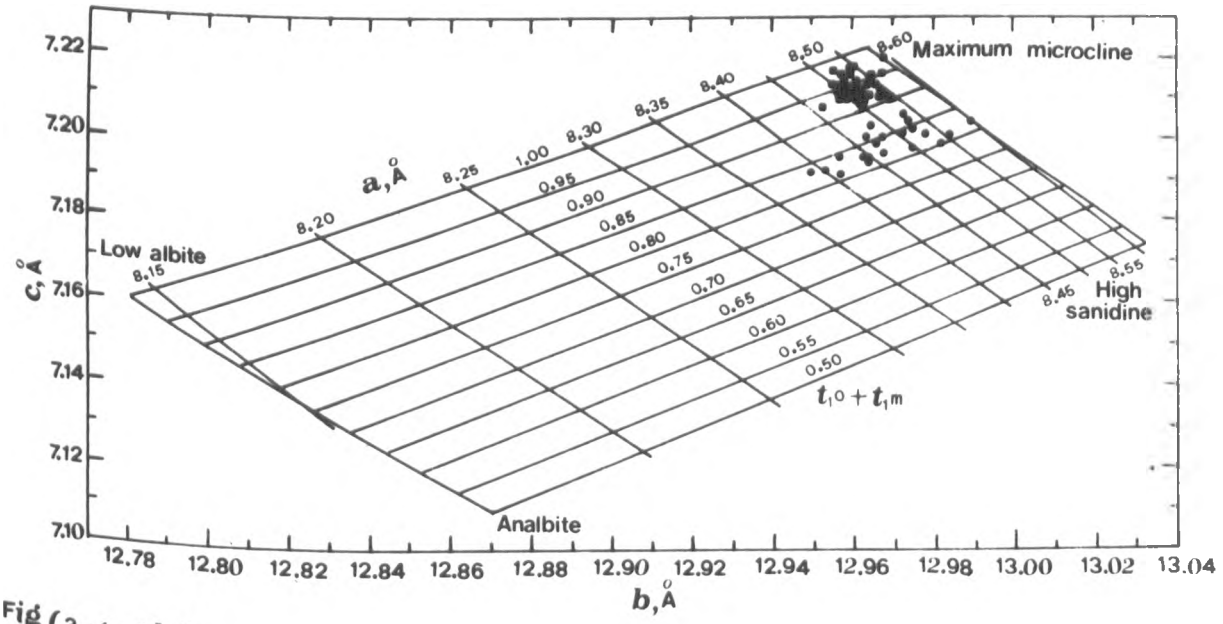

Fig (3-1-3b)

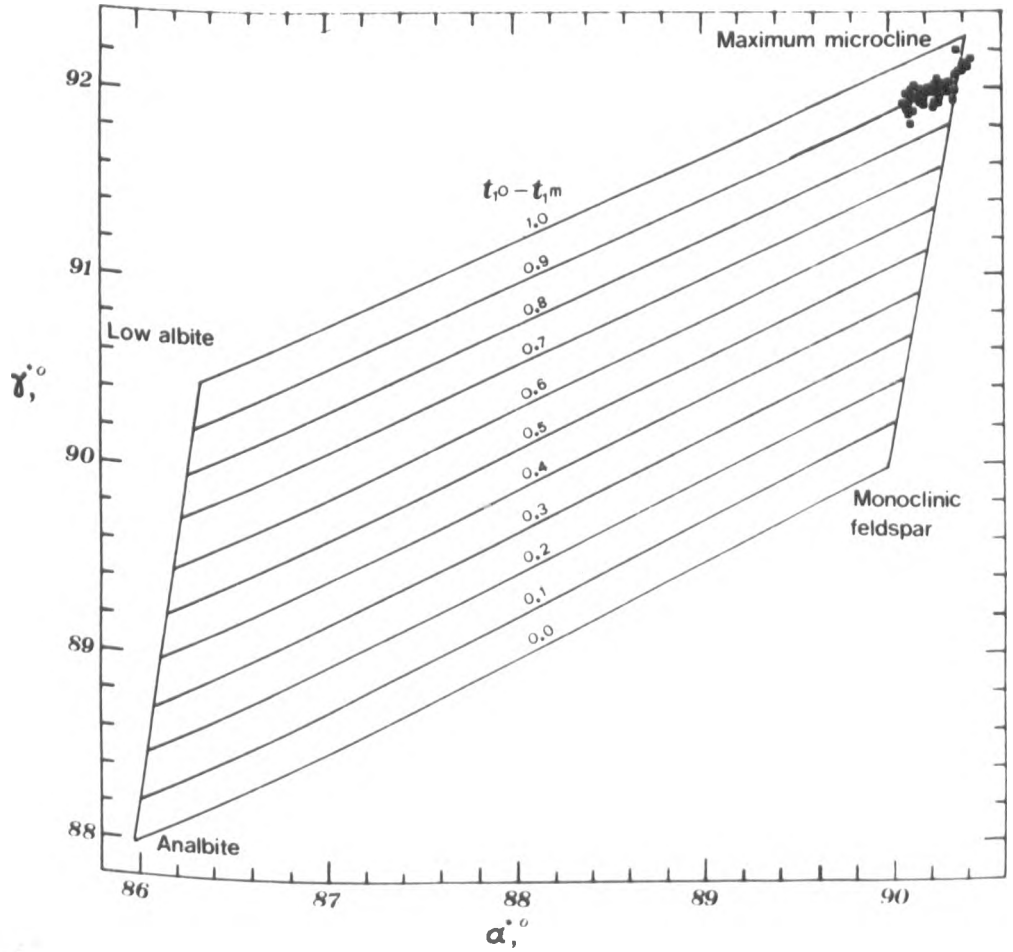

Fig (3-1-3c)

calculated contents of aluminium in $t_{1o} + t_{1m}$ sites may possibly arise due to the problem of using just two reflections of the powder diffraction pattern in the former method. Reference to the fig. (3-1-3a) shows that the intensity of the $(1\bar{3}1)$ reflection of the triclinic feldspars is small and therefore may be subject to quite a range of possible measuring errors. The second method, which depends upon the whole diffraction pattern is much more precise and therefore these data are to be preferred.

The triclinic samples have been plotted on to a $\alpha^* - \gamma^*$ diagram (fig. 3-1-3c, after Stewart and Wright, 1974). All the potassium feldspars are very tightly grouped close to the values for maximum microcline. There appears to be some dispersion of the α^* parameters (α^*, 90.042 to 90.505) but little or no variation in γ^*. This diagram (fig. 3-1-3c) has been used to discriminate between orthoclase, intermediate microcline, and maximum microcline (Stewart and Wright, 1974; Cherry and Trembath, 1978).

It is possible to determine the Al/si order in potassium feldspar by calculating the Al distribution in the tetrahedral sites (t_{1o}, t_{1m}, t_{2o}, t_{2m}) in the structure, by combining the following equations (Stewart and Wright, 1974).

$$t_{1o} + t_{1m} = \frac{C - 0.45132b - 1.22032}{1.6095 - 0.11252\ b}$$

$$t_{1o} - t_{1m} = \frac{\alpha^* - 1.99754\gamma^* + 89.77811}{0.24614\ \gamma^* - 26.8196}$$

Aluminium is found in the tetrahedral sites of the potassium feldspar sites such that

$$t_{1O} + t_{1m} + t_{2O} + t_{2m} = 1.0$$

from the chemical formula ($KAlSi_3O_8$). It has been noted from structural refinements of site occupancy that the amount of aluminium in t_{2O} is the same as that in t_{2m} (Smith, 1974) therefore it is possible to display the tetrahedral site occupancy in a triangle with apices representing t_{1O}, t_{1m} and $t_{2O} + t_{2m}$ (fig. 3-1-3f). Only the lower portion of the triangle is used and hence appears as a quadrilateral.

The calculated data (for t_{1O}, t_{1m}, t_{2O}, t_{2m}) are given in tables (3-1-3c) for triclinic and (3-1-3d) for monoclinic feldspars. For ten of thirty-six triclinic samples, the difference t_{1O}-t_{1m} was larger than the $t_{1O} + t_{1m}$. This happens in data from the Serres-Drama granitic complex only at high values of $t_{1O} + t_{1m} \gtrsim 0.91$. It is possible that this may occur because of the errors in measurement of the cell parameters and the propagation of errors using the Stewart-Ribbe method. Stewart and Wright (1974) state that

> "The problem is most common with strained feldspars and in some cases is clearly a strain phenomenon; ... The Stewart-Ribbe method may be erroneous for some strained aggregates, and may yield errors in t_{1m} as high as $\pm$ 0.05 in a few highly ordered strained samples."

Stewart and Wright (1974) established an index to characterize the strain in alkali feldspars where $\Delta a = a_{observed} - a_{estimated}$, the $a_{estimated}$ is calculated from the contours on the b-c plot. They established as a

TABLE: (3-1-3c) Tetrahedral site occupancy values(t_1O, t_2O, t_1m, t_2m), the index of strain (Δa), the triclinicity (Δ), the composition of potassium phase (mol % Or), the bulk composition in molecular % of Or (bulk c.d.) and the bulk composition in weight % of Or (bulk c.c.), calculated from the X-ray diffraction data of triclinic K-feldspars from the Serres-Drama granitic complex.

Samp No.	No of reflect	t_1O+t_1m	t_1O-t_1m	t_1O	t_1m	t_2O+t_2m	Δa	Δ	mol% Or	$d_{(\bar{2}01)}$	bulk c.d.	bulk c.c.
2	15	0.94	0.92	0.93	0.01	0.06	0.09	0.969	87	-	-	-
6a	14	0.93	0.88	0.91	0.02	0.07	0.05	0.838	91	-	-	-
46	15	0.92	0.97	-	-	0.08	0.07	0.844	88	-	-	-
114	21	0.92	0.95	-	-	0.08	0.06	0.768	91	-	-	-
115	18	0.89	0.88	0.89	0.01	0.11	0.03	0.711	94	-	-	-
118	20	0.92	0.97	-	-	0.08	0.06	0.763	90	-	-	-
119	19	0.95	0.93	0.94	0.01	0.05	0.02	0.807	89	4.205	78	80
120	20	0.93	0.94	-	-	0,08	0.07	0.809	91	-	-	-
121	14	0.93	0.90	0.91	0.02	0.07	0.07	0.821	89	-	-	-
129	19	0.94	0.90	0.92	0.02	0.06	0.05	0.888	92	-	-	-
130	18	0.92	0.90	0.91	0.01	0.08	0.06	0.876	92	-	-	-
132	21	0.94	0.91	0.93	0.02	0.06	0.03	0.866	91	-	-	-
165	14	0.96	0.92	0.94	0.02	0.04	0.00	0.809	94	-	-	-
171	20	0.95	0.97	-	-	0.05	0.01	0.936	90	4.204	78	79.5
206	18	0.91	0.93	-	-	0.09	0.03	0.707	93	-	-	-
207	20	0.92	0.94	-	-	0.08	0.05	0.732	91	-	-	-
209	17	0.91	0.87	0.89	0.02	0.09	0.04	0.716	97	-	-	-
210	16	0.90	0.81	0.86	0.05	0.10	0.05	0.686	95	-	-	-

TABLE: (3-1-3c) Tetrahedral site occupancy values ($t_1$0, $t_2$0, t_1m, t_2m), the index of strain (Δ a), the triclinicity (Δ), the composition of potassium phase (mol % Or), the bulk composition in molecular % of Or (bulk c.d.) and the bulk composition in weight % of Or (bulk c.c.), calculated from the X-ray diffraction data of triclinic K-feldspars from the Serres-Drama granitic complex. (cont)

Samp No	No of reflect	$t_1$0+ t_1m	$t_1$0- t_1m	$t_1$0	t_1m	$t_2$0+ t_2m	Δa	Δ	mol% Or	$d_{(\bar{2}01)}$	bulk c.d.	bulk c.c.
212	19	0.91	0.93	-	-	0.09	0.03	0.745	93	-	-	-
213	18	0.98	0.90	0.94	0.04	0.02	0.05	0.769	95	4.210	80	82
215	16	0.95	0.89	0.92	0.03	0.05	0.05	0.764	93	4.201	77.5	78
216	16	0.98	0.93	0.96	0.03	0.02	0.02	0.835	93	-	-	-
218	19	0.95	0.94	0.95	0.01	0.05	0.04	0.768	91	-	-	-
222	20	0.97	0.92	0.95	0.03	0.03	-	0.822	95	-	-	-
224	18	0.93	0.91	0.92	0.01	0.08	0.06	0.768	93	-	-	-
226	15	0.92	0.88	0.90	0.02	0.08	0.04	0.698	92	-	-	-
238	17	0.95	0.95	-	-	0.06	0.05	0.768	91	-	-	-
239	17	0.93	0.91	0.92	0.01	0.07	0.02	0.945	93	4.201	77.5	78
272	14	0.98	0.85	0.91	0.06	0.02	0.02	0.772	90	-	-	-
273	17	0.96	0.90	0.93	0.03	0.04	0.06	0.816	93	4.205	78	80
277	14	0.94	0.88	0.91	0.03	0.06	0.07	0.843	92	4.197	76	76
279	22	0.98	0.94	0.96	0.02	0.02	0.04	0.922	93	-	-	-
289	13	0.92	0.93	-	-	0.08	0.03	0.876	88	4.198	77	77
307	17	0.93	0.87	0.90	0.04	0.07	0.05	0.839	90	-	-	-
312	14	0.94	0.93	0.94	0.01	0.06	0.06	0.925	90	-	-	-
315	16	0.93	0.90	0.92	0.01	0.07	0.04	0.896	90	4.207	79	81

TABLE: (3-1-3d). Tetrahedral site occupancy values (t_1O, t_2O, t_1m, t_2m), the index of strain (Δ a), the composition potassium phase (mol % Or), the bulk composition in molecular % of Or (bulk c.d.) and the bulk composition in weight % of Or (bulk c.c.), calculated from the X-ray diffraction data of monoclinic K-feldspars from the Serres-Drama granitic complex.

Sample Number	No. of reflect	t_1O+t_1m	t_1O	t_2O+t_2m	Δa	mol % Or	$d_{(\bar{2}01)}$	bulk c.d.	bulk c.c
1	24	0.83	0.41	0.17	0.07	89	-	-	-
124	27	0.78	0.39	0.22	0.01	87	-	-	-
126	28	0.82	0.41	0.18	0.10	84	4.196	75	76
127	26	0.81	0.41	0.19	0.09	87	-	-	-
140	21	0.88	0.44	0.12	0.01	89	4.198	77	77
184	26	0.77	0.39	0.23	0.05	87	4.197	76	76
185	15	0.82	0.41	0.18	-	97	-	-	-
186	20	0.86	0.43	0.14	0.03	92	-	-	-
187	19	0.82	0.41	0.18	0.04	93	-	-	-
188	17	0.79	0.40	0.21	0.14	88	-	-	-
201	18	0.81	0.40	0.19	0.01	92	4.198	77	77
204	18	0.82	0.41	0.18	0.10	86	4.201	77.5	78
321	23	0.82	0.41	0.18	0.16	81	-	-	-
330	23	0.87	0.44	0.13	0.03	84	-	-	-
342	23	0.83	0.41	0.18	0.01	89	-	-	-
350	24	0.82	0.41	0.18	0.13	84	-	-	-
356	25	0.82	0.41	0.18	0.11	87	-	-	-
360	23	0.85	0.43	0.15	0.07	86	4.207	79	81
366	22	0.84	0.42	0.16	0.03	92	-	-	-
367	26	0.84	0.42	0.16	0.12	85	-	-	-
368	24	0.85	0.42	0.15	0.15	85	-	-	-

threshold value $\Delta a = 0.05$. In the present study, the data of Δa listed in table (3-1-3c) and (3-1-3d) indicate that monoclinic potassium feldspars are more strained than the triclinic potassium feldspars. This has been observed by many other workers (Cherry and Trembath, 1978; Stewart and Wright, 1974).

From the above ten triclinic samples mentioned, four were strained. From eight triclinic megacrysts, three were found to be strained and from six monoclinic megacrysts, three were strained. Two samples from xenoliths (No.1 and 315) within the quartz monzonite were also found to be strained, one (sample No.1) is monoclinic in structural state and the other (sample No.315) is triclinic.

Many authors (Parsons and Boyd, 1971; Steward and Wright, 1974; Cherry and Trembath, 1978) have argued that the degree of $Al/_{Si}$ order in natural feldspars is influenced by several factors, such as temperature, presence of volatiles, bulk composition and shearing stress. It is thought that the degree of order may have preserved a record of the cooling history of the magma. The amount of aluminium in the various tetrahedral sites of potassium feldspars is thought to be primarily a function of the cooling history of that particular feldspar. As the temperature falls the Al is ordered first in the T_1 sites and finally into the T_{1O} sites. Therefore a calculation of the distribution of Al among the tetrahedral sites will indicate the temperature at which the ordering process ceased. The amount of aluminium in the T_1 sites in alkali feldspars from the Serres-Drama granitic complex as a function of temperature, are plotted in fig. (3-1-3d). The plots are

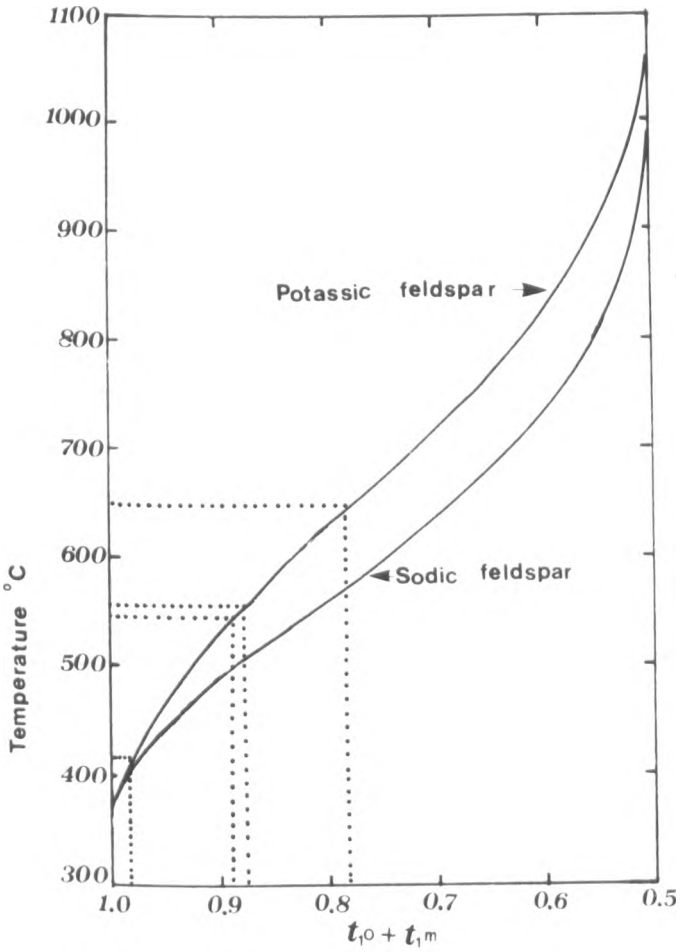

Fig (3-1-3d)

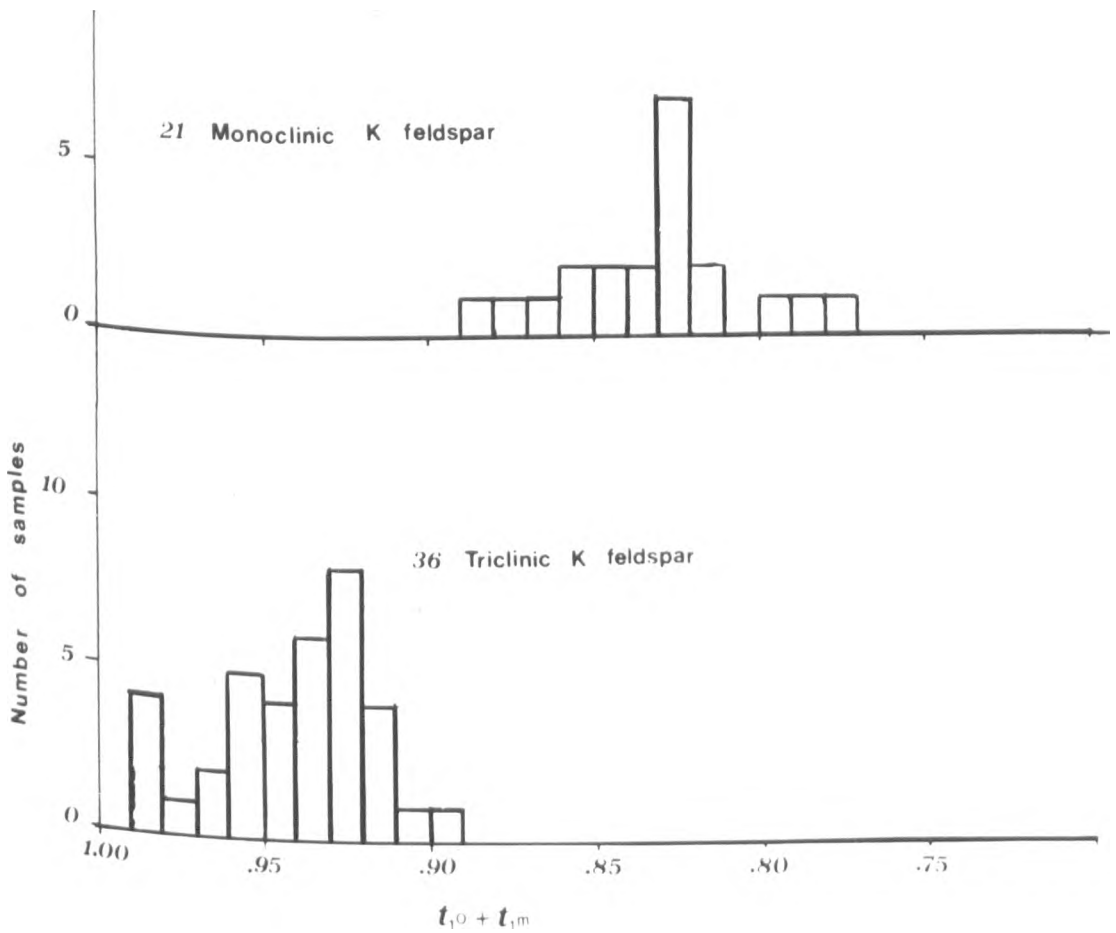

Fig (3-1-3e)

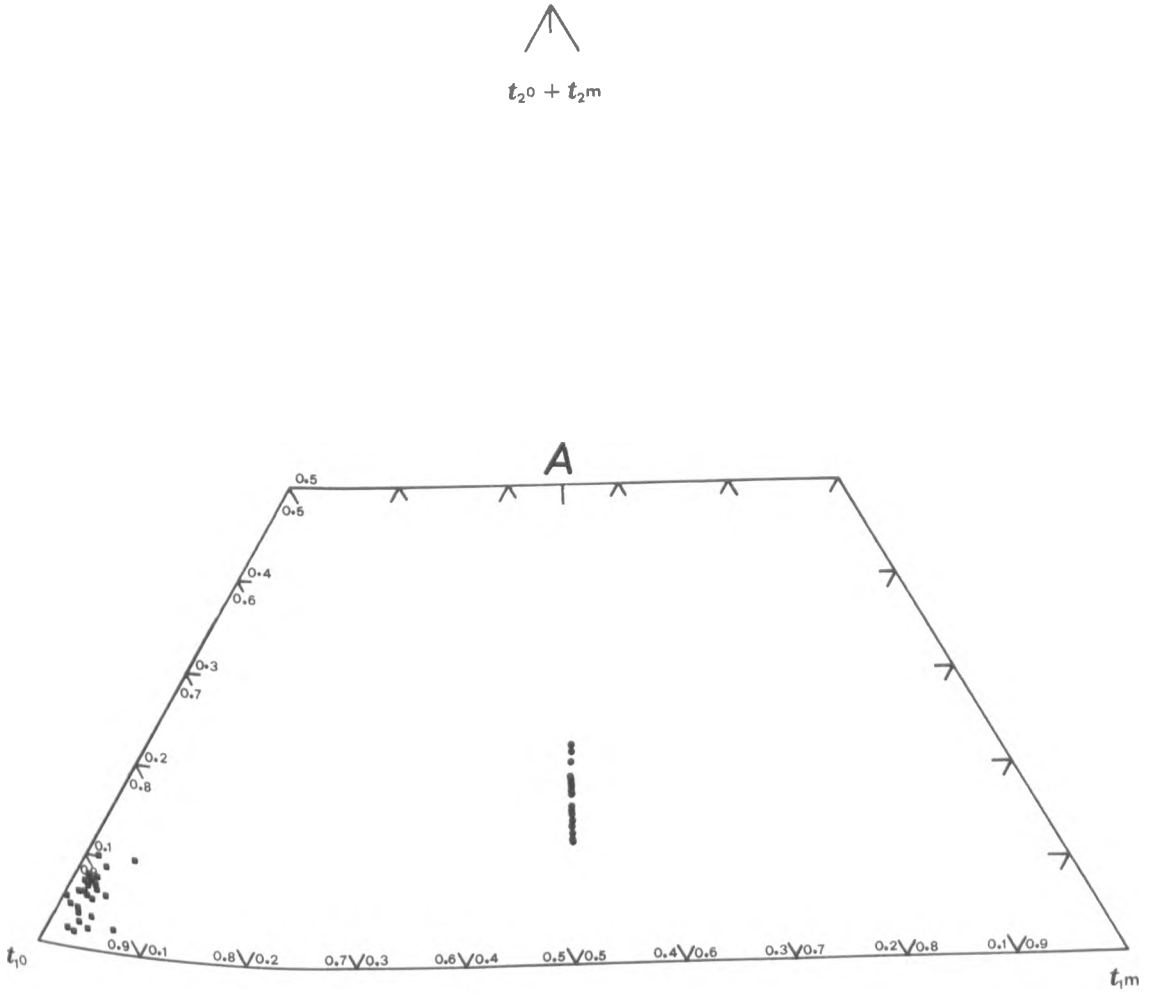
$t_{20} + t_{2m}$
A
0.5
0.5
0.4
0.6
0.3
0.7
0.2
0.8
0.1
0.9
t_{10}
0.9 0.1
0.8 0.2
0.7 0.3
0.6 0.4
0.5 0.5
0.4 0.6
0.3 0.7
0.2 0.8
0.1 0.9
t_{1m}

Fig (3-1-3f)

from Stewart and Wright (1974). The range of temperature for orthoclase is from 650° C for the most disordered, to 545° C for the most ordered monoclinic polymorph. For microcline the range of temperature is from 540° C to 420° C.

The data in table (3-1-3c) indicate a small range in Al/Si order ($t_{2o} + t_{2m}$ = 0.02 to 0.11) for the triclinic samples. The monoclinic samples in table (3-1-3d) display a small range in Al/Si order but slightly larger than that for the triclinic samples ($t_{2o} + t_{2m}$ = 0.12 to 0.23). According to Stewart and Wright (1974) it is possible to derive the ordering process which has taken place in the cooling feldspars by displaying the tetrahedral site occupancies on a quadrilateral (fig. 3-1-3f). The data for the Serres-Drama potassium feldspars are plotted onto this quadrilateral (fig. 3-1-3f). Completely ordered triclinic feldspars (maximum microcline) plot at the t_{1o} vertex. The monoclinic potassium feldspars, however, plot on a vertical line which connects the completely disordered monoclinic feldspar at the point (A) $t_{1o} = t_{1m} = t_{2o} = t_{2m}$ = 0.25.

The ordering process in monclinic samples is indicated by a line from the point of complete disorder (A) toward the base of the quadrilateral, with Al migrating in equal amounts into t_{1o} and t_{1m} sites.

The triclinic samples do not show sufficient variation in their structural state to establish an ordering

path, being tightly grouped on the diagram as highly ordered potassium feldspars. No intermediate microclines were found to complete the ordering path or indeed to indicate which path may have been followed by the Serres-Drama potassium feldspars, as in the example of Guidotti et al (1973, in Stewart and Wright, 1974). Polymorphic potassium feldspars in the same rock-type were not observed.

If we compare the ordering process in feldspars from metamorphic rocks (Stewart and Wright, 1974) with the ordering process in the feldspars from the igneous rocks of the present study, a similar pattern is found. From the present study it is possible to state whether the maximum microcline feldspars arise from a simple ordering event, i.e. a line connecting the present monoclinic feldspar to the triclinic feldspar, with a series of intermediate microclines between the two, or whether it was a two stage process where the monoclinic feldspars reached a state of order close to the base of the quadrilateral and then ordered to the maximum microcline state.

According to Stewart and Wright (1974) it is possible to use either the a axis or the cell volume to calculate the orthoclase content of alkali feldspars. From the cell parameters of the potassic phase of the alkali feldspars from the Serres-Drama granitic complex the cell volume (VA^{o3}) was calculated using the following equation (Stewart and Wright, 1974).

$$\text{Or (mole per cent)} = \frac{0.2962 - \sqrt{0.953131 - 0.0013V}}{0.0018062}$$

The calculation of orthoclase content of the potassic phase of these microperthitic alkali feldspars are from the cell volume.

The composition was determined by using the equations for the calculation of unit cell volume for both triclinic and monoclinic samples and the obtained values are listed respectively in tables (3-1-3a) and (3-1-3b). The mean value for the triclinic samples (Or=91.67%) is larger than the mean value for monoclinic samples (Or=87.81%). The range of orthoclase content (mole per cent) is: 87% to 97% for triclinic and 81% to 97% for monoclinic potassium feldspars. No variation in the composition of the potassium phase in the alkali feldspar with rock-type has been observed.

Parsons (1978, a) suggested that in alkali feldspars "bulk composition will depend on magma composition and the P-T regime under which the feldspar grew from melt, ...". As already cited (Stewart and Wright, 1974) the $d_{\bar{2}01}$ parameter of alkali feldspars is strongly dependent upon composition, therefore reflections such as ($\bar{2}$01) will be affected by variation in the K/Na ratios of alkali feldspars, i.e. the orthoclase content. The ($\bar{2}$01) reflection can therefore be used to obtain the composition of homogenized alkali feldspars. By use of the mean value of $d_{\bar{2}01}$, the bulk composition of the fifteen heat treated samples was determined using fig. (3-1-3g) from Jones et al (1969, in Hutchinson, 1974). The above method is preferred to that of Orville (1967, in Hutchinson, 1974) because compositions of

homogeneous natural alkali feldspars are used rather than the synthetic equivalents used by Orville (op.cit.)

The orthoclase percentage can be calculated using the following equation (Jones et al, 1969, in Hutchinson, 1974).

$$Or\% = 465.5 \times d_{(\bar{2}01)} - 1877.5$$

The data obtained by graphic and calculation methods (Jones et al, 1969) are listed in tables (3-1-3c) for triclinic and (3-1-3d) for monoclinic potassium feldspar. The difference between the above values for the two methods only range from 0% to 2%. The results obtained by calculation are probably the more accurate.

Robin (1974) observed, using the transmission electron microscope, that in cryptoperthitic alkali feldspars the exsolution lamellae are fully coherent and full continuity is present in their lattices. According to Robin (op. cit.) use of the $(\bar{2}01)$ method for composition determination gives results that exaggerates the potassium content of that phase and underrates that of the Na-rich phase in cryptoperthites. This may indeed be so for microperthites as in samples from Serres-Drama analysed by electron microprobe the X-ray results do appear to be slightly higher than the chemical analyses (see below).

Consider a point A, fig. (3-1-3h), exsolution starts when the falling temperature (t) meets the hydrostatic solvus at point B. At this point the sodic phase has a composition X. If the sample is not strained then the temperature follows the hydrostatic curve from B to C with a corresponding

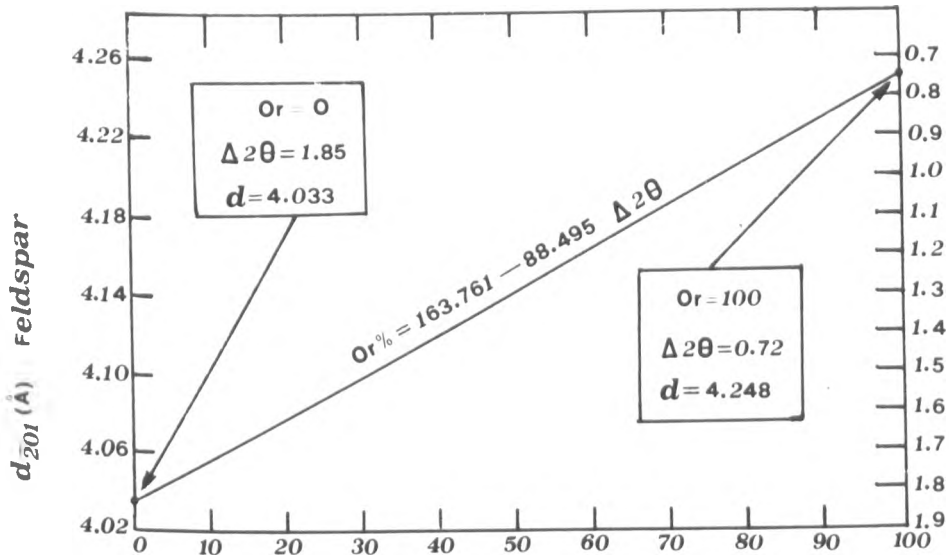

Fig. (3-1-3g) (Jones et al. 1969)

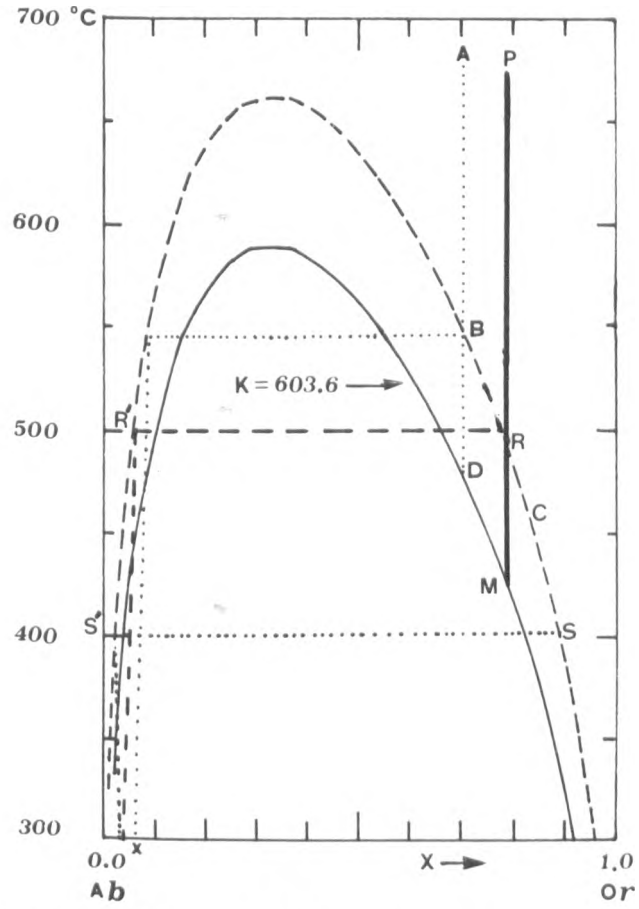

Fig (3-1-3h) (Robin , 1974)

change in composition of the sodic phase. However, if the sample is strained then the temperature follows the line B to D.

Considering a potassium composition of approximately 78% (mean bulk composition of K-feldspar phase for all cell refinements which have been made in the present study). On the T-X graph (fig. 3-1-1h, after Robin, 1974), this composition is represented by point P. Under conditions of no strain, unmixing will start when the temperature has fallen far enough for the composition line through P to intersect the hydrostatic solvus curve (point R, $\sim 500^{o}$). The compositions of the albite rich phase is $\sim Or_5$ (point R'). As temperature falls further the compositions of the Or-rich and Ab-rich phases change along the hydrostatic curve towards S and S'. However, under conditions of strain the composition of the Or-rich phase will follow the line R to M, on the theoretical thermodynamically derived coherent solvus (Robin (op.cit.) for definition), which will give coexisting lamellae of less extreme compositions for the same temperature as those on the hydrostatic solvus.

3-1-4 Microprobe analysis

The general chemical formula for alkali feldspars is $(K, Na, Ca)_4 (Al, Si)_{16} O_{32}$ (Deer et al, 1963, Vol.4) or $M_4 T_{16} O_{32}$. The M cations should be large, with a radius between $0.9A^{o}$ and $1.5A^{o}$ and are either mono- or di-valent. In most cases M=K, Na, Ca with a value not less than 3.9. The T cations

should be small, with radius between 0.2A^{o} and 0.7A^{o} and are tri- or quadri-valent. In most cases T = Si, Al, Ti, Fe^{+3} with a value of 16.0. The above values were calculated on the basis of 32 oxygens. Usually the general formula is expressed as follows:

$$MT_4O_8$$

The following elements were determined by electron microprobe analysis: Si, Ti, Al, Fe, Mn, Mg, Ca, Na, and K and subsequently recalculated to oxides. The data obtained are listed in table (3-1-4a).

For comparison purposes, microprobe analyses of potassium feldspar from other granitic complexes from the Rhodope massif are given in table (3-1-4b) (Christofides, 1977) and table (3-1-4c) (Sklavounos, 1981).

The mean SiO_2 values are 63.73% (Sklavounos, 1981), 64.57% (Christofides, 1977) and in the present study 65.13%. The difference between the mean of Al_2O_3 values is low ($<$ 0.4%).

The valence state of titanium is unknown in feldspars, but the assumption is that tetravalent ions probably occupy T sites. Smith (1974, Vol.2) suggests that titanium enters the feldspar structure, but it is not clear what petrological factors control the degree of substitution. However, the titanium content is low, Sklavounos (1981) did not analyse for this element. The mean TiO_2 values are 0.39% (in Christofides, 1977, who determined TiO_2 in six of the seventeen analyses) and in the present study 0.13%, although only twenty-three out of the fifty-three analyses

TABLE: (3-1-4a) Microprobe analyses of potassium feldspars from the Serres-Drama granitic complex

	119R A1	119R B31	119R B32	119R C43	119R C44	119R C45	119R C46	119R C47	119R C48
SiO_2	65•17	64•73	64•96	63•62	65•02	65•05	64•67	64•71	64•90
TiO_2	0•40	0•18	0•24	0•35	-	0•20	-	-	-
Al_2O_3	19•33	18•40	18•21	18•66	18•83	18•47	18•38	18•33	18•57
*FeO	-	-	-	-	-	-	-	-	0•30
CaO	-	-	-	0•56	-	-	-	-	-
Na_2O	1•95	0•82	0•93	2•60	1•58	0•69	0•46	-	0•64
K_2O	13•46	14•91	14•97	11•27	14•06	15•40	14•86	15•58	15•27
Total	100•31	99•04	99•31	97•06	99•49	99•81	98•37	98•62	99•68
	Numbers of ions on the basis of 8(O)								
Si	2•969	3•001	3•005	2•975	2•992	2•999	3•012	3•014	2•997
Al	1•038	1•006	0•993	1•029	1•021	1•004	1•009	1•006	1•011
Ti	0•014	0•006	0•008	0•012	-	0•007	-	-	-
Fe	-	-	-	-	-	-	-	-	0•012
Ca	-	-	-	0•028	-	-	-	-	-
Na	0•173	0•074	0•088	0•236	0•141	0•061	0•042	-	0•058
K	0•782	0•882	0•883	0•672	0•825	0•906	0•883	0•926	0•900
				Mol%					
An	-	-	-	2•99	-	-	-	-	-
Ab	18•12	7•74	9•06	25•21	14•60	6•31	4•54	-	6•05
Or	81•89	92•26	90•94	71•80	85•40	93•69	95•46	100•00	93•95

Rock types: Quartz monzonite(119R); monzonite(126R, 184R, 202R)
Symbols: R = rock
* total iron as FeO

TABLE: (3-1-4a) Microprobe analyses of potassium feldspars from the Serres-Drama granitic complex (continued)

	119R C49	119R C50	119R C51	119R D52	119R D53	119R D54	119R D55	119R D56	119R D57
SiO_2	64•99	64•73	64•84	65•18	64•80	65•04	65•02	64•55	64•82
TiO_2	-	0•33	0•23	0•21	0•26	0•32	0•34	0•40	0•22
Al_2O_3	18•04	18•44	18•49	18•92	18•43	18•51	18•59	18•47	18•32
*FeO	-	-	-	-	-	-	-	-	-
CaO	-	-	-	-	-	-	-	-	-
Na_2O	2•31	1•25	0•96	-	0•56	1•16	0•94	1•45	1•43
K_2O	13•32	14•76	15•18	15•58	15•07	14•61	14•76	13•89	14•04
Total	98•66	99•51	99•70	99•89	99•12	99•64	99•65	98•76	98•83
	Numbers of ions on the basis of 8(O)								
Si	3•012	2•990	2•993	2•996	3•001	2•995	2•994	2•991	3•002
Al	0•985	1•004	1•006	1•025	1•006	1•005	1•009	1•009	1•000
Ti	-	0•011	0•008	0•007	0•009	0•011	0•012	0•014	0•008
Fe	-	-	-	-	-	-	-	-	-
Ca	-	-	-	-	-	-	-	-	-
Na	0•207	0•114	0•086	-	0•050	0•104	0•084	0•130	0•128
K	0•788	0•870	0•894	0•914	0•890	0•858	0•867	0•821	0•830
	Mol%								
An	-	-	-	-	-	-	-	-	-
Ab	20•80	11•59	8•78	-	5•32	10•81	8•83	13•67	13•36
Or	79•20	88•33	91•22	100•00	94•68	89•19	91•17	86•33	86•64

TABLE: (3-1-4a) Microprobe analyses of potassium feldspars from the Serres-Drama granitic complex (continued)

	119R	126R	126R	126R	126R	126R	126R	126R	184R
	average	A1	A2	A3	A4	B35	B36	average	A21
SiO_2	64•82	65•42	65•74	65•44	65•56	65•71	65•71	65•60	67•25
TiO_2	0•20	-	-	0•27	-	-	-	0•05	-
Al_2O_3	18•52	18•75	18•55	18•61	18•68	18•38	18•63	18•60	18•81
*FeO	0•02	-	-	-	-	-	-	-	-
CaO	0•03	-	-	-	-	-	-	-	-
Na_2O	1•10	1•31	0•90	1•60	1•13	1•54	0•88	1•23	4•85
K_2O	14•50	14•47	15•03	13•99	14•91	14•06	14•62	14•51	9•02
Total	-	99•95	100•22	99•91	100•28	99•69	99•84	-	99•93
				Numbers of ions on the basis of 8(O)					
Si	-	3•000	3•010	2•997	3•001	3•009	3•012	-	3•019
Al	-	1•013	1•001	1•005	1•008	1•000	1•006	-	0•995
Ti	-	-	-	-	-	-	-	-	-
Fe	-	-	-	-	-	-	-	-	-
Ca	0•002	-	-	-	-	-	-	-	-
Na	0•099	0•117	0•080	0•142	0•101	0•138	0•078	0•109	0•422
K	0•855	0•846	0•878	0•817	0•870	0•828	0•855	0•849	0•517
				Mol%					
An	0•17	-	-	-	-	-	-	-	-
Ab	10•27	12•15	8•35	14•81	10•40	14•29	8•36	11•39	44•94
Or	89•56	87•85	91•65	85•19	89•60	85•71	91•64	88•61	55•06

TABLE: (3-1-4a)Microprobe analyses of potassium feldspars from the Serres-Drama granitic complex (continued)

	184R A22	184R A23	184R B53	184R B54	184R B55	184R B56	184R B57	184R B58	184R B59
SiO_2	65•45	65•88	65•14	64•54	65•68	65•68	64•84	65•04	65•03
TiO_2	-	-	-	-	-	-	-	-	0•22
Al_2O_3	18•60	18•91	18•71	18•43	18•21	18•53	18•61	18•55	18•69
*FeO	0•22	-	-	0•22	-	0•30	0•21	-	0•26
CaO	-	-	-	-	-	-	-	-	-
Na_2O	0•25	1•24	1•18	1•22	2•52	1•79	1•41	1•73	1•65
K_2O	13•58	15•27	14•47	14•25	12•74	13•98	14•22	13•72	13•35
Total	98•10	101•30	99•50	98•66	99•15	100•28	99•29	99•04	99•20
	Numbers of ions on the basis of 8(O)								
Si	2•995	2•992	3•000	3•000	3•018	3•002	2•995	3•002	2•994
Al	1•003	1•012	1•015	1•010	0•986	0•998	1•013	1•009	1•014
Ti	-	-	-	-	-	-	-	-	0•008
Fe	0•008	-	-	0•009	-	0•012	0•008	-	0•010
Ca	-	-	-	-	-	-	-	-	-
Na	0•200	0•110	0•105	0•110	0•224	0•158	0•127	0•155	0•147
K	0•793	0•885	0•850	0•845	0•747	0•815	0•838	0•808	0•784
	Mol%								
An	-	-	-	-	-	-	-	-	-
Ab	20•14	11•06	11•00	11•52	23•07	16•24	13•16	16•10	15•79
Or	79•86	88•95	89•01	88•48	76•93	83•76	86•84	83•90	84•21

TABLE: (3-1-4a) Microprobe analyses of potassium feldspars from the Serres-Drama granitic complex (continued)

	184R C60	184R D63	184R D64	184R D65	184R average	202R A34	202R A35	202R A36	202R A37
SiO_2	65•22	64•28	64•39	64•17	65•19	65•36	64•70	65•04	65•32
TiO_2	-	0•43	0•52	0•44	0•12	-	-	0•17	-
Al_2O_3	18•47	18•82	19•09	18•66	18•65	19•17	18•76	18•67	18•72
*FeO	-	0•25	0•24	0•25	0•14	-	-	-	-
CaO	-	-	-	-	-	0•39	-	-	-
Na_2O	3•31	1•83	2•12	1•85	1•93	2•94	2•22	2•71	2•90
K_2O	11•46	12•89	12•67	12•83	13•18	11•71	13•08	12•48	12•35
Total	98•46	98•50	99•03	98•20	-	99•57	98•76	99•07	99•29
				Numbers of ions on the basis of 8(O)					
Si	3•005	2•978	2•966	2•982	-	2•982	2•991	2•991	2•996
Al	1•003	1•028	1•036	1•022	-	1•031	1•022	1•012	1•016
Ti	-	0•015	0•018	0•015	-	-	-	0•006	-
Fe	-	0•010	0•009	0•010	-	-	-	-	-
Ca	-	-	-	-	-	0•019	-	-	-
Na	0•296	0•165	0•189	0•167	0•184	0•260	0•199	0•242	0•258
K	0•674	0•762	0•745	0•761	0•773	0•682	0•771	0•732	0•722
				Mol%					
An	-	-	-	-	-	1•98	-	-	-
Ab	30•83	17•80	20•24	18•00	19•28	27•06	20•52	24•85	26•33
Or	70•21	82•20	79•76	82•00	80•80	70•97	79•49	75•46	73•67

TABLE: (3-1-4a) Microprobe analyses of potassium feldspars from the Serres-Drama granitic complex (continued)

	202R A38	202R A39	202R B44	202R B45	202R B46	202R B47	202R C48	202R C49	202R C50
SiO_2	64·70	64·26	65·55	65·52	64·88	65·85	63·94	64·47	63·44
TiO_2	-	0·42	-	-	-	-	0·56	0·52	0·36
Al_2O_3	18·94	18·66	19·00	18·93	18·74	18·73	19·06	19·07	20·07
*FeO	-	-	0·23	-	0·26	-	-	-	0·21
CaO	0·21	-	-	-	-	-	-	-	1·33
Na_2O	3·30	1·76	2·00	0·76	1·99	1·22	1·53	1·72	3·17
K_2O	11·63	13·01	13·63	15·28	13·47	14·88	13·54	13·34	10·35
Total	98·78	98·11	100·41	100·49	99·34	100·68	98·63	99·12	98·93
	Numbers of ions on the basis of 8(O)								
Si	2·979	2·986	2·988	2·995	2·989	3·002	2·965	2·971	2·914
Al	1·028	1·022	1·021	1·020	1·018	1·006	1·042	1·036	1·087
Ti	-	0·015	-	-	-	-	0·019	0·018	0·012
Fe	-	-	0·009	-	0·010	-	-	-	0·008
Ca	0·010	-	-	-	-	-	-	-	0·065
Na	0·294	0·159	0·177	0·067	0·178	0·108	0·138	0·153	0·282
K	0·683	0·771	0·792	0·891	0·792	0·865	0·801	0·784	0·606
	Mol%								
An	0·01	-	-	-	-	-	-	-	0·07
Ab	29·79	17·10	0·18	6·99	18·35	11·10	14·70	16·33	29·59
Or	69·20	82·90	0·79	93·01	81·65	88·90	85·30	83·67	63·59

TABLE: (3-1-4a) Microprobe analyses of potassium feldspars from the Serres-Drama granitic complex (continued)

	202R C51	202R C52	202R average	119R, 126R 184R, 202R average
SiO_2	65•17	65•35	64•90	65•13
TiO_2	-	-	0•14	0•13
Al_2O_3	19•09	18•65	18•95	18•73
*FeO	-	0•29	0•07	0•06
CaO	-	-	0•13	0•04
Na_2O	1•66	1•55	2•10	1•59
K_2O	13•85	14•11	13•11	13•83
Total	99•77	99•95	-	-
		Numbers of ions on the basis of 8(O)		
Si	2•987	2•998	-	-
Al	1•031	1•008	-	-
Ti	-	-	-	-
Fe	-	0•011	-	-
Ca	-	-	0•060	-
Na	0•147	0•138	0•187	-
K	0•810	0•825	0•768	-
				Mol%
An	-	-	0•14	-
Ab	15•36	14•33	19•38	-
Or	84•64	85•67	79•99	-

TABLE: (3-1-4b) Microprobe analyses of potassium feldspars from the Xanthi plutonic complex (Christofides, 1977)

	250-1	250-2	125-1	84-1	84-2	210-1	210-2	42-1	42-2
SiO_2	64·67	64·13	64·74	64·37	64·83	63·70	64·89	65·58	64·60
TiO_2	n.a.	n.a.	n.a.	n.a.	n.a.	0·76	0·16	n.a.	n.a.
Al_2O_3	18·80	18·99	18·56	18·76	18·66	19·07	18·14	18·45	18·62
FeO	0·00	0·17	0·00	0·12	0·00	0·19	0·13	0·00	0·25
CaO	0·05	0·15	0·11	0·15	0·15	0·14	0·15	0·21	0·18
K_2O	14·45	14·32	14·08	14·28	13·36	13·47	14·36	13·36	13·42
Na_2O	1·43	1·34	1·97	1·66	2·26	1·89	1·29	2·27	2·00
BaO	0·40	0·57	0·00	0·00	0·00	n.a.	n.a.	0·69	0·85
Total	99·80	99·67	99·46	99·34	99·26	99·22	99·12	100·56	99·22
				Numbers of ions on the basis of 32(O)					
Si	11·935	11·879	11·951	11·914	11·953	11·781	12·016	11·992	11·924
Ti	n.a.	n.a.	n.a.	n.a.	n.a.	0·106	0·022	n.a.	n.a.
Al	4·090	4·146	4·040	4·093	4·056	4·158	3·960	3·976	4·051
Fe^{2+}	0·000	0·027	0·000	0·019	0·000	0·029	0·020	0·000	0·039
Ca	0·010	0·023	0·022	0·031	0·030	0·028	0·030	0·041	0·035
K	3·402	3·383	3·317	3·372	3·143	3·179	3·393	3·116	3·160
Na	0·511	0·481	0·705	0·592	0·808	0·678	0·463	0·805	0·715
Ba	0·029	0·041	0·000	0·000	0·000	n.a.	n.a.	0·049	0·061
				Mol%					
Or	86·82	87·17	82·02	84·40	78·95	81·83	87·31	78·91	81·11
Ab	12·93	12·24	17·44	14·82	20·30	17·45	11·92	20·07	18·01
An	0·25	0·59	0·54	0·78	0·75	0·72	0·77	1·02	0·88

TABLE: (3-1-4b) Microprobe analyses of potassium feldspars from the Xanthi plutonic complex (Christofides, 1977) (continued)

	44-1	44-2	55-1	55-2	19-1	19-2	280-1	280-2
SiO_2	63·29	63.98	65·02	65·22	65·29	64·59	64·74	64·05
TiO_2	n.a.	n.a.	0.12	0·25	n.a.	n.a.	0·59	0·46
Al_2O_3	19·20	18·71	18·67	18·93	18·24	18·90	19·45	19·51
FeO	0·41	0·21	0·35	-	-	-	0·26	-
CaO	0·99	0·40	0·18	0·23	0·30	1·03	0·68	1·36
K_2O	11·58	12·01	13·64	13·29	12·55	10·47	11·20	10·78
Na_2O	2·86	2·63	1·89	1·99	2·52	3·73	3·27	3·02
BaO	0·69	1·28	n.a.	n.a.	0·32	0·52	n.a.	n.a.
Total	99·02	99·22	99·87	99·91	99·22	99·24	100·19	99·18
			Numbers of ions on the basis of 32(O)					
Si	11·750	11·858	11·938	11·928	12·826	11·866	11·767	11·740
Ti	n.a.	n.a.	0·017	0·034	n.a.	n.a.	0·081	0·063
Al	4·201	4·087	4·042	4·082	3·960	4·092	4·168	4·216
Fe^{2+}	0·064	0·032	0·054	-	-	-	0·040	-
Ca	0·197	0·079	0·035	0·045	0·059	0·203	0·132	0·267
K	2·742	2·840	3·196	3·101	2·948	2·454	2·598	2·521
Na	1·030	0·945	0·673	0·706	0·900	1·329	1·153	1·074
Ba	0·050	0·092	n.a.	n.a.	0·023	0·038	n.a.	n.a.
			Mol%					
Or	69·47	74·11	81·86	80·50	75·60	61·93	66·91	65·28
Ab	25·63	23·89	17·24	18·33	22·90	33·03	29·69	27·81
An	4·90	2·00	0·90	1·17	1·50	5·04	3·40	6·91

TABLE: (3-1-4c) Microprobe analyses of potassium feldspars from the Paranesti (Dipotamos) granite (Sklavounos, 1981)

	29A	29B	30	32	34	35	37	38	39	42
SiO_2	63•19	63•79	63•86	63•84	63•79	63•88	63•75	63•86	63•86	63•88
Al_2O_3	18•49	18•40	18•46	18•44	18•38	18•47	18•37	18•46	18•46	18•47
K_2O	15•42	15•11	15•34	15•31	15•33	15•20	15•81	15•31	15•37	14•84
Na_2O	1•03	0•97	0•96	1•10	1•06	1•04	0•70	1•05	0•94	1•29
CaO	0•04	0•04	0•02	0•03	0•03	0•04	-	0•04	0•04	0•04
Total	98•17	98•31	98•64	98•72	98•59	98•63	98•63	98•72	98•67	98•52
				Numbers of ions on the basis of 32(O)						
Si	11•897	11•955	11•943	11•936	11•944	11•942	11•947	11•937	11•941	11•941
Al	4•105	4•065	4•070	4•065	4•056	4•071	4•058	4•068	4•069	4•070
K	3•704	3•613	3•659	3•651	3•660	3•626	3•779	3•650	3•667	3•538
Na	0•375	0•353	0•348	0•397	0•384	0•377	0•254	0•380	0•341	0•467
Ca	0•008	0•008	0•005	0•006	0•006	0•008	-	0•008	0•008	0•008
				Mol%						
Or	90•78	91•00	91•24	90•14	90•37	90•42	93•77	90•34	91•44	88•22
Ab	9•19	8•89	8•67	9•80	9•48	9•40	6•30	9•40	8•50	11•64
An	0•19	0•20	0•12	0•14	0•15	0•19	-	0•20	0•19	0•20

TABLE: (3-1-4c) Microprobe analyses of potassium feldspars from the Paranesti (Dipotamos) granite (Sklavounos, 1981) (continued)

	43	43	44	45A	45B	45C	47	48	49
SiO_2	64•20	63•79	63•79	63•84	63•08	62•90	63•86	63•81	63•81
Al_2O_3	18•51	18•44	18•40	18•42	18•29	18•29	18•46	18•46	18•42
K_2O	14•32	14•94	15•33	15•02	14•98	14•99	15•20	15•29	15•28
Na_2O	0•90	1•23	0•67	1•38	1•26	1•26	1•28	0•84	1•08
CaO	0•03	0•02	0•03	0•04	0•07	0•07	0•03	0•04	0•04
Total	97•96	98•42	98•22	98•70	97•68	97•51	98•83	98•44	98•63
				Numbers of ions on the basis of 32(O)					
Si	12•002	11•942	11•967	11•932	11•919	11•910	11•926	11•950	11•939
Al	4•080	4•069	4•069	4•059	4•073	4•082	4•065	4•075	4•063
K	3•415	3•568	3•668	3•580	3•610	3•620	3•623	3•653	3•647
Na	0•326	0•445	0•243	0•500	0•461	0•462	0•464	0•306	0•391
Ca	0•006	0•005	0•006	0•008	0•014	0•013	0•006	0•008	0•008
				Mol%					
Or	91•06	88•75	93•57	87•74	88•48	88•50	88•58	92•24	90•27
Ab	8•69	11•06	6•19	12•25	11•29	11•29	11•34	7•72	9•67
An	0•16	0•12	0•15	0•19	0•34	0•31	0•14	0•20	0•19

have TiO_2 above the detection limit of the energy dispersive electron microprobe system.

Iron may occur in both divalent and trivalent states. In potassium feldspars, most of the iron is probably trivalent. Smith (1974, Vol.2) suggests that the iron content, if it is indeed in the structure of alkali feldspars, may correlate with the temperature of equilibration. Iron may however be in small defects or along cleavage planes within the feldspars. The entrance of iron ions into alkali feldspars is complex and is thought to be related both to the host rock and the oxidation state of the feldspars. The iron content of potassium feldspars from granitic rocks is low. However, Sklavounos (1981) did not analyse for iron. The mean FeO values in Christofides (1977) are 0.14% and in the present study 0.06%. Only twelve analyses have iron as FeO above the detection limit.

The small amount of the CaO combines with Na_2O in the plagioclase phase of microperthite in the potassic-rich feldspars. The mean CaO values are 0.38% (in Christofides, 1977), 0.04% (in Sklavounos, 1981) and in the present study, 0.04%, although only four out of the fifty-three analyses have CaO present above the detection limit. In addition to the above elements Mn and Mg were also analysed for but none was detected.

The degree of substitution of K by Na depends upon two conditions: the bulk composition of the system and the effects of falling temperature. The mean K_2O and Na_2O values for the Xanthi granitic complex are respectively

12.98% and 2.24% (in Christofides, 1977), 15.18% and 1.06% for the Paranesti (Dipotamos) complex (in Sklavounos, 1981), 13.83% and 1.59% in the present study. Only Sklavounos's analysis is richer in potassium.

The electron microprobe results for three of the samples are presented in table (3-1-4a). Comparison of these data with that from the X-ray study shows good agreement for the third. The mean of the unnormalized molecular percentage for each sample has been used for comparison with the orthoclase percentage, using the cell volume method. In sample No. 119 the percentage of orthoclase determined by microprobe analysis is 3% lower than that determined by the cell volume method. Similarly, sample No.184 is lower by 9%, but for sample No. 126 the two methods give the same result.

Although one of the results is a little low, it is probably satisfactory to place some reliance on the composition of the potassium phase determined using the X-ray methods.

3-1-5 Discussion

The polymorphic potassium feldspars are distinctly separated into two areas in the Serres-Drama granitic complex. The presence of both monoclinic and triclinic potassium feldspars in the same rock type were not observed. Goldsmith and Laves (1954) suggested that microcline is the

stable potassium feldspars polymorph at low temperatures and sanidine is the stable form at high temperatures. In Stewart and Wright (1974) orthoclase is stable at higher temperatures than microcline. The thermal stabilities of the polymorphs suggest that Al/Si ordering is a function of the potassium feldspar. Studies of naturally occurring potassium feldspars indicate that several other factors influence the degree of Al/Si order.

Marmo (1959, in Parsons and Boyd, 1971) observed that orthoclase-bearing granites are usually cut by aplitic veins that contain microcline of high triclinicity. Similarly, in the Serres-Drama granitic complex, the 'intermediate' group of rocks are cut by aplitic veins containing potassium feldspars whose structural state is close to maximum microcline. However, the structure state of the potassium feldspar in the host rocks is not monoclinic but triclinic.

Tilling (1968) has studied in detail the Rader Creek granodiorite pluton within the Boulder batholith, Montana, U.S.A. He concluded that those rocks containing more potash-rich K-feldspars (Or 84% to 85% - bulk composition) showed only the monoclinic structural state (orthoclase) whilst more soda-rich K-feldspars (Or 66% to 78% - bulk composition) contain dominant microcline (triclinic structural state). In the Serres-Drama pluton the difference in bulk composition between the monoclinic and triclinic k-feldspars is very much less marked, i.e. 75% to 79% bulk composition for monoclinic (mean is 76.9%) and 76% to 80% bulk composition for triclinic (mean is 77.9%). This difference is

so small that it is probably not significant. Whether the difference is accepted as a real one or not, the evidence from Serres-Drama contradicts the finding of Tilling (op. cit).

Vorma (1971) has observed in the large rapakivi granitic complexes in Finland that there is a close relationship between increasing silica, falling calcium content and the appearance of microcline in the perthitic alkali feldspars, at the expense of orthoclase. He interpreted this relationship with the parallel processes of concentration of volatiles and of fractionation, i.e. that there is a close relationship between bulk rock chemical composition and k-feldspar structural state. Dietrich (1962, in Parsons and Boyd, 1971) also observed increasing triclinicity with fractionation in the Boulder Batholith. Potassium feldspar content increases with the quartz content of the rocks. In the Serres-Drama complex the monoclinic K-feldspars are restricted to the rocks of the 'basic' group, while the triclinic polymorphs occur in the rocks of the 'intermediate' group. Thus there appears to be a relationship with bulk rock SiO_2 content and with the increasing volatile content of the magma, as shown by the change from anhydrous to hydrous mafic mineral phases.

Eggleton (1979) suggests that after the crystal became triclinic, there is discontinuity in the ordering path with regard to γ. This accounts for a gap in $\Delta\alpha^* \gamma^*$ between 0.45 and 0.8. The K-feldspars of the present study likewise separate clearly into two groups (fig. 3-1-1c)

with (t_{1O}-t_{1m}) values of 0.0 and ~0.9 for the monoclinic and triclinic groups respectively.

Cherry and Trembath (1978) suggest that slower cooling controlled the ordering in the alkali feldspars. It must be stressed that the ordering process is a complex one and must be separately determined for each alkali feldspar.

Iball and Hubbard (1982) concluded that the major controlling influence on the pattern of lattice structural change in potassium feldspars was the level of hydration of the containing rock. The evidence from Serres-Drama complex would appear to be in agreement with this.

The role of water in the two types of ordering process is different. Parsons (1978a) suggested that "orthoclase persists in rocks that had 'dry' histories as they entered the thermal stability range of microcline".

Parsons and Boyd (1971) suggest that

> "the presence of volatile (or peralkaline or peraluminous) components in the melt at the time of initial crystal growth can control details of the structure of the feldspar that determine the ease with which microcline can evolve on cooling... ... the presence or absence of volatiles during this part of the history of a k-feldspar will be one control of the degree of order achieved".

If this control were active in the Serres-Drama granitic complex, the distribution of the potassium feldspar polymorphs, does indicate that a volatile phase was reduced in the monzonite. There is evidence for variation in volatile content in the magma in that the monzonite

contains fresh clinopyroxene, whilst the other rock-types contain only hydrated mafic minerals, e.g. amphibole and biotite. These latter rocks also contain aplite veins implying higher water contents.

It could be interpreted that there was a difference in the stage of crystallization at which the volatiles became a separate phase. This removal of the volatile content from the monzonite could have been accompanied by a decrease in pressure. Removal of the volatiles from the monzonite, prohibited, or at least inhibited, the ordering process in the potassium feldspars from monoclinic to triclinic symmetry. The volatile phase in the granite, granodiorite and quartz-monzonite body, however, may not have been lost, thus allowing the ordering process in the potassium feldspars to proceed.

This interpretation, however, runs counter to the evidence shown by the plagioclase feldspars (Section 3-2) where the high Ca content of these minerals is thought to be due to high water pressures present during crystallisation.

3-1-6 Summary

From the optical and X-ray diffraction studies, it is possible to conclude that monoclinic potassium feldspar occurs in the monzonite, which may have cooled with a much lower volatile content, whilst the triclinic potassium

feldspars occur in the granodiorite, granite and quartz-monzonite, which probably cooled in the presence of a greater volatile content.

An ordering process has been observed which increases with the quartz content of the rocks.

Experimental data and field studies are consistent with the interpretation that the degree of ordering increases with the degree of differentiation.

3-2 PLAGIOCLASE FELDSPARS

3-2-1 Introduction

Petrographic studies show that plagioclase feldspar occurs in all the rock-types, including the aplite and pegmatite veins and dioritic zenoliths. Plagioclase examined under crossed nicols reveals extinction contours resulting from chemical variation(fig. (2-3-1f) and fig. (2-3-1g)). Usually the average trend is from a calcic core to a more sodic margin. Simple progress from a calcic core to a sodic rim is regarded as normal zoning and this is the most common appearance of plagioclase feldspar in the Serres-Drama granitic complex. The reverse of this process i.e. sodic core and a calcic rim is known as reverse zoning. The phenomenon of reverse zoning has not been noted in the Serres-Drama complex. Very commonly there is oscillatory zoning present with oscillation in Na and Ca contents in adjacent zones.

Plagioclase zoning was thought to be most useful in making inferences about environmental variables of the magma chamber and many theories have been developed to explain zoning types (Bowen, 1913, 1928; Harloff, 1927; Hills, 1963; Vance, 1962, 1965; Bottinga et al, 1966; Lofgren, 1974a); Sibley et al, 1976).

Bowen (1913), in addition to describing experiments on the equilibrium crystallisation of plagioclase feldspars

also explained the production of normal zoning by incomplete reaction of solid and liquid. These ideas have gained wide acceptance for the origin of normal zoning. Oscillatory zoning has on the contrary been the subject of intense debate. In 1928 Bowen explained normal oscillatory zoning as being the result of cyclical sinking of the plagioclase crystal in a magma, during which the crystal reaches a hotter part of the magma causing growth of a more calcic plagioclase. Every sinking cycle is followed by a surge during which the crystal enters a more sodic part of the magma. Over the period of crystallisation the bulk magma tends to a more sodic composition with the result of overall normal zoning.

Harloff (1927) initiated the theory that the regular, closely-spaced oscillatory zoning was due to kinetic factors of crystallisation and diffusion rather than adjustments to physicochemical changes as in Bowen's work. Later interpretations of the phenomenon of oscillatory zoning in plagioclase feldspar have emphasized the role of kinetics of diffusion of chemical species linked to disequilibrium crystallisation (Hills, 1936; Vance, 1962, 1965; Bottinga, Kudo and Weill, 1966). The most recent advances made in the understanding of this type of zoning follow from the experiments of Lofgren (1974a). Lofgren (ibid) and Sibley et al (1976) propose a process known as constitutional supercooling which is supersaturation that results from a concentration gradient in the melt at the crystal-melt interface. When the liquid in contact with

an advancing solid-liquid interface is different in composition from the bulk composition of the liquid, constitutional supercooling occurs (Rutter and Chalmers, 1953; Tiller, Jackson, Rutter and Chalmers, 1963; Chalmers, 1964; Flemings, 1974). This process appears to be gaining wide acceptance among petrologists.

This idea of constitutional supercooling is best understood by starting with an equilibrium phase diagram and considering deviation from equilibrium. We start with a binary solid solution series from two components A and B, fig. (3-2-1a).

Crystallisation from a liquid of composition X begins with formation of stable nuclei only after some degree of supercooling (T_o-T_1) has occurred. A concentration gradient gradually occurs in the melt away from the crystal, if the diffusion rate of B away from the solid - liquid interface or diffusion of A to the interface is not as great as the growth rate. In fig. (3-2-1b) is illustrated the possible distribution of B in the liquid away from solid-liquid interface in a constitutionally supercooled liquid. The boundary layer that occurs shows the zone of increased B concentration. The bulk liquid (L_2) has composition between the boundary layer and the initial composition X.

The degree of supercooling is the major factor affecting the growth rate. Crystallisation is rapid when the degree of constitutional supercooling is large (L_3 at T_1, in fig. 3-2-1a), whereas at equilibrium (L_1 at T_1,

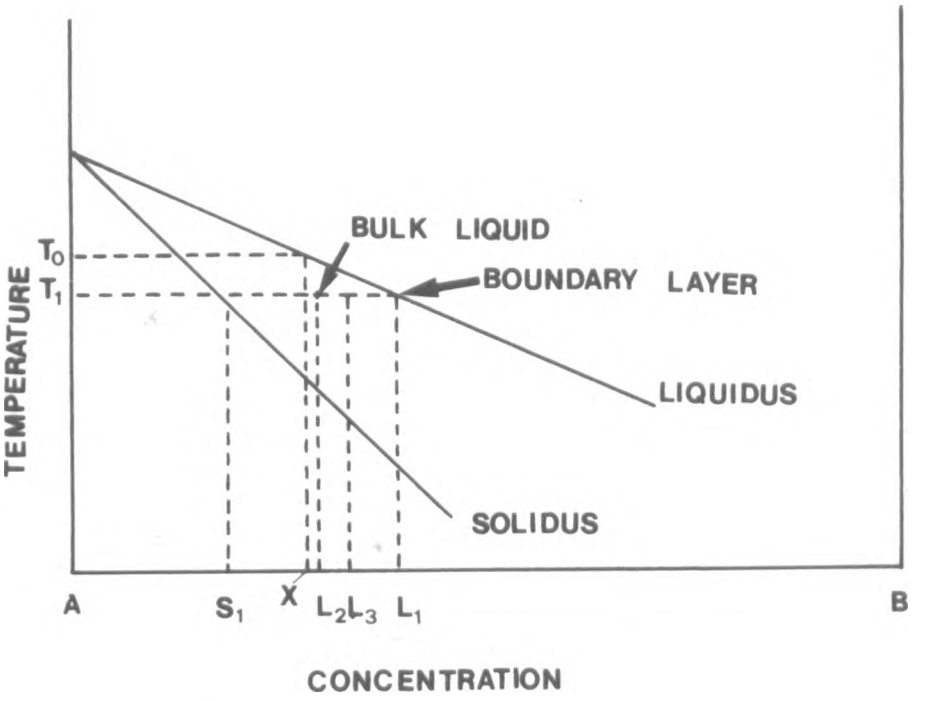

Fig. [3-2-1a] [from Sibley et al, 1976]

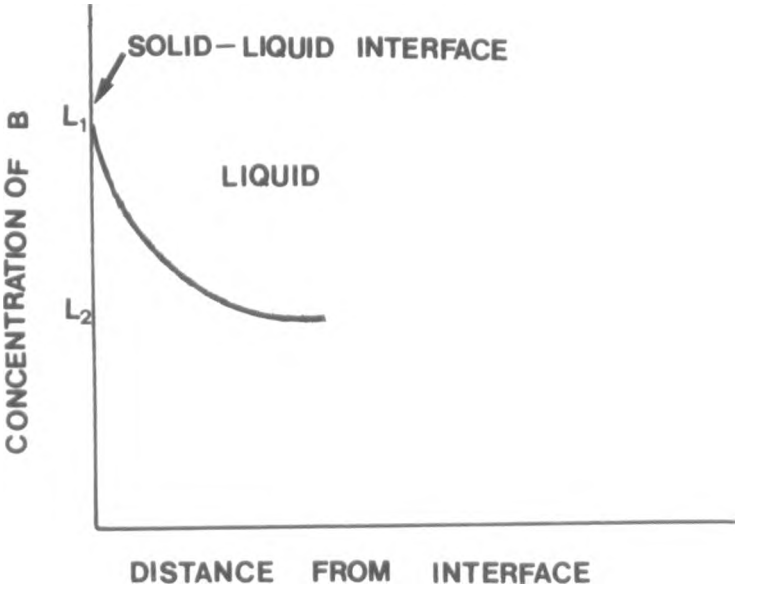

Fig. [3-2-1b] [from Sibley et al , 1976]

fig. 3-2-1a) the growth ceases. This fact, along with planar nature of the plagioclase solid/liquid interface, provides the explanation of the driving force for oscillatory zoning.

3-2-2- Electron microprobe analysis results.

A limited study of the plagioclase feldspars was done by electron microprobe analysis to discover:

I the type of zoning present and the range of chemical composition and

II to explain the genesis of the plagioclase feldspars and their zoning.

The microprobe analysis data confirms the extinction contours noted during the optical study and reveals the presence of both normal and oscillatory zoning developed in the plagioclase feldspars of the Serres-Drama complex.

Plagioclase forms a chemical series ranging from pure albite $Na\ AlSi_3\ O_8$ to pure anorthite $Ca\ Al_2\ Si_2\ O_8$, but they include in very limited amounts, the ions Ti, Fe^{+3}, Fe^{+2}, Mn, Mg, Ba, Sr and may also contain a small amount of potassium. During this microprobe analysis the following elements were determined, Si, Ti, Al, Fe, Mn, Mg, Ca, Na and K and subsequently recalculated to weight percentage of oxides.

The obtained data are given in table (3-2-2a). Microprobe analyses of plagioclase from other granitic complexes from the Rhodope massif area are given in tables

TABLE: (3-2-2a) Microprobe analyses of plagioclases from the Serres-Drama granitic complex.

	119R A25c	119R A26	119R A27	119R A28	119R A29r	119R C33c	119R C34	119R C35
SiO_2	56·55	56·48	59·89	59·71	59·68	54·01	54·06	59·11
Al_2O_3	28·34	27·81	25·54	25·80	25·36	29·59	29·20	26·03
*FeO	0·31	-	0·24	-	0.26	-	0.22	-
CaO	10·39	10·09	7·69	7·78	7·47	11·99	11·77	7·90
Na_2O	5·19	5·51	6·68	6·82	6·81	4·37	4·78	6·61
K_2O	0·26	0·22	0·24	0·16	0·25	0·14	0·16	0·25
Total	101·04	100·11	100·28	100·27	99·83	100·10	100·19	99·90
			Numbers of ions on the basis of 8(O)					
Si	2·516	2·532	2·662	2·653	2·664	2·434	2·439	2·638
Al	1·486	1·470	1·332	1·351	1·335	1·572	1·553	1·369
Fe	0·011	-	0·009	-	0·010	-	0.008	-
Ca	0·495	0·485	0·366	0·370	0·357	0·579	0·569	0·378
Na	0·448	0·479	0·576	0·588	0·590	0·381	0·418	0·572
K	0·015	0·013	0·014	0·009	0·014	0·008	0·009	0·014
				Mol%				
An	51·65	49·64	38·29	38·26	37·15	59·81	57·71	39·21
Ab	46·76	49·03	60·25	60·81	61·39	39·36	42·39	59·34
Or	1·57	1·33	1·46	0·93	1·46	0·83	0·91	1·45

Rock types: Quartz monzonite(119R); monzonite(126R,184R,202R); Xenolith(126X,6bX); gabbro(152R)
Symbols: R = Rock, X = xenolith, c = core, r = rim
* total iron as FeO

TABLE: (3-2-2a) Microprobe analyses of plagioclases from the Serres-Drama granitic complex (cont.)

	119R C36r	119R D37	119R D38	119R D39	119R L40c	119R L41	119R L42	119R E60r
SiO_2	59•33	59•71	59•63	60•27	58•15	59•46	58•93	60•34
Al_2O_3	25•59	25•26	25•52	24•69	26•22	25•14	25•21	24•72
*FeO	0•25	-	0•32	0•34	-	-	0•23	0•21
CaO	7•53	7•49	7•39	6•82	8•27	7•54	7•51	6•81
Na_2O	6•92	7•13	7•40	7•16	5•88	6•28	6•68	7•18
K_2O	0•23	0•28	0•17	0•20	0•31	0•42	0•37	0•31
Total	99•85	99•87	100•43	99•48	98•83	98•84	98•93	99•57
			Numbers of ions on the basis of 8(O)					
Si	2•654	2•666	2•653	2•696	2•622	2•675	2•658	2•696
Al	1•348	1•329	1•338	1•301	1•394	1•333	1•340	1•302
Fe	0•009	-	0•012	0•013	-	-	0•009	0.008
Ca	0•360	0•358	0•352	0•327	0•399	0•364	0•363	0•326
Na	0•599	0•617	0•638	0•621	0•514	0•548	0•584	0•622
K	0•013	0•016	0•010	0•012	0•018	0•024	0•021	0•018
				Mol%				
An	36•66	36•13	35•20	34•06	42•86	38•89	37•50	33•75
Ab	61•00	62•26	63•80	64•69	55•21	58•55	60•33	64•39
Or	1•32	1•62	1•00	1•25	1•93	2•56	2•17	1•86

TABLE: (3-2-2a) Microprobe analyses of plagioclases from the Serres-Drama granitic complex (cont.)

	119R E61	119R E62	119R E63	119R E64c	119R F67c	119R F68	119R F69r	119R G74
SiO_2	60·53	60·24	58·84	58·49	58·12	58·88	60·28	53·67
Al_2O_3	25·21	24·93	26·81	26·40	25·89	25·49	26·51	29·68
*FeO	-	0·30	0·38	-	0·17	0·27	0·27	0·36
CaO	7·27	7·13	8·48	6·07	8·11	7·71	7·68	12·29
Na_2O	7·28	6·80	6·40	6·34	6·46	6·81	7·16	4·72
K_2O	0·24	0·38	0·09	0·17	0·17	0·22	0·22	0·16
Total	100·53	99·78	101·00	97·47	98·92	99·38	102·12	100·88
			Numbers of ions on the basis of 8(O)					
Si	2·681	2·688	2·604	2·614	2·626	2·645	2·636	2·412
Al	1·316	1·311	1·398	1·391	1·379	1·350	1·366	1·573
Fe	-	0·011	0·014	-	-	0·010	0·010	0·014
Ca	0·345	0·341	0·402	0·407	0·392	0·371	0·360	0·592
Na	0·625	0·589	0·549	0·549	0·566	0·593	0·607	0·412
K	0·013	0·022	0·005	0·010	0·010	0·012	0·012	0·009
				Mol%				
An	35·10	35·82	42·05	42·13	40·50	38·01	36·77	58·44
Ab	63·58	61·87	57·43	56·83	58·47	60·76	62·00	40·49
Or	1·32	2·31	0·52	1·04	1·03	1·25	1·23	0·89

TABLE: (3-2-2a) Microprobe analyses of plagioclases from the Serres-Drama granitic complex (cont.)

	119R G75	119R G76	119R G77r	119R H78c	119R J79c	119R J80	119R J81	119R J82r
SiO_2	54•85	60•12	60•38	58•78	59•52	59•28	60•41	60•66
Al_2O_3	28•55	25•30	25•24	26•17	25•53	25•00	25•16	24•95
*FeO	0•30	0•27	0•29	0•25	0•32	0•22	0•33	0•32
CaO	11•33	7•30	7•20	8•37	7•49	7•51	6•98	6•88
Na_2O	5•02	7•03	7•22	6•48	6•88	6•96	6•99	7•36
K_2O	0•18	0•30	0•19	0•18	0•33	0•39	0•55	0•39
Total	100•23	100•32	100•52	100•23	100•07	99•36	100•42	100•56
			Numbers of ions on the basis of 8(O)					
Si	2•471	2•672	2•677	2•621	2•655	2•665	2•682	2•689
Al	1•516	1•325	1•319	1•375	1•342	1•325	1•317	1•304
Fe	0•011	0•010	0•011	0•009	0•012	0•008	0•012	0•012
Ca	0•547	0•347	0•342	0•400	0•358	0•362	0•332	0•327
Na	0•439	0•606	0•621	0•560	0•595	0•606	0•601	0•632
K	0•010	0•017	0•011	0•010	0•019	0•022	0•031	0•022
				Mol%				
An	54•92	36•15	35•11	41•24	37•21	36•57	34•44	33•33
Ab	44•08	63•13	63•76	57•73	61•85	61•21	62•34	64•42
Or	1•00	1•77	1•13	1•03	1•98	2•22	3•22	2•24

TABLE: (3-2-2a) Microprobe analyses of plagioclases from the Serres-Drama granitic complex (cont.)

	119R K83c	119R K84	126R A5r	126R A6	126R A7c	126R B8c	126R B9r	126R C10c
SiO_2	56•63	58•49	60•93	60•00	59•65	61•04	61•23	59•99
Al_2O_3	27•89	27•21	24•56	25•41	25•62	24•67	24•48	25•33
*FeO	0•25	0•27	0•24	0•32	0•30	0•30	-	0•33
CaO	9•89	8•95	6•61	7•15	7•54	6•50	6•16	7•46
Na_2O	5•62	6•16	7•39	7•07	7•22	7•61	7•26	6•92
K_2O	0•12	0•21	0•37	0•40	0•32	0•31	0•40	0•39
Total	100•40	101•29	100•10	100•35	100•65	100•43	99•53	100•42
			Numbers of ions on the basis of 8(O)					
Si	2•532	2•586	2•708	2•667	2•649	2•706	2•727	2•666
Al	1•470	1•418	1•287	1•332	1•341	1•289	1•285	1•327
Fe	0•009	0•010	0•009	0•012	0•011	0•011	-	0•012
Ca	0•474	0•424	0•315	0•341	0•359	0•309	0•294	0•355
Na	0•488	0•528	0•639	0•609	0•622	0•654	0•627	0•596
K	0•007	0•012	0•021	0•022	0•018	0•018	0•023	0•022
				Mol%				
An	48•92	43•98	32•37	35•08	35•94	31•50	31•14	36•49
Ab	50•36	54•77	65•47	62•65	62•26	66•67	66•42	61•25
Or	0•72	1•23	2•16	2•26	1•80	1•84	2•44	2•26

TABLE: (3-2-2a) Microprobe analyses of plagioclases from the Serres-Drama granitic complex (cont.)

	126R C11r	126R D14r	126R D15c	184R A24c	184R A25	184R A26	184R A27	184R A28r
SiO_2	60•97	60•90	61•08	59•14	58•72	58•08	59•81	62•17
Al_2O_3	24•55	24•86	24•83	27•03	26•18	26•77	26•34	24•11
*FeO	0•21	0•33	0•26	0•22	0•33	0•21	0•32	-
CaO	6•61	6•56	6•55	8•71	8•28	9•08	7•91	5•75
Na_2O	7•12	7•75	7•63	6•74	6•24	6•06	6•96	7•88
K_2O	0•21	0•26	0•41	0•21	0•13	0•19	0•18	0•25
Total	99•67	100•66	100•76	102•05	99•88	100•39	101•52	100•16
			Numbers of ions on the basis of 8(O)					
Si	2•715	2•696	2•700	2•596	2•624	2•590	2•632	2•749
Al	1•289	1•297	1•294	1•398	1•379	1•407	1•366	1•257
Fe	0•008	0•012	0•010	0•008	0•012	0•008	0•012	-
Ca	0•315	0•311	0•310	0•409	0•396	0•434	0•373	0•272
Na	0•615	0•665	0•654	0•574	0•541	0•524	0•594	0•675
K	0•012	0•015	0•023	0•012	0•007	0•010	0•010	0•014
				Mol%				
An	33•44	31•38	31•41	41•11	41•95	44•84	38•18	28•30
Ab	65•29	67•10	66•26	57•69	57•31	54•13	60•80	70•24
Or	1•27	1•51	2•33	1•21	0•74	1•03	1•02	1•46

TABLE: (3-2-2a) Microprobe analyses of plagioclases from the Serres-Drama granitic complex (cont.)

	184R B29c	184R B30	184R B31r	184R C32c	184R C33	184R C34	184R C35	184R C36r
SiO_2	58•23	58•75	61•77	57•13	55•29	54•21	58•58	63•59
Al_2O_3	27•14	27•75	24•30	26•61	28•84	28•55	26•38	22•36
*FeO	0•41	0•32	-	0•24	0•54	0•52	0•28	0•43
CaO	9•39	9•13	5•97	8•79	10•96	11•43	8•10	3•87
Na_2O	6•04	5•98	7•95	6•30	5•43	4•43	6•25	8•92
K_2O	0•25	0•29	0•25	0•30	0•17	0•17	0•21	0•39
Total	101•46	102•22	100•24	99•37	101•23	99•31	99•80	99•56
			Numbers of ions on the basis of 8(O)					
Si	2•575	2•574	2•734	2•579	2•469	2•463	2•619	2•824
Al	1•415	1•433	1•268	1•416	1•518	1•529	1•390	1•170
Fe	0•015	0•012	-	0•009	0•020	0•020	0•011	0•016
Ca	0•445	0•429	0•283	0•425	0•524	0•560	0•388	0•184
Na	0•518	0•508	0•682	0•552	0•470	0•390	0•541	0•768
K	0•014	0•016	0•014	0•017	0•009	0•010	0•012	0•022
				Mol%				
An	45•55	45•02	28•91	42•76	52•24	58•33	41•23	18•89
Ab	53•02	53•31	69•66	55•53	46•86	40•63	57•49	78•85
Or	1•43	1•68	1•43	1•71	0•90	1•04	1•28	2•26

TABLE: (3-2-2a) Microprobe analyses of plagioclases from the Serres-Drama granitic complex (cont.)

	184R D37r	184R D38	184R D39	184R D40c	184R D41	184R E42c	184R E43	184R E44
SiO_2	63•76	63•62	60•16	59•34	61•65	56•39	58•58	60•81
Al_2O_3	22•34	21•87	24•05	25•37	23•57	26•90	26•04	23•66
*FeO	0•38	-	0•42	0•39	0•24	0•30	0•31	-
CaO	3•89	3•94	6•35	7•28	5•07	9•27	8•26	5•43
Na_2O	8•73	8•76	7•18	6•73	8•33	5•93	6•29	7•46
K_2O	0•33	0•28	0•30	0•34	0•21	0•20	0•19	0•30
Total	99•43	98•47	98•46	99•45	99•07	98•99	99•67	97•66
			Numbers of ions on the basis of 8(O)					
Si	2•831	2•846	2•717	2•661	2•758	2•557	2•625	2•753
Al	1•169	1•154	1•280	1•341	1•243	1•438	1•375	1•262
Fe	0•014	-	0•016	0•014	0•009	0•011	0•012	-
Ca	0•185	0•189	0•307	0•350	0•243	0•450	0•397	0•264
Na	0•751	0•760	0•629	0•585	0•723	0•521	0•547	0•655
K	0•019	0•016	0•017	0•020	0•012	0•011	0•011	0•018
				Mol%				
An	19•37	19•59	32•31	36•65	24•85	45•83	41•57	28•18
Ab	78•64	78•76	66•00	61•26	73•93	53•06	57•28	69•90
Or	1•99	1•66	1•78	2•09	1•23	1•12	1•15	1•92

TABLE: (3-2-2a) Microprobe analyses of plagioclases from the Serres-Drama granitic complex (cont.)

	184R E45	184R E46	184R E47	184R E48r	184R F49c	184R F50	184R F51r	202R A22r
SiO_2	57·90	60·76	61·39	64·89	58·31	58·78	63·85	60·85
Al_2O_3	25·70	24·29	23·87	22·26	26·10	25·58	22·08	24·94
*FeO	0·35	0·37	0·35	-	0·29	0·44	0·36	0·25
CaO	8·06	6·28	5·95	3·65	8·27	7·71	3·64	6·74
Na_2O	6·30	7·43	7·38	9·14	5·90	6·70	8·79	7·63
K_2O	0·28	0·36	0·39	0·43	0·43	0·45	0·48	0·20
Total	98·59	99·49	99·33	100·37	99·30	99·66	99·20	100·61
			Numbers of ions on the basis of 8(O)					
Si	2·625	2·717	2·743	2·850	2·623	2·639	2·842	2·693
Al	1·374	1·280	1·257	1·152	1·384	1·354	1·158	1·301
Fe	0·013	0·014	0·013	-	0·011	0·016	0·013	0·009
Ca	0·391	0·301	0·285	0·172	0·399	0·371	0·174	0·320
Na	0·554	0·644	0·639	0·778	0·514	0·583	0·759	0·655
K	0·016	0·021	0·022	0·024	0·024	0·026	0·027	0·012
				Mol%				
An	40·69	31·16	30·13	17·66	42·58	37·86	18·32	32·42
Ab	57·65	66·67	67·55	79·88	54·86	59·49	79·90	66·36
Or	1·67	2·17	2·33	2·46	2·56	2·65	2·84	1·22

TABLE: (3-2-2a) Microprobe analyses of plagioclases from the Serres-Drama granitic complex (cont.)

	202R A23	202R A24c	202R B25c	202R B26	202R B27	202R B28r	202R C29c	202R C30
SiO_2	59•54	58•81	56•01	55•70	56•45	58•20	57•48	58•40
Al_2O_3	25•61	25•78	28•25	27•70	27•42	27•05	27•03	26•55
*FeO	0•22	0•25	0•46	0•32	-	0•29	0•36	0•25
CaO	7•44	7•96	10•42	10•17	10•02	8•96	9•20	8•65
Na_2O	6•91	6•42	5•56	5•60	5•80	6•27	6•24	6•27
K_2O	0•29	0•24	0•18	0•21	0•19	0•12	0•22	0•31
Total	101•01	99•46	100•88	99•70	99•88	100•89	100•53	100•43
			Numbers of ions on the basis of 8(O)					
Si	2•655	2•639	2•503	2•520	2•539	2•583	2•568	2•603
Al	1•346	1•363	1•488	1•471	1•454	1•415	1•423	1•395
Fe	0•008	0•009	0•017	0•012	-	0•011	0•013	0•009
Ca	0•355	0•383	0•499	0•491	0•483	0•426	0•440	0•413
Na	0•597	0•559	0•482	0•489	0•506	0•539	0•540	0•542
K	0•016	0•014	0•010	0•012	0•011	0•007	0•013	0•017
				Mol%				
An	36•67	40•06	50•35	49•50	48•30	43•83	44•31	42•49
Ab	61•67	58•47	48•64	49•29	50•60	55•45	54•38	55•76
Or	1•65	1•46	1•01	1•21	1•10	0•72	1•31	1•75

TABLE: (3-2-2a) Microprobe analyses of plagioclases from the Serres-Drama granitic complex (cont.)

	202R C31r	202R D32r	202R D33c	202R E40c	202R E41r	202R F42c	202R F43r	202R G53c
SiO_2	59•68	60•10	59•71	58•31	61•66	56•02	58•30	59•33
Al_2O_3	25•30	25•04	25•94	25•71	23•30	28•97	26•59	26•42
*FeO	0•88	-	0•29	-	-	-	0•26	0•29
CaO	7•11	6•81	7•48	8•02	5•53	10•24	8•30	8•14
Na_2O	6•94	7•22	6•77	6•46	7•95	5•30	6•20	6•78
K_2O	0•20	0•29	0•30	0•23	0•18	0•14	0•21	0•24
Total	100•11	99•46	100•49	98•73	98•62	100•67	99•86	101•20
			Numbers of ions on the basis of 8(O)					
Si	2•663	2•687	2•649	2•634	2•767	2•514	2•608	2•621
Al	1•330	1•319	1•357	1•369	1•233	1•496	1•402	1•376
Fe	0•033	-	0•011	-	-	-	0•010	0•011
Ca	0•340	0•326	0•356	0•388	0•266	0•492	0•398	0•385
Na	0•601	0•626	0•582	0•566	0•692	0•462	0•537	0•581
K	0•012	0•017	0•017	0•013	0•010	0•008	0•012	0•014
				Mol%				
An	35•68	33•64	37•28	40•12	27•48	51•14	42•03	39•29
Ab	63•06	64•60	60•94	58•53	71•49	48•03	56•71	59•29
Or	1•26	1•75	1•78	1•34	1•03	0•83	1•27	1•43

TABLE: (3-2-2a) Microprobe analyses of plagioclases from the Serres-Drama granitic complex (cont.)

	202R G54r	126X Z26r	126X Z27c	126X Y28c	126X Y29r	126X X30c	126X X31r	126X W32c
SiO_2	59•58	60•82	60•68	59•22	61•58	58•96	61•24	59•20
Al_2O_3	26•36	24•83	25•07	25•90	24•42	26•31	24•63	25•95
*FeO	0•31	-	-	0•26	-	0•31	-	0•53
CaO	8•09	6•81	6•97	7•79	6•39	8•40	6•57	7•93
Na_2O	6•81	7•43	7•02	6•56	7•90	6•42	7•57	6•48
K_2O	0•27	0•21	0•18	0•33	0•15	0•25	0•27	0•25
Total	101•42	100•10	99•92	100•06	100•44	100•65	100•28	100•34
			Numbers of ions on the basis of 8(O)					
Si	2•627	2•701	2•696	2•641	2•723	2•619	2•713	2•636
Al	1•369	1•300	1•313	1•361	1•273	1•378	1•286	1•362
Fe	0•011	-	-	0•010	-	0•012	-	0•020
Ca	0•382	0•324	0•332	0•372	0•303	0•400	0•312	0•378
Na	0•582	0•640	0•605	0•567	0•677	0•553	0•650	0•560
K	0•015	0•012	0•010	0•019	0•008	0•014	0•015	0•014
				Mol%				
An	39•02	33•20	35•06	38•83	30•67	41•37	31•93	39•71
Ab	59•45	65•57	63•89	59•19	68•52	57•19	66•53	58•82
Or	1•53	1•23	1•06	1•98	0•81	1•45	1•54	1•42

TABLE: (3-2-2a) Microprobe analyses of plagioclases from the Serres-Drama granitic complex (cont.)

	126X W33	126X W34r	6bX A1c	6bX A2	6bX A3	6bX A4r	6bX B5c	6bX B6
SiO_2	60•69	61•03	58•76	60•24	61•47	61•47	57•23	59•54
Al_2O_3	25•84	24•47	27•20	25•35	24•58	23•82	27•43	25•12
*FeO	0•24	0•30	0•40	0•40	0•32	0•34	0•26	0•34
CaO	7•06	6•51	9•17	7•19	6•31	5•48	9•53	7•06
Na_2O	6•89	7•47	6•49	7•42	7•64	7•90	5•63	7•28
K_2O	0•19	0•27	0•16	0•33	0•28	0•25	0•23	0•30
Total	100•91	100•05	102•18	100•93	100•60	99•26	100•31	99•64
	Numbers of ions on the basis of 8(O)							
Si	2•673	2•713	2•581	2•667	2•717	2•747	2•558	2•667
Al	1•342	1•282	1•408	1•322	1•281	1•255	1•445	1•326
Fe	0•008	0•011	0•015	0•015	0•012	0•013	0•010	0•013
Ca	0•333	0•310	0•432	0•341	0•299	0•262	0•456	0•339
Na	0•588	0•644	0•552	0•637	0•655	0•685	0•488	0•633
K	0•011	0•015	0•009	0•019	0•016	0•014	0•013	0•017
				Mol%				
An	35•73	31•99	43•51	34•20	30•83	27•26	47•65	34•28
Ab	63•09	66•46	55•59	63•89	67•53	71•28	50•99	64•00
Or	1•18	1•55	0•91	1•91	1•65	1•46	1•36	1•72

TABLE: (3-2-2a) Microprobe analyses of plagioclases from the Serres-Drama granitic complex (cont.)

	6bX B7r	6bX C8c	6bX C9r	6bX D20c	6bX D21r	6bX E22c	6bX E23	152R A10r
SiO_2	61•68	58•61	60•45	60•05	61•76	61•78	61•70	46•38
Al_2O_3	23•85	25•44	24•60	25•61	23•98	24•05	23•83	34•68
*FeO	0•32	0•30	0•36	-	-	0•37	0•49	0•67
CaO	5•56	7•51	6•61	7•42	5•63	5•58	5•60	18•34
Na_2O	8•04	7•17	7•34	7•04	7•49	7•84	8•04	1•11
K_2O	0•19	-	0•17	0•21	0•22	0•26	0•29	0•10
Total	99•64	99•03	99•53	100•33	99•08	99•88	99•95	101•28
			Numbers of ions on the basis of 8(O)					
Si	2•746	2•642	2•702	2•665	2•755	2•744	2•743	2•115
Al	1•252	1•352	1•296	1•339	1•261	1•259	1•249	1•864
Fe	0•012	0•011	0•014	-	-	0•014	0•018	0•026
Ca	0•265	0•363	0•316	0•353	0•269	0•265	0•267	0•896
Na	0•694	0•627	0•636	0•606	0•648	0•675	0•693	0•098
K	0•011	-	0•010	0•012	0•012	0•015	0•017	0•006
				Mol%				
An	27•32	36•67	32•85	36•35	28•96	27•75	27•33	89•60
Ab	71•55	63•33	66•11	62•41	69•75	70•68	70•93	9•80
Or	1•13	-	1•04	1•24	1•29	1•57	1•74	0•60

TABLE: (3-2-2a) Microprobe analyses of plagioclases from the Serres-Drama granitic complex (cont.)

	152R A11	152R A12c	152R B13c	152R B14	152R B15r	152R C16c	152R C17r	152R D18c
SiO_2	46•11	46•02	45•04	44•85	45•59	45•48	44•71	45•66
Al_2O_3	34•85	34•59	34•73	34•58	34•80	35•19	34•97	35•29
*FeO	0•31	0•54	0•57	0•55	0•25	0•44	0•34	0•32
CaO	18•20	18•05	18•51	18•36	18•52	18•62	18•52	18•62
Na_2O	1•00	0•87	0•71	0•93	0•89	0•82	1,08	0•98
K_2O	-	-	-	-	-	-	0•16	-
Total	100•47	100•07	99•56	99•27	100•05	100•55	99•78	100•87
	Numbers of ions on the basis of 8(O)							
Si	2•113	2•118	2•089	2•088	2•101	2•088	2•073	2•089
Al	1•883	1•877	1•899	1•897	1•890	1•904	1•911	1•903
Fe	0•012	0•021	0•022	0•021	0•010	0•017	0•013	0•012
Ca	0•893	0•890	0•920	0•916	0•914	0•916	0•920	0•913
Na	0•089	0•078	0•064	0•084	0•079	0•073	0•097	0•087
K	-	-	-	-	-	-	0•009	-
	Mol%							
An	90•94	91•94	93•50	92•53	92•04	92•62	89•67	91•30
Ab	9•06	8•06	6•50	8•49	7•96	7•38	9•45	8•70
Or	-	-	-	-	-	-	0•88	-

TABLE: (3-2-2a) Microprobe analyses of plagioclases from the Serres-Drama granitic complex (cont.)

	152R D19r	152R E20r	152R E21c
SiO_2	45•58	45•03	45•09
Al_2O_3	34•43	34•56	34•70
*FeO	-	-	0•76
CaO	18•21	18•69	18•97
Na_2O	0•98	0•81	0•69
K_2O	0•10	-	-
Total	99•30	99•09	100•21
	Numbers of ions on the basis of 8(O)		
Si	2•113	2•089	2•083
Al	1•882	1•890	1•890
Fe	-	0•023	0•029
Ca	0•904	0•929	0•939
Na	0•088	0•073	0•062
K	0•006	-	-
	Mol%		
An	90•58	92•72	93•81
Ab	8•82	7•29	6•19
Or	0•60	-	-

TABLE: (3-2-2b) Microprobe analyses of plagioclases from the Xanthi plutonic complex (Christofides, 1977)

	41-1r	41-2c	41-3r	41-4c	210-1c	210-2r	125-1	125-2c	125-21
SiO_2	57·66	55·61	56·21	57·39	57·46	60·36	55·52	57·05	58·10
TiO_2	n.a.	n.a.	n.a.	n.a.	-	-	-	-	-
Al_2O_3	26·27	27·68	27·19	25·95	25·97	24·51	27·56	26·99	26·43
FeO	0·43	0·40	0·39	0·59	0·22	0·30	0·35	0·22	0·31
CaO	8·10	9·78	9·43	7·82	8·64	7·02	10·07	9·51	8·06
K_2O	0·24	0·33	0·32	1·26	0·24	0·31	0·33	0·13	0·41
Na_2O	6·78	5·84	5·94	6·32	6·61	7·70	5·74	6·16	6·62
Total	99·48	99·64	99·46	99·33	99·14	100·20	99·57	100·06	99·93
	Numbers of ions on the basis of 32(O)								
Si	10·391	10·061	10·168	10·405	10·396	10·759	10·057	10·240	10·414
Ti	n.a.	n.a.	n.a.	n.a.	-	-	-	-	-
Al	5·582	5·904	5·799	5·547	5·540	5·151	5·886	5·712	5·585
Fe^{2+}	0·065	0·061	0·059	0·089	0·033	0·045	0·053	0·033	0·046
Ca	1·564	1·896	1·828	1·519	1·675	1·341	1·955	1·829	1·548
K	0·055	0·076	0·074	0·292	0·055	0·071	0·076	0·030	0·094
Na	2·370	2·050	2·077	2·223	2·320	2·662	2·017	2·145	2·302
				Mol%					
Or	1·38	1·89	1·86	7·24	1·36	1·74	1·88	0·75	2·38
Ab	59·41	50·97	52·20	55·11	57·28	65·34	49·83	53·57	58·37
An	39·21	47·14	45·94	37·65	41·36	32·92	48·29	45·68	39·25

n.a = not analysed
Symbols: r = rim; c = core

TABLE: (3-2-2b) Microprobe analyses of plagioclases from the Xanthi plutonic complex (Christofides, 1977) (cont.)

	125-22	125-23r	125-3	125-4	250-1r	250-2	250-3c	156-1	156-2
SiO_2	56·71	59·07	59·26	59·26	61·87	57·20	57·14	56·30	57·44
TiO_2	-	-	-	-	n.a.	n.a.	n.a.	-	-
Al_2O_3	26·61	25·83	25·32	25·17	23·37	26·27	26·29	27·31	26·65
FeO	0·28	0·30	0·22	0·22	0·20	-	0·28	0·45	0·38
CaO	9·74	8·57	7·33	7·33	5·25	8·78	9·01	10·36	9·02
K_2O	0·25	0·31	0·38	0·38	0·23	0·13	0·25	0·14	0·23
Na_2O	5·88	6·48	6·98	7·08	8·28	6·59	6·13	5·60	6·35
Total	99·47	100·56	99·49	99·44	99·20	98·97	99·10	100·16	100·07
				Numbers of ions on the basis of 32(O)					
Si	10·251	10·516	10·632	10·642	11·057	10·355	10·343	10·126	10·308
Ti	-	-	-	-	n.a.	n.a.	n.a.	-	-
Al	5·671	5·421	5·356	5·329	4·924	5·607	5·611	5·791	5·639
Fe^{2+}	0·042	0·045	0·033	0·033	0·030	-	0·042	0·068	0·057
Ca	1·887	1·635	1·409	1·411	1·005	1·703	1·748	1·997	1·735
K	0·058	0·070	0·087	0·087	0·052	0·030	0·058	0·032	0·053
Na	2·062	2·238	2·429	2·466	2·870	2·314	2·152	1·954	2·211
				Mol%					
Or	1·45	1·77	2·22	2·19	1·32	0·74	1·47	0·80	1·33
Ab	51·46	56·76	61·88	62·21	73·09	57·18	54·37	49·06	55·29
An	47·09	41·47	35·90	35·60	25·59	42·08	44·16	50·14	43·38

TABLE: (3-2-2b) Microprobe analyses of plagioclases from the Xanthi plutonic complex (Christofides, 1977) (cont.)

	46-1	46-2	46-3	19-1	19-2	280-1	280-2	277-1	277-2
SiO_2	56·08	57·08	54·82	52·48	55·19	54·43	54·73	54·24	54·10
TiO_2	-	-	-	-	-	-	0·15	-	-
Al_2O_3	27·73	26·75	28·67	29·70	26·69	27·69	27·97	28·28	28·68
FeO	0·21	0·32	0·38	n.a.	n.a.	0·41	0·31	0·39	0·39
CaO	11·00	8·64	11·01	11·70	9·44	10·47	11·05	11·70	11·06
K_2O	0·28	0·29	0·21	0·39	2·12	0·48	0·48	0·53	0·47
Na_2O	5·43	6·47	5·24	4·67	4·79	5·17	4·99	4·60	4·99
Total	100·73	99·55	100·33	98·94	99·23	99·65	99·68	99·74	99·69
	Numbers of ions on the basis of 32(O)								
Si	10·046	10·292	9·872	9·606	10·064	10·037	9·928	9·852	9·822
Ti	-	-	-	-	-	-	0·020	-	-
Al	5·857	5·687	6·087	6·410	5·953	5·911	5·982	6·056	6·139
Fe^{2+}	0·031	0·048	0·057	n.a.	n.a.	0·062	0·047	0·059	0·059
Ca	2·112	1·670	2·125	2·295	1·845	2·032	2·148	2·277	2·152
K	0·064	0·067	0·048	0·091	0·493	0·111	0·111	0·123	0·109
Na	1·887	2·263	1·831	1·658	1·694	1·816	1·756	1·621	1·757
	Mol%								
Or	1·58	1·67	1·20	2·25	12·23	2·80	2·76	3·06	2·71
Ab	46·44	56·57	45·73	41·00	42·01	45·87	43·74	40·31	43·73
An	51·98	41·76	53·07	56·75	45·76	51·33	53·50	56·63	53·56

TABLE: (3-2-2b) Microprobe analyses of plagioclases from the Xanthi plutonic complex (Christofides, 1977) (cont.)

	277-3	28-1r	28-2c	28-3r	28-5c	28-6	58-1	58-2	P_3-1r	P_3-3c
SiO_2	54·56	54·56	49·05	56·44	48·26	55·09	54·83	52·99	60·94	50·16
TiO_2	0·11	-	-	-	-	-	0·17	-	0·11	-
Al_2O_3	28·61	28·76	31·91	26·32	32·59	28·09	28·10	29·42	24·13	30·77
FeO	0·38	0·44	0·35	0·26	0·43	0·27	0·43	0·49	0·25	0·40
CaO	11.16	12·09	16·10	9·63	15·82	11·50	11·55	12·36	6·37	14·66
K_2O	0·48	0·16	-	0·29	-	0·14	0·30	0·23	0·35	0·12
Na_2O	4·89	4·40	2·42	5·90	2·49	4·83	4·80	4·47	7·91	3·02
Total	100·19	100·41	99·83	98·84	99·59	99·92	100·18	99·96	100·06	99·13
				Numbers of ions on the basis of 32(O)						
Si	9·851	9·826	8·998	10·268	8·881	9·949	9·901	9·626	10·854	9·235
Ti	0·015	-	-	-	-	-	0·023	-	0·015	-
Al	6·091	6·107	6·902	5·646	7·071	5·981	5·983	6·301	5·067	6·680
Fe^{2+}	0·057	0·066	0·054	0·040	0·066	0·041	0·065	0·074	0·037	0·062
Ca	2·159	2·333	3·165	1·878	3·120	2·226	2·235	2·406	1·216	2·893
K	0·111	0·037	-	0·067	-	0·032	0·069	0·053	0·080	0·028
Na	1·713	1·537	0·861	2·082	0·889	1·692	1·681	1·575	2·733	1·079
				Mol%						
Or	2·79	0·95	0·00	1·66	0·00	0·81	1·73	1·32	1·99	0·70
Ab	43·01	39·34	21·39	51·70	22·18	42·84	42·18	39·04	67·83	26·97
An	54·20	59·71	78·61	46·64	77·82	56·35	56·09	59·64	30·18	72·33

TABLE: (3-2-2b) Microprobe analyses of plagioclases from the Xanthi plutonic complex (Christofides, 1977) (cont.)

	294-1	294-3	42	42-1	42-2	42-3	44-1	44-2	44-3
SiO_2	56·16	55·78	60·04	58·68	57·00	55·56	55·03	55·11	51·94
TiO_2	-	-	n.a.	n.a.	n.a.	n.a.	n.a.	n.a.	n.a.
Al_2O_3	27·33	27·07	24·67	25·75	26·76	28·01	27·58	27·36	29·86
FeO	0·37	0·24	0·26	0·23	0·22	0·34	0·32	0·49	0·53
CaO	10·35	10·52	7·09	7·94	9·12	10·48	10·33	10·33	12·38
K_2O	0·22	0·29	0·61	0·38	0·39	0·31	0·30	0·24	0·17
Na_2O	5·56	5·16	7·07	6·76	5·95	5·36	5·37	5·46	4·35
Total	99·99	99·06	99·74	99·74	99·44	100·06	98·93	98·99	99·23
				Numbers of ions on the basis of 32(O)					
Si	10·119	10·135	10·746	10·525	10·287	10·012	10·029	10·046	9·512
Ti	-	-	n.a.	n.a.	n.a.	n.a.	n.a.	n.a.	n.a.
Al	5·806	5·799	5·206	5·445	5·694	5·951	5·926	5·880	6·447
Fe^{2+}	0·056	0·036	0·039	0·035	0·033	0·051	0·049	0·075	0·081
Ca	1.998	2.048	1·360	1·526	1·764	0·024	2·017	2·018	2·430
K	0·051	0·067	0·139	0·087	0·090	0·071	0·070	0·056	0·040
Na	1·943	1·819	2·455	2·352	2·083	1·874	1·898	1·931	1·545
				Mol%					
Or	1·28	1·70	3·52	2·19	2·29	1·79	1·76	1·40	1·00
Ab	48·67	46·24	62·09	59·32	52·91	47·22	47·63	48·21	38·48
An	50·05	52·06	34·39	38·49	44·80	50·99	50·61	50·39	60·52

TABLE: (3-2-2c) Microprobe analyses of plagioclases from Paranesti (Dipotamos) granite (Sklavounos, 1981)

	29A	29B	30A	30B	31	32	34	35A	35B	36	37
SiO_2	64•61	64•71	63•91	62•51	63•07	64•61	63•20	63•36	61•86	61•20	63•38
Al_2O_3	22•02	22•07	21•33	23•31	22•88	20•78	22•88	22•90	22•63	22•08	22•80
K_2O	0•24	0•26	0•28	0•28	0•28	0•22	0•32	0•19	0•25	0•24	0•19
Na_2O	9•51	9•55	10•29	8•82	9•24	9•48	9•15	9•02	8•27	9•95	9•58
CaO	2•89	3•64	4•21	5•10	3•05	3•86	3•48	3•97	5•50	2•57	3•40
Total	99•27	100•23	100•02	100•02	98•52	98•95	99•03	99•44	98•51	99•05	99•36
					Numbers of ions on the basis of 32(O)						
Si	11•446	11•391	11•349	11•085	11•275	11•523	11•257	11•243	11•133	11•413	11•258
Al	4•599	4•580	4•464	4•874	4•821	4•368	4•803	4•790	4•801	4•627	4•775
K	0•053	0•059	0•064	0•064	0•064	0•049	0•072	0•042	0•058	0•055	0•044
Na	3•266	3•260	3•542	3•032	3•203	3•279	3•159	3•103	2•885	3•429	3•300
Ca	0•548	0•686	0•801	0•968	0•584	0•737	0•664	0•755	1•061	0•489	0•646
					Mol%						
Or	1•31	1•47	1•45	1•57	1•66	1•20	1•85	1•07	1•45	1•38	1•10
Ab	84•61	81•50	80•50	74•67	83•19	80•76	81•20	79•56	72•05	86•37	82•70
An	14•19	17•15	18•20	23•84	15•16	18•15	17•06	19•35	26•50	12•31	16•19

TABLE: (3-2-2c) Microprobe analyses of plagioclases from Paranesti (Dipotamos) granite (Sklavounos, 1981) (cont.)

	38	39	40A	40B	42	44	45	47	48	49
SiO_2	60•43	64•79	61•50	60•39	64•79	64•90	61•69	63•58	64•73	64•09
Al_2O_3	25•25	21•48	23•50	24•88	22•10	22•18	23•97	22•55	22•10	22•65
K_2O	0•31	0•23	0•40	0•21	0•28	0•21	0•32	0•34	0•21	0•33
Na_2O	8•50	10•17	8•78	8•33	9•63	9•84	8•71	9•55	9•51	9•77
CaO	5•35	4•00	4•52	4•75	3•14	2•44	4•91	2•85	3•22	3•41
Total	99•84	100•67	98•70	98•56	99•94	99•57	99•60	98•87	99•77	100•25
				Numbers of ions on the basis of 32 (O)						
Si	10•762	11•400	11•046	10•851	11•420	11•454	10•987	11•330	11•422	11•295
Al	5•301	4•455	4•975	5•271	4•592	4•615	5•032	4•737	4•597	4•706
K	0•070	0•050	0•090	0•047	0•063	0•046	0•072	0•077	0•046	0•074
Na	2•934	3•470	3•058	2•902	3•292	3•368	3•007	3•300	3•253	3•338
Ca	1•020	0•753	0•869	0•914	0•593	0•461	0•937	0•544	0•608	0•643
				Mol%						
Or	1•74	1•17	2•24	1•21	1•59	1•18	1•79	1•96	1•17	1•82
Ab	72•98	81•26	76•26	75•18	83•55	87•02	74•98	84•18	83•41	82•41
An	25•37	17•63	21•67	23•67	15•05	11•91	23•36	13•87	15•58	15•87

(3-2-2b) (from Christofides, 1977) and (3-2-2c) (from Sklavounos, 1981) for comparison with the present study.

The range of composition in terms of anorthite, albite and orthoclase content for granitic complexes from the Rhodope massif are as follows:

Xanthi (Christofides, 1977)

An_{26-79} Ab_{21-73} Or_{0-12}

Paranesti (Dipotamos) (Sklavounos), 1981)

An_{12-27} Ab_{72-87} Or_{1-2}

Serres-Drama (Present Study)

An_{18-94} Ab_{6-80} Or_{0-3}

The range of rock type in the three complexes are granodiorite to granite (Paranesti), gabbro to granite (Xanthi) and gabbro-granite/aplite in the Serres-Drama complex. Of all the analyses of the Serres-Drama complex, the most albitic is a rim composition (An_{18} Ab_{80} Or_2) from a monzonite (sample No.184) collected a few metres from the contact with the country rocks at Papazora. The range of composition of plagioclase feldspar in these complexes does seem to be closely related to rock type.

There is an interesting contrast between the composition of plagioclase in the gabbro from Xanthi and that in the gabbro of the present study, for which an explanation is given below.

A comparison between the compositions determined using the universal stage (Papadakis, 1965) and those

obtained by the electron microprobe is instructive:

	Papadakis, 1965	Present Study
Gabbro	An_{85-95}	An_{90-94}
Monzonite	An_{36-45}	An_{18-58}
Quartz monzonite	An_{28-42}	An_{33-60}
Granodiorite	An_{28-42}	not analysed
Granite	included in quartz monzonite	not analysed
Diorite Xenolith	not determined	An_{27-48}

The electron microprobe has revealed more extreme zoning than the optical methods and plagioclase feldspar both from the monzonite and quartz monzonite have very calcic cores (up to An_{60}).

The iron values in the plagioclase feldspars of the 'granitic' rocks are low (0-0.033 atoms Fe). This upper figure may be aberrant in that it is the only analysis significantly above a mean value of 0.010. Indeed, of 123 analyses of plagioclase, 28 are below the detection limit for iron. A more appreciable amount of iron has been determined in the gabbro with maximum concentration of 0.029 atoms, a similar observation was made by Lewis (1969) in plagioclase feldspars from plutonic blocks of the Soufriere Volcano, St. Vincent, West Indies. It is quite reasonable to assume that the iron ion is trivalent ($r = 0.64A^{o}$) and hence will substitute for the aluminium ($r = 0.51A^{o}$) in anorthite.

The Ti, Mn and Mg contents of the plagioclase feldspars were found to be below the detection limit for the E.D.S. microprobe technique.

The mean K values are also low (mean Or = 1.38%), but it is lowest in the gabbro (mean Or = 0.17%). The low content of potassium in plagioclase feldspars from gabbroic rocks is probably not a chemical control but a structural one, in spite of their high temperature of crystallisation. The probable explanation may be found in the greater ionic radius of K ($r \simeq 1.33A^{O}$) compared to Ca ($r = 0.99A^{O}$) and to the very tightly coordinated group around the Ca ion in the anorthite structure (Lewis, 1969). It is therefore unlikely that the very low potassium content in calcic plagioclase is related to the particular magma chamber from which it crystallised.

The data from the table (3-2-2a) are plotted onto a triangle with apices representing Ab, An, Or in fig. (3-2-2a). The molecular percentage Ab: An: Or has been calculated according to the formula:

$$\frac{Ca}{Na + K + Ca}, \text{ etc.}$$

The plagioclase feldspars (fig. 3-2-2a) show a very wide range of composition (An_{18-94}) but several important features can be noted: (1) the plagioclase feldspars in the gabbro are extremely anorthitic and there does seem to be a compositional gap ($\sim$ 30% in An content) between these minerals and those developed in the 'granitic' rock, (2) within the granitoid rocks there appears

Plagioclases

● from monzonite

■ from quartz monzonite

▽ from xenolith

✱ from gabbro.

Fig (3 2 2a)

to be a good deal of overlap between the composition of plagioclase in the more basic members (monzonite and dioritic xenoliths) and the more acid (quartz monzonite). The most anorthitic composition of plagioclase in both the monzonite and quartz monzonite is An_{60} which is extremely calcic for rock of these compositions, (3) plagioclase compositions from the dioritic xenoliths are less anorthitic (An_{27-48}) than those from the monzonite (An_{18-58}) although in terms of bulk rock chemical composition the diorites are more basic, (4) the plot does emphasize the very low orthoclase content of these plagioclase feldspars.

If we consider the range in compositions (An_{18-94}) in the 'basic' group (gabbro-diorite-monzonite) it is far greater (An_{33-60}) than in the intermediate group (quartz monzonite).

Chemical compositions of zoned plagioclase feldspars have been obtained for most of the rock types in the Serres-Drama complex, but a much more detailed traverse was performed on an oscillatory zoned crystal from a granite (sample No.110). There are 41 spot analyses across this single grain, displaying wide variation in composition (figure, 3-2-3d). These analyses are not represented in the table (3-2-2a).

One major problem when analysing zoned crystals is that it is often very difficult to know before analysis whether the core of the crystal has been sectioned in the process of polishing the sample for the electron microprobe.

Therefore it is often necessary to analyse several grains to obtain in the case of the plagioclase feldspars the most anorthitic composition.

In the present study six grains were analysed from sample No.184 (monzonite), collected near the contact with the country rocks. Two of them (grain B = 53 to 70 Ab% and grain F = 55 to 80 Ab%) are normally zoned i.e. calcic cores and sodic rims. It is possible that the results of the three analyses of each of these two grains do not represent the true type of zoning, since the two grains had either insufficient analyses performed upon them to show the full range of variation in composition or type of zoning. The other four (A, C, D and E) grains have oscillatory zones. The transition from normal to oscillatory zoning is abrupt. The range of albite content (%) in the six grains is as follows:

	Core Ab%	rim Ab%
grain A	57	70
" B	53	70
" C	41	79
" D	61	79
" E	53	80
" F	55	80

Four of these grains have the same rim composition and the other two some 10% Ab less. The changes in composition from zone to zone are abrupt and in three of the grains (C, D and E) there is a sharp decrease in Ab content from the rims (79-80 Ab%) to the next zone inside the

crystal (grain C = 57 to 79 Ab%; grain D = 66 to 79 Ab%; grain E = 68 to 80 Ab%).

The plagioclase feldspar compositions from the oscillatory zoned grains show abrupt changes across the crystals as indicated below:

Spot analyses from individual zones within each grain								Ab%
grain	A	58	57	54	61	70		
"	C	56	47	41	57	79		
"	D	74	61	66	79	79		
"	E	53	57	70	58	67	68	80

Only normal zoning has been noted in samples 126R, 202R (both monzonite), 119R (quartz monzonite), 126x, 6-bx (both dioritic xenolith). The range in albite composition (%) is as follows:

Sample	126R	61	to	67	Ab%
"	202R	48	to	71	"
"	119R	39	to	65	"
"	126x	57	to	69	"
"	6-bx	51	to	72	"

There does not appear to be any relationship between the composition of the plagioclase feldspar and the silica content of the rocks i.e. sample 119R which has the most basic core composition is from a quartz monzonite which is more evolved than the monzonite and the dioritic xenoliths. It is difficult to assign any real significance to these ranges of composition particularly those of the core, because of the problem outlined earlier in relationship to

the sectioning of the core of these crystals. More reliance however can be placed upon the great similarity between the rim compositions of all these samples.

Plagioclase feldspar analyses for crystals from a dioritic xenolith and its host monzonite (sample No.126) indicate a complete overlap in composition. Two possible explanations can be put forward for this overlap: 1) that the xenoliths represent a magma with a separate but similar crystallisation history to that of the ultimate host rock, 2) the xenoliths were partly recrystallised after being incorporated into the host rock magma and that the outer zone compositions represent growth or equilibrium reaction with the host rock magma. There is little doubt that some recrystallisation has taken place because the rock texture of the xenolith now appears to be metamorphic rather than igneous. Although this texture is present in all the xenoliths there does appear to be a late phase of growth of potassium feldspar within the host rock but they do not cross the boundary into the xenolith, therefore any exchange in elements between xenolith and host appears minimal.

The composition of plagioclase feldspar from the gabbro (sample No.152) range in composition from An_{94-90}. All the grains exhibit normal zoning.

3-2-3 Discussion

Two major problems have been highlighted in the

previous section: 1) the presence of normal and oscillatory zoning and 2) the calcic composition of the plagioclase feldspars. In the following discussion these two subjects will be taken in turn.

It is obvious that zoning occurs in different environments. According to Sibley et al (1976) the zoning in plagioclase is due to two major mechanisms: 1) changes in general environmental variables, such as magma composition, temperature and pressure and 2) constitutional supercooling. The width and compositional range of each zone are interpreted as being a function of diffusion rates in the interface liquid. They explained that the periodic zoning resulted from an interplay between the nature of solid-liquid interface and the amount of supersaturation, growth and diffusion rates. In their model (figures 3-2-1a and 3-2-1b), the maximum albite content in each zone should indicate crystallisation from the equilibrium composition, L_1, while minimum albite composition should indicate crystallisation from a constitutionally supercooled liquid L_2. The interface liquid at equilibrium would have a relatively constant composition. In consequence, zoning due to constitutional supercooling means that maximum albite content in each zone must be constant. If the zoning is due to external changes, an abrupt increase would arise in the maximum albite content accompanied by a drop in temperature or pressure.

Their suggested criteria for determining whether zoning is due to external changes or to constitutional

supercooling is that in zoning that results from a constitutionally supercooled liquid the maximum albite content in each zone should be nearly constant, but zoning due to external changes will show a considerable variation, fig. (3-2-3a). In fig. (3-2-3b) is illustrated (A) oscillatory zoning with three anomalously high albite zones. In (B) the transition from the inner core to the outer zone D is shown to be clearly due to changing external factors.

It appears from the plagioclase data for the Serres-Drama granitic complex, that there are examples of both the major mechanisms outlined by Sibley et al (op.cit). Sample No.184 appears to show considerable variation in chemical composition between zones with an abrupt change in composition of albite (grain C = 57 to 79 Ab%; grain D = 66 to 79 Ab%; and grain E = 53 to 80 Ab%) which can be interpreted as being a result of a change in external factors, such as a change in temperature or pressure (including water pressure) and magma composition. This conclusion is quite reasonable because the monzonite (sample No.184) was collected close to the contact of the complex where a drop in temperature would be expected. The rim composition of the plagioclase feldspar is more albitic than any of the other analyses and the phenomenon exhibited is comparable to that of figure (3-2-3a, after Sibley et al, 1976), therefore it can be interpreted that it is due to external factors.

The second major mechanism of Sibley et al (op.cit)

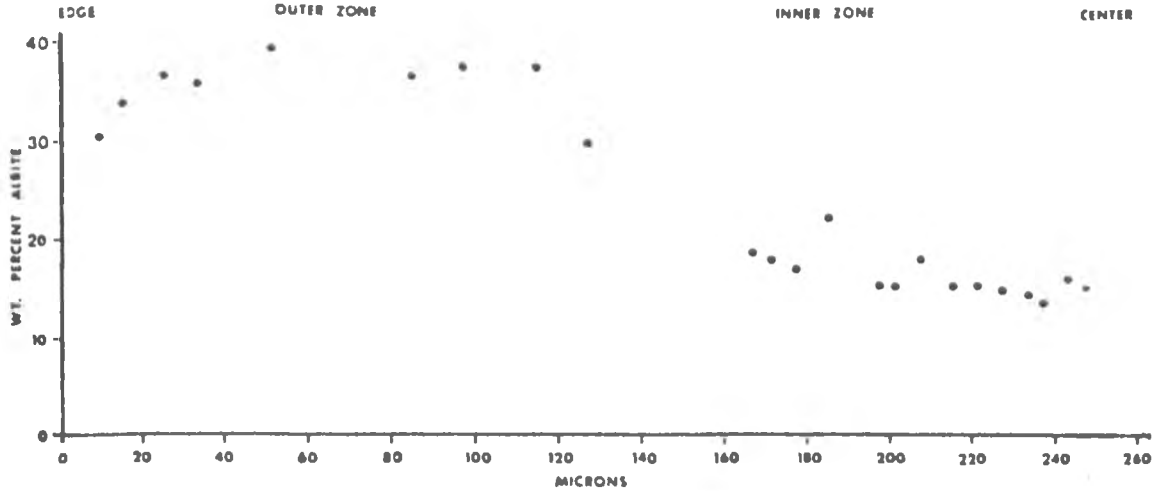

Fig [3–2–3a] Plot of the maximum albite content of zones across a zoned plagioclase phenocryst from the center to the edge of the crystal. Regions of the crystal where the maximum albite content of the zones are constant or slightly increasing indicate zoning attributable to constitutional supercooling. **[Sibley et al, 1976]**

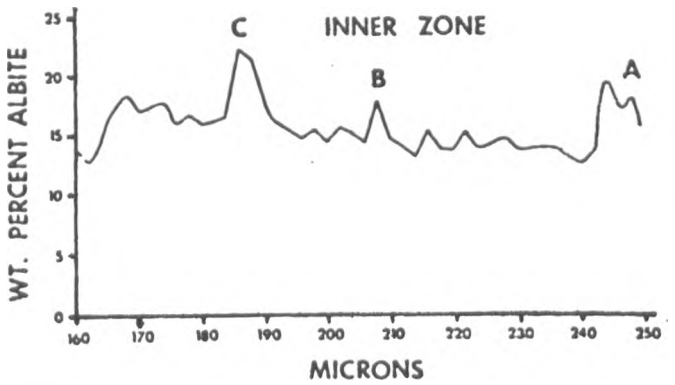

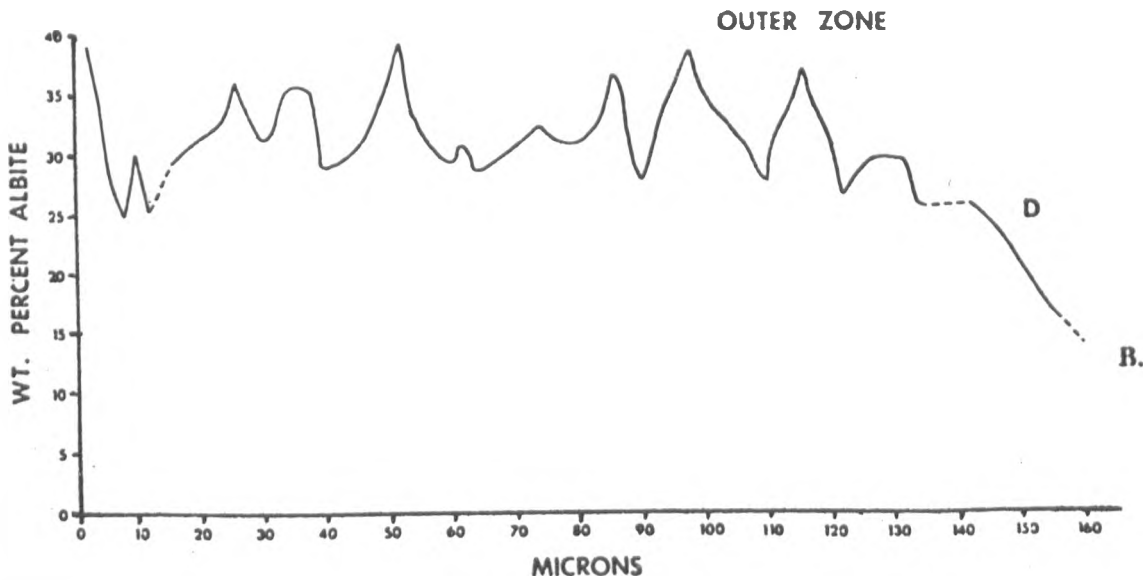

Fig [3–2–3b] A. Plot of compositional variation in wt percent albite across the inner zone of phenocryst.

B. Compositional variation plotted across outer zone of phenocryst. Major discontinuities are probably the result of changes in external factors, while the fine, oscillatory zoning can be explained by constitutional supercooling. **[Sibley et al, 1976]**

is that of constitutional supercooling and appears to explain the oscillatory zoning of plagioclase feldspar in the granite (sample No.110, fig. 3-2-3d). The compositions are symmetrically disposed and there is no patch zoning present (Vance, 1962, 1966). The rim composition of this crystal is Ab_{75}. There are several anomalous compositions in zones across the crystal. In particular, there is a zone of composition Ab_{72} close to the core of the crystal which is very similar to the rim. There is also an anomalously low albite zone (Ab_{50}) surrounded by two zones of similar composition (Ab_{60}). These observations are the same as shown in fig. (3-2-3b) after Sibley et al (op.cit) and may be interpreted as being due to constitutional supercooling. One criterion used by Sibley et al (op.cit) is that the maximum albite content in the zoning should be constant and indeed within this crystal it appears to be so.

Bowen (1913) explained the formation of normal zoning, using his experimental data, of the Ab-An system. If the crystals did not completely equilibrate their composition with the liquid, normal zoning would occur.

Wills (1974) said that falling temperature and loss of volatiles from the liquid results in the gradual increase in sodium content and also results in a viscosity increase. The density difference between plagiolcase and magma will be less than for any other phase, except quartz; so as the viscosity increases during cooling, plagiolcase crystals will tend to remain in contact with a localised

magma environment. The settling of the plagioclase crystals will be retarded in relation to other phases.

There is little doubt that the plagioclase feldspars present in all the rock types are much more calcic than one would expect from the compositions of the rocks. The plagioclase from the gabbros are extremely anorthitic (An_{90-94}) and although their compositions do vary across the crystals, the zoning is of a very limited nature. The plagioclase from the monzonite and quartz monzonite has zones which are up to An_{60}, an extremely calcic composition for such evolved rock types. Most workers explanations (Yoder, 1969; Lewis, 1969; Arculus and Wills, 1980; Johannes, 1978) for these observations involve the presence of a high water vapour pressure to lower both the solidus and liquidus surfaces relative to the anhydrous systems.

Lewis (1969) described 'sodic anorthites' from plutonic blocks which had been brought up by the Soufriere Volcano in the West Indies and he suggested that there is no reason to believe that the formation of anorthite in igneous rocks needs to be explained by contamination or special magmas. Lewis (ibid) concluded that anorthite (An_{90-100}) may possibly be the first plagioclase to be precipitated from a silica-saturated basaltic magma, under the conditions of high temperature and a high water vapour pressure, this being so provided that equilibrium is maintained. Other phases will be precipitated as well according to the physical conditions within the magma.

Arculus and Wills (1980) stated that several parameters are important in the equilibrium:

$$\mu^{\text{Plagioclase}}_{Ca\,Al_2\,Si_2\,O_8} = \mu^{\text{melt}}_{Ca\,Al_2\,Si_2\,O_8}$$

(Where μ_i^a is the chemical potential of component i in phase a)

These parametes are a) activities of the anorthite component in the solid and melt phase, b) temperature and c) pressure of equilibration.

Yoder (1969) made an attempt to explain the An-rich nature of plagioclase by examining the influence of water on parameter a. He suggested that for any given bulk composition (e.g. An_{40}, see fig. 3-2-3c) to produce an An-rich plagioclase, its melting loop would have to be lowered and this would best be done by increasing the water vapour pressure. There are several inadequacies in this explanation, however, which are apparent in fig. (3-2-3c), where the lower melting loop is the hydrous and the upper is the anhydrous case. The tie line at a fixed temperature (To) demonstrates that Yoder's (1969) explanation is only one example applied to a fixed melting loop. In the hydrous case only a few crystals of An_{74} coexist with abundant melt of An_{40}, whilst in anhydrous cases a reduced volume of melt (e.g. An_{20}) coexists with larger numbers of relatively An-poor (An_{60}) crystals.

If the narrow range of temperature of crystallisation is relaxed and the alternative requirement of equivalent modal proportions of crystal and melt are applied to fig. (3-2-3c), it can be seen from this diagram that

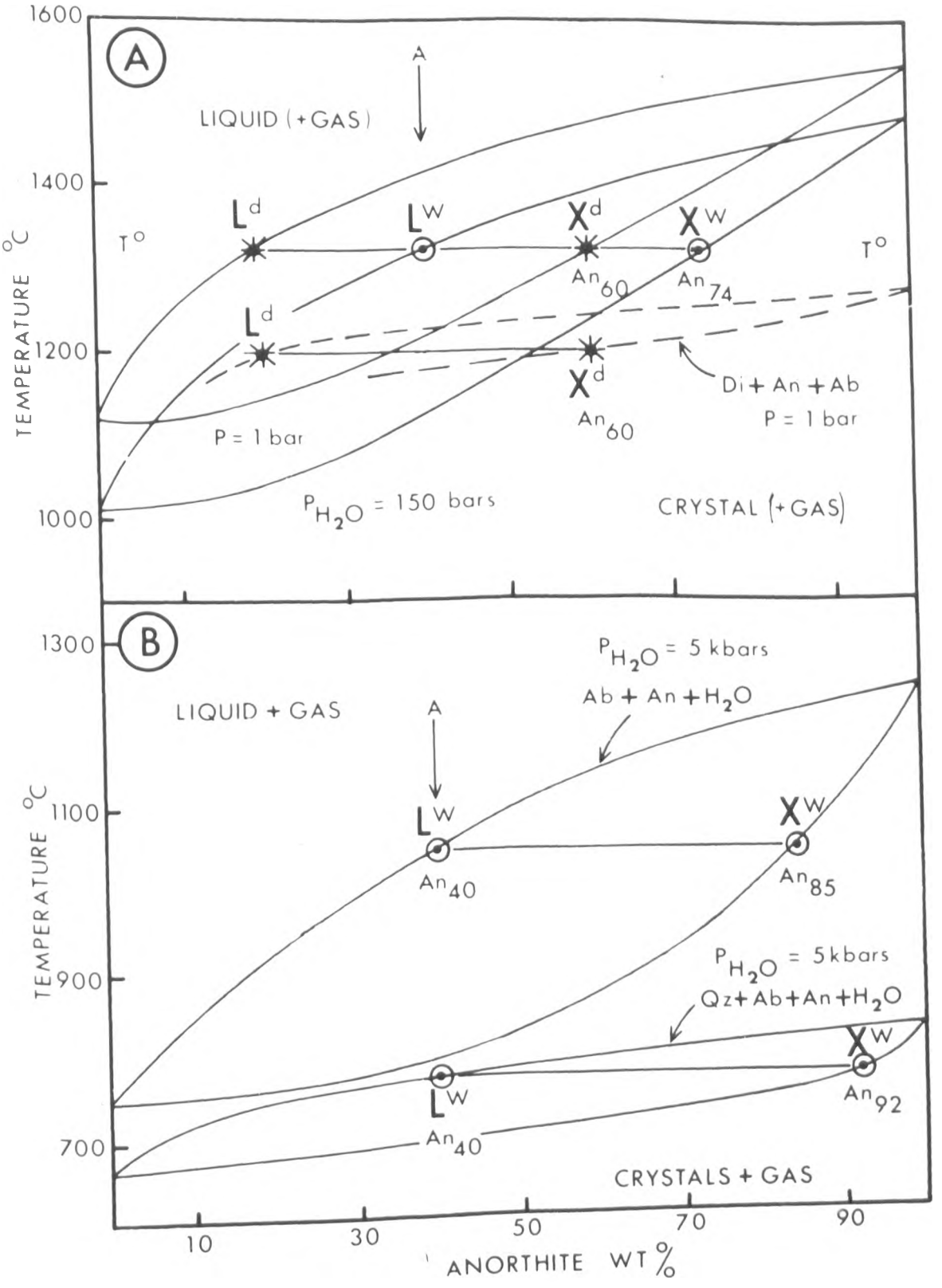

Fig (3-2-3c) (From R. Arculus and K.Wills , 1980)

Phase relations of plagioclase (An–Ab) and plagioclase-bearing systems after Bowen (1913, 1915), Yoder *et al.* (1957) and Johannes (1978). In (A), the symmetrical melting loops for the pure An–Ab system are presented as drawn by Yoder (1969). The dashed curves are the projected melting loop for the diopside–albite–anorthite system as determined by Bowen (1915). Note that the anhydrous melts (L^d) and crystals (X^d) are compositionally identical in the An–Ab and Di–An–Ab system at equivalent per cent crystallization. The melting loops drawn in (B) are from Johannes (1978). Note the contrast in symmetry of melting loops in (A) and (B) and the differences in hydrous melt-crystal (L^w and X^w respectively) compositions compared with the anhydrous situations at equivalent per cent crystallization.

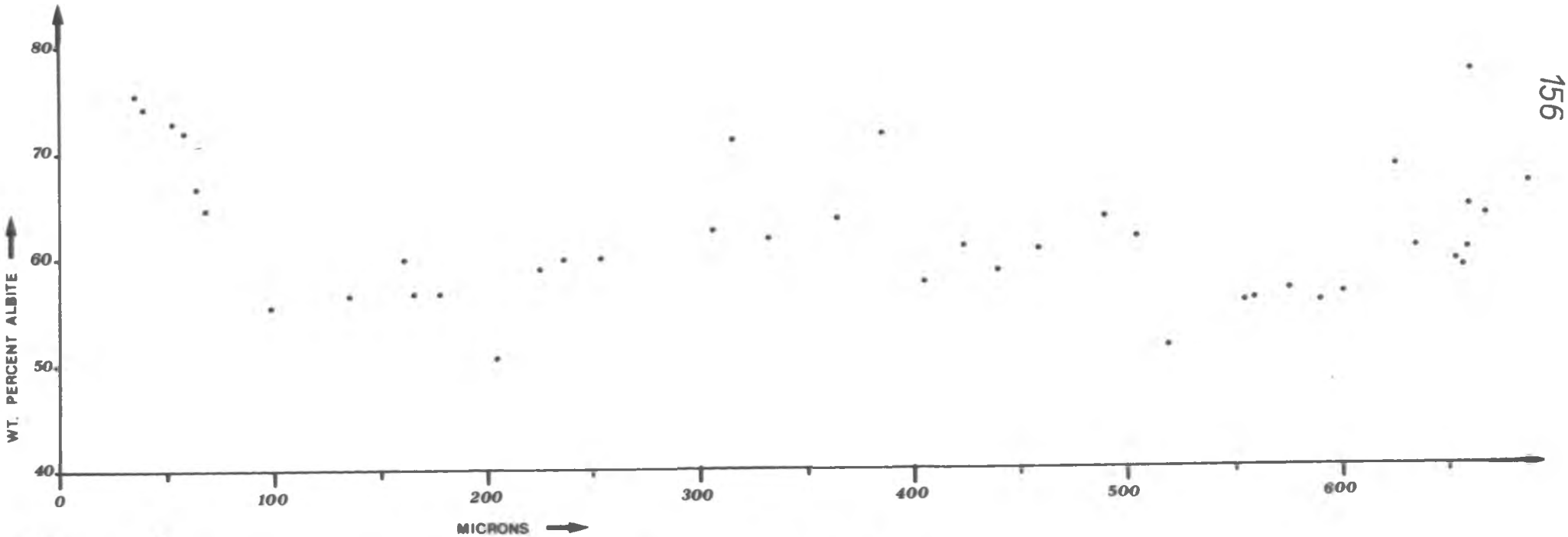

Fig. (3-2-3d)
Plot of the albite content across a zoned plagioclase feldspar from one edge to the other (sample No. 110).

identical crystal compositions occur in both hydrous and anhydrous cases, as the melting loop has an identical symmetry.

Yoder (1969) suggested that the role of water in calc-alcaline suites is crucial in determining the nature of plagioclase composition. Arculus and Wills (1980) concluded that this suggestion may be correct for the following reasons:

It is obvious that there is a critical difference in symmetry between the melting loops' cases, this is shown in fig. (3-2-3c). Johannes (1978) has demonstrated by experimental work that the solidus, as illustrated in fig. (3-2-3c) after Yoder et al (1957), is incorrect. Revised solidi for the Qz-Ab-An-H_2O and Ab-An-H_2O systems for comparison with the anhydrous Ab-An system show that for a given melt composition the An content of a crystal in equilibrium is higher in the hydrous than anhydrous conditions. Burnham (1975a, in Arculus and Wills, 1980) demonstrated a solution mechanism of water in aluminosilicate melts which depends on analogies with the Na Al Si_3 O_8 - H_2O system. This interaction is shown by the following equation:

$$Na\ Al\ Si_3\ O_8 + H_2O = Al\ Si_3\ O_7\ (OH) + Na\ (OH)$$

where the exchange reaction $Na^+ \rightleftharpoons H^+$ is critical. The equivalent reaction energetics involving Ca^{+2} as the exchangeable cation cannot be the same as for Na^+ and we can see from the phase diagrams of Johannes (1978) that

the solution of water in silica melts results in the lowering of a $^{melt}_{Na\ Al\ Si_3\ O_8}$ to a greater extent than a $^{melt}_{Ca\ Al_2\ Si_2\ O_8}$. Burnham (1975b, in Arculus and Wills, 1980) demonstrated experimentally that lack of exchangeable cations preclude any similarity of solution mechanism with the Ab-H_2O system to be expected.

Arculus and Wills (1980) concluded that the

> "greatly differing plagioclase compositions is apparently due to the crucial role of H_2O in disturbing the relationship of the chemical potentials of the An and Ab components of the respective melt compositions".

It would seem that the role of water is crucial in the formation of anorthite rich plagioclase. According to Johannes' (1978) interpretation of the hydrous melting loop (see, fig. 3-2-3c) if we initially accept that the plagioclases are crystallised from a melt composition of An (40%) under hydrous conditions (P_{H_2O} = 5Kb), resultant plagioclase will be 92% An in composition.

If we are to accept that the plagioclase of the sample No.152 (gabbro) in the present study began to crystallise from a similar melt composition to that of Johannes' (1978) then we can explain the range of plagioclase compositions (An_{90-94}).

If high water vapour pressure is considered to be the important factor in generating anorthitic plagioclase then we should also consider the effect on the phases which are crystallising together with the plagioclase feldspars in the gabbro (clinopyroxene and hornblende). In both the plutonic blocks brought to the surface by the Soufriere volcano

(Lewis, 1969) and in the present complex, primary hornblende crystallises together with anorthite in the gabbroic rocks. Although clinopyroxene is present in the Serres-Drama gabbros it has been replaced by hornblende (Chapter 2) and also the proportion of clinopyroxene is low, compared to anhydrous gabbros. The bulk rock chemistry of the gabbros does not indicate that they are of a highly calcic nature, therefore if anorthite is abstracting a large amount of calcium from the magma, then a less calcic mafic phase is required to take up sodium. It therefore appears reasonable to conclude that a reaction is taking place in the hydrous magma to suppress the clinopyroxene:

$$\underset{\text{clinopyroxene}}{Ca\ Mg\ Si_2\ O_6} + \underset{\text{labradorite}}{(Ca\ Al_2\ Si_2\ O_8 + Na\ Al\ Si_3\ O_8)} + H_2O \rightleftharpoons$$

$$\underset{\text{pargasite}}{Na\ Ca_2\ Mg_4\ Al\ Si_6\ Al_2\ O_{22}\ (OH)_2} + \underset{\text{anorthite}}{Ca\ Al_2\ Si_2\ O_8}$$

(equation unbalanced)

This reaction can be interpreted such that increased P_{H_2O} will drive the equilibrium to the right and reduced P_{H_2O} will favour the left hand side of the equation.

A similar situation can also be suggested to account for the core composition of the plagioclase feldspars in the monzonitic rocks, although they are more evolved (An_{60}), where clinopyroxenes, hornblende and plagioclase are crystallising. The texture of the monzonite does not imply that any of these phases was the first to crystallise (i.e. lack of any poikilitic texture).

The presence of a high water vapour pressure could also be used to explain the presence of oscillatory zoning of the plagioclase feldspars in the monzonites, and the 'intermediate' group of rocks. At high values of P_{H_2O} the compositions of the plagioclase became more anorthite rich and as P_{H_2O} reduced, the feldspar responded by becoming more albitic. For the P_{H_2O} to be reduced, a phase must be crystallising which is taking water into its lattice (i.e. hornblende). Therefore a tentative conclusion may be that there is a delicate balance between the P_{H_2O} and the particular phase crystallising.

This evidence from the plagioclase feldspars in the 'granitic' rocks may therefore appear to contrast with that of the potassium feldspars where it was suggested that the monoclinic symmetry of the potassium feldspars from the monzonite was related to a reduced water content compared to the triclinic symmetry of potassium feldspars from the more evolved rock types. The potassium feldspar polymorphs are, however, the latest phases to crystallise in these magmas, overprinting and often incorporating all the earlier crystallised phases. Therefore, either the potassium feldspar in the monzonites was crystallising where either the water content or P_{H_2O} was very low compared to the more evolved rocks or water is not as important in determining the final symmetry of the potassium feldspar polymorph, as suggested by Parsons and Boyd (1971).

3-2-4 Summary

In the present study it has been observed that there are plagioclase feldspars with oscillatory zoning and normal zoning. The oscillatory zoning is interpreted as being due to external factors and to constitutional supercooling. The normal zoning is explained by the incomplete reaction of solid and liquid, but the plagioclases with high anorthite content can be attributed to the crucial role of water which influences the relationship between anorthite and albite in the high water pressure melt compositions.

3-3 AMPHIBOLES

3-3-1 Introduction

Amphiboles were named by Hatly (1801) from the Greek "amphibolos" meaning ambiguous.

From the petrographic studies it is apparent that amphiboles are very common and widely distributed minerals in all the rock-types, usually as primary but sometimes as secondary minerals.

Amphiboles have a large variety of chemical compositions and therefore it is paramount to first of all classify these minerals. Microprobe analysis has been used to determine the chemistry of these phases and they have been classified according to the I.M.A. nomenclature (Leake, 1978) and also to attempt to find some evidence for their formation.

3-3-2 A short review of the structure of the amphiboles.

The amphibole group of minerals are both orthorhombic and monoclinic in symmetry. The structure consists of double chains of tetrahedrally co-ordinated cations of infinite length parallel to the "c" crystallographic axis. An entirely schematic diagram structure, common to all amphiboles, is illustrated in fig. (3-3-2a). This is the projection of the monoclinic amphibole crystal structure on the (001) and (100), modified after Colville et al

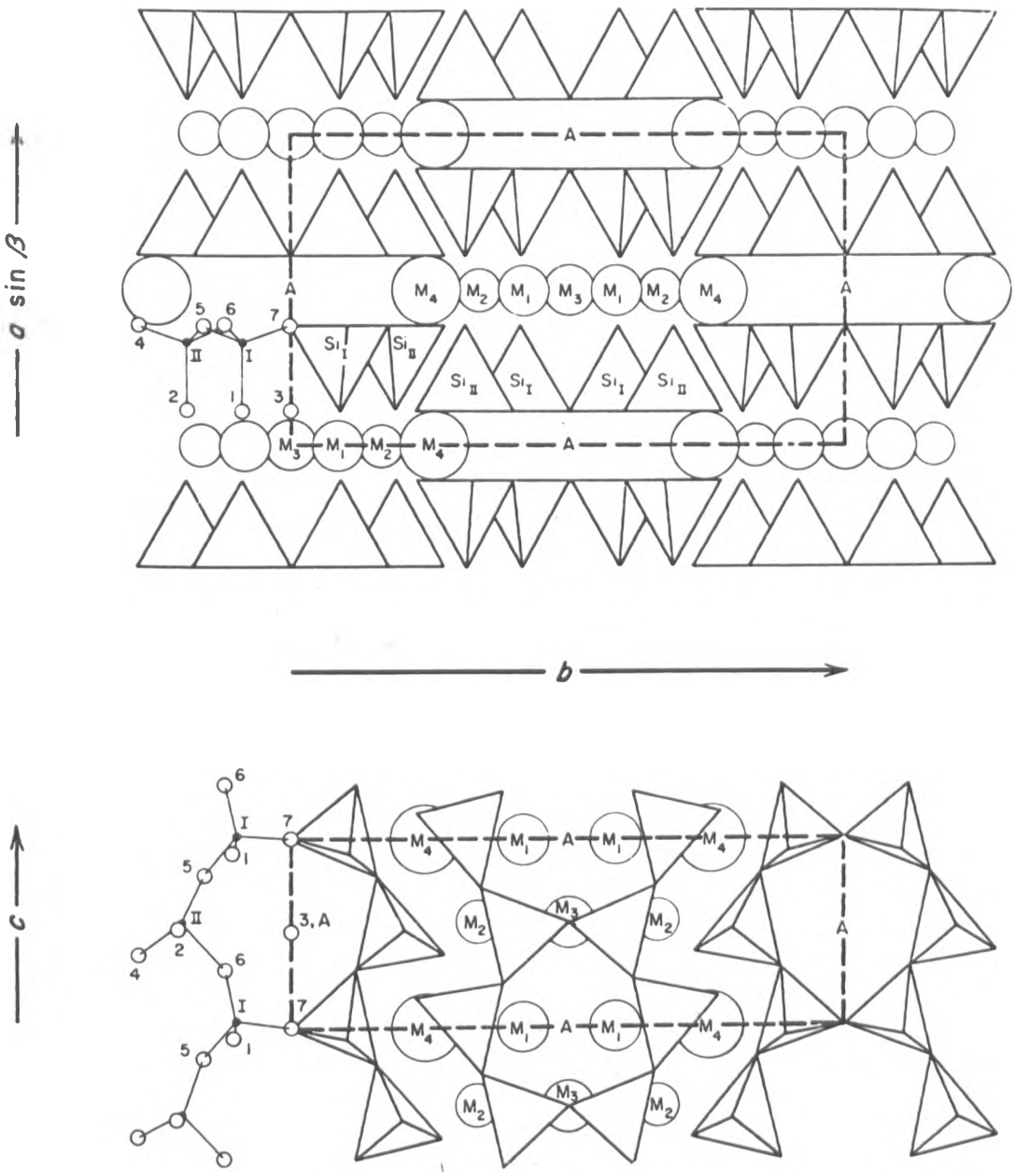

Fig (3-3-2a) Schematic diagram of the structure of the amphiboles, (after Ernst, 1968, from Rowbotham, 1973)

(1966, in Ernst, 1968). The chains consists of six connected rings surrounding a central void. The two different tetrahedral sites are designated S_I and S_{II}; tetrahedrally co-ordinated cation sites are illustrated as small solid circles, as shown in fig. (3-3-2a). There are octahedrally co-ordinated M_1, M_2 and M_3 sites: six-eight fold co-ordinated M_4 and ten-twelve fold sites shown by the letter (A). Anion sites are illustrated on the diagram by small open circles numbered 1 to 7. The O_3 anion site generally contain monovalent OH or F.

3-3-3 General classification of the amphiboles.

The classification of the amphibole group is based on the chemical composition of the minerals, as the physical properties, such as optics and X-ray powder diffraction, cannot differentiate totally between the different compositions.

The classification is based on the chemical composition of a standard amphibole formula calculated on the basis of 24 (O, OH, F, Cl), where OH + F + Cl is 2.00 atoms but it is understood that, where there is no determination of H_2O+ or there is reason to suppose that the reported H_2O+ is erroneous, or there is substantial unreported F or Cl, then the cation composition of the standard chemical formula is calculated on the basis of 23 (O).

The standard amphibole chemical formula contains eight tetrahedral sites and the general form is:

$$A_{0-1}\ B_2\ C_5^{VI}\ T_8^{IV}\ O_{22}\ (OH, F, Cl)_2$$

The standard amphibole chemical formula is best calculated using the following procedure (after Leake, 1978):

1) If there is a complete analysis including Fe^{3+}, H_2O^+, F^-, Cl^- etc. the recalculation should be made on the basis of 24(O).

2) If there is incomplete analysis then the recalculation should be on the basis of 23(O).

3) Sum T to 8.00 using Si, then Al, then Cr^3, then Fe^3, then Ti^4.

4) Sum C to 5.00 using excess Al, Cr, Ti, Fe^3 from (3), then Mg, then Fe^2 and then Mn.

5) Sum B to 2.00 using excess Fe^2, Mn, Mg from (4), then Ca, then Na.

6) Excess Na from (5) is assigned to A, then all K. Total A should be between 0.00 and 1.00, inclusive.

When a standard amphibole formula has been determined, on the basis of the numbers of atoms of $(Ca + Na)_B$, it is classified into one of four principal amphibole groups.

These assignments normally correspond to the occupancies of the tetrahedral sites (T), the $M_1+M_2+M_3$ sites (C), the M_4 sites (B) and the A sites (A).

The four principal amphibole groups on the basis of the numbers of atoms of $(Ca + Na)_B$ and Na_B are defined by Leake (1978):

"a) When $(Ca + Na)_B < 1.34$, then the amphibole is a member of the iron-magnesium-manganese amphibole group.

b) When $(Ca + Na)_B \geqslant 1.34$ and $Na_B < 0.67$, then the amphibole is a member of the calcic amphibole group. Nearly all such natural amphiboles have $Ca_B \geqslant 1.34$.

c) When $(Ca + Na)_B \geqslant 1.34$ and $0.67 \ll Na_B < 1.34$, then the amphibole is a member of the sodic-calcic amphibole group. Such natural amphiboles usually contain $0.67 < Ca_B < 1.34$.

d) When $Na_B \geqslant 1.34$, then the amphibole is a member of the alkali amphibole group".

The axes chosen for the classification of the calcic, sodic-calcic and alkali amphibole groups are Na_B, $(Na+k)_A$ and (8-Si) respectively and are illustrated in fig. (3-3-3a).

All the amphiboles of the present study are members of the monoclinic calcic amphibole group. It was considered useful to classify this group of amphiboles in tabulated form as shown in fig. (3-3-3b). Subsequent nomenclature is governed by the variation in Ti and $(Na + K)_A$ content, also shown in fig. (3-3-3b) (A, B, C and D). Any further sub-division depends upon $Mg / Mg + Fe^2$ ratio and Si content, which gives the more commonly used name of the particular amphibole.

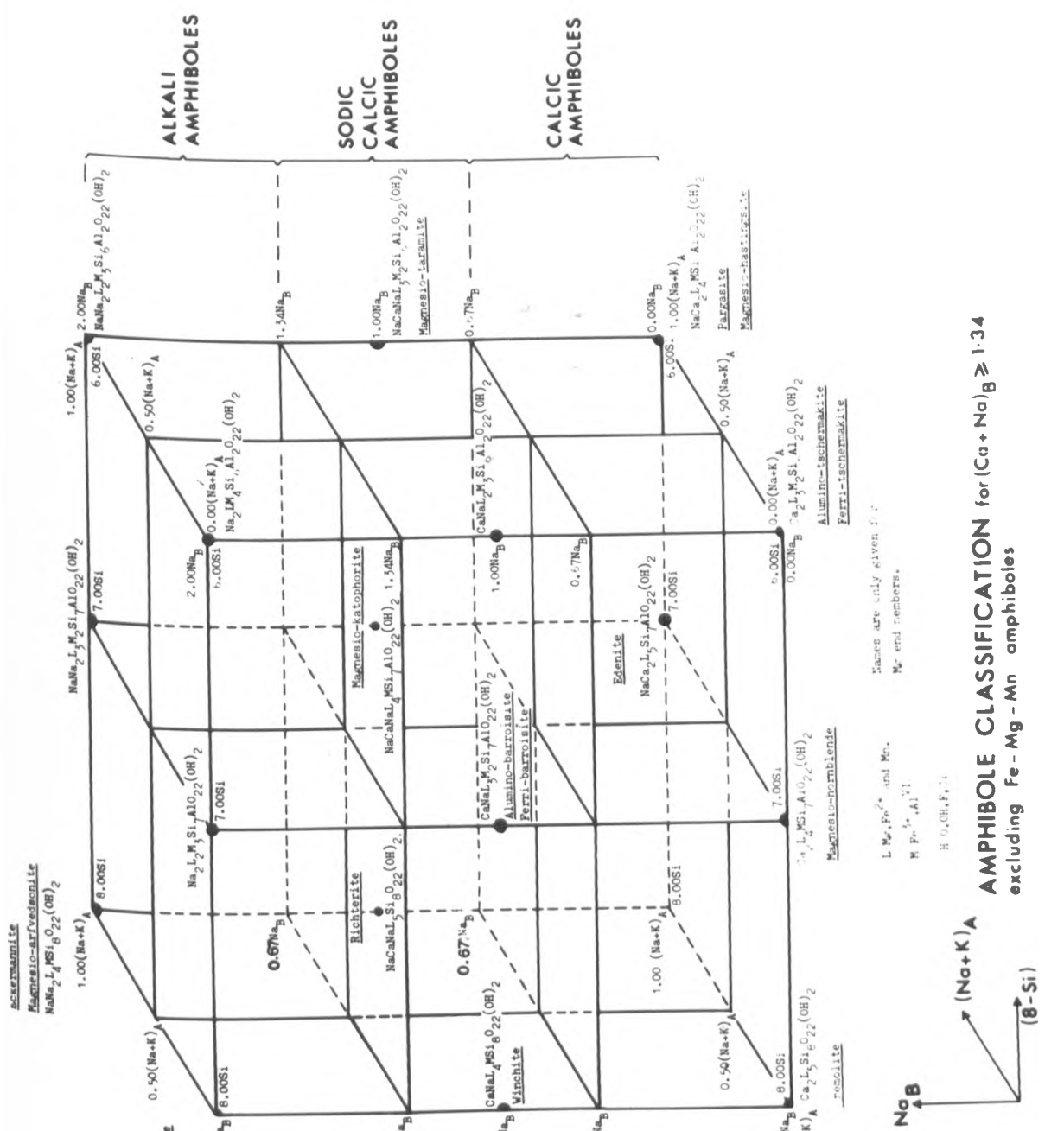

Fig. (3-3-3a) Leake (1978)

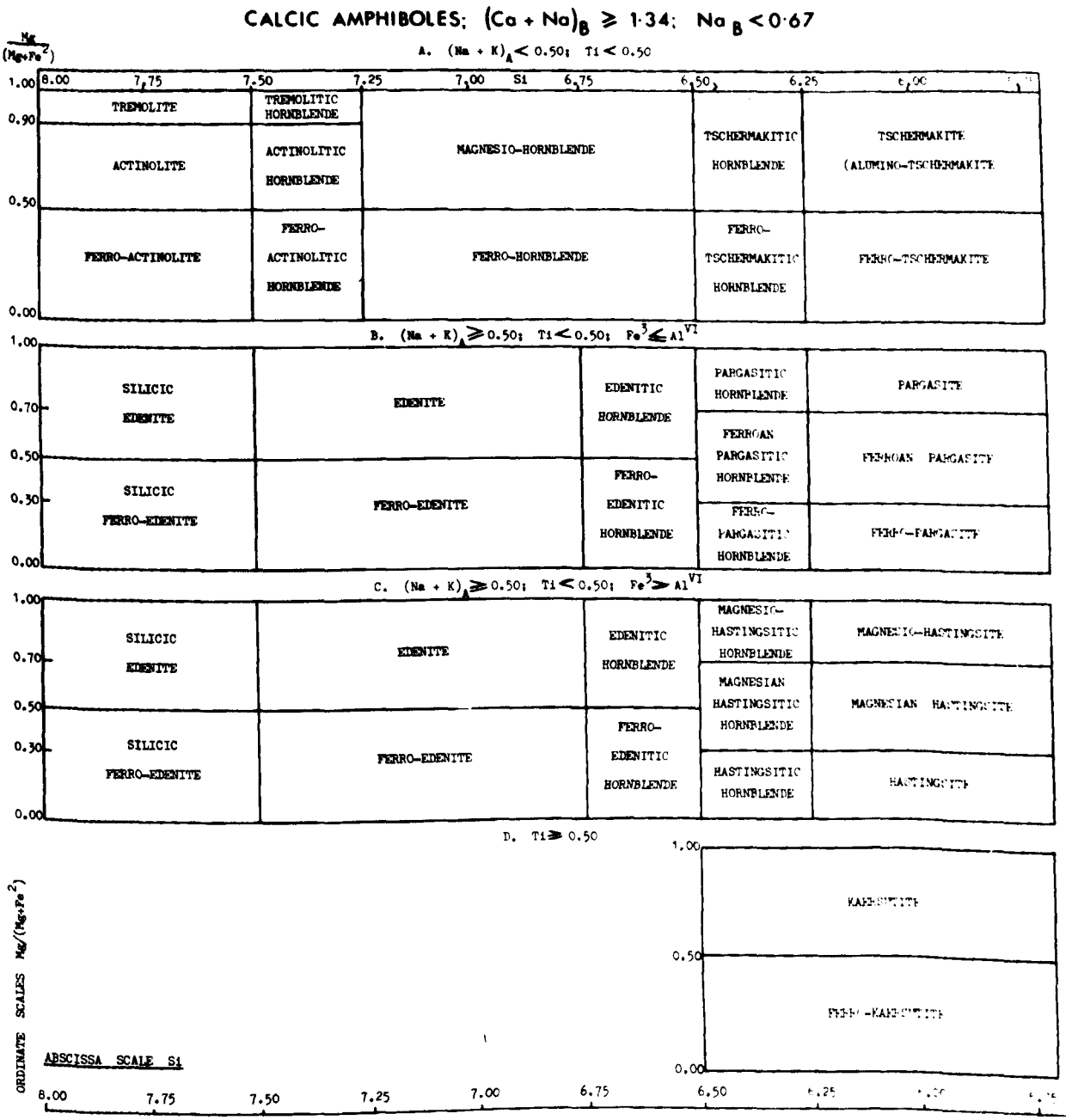

Fig. (3-3-3b) **Leake(1978)**

3-3-4 Electron microprobe analysis results

The obtained data for fifty-five amphibole analyses by electron microprobe, using twenty grains of seven amphibole-bearing samples are given in table (3-3-4a). Out of the fifty-five analyses, fourteen of these were from quartz monzonite (sample No.119) from five grains, fourteen were from monzonites (samples No.126R, No.184R, No.202R) from five grains, fourteen were xenoliths (samples No.126x, No.6-X) from six grains and thirteen were from gabbro (sample No.152R) from four grains. The values FeO and Fe_2O_3 were estimated using the computer programme of Papike et al (1974). These analyses were then recalculated on an anhydrous basis.

From the computer results (Papike et al, 1974), the ratio $Mg / Mg + Fe^2$ and the (X+Y) and (Y+Z) for Phillips' compositional space (X=Na in M_4 sites, $Y=Fe^3+Al^{VI}$ in octahedral sites, $Z=Al^{IV}$, Al^{IV} in tetrahedral sites) have been calculated as shown in table (3-3-4c).

The $Mg / Mg + Fe^2$ ratio increases from 0.49 to 0.80 if we consider all the amphibole analyses, but in the quartz monzonite the range is from 0.62 to 0.70, in the monzonite from 0.57 to 0.80, in the dioritic xenoliths from 0.60 to 0.67 and in the gabbro from 0.49 to 0.61. This ratio therefore increases with fractionation. The Si ranges between 6.11 and 7.74, while the host rock silica (SiO_2) varies between 46.5% and 68.3%.

The natural amphiboles from the Serres-Drama granitic

TABLE: (3-3-4a) Microprobe analyses of amphiboles from Serres-Drama granitic complex

	119R A13	119R A14	119R A15	119R B16	119R B17	119R B18	119R C19	119R D20	119R D21	119R D22
SiO_2	49·18	49·17	48·63	47·29	46·73	47·35	46·91	47·94	47·49	46·48
Al_2O_3	6·01	5·70	6·25	7·48	7·49	6·83	7·31	6·96	7·04	7·34
FeO	10·71	11·90	12·25	13·35	12·70	12·09	13·51	11·56	12·65	12·04
Fe_2O_3	4·23	2·65	2·46	2·12	2·83	3·84	2·16	3·79	2·59	3·22
MgO	13·86	13·45	13·20	12·28	12·29	12·55	12·42	13·11	12·73	12·55
MnO	0·60	0·65	0·67	0·56	0·65	0·62	0·54	0·58	0·53	0·61
TiO	0·87	0·85	0·79	1·32	1·25	0·87	1·19	1·04	1·16	1·15
CaO	12·04	12·13	12·20	12·06	12·07	11·96	11·90	11·91	12·05	11·97
Na_2O	1·10	1·03	1·11	1·27	1·08	1·11	1·73	1·36	1·24	1·23
K_2O	0·74	0·55	0·66	0·84	1·04	0·85	0·91	0·77	0·88	0·89
Total	99·34	98·08	98·22	98·57	98·13	98·07	98·58	99·02	98·36	97·48
	Numbers of ions on the basis of 23(O)									
Si_{iv}	7·085	7·176	7·109	6·936-	6·894	6·972	6·906	6·966	6·967	6·889
Al^{iv}	0·915	0·824	0·891	1·064	1·106	1·028	1·094	1·034	1·033	1·111
Al^{vi}	0·106	0·156	0·186	0·229	0·198	0·158	0·174	0·158	0·185	0·172
Fe_2	1·291	1·453	1·497	1·637	1·566	1·489	1·663	1·404	1·552	1·492
Fe^3	0·459	0·291	0·271	0·234	0·314	0·426	0·239	0·414	0·286	0·360
Mg	2·977	2·926	2·877	2·684	2·702	2·754	2·725	2·839	2·783	2·772
Mn	0·073	0·080	0·083	0·070	0·082	0·077	0·068	0·071	0·066	0·076
Ti	0·094	0·094	0·086	0·146	0·138	0·096	0·131	0·114	0·128	0·128
Ca	1·859	1·897	1·911	1·895	1·908	1·887	1·877	1·854	1·895	1·901
$Na(M_4)$	0·141	0·103	0·089	0·105	0·092	0·113	0·123	0·146	0·105	0·099
Na(A)	0·167	0·190	0·227	0·257	0·215	0·204	0·371	0·238	0·247	0·254
K	0·136	0·103	0·124	0·157	0·196	0·160	0·170	0·143	0·165	0·169

TABLE: (3-3-4a) Microprobe analyses of amphiboles from Serres-Drama granitic complex (continued)

	119R E23	119R E24	119R F72	119R F73	126R A12	126R A13	184R A4	184R A5	184R A6	184R B7
SiO_2	46·39	46·21	48·32	48·92	46·61	47·14	52·50	52·75	54·03	54·77
Al_2O_3	7·36	7·43	5·84	5·69	7·24	7·54	3·34	3·41	2·27	2·11
FeO	12·46	12·61	12·51	11·96	12·79	13·36	9·32	8·70	9·34	9·63
Fe_2O_3	3·05	3·42	1·69	1·88	2·20	1·64	2·34	2·74	2·07	0·87
MgO	12·28	12·30	13·27	13·54	12·52	12·67	16·17	16·46	16·89	17·20
MnO	0·32	0·57	0·57	0·62	0·58	0·68	0·74	0·89	0·34	0·47
TiO	1·17	1·34	0·70	0·50	1·26	1·37	0·36	0·54	-	-
CaO	11·90	12·08	12·21	12·20	11·84	12·12	12·44	12·10	12·67	12·85
Na_2O	1·07	1·25	1·11	1·01	1·48	1·63	0·84	1·28	0·61	0·56
K_2O	0·88	0·92	0·62	0·60	0·95	0·94	0·36	0·34	0·16	0·18
Total	96·88	98·13	96·84	96·92	97·47	99·09	98·41	99·21	98·38	98·64
	Numbers of ions on the basis of 23(O)									
Si	6·912	6·834	7·162	7·216	6·918	6·892	7·500	7·470	7·673	7·739
Al^{iv}	1·088	1·176	0·848	0·784	1·082	1·108	0·500	0·530	0·327	0·261
Al^{vi}	0·206	0·129	0·182	0·206	0·185	0·191	0·064	0·040	0·053	0·091
Fe^2	1·553	1·559	1·550	1·476	1·587	1·633	1·114	1·031	1·109	1·138
Fe^3	0·342	0·381	0·188	0·209	0·245	0·181	0·252	0·292	0·222	0·092
Mg	2·728	2·711	2·930	2·976	2·770	2·760	3·443	3·474	3·575	3·622
Mn	0·041	0·071	0·072	0·078	0·072	0·085	0·089	0·106	0·041	0·057
Ti	0·131	0·149	0·078	0·056	0·141	0·150	0·038	0·057	-	-
Ca	1·901	1·914	1·938	1·929	1·883	1·898	1·905	1·836	1·928	1·946
Na (M_4)	0·099	0·096	0·062	0·071	0·117	0·102	0·095	0·164	0·072	0·054
Na (A)	0·210	0·271	0·256	0·217	0·309	0·361	0·138	0·187	0·097	0·099
K	0·168	0·173	0·118	0·112	0·179	0·176	0·065	0·061	0·028	0·032

TABLE: (3-3-4a) Microprobe analyses of amphiboles from Serres-Drama granitic complex (continued)

	184R B8	184R B9	184R C16	184R C17	184R C18	202R A19	202R A20	202R A21	126X Z20	126X Z21
SiO_2	51·38	53·10	50·48	50·22	54·05	41·50	41·64	42·96	47·34	45·92
Al_2O_3	4·51	2·57	4·81	4·87	2·53	10·83	10·65	9·59	6·77	7·93
FeO	8·31	8·13	8·12	9·68	7·58	13·80	14·77	13·56	11·36	12·65
Fe_2O_3	3·97	3·26	4·89	3·43	3·98	2·89	1·71	3·62	3·42	3·27
MgO	15·82	16·64	15·49	14·76	16·94	10·70	10·88	11·03	13·20	12·40
MnO	0·83	0·67	0·87	0·97	0·76	0·38	0·42	0·56	0·66	0·56
TiO	0·71	0·33	0·90	0·98	-	1·18	1·24	0·67	1·10	1·20
CaO	12·12	12·19	11·98	11·85	12·18	11·83	12·23	11·93	12·24	12·08
Na_2O	1·08	0·73	1·13	1·32	0·73	1·89	2·08	1·77	1·03	1·53
K_2O	0·39	0·23	0·50	0·46	0·26	1·77	1·62	1·54	0·77	1·05
Total	99·12	97·85	99·17	98·54	99·01	96·78	97·24	97·23	97·89	98·59
	Numbers of ions on the basis of 23(O)									
Si	7·303	7·586	7·203	7·238	7·616	6·337	6·344	6·513	6·958	6·770
Al^{iv}	0·697	0·414	0·797	0·762	0·384	1·663	1·656	1·487	1·042	1·230
Al^{vi}	0·059	0·019	0·011	0·066	0·037	0·286	0·256	0·227	0·131	0·149
Fe^2	0·988	0·971	0·969	1·167	0·893	1·762	1·882	1·719	1·396	1·559
Fe^3	0·425	0·350	0·525	0·372	0·422	0·332	0·196	0·412	0·378	0·363
Mg	3·351	3·544	3·293	3·171	3·557	2·436	2·471	2·493	2·891	2·726
Mn	0·100	0·081	0·105	0·118	0·091	0·049	0·054	0·072	0·082	0·070
Ti	0·077	0·035	0·097	0·106	-	0·135	0·141	0·077	0·122	0·133
Ca	1·846	1·866	1·832	1·829	1·840	1·935	1·996	1·938	1·927	1·908
Na (M_4)	0·154	0·134	0·168	0·171	0·160	0·065	0·004	0·062	0·073	0·092
Na (A)	0·144	0·068	0·146	0·198	0·039	0·494	0·611	0·458	0·220	0·346
K	0·070	0·041	0·090	0·084	0·046	0·345	0·314	0·298	0·134	0·198

TABLE: (3-3-4a) Microprobe analyses of amphiboles from Serres-Drama granitic complex (continued)

	126X Z22	126X Y23	6-bX A10	6-bX A11	6-bX A12	6-bX A13	6-bX B14	6-bX B15	6-bX C24	6-bX C25
SiO_2	46·38	46·38	46·53	46·09	46·17	46·46	46·24	46·80	46·80	46·21
Al_2O_3	7·84	7·30	6·96	6·76	7·12	7·43	6·96	7·39	7·29	7·59
FeO	13·55	14·38	12·25	12·43	12·40	12·57	11·44	13·05	13·43	13·24
Fe_2O_3	2·23	1·24	3·11	2·28	2·73	2·33	3·61	3·71	1·97	2·45
MgO	12·14	12·12	12·49	12·57	12·36	12·37	12·62	12·01	12·58	12·27
MnO	0·63	0·58	0·55	0·78	0·79	0·63	0·55	0·72	0·71	0·72
TiO	1·27	1·44	1·34	1·41	1·35	1·00	1·27	1·11	1·43	1·38
CaO	12·39	12·24	11·77	11·71	11·80	11·94	11·73	12·10	12·01	11·89
Na_2O	1·19	1·40	1·27	1·57	1·45	1·28	1·16	1·24	1·80	1·77
K_2O	1·00	1·07	0·90	0·89	0·86	0·90	0·83	0·90	0·91	0·92
Total	98·62	98·15	97·17	96·49	97·03	96·91	96·41	99·03	98·93	98·44
			Numbers of ions on the basis of 23(O)							
Si	6·834	6·884	6·921	6·917	6·891	6·926	6·915	6·870	6·872	6·827
Al^{iv}	1·166	1·116	1·079	1·083	1·109	1·074	1·085	1·130	1·128	1·173
Al^{vi}	0·197	0·162	0·141	0·114	0·145	0·232	0·141	0·149	0·134	0·149
Fe^2	1·669	1·784	1·524	1·560	1·548	1·567	1·430	1·602	1·649	1·636
Fe^3	0·247	0·138	0·348	0·257	0·306	0·261	0·406	0·410	0·218	0·272
Mg	2·667	2·682	2·768	2·811	2·750	2·748	2·811	2·627	2·753	2·701
Mn	0·079	0·073	0·069	0·099	0·100	0·079	0·069	0·089	0·088	0·089
Ti	0·141	0·161	0·150	0·159	0·151	0·113	0·143	0·123	0·158	0·153
Ca	1·956	1·946	1·876	1·883	1·886	1·907	1·879	1·903	1·889	1·883
Na (M_4)	0·044	0·054	0·124	0·117	0·114	0·093	0·121	0·097	0·111	0·117
Na (A)	0·296	0·347	0·243	0·340	0·306	0·278	0·216	0·254	0·400	0·390
K	0·189	0·202	0·171	0·171	0·163	0·172	0·158	0·168	0·170	0·173

TABLE (3-3-4a) *Microprobe analyses of amphiboles from Serres-Drama granitic complex (continued)*

	6-bX	6-bX	152R	152R	152R	152R	152R	152R	152R	152R
	D26	D27	A6	A7	A8	A9	B28	B29	C32	C33
SiO_2	46·18	46·38	41·22	40·61	40·92	40·41	41·07	41·73	41·75	41·46
Al_2O_3	7·14	7·17	13·07	13·13	12·79	12·83	12·08	11·60	13·39	13·27
FeO	13·56	13·27	12·90	13·17	16·20	16·06	15·08	14·78	14·07	13·20
Fe_2O_3	1·55	1·46	2·62	3·30	1·80	2·49	4·16	3·86	1·13	2·15
MgO	12·47	12·42	10·94	10·35	8·96	8·66	9·64	9·78	10·94	10·98
MnO	0·62	0·73	-	0·27	-	-	-	-	0·22	-
TiO	1·34	1·30	2·65	2·35	2·45	2·07	0·94	1·08	2·80	2·70
CaO	11·93	12·13	12·25	12·36	12·20	12·24	12·22	12·17	12·64	12·72
Na_2O	1·81	1·34	1·66	1·55	1·35	1·19	1·74	1·43	1·73	1·38
K_2O	0·92	0·93	1·27	1·30	1·37	1·39	1·58	1·46	1·38	1·29
Total	97·52	97·13	98·58	98·39	98·04	97·34	98·51	97·89	100·05	99·15
			Numbers of ions on the basis of 23(O)							
Si_{iv}	6·882	6·919	6·111	6·068	6·179	6·158	6·199	6·305	6·115	6·111
Al^{iv}	1·118	1·081	1·889	1·932	1·821	1·842	1·801	1·695	1·885	1·889
Al^{vi}_2	0·137	0·181	0·395	0·380	0·455	0·463	0·349	0·370	0·427	0·416
Fe_3	1·690	1·656	1·600	1·645	2·046	2·047	1·904	1·867	1·724	1·627
Fe	0·174	0·164	0·293	0·371	0·205	0·285	0·472	0·438	0·125	0·239
Mg	2·771	2·761	2·417	2·306	2·016	1·968	2·169	2·202	2·388	2·411
Mn	0·078	0·092	-	0·034	-	-	-	-	0·027	-
Ti	0·150	0·146	0·295	0·264	0·278	0·238	0·106	0·123	0·309	0·299
Ca	1·904	1·939	1·947	1·978	1·973	1·999	1·976	1·971	1·984	2·008
Na (M_4)	0·096	0·061	0·053	0·022	0·027	0·001	0·024	0·029	0·016	-
Na (A)	0·427	0·328	0·424	0·428	0·368	0·351	0·486	0·389	0·475	0·394
K	0·175	0·176	0·240	0·247	0·264	0·270	0·305	0·282	0·257	0·243

TABLE: (3-3-4a) Microprobe analyses of amphiboles from Serres-Drama granitic complex (continued)

	152R C34	152R C35	152R C36	152R D39	152R D40
SiO_2	41•77	42•69	44•11	43•39	43•58
Al_2O_3	12•26	11•56	11•24	10•83	10•31
FeO	12•47	13•35	15•93	15•04	15•45
Fe_2O_3	3•63	3•49	2•65	1•66	0•88
MgO	10•75	10•50	9•93	11•38	11•01
MnO	0•26	-	-	-	0•27
TiO	1•17	1•67	0•74	1•55	1•56
CaO	12•24	12•29	12•50	12•34	12•21
Na_2O	1•25	0•81	1•24	2•18	2•01
K_2O	1•52	1•43	1•31	1•37	1•29
Total	97•32	97•79	99•65	99•74	98•57

Numbers of ions on the basis of 23(O)

Si	6•277	6•378	6•514	6•402	6•502
Al^{iv}	1•723	1•622	1·486	1•598	1•498
Al^{vi}	0•450	0•414	0•471	0•285	0•315
Fe^2	1•567	1•669	1•967	1•856	1•928
Fe^3	0•410	0•392	0•295	0•185	0•099
Mg	2•408	2•338	2•185	2•502	2•449
Mn	0•033	-	-	-	0•034
Ti	0•132	0•187	0•082	0•172	0•175
Ca	1•971	1•968	1•978	1•951	1•953
Na (M_4)	0•029	0•032	0•022	0•049	0•047
Na (A)	0•337	0•202	0•333	0•576	0•534
K	0•291	0•272	0•247	0•258	0•246

complex are calcic amphiboles because they contain $(Ca + Na)_B \geq 1.34$ and $Na_B < 0.67$, according to the International Mineralogical Association Commission, (I.M.A.C.) classification (Leake, 1978). The classification of the calcic amphibole group (as shown in detail in fig. 3-3-3b) has been used to classify the analyses into three subgroups, as follows:

1) If they contain $(Na + K)_A < 0.50$ and $Ti < 0.50$, then of all the analyses, thirty-one (56.4%), when plotted, fall within this subgroup (fig. 3-3-4a). The above thirty-one analyses can be classified as follows:

Twenty-three are magnesio-hornblendes, present in quartz monzonite (13 analyses), monzonite (3 analyses) and diroitic xenolith (7 analyses) (see, table 3-3-4c); two are actinolitic hornblende, both from monzonite; four are actinolite, all from monzonite; one is tschermakitic hornblende from gabbro and one from the monzonite lies on the border between actinolite and actinolitic hornblende.

2) if they contain $(Na + k)_A \geq 0.50$, $Ti < 0.50$ and $Fe^3 \ll Al^{VI}$, fourteen analyses (25.5%), when plotted, fall within this subgroup (fig. 3-3-4b). The above fourteen analyses can be classified as follows:

Three of the amphibole analyses are edenite, obtained from monzonite (1 analysis) and dioritic xenolith (2 analyses); three are ferroan pargasitic hornblende, obtained from monzonite (1 analysis) and gabbro (2 analyses); six are ferroan pargasite, all from gabbro; one is edenitic hornblende from gabbro and one lies on the border between edenite and ferroan pargasitic hornblende

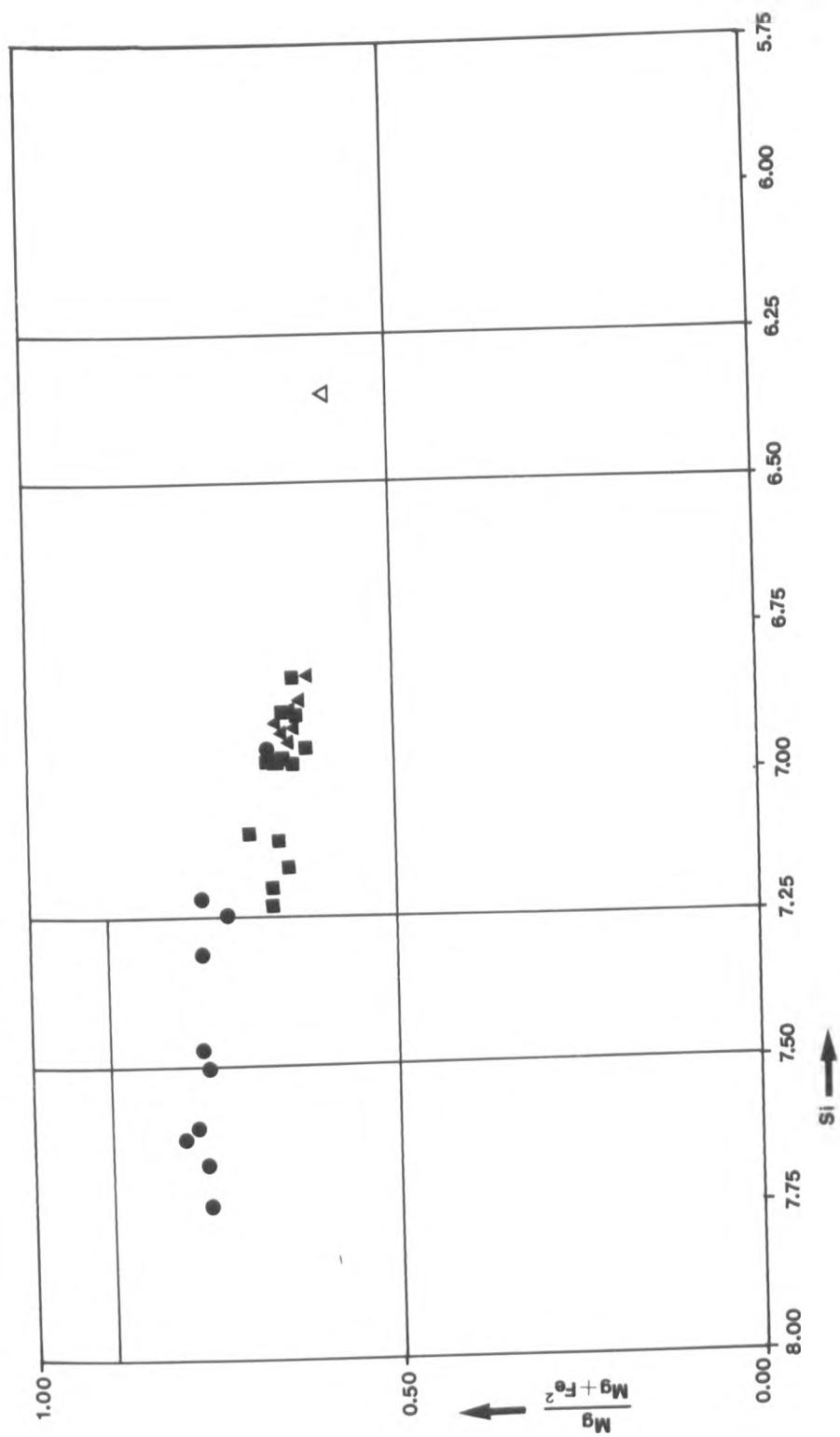
CALCIC AMPHIBOLES; $(Ca+Na)_B \geqslant 1.34$; $Na_B < 0.67$ (Leake, 1978)
A. $(Na+K)_A < 0.50$; Ti < 0.50
1.00
0.50
0.00
$\frac{Mg}{Mg+Fe^{2}}$
8.00
7.75
7.50
7.25
7.00
6.75
6.50
6.25
6.00
5.75
Si
Amphiboles: ● from monzonite; ■ from quartz monzonite; ▲ from xenolith; △ from gabbro.

Fig. (3-3-4a)

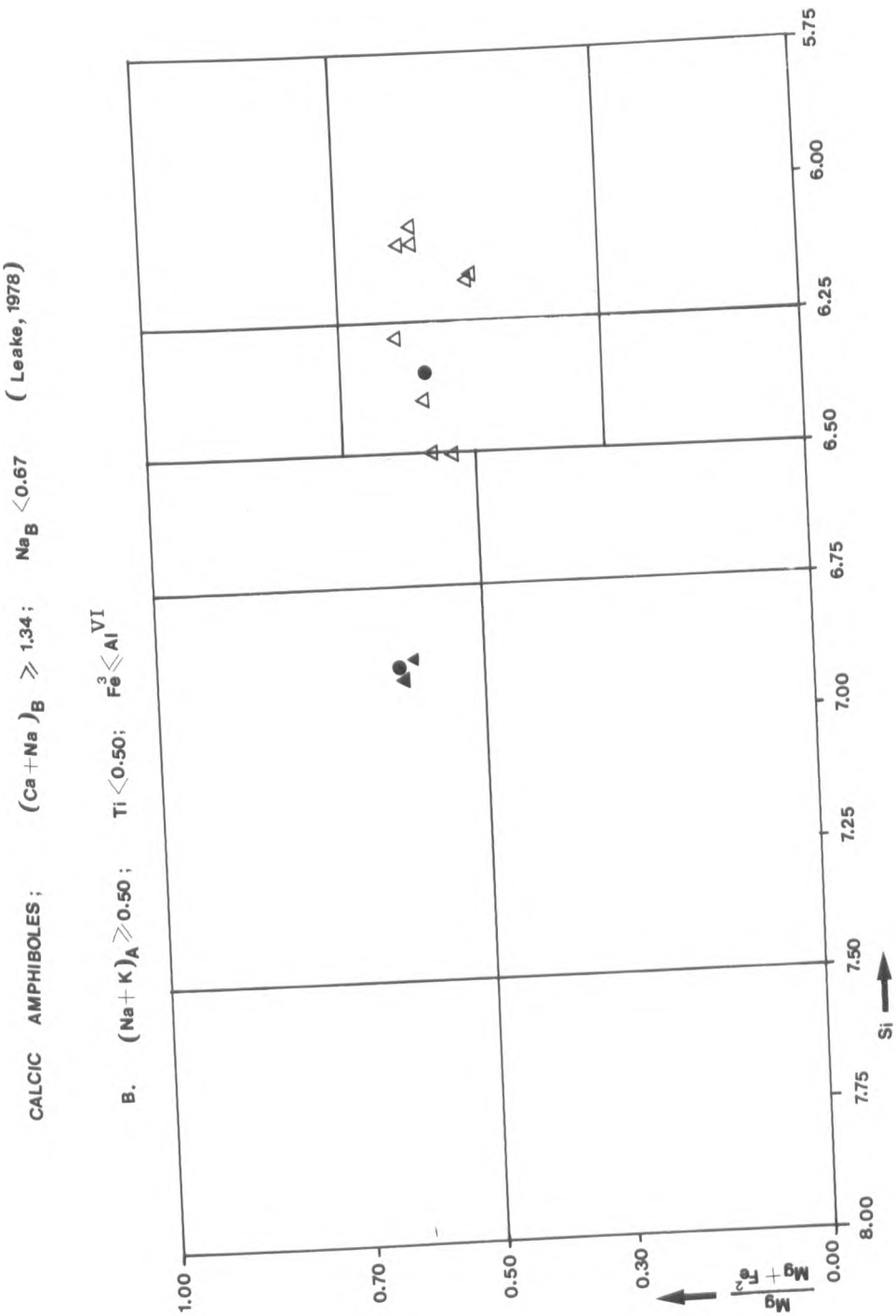
CALCIC AMPHIBOLES; $(Ca+Na)_B \geqslant 1.34$; $Na_B < 0.67$ (Leake, 1978)
B. $(Na+K)_A \geqslant 0.50$; Ti < 0.50; $Fe^3 \leqslant Al^{VI}$
1.00
0.70
0.50
0.30
0.00
$\frac{Mg}{Mg+Fe^{2+}}$
8.00
7.75
7.50
7.25
7.00
6.75
6.50
6.25
6.00
5.75
Si
Amphiboles: ● from monzonite; ■ from quartz monzonite; ▲ from xenolith; △ from gabbro.

Fig. (3-3-4b)

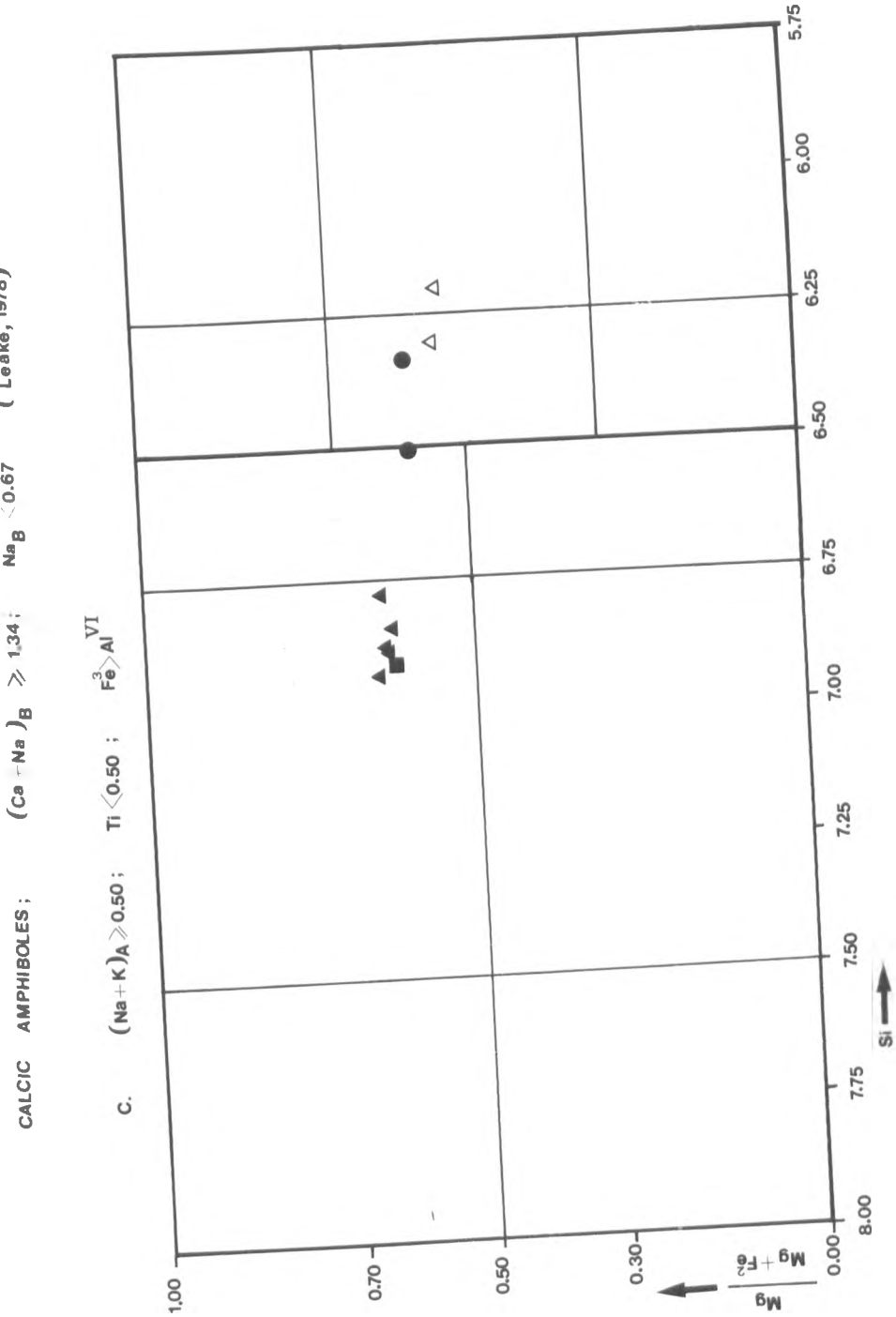
CALCIC AMPHIBOLES ; (Ca + Na)B ⩾ 1.34 ; NaB < 0.67 (Leake, 1978)
C. (Na+K)A ⩾ 0.50 ; Ti < 0.50 ; Fe3 > AlVI
1.00
0.70
0.50
0.30
0.00
Mg / Mg + Fe2
8.00
7.75
7.50
7.25
7.00
6.75
6.50
6.25
6.00
5.75
Si
Amphiboles: ● from monzonite; ■ from quartz monzonite; ▲ from xenolith; △ from gabbro.

Fig. (3-3-4c)

from gabbro.

3) if they contain $(Na + k)_A \gg 0.50$, $Ti < 0.50$ and $Fe^3 \gg Al^{VI}$, ten analyses (18.1%), when plotted, fall within this subgroup (fig. 3-3-4c). The above ten analyses can be classified as follows:

Six are edenite, obtained from quartz monzonite (1 analysis) and dioritic xenolith (5 analyses); two are magnesian hastingsitic hornblende, from monzonite (1 analysis) and gabbro (1 analysis); one is edenitic hornblende from monzonite and one is magnesian hastingsite from gabbro.

In summary, the range of amphibole compositions vary quite considerably but there is quite a large amount of overlap between compositions in the different 'granitic' rock types table (3-3-4c).

The results of the ratio $Mg/_{Mg + Fe^{2+}}$ of table (3-3-4c) are plotted against the host rock silica content in fig. (3-3-4e). It can be observed that the ratio increases with increase in the host rock silica.

For comparison with the present study the $Mg/_{Mg + Fe^{2+}}$ ratio has been calculated table(3-3-4b) for Christofides (1977) analyses. The number of silicon ions ranges between 7.141 and 7.584 and the ratio $Mg/_{Mg+Fe^{2+}}$ varies between 0.729 and 0.764. The above Si and $Mg/_{Mg+ Fe^{2+}}$ values have been plotted in fig. (3-3-4f). The above analyses can be classified as follows:

One is actinolite, two actinolitic hornblende and two magnesio-hornblende. These minerals are of the same composition as in the present study, except that the

TABLE: (3-3-4b) Microprobe analyses of amphiboles from the Xanthi plutonic complex (Christofides, 1977)

	A210	A125	156	A250	B41
SiO_2	53·49	51·56	50·66	50·02	48·94
TiO_2	0·36	0·48	0·80	0·88	1·31
Al_2O_3	3·01	3·77	4·47	4·57	5·22
Fe_2O_3	1·79	2·02	3·81	3·66	3·22
FeO	9·21	10·23	9·49	9·55	9·98
MnO	0·70	0·86	0·56	0·74	0·75
MgO	16·76	15·80	15·28	15·17	14·97
CaO	12·26	12·07	12·22	11·87	11·33
K_2O	0·19	0·29	0·39	0·43	0·61
Na_2O	0·81	0·68	0·63	1·17	1·08
Total	98·58	97·46	98·31	98·06	97·41
	Numbers of ions on the basis of 23(O)				
Si	7·584	7·459	7·287	7·237	7·141
Al	0·416	0·541	0·713	0·763	0·859
Al	0·087	0·102	0·045	0·017	0·039
Ti^{3+}	0·038	0·052	0·087	0·096	0·144
Fe^{2+}	0·191	0·220	0·412	0·399	0·354
Mg	1·092	1·238	1·142	1·156	1·208
Mn	3·541	3·342	3·275	3·271	3·255
	0·051	0·046	0·039	0·061	-
Ca_{2+}	1·863	1·871	1·884	1·840	1·772
Fe^{2+}	-	-	-	-	0·010
Mn	0·033	0·059	0·068	0·030	0·093
Na	0·104	0·070	0·048	0·130	0·125
Na	0·119	0·121	0·128	0·198	0·181
K	0·034	0·054	0·072	0·079	0·114

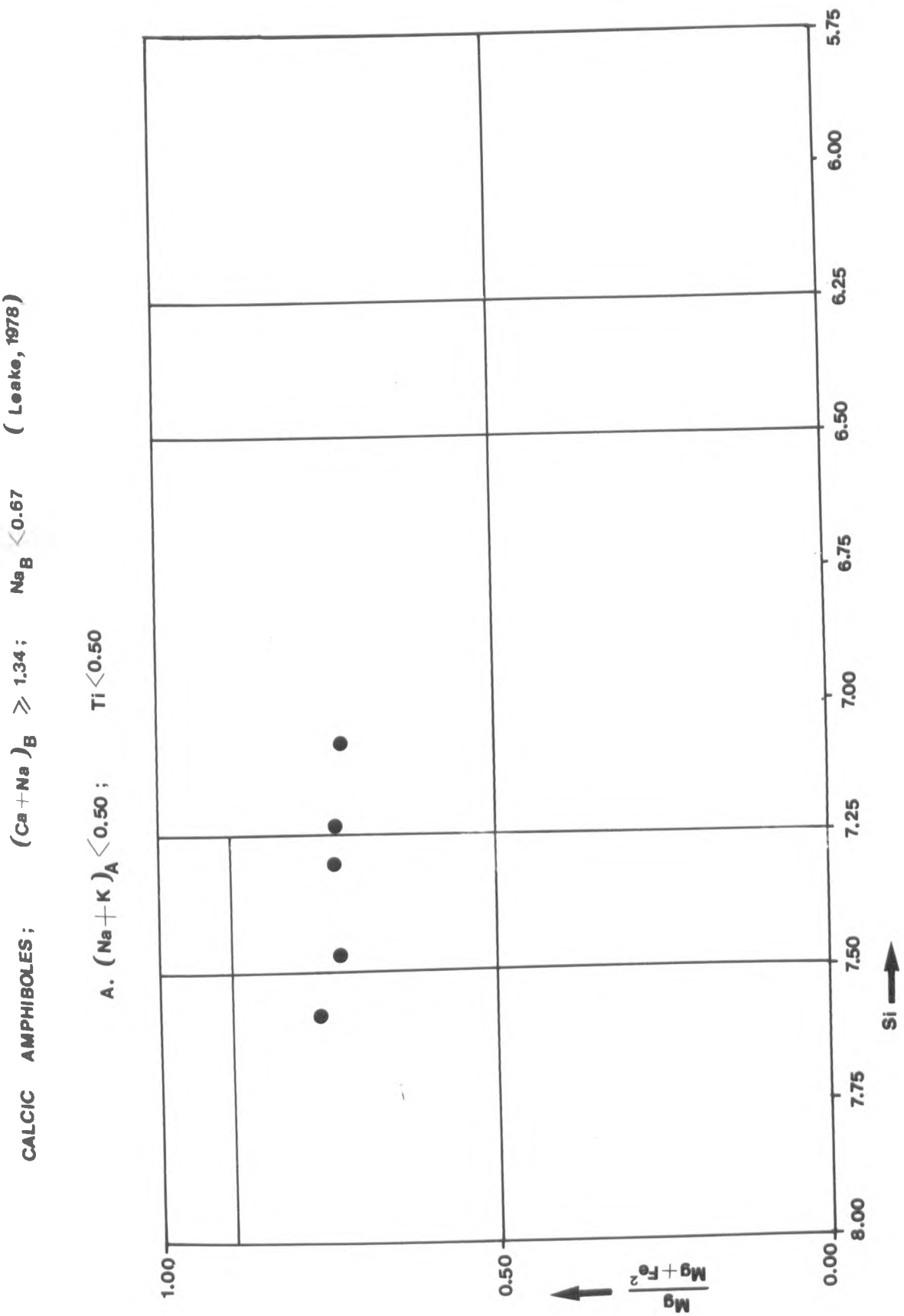
CALCIC AMPHIBOLES; $(Ca+Na)_B \geqslant 1.34$; $Na_B < 0.67$ (Leake, 1978)
A. $(Na+K)_A < 0.50$; Ti < 0.50
1.00
0.50
0.00
$\frac{Mg}{Mg+Fe^{2}}$
8.00
7.75
7.50
7.25
7.00
6.75
6.50
6.25
6.00
5.75
Si

Fig. (3-3-41)

TABLE: (3-3-4c) Atomic ratios ($Mg/Mg + Fe^2$), coupled substitution and co-ordinates (X + Y)(Y + Z) of the amphiboles of the Serres-Drama granitic complex.

Sample No.	$Mg/Mg+Fe^2$	X+Y	Y+Z	$(Na+K)_A$	$Na^{(A)}+Al^{iv}$	Mg+Si	Nomenclature
			Quartz monzonite				
119/A13	0.70	0.70	1.47	0.302	1.08	10.06	magnesio hornblende
119/A14	0.67	0.55	1.27	0.292	1.01	10.10	magnesio hornblende
119/A15	0.66	0.55	1.35	0.350	1.12	9.99	magnesio hornblende
119/B16	0.62	0.56	1.52	0.414	1.32	9.62	magnesio hornblende
119/B17	0.63	0.60	1.62	0.411	1.32	9.60	magnesio hornblende
119/B18	0.65	0.69	1.61	0.365	1.23	9.73	magnesio hornblende
119/C19	0.62	0.53	1.50	0.541	1.47	9.63	edenite
119/D20	0.67	0.72	1.60	0.380	1.27	9.80	magnesio hornblende
119/D21	0.64	0.53	1.50	0.412	1.28	9.75	magnesio hornblende
119/D22	0.65	0.63	1.64	0.423	1.36	9.66	magnesio hornblende
119/E23	0.64	0.65	1.64	0.378	1.30	9.64	magnesio hornblende
119/E24	0.63	0.60	1.69	0.444	1.44	9.54	magnesio hornblende
119/F72	0.65	0.43	1.21	0.374	1.09	10.09	magnesio hornblende
119/F73	0.67	0.43	1.19	0.329	1.00	10.19	magnesio hornblende

TABLE: (3-3-4c) Atomic ratios ($Mg/Mg + Fe^2$), coupled substitution and co-ordinates $(X + Y)(Y + Z)$ of the amphiboles of the Serres-Drama granitic complex (continued)

Sample No.	$Mg/Mg+Fe^2$	X+Y	Y+Z	$(Na+K)_A$	Na^A+Al^{iv}	Mg+Si	Nomenclature
			Monzonite				
126/A12	0.64	0.55	1.51	0.488	1.39	9.69	magnesio hornblende
126/A13	0.63	0.47	1.48	0.537	1.47	9.65	edenite
184/A4	0.76	0.41	0.81	0.203	0.64	10.94	actinolite/actinolitic hornblende
184/A5	0.77	0.49	0.86	0.248	0.72	10.94	actinolitic hornblende
184/A6	0.76	0.34	0.60	0.125	0.42	11.25	actinolite
184/B7	0.76	0.24	0.44	0.131	0.36	11.36	actinolite
184/B8	0.77	0.63	1.18	0.214	0.84	10.65	actinolitic hornblende
184/B9	0.78	0.50	0.79	0.109	0.48	11.13	actinolite
184/C16	0.77	0.71	1.34	0.236	0.94	10.50	magnesio hornblende
184/C17	0.73	0.61	1.20	0.282	0.96	10.41	magnesio hornblende
184/C18	0.80	0.62	0.84	0.085	0.42	11.17	actinolite
202/A19	0.58	0.68	2.29	0.839	2.16	8.77	magnesium hastingsitic hornblende
202/A20	0.57	0.45	2.11	0.925	2.27	8.81	ferroan paragasitic hornblende
202/B21	0.59	0.70	2.13	0.757	1.95	9.01	edenitic hornblende

TABLE: (3-3-4c) Atomic ratios ($Mg/Mg + Fe^2$), coupled substitution and co-ordinates $(X + Y)(Y + Z)$ of the amphiboles of the Serres-Drama granitic complex (continued)

Sample No.	$Mg/Mg+Fe^2$	X+Y	Y+Z	$(Na+K)_A$	Na^A+Al^{iv}	Mg+Si	Nomenclature
				Xenolith			
126/Z20	0.67	0.58	1.55	0.364	1.26	9.85	magnesio hornblende
126/Z21	0.64	0.60	1.74	0.544	1.58	9.50	edenite
126/Z22	0.62	0.48	1.61	0.485	1.46	9.50	magnesio hornblende
126/Y23	0.60	0.35	1.42	0.549	1.46	9.57	edenite
6B/A10	0.65	0.61	1.57	0.414	1.32	9.69	magnesio hornblende
6B/A11	0.64	0.49	1.45	0.511	1.42	9.73	edenite
6B/A12	0.64	0.56	1.56	0.469	1.41	9.64	magnesio hornblende
6B/A13	0.64	0.58	1.56	0.450	1.35	9.67	magnesio hornblende
6B/B14	0.66	0.67	1.64	0.374	1.30	9.73	magnesio hornblende
6B/B15	0.62	0.66	1.69	0.423	1.38	9.50	magnesio hornblende
6B/C24	0.63	0.46	1.48	0.570	1.53	9.63	edenite
6B/C25	0.62	0.54	1.59	0.563	1.56	9.53	edenite
6B/D26	0.62	0.41	1.43	0.602	1.55	9.65	edenite
6B/D27	0.62	0.40	1.42	0.504	1.41	9.68	edenite

TABLE: (3-3-4c) Atomic ratios ($Mg/Mg + Fe^2$), coupled substitution and co-ordinates $(X + Y)(Y + Z)$ of the amphiboles of the Serres-Drama granitic complex (continued)

Sample No	$Mg/Mg+Fe^2$	X+Y	Y+Z	$(Na+K)_A$	Na^A+Al^{iv}	Mg+Si	Nomenclature
				Gabbro			
152/A6	0.60	0.74	2.58	0.664	2.31	8.53	ferroan pargasite
152/A7	0.58	0.77	2.68	0.675	2.36	8.37	ferroan pargasite
152/A8	0.50	0.69	2.48	0.632	2.19	8.19	ferroan pargasite
152/A9	0.49	0.75	2.59	0.621	2.19	8.13	ferroan pargasite
152/B28	0.53	0.84	2.62	0.791	2.29	8.37	magnesian hastingsite
152/B29	0.54	0.84	2.51	0.670	2.08	8.51	magnesian hastingsitic hornblende
152/C32	0.58	0.57	2.44	0.732	2.36	8.50	ferroan pargasite
152/C33	0.60	0.66	2.55	0.637	2.28	8.52	ferroan pargasite
152/C34	0.61	0.89	2.58	0.628	2.06	8.69	ferroan pargasitic hornblende
152/C35	0.58	0.84	2.43	0.474	1.82	8.72	tschermakitic hornblende
152/C36	0.53	0.79	2.26	0.579	1.82	8.70	edenite hornblende
152/D39	0.57	0.52	2.07	0.834	2.17	8.90	ferroan pargasitic hornblende
152/D40	0.56	0.46	1.91	0.780	2.03	8.95	edenite hornblende/ferroan pargasitic hornblende

amphiboles of the Serres-Drama granitic complex have a larger range of compositions.

According to the scheme of Rowbotham, (1973), the (X+Y) and (Y+Z) values from table (3-3-4c) have been plotted on the Phillips' compositional space as shown in fig. (3-3-4d). As illustrated in the above figure, the distribution of chemical compositions of the amphiboles range approximately between pargasite and tremolite.

From the distribution of the compositions of the calcic amphiboles, it is apparent that there are present several important substitutions:

$$Fe^{2+} \rightleftharpoons Mg$$

$$Na^{A}\ Al^{IV} \rightleftharpoons \square\ Si \quad \text{(edenite substitution)}$$

$$Al^{IV}\ Al^{VI} \rightleftharpoons (Mg,\ Fe^{2+})\ Si \quad \text{(tschermakite substitution)}$$

$$(Fe,Mg)\ Ti \rightleftharpoons Al^{IV}\ Al^{VI}$$

In summary the amphiboles in the early fractionated rocks in the Serres-Drama complex are higher in ferrous iron and titanium and in the proportion of "edenite" and "tschermakite" than the calcic amphiboles from the more evolved rocks. The two dominant substitutions (edenitic and tschermakitic) are represented in figures (3-3-5a and 3-3-5b) respectively. There is almost a complete solid solution series along the two trends with a small gap in compositions between 6.00 and 6.50 atoms of Si. Although there is a large compositional variation in the amphiboles there is little observed continuous or discontinuous zoning in these minerals.

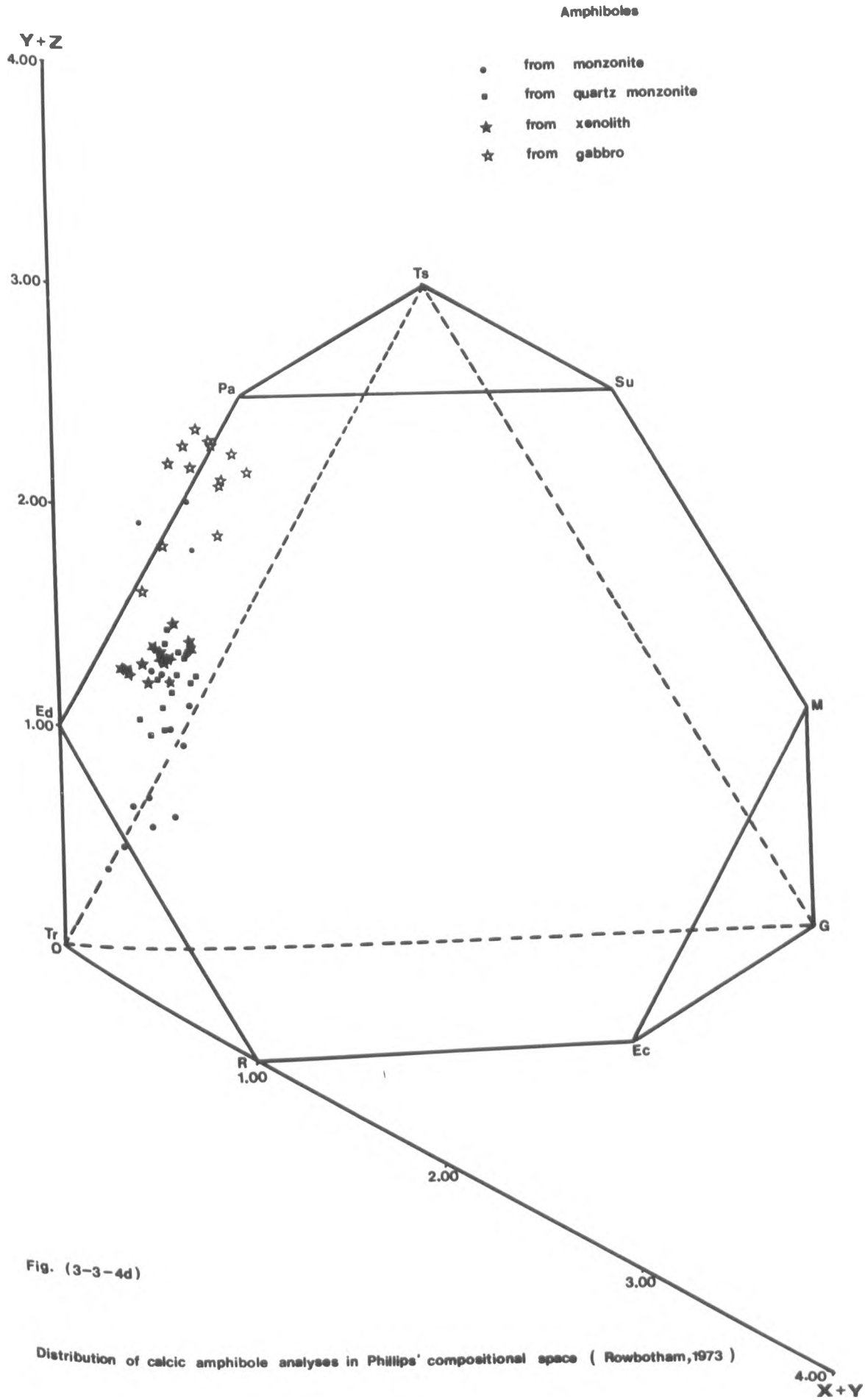

Fig. (3-3-4d)

Distribution of calcic amphibole analyses in Phillips' compositional space (Rowbotham, 1973)

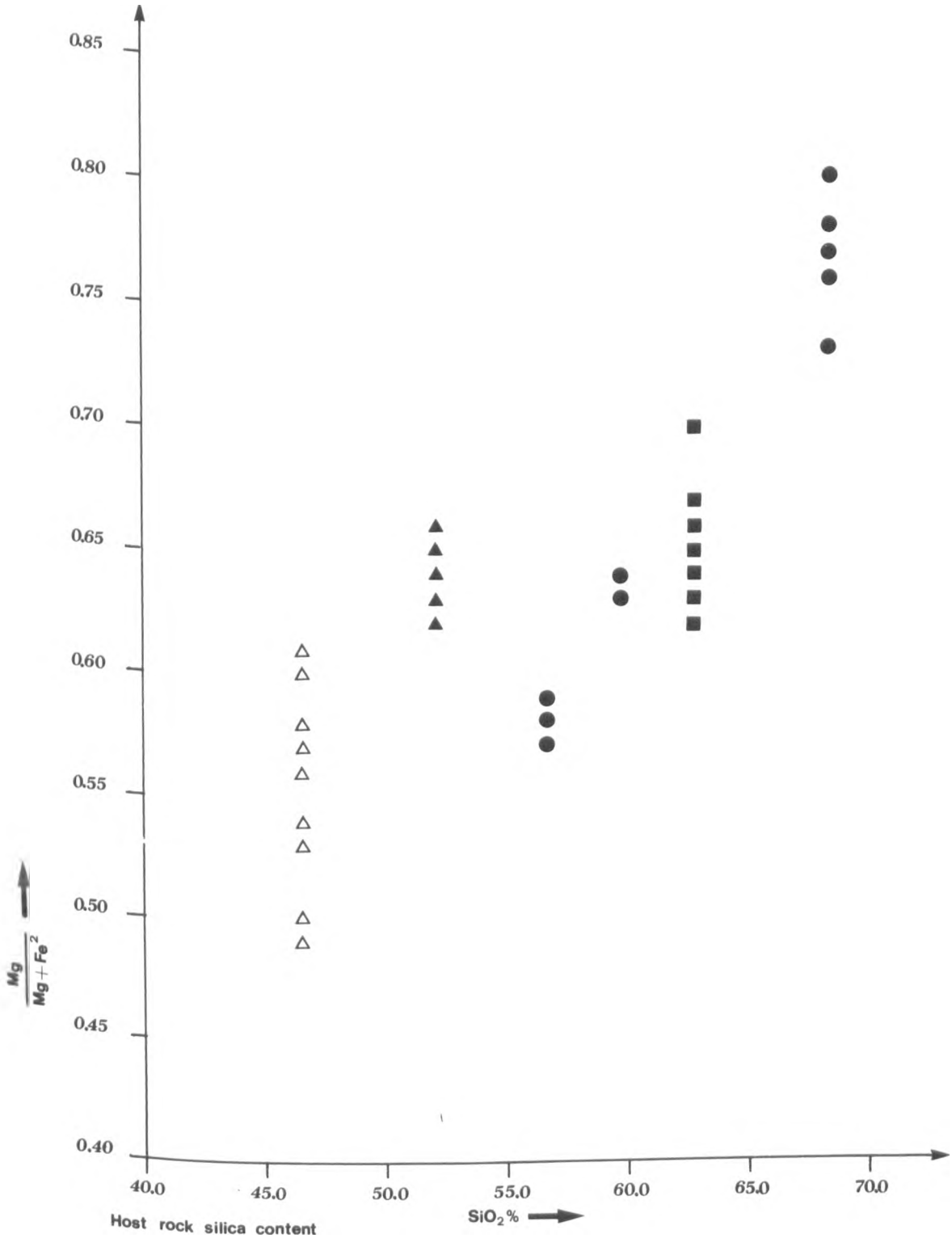

Fig (3-3-4e)

Amphiboles: ● from monzonite; ■ from quartz monzonite; ▲ from xenolith; △ from gabbro

3-3-5 Discussion and conclusion

Systematic analyses of amphiboles from calc-alkaline plutonic rocks have been described by Dodge, Papike and Mays (1968), Czamanske and Wones (1973), Czamanske, Ishihara and Atkin (1981), Chivas (1981) among many other authors and the calcic amphibole compositions are comparable to those present in the Serres-Drama complex.

Dodge, Papike and Mays (1968) reported that the composition of hornblendes from the Sierra Nevade batholith, USA, reveal only a limited correlation with the chemistry of the host rock. This is counter to that observed in the present study, where there is a close correlation between amphibole and bulk rock compositions. In rocks of the same compositon from within the Sierra Nevada batholith, Dodge et. al (op.cit), have found a wide range of compositions, particularly the amount of aluminium in tetrahedral co-ordination ($\langle .75 \rangle$ 1.00 Al^{IV}). The presence of increasing aluminium in tetrahedral sites has been correlated with increasing temperature of origin of the amphibole (Thompson, 1947; Harry, 1950; Leake, 1965, amongst others). This correlation has also been demonstrated experimentally by Helz (1973), who also showed that entry of Ti into the amphibole structure was favoured by high temperature. These observations can be seen in the Serres-Drama complex, where both the highest Al^{IV} and Ti contents are found in primary amphiboles in the gabbro which have crystallised with anorthitic plagioclase. There are compositions close to these also in the monzonite. Both these

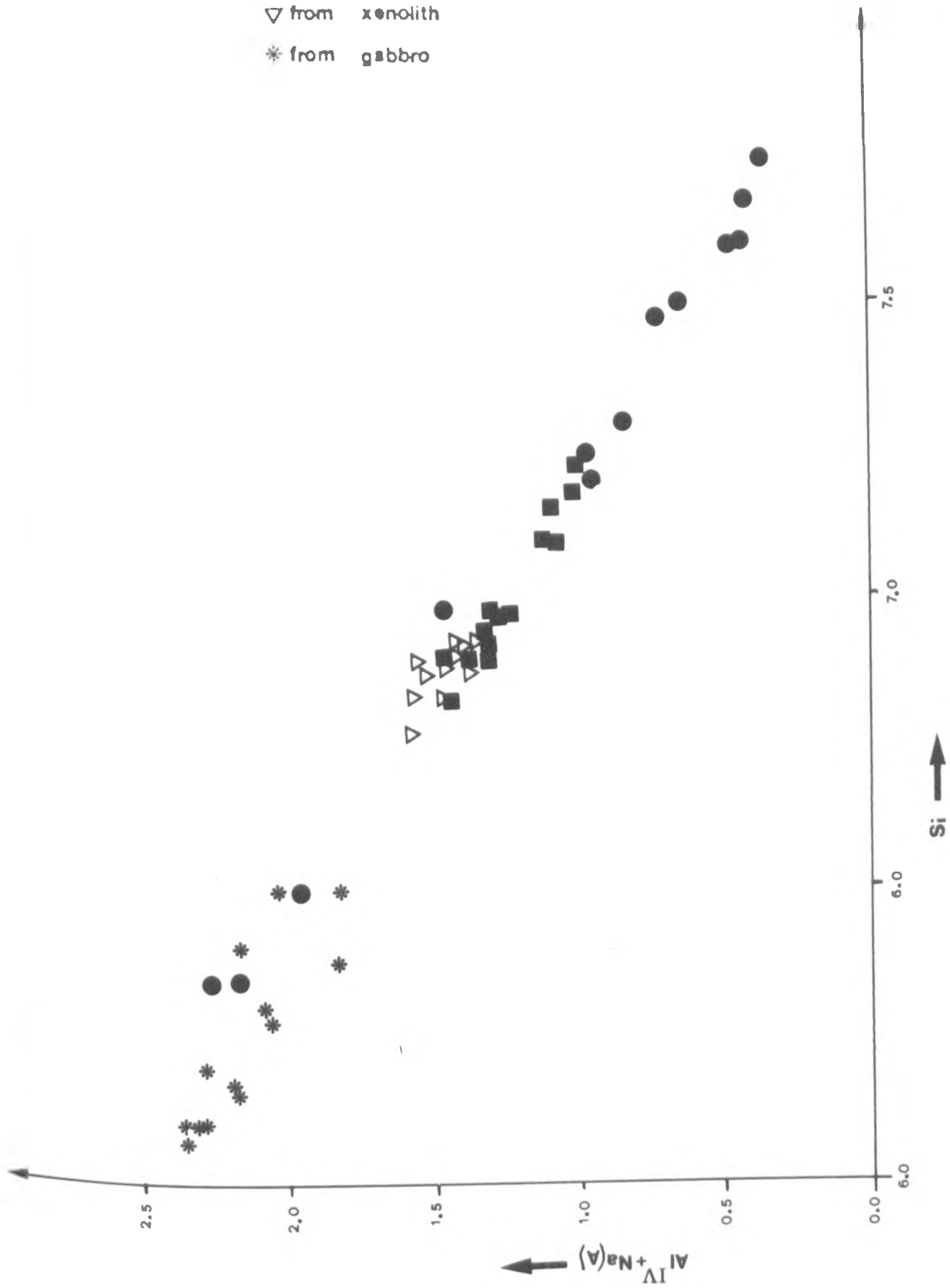
from monzonite
from quartz monzonite
from xenolith
from gabbro
Si
$Al^{IV}+Na(A)$
6.0
7.0
7.5
6.0
0.0
0.5
1.0
1.5
2.0
2.5

Fig. (3-3-5a)

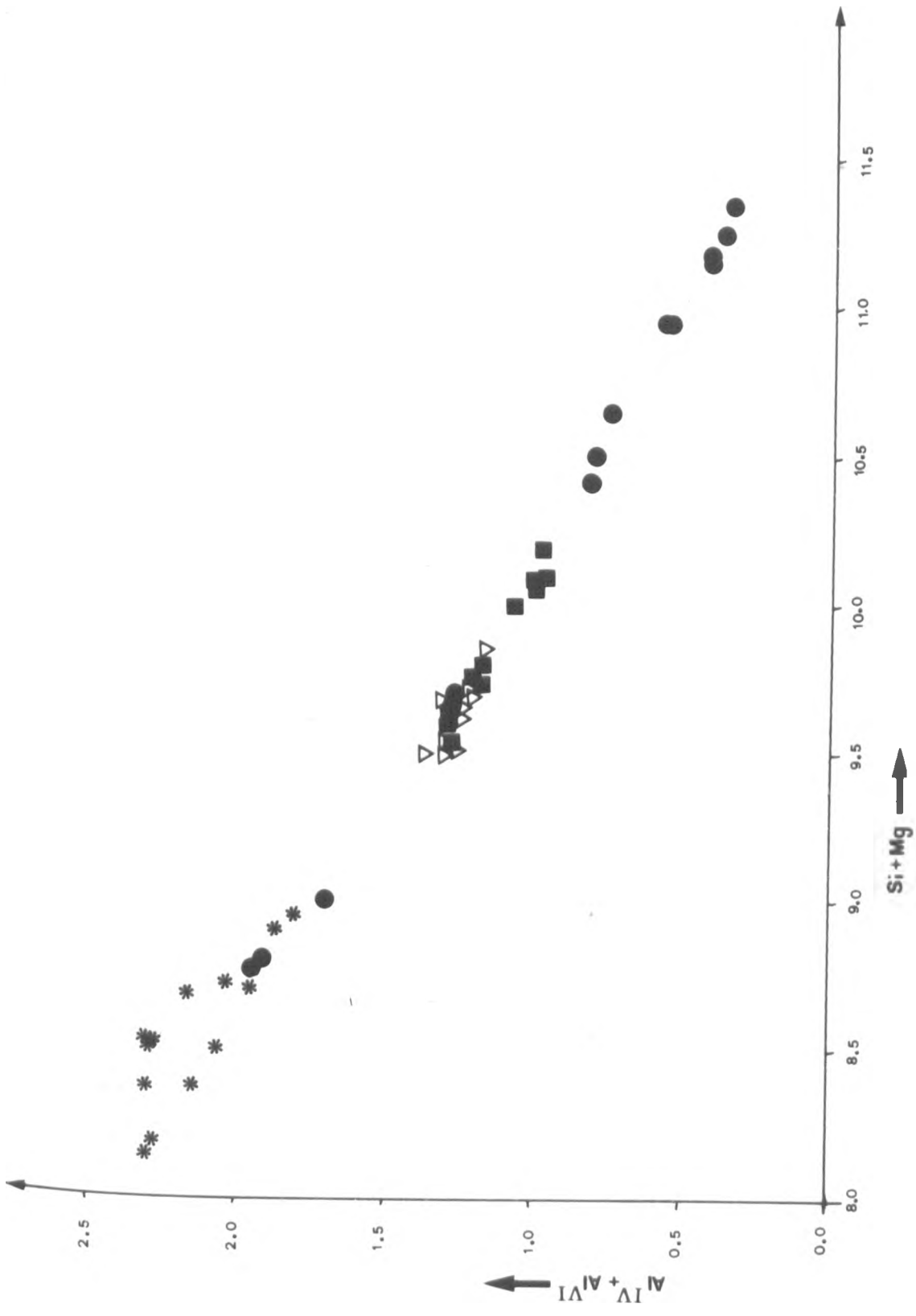
from monzonite
from quartz monzonite
from xenolith
from gabbro
Si + Mg
$Al^{IV} + Al^{VI}$
8.0
8.5
9.0
9.5
10.0
10.5
11.0
11.5
0.0
0.5
1.0
1.5
2.0
2.5

Fig. (3-3-5b)

rock types are thought to be formed at higher temperatures than the rest of the complex.

The following substitutions, as noted in the previous section, are dominant in the Serres-Drama complex:

$$^{A}Na + Al^{IV} \rightleftharpoons \square\ Si \quad (\square \text{ indicates vacancy})$$

edenite substitution

$$Al^{IV} + Al^{VI} \rightleftharpoons (Mg, Fe^{2+})\ S_1$$

tschermakite substitution

Czamanske, Ishihara and Atkin (1981) and Chivas (1981) also show that 'edenite' and 'tschermakite' substitutions are predominant in their amphiboles. These substitutions are obviously linked with temperature of origin, i.e. amphiboles with high, 'edenite' and 'tschermakite' components form at higher temperature and vice versa. Helz (op. cit) also noted this phenomenon in her experiments on hydrous basalt.

Czamanske and Wones (1973) in their analysis of amphiboles (from monzonite and granodiorite) from the Finnemarka complex of Norway also interpreted the compositional trends, particulary ($Fe \rightleftharpoons Mg$), as reflecting crystallisation under progressively more oxidizing conditions with decreasing temperatures.

Amphiboles could be involved in oxidation reactions and also reflect the oxidation-reduction processes occuring in the various stages of magmatic evolution.

Czamanske, Ishihara and Atkin (1981) suggest that oxidation of the magnetite bearing rocks may have occurred during crystallisation near the level of intrusion, due to

secondary boiling and/or differential loss of hydrogen. This suggestion is based on the constant or increasing $Mg/M_g + Fe^2$ ratio for amphiboles, coupled with the increase in host silica content and the absence of early formed magnetite and sphene. Although this conclusion may be put forward for the Serres-Drama complex, it must be borne in mind that magnetite and sphene are early formed crystals as they are often euhedral.

The data of table (3-3-4a) indicate that amphibole compositions have been significantly influenced by the magmatic oxidation state (e.g. fig.3-3-4e). The oxygen fugacity increases with the differentiation of magma. The iron in the magma becomes progressively more Fe^{+3} rich according to the equation $Fe^{+2} \rightleftharpoons Fe^{+3}$ so that the amphiboles become more Mg rich because the $Mg/Mg + Fe^{+2}$ ratio increases in the magma.

3-4 BIOTITES

3-4-1 Introduction

The second most abundant mafic mineral after amphibole, observed from petrographic studies, is biotite. The content of biotite is greatest in granite and quartz-monzonite, less in granodiorite and rare in monzonite and gabbro.

The biotites are defined as monoclinic in symmetry with considerable variation in chemical and physical

properties. The general chemical formula for biotites is:

$$K_2 (Fe^{+2}, Mg)_{6-4} (Fe^{+3}, Al, T_1)_{0-2} (Si_{6-5}Al_{2-3}) O_{20-22} (OH,F)_{4-2}$$

(From Deer et al, 1962)

The majority of specimens fall within a field outlined by four end-members, phlogopite, annite, eastonite and siderophyllite (fig. (3-4-2a)).

A limited study of the biotites was done by electron microprobe analysis to determine the chemical composition, to classify the specimens and to attempt to find some evidence for their genesis.

The work by Czamanske, Ishihara and Atkin (1981), shows very close parallels to the Serres-Drama granitic complex and, because of this, the work will be extensively referred to.

3-4-2 Biotites electron microprobe analysis results.

The data for thirty-three biotite analyses by electron microprobe from thirteen grains of four biotite-bearing samples are listed in table (3-4-2a). For comparative purposes, microprobe analyses from the Rhodope massif granitic complexes are given in tables (3-4-2b) (from Christofides, 1977) and (3-4-2c) (from Sklavounos, 1981)

According to the scheme of Deer et al (1962); using the data from table (3-4-2a), Mg / Fe_{total} against Si has been plotted, fig. (3-4-2a). All the analyses fall into the biotite field. The division between biotite-phlogopite compositional fields is arbitrarily

TABLE: (3-4-2a) Microprobe analyses of biotites from the Serres-Drama granitic complex

	119R A1	119R A2	119R A3	119R A4	119R B5	119R B6	119R B7	119R C8	119R D9	119R D10
SiO_2	37·58	37·75	37·78	37·92	38·03	37·67	37·88	37·59	37·71	37·53
TiO_2	3·73	3·58	3·76	3·79	3·33	3·21	2·23	3·06	3·54	3·41
Al_2O_3	14·68	14·08	14·18	14·40	14·19	14·56	14·85	14·42	14·47	14·20
FeO	17·99	18·31	18·16	17·65	18·10	18·28	17·50	17·80	17·02	17·29
MnO	0·26	0·49	0·40	0·44	0·41	0·45	0·59	0·40	0·35	0·37
MgO	12·08	11·92	12·32	12·86	12·45	12·21	12·56	12·45	12·95	13·15
Na_2O	-	-	-	-	-	-	-	-	-	-
K_2O	9·64	9·49	9·60	9·54	9·34	9·18	9·20	8·95	9·42	9·56
Cl	-	-	-	0·17	0·21	0·17	0·17	0·17	0·15	0·12
Total	95·96	95·62	96·20	96·77	96·06	95·73	94·98	94·84	95·61	95·63
	Numbers of ions on the basis of 22(O)									
Si	5·658	5·715	5·681	5·660	5·725	5·690	5·743	5·712	5·676	5·664
Al	2·605	2·513	2·513	2·534	2·517	2·592	2·655	2·583	2·568	2·526
Ti	0·422	0·407	0·425	0·425	0·377	0·365	0·255	0·350	0·400	0·387
Fe_t	2·265	2·319	2·284	2·203	2·278	2·309	2·219	2·263	2·142	2·183
Mn	0·033	0·063	0·051	0·055	0·052	0·058	0·075	0·051	0·044	0·047
Mg	2·711	2·689	2·761	2·862	2·794	2·750	2·838	2·820	2·904	2·959
Na	-	-	-	-	-	-	-	-	-	-
K	1·851	1·833	1·842	1·816	1·973	1·769	1·779	1·734	1·808	1·840
Cl	-	-	-	0·044	0·207	0·044	0·043	0·045	0·037	0·031
Mg/Fe_t	1·197	1·160	1·209	1·299	1·227	1·191	1·279	1·246	1·356	1·355
$Mg/Mg+Fe_t$	0·545	0·537	0·547	0·565	0·551	0·544	0·561	0·555	0·576	0·575

TABLE: (3-4-2a) Microprobe analyses of biotites from the Serres-Drama granitic complex (continued)

	119R E11	119R E12	119R F70	119R F71	184R A1	184R A2	184R A3	184R B12	184R B13	184R B14
SiO_2	38·18	37·60	36·81	36·70	37·09	37·28	37·19	38·10	37·04	36·71
TiO_2	3·70	3·68	2·98	3·59	4·90	4·70	4·45	4·37	4·74	4·82
Al_2O_3	14·64	14·38	15·07	14·92	14·23	14·56	14·09	14·66	14·09	14·01
FeO	17·07	16·58	17·67	18·15	18·37	18·16	17·94	16·69	18·06	17·50
MnO	0·36	0·43	0·45	0·51	0·44	0·35	0·41	0·42	0·32	0·42
MgO	12·91	12·52	10·21	10·48	12·80	12·89	12·90	12·17	12·76	12·97
Na_2O	-	-	-	-	0.70	-	-	-	-	-
K_2O	9·30	9·09	9·44	9·47	9.28	9·48	9·55	8·59	9·38	9·11
Cl	0·17	0·15	0·15	0·12	-	-	-	-	-	-
Total	96·33	94·43	92·78	93·94	97·81	97·42	96·53	95·00	96·39	95·54

Numbers of ions on the basis of 22(O)

Si	5·698	5·711	5·738	5·669	5·508	5·537	5·579	5·716	5·562	5·548
Al	2·573	2·574	2·768	2·412	2·491	2·548	2·492	2·592	2·494	2·495
Ti	0·414	0·420	0·349	0·417	0·548	0·525	0·502	0·494	0·536	0·548
Fe_{tot}	2·129	2·106	2·304	2·344	2·282	2·256	2·251	2·094	2·268	2·212
Mn	0·046	0·055	0·059	0·067	0·056	0·044	0·052	0·054	0·041	0·054
Mg	2·868	2·835	2·372	2·412	2·834	2·855	2·883	2·722	2·856	2·922
Na	-	-	-	-	0·203	-	-	-	-	-
K	1·768	1·762	1·876	1·866	1·759	1·797	1·828	1·644	1·796	1·756
Cl	0·042	0·039	0·039	0·031	-	-	-	-	-	-
Mg/Fe_t	1·347	1·346	1·030	1·029	1·242	1·266	1·281	1·300	1·259	1·321
$Mg/Mg+Fe_t$	0·574	0·574	0·507	0·507	0·554	0·559	0·562	0·565	0·557	0·569

TABLE: (3-4-2a) Microprobe analyses of biotites from the Serres-Drama granitic complex(continuted)

	184R B15	202R A13	202R A14	202R A15	202R B16	202R B17	202R B18	202R C55	202R C56	6-bX A16
SiO_2	37·08	36·59	37·82	38·14	38·11	38·10	37·24	37·96	37·56	38·27
TiO_2	4·88	2·92	3·01	3·00	2·88	2·82	3·07	2·62	2·80	3·44
Al_2O_3	14·29	14·21	13·63	13·54	13·49	13·70	13·77	14·15	13·74	14·11
FeO	16·89	17·31	17·02	16·26	15·67	16·18	16·96	16·06	16·06	18·08
MnO	0·51	-	-	0·47	0·30	0·36	0·42	0·47	0·56	0·58
MgO	12·50	13·72	14·20	14·78	14·43	14·77	14·27	14·49	14·06	11·49
Na_2O	-	-	-	-	-	-	-	-	-	-
K_2O	9·02	9·37	9·59	9·69	9·83	9·53	9·72	9·62	9·81	9·49
Cl	-	-	-	-	-	-	-	-	-	-
Total	95·17	94·12	95·27	95·88	94·71	95·46	95·45	95·37	94·59	95·46

Numbers of ions on the basis of 22(O)

Si	5·599	5·606	5·707	5·710	5·761	5·718	5·632	5·703	5·709	5·788
Al	2·543	2·566	2·425	2·390	2·403	2·423	2·456	2·505	2·462	2·516
Ti	0·555	0·336	0·342	0·337	0·327	0·319	0·349	0·295	0·320	0·392
Fe_{total}	2·132	2·218	2·148	2·036	1·981	2·030	2·145	2·018	2·041	2·287
Mn	0·065	-	-	0·059	0·038	0·046	0·054	0·060	0·072	0·074
Mg	2·813	3·133	3·194	3·300	3·253	3·303	3·216	3·246	3·186	2·591
Na	-	-	-	-	-	-	-	-	-	-
K	1·737	1·831	1·847	1·851	1·895	1·825	1·718	1·844	1·902	1·830
Cl	-	-	-	-	-	-	-	-	-	-
Mg/Fe_{total}	1·319	1·413	1·487	1·621	1·642	1·627	1·499	1·609	1·561	1·133
$Mg/Mg+Fe_{tot}$	0·569	0·585	0·598	0·618	0·622	0·619	0·600	0·617	0·610	0·531

TABLE: (3-4-2a) Microprobe analyses of biotites from the Serres-Drama granitic complex (continued)

	6-bX A17	6-bX B18	6-bX B19
SiO_2	38·26	37·19	37·67
TiO_2	3·29	4·36	3·88
Al_2O_3	14·00	14·31	14·48
FeO	18·26	19·48	18·90
MnO	0·36	0·60	0·59
MgO	11·77	10·20	10·53
Na_2O	-	-	-
K_2O	9·58	9·71	9·50
Cl	-	-	-
Total	95·52	95·85	95·55

Numbers of ions on the basis of 22(O)

Si	5·787	5·665	5·722
Al	2·496	2·569	2·592
Ti	0·374	0·500	0·443
Fe_{total}	2·309	2·482	2·401
Mn	0·046	0·077	0·075
Mg	2·653	2·316	2·384
Na	-	-	-
K	1·849	1·886	1·841
Cl	-	-	-
Mg/Fe_{total}	1·149	0·933	0·993
$Mg/Mg+Fe_{tot}$	0·535	0·483	0·498

TABLE: (3-4-2b) Microprobe analyses of biotites from the Xanthi plutonic complex (Christofides, 1977)

	250	A41	156	210	A125	280	A44	A58	42	44
SiO_2	36.48	36.85	37.14	37.23	38.13	37.22	37.39	37.50	37.69	37.82
TiO_2	4.75	4.91	5.32	5.25	4.28	6.61	4.80	5.26	4.83	4.36
Al_2O_3	13.78	13.46	13.19	13.72	13.52	13.02	13.59	14.10	13.26	13.34
Fe_2O_3	2.99	3.63	4.16	3.85	0.59	3.11	1.33	2.78	4.99	1.36
FeO	15.36	14.79	15.03	14.14	17.47	18.46	15.52	9.52	13.65	15.52
MnO	0.37	0.53	0.47	0.41	0.52	-	0.12	-	0.32	0.21
MgO	12.44	12.39	12.57	13.03	12.92	10.01	14.11	17.32	12.93	13.92
CaO	0.11	-	-	-	0.11	0.22	-	0.23	0.20	0.17
K_2O	9.31	9.36	9.56	9.52	9.65	9.44	9.43	8.47	9.37	9.39
Na_2O	0.23	0.31	0.11	0.17	0.21	0.31	0.33	0.43	0.31	0.29
total	95.82	96.23	97.55	97.32	97.40	98.40	96.62	95.61	97.55	96.38
				Number of ions on the basis of 22(O)						
Si_{IV}	5.502	5.531	5.512	5.504	5.628	5.538	5.558	5.469	5.557	5.633
Al^{3+}	2.451	2.382	2.308	2.391	2.372	2.284	2.382	2.424	2.305	2.343
Fe_{VI}	0.047	0.087	0.180	0.105	-	0.178	0.060	0.107	0.138	0.024
Al	-	-	-	-	0.012	-	-	-	-	-
Ti	0.539	0.554	0.594	0.584	0.482	0.740	0.537	0.577	0.536	0.488
Fe^{3+}	0.292	0.323	0.285	0.323	0.066	0.170	0.089	0.198	0.416	0.128
Fe^{2+}	1.938	1.857	1.866	1.748	2.186	2.297	1.930	1.161	1.683	1.933
Mg	2.796	2.772	2.780	2.871	2.880	2.220	3.126	3.764	2.841	3.090
Mn	0.047	0.067	0.059	0.051	0.066	-	0.015	-	0.040	0.026
K	1.792	1.793	1.810	1.796	1.829	1.792	1.789	1.576	1.763	1.785
Ca	0.018	-	-	-	0.018	0.035	-	0.036	0.032	0.027
Na	0.067	0.090	0.032	0.049	0.061	0.089	0.095	0.122	0.089	0.084
$\frac{Fetot}{Fetot + Mg}$	0.44	0.44	0.44	0.42	0.44	0.53	0.39	0.42	0.425	0.40

TABLE: (3-4-2c) Microprobe analyses of Biotites from the Paranesti (Dipotamos) granite (Sklavounos, 1981)

	29A	29B	30	32	34A	34B	35	36
SiO_2	34.84	38.61	36.09	34.25	33.12	34.91	35.15	37.18
Al_2O_3	16.53	16.80	16.33	17.18	17.41	17.45	15.60	16.23
Fe_2O_3	22.23	19.82	22.03	27.00	2.18	25.39	22.41	20.69
FeO					25.15			
TiO_2	3.27	3.30	2.91	3.52	3.73	3.75	3.79	2.85
MnO^2	0.70	0.67	0.60	0.38	0.59	0.49	0.69	0.70
MgO	7.93	6.67	8.38	4.71	5.27	5.32	7.84	8.63
CaO	0.05	0.07	0.06	0.03	0.06	0.08	0.05	0.18
Na_2O	0.10	0.12	0.11	0.06	0.07	0.10	0.08	0.10
K_2O	9.56	9.62	9.52	9.78	9.08	9.52	9.76	9.52
Total	95.21	95.68	96.03	96.91	96.66	97.01	95.37	96.08

Number of ions on the basis of 22(O)

Si_{IV}	5.518	5.846	5.548	5.366	5.213	5.403	5.487	5.662
Al_{+3}	2.482	2.154	2.452	2.634	2.787	2.597	2.513	2.338
Fe_{VI}	-	-	-	-	-	-	-	-
Al	0.510	0.845	0.508	0.538	0.444	0.587	0.357	0.575
Ti_{+3}	0.377	0.376	0.336	0.415	0.442	0.436	0.445	0.327
Fe_{+2}	2.854	2.510	2.832	3.537	0.257	3.286	2.295	2.635
Fe					3.229			
Mn	0.091	0.086	0.079	0.051	0.079	0.064	0.091	0.091
Mg	1.815	1.505	1.919	1.099	1.232	1.227	1.823	1.958
Ca	0.008	0.011	0.010	0.005	0.010	0.013	0.008	0.029
Na	0.030	0.034	0.033	0.018	0.021	0.030	0.024	0.029
K	1.873	1.858	1.867	1.954	1.823	1.880	1.943	1.850
$\frac{Fetot}{Fetot+Mg}$	0.61	0.62	0.59	0.76	0.73	0.73	0.55	0.57

TABLE: (3-4-2c) Microprobe analyses of Biotites from the Paranesti (Dipotamos) granite(Sklavounos, 1981)

	37	39	40	44	47	48	49
SiO_2	34.61	34.88	34.63	38.35	31.44	35.58	34.23
Al_2O_3	17.65	17.08	17.24	16.62	14.01	15.72	17.03
Fe_2O_3	1.01	3.00	1.85	17.83	17.26	3.85	25.85
FeO	25.88	23.15	23.00		10.21	18.62	
TiO_2	4.80	3.22	3.41	2.26	0.40	2.55	3.81
MnO	0.35	0.30	0.22	1.63	8.27	1.08	0.61
MgO	4.32	5.19	6.06	9.75	9.18	8.93	4.83
CaO	-	0.05	0.07	0.18	0.51	0.04	0.01
Na_2O	0.07	0.09	0.11	0.14	0.15	0.08	0.09
K_2O	9.30	9.50	9.52	9.66	5.40	9.60	9.56
total	98.19	96.46	96.11	96.42	96.83	96.05	96.02

Numbers of ions on the basis of 22(O)

Si_{IV}	5.316	5.448	5.398	5.747	5.084	5.511	5.385
Al^{+3}	2.684	2.552	2.602	2.253	2.670	2.484	2.615
Fe_{VI}	-	-	-	-	0.246	-	-
Al	0.548	0.585	0.566	0.683	-	0.381	0.544
Ti	0.554	0.378	0.400	0.255	0.049	0.297	0.451
Fe^{+3}	0.116	0.352	0.215	2.235	1.773	0.448	3.401
Fe^{+2}	3.303	3.010	2.991		1.327	2.398	
Mn	0.045	0.039	0.029	0.207	1.133	0.141	0.081
Mg	0.988	1.208	1.408	2.177	2.213	2.062	1.133
Ca	-	0.008	0.011	0.029	0.047	0.007	0.002
Na	0.021	0.028	0.034	0.041	1.114	0.024	0.028
K	1.822	1.892	1.894	1.848	0.049	1.897	1.919
$\frac{Fetot}{Fetot+Mg}$	0.77	0.73	0.69	0.50	0.58	0.58	0.75

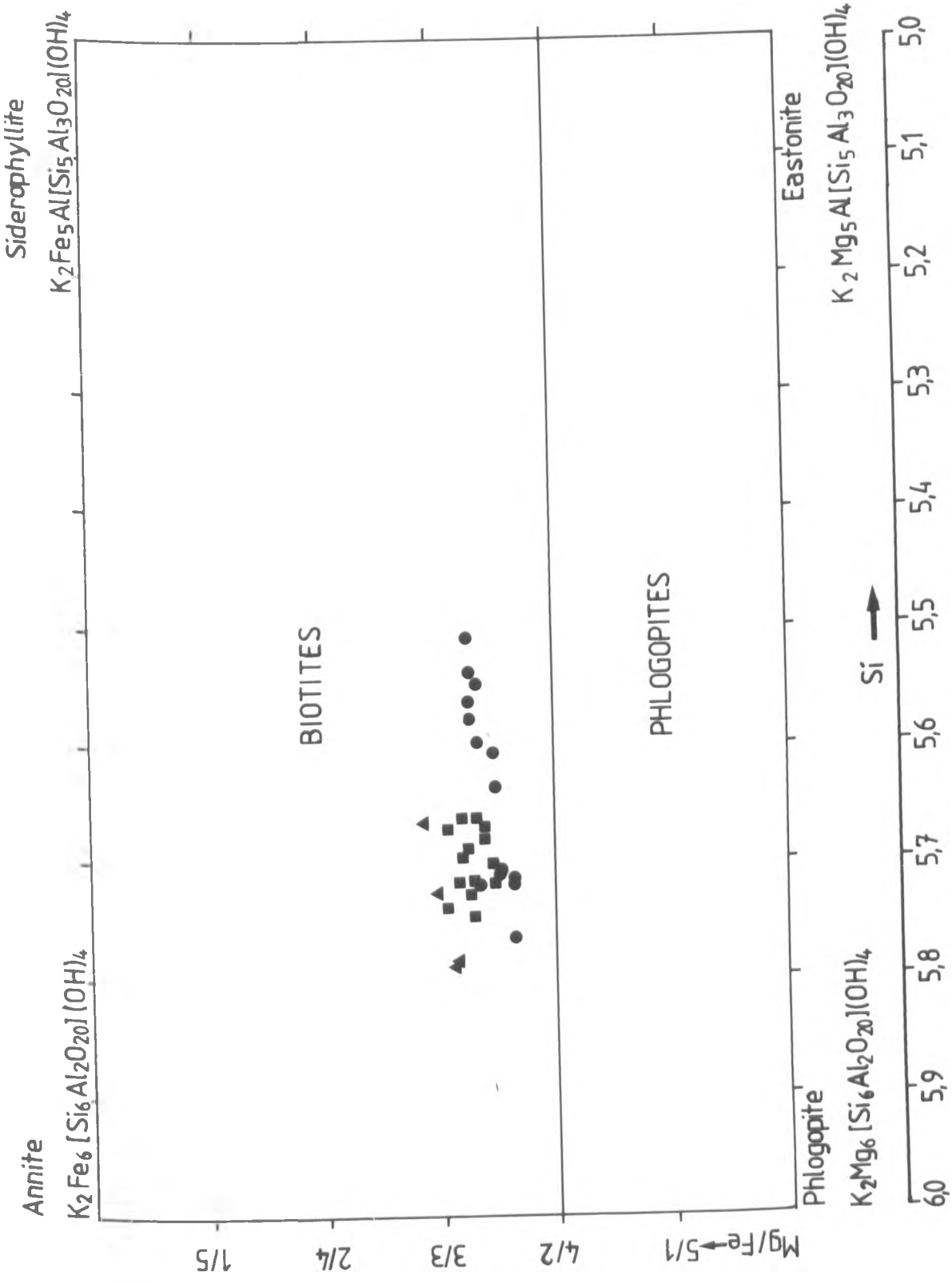

Fig. (3-4-2a) (From Deer et. al. 1962)

Biotites :

- ■ from quartz monzonite
- ● from monzonite
- ▲ from xenolith

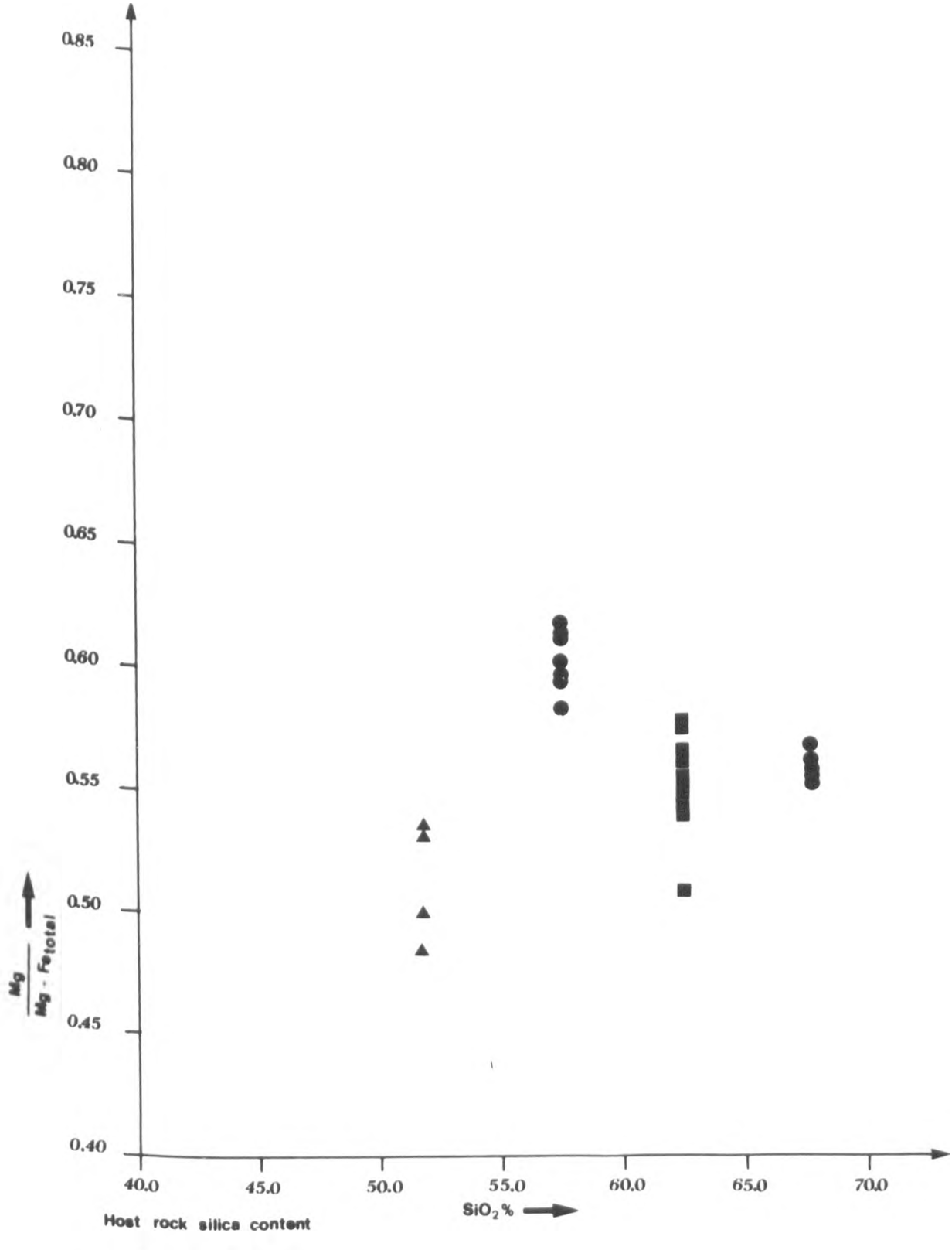

Fig. (3-4-2 b)

Biotites: ● from monzonite; ■ from quartz monzonite; ▲ from xenolith;

chosen to be where Mg: Fe = 2:1. The range in silica content in tetrahedral sites is from 5.51 to 5.79 and the range in ratio $Mg/_{Fe\ total}$ is from 0.93 to 1.64.

The ratio $Mg/_{Mg + Fe\ total}$ against the host rock silica content has also been plotted, fig. (3-4-2b). In the above diagram it can be seen that there is no substantial difference between samples in the ratio $Mg/_{Mg + Fe\ total}$.

The range of Mg, Fe total and Al^{IV} in tetrahedral sites) atoms per formula unit are correspondingly 2.220 to 3.764, 1.359 to 2.467 and 2.284 to 2.451 (in Christofides, 1977), 0.988 to 2.213, 2.510 to 3.486 and 2.154 to 2.787 (in Skalavounos, 1981) and 2.316 to 3.303, 1.981 to 2.482 and 2.390 to 2.605 in the present study, including the dioritic xenolith.

3.4.3 Discussion and conclusion

Intermediate rocks of calc-alkaline affinities are characterised by biotite which occurs in a wide range of rocks of hybrid origin (Deer et al, 1962, Vol.3).

Gokhale (1968) concluded that the chemical composition of biotite reflected the environment in which it was formed and also that of its host rock. Biotites are the ferromagnesian minerals which are found most commonly in granitic rocks.

Dodge, Smith and Mays (1969) in their study of

biotites of central Sierra Nevada and Inyo mountains of California, observed a compositional trend which suggested that oxygen fugacities in the magma during the crystallisation of biotites were a little higher than those within the definition of the Ni-NiO buffer. In addition, it seemed that the magma was "buffered" as regards oxygen by oxides which exist inside the magma.

As an inferred temperature indicator, the correlation between the ratio Fe/Fe + Mg and other elements is poor; consequently factors, apart from temperature during the crystallisation, must have had a significant influence on the composition of the biotites.

Czamanske and Wones (1973) observed a comparative trend in biotites (from monzonite and granodiorite) which they interpreted as reflecting crystallisation under increasingly oxidizing conditions. The average ratio Fe/Fe + Mg for biotites from successively more silicic rock types changes from 0.64 → 0.35 → 0.28. In comparison, this ratio in the Serres-Drama complex also decreases although the range is much smaller.

Ishihara (1977, in Czamanske et al, 1981) in his study of a 'magnetite' series calc-alkaline plutonic belt along the Japan Sea side of Southwest Japan has found that "it has been characterised by progressive oxidation during crystallisation and magmatic differentiation". The evidence cited by Ishihara (op.cit.) is largely based upon the decrease in $Fe/_{Fe + Mg}$ in coexisting biotites and amphiboles. Czamanske, Ishihara and Atkin (1981) observed a

constant or decreasing ratio of $Fe/_{Fe + Mg}$ for biotite with increasing host silica content.

Lack of substantial change in Al^{IV} and the ratio $Fe/_{Fe + Mg}$ content in biotites from the Serres-Drama complex suggests that "they do not record significant changes in crystallisation history".

The most significant aspect of the variations in biotite chemistry in biotites of the Serres-Drama complex is the constant or decreasing ratio Fe/Mg + Fe which is coupled with increasing host rock silica content, and this can be correlated with other examples of the 'magnetite' series, as defined by Ishihara (op.cit). As shown in fig. (3-4-2b), the variation in biotite composition appears to have been influenced by progressive oxidation during the magmatic crystallisation, as in the amphiboles.

3-5 PYROXENES

3-5-1 Introduction

Pyroxenes were named by Haüy from the Greek, "pyro" meaning fire and "xenos", meaning stranger.

Pyroxenes are an important group of rock-forming ferromagnesian silicates and include orthopyroxenes (orthorhombic in symmetry) and clinopyroxenes (monoclinic in symmetry).

Clinopyroxenes have been observed from petrographic

Nomenclature of clinopyroxenes in the system $CaMgSi_2O_6$–$CaFeSi_2O_6$–$Mg_2Si_2O_6$–$Fe_2Si_2O_6$ (after Poldervaart and Hess, 1951).

Fig. (3—5—1a) From Deer et al. (1978)

studies, in monzonites, gabbros and dioritic xenoliths of the Serres-Drama granitic complex.

The classification of the clinopyroxenes is based on the chemical composition, according to the scheme of Deer et al (1978) fig. (3-5-1a). The diopside-salite-ferrosalite-hedenbergite minerals form a complete solid solution series between Ca Mg Si_2 O_6 and Ca Fe^{+2} Si_2 O_6, but most of them contain other ions.

The pyroxenes' structural formula is M_2 M_1 $(Si,Al)_2O_6$ and in calcic pyroxenes the calcium ions occupy more than two-thirds of M_2 positions.

A short study of clinopyroxenes was undertaken, using electron microprobe analysis. The main aim was to determine the chemical compositions (fig. 3-5-1a) in order to classify them and to look for evidence for their genesis.

3-5-2 Clinopyroxenes electron microprobe analysis results.

Table (3-5-2a) lists thirty analyses from fifteen grains, from clinopyroxene-bearing samples (202R monzonite, 4 grains; 126X xenolith in monzonite, 3 grains; 152R gabbro, 8 grains). Microprobe analyses from the Xanthe complex are given in table (3-5-2b) (from Christofides, 1977) for comparison.

The data from table (3-5-2a) have been plotted on the triangle Mg, Fe(M) and Ca, fig. (3-5-2a). Twenty-six

TABLE: (3-5-2a) Microprobe analyses of clinopyroxenes from the Serres-Drama granitic complex

	202R A1	202R A2	202R A3r	202R B4c	202R B5	202R B6r	202R C7	202R C8	202R C9	202R D10
SiO_2	51·65	51·67	51·50	52·96	52·13	51·91	51·34	51·93	50·56	51·08
TiO_2	0·27	-	-	-	-	-	0·24	-	0·46	0·29
Al_2O_3	1·57	0·80	0·83	0·72	0·59	0·74	1·52	1·70	1·82	1·90
FeO	10·75	9·22	9·22	9·57	9·50	9·57	11·06	10·77	11·14	11·26
MnO	0·57	0·73	0·61	0·53	0·54	0·59	0·48	0·55	0·57	0·47
MgO	11·65	11·59	12·29	12·13	12·14	11·77	11·16	11·37	11·15	11·23
CaO	23·67	23·40	23·71	24·18	24·05	23·82	23·41	23·45	23·37	23·63
Na_2O	1·06	0·60	0·64	0·67	0·66	0·75	0·92	0·78	0·66	0·66
K_2O	-	-	-	-	-	-	-	-	-	-
Total	101·19	98·01	98·80	100·76	99·61	99·15	100·13	100·55	99·73	100·52

Numbers of ions on the basis of 6(O)

Si_{iv}	1·940	1·987	1·968	1·982	1·977	1·978	1·950	1·957	1·931	1·934
Al^{iv}	0·060	0·013	0·032	0·018	0·023	0·022	0·050	0·043	0·069	0·066
Al^{vi}	0·010	0·023	0·006	0·014	0·004	0·011	0·018	0·032	0·013	0·019
Ti	0·007	-	-	-	-	-	0·007	-	0·013	0·008
Fe	0·338	0·296	0·295	0·300	0·301	0·305	0·351	0·340	0·356	0·357
Mn	0·018	0·024	0·020	0·017	0·017	0·019	0·015	0·018	0·018	0·015
Mg	0·653	0·665	0·700	0·677	0·686	0·669	0·632	0·639	0·635	0·634
Ca	0·953	0·964	0·971	0·970	0·977	0·973	0·953	0·947	0·956	0·959
Na	0·077	0·045	0·047	0·049	0·048	0·055	0·067	0·057	0·049	0·049
K	-	-	-	-	-	-	-	-	-	-
$Mg/Mg+Fe_t$	0·659	0·692	0·704	0·693	0·695	0·687	0·643	0·653	0·641	0·640
Fe_t(Mn)%	18·1	16·4	15·9	16·1	16·1	16·5	18·8	18·4	19·0	18·9
Mg%	33·3	34·1	35·2	34·5	34·6	34·0	32·4	32·9	32·3	32·3
Ca%	48·6	49·5	48·9	49·4	49·3	49·5	48·8	48·7	48·7	48·8

TABLE: (3-5-2a) Microprobe analyses of clinopyroxenes from the Serres-Drama granitic complex

	202R D11	202R D12	126X Z16c	126X Z17r	126X Y18	126X Y19	126X X24	126X X25	152R A1	152R B2
SiO_2	52·27	52·44	52·96	52·96	52·93	53·40	53·27	52·68	52·01	51·51
TiO_2	0·24	-	-	-	-	-	-	-	-	0·38
Al_2O_3	1·10	1·06	0·91	0·41	0·64	0·83	0·52	0·45	3·99	2·15
FeO	10·18	10·46	8·42	9·10	9·11	8·91	8·73	8·78	9·83	7·95
MnO	0·52	0·50	0·66	0·75	0·66	0·72	0·67	0·74	0·30	-
MgO	12·03	11·99	13·20	12·99	12·78	13·20	13·13	12·91	13·18	12·75
CaO	23·74	23·70	23·79	23·64	23·71	23·95	23·52	23·72	22·82	23·48
Na_2O	0·66	0·52	-	-	0·49	0·50	-	-	0·52	-
K_2O	-	-	-	-	0·10	0·12	-	-	0·13	-
Total	100·74	100·67	99·94	99·85	100·42	101·63	99·84	99·28	102·78	98·22
	Numbers of ions on the basis of 6(O)									
Si	1·963	1·970	1·982	1·991	1·983	1·975	1·996	1·991	1·900	1·954
Al^{iv}	0·037	0·030	0·018	0·009	0·017	0·025	0·004	0·009	0·100	0·046
Al^{vi}	0·011	0·017	0·028	0·009	0·011	0·011	0·019	0·011	0·072	0·050
Ti	0·007	-	-	-	-	-	-	-	-	-
Fe	0·320	0·328	0·264	0·286	0·285	0·276	0·274	0·277	0·300	0·252
Mn	0·017	0·016	0·021	0·024	0·021	0·022	0·021	0·024	0·009	-
Mg	0·673	0·672	0·737	0·728	0·714	0·728	0·734	0·727	0·718	0·721
Ca	0·955	0·954	0·954	0·952	0·952	0·949	0·944	0·960	0·893	0·954
Na	0·048	0·038	-	-	0·036	0·036	-	-	0·037	-
K	-	-	-	-	0·005	0·006	-	-	0·006	-
$Mg/Mg+Fe_t$	0·678	0·672	0·736	0·718	0·715	0·725	0·728	0·724	0·705	0·741
Fe_t(Mn)%	17·2	17·5	14·4	15·6	15·5	15·1	15·0	15·1	16·1	13·1
Mg%	34·2	34·1	37·3	36·6	36·2	36·9	37·2	36·6	37·4	37·4
Ca %	48·6	48·4	48·3	47·8	48·3	48·0	47·8	48·3	46·5	49·5

TABLE: (3-5-2a) Microprobe analyses of clinopyroxenes from the Serres-Drama granitic complex

	152R C3	152R D4	152R E22	152R E23	152R E24	152R F25	152R F26	152R F27	152R G37	152R H38
SiO_2	51·44	53·07	52·15	51·62	53·99	53·70	52·44	53·07	52·69	52·51
TiO_2	-	0·23	-	0·21	0·19	-	0·17	-	0·31	-
Al_2O_3	3·48	1·75	0·55	1·08	1·26	1·02	0·91	0·31	1·78	1·15
FeO	9·93	9·00	7·70	7·68	8·05	8·96	7·97	7·43	8·15	7·91
MnO	0·22	0·28	-	-	-	0·21	-	0·29	-	0·22
MgO	13·17	13·62	13·06	13·04	13·44	13·52	13·57	13·44	13·08	13·26
CaO	21·19	23·80	24·56	24·15	25·11	25·15	24·47	25·16	24·24	24·41
Na_2O	-	-	-	-	0·64	-	0·47	-	-	0·57
K_2O	0·34	-	-	-	-	-	-	-	0·12	-
Total	99·77	101·75	98·02	97·77	102·68	102·56	100·00	99·70	100·37	100·03

Numbers of ions on the basis of 6(O)

Si_{iv}	1·928	1·952	1·987	1·970	1·966	1·965	1·963	1·989	1·959	1·965
Al^{iv}	0·072	0·048	0·013	0·030	0·034	0·035	0·037	0·011	0·041	0·035
Al^{vi}	0·082	0·028	0·012	0·019	0·020	0·009	0·003	0·003	0·037	0·016
Ti	-	0·006	-	0·006	0·005	-	0·005	-	0·005	-
Fe	0·311	0·277	0·245	0·245	0·245	0·274	0·249	0·233	0·253	0·248
Mn	0·007	0·009	-	-	-	0·006	-	0·009	-	0·001
Mg	0·736	0·747	0·741	0·742	0·729	0·738	0·757	0·751	0·725	0·740
Ca	0·851	0·938	1·003	0·988	0·979	0·986	0·981	1·010	0·966	0·979
Na	-	-	-	-	0·045	-	0·034	-	-	0·041
K	-	-	-	-	-	-	-	-	0·005	-
$Mg/Mg+Fe_t$	0·703	0·729	0·752	0·752	0·748	0·729	0·752	0·763	0·741	0·749
Fe(Mn)%	16·7	14·5	12·3	12·4	12·5	14·0	12·5	12·1	13·0	12·7
Mg %	38·6	37·9	37·3	37·6	37·3	36·8	38·1	37·5	37·3	37·6
Ca %	44·7	47·6	50·4	50·0	50·1	49·2	49·4	50·4	49·7	49·7

TABLE: (3-5-2b) Microprobe analyses of clinopyroxenes from the Xanthi plutonic complex (Christofides, 1977)

	42	294	19	58	280	277	46	44	P_3
SiO_2	53·32	53.21	52·27	52·24	51·91	51·72	51·54	51·53	51·39
Al_2O_3	0·62	0·62	1·19	2·18	1·95	1·75	1·82	1·87	2·43
Fe_2O_3	-	-	-	1·38	1·57	0·94	-	-	-
FeO	10·56	7·97	11·16	7·04	9·34	8·53	11·13	11·53	9·24
MgO	13·05	13·98	13·61	14·67	13·91	14·10	14·01	13·18	14·35
MnO	0·63	0·67	0·41	0·34	0·43	0·43	0·51	0·45	0·49
TiO_2	-	-	0·39	0·69	0·92	0·57	0·47	0·93	0·70
CaO	22·02	23·11	20·21	21·73	20·65	20·97	20·21	19·97	20·41
Na_2O	-	-	0·38	-	-	0·53	-	-	0·63
Total	100·20	99·56	99·62	100·27	100·68	99·54	99·69	99·46	99·64

Numbers of ions on the basis of 6(O)

Si	1·997	1·991	1·969	1·931	1·929	1·940	1·941	1·946	1·925
Al	0·003	0·009	0·031	0·069	0·071	0·060	0·059	0·054	0·075
Al	0·024	0·018	0·022	0·026	0·014	0·017	0·022	0·029	0·032
Ti	-	-	0·011	0·019	0·026	0·016	0·013	0·026	0·020
Fe^{3+}	-	-	-	0·038	0·044	0·027	-	-	-
Fe^{2+}	0·331	0·249	0·352	0·218	0·290	0·268	0·351	0·364	0·289
Mg	0·728	0·779	0·764	0·808	0·770	0·788	0·786	0·742	0·801
Mn	0·020	0·021	0·013	0·011	0·014	0·014	0·016	0·014	0·016
Ca	0·884	0·926	0·816	0·861	0·822	0·843	0·816	0·808	0·819
Na	-	-	0·028	-	-	0·039	-	-	0·046
Ca%	45·02	46·87	41·95	44·47	43·36	44·08	41·43	41·91	42·55
Mg%	37·11	39·43	39·29	41·74	40·62	41·22	39·94	38·46	41·61
Fe_{tot}(Mn)%	17·87	13·69	18·75	13·79	16·02	14·71	18·63	19·63	15·84

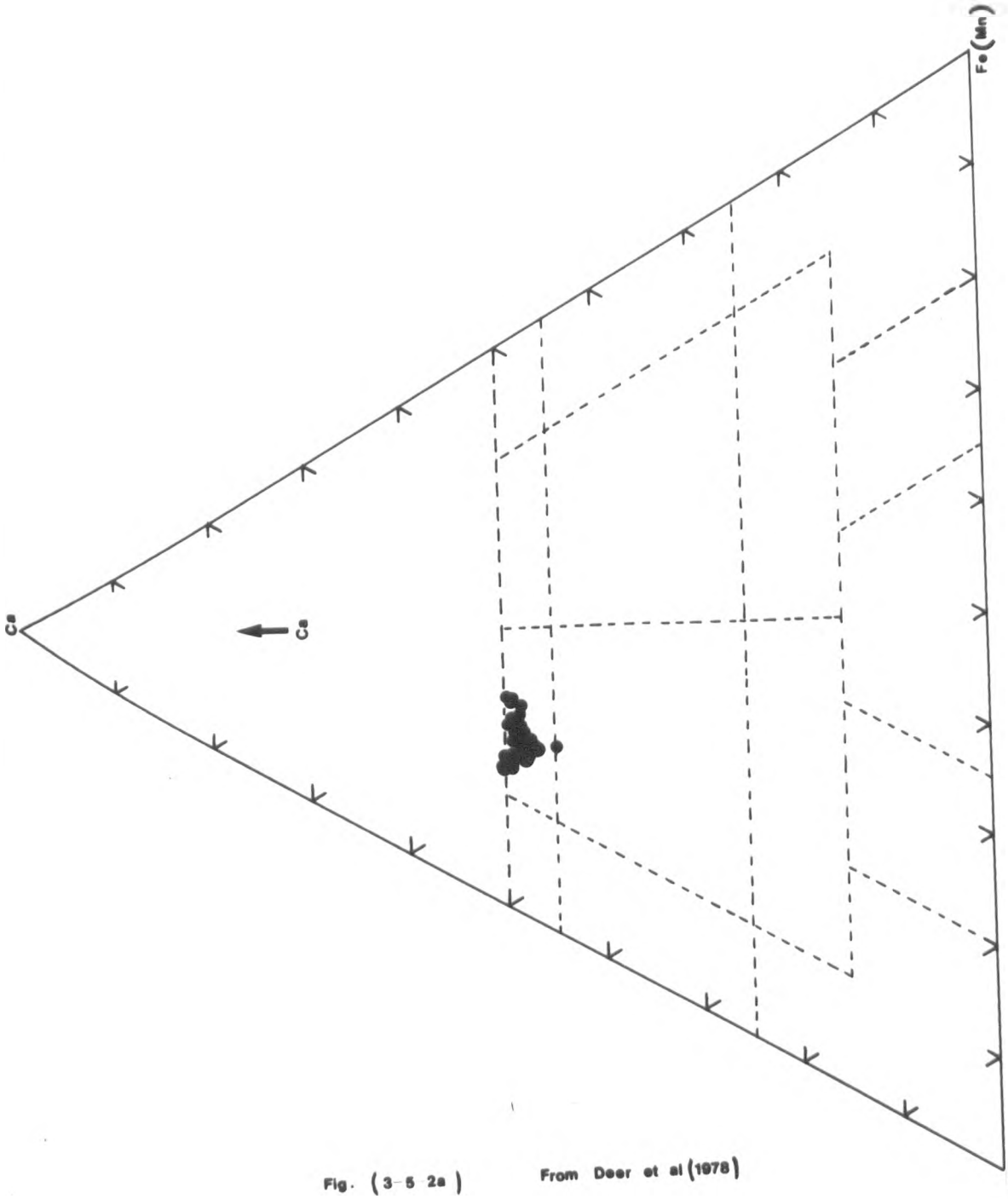

Fig. (3-5 2a) From Deer et al (1978)

analyses (86.7%), when plotted, fall into the compositional fields of salite, the remaining four from gabbro, fall close to but outside the artificial boundary. But, as the divisions between compositional fields are arbitrary, they can be classified as salite.

As expected in the present study, the clinopyroxenes have high CaO (ranging from 21.19% to 25.99%) and low Al_2O_3 (ranging from 0.31% to 3.99%) contents. In Christofides' (1977) analyses the CaO is a slightly less (ranging from 19.77% to 23.11%) but the Al_2O_3 has a smaller range (0.62% to 2.43%) which lies between the extreme values of the present study. Also the TiO_2 content is very low, only being found in eleven out of thirty analyses.

The range of Al^{IV}, Mg and Fe total atoms per formula unit are correspondingly 0.003 to 0.075, 0.728 to 0.808 and 0.249 to 0.757 (in Christofides, 1977), 0.004 to 0.072, 0.632 to 0.757 and 0.233 to 0.357 in the present study.

From the above comparison it can be seen that the ranges for Al^{IV} and Fe total are the same. In the present study, however, although the range of Mg content in the Serres-Drama clinopyroxenes is greater, the clinopyroxenes from Xanthe are more magnesian-rich.

From nine of Christofides' (1977) analyses (Poldervaart and Hess, 1951, from Deer et al, 1978), seven fall into the augite compositional field and the remaining

two into the salite compositional field. Therefore the Serres-Drama plutonic clinopyroxenes are more calcic.

The ratio Mg/Mg + Fe total ranges from 0.640 to 0.763 in the present study, including the xenolith.

3-5-3 Discussion and conclusion

Deer et al (1978, p.257) reported that "the members of the diopside-hedenbergite series cannot always be distinguished from clinopyroxenes of augite and ferroaugite composition (see p.294) but in general the diopside-hedenbergite minerals have higher optic axial angles than those of augite and ferroaugite with comparable refractive indices". This is probably the reason why Papadakis (1965) characterised the clinopyroxenes in the Serres-Drama complex as augite rather than salite.

Czamanske and Wones (1973) reported that pyroxenes are present only in the monzonite of the Finnmarke complex, Oslo area of Norway. Both hypersthene and augite formed early and partial replacement of some grains by amphibole and subordinate biotite occurs. The range of $Fe/_{Fe + Mg}$ values for orthopyroxene and clinopyroxenes fits logically into the same pattern as the amphiboles and biotites, as in the Serres-Drama complex.

Czamanske, Ishihara and Atkin (1981) observed that the ratio $Fe/_{Fe + Mg}$ for clinopyroxenes from calc-alkaline plutonic rocks in southwestern Japan is lower than the

coexisting amphiboles. The clinopyroxenes are uniformly low in TiO_2 and Al_2O_3 and high in CaO compared to clinopyroxenes which have crystallised from anhydrous tholeiitic and alkaline basaltic magmas (Deer et al, 1978).

The clinopyroxenes of the present study, as illustrated in fig. (3-5-2a), are characterised from their chemical composition as salite. Some grains of these early formed clinopyroxenes are partially replaced by amphiboles.

3-6 SPHENE

Sphene, is named from the Greek "sphenos", meaning wedge. It crystallises in the monoclinic system has the ideal chemical formula Ca Ti Si O_5 and usually occurs in euhedral crystals, with an acute rhombic cross section in the Serres-Drama granitic complex.

The data for two grains obtained by electron microprobe analysis (sample No.119, quartz monzonite) are given in table (3-6a). As a comparison with the present study, sphene microprobe analyses from the Xanthe complex are displayed in table (3-6b) (from Christofides, 1977). It can be seen that the two sets of results show that the chemical compositions are similar. The compositions of all the sphenes from the Rhodope massif are essentially pure (CaTi Si O_5) with only small concentration of iron ($\sim$0.2 atoms per 4 formula units) and aluminium ($\sim$0.2 atoms per 4 formula units).

TABLE: (3-6a) Microprobe analyses of sphenes from the Serres-Drama granitic complex

	119R 58	119R 59
SiO_2	29•83	29•39
TiO_2	36•64	36•04
Al_2O_3	1•29	1•27
FeO_{total}	2•06	1•82
MnO	-	-
MgO	-	-
CaO	27•73	27•27
Na_2O	-	-
K_2O	0•13	-
Total	97•68	95•79

Numbers of ions on the basis of 20(O)

Si	4•015	4•027
Al	0•204	0•205
Ti	3•710	3•713
Fe^{2+}	0•232	0•209
Mn	-	-
Mg	-	-
Ca	4•000	4•003
Na	-	-
K	0•023	-

TABLE: (3-6b) Microprobe analyses of sphenes from the Xanthi plutonic complex (Christofides, 1977)

	125	41
SiO_2	29•97	29•75
TiO_2	37•32	36•82
Al_2O_3	1•49	1•76
FeO_{total}	1•78	1•72
MnO	-	0•13
MgO	-	-
CaO	27•73	26•63
Na_2O	-	-
K_2O	-	-
V_2O_5	-	0•30
Total	99•29	97•11

Numbers of ions on the basis of 20 (O)

Si	3•998	4•008
Ti	3•744	3•731
Al	0•234	0•280
Fe^{2+}	0•199	0•194
Mn	-	0•015
Mg	-	-
Ca	3•964	3•844
Na	-	-
K	-	-
V	-	0•032

3-7 ORE MINERALS

Microprobe analyses for two ore mineral grains from a dioritic xenolith are listed in table (3-7a). It is obvious that they are magnetite. In both analyses the TiO_2 is found to be zero. Although only two analyses are given in table (3-7a) many ore grains were tested for the presence of Ti and none was found.

Czamanske, Ishihara and Atkin (1981) have correlated a decrease in the ratio $Fe/_{Fe + Mg}$ in amphibole and biotite with an increase in the host rock silica content and suggest that this characterises a calc-alkaline "magnetite series" to distinguish it from an "ilmenite series" of calc-alkaline rocks (Ishihara, 1977, from Takahashi et al, 1980). This is also observed in the present study. Therefore we can conclude that the Serres-Drama complex is a member of the magnetite series of Ishihara (op. cit).

3-8 EPIDOTE

The secondary accessory minerals in the present study are epidote and chlorite.

Epidote was named by Haüy from the Greek "epidosis" meaning increase.

The variation in the chemical composition of the epidote-clinozoisite series of minerals are restricted to the range between $Ca_2 Fe^{+3} Al_2 Si_3 O_{12} (OH)$ and $Ca_2Al_3Si_3O_{12} (OH)$ and the data for five epidotes analysed by electron microprobe (two grains from quartz monzonite and three grains from gabbro) are given in table (3-8a).

TABLE (3-7a) Microprobe analyses of magnetite from the Serres-Drama granitic complex

	6-b,R 28	6-b,R 29
SiO_2	0.29	0.24
TiO_2	-	-
Al_2O_3	0.22	-
FeO total	90.32	90.17
MnO	0.24	0.28
MgO	-	-
CaO	-	0.13
Na_2O	-	-
K_2O	-	-
Total	91.07	90.82
Numbers of ions on the basis of 4(O)		
Si	0.015	0.012
Al	0.013	-
Ti	-	-
Fe total	3.939	3.955
Mg	-	-
Mn	0.011	0.013
Ca	-	0.007
Na	-	-
K	-	-

TABLE (3-8a) Microprobe analyses of Epidotes from the Serres-Drama granitic complex

	119R 65	119R 66	152 29	152 30	152 31
SiO_2	38.22	37.85	43.50	37.92	37.46
TiO_2	-	-	-	-	0.25
Al_2O_3	22.28	22.63	32.18	24.70	24.43
FeO total	13.77	12.87	2.61	10.49	10.91
MnO	0.33	-	-	-	-
MgO	-	-	-	-	-
CaO	23.61	23.74	19.57	23.60	23.43
Na_2O	-	-	0.59	-	-
K_2O	0.13	0.16	0.14	0.14	0.12
Total	98.34	97.25	98.59	96.84	96.60

Number of ions on the basis of 12.5 (O)

Si	3.122	3.113	3.242	3.085	3.064
Al	2.145	2.193	2.827	2.369	2.356
Ti	-	-	-	-	0.016
Fe^{2+}	0.941	0.885	0.162	0.714	0.747
Mn	0.023	-	-	-	-
Mg	-	-	-	-	-
Ca	2.067	2.092	1.563	2.057	2.054
Na	-	-	0.086	-	-
K	0.013	0.017	0.014	0.014	0.013

Four of the five analyses have high concentration of $Ca_2 Fe^{3+} Al_2 Si_3 O_{12} (OH)$ (0.714 ⟶ 0.941 atoms of Fe^{2+}) which are typical values for hydrothermal epidotes (Exley, 1980). The fifth analysis appears to be spurious.

3-9 CHLORITES

Chlorites were named from the Greek "chloros", meaning green.

This group of minerals occurs as a common product of hydrothermal alteration of pyroxenes, amphiboles and biotites in igneous rocks. Partial and complete chloritisation of biotites is particularly common in granites. In the Serres-Drama granitic complex it occurs only very rarely.

The chemistry of the chlorite group minerals can be described according to a chlorite with the hypothetical composition of $Mg_6 Si_8 O_{20} (OH)_4 + Mg_6 (OH)_{12}$ which has equal numbers of talc and brucite layers. In these minerals a wide range of substitutions occur within the tetrahedral and octahedral sites. The ratio $Fe^{+2} / Fe^{+2} + Mg$ can lie between zero and unity.

Hey (1954, from Deer et al, 1971) suggested a classification scheme (fig. 3-9a) using the Si per formula unit and total iron or the ratio Fe total/ Fe total + Mg. The boundaries between composition fields are to a great extent, arbitrary. A first subdivision was between

chlorites with more than four per cent Fe_2O_3 which are termed oxidized and less than four per cent are termed unoxidized. Many authors have used this classification (Bevins, 1979; Foster, 1962).

The data for four analyses by electron microprobe are listed in table (3-9a). Two of these (184R,10 and 184R,11) are from chlorites replacing hornblendes. There is little difference in chemical composition of the chlorite whether it replaces biotite or hornblende.

The data from table (3-9a) have been plotted on the Hey (1954) classification, fig. (3-9b). Three analyses fall into the compositional field of pycnochlorite and the fourth, in the ccompositional field of diabantite but close to the boundary.

For comparison with the present study, microprobe analyses of chlorites from the Xanthi complex (Christofides, 1977) are listed in table (3-9b). The above data also fall into the compositional field of pycnochlorite, fig. (3-9b).

The range of Si per formula unit and the ratio Fe total/Fe total + Mg are correspondingly 5.712 to 6.236 and 0.370 to 0.441 (in present study), 5.707 to 5.817 and 0.372 to 0.385 (in Christofides, 1977) and 5.277 to 6.031 and 0.378 to 0.990 (in Czamanske et al, 1981).

If we compare the chlorites from the Rhodope massif area with the corresponding chlorites from the Cretaceous Paleocene batholith in southwestern Japan, the former are found to be more closely grouped. The data of Czamanske et al, (1981, p.10445) indicate that the chlorites may be classified as pycnochlorites, ripidolites, brunsvigites and

TABLE (3-9a) Microprobe analyses of chlorites from the Serres-Drama granitic complex

	184R 10	184R 11	184R 19	184R 20
SiO_2	29.37	28.11	29.57	29.77
TiO_2	-	-	-	-
Al_2O_3	19.06	20.65	17.21	17.68
FeO_{total}	20.17	19.67	22.45	21.61
MnO	0.63	0.82	0.68	0.62
MgO	19.30	18.73	17.60	16.18
CaO	-	-	-	0.17
Na_2O	-	-	-	-
K_2O	-	-	-	-
Total	88.53	87.98	87.51	86.03
	Numbers of ions on the basis of 28(O)			
Si	5.936	5.712	6.126	6.236
Al^{iv}	2.064	2.288	1.874	1.864
Al^{vi}	2.466	2.658	2.330	2.600
Ti	-	-	-	-
Fetot	3.410	3.344	3.890	3.986
Mn	0.108	0.140	0.120	0.110
Mg	5.814	5.674	5.434	5.052
Ca	-	-	-	0.038
Na	-	-	-	-
K	-	-	-	-
$\frac{Fetot}{Mg+ Fetot}$	0.370	0.371	0.417	0.441

TABLE (3-9b) Microprobe analyses of chlorites from the Xanthi plutonic complex (Christofites, 1977)

	250	28	41
SiO_2	27.50	28.52	28.11
TiO_2	-	-	0.23
Al_2O_3	18.56	18.48	18.80
FeO_{tot}	20.89	21.22	21.12
MnO	1.17	0.47	0.46
MgO	18.74	19.18	19.97
CaO	-	0.23	0.17
Na_2O	-	0.44	-
K_2O	-	0.20	0.13
Total	86.86	88.74	88.99

Numbers of ions on the basis of 28 (O)

Si	5.736	5.817	5.707
Al^{iv}	2.264	2.183	2.293
Al^{vi}	2.300	2.261	2.207
Ti	-	-	0.035
Fetot	3.645	3.620	3.586
Mn	0.207	0.081	0.079
Mg	5.826	5.830	6.042
Ca	-	0.05o	0.037
Na	-	0.174	-
K	-	0.052	0.034
$\frac{Fetot}{Mg+Fetot}$	0.385	0.383	0.372

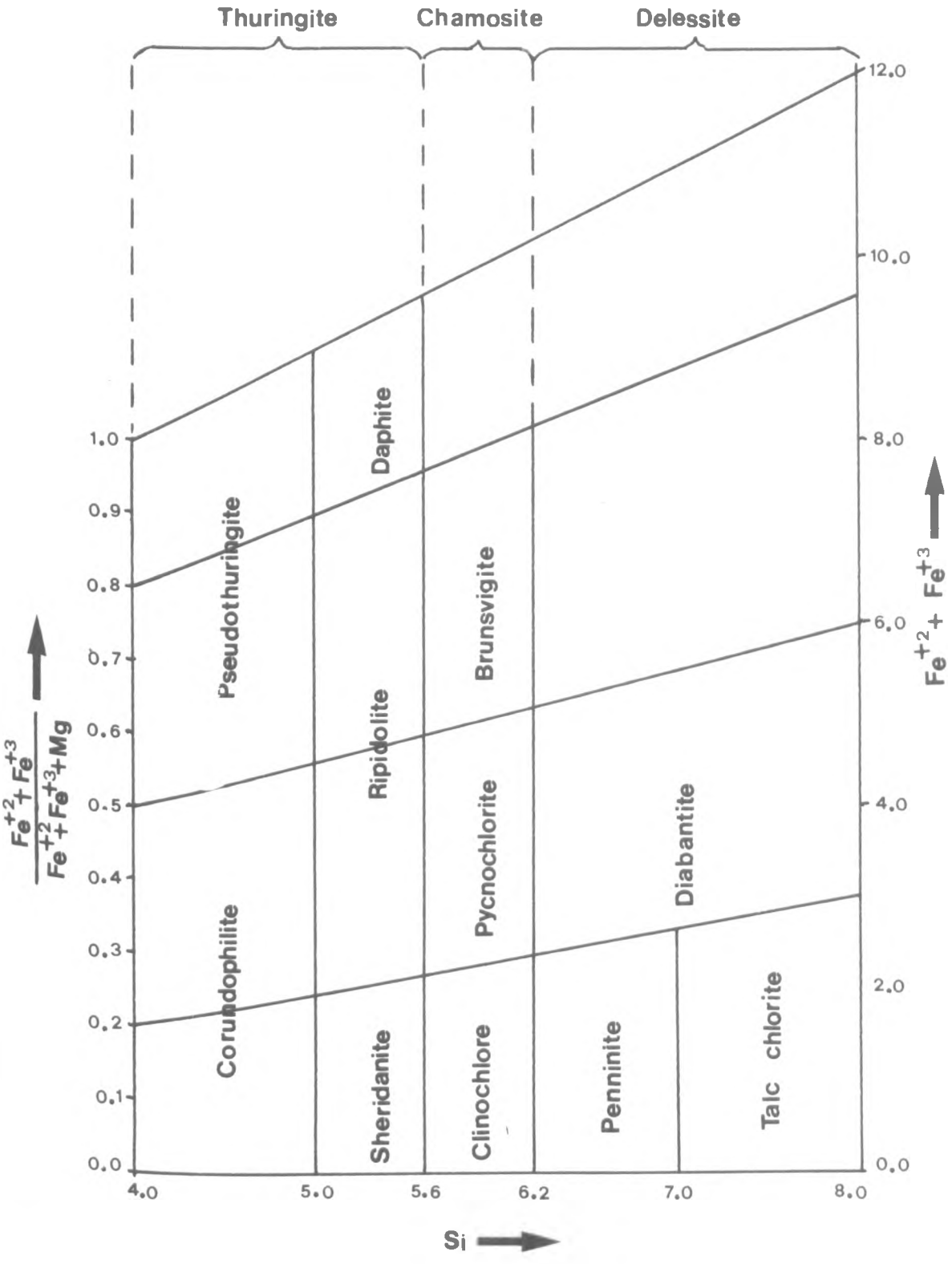

Fig. (3–9a) Nomenclature of orto-chlorites and oxidized chlorite (after Hey, 1954, from Deer et al, 1962)

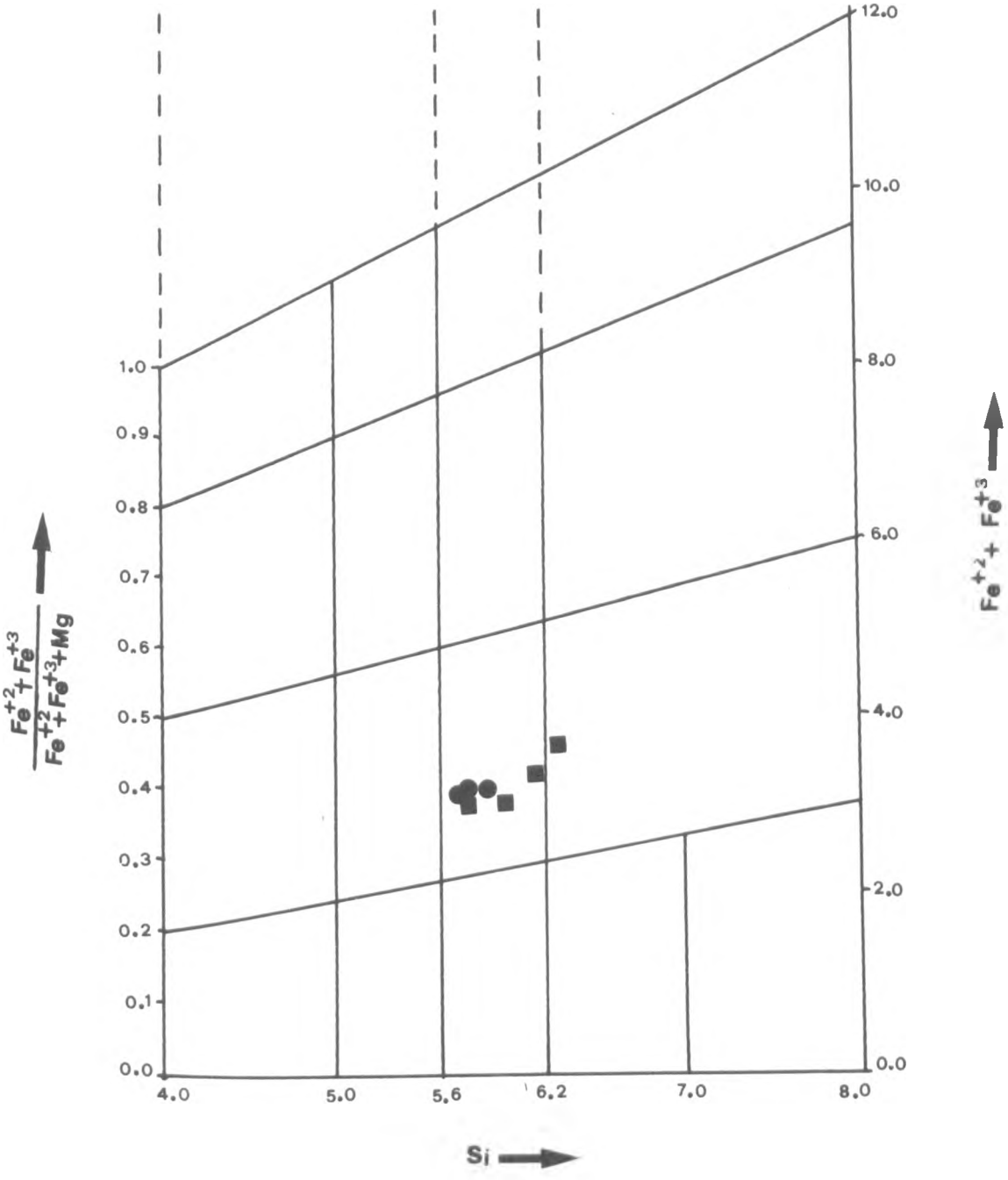

Fig (3–9b) Chlorites: ■ from Author, ● from Christofides

daphnites, Bevins (1979) found that the composition of chlorite appeared to depend upon the total iron content of the rock. There are, however, too few results from this complex to make any sensible conclusions.

From the analytical data it has been observed that there is nothing particularly distinctive about any of these chlorites.

CHAPTER IV : MAJOR ELEMENT GEOCHEMISTRY

CHAPTER IV

MAJOR ELEMENT GEOCHEMISTRY

4-1-1 Introduction

One hundred and seventy four samples from the Serres-Drama granitic complex have been analysed, by X-ray flurrescence and wet chemical techniques (details of analytical techniques and sample preparation can be found in Appendix C), for twelve major element oxides (SiO_2, TiO_2, Al_2O_3, Fe_2O_3, FeO, MnO, MgO, CaO, Na_2O, K_2O, P_2O_5, H_2O^+ as L.O.I.). H_2O^+ was not determined directly. Loss on ignition at 1000^{o} C was corrected for the oxidation of FeO in the rock and CO_2 (none present). This figure was used as the H_2O^+ content (for further details see Appendix C).

Of the above mentioned samples: sixty nine samples were of monzonite composition; fifty samples of quartz monzonite composition; twenty samples of granodiorite composition; eighteen samples of granite composition; five samples of gabbro composition; four samples of aplite composition and eight samples of dioritic xenolith material.

The samples were collected to include the full range of rock-types present in the Serres-Drama granitic complex. The samples are identified by station numbers and a symbol to denote rocktype (sample locations are shown in fig. (4-1-1a).

In the discussion that follows the rock-types described from the complex have been divided into two groups

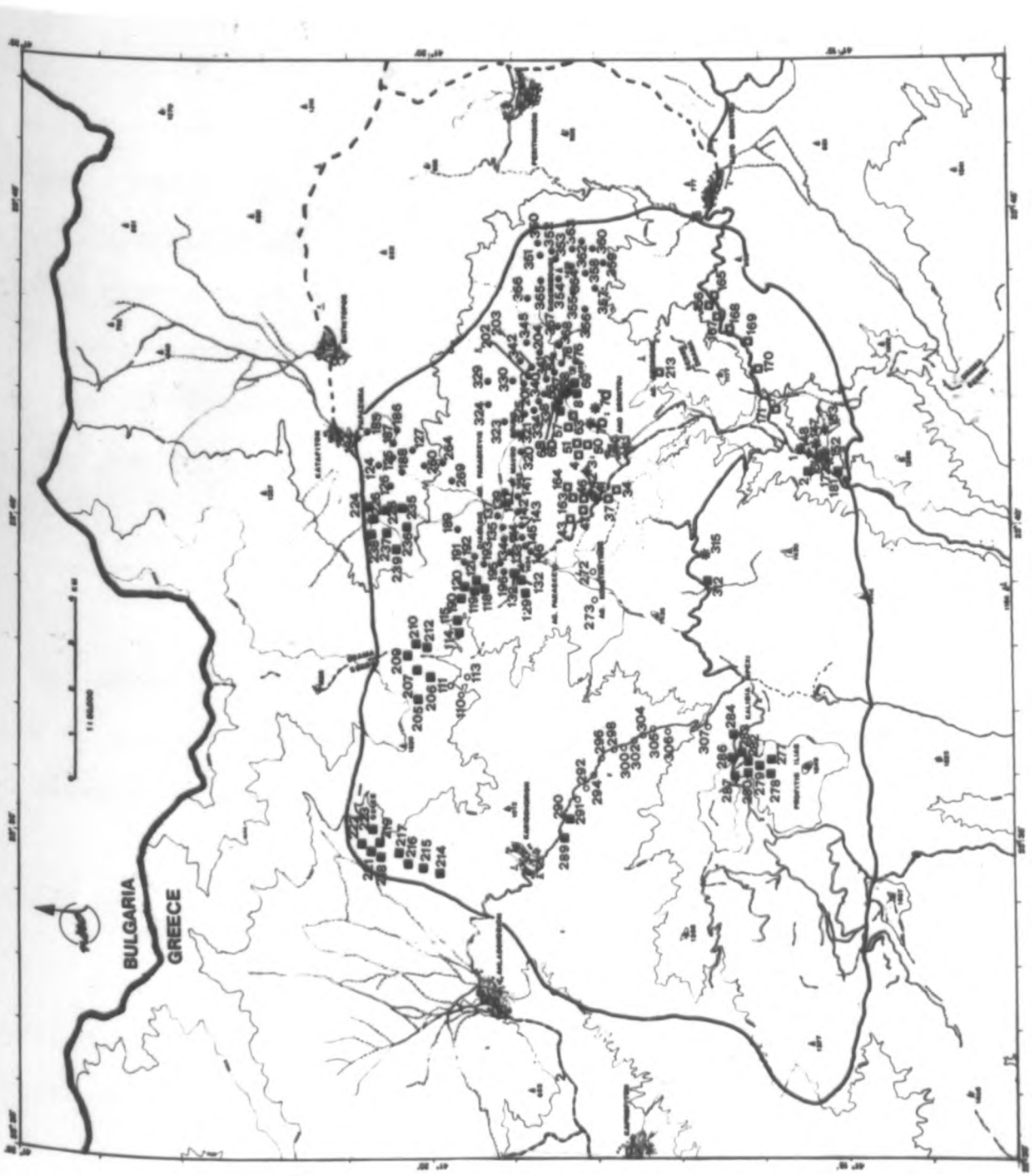

Fig. (4–1–1a)

- Quartz monzonite
- Granite
- Granodiorite
- Monzonite
- Aplite
- Xenolith
- Gabbro

which are thought to have real geological significance (for discussion see the chapters on petrography and mineralogy). These groups have been designated the "basic group" comprising the gabbro, dioritic xenoliths and monzonite and characterised by low SiO_2 contents, and the "intermediate group", comprising the quartz monzonite, granodiorite and granite charcterised by higher SiO_2 contents.

The geochemistry of the Serres-Drama granitic complex was investigated to explore:

a) the variation of chemical composition throughout the complex;

b) the compositional differences between the rock-types; and

c) to determine whether the original magma which gave rise to the complex was of possible igneous origin (I-type) or sedimentary origin (S-type).

4-1-2 Results of major element analysis

For each rock-type the major elements and the calculated norms are tabulated as follows: quartz monzonites in table (4-1-2a), granites in table (4-1-2b), granodiorites in table (4-1-2c), monzonites in table(4-1-2d), aplites in table (4-1-2f), gabbros in table (4-1-2e) and diorite xenoliths in table (4-1-2g).

The range of SiO_2 content in the whole granitic complex is between 46.5% (gabbro, sample No.153) and 76.8% (aplite, sample No.42). The mean SiO_2 value is

TABLE: (4-1-2a) Major element analyses and C.I.P.W. Norms of quartz monzonite from Serres-Drama granitic complex.

	6a3	6b3	8	64	66	67
SiO_2	61•26	62•78	62•26	67•34	64•69	63•03
TiO_2	0•51	0•49	0•47	0•32	0•38	0•42
Al_2O_3	17•08	17•39	16•77	15•25	16•94	16•76
Fe_2O_3	1•31	0•98	1•22	1•26	2•42	2•20
FeO	3•11	2•85	3•00	1•58	1•35	1•45
MnO	0•14	0•14	0•15	0•12	0•12	0•13
MgO	1•44	1•89	1•47	1•38	1•43	1•51
CaO	4•13	3•98	3•90	3•38	3•12	3•25
Na_2O	3•91	3•88	3•82	3•58	3•62	3•53
K_2O	4•94	4•91	4•92	3•67	5•79	5•40
P_2O_5	0•25	0•24	0•18	0•25	0•16	0•15
H_2O^+	0•66	0•69	0•70	0•76	0•69	0•81
Total	98•74	100•22	98•86	98•89	100•71	98•64

C.I.P.W. Norms

Qz	8•42	9•55	10•24	23•28	13•39	13•12
Co	-	-	-	-	-	-
Or	29•19	29•03	29•06	21•68	34•24	31•91
Ab	33•08	32•85	32•30	30•26	30•62	29•89
An	14•47	15•52	14•09	14•73	12•87	13•92
Ne	-	-	-	-	-	-
Mg-Di	1•85	1•26	1•75	0•23	1•21	0•88
Fe-Di	1•82	0•91	1•66	0•09	0•02	0•08
Wo	-	-	-	-	-	-
En	2•73	4•11	2•86	3•33	3•00	3•35
Fs	3•08	3•39	3•12	1•51	0•07	0•34
Fo	-	-	-	-	-	-
Fa	-	-	-	-	-	-
Mt	1•91	1•42	1•77	1•82	3•51	3•19
Il	0•96	0•92	0•89	0•60	0•71	0•81
Hm	-	-	-	-	-	-
Ap	0•59	0•57	0•41	0•59	0•37	0•35
H_2O	0•66	0•69	0•70	0•76	0•69	0•81

TABLE: (4-1-2a) Major element analyses and C.I.P.W. Norms of quartz monzonite from Serres-Drama granitic complex. (cont.)

	68	69	118	119	120	121
SiO_2	61·60	62·03	60·88	62·30	61·06	60·56
TiO_2	0·47	0·45	0·55	0·54	0·52	0·51
Al_2O_3	16·92	17·58	16·75	17·21	16·42	18·22
Fe_2O_3	2·81	2·59	2·68	3·31	2·40	2·82
FeO	1·80	1·91	2·07	2·30	2·22	2·00
MnO	0·14	0·14	0·15	0·15	0·15	0·14
MgO	1·87	1·99	2·71	2·65	2·61	1·86
CaO	3·76	4·28	4·43	4·96	4·61	4·37
Na_2O	3·54	3·87	3·18	3·57	3·42	3·06
K_2O	5·03	4·95	4·98	4·02	4·50	6·13
P_2O_5	0·23	0·24	0·10	0·23	0·24	0·20
H_2O^+	0·76	0·51	1·38	0·30	0·88	0·84
Total	98·93	100·54	99·86	101·54	99·03	100·71

C.I.P.W. Norms

Qz	11·72	9·51	10·65	12·69	11·27	7·91
Co	-	-	-	-	-	-
Or	29·74	29·27	29·44	23·77	26·62	36·25
Ab	29·97	32·77	26·88	30·21	28·93	25·90
An	15·41	15·95	16·73	19·05	16·15	17·86
Ne	-	-	-	-	-	-
Mg-Di	1·25	2·52	3·22	2·86	3·41	1·74
Fe-Di	0·11	0·39	0·40	0·33	0·69	0·25
Wo	-	-	-	-	-	-
En	4·07	3·79	5·25	5·27	4·91	3·82
Fs	0·41	0·67	0·75	0·70	1·15	0·63
Fo	-	-	-	-	-	-
Fa	-	-	-	-	-	-
Mt	4·08	3·75	3·88	4·80	3·49	4·09
Il	0·90	0·86	1·04	1·03	0·98	0·96
Hm	-	-	-	-	-	-
Ap	0·55	0·57	0·24	0·54	0·56	0·47
H_2O	0·76	0·51	1·38	0·30	0·88	0·84

TABLE: (4-1-2a) Major element analyses and C.I.P.W. Norms of quartz monzonite from Serres-Drama granitic complex (cont.).

	129	130	132	181	190	205
SiO_2	57·88	61·93	63·91	62·51	64·91	65·32
TiO_2	0·45	0·51	0·44	0·54	0·44	0·47
Al_2O_3	18·26	17·99	17·17	16·58	16·46	16·20
Fe_2O_3	3·75	2·99	2·39	2·49	1·78	2·02
FeO	2·65	1·98	1·82	2·31	1·76	1·94
MnO	0·27	0·21	0·18	0·15	0·13	0·13
MgO	2·91	2·09	1·96	1·81	1·35	1·38
CaO	5·64	4·66	4·04	4·95	4·17	4·00
Na_2O	3·99	3·89	3·66	3·67	3·64	3·51
K_2O	3·84	4·76	5·26	3·75	3·91	4·06
P_2O_5	0·31	0·22	0·17	0·21	0·11	0·13
H_2O^+	0·97	0·60	0·56	0·60	0·51	0·54
Total	100·92	101·83	101·56	99·57	99·17	99·70

C.I.P.W. Norms

Qz	4·89	9·13	11·82	14·59	18·21	19·03
Co	-	-	-	-	-	-
Or	22·67	28·13	31·10	22·15	23·12	23·99
Ab	33·80	32·95	30·98	31·05	30·77	29·69
An	20·57	17·55	14·86	17·69	17·04	16·46
Ne	-	-	-	-	-	-
Mg-Di	3·58	2·94	2·75	3·36	1·77	1·53
Fe-Di	0·66	0·35	0·48	1·04	0·59	0·53
Wo	-	-	-	-	-	-
En	5·59	3·85	3·60	2·94	2·54	2·73
Fs	1·19	0·53	0·72	1·04	0·97	1·09
Fo	-	-	-	-	-	-
Fa	-	-	-	-	-	-
Mt	5·43	4·33	3·47	3·60	2·58	2·93
Il	0·85	0·97	0·83	1·02	0·83	0·88
Hm	-	-	-	-	-	-
Ap	0·74	0·51	0·41	0·50	0·27	0·30
H_2O	0·97	0·60	0·56	0·60	0·51	0·54

TABLE: (4-1-2a) Major element analyses and C.I.P.W. Norms of quartz monzonite from Serres-Drama granitic complex (cont.).

	206	207	209	212	214	215
SiO_2	63·09	65·36	64·00	64·35	63·54	62·98
TiO_2	0·49	0·52	0·47	0·50	0·41	0·37
Al_2O_3	16·89	17·12	16·41	17·07	17·83	17·30
Fe_2O_3	2·67	2·63	2·22	2·25	2·49	2·34
FeO	2·00	2·01	1·93	1·93	1·36	1·19
MnO	0·15	0·15	0·14	0·13	0·12	0·12
MgO	1·62	1·65	1·50	1·54	0·78	0·44
CaO	4·43	4·35	4·13	4·52	3·93	3·33
Na_2O	3·57	3·46	3·62	3·68	4·34	4·30
K_2O	3·95	4·02	4·11	3·91	4·21	4·42
P_2O_5	0·14	0·17	0·12	0·12	0·13	0·10
H_2O^+	0·54	0·61	0·62	0·52	0·68	0·86
Total	99·54	102·05	99·27	100·52	99·82	97·75

C.I.P.W. Norms

Qz	15·84	18·36	16·65	16·51	13·39	13·76
Co	-	-	-	-	-	-
Or	23·36	23·78	24·27	23·08	24·89	26·14
Ab	30·21	29·30	30·62	31·17	36·68	36·38
An	18·39	19·28	16·39	18·50	16·76	14·84
Ne	-	-	-	-	-	-
Mg-Di	1·76	0·80	2·07	1·97	1·45	0·79
Fe-Di	0·36	0·16	0·58	0·50	-	-
Wo	-	-	-	-	-	-
En	3·21	3·73	2·78	2·93	1·28	0·73
Fs	0·75	0·85	0·90	0·85	-	-
Fo	-	-	-	-	-	-
Fa	-	-	-	-	-	-
Mt	3·87	3·81	3·22	3·26	3·60	3·17
Il	0·94	0·99	0·88	0·94	0·78	0·69
Hm	-	-	-	-	0·01	0·15
Ap	0·34	0·40	0·29	0·29	0·31	0·25
H_2O	0·54	0·61	0·62	0·52	0·68	0·86

TABLE: (4-1-2a) Major element analyses and C.I.P.W. Norms of quartz monzonite from Serres-Drama granitic complex (cont.).

	216	217	218	219	221	222
SiO_2	64·58	66·05	62·64	64·46	66·43	65·95
TiO_2	0·33	0·43	0·40	0·32	0·29	0·36
Al_2O_3	18·46	17·71	18·33	18·62	17·46	15·96
Fe_2O_3	2·52	2·44	2·37	2·74	2·34	2·04
FeO	0·82	1·06	1·24	0·84	1·04	1·37
MnO	0·08	0·11	0·13	0·12	0·10	0·11
MgO	0·38	0·48	0·61	0·17	0·49	0·69
CaO	3·08	3·38	4·14	3·43	3·30	3·25
Na_2O	4·45	4·73	4·63	4·79	4·63	4·25
K_2O	5·03	4·49	4·74	4·36	3·91	4·31
P_2O_5	0·10	0·11	0·11	0·11	0·10	0·10
H_2O^+	0·74	0·63	0·55	0·66	0·43	0·35
Total	100·57	101·62	99·89	100·62	100·52	98·74

C.I.P.W. Norms

Qz	12·57	14·21	9·07	12·61	17·14	17·65
Co	0·27	-	-	0·04	-	-
Or	29·74	26·52	28·03	25·75	23·09	25·45
Ab	37·62	39·99	39·20	40·57	39·14	35·94
An	14·63	13·84	15·22	16·28	15·33	11·77
Ne	-	-	-	-	-	-
Mg-Di	-	1·72	3·27	-	0·30	2·42
Fe-Di	-	-	-	-	-	0·54
Wo	-	-	0·16	-	-	-
En	0·95	0·40	-	0·43	1·08	0·59
Fs	-	-	-	-	-	0·15
Fo	-	-	-	-	-	-
Fa	-	-	-	-	-	-
Mt	1·94	2·55	3·27	2·16	2·84	2·95
Il	0·63	0·81	0·76	0·16	0·54	0·68
Hm	1·18	0·68	0·12	1·25	0·39	-
Ap	0·23	0·26	0·27	0·26	0·24	0·24
H_2O	0·74	0·63	0·55	0·66	0·43	0·35

TABLE: (4-1-2a) Major element analyses and C.I.P.W. Norms of quartz monzonite from Serres-Drama granitic complex (cont.).

	223	226	228	235	236	237
SiO_2	61•54	66•44	65•52	66•36	66•46	66•30
TiO_2	0•40	0•44	0•49	0•43	0•46	0•46
Al_2O_3	18•26	16•45	16•73	15•94	16•21	16•15
Fe_2O_3	2•88	2•11	0•40	2•07	2•38	2•15
FeO	1•25	1•14	0•59	1•32	1•69	1•83
MnO	0•13	0•05	0•05	0•09	0•10	0•10
MgO	0•74	1•32	1•12	1•15	1•40	1•36
CaO	3•76	4•32	5•24	4•03	3•94	4•01
Na_2O	4•68	3•75	4•05	3•72	3•64	3•67
K_2O	4•08	4•04	4•19	3•78	4•00	3•73
P_2O_5	0•12	0•12	0•13	0•11	0•11	0•11
H_2O^+	0•82	0•50	0•46	0•65	0•61	0•45
Total	98•66	100•68	98•97	99•65	101•00	100•32

C.I.P.W. Norms.

Qz	10•10	19•26	15•53	20•94	20•09	20•47
Co	-	-	-	-	-	-
Or	24•12	23•88	24•77	22•33	23•62	22•06
Ab	39•63	31•73	34•29	31•48	30•84	31•04
An	16•76	16•12	15•08	15•64	16•07	16•59
Ne	-	-	-	-	-	-
Mg-Di	0•88	3•53	6•02	2•69	1•92	1•64
Fe-Di	-	-	0•08	0•14	0•27	0•42
Wo	-	-	0•94	-	-	-
En	1•44	1•64	-	1•61	2•59	2•63
Fs	-	-	-	0•09	0•41	0•78
Fo	-	-	-	-	-	-
Fa	-	-	-	-	-	-
Mt	3•30	2•59	0•58	3•00	3•45	3•12
Il	0•76	0•83	0•93	0•82	0•88	0•87
Hm	0•60	0•33	-	-	-	-
Ap	0•27	0•28	0•30	0•27	0•26	0•27
H_2O	0•82	0•50	0•46	0•65	0•61	0•45

TABLE: (4-1-2a) Major element analyses and C.I.P.W. Norms of quartz monzonite from Serres-Drama granitic complex (cont.).

	238	239	277	278	279	280
SiO_2	65•51	66•37	67•72	67•96	66•72	66•01
TiO_2	0•44	0•46	0•40	0•41	0•41	0•43
Al_2O_3	16•10	15•92	16•26	16•30	15•74	16•15
Fe_2O_3	2•06	2•21	1•85	1•23	1•62	1•85
FeO	1•71	1•75	1•44	2•31	1•52	1•53
MnO	0•09	0•10	0•12	0•12	0•11	0•12
MgO	1•28	1•34	0•75	0•57	0•56	0•87
CaO	3•90	3•97	2•47	2•87	2•75	2•90
Na_2O	3•68	3•48	3•77	3•87	3•98	4•10
K_2O	3•73	3•86	5•01	4•88	5•38	5•11
P_2O_5	0•11	0•12	0•22	0•08	0•22	0•22
H_2O^+	0•50	0•49	0•87	0•67	0•59	0•69
Total	99•11	100•07	100•88	101•27	99•60	99•98

C.I.P.W. Norms.

Qz	19•97	21•35	20•55	18•97	17•06	15•88
Co	-	-	0•52	-	-	-
Or	22•02	22•79	29•59	28•84	31•81	30•21
Ab	31•14	29•46	31•87	32•72	33•67	34•67
An	16•40	16•43	10•84	12•70	9•20	10•57
Ne	-	-	-	-	-	-
Mg-Di	1•43	1•66	-	0•32	1•55	1•46
Fe-Di	0•43	0•35	-	0•54	0•95	0•46
Wo	-	-	-	-	-	-
En	2•53	2•58	1•86	1•28	0•68	1•48
Fs	0•70	0•63	0•67	2•49	0•48	0•54
Fo	-	-	-	-	-	-
Fa	-	-	-	-	-	-
Mt	2•98	3•21	2•69	1•78	2•34	2•68
Il	0•84	0•87	0•77	0•78	0•78	0•82
Hm	-	-	-	-	-	-
Ap	0•27	0•27	0•51	0•19	0•51	0•51
H_2O	0•50	0•49	0•87	0•67	0•59	0•69

TABLE: (4-1-2a) Major element analyses and C.I.P.W. Norms of quartz monzonite from Serres-Drama granitic complex (cont.).

	282	283	284	286	287	289
SiO_2	68•24	61•42	68•41	67•50	67•22	67•66
TiO_2	0•36	0•79	0•37	0•36	0•37	0•43
Al_2O_3	16•25	15•87	15•53	15•80	15•63	16•66
Fe_2O_3	1•82	2•91	1•76	1•57	1•57	1•87
FeO	1•46	2•95	1•36	1•40	1•21	1•24
MnO	0•11	0•17	0•12	0•11	0•10	0•12
MgO	0•82	2•02	0•73	0•71	0•50	0•70
CaO	2•83	4•31	2•59	2•73	2•33	3•10
Na_2O	4•18	3•79	4•07	4•18	4•11	4•31
K_2O	4•76	5•17	4•64	4•78	5•34	4•11
P_2O_5	0•20	0•50	0•17	0•19	0•20	0•22
H_2O^+	0•48	0•83	0•55	0•48	0•66	0•73
Total	101•51	100•73	100•30	99•81	99•24	101•15

C.I.P.W. Norms.

Qz	18•94	9•32	20•82	18•57	17•86	19•74
Co	-	-	-	-	-	0•02
Or	28•11	30•58	27•43	28•22	31•55	24•29
Ab	35•33	32•10	34•42	35•39	34•79	36•43
An	11•54	10•99	10•42	10•24	8•44	13•90
Ne	-	-	-	-	-	-
Mg-Di	0•70	4•26	0•83	1•15	1•11	-
Fe-Di	0•24	1•50	0•26	0•51	0•39	-
Wo	-	-	-	-	-	-
En	1•70	3•06	1•42	1•23	0•72	1•75
Fs	0•65	1•24	0•51	0•62	0•29	0•23
Fo	-	-	-	-	-	-
Fa	-	-	-	-	-	-
Mt	2•64	4•22	2•55	2•28	2•27	2•71
Il	0•69	1•49	0•70	0•68	0•70	0•82
Hm	-	-	-	-	-	-
Ap	0•48	1•17	0•39	0•45	0•46	0•53
H_2O	0•48	0•83	0•55	0•48	0•66	0•73

TABLE: (4-1-2a) Major elemental analyses and C.I.P.W. Norms of quartz monzonite from Serres-Drama granitic complex (cont.).

	290	312
SiO_2	66•07	60•36
TiO_2	0•38	0•49
Al_2O_3	16•62	18•34
Fe_2O_3	1•95	3•24
FeO	1•40	1•41
MnO	0•13	0•61
MgO	0•89	0•93
CaO	2•89	4•78
Na_2O	4•28	4•12
K_2O	5•01	3•63
P_2O_5	0•20	0•16
H_2O^+	0•39	0•83
Total	100•21	98•90

C.I.P.W. Norms.

Qz	15•16	11•72
Co	-	-
Or	29•61	21•45
Ab	36•18	34•89
An	11•35	20•82
Ne	-	-
Mg-Di	1•10	1•43
Fe-Di	0•25	-
Wo	-	-
En	1•70	1•65
Fs	0•44	-
Fo	-	-
Fa	-	-
Mt	2•82	3•67
Il	0•72	0•92
Hm	-	0•71
Ap	0•47	0•38
H_2O	0•39	0•83

TABLE: (4-1-2b) Major element analyses and C.I.P.W. Norms of granite from Serres-Drama granitic complex.

	110	111	113	114	115	272
SiO_2	64•46	64•45	65•06	66•00	66•27	68•75
TiO_2	0•45	0•47	0•40	0•41	0•41	0•29
Al_2O_3	16•79	16•90	16•99	16•06	16•90	16•04
Fe_2O_3	2•02	2•36	1•97	2•15	2•25	1•72
FeO	1•90	1•73	1•73	1•61	1•60	1•00
MnO	0•13	0•14	0•13	0•13	0•13	0•12
MgO	1•96	2•21	1•71	1•19	1•85	-
CaO	4•05	4•36	3•78	3•63	3•92	3•32
Na_2O	3•62	3•74	3•69	3•65	3•62	3•71
K_2O	4•03	3•67	4•25	4•61	4•22	3•92
P_2O_5	0•11	0•12	0•11	0•13	0•11	0•05
H_2O^+	0•42	0•64	0•48	0•48	0•42	0•41
Total	99•94	100•79	100•30	100•05	101•70	99•33

C.I.P.W. Norms.

Qz	16•49	16•54	16•61	18•33	18•20	25•49
Co	-	-	-	-	-	-
Or	23•80	21•68	25•13	27•24	24•93	23•14
Ab	30•62	31•65	31•26	30•86	30•64	31•39
An	17•67	18•49	17•21	13•83	17•39	15•55
Ne	-	-	-	-	-	-
Mg-Di	1•09	1•69	0•54	2•19	0•97	-
Fe-Di	0•26	0•19	0•13	0•48	0•12	0•30
Wo	-	-	-	-	-	0•51
En	4•36	4•71	4•01	1•94	4•16	-
Fs	1•18	0•60	1•07	0•49	0•59	-
Fo	-	-	-	-	-	-
Fa	-	-	-	-	-	-
Mt	2•93	3•43	2•85	3•11	3•27	2•49
Il	0•85	0•90	0•75	0•78	0•77	0•55
Hm	-	-	-	-	-	-
Ap	0•27	0•28	0•26	0•30	0•25	0•13
H_2O	0•42	0•64	0•48	0•48	0•42	0•41

TABLE: (4-1-2b) Major element analyses and C.I.P.W. Norms of granite from Serres-Drama granitic complex (cont.).

	273	291	292	294	296	298
SiO_2	68•93	67•01	67•36	70•01	67•68	66•27
TiO_2	0•28	0•35	0•41	0•32	0•36	0•39
Al_2O_3	16•17	15•94	15•15	16•05	16•08	16•09
Fe_2O_3	0•29	1•45	1•79	1•58	1•68	1•75
FeO	2•31	1•25	1•34	1•10	1•22	1•40
MnO	0•12	0•10	0•12	0•11	0•11	0•11
MgO	0•57	0•77	0•61	0•57	0•78	0•73
CaO	3•10	2•39	2•70	2•27	2•66	2•66
Na_2O	3•87	3•98	3•99	3•97	4•36	4•17
K_2O	4•04	5•48	4•85	5•33	5•01	5•04
P_2O_5	0•08	0•06	0•23	0•17	0•16	0•21
H_2O^+	0•67	0•40	0•52	0•50	0•32	0•59
Total	100•43	99•18	99•00	101•98	100•42	99•41

C.I.P.W. Norms.

Qz	22•02	16•93	19•94	21•16	17•13	16•56
Co	-	-	-	0•03	-	-
Or	23•84	32•37	28•64	31•48	29•58	29•76
Ab	32•72	33•64	33•72	33•56	36•87	35•30
An	14•84	9•47	9•13	10•14	9•54	10•30
Ne	-	-	-	-	-	-
Mg-Di	-	1•21	1•71	-	1•70	0•92
Fe-Di	-	0•39	0•50	-	0•35	0•30
Wo	-	-	-	-	-	-
En	1•42	1•36	0•73	1•41	1•16	1•38
Fs	3•76	0•50	0•25	0•38	0•27	0•51
Fo	-	-	-	-	-	-
Fa	-	-	-	-	-	-
Mt	0•42	2•10	2•60	2•29	2•44	2•54
Il	0•53	0•67	0•78	0•61	0•68	0•75
Hm	-	-	-	-	-	-
Ap	0•20	0•14	0•54	0•40	0•39	0•49
H_2O	0•67	0•40	0•52	0•50	0•32	0•59

TABLE: (4-1-2b) Major element analyses and C.I.P.W. Norms of Granite from Serres-Drama granitic complex (cont.).

	300	302	304	305	306	307
SiO_2	66·04	66·22	67·35	68·16	67·92	68·70
TiO_2	0·38	0·39	0·37	0·34	0·33	0·31
Al_2O_3	16·07	15·70	15·88	14·92	15·19	15·42
Fe_2O_3	1·27	1·58	1·49	1·50	1·53	1·57
FeO	1·46	1·32	1·30	0·96	1·03	1·03
MnO	0·11	0·12	0·12	0·10	0·11	0·10
MgO	0·68	0·73	0·70	0·43	0·61	0·63
CaO	2·52	2·67	2·67	2·20	2·33	2·33
Na_2O	4·18	4·19	4·17	3·90	4·09	3·93
K_2O	4·99	4·61	4·85	5·31	4·75	5·11
P_2O_5	0·19	0·18	0·21	0·15	0·15	0·16
H_2O^+	0·61	0·48	0·37	0·39	0·62	0·25
Total	98·50	98·19	99·48	98·36	98·66	99·54

C.I.P.W. Norms.

Qz	16·38	17·94	18·36	20·65	20·69	20·95
Co	-	-	-	-	-	-
Or	29·48	27·23	28·63	31·39	28·08	30·22
Ab	35·40	35·48	35·30	33·01	34·58	33·24
An	10·34	10·42	10·28	7·52	9·06	9·33
Ne	-	-	-	-	-	-
Mg-Di	0·47	1·00	0·95	1·73	1·03	0·81
Fe-Di	0·29	0·33	0·36	0·21	0·17	0·12
Wo	-	-	-	-	-	-
En	1·47	1·35	1·31	0·27	1·03	1·19
Fs	1·06	0·52	0·57	0·04	0·20	0·20
Fo	-	-	-	-	-	-
Fa	-	-	-	-	-	-
Mt	1·85	2·29	2·16	2·17	2·21	2·28
Il	0·72	0·74	0·71	0·64	0·62	0·58
Hm	-	-	-	-	-	-
Ap	0·44	0·43	0·49	0·34	0·36	0·38
H_2O	0·61	0·48	0·37	0·39	0·62	0·25

TABLE: (4-1-2c) Major element analyses and C.I.P.W. Norms of granodiorite from Serres-Drama granitic complex.

	4	34	37	46	47	48
SiO_2	59·71	63·97	67·19	59·12	68·07	67·13
TiO_2	0·55	0·39	0·32	0·53	0·30	0·31
Al_2O_3	17·16	16·45	15·68	18·31	15·91	16·56
Fe_2O_3	0·91	2·29	0·75	2·60	1·52	1·96
FeO	4·09	1·44	2·04	2·13	1·43	1·14
MnO	0·17	0·13	0·13	0·15	0·13	0·11
MgO	2·58	1·36	0·90	2·13	1·33	1·27
CaO	4·73	2·82	3·50	5·14	3·32	3·31
Na_2O	3·74	3·83	3·83	3·96	3·85	3·90
K_2O	4·76	6·09	3·80	5·28	3·69	4·79
P_2O_5	0·26	0·15	0·11	0·22	0·17	0·18
H_2O^+	0·89	0·62	0·87	0·54	0·59	0·49
Total	99·55	99·54	99·12	100·11	100·31	101·15

C.I.P.W. Norms.

Qz	4·94	11·32	21·06	3·41	22·47	17·96
Co	-	-	-	-	-	-
Or	28·11	36·01	22·44	31·18	21·81	28·30
Ab	31·67	32·37	32·39	33·51	32·55	32·96
An	15·97	9·71	14·39	16·60	15·24	13·56
Ne	-	-	-	-	-	-
Mg-Di	2·61	2·35	0·89	4·99	0·09	1·25
Fe-Di	2·19	0·21	0·99	0·95	0·03	0·06
Wo	-	-	-	-	-	-
En	5·21	2·29	1·82	2·99	3·27	2·58
Fs	5·01	0·24	2·31	0·65	1·10	0·13
Fo	-	-	-	-	-	-
Fa	-	-	-	-	-	-
Mt	1·32	3·32	1·09	3·77	2·20	2·85
Il	1·05	0·73	0·61	1·01	0·58	0·58
Hm	-	-	-	-	-	-
Ap	0·62	0·36	0·26	0·51	0·39	0·43
H_2O	0·89	0·62	0·87	0·54	0·59	0·49

TABLE: (4-1-2c) Major element analyses and C.I.P.W. Norms of granodiorite from Serres-Drama granitic complex (cont.).

	50	51	57	63	163	164
SiO_2	65•40	57•04	65•85	60•36	67•63	67•82
TiO_2	0•41	0•61	0•36	0•48	0•31	0•29
Al_2O_3	16•70	18•49	16•09	18•19	16•40	16•62
Fe_2O_3	2•59	4•07	2•43	3•06	1•58	1•72
FeO	1•43	2•70	1•32	2•15	1•27	1•25
MnO	0•15	0•19	0•13	0•17	0•12	0•12
MgO	1•65	3•22	1•10	2•31	0•64	0•54
CaO	4•23	6•00	3•44	4•78	3•31	3•46
Na_2O	3•89	3•30	3•95	3•89	3•76	3•88
K_2O	3•65	4•43	4•45	4•86	4•00	3•85
P_2O_5	0•19	0•33	0•15	0•25	0•08	0•09
H_2O^+	0•55	0•82	0•49	0•40	0•62	0•86
Total	100•84	101•20	99•76	100•90	99•72	100•50

C.I.P.W. Norms.

Qz	18•31	4•83	17•87	6•65	22•28	22•25
Co	-	-	-	-	0•05	-
Or	21•58	26•16	26•32	28•73	23•64	22•76
Ab	32•90	27•95	33•44	32•88	31•82	32•86
An	17•32	22•56	13•02	17•84	15•90	16•53
Ne	-	-	-	-	-	-
Mg-Di	1•83	3•59	2•33	2•97	-	0•03
Fe-Di	0•03	0•37	0•05	0•42	-	0•01
Wo	-	-	-	-	-	-
En	3•27	6•35	1•67	4•37	1•60	1•34
Fs	0•07	0•74	0•04	0•71	0•75	0•61
Fo	-	-	-	-	-	-
Fa	-	-	-	-	-	-
Mt	3•75	5•90	3•53	4•44	2•29	2•49
Il	0•79	1•16	0•68	0•92	0•58	0•56
Hm	-	-	-	-	-	-
Ap	0•46	0•78	0•36	0•58	0•19	0•21
H_2O	0•55	0•82	0•49	0•40	0•62	0•86

TABLE: (4-1-2c) Major element analyses and C.I.P.W. Norms of granodiorite from Serres-Drama granitic complex (cont.).

	165	166	167	168	169	170
SiO_2	67•27	68•72	65•61	66•14	64•50	65•24
TiO_2	0•30	0•26	0•34	0•33	0•39	0•42
Al_2O_3	16•53	15•82	16•62	17•10	17•54	16•47
Fe_2O_3	2•15	2•20	2•38	2•52	2•63	2•11
FeO	0•82	0•45	1•04	1•01	0•89	1•63
MnO	0•10	0•07	0•11	0•13	0•15	0•15
MgO	0•56	0•39	0•65	0•71	0•64	1•02
CaO	2•93	2•43	3•22	3•48	3•51	3•56
Na_2O	3•95	3•64	3•90	4•01	4•29	3•63
K_2O	4•78	4•92	4•54	4•42	4•49	4•02
P_2O_5	0•10	0•08	0•12	0•13	0•10	0•13
H_2O^+	0•52	0•61	0•56	0•59	0•75	0•72
Total	100•01	99•59	99•09	100•57	99•88	99•10

C.I.P.W. Norms.

Qz	19•34	23•14	18•16	17•93	14•46	19•58
Co	-	0•21	-	-	-	-
Or	28•24	29•08	26•85	26•10	26•52	23•76
Ab	33•38	30•82	33•00	33•94	36•31	30•74
An	13•27	11•53	14•43	15•60	15•34	16•76
Ne	-	-	-	-	-	-
Mg-Di	0•47	-	0•61	0•67	1•14	0•02
Fe-Di	-	-	-	-	-	-
Wo	-	-	-	-	-	-
En	1•18	0•96	1•33	1•46	1•08	2•54
Fs	-	-	-	-	-	0•83
Fo	-	-	-	-	-	-
Fa	-	-	-	-	-	-
Mt	2•10	0•93	2•70	2•71	2•24	3•06
Il	0•56	0•49	0•65	0•63	0•74	0•72
Hm	0•70	1•56	0•52	0•65	1•09	-
Ap	0•24	0•19	0•27	0•30	0•23	0•32
H_2O	0•52	0•61	0•56	0•59	0•75	0•72

TABLE: (4-1-2c) Major element analyses and C.I.P.W. Norms of granodiorite from Serres-Drama granitic complex (cont.).

	171	213
SiO_2	63•91	69•17
TiO_2	0•50	0•30
Al_2O_3	17•09	15•44
Fe_2O_3	2•40	1•44
FeO	2•27	1•22
MnO	0•18	0•12
MgO	1•38	0•69
CaO	4•45	2•96
Na_2O	3•47	3•79
K_2O	3•47	3•59
P_2O_5	0•16	0•09
H_2O^+	0•63	0•45
Total	99•91	99•26

C.I.P.W. Norms.

Qz	18•59	25•93
Co	-	0•12
Or	20•52	21•23
Ab	29•34	32•03
An	20•81	14•11
Ne	-	-
Mg-Di	0• 13	-
Fe-Di	0•06	-
Wo	-	-
En	3•37	1•71
Fs	1•67	0•77
Fo	-	-
Fa	-	-
Mt	3•47	2•09
Il	0•95	0•57
Hm	-	-
Ap	0•38	0•20
H_2O	0•63	0•45

TABLE: (4-1-2d) Major element analyses and C.I.P.W. Norms of monzonite from Serres-Drama granitic complex.

	76	78	82	124	125	126
SiO_2	56·45	57·05	66·02	63·76	63·56	59·54
TiO_2	0·59	0·62	0·40	0·44	0·45	0·53
Al_2O_3	18·32	18·21	16·78	16·56	16·08	17·41
Fe_2O_3	3·56	3·70	2·43	2·11	2·19	2·72
FeO	2·87	3·16	1·37	1·84	1·78	2·20
MnO	0·18	0·19	0·15	0·11	0·13	0·15
MgO	2·93	3·19	1·29	1·68	1·91	2·36
CaO	5·94	6·24	3·76	3·64	3·97	5·18
Na_2O	3·34	3·51	3·90	3·45	3·72	3·93
K_2O	4·76	4·15	4·48	4·91	4·54	4·42
P_2O_5	0·28	0·29	0·17	0·12	0·17	0·21
H_2O^+	0·86	0·62	0·49	0·74	0·77	0·55
Total	100·08	100·93	101·24	99·36	99·27	99·20

C.I.P.W. Norms

Qz	3·18	4·09	17·21	14·85	14·27	6·82
Co	-	-	-	-	-	-
Or	28·14	24·55	26·45	29·03	26·81	26·14
Ab	28·28	29·67	32·96	29·22	31·50	33·23
An	20·92	21·69	15·08	15·16	13·75	16·80
Ne	-	-	-	-	-	-
Mg-Di	4·43	4·80	1·87	1·36	3·29	5·07
Fe-Di	0·90	1·10	0·06	0·32	0·57	0·91
Wo	-	-	-	-	-	-
En	5·24	5·72	2·35	3·36	3·23	3·53
Fs	1·22	1·50	0·09	0·96	0·65	0·72
Fo	-	-	-	-	-	-
Fa	-	-	-	-	-	-
Mt	5·16	5·36	3·53	3·06	3·18	3·94
Il	1·11	1·17	0·75	0·83	0·86	1·00
Hm	-	-	-	-	-	-
Ap	0·67	0·68	0·40	0·29	0·39	0·50
H_2O	0·86	0·62	0·49	0·74	0·77	0·55

TABLE: (4-1-2d) Major element analyses and C.I.P.W. Norms of monzonite from Serres-Drama granitic complex (continued).

	127	133	134	135	137	139
SiO_2	63·00	59·86	57·78	60·53	60·14	59·98
TiO_2	0·49	0·48	0·53	0·38	0·44	0·48
Al_2O_3	17·34	18·87	18·90	19·31	18·80	18·00
Fe_2O_3	2·43	2·64	2·77	2·23	1·81	2·47
FeO	1·94	1·23	1·75	1·00	1·01	1·46
MnO	0·13	0·13	0·19	0·08	0·14	0·12
MgO	2·06	1·16	1·93	0·83	0·57	1·21
CaO	4·51	4·36	4·95	3·50	3·95	4·15
Na_2O	4·06	4·11	4·20	4·07	3·42	4·10
K_2O	4·47	6·42	5·08	6·72	7·73	6·36
P_2O_5	0·16	0·15	0·23	0·12	0·19	0·19
H_2O^+	0·40	0·47	0·58	0·56	0·65	0·36
Total	100·99	99·88	98·89	99·33	98·85	98·88

C.I.P.W. Norms.

Qz	10·72	2·15	2·05	3·20	3·04	3·23
Co	-	-	-	-	-	-
Or	26·39	37·93	29·99	39·69	45·66	37·58
Ab	34·38	34·78	35·56	34·41	28·92	34·66
An	15·89	14·09	17·73	14·60	13·13	11·94
Ne	-	-	-	-	-	-
Mg-Di	3·69	5·12	3·90	1·56	3·07	5·64
Fe-Di	0·63	-	0·28	-	-	0·10
Wo	-	-	-	-	0·54	-
En	3·41	0·52	3·00	1·35	-	0·41
Fs	0·66	-	0·25	-	-	0·01
Fo	-	-	-	-	-	-
Fa	-	-	-	-	-	-
Mt	3·52	3·00	4·02	2·40	2·45	3·58
Il	0·92	0·91	1·01	0·72	0·83	0·92
Hm	-	0·56	-	0·57	0·12	-
Ap	0·39	0·35	0·55	0·28	0·45	0·46
H_2O	0·40	0·47	0·58	0·56	0·65	0·36

TABLE: (4-1-2d) Major element analyses and C.I.P.W. Norms of monzonite from Serres-Drama granitic complex (continued).

	140	141	142	143	144	145
SiO_2	60·09	60·00	60·18	57·32	58·89	58·65
TiO_2	0·56	0·51	0·46	0·61	0·42	0·46
Al_2O_3	18·08	18·70	18·64	18·75	18·90	18·97
Fe_2O_3	2·50	2·94	2·02	3·89	3·36	3·34
FeO	1·75	1·75	1·24	2·78	1·88	2·17
MnO	0·15	0·16	0·13	0·19	0·15	0·17
MgO	1·57	1·32	0·56	1·96	1·20	1·21
CaO	6·16	5·03	3·99	5·19	4·37	4·43
Na_2O	4·45	4·28	3·99	3·41	3·84	3·80
K_2O	4·88	5·03	6·38	4·87	5·72	5·71
P_2O_5	0·20	0·22	0·14	0·32	0·24	0·26
H_2O^+	0·39	0·46	0·47	1·69	0·66	0·70
Total	100·78	100·40	98·20	100·98	99·63	99·87

C.I.P.W. Norms.

Qz	3·38	5·00	4·56	5·61	4·65	4·32
Co	-	-	-	-	-	-
Or	28·84	29·74	37·71	28·79	33·83	33·73
Ab	37·69	36·24	33·75	28·85	32·46	32·12
An	14·92	16·94	14·11	21·48	17·46	17·85
Ne	-	-	-	-	-	-
Mg-Di	8·45	4·86	3·01	1·42	1·95	1·60
Fe-Di	0·93	0·32	0·17	0·31	0·15	0·36
Wo	1·03	-	0·30	-	-	-
En	-	1·04	-	4·23	2·08	2·27
Fs	-	0·08	-	1·07	0·18	0·58
Fo	-	-	-	-	-	-
Fa	-	-	-	-	-	-
Mt	3·62	4·27	2·92	5·64	4·86	4·84
Il	1·07	0·97	0·88	1·16	0·80	0·88
Hm	-	-	-	-	-	-
Ap	0·46	0·51	0·32	0·76	0·56	0·61
H_2O	0·39	0·46	0·47	1·69	0·66	0·70

TABLE: (4-1-2d) Major element analyses and C.I.P.W. Norms of monzonite from Serres-Drama granitic complex (continued).

	146	184	185	186	187	188
SiO_2	57•31	68•26	65•12	62•63	58•79	64•66
TiO_2	0•50	0•37	0•41	0•44	0•56	0•43
Al_2O_3	19•08	16•13	16•71	16•70	18•68	16•94
Fe_2O_3	3•68	1•96	2•05	2•31	2•86	2•32
FeO	2•51	1•32	1•67	1•63	2•11	1•61
MnO	0•18	0•07	0•12	0•12	0•17	0•10
MgO	1•80	0•80	1•19	1•22	1•55	1•20
CaO	5•17	3•22	3•96	4•10	6•67	4•18
Na_2O	3•70	3•82	3•92	3•97	4•32	4•05
K_2O	5•31	4•42	4•76	4•65	4•81	4•66
P_2O_5	0•30	0•10	0•14	0•15	0•20	0•16
H_2O^+	0•67	0•26	0•46	0•47	0•39	0•44
Total	100•2 1	100•73	100•51	98•39	101•11	100•75

C.I.P.W. Norms.

Qz	2•94	21•48	14•87	12•47	1•92	13•92
Co	-	-	-	-	-	-
Or	31•37	26•09	28•11	27•46	28•41	27•54
Ab	31•27	32•36	33•18	33•61	36•56	34•24
An	19•79	13•81	13•95	14•01	17•38	14•31
Ne	-	-	-	-	-	-
Mg-Di	2•57	1•06	3•02	3•63	8•34	3•72
Fe-Di	0•54	0•15	0•81	0•60	1•71	0•56
Wo	-	-	-	-	0•74	-
En	3•30	1•50	1•55	1•36	-	1•27
Fs	0•79	0•25	0•48	0•26	-	0•22
Fo	-	-	-	-	-	-
Fa	-	-	-	-	-	-
Mt	5•33	2•84	2•98	3•35	4•14	3•36
Il	0•95	0•69	0•78	0•84	1•05	0•82
Hm	-	-	-	-	-	-
Ap	0•71	0•23	0•33	0•36	0•48	0•37
H_2O	0•67	0•26	0•46	0•47	0•39	0•44

TABLE: (4-1-2d) Major element analyses and C.I.P.W. Norms of monzonite from Serres-Drama granitic complex (continued).

	189	191	192	193	195	196
SiO_2	65•81	64•84	59•63	61•84	59•50	59•68
TiO_2	0•39	0•50	0•43	0•52	0•50	0•54
Al_2O_3	16•26	16•88	17•33	17•30	17•60	17•50
Fe_2O_3	2•05	2•23	2•75	2•56	2•67	2•74
FeO	1•63	2•24	2•24	2•19	2•07	2•23
MnO	0•12	0•16	0•15	0•14	0•14	0•17
MgO	1•12	1•64	1•53	1•90	1•42	1•62
CaO	3•82	4•42	4•49	4•71	4•55	5•15
Na_2O	3•68	3•59	3•60	3•44	3•10	4•02
K_2O	3•98	3•55	5•19	4•86	5•99	4•50
P_2O_5	0•11	0•12	0•17	0•21	0•18	0•18
H_2O^+	0•63	0•58	0•48	0•80	0•79	0•41
Total	99•60	100•75	97•99	100•47	98•51	98•74

C.I.P.W. Norms.

Qz	19•68	18•35	7•93	11•32	7•81	7•31
Co	-	-	-	-	-	-
Or	23•51	21•00	30•68	28•73	35•39	26•57
Ab	31•16	30•40	30•45	29•08	26•22	34•00
An	16•09	19•44	15•81	17•41	16•44	16•43
Ne	-	-	-	-	-	-
Mg-Di	1•36	0•98	3•24	2•92	3•15	5•01
Fe-Di	0•37	0•37	1•05	0•71	0•80	1•35
Wo	-	-	-	-	-	-
En	2•17	3•63	2•32	3•37	2•07	1•70
Fs	0•68	1•55	0•86	0•94	0•60	0•52
Fo	-	-	-	-	-	-
Fa	-	-	-	-	-	-
Mt	2•97	3•24	3•98	3•71	3•87	3•98
Il	0•74	0•94	0•81	0•99	0•96	1•03
Hm	-	-	-	-	-	-
Ap	0•26	0•29	0•41	0•50	0•43	0•42
H_2O	0•63	0•58	0•48	0•80	0•79	0•41

TABLE: (4-1-2d) Major element analyses and C.I.P.W. Norms of monzonite from Serres-Drama granitic complex (continued).

	201	202	203	204	260	264
SiO_2	54•16	56•60	63•90	55•53	59•98	62•64
TiO_2	0•73	0•57	0•37	0•58	0•55	0•55
Al_2O_3	17•10	17•57	18•10	18•63	18•38	16•54
Fe_2O_3	3•53	2•79	2•21	3•94	3•29	2•98
FeO	3•38	2•68	1•69	2•52	1•97	1•85
MnO	0•18	0•16	0•14	0•16	0•12	0•15
MgO	3•63	2•32	0•85	1•80	1•47	1•40
CaO	9•03	6•53	3•47	7•40	4•94	4•07
Na_2O	3•15	3•75	4•20	3•76	3•88	3•61
K_2O	4•10	5•49	5•56	4•54	5•14	4•44
P_2O_5	0•43	0•33	0•17	0•32	0•22	0•18
H_2O^+	0•56	0•64	0•48	0•35	0•51	1•06
Total	99•98	99•43	101•14	99•53	100•45	99•47

C.I.P.W. Norms.

Qz	0•13	–	9•99	1•36	6•69	14•90
Co	–	–	–	–	–	–
Or	24•25	32•44	32•88	26•81	30•37	26•22
Ab	26•69	31•71	35•50	31•84	32•82	30•58
An	20•37	14•92	14•11	20•54	17•58	15•81
Ne	–	–	–	–	–	–
Mg-Di	13•96	9•50	1•17	9•69	4•08	2•34
Fe-Di	3•27	2•81	0•45	1•33	0•22	0•18
Wo	–	–	–	0•06	–	–
En	2•57	0•54	1•57	–	1•76	2•40
Fs	0•69	0•18	0•69	–	0•11	0•21
Fo	–	0•58	–	–	–	–
Fa	–	0•22	–	–	–	–
Mt	5•12	4•05	3•20	5•71	4•77	4•31
Il	1•39	1•09	0•69	1•11	1•04	1•05
Hm	–	–	–	–	–	–
Ap	1•03	0•77	0•39	0•76	0•53	0•42
H_2O	0•56	0•64	0•48	0•35	0•51	1•06

TABLE: (4-1-2d) Major element analyses and C.I.P.W. Norms of monzonite from Serres-Drama granitic complex (continued).

	269	320	321	323	324	325
SiO_2	61•31	62•22	58•93	56•63	57•93	55•59
TiO_2	0•50	0•34	0•51	0•61	0•61	0•66
Al_2O_3	17•92	18•00	19•55	17•33	18•35	17•31
Fe_2O_3	2•56	2•11	3•10	3•32	3•01	3•21
FeO	1•92	1•31	1•82	2•25	2•41	2•89
MnO	0•15	0•12	0•14	0•16	0•16	0•16
MgO	1•42	0•65	1•34	2•31	2•19	2•70
CaO	4•29	3•14	4•61	6•11	6•22	7•33
Na_2O	3•71	4•24	4•33	4•09	4•08	3•61
K_2O	5•16	5•78	5•72	5•48	6•09	5•01
P_2O_5	0•17	0•16	0•25	0•35	0•32	0•38
H_2O^+	0•63	0•56	0•46	0•45	0•47	0•61
Total	99•73	98•63	100•76	99•09	101•84	99•46

C.I.P.W. Norms.

Qz	9•46	7•87	1•51	-	-	-
Co	-	-	-	-	-	-
Or	30•48	34•21	33•81	32•35-	36•01	29•61
Ab	31•37	35•91	36•62	33•64	30•52	30•54
An	17•02	12•70	17•03	12•76	13•78	16•22
Ne	-	-	-	0•53	2•15	-
Mg-Di	2•09	1•22	3•12	10•91	9•98	11•33
Fe-Di	0•44	0•20	0•17	1•11	1•94	2•75
Wo	-	-	-	-	-	-
En	2•56	1•06	1•89	-	-	0•71
Fs	0•62	0•20	0•12	0•49	-	0•20
Fo	-	-	-	0•06	0•59	0•52
Fa	-	-	-	4•81	0•14	0•16
Mt	3•71	3•11	4•49	4•81	4•36	4•66
Il	0•95	0•63	0•96	1•17	1•17	1•25
Hm	-	-	-	-	-	-
Ap	0•39	0•37	0•59	0•83	0•76	0•91
H_2O	0•63	0•56	0•46	0•45	0•47	0•61

TABLE: (4-1-2d) Major element analyses and C.I.P.W. Norms of monzonite from Serres-Drama granitic complex (continued).

	329	330	334	338	340	341
SiO_2	55•58	55•46	54•17	56•96	56•50	56•52
TiO_2	0•44	0•64	0•73	0•64	0•66	0•64
Al_2O_3	17•59	17•65	17•95	17•50	17•83	17•34
Fe_2O_3	3•65	3•58	3•79	3•22	3•55	3•25
FeO	2•69	2•79	3•15	2•79	2•74	2•65
MnO	0•16	0•17	0•18	0•17	0•17	0•16
MgO	2•22	2•29	3•34	2•79	2•75	2•84
CaO	7•61	7•88	8•80	6•95	7•26	7•00
Na_2O	3•69	3•68	3•39	3•89	3•79	3•89
K_2O	4•80	4•57	4•33	5•14	4•19	5•24
P_2O_5	0•38	0•40	0•45	0•36	0•37	0•37
H_2O^+	0•35	0•44	0•53	0•58	0•47	0•47
Total	99•16	99•55	99•91	101•00	101•00	100•37

C.I.P.W. Norms.

Qz	0•42	0•74	-	-	-	-
Co	-	-	-	-	-	-
Or	28•34	27•00	25•58	30•36	29•03	30•99
Ab	31•21	31•10	28•24	32•89	32•09	31•54
An	17•29	18•17	18•52	15•14	17•12	14•37
Ne	-	-	0•23	-	-	0•74
Mg-Di	11•61	11•99	14•89	11•16	11•16	12•09
Fe-Di	2•75	2•60	2•77	2•40	1•88	2•13
Wo	-	-	-	-	-	-
En	0•16	0•15	-	0•47	1•65	-
Fs	0•04	0•04	-	0•12	0•32	-
Fo	-	-	1•00	0•90	0•02	1•02
Fa	-	-	0•23	0•25	-	0•23
Mt	5•29	5•19	5•50	4•67	5•14	4•72
Il	0•83	1•22	1•39	1•22	1•26	1•21
Hm	-	-	-	-	-	-
Ap	0•89	0•95	1•05	0•86	0•89	0•88
H_2O	0•35	0•44	0•53	0•58	0•47	0•47

TABLE: (4-1-2d) Major element analyses and C.I.P.W. Norms of monzonite from Serres-Drama granitic complex (continued).

	342	345	346	350	351	352
SiO_2	57·03	60·63	59·65	62·19	59·38	60·04
TiO_2	0·59	0·45	0·48	0·43	0·48	0·46
Al_2O_3	17·50	18·65	18·83	17·62	17·77	17·54
Fe_2O_3	2·81	2·84	2·80	3·12	3·43	1·02
FeO	2·66	1·96	2·12	2·16	2·27	2·37
MnO	0·15	0·14	0·14	0·16	0·17	0·16
MgO	2·54	1·18	1·27	1·68	1·66	1·74
CaO	6·54	4·10	4·16	4·30	4·59	4·57
Na_2O	4·03	4·41	4·30	3·65	3·77	3·86
K_2O	5·50	5·34	5·40	5·05	4·86	4·98
P_2O_5	0·35	0·23	0·23	0·21	0·20	0·19
H_2O^+	0·51	0·59	0·46	0·91	0·86	0·50
Total	100·12	100·51	99·84	101·47	99·44	97·43

C.I.P.W. Norms.

Qz	-	5·05	4·01	10·76	7·61	6·51
Co	-	-	-	-	-	-
Or	32·48	31·53	31·89	29·82	28·74	29·44
Ab	32·26	37·33	36·37	30·89	31·91	32·64
An	13·42	15·32	16·14	16·79	17·19	15·85
Ne	1·00	-	-	-	-	-
Mg-Di	10·34	2·31	1·84	2·12	2·88	2·82
Fe-Di	2·67	0·54	0·54	0·43	0·52	1·73
Wo	-	-	-	-	-	-
En	-	1·88	2·30	3·20	2·81	3·03
Fs	-	0·50	0·77	0·74	0·58	2·14
Fo	-	-	-	-	-	-
Fa	-	-	-	-	-	-
Mt	4·08	4·11	4·05	4·52	4·97	1·47
Il	1·11	0·85	0·91	0·82	0·91	0·87
Hm	-	-	-	-	-	-
Ap	0·83	0·53	0·55	0·49	0·48	0·45
H_2O	0·51	0·59	0·46	0·91	0·86	0·50

TABLE: ((4-1-2d) Major element analyses and C.I.P.W. Norms of monzonite from Serres-Drama granitic complex (continued).

	353	354	355	356	357	358
SiO_2	60•72	60•85	60•36	59•89	59•80	61•44
TiO_2	0•48	0•47	0•48	0•48	0•49	0•51
Al_2O_3	17•49	18•34	17•60	16•98	16•85	17•40
Fe_2O_3	2•91	3•37	2•94	3•00	3•18	3•56
FeO	2•22	2•19	2•32	2•20	2•29	2•07
MnO	0•17	0•17	0•17	0•17	0•17	0•16
MgO	1•49	1•53	1•54	1•59	1•69	1•63
CaO	4•66	4•96	4•45	4•43	5•03	5•01
Na_2O	3•84	3•88	3•89	3•78	3•80	3•81
K_2O	4•95	5•06	4•92	5•37	4•90	4•97
P_2O_5	0•20	0•19	0•20	0•19	0•19	0•20
H_2O^+	0•53	0•53	0•63	0•54	0•45	0•74
Total	99•66	101•54	99•50	98•62	98•84	101•50

C.I.P.W. Norms.

Qz	8•54	7•46	8•04	7•07	7•67	9•21
Co	-	-	-	-	-	-
Or	29•26	29•88	29•09	31•75	28•96	29•35
Ab	32•50	32•80	32•92	32•02	32•16	32•27
An	15•86	17•70	16•03	13•49	14•45	15•69
Ne	-	-	-	-	-	-
Mg-Di	3•72	3•80	2•90	4•68	6•03	5•76
Fe-Di	1•04	0•68	0•89	1•11	1•37	0•41
Wo	-	-	-	-	-	-
En	1•99	2•04	2•49	1•78	1•42	1•39
Fs	0•64	0•42	0•88	0•49	0•37	0•11
Fo	-	-	-	-	-	-
Fa	-	-	-	-	-	-
Mt	4•21	4•89	4•26	4•35	4•62	5•16
Il	0•91	0•89	0•92	0•92	0•92	0•96
Hm	-	-	-	-	-	-
Ap	0•48	0•46	0•48	0•45	0•44	0•48
H_2O	0•53	0•53	0•63	0•54	0•45	0•74

TABLE: (4-1-2d) Major element analyses and C.I.P.W. Norms of monzonite from Serres-Drama granitic complex (continued).

	359	360	362	363	364	365
SiO_2	60•66	60•19	60•32	59•44	59•18	61•20
TiO_2	0•46	0•51	0•44	0•46	0•50	0•48
Al_2O_3	17•98	17•79	17•48	17•12	17•53	17•65
Fe_2O_3	3•35	3•32	2•76	3•03	3•38	3•05
FeO	2•02	2•46	2•10	2•20	2•23	2•37
MnO	0•16	0•18	0•16	0•17	0•18	0•16
MgO	1•69	1•75	0•84	1•47	1•86	1•51
CaO	4•47	5•01	4•42	4•88	4•88	4•92
Na_2O	3•73	3•90	3•72	3•80	3•91	3•85
K_2O	4•96	4•61	5•27	5•33	5•16	5•01
P_2O_5	0•20	0•22	0•22	0•20	0•21	0•20
H_2O^+	0•65	0•63	0•52	0•64	0•35	0•55
Total	100•33	100•57	98•25	98•74	99•37	100•95

C.I.P.W. Norms.

Qz	8•96	7•88	8•96	6•32	5•41	8•30
Co	-	-	-	-	-	-
Or	29•31	27•23	31•15	31•49	30•47	29•62
Ab	31•53	32•98	31•50	32•14	33•04	32•60
An	17•67	17•45	15•42	13•92	15•08	16•07
Ne	-	-	-	-	-	-
Mg-Di	2•26	3•80	2•76	5•69	5•35	4•29
Fe-Di	0•22	0•97	1•33	1•49	0•81	1•33
Wo	-	-	-	-	-	-
En	3•15	2•59	0•82	1•02	2•14	1•76
Fs	0•36	0•76	0•45	0•31	0•37	0•63
Fo	-	-	-	-	-	-
Fa	-	-	-	-	-	-
Mt	4•86	4•81	4•00	4•39	4•90	4•43
Il	0•88	0•97	0•83	0•87	0•95	0•92
Hm	-	-	-	-	-	-
Ap	0•48	0•51	0•53	0•48	0•49	0•48
H_2O	0•65	0•63	0•52	0•64	0•35	0•55

TABLE: (4-1-2d) Major element analyses and C.I.P.W. Norms of monzonite from Serres-Drama granitic complex (continued).

	366	367	368
SiO_2	61•11	60•61	60•82
TiO_2	0•45	0•45	0•44
Al_2O_3	17•42	18•38	17•67
Fe_2O_3	2•82	2•85	2•29
FeO	2•37	2•01	1•85
MnO	0•16	0•15	0•14
MgO	1•45	1•04	1•20
CaO	4•56	4•00	3•24
Na_2O	3•84	4•30	4•04
K_2O	4•83	5•25	5•99
P_2O_5	0•20	0•23	0•20
H_2O^+	0•55	0•46	0•95
Total	99•76	99•73	98•83

C.I.P.W. Norms

Qz	9•34	6•28	6•25
Co	-	-	-
Or	28•57	31•02	35•39
Ab	32•46	36•38	34•22
An	16•04	15•36	12•38
Ne	-	-	-
Mg-Di	3•08	1•87	1•48
Fe-Di	1•18	0•55	0•45
Wo	-	-	-
En	2•19	1•72	2•30
Fs	0•96	0•58	0•80
Fo	-	-	-
Fa	-	-	-
Mt	4•08	4•13	3•32
Il	0•85	0•85	0•83
Hm	-	-	-
Ap	0•47	0•53	0•47
H_2O	0•55	0•46	0•95

TABLE: (4-1-2e) Major element analyses and C.I.P.W. Norms of gabbro from Serres-Drama granitic complex

	147	151	152	153	172
SiO_2	59•29	48•38	46•51	46•49	46•83
TiO_2	0•79	0•78	0•87	1•11	1•05
Al_2O_3	18•76	14•02	13•70	13•51	12•61
Fe_2O_3	0•97	3•76	4•08	5•82	5•99
FeO	1•97	5•48	5•94	4•97	6•72
MnO	0•15	0•22	0•20	0•25	0•22
MgO	2•40	7•34	7•69	7•48	7•88
CaO	8•16	17•91	19•20	18•79	17•98
Na_2O	2•97	0•63	0•54	0•33	0•41
K_2O	3•30	0•49	0•40	0•40	0•45
P_2O_5	0•22	0•38	0•07	0•33	0•03
H_2O^+	0•99	1•99	1•52	1•91	1•59
Total	99•97	101•38	100•72	101•39	101•76

C.I.P.W. Norms.

Qz	10•46	3•13	1•10	3•51	2•29
Co	-	-	-	-	-
Or	19•47	2•88	2•38	2•33	2•63
Ab	25•16	5•34	4•54	2•78	3•45
An	28•12	33•99	33•79	34•21	31•26
Ne	-	-	-	-	-
Mg-Di	6•95	32•55	33•72	39•51	36•37
Fe-Di	1•83	9•44	9•90	5•45	9•81
Wo	-	-	-	-	-
En	2•77	3•19	3•53	0•32	2•75
Fs	0•83	1•06	1•19	0•05	0•85
Fo	-	-	-	-	-
Fa	-	-	-	-	-
Mt	1•40	5•45	5•92	8•44	8•68
Il	1•49	1•48	1•66	2•11	2•00
Hm	-	-	-	-	-
Ap	0•51	0•90	2•54	0•77	0•08
H_2O	0•99	1•99	1•52	1•91	1•59

TABLE: (4-1-2f) Major element analyses and C.I.P.W. Norms of aplite from Serres-Drama granitic complex

	3	41	42	148
SiO_2	75•70	76•38	76•77	72•83
TiO_2	0•06	0•07	0•04	0•14
Al_2O_3	12•94	13•59	13•57	14•19
Fe_2O_3	0•17	0•19	0•06	0•80
FeO	0•28	0•25	0•20	0•60
MnO	0•02	0•02	0•01	0•03
MgO	0•25	0•16	0•09	0•09
CaO	0•59	0•94	0•66	1•45
Na_2O	3•82	3•72	3•07	3•44
K_2O	5•24	5•07	6•37	4•50
P_2O_5	0•04	0•07	0•06	0•04
H_2O^+	0•50	0•35	0•40	0•62
Total	99•61	100•81	101•30	98•73

C.I.P.W. Norms.

Qz	31•75	33•20	33•01	32•33
Co	0•01	0•35	0•44	0•88
Or	30•98	29•97	37•66	26•62
Ab	32•35	31•46	25•99	29•12
An	2•63	4•18	2•90	6•92
Ne	-	-	-	-
Mg-Di	-	-	-	-
Fe-Di	-	-	-	-
Wo	-	-	-	-
En	0•62	0•40	0•23	0•22
Fs	0•31	0•23	0•27	0•26
Fo	-	-	-	-
Fa	-	-	-	-
Mt	0•25	0•28	0•09	1•16
Il	0•12	0•12	0•07	0•26
Hm	-	-	-	-
Ap	0•10	0•17	0•14	0•09
H_2O	0•50	0•35	0•40	0•62

TABLE: (4-1-2g) Major element analyses and C.I.P.W. Norms of dioritic xenolith from Serres-Drama granitic complex

	1	6a1	6a2	6b1
SiO_2	54.53	53.67	52.86	52.02
TiO_2	0.68	0.90	0.86	0.87
Al_2O_3	18.31	17.55	17.08	18.49
Fe_2O_3	0.62	1.24	0.85	1.97
FeO	6.18	7.87	8.19	7.13
MnO	0.22	0.39	0.38	0.33
MgO	3.61	3.98	3.86	4.30
CaO	7.65	8.32	8.18	8.02
Na_2O	3.69	4.67	4.54	5.01
K_2O	3.51	0.74	0.90	0.63
P_2O_5	0.32	0.22	0.33	0.37
H_2O+	0.98	1.13	1.57	1.45
Total	100.30	99.55	99.60	100.59

C.I.P.W. Norms

Qz	-	-	-	-
Co	-	-	-	-
Or	20.76	4.35	5.33	3.73
Ab	31.18	39.54	38.42	42.18
An	23.04	24.75	23.55	26.11
Ne	-	-	-	0.10
Mg-Di	5.39	5.59	5.57	5.00
Fe-Di	5.29	6.62	6.89	4.33
Wo	-	-	-	-
En	0.96	3.83	3.26	-
Fs	1.09	4.88	4.62	-
Fo	3.88	2.34	2.64	5.89
Fa	4.81	3.29	4.12	6.44
Mt	0.89	1.80	1.24	2.85
Il	1.28	1.71	1.62	1.65
Hm	-	-	-	-
Ap	0.75	0.52	0.78	0.87
H_2O	0.98	1.13	1.57	1.45

TABLE: (4-1-2g) Major element analyses and C.I.P.W. Norms of dioritic xenolith from Serres-Drama granitic complex (cntd)

	6b2	7b	7d	315
SiO_2	52.67	54.17	54.08	57.05
TiO_2	0.78	0.83	0.84	0.64
Al_2O_3	18.16	18.03	17.89	18.98
Fe_2O_3	2.49	0.63	0.67	5.07
FeO	6.71	7.36	7.12	1.98
MnO	0.32	0.29	0.28	0.21
MgO	4.26	3.37	3.34	1.28
CaO	7.71	6.97	6.86	7.07
Na_2O	4.99	4.38	4.28	3.67
K_2O	0.69	1.76	1.77	3.16
P_2O_5	0.36	0.20	0.21	0.31
H_2O^+	1.59	1.48	1.55	0.82
Total	100.73	99.47	98.89	100.24

C.I.P.W.Norms

Qz	-	-	-	8.97
Co	-	-	-	-
Or	4.07	10.42	10.47	18.65
Ab	42.19	37.08	36.18	31.05
An	25.13	24.31	24.39	25.99
Ne	-	-	-	-
Mg-Di	4.99	3.31	3.11	5.53
Fe-Di	3.92	4.18	3.80	-
Wo	-	-	-	-
En	2.62	5.17	6.60	0.62
Fs	2.36	7.51	9.25	-
Fo	3.98	1.18	0.19	-
Fa	3.96	1.88	0.30	-
Mt	3.61	0.92	0.97	5.22
Il	1.48	1.58	1.60	1.21
Hm	-	-	-	1.47
Ap	0.85	0.48	0.50	0.72
H_2O	1.59	1.48	1.55	0.82

TABLE: (4-1-2h) Average major element compositions of the whole complex, quartz monzonite (Qm) + granite (Gr) + granodiorite (Gd) and individual rock-suites from the Serres-Drama granitic complex.

	Aver w.r.s	Aver Qm,Gr, Gd Samp88	Aver Qm Sam50	Aver Gr Sam18	Aver Gd Sam20	Aver Mon Sam69	Aver Apl Samp4	Aver Gab Samp5	Aver Xen Samp8
SiO_2	$^{62.32}_{-5.10}$	$^{65.08}_{-2.76}$	$^{64.39}_{-2.49}$	$^{67.04}_{-1.57}$	$^{64.99}_{-3.42}$	$^{59.96}_{-2.88}$	$^{75.42}_{-1.79}$	$^{49.50}_{-5.53}$	$^{53.88}_{-1.54}$
TiO_2	$^{0.47}_{-0.16}$	$^{0.41}_{-0.09}$	$^{0.44}_{-0.08}$	$^{0.37}_{-0.05}$	$^{0.39}_{-0.10}$	$^{0.50}_{-0.09}$	$^{0.08}_{-0.04}$	$^{0.92}_{-0.15}$	$^{0.80}_{-0.10}$
Al_2O_3	$^{17.02}_{-1.25}$	$^{16.65}_{-0.87}$	$^{16.84}_{-0.87}$	$^{16.02}_{-0.61}$	$^{16.76}_{-0.85}$	$^{17.75}_{-0.79}$	$^{13.57}_{-0.51}$	$^{14.52}_{-2.43}$	$^{18.06}_{-0.58}$
Fe_2O_3	$^{2.40}_{-0.94}$	$^{2.08}_{-0.65}$	$^{2.20}_{-0.63}$	$^{1.66}_{-0.45}$	$^{2.17}_{-0.74}$	$^{2.87}_{-0.58}$	$^{0.31}_{-0.33}$	$^{4.12}_{-2.03}$	$^{1.69}_{-1.53}$
MnO	$^{0.15}_{-0.05}$	$^{0.13}_{-0.03}$	$^{0.13}_{-0.04}$	$^{0.12}_{-0.01}$	$^{0.13}_{-0.03}$	$^{0.15}_{-0.02}$	$^{0.02}_{-0.01}$	$^{0.21}_{-0.04}$	$^{0.30}_{-0.07}$
MgO	$^{1.63}_{-1.25}$	$^{1.21}_{-0.68}$	$^{1.29}_{-0.66}$	$^{0.93}_{-0.60}$	$^{1.25}_{-0.77}$	$^{1.69}_{-0.65}$	$^{0.15}_{-0.08}$	$^{6.56}_{-2.33}$	$^{3.50}_{-0.97}$
CaO	$^{4.67}_{-2.62}$	$^{3.62}_{-0.84}$	$^{3.81}_{-0.76}$	$^{2.98}_{-0.69}$	$^{3.73}_{-0.89}$	$^{5.04}_{-1.32}$	$^{0.91}_{-0.39}$	$^{16.41}_{-4.64}$	$^{7.60}_{-0.57}$
Na_2O	$^{3.81}_{-0.62}$	$^{3.89}_{-0.33}$	$^{3.90}_{-0.40}$	$^{3.93}_{-0.23}$	$^{3.82}_{-0.21}$	$^{3.85}_{-0.28}$	$^{3.51}_{-0.34}$	$^{0.98}_{-1.12}$	$^{4.40}_{-0.52}$
K_2O	$^{4.54}_{-1.16}$	$^{4.52}_{-0.61}$	$^{4.51}_{-0.61}$	$^{4.67}_{-0.54}$	$^{4.39}_{-0.65}$	$^{5.11}_{-0.67}$	$^{5.30}_{-0.78}$	$^{1.01}_{-1.28}$	$^{1.65}_{-1.14}$
P_2O_5	$^{0.20}_{-0.11}$	$^{0.16}_{-0.07}$	$^{0.17}_{-0.07}$	$^{0.14}_{-0.05}$	$^{0.15}_{-0.07}$	$^{0.23}_{-0.08}$	$^{0.05}_{-0.02}$	$^{0.41}_{-0.40}$	$^{0.29}_{-0.07}$
H_2O	$^{0.65}_{-0.30}$	$^{0.61}_{-0.18}$	$^{0.64}_{-0.18}$	$^{0.48}_{-0.12}$	$^{0.63}_{-0.15}$	$^{0.58}_{-0.20}$	$^{0.47}_{-0.12}$	$^{1.60}_{-0.40}$	$^{1.32}_{-0.30}$

* ($^{+}_{-}5.10$) = Standard deviation

TABLE: (4-1-2i) Chemical analyses of quartz monzonite, granodiorite, monzonite and gabbro from the Serres-Drama pluton. (Papadakis 1965, table 25, p 83).

	Qz monzonite	Granodiorite	Monzonite	Gabbro
SiO_2	65•92	63•76	59•58	43•69
Al_2O_3	15•51	18•11	20•02	20•57
Fe_2O_3	1•32	1•49	1•92	3•20
FeO	2•14	1•90	2•23	8•35
MnO	0•08	0•07	0•12	0•14
MgO	1•25	1•64	2•20	7•20
CaO	3•36	4•50	4•41	12•54
Na_2O	3•84	3•89	3•75	1•62
K_2O	4•63	3•41	5•06	0•78
TiO_2	0•39	0•33	0•37	0•93
P_2O_5	0•38	0•40	0•43	0•17
$+H_2O$	0•36	0•46	0•26	0•69
Total	99•18	99•96	100•35	99•88

62.3%. However for each of the component rock-types the SiO_2 content is as follows:

	Rock-type	Range of SiO_2%	Mean of SiO_2%
	Aplite	72.8-76.8	75.4
'intermediate group'	(granite	64.5-70.0	67.0
	(granodiorite	57.0-69.2	65.0
	(quartz monzonite	57.9-68.4	64.4
	(monzonite	54.2-68.3	59.9
'basic group'	(dioritic (xenoliths	52.0-57.1	53.9
	(gabbro	46.5-59.3*	49.5

(* this figure is from gabbro No.147 with a leucocratic vein running through it.)

The average major element oxide percentages for the whole complex, the 'intermediate' group, and each individual rock suite are listed in table (4-1-2h), together with their standard deviations.

It can be seen from this table that in the 'intermediate' group some variation in major element oxide concentrations occurs between the periphery and centre of the outcrop of these rocks. SiO_2 and probably K_2O increased from the periphery towards the centre, although the mean values for K_2O do in fact increase, when consideration is taken of the standard deviation of this oxide (table, 4-1-2h), the increase is less certain; Na_2O remains fairly constant; the other oxides, including H_2O^+, decrease.

From table (4-1-2h), the comparison of the average analyses for the 'intermediate' rocks and monzonite show

that in the 'intermediate' rocks the SiO_2 is higher, but all the other oxides are lower than in the monzonite. Consequently, on the basis of chemical composition of the major elements the 'intermediate' rocks are different from the monzonite, as expected.

From their chemical composition it is obvious that the gabbro, dioritic xenoliths and aplite are distinct from each other and from all other rock-types. From the table (4-1-2h) it can be seen that the highes values of TiO_2, CaO, MgO and total iron are to be found in the gabbro. These oxides decrease with increasing differentiation. The Na_2O values are low in gabbro, as shown in fig. (4-1-2i).

Papadakis' (1965) analyses are given in table (4-1-2i) as a comparison with the average analyses of the present study. His silica values are similar except for the gabbro which is lower than the present study (possibly because the impure sample No.147 is included in the present study). The other major element oxides are not significantly different.

Various parameters have been put forward as possible indices of differentiation. For plutonic complexes, indices which have been suggested are variation in SiO_2 content (Bateman and Dodge, 1970; Shaw and Flood, 1981; Brown, 1982), modified Larsen index (Nockolds and Allen, 1953) and differentiation index of Thornton and Tuttle (Brown, M. et al, 1981). In this study SiO_2 has been used as a measure of differentiation because the range is wide enough to bring out the essential features and for simplicity. Comparison

between the indices above have shown that the SiO_2 and modified Larsen index are almost identical, whereas the Thornton and Tuttle index is slightly different but still very similar.

The analytical data for the major element oxides are plotted in the following figures (4-1-2a) to (4-1-21). All the major elements, with the exception of the alkalis, show a trend of decreasing concentration with increasing differentiation. TiO_2, total iron, MgO, CaO show good negative correlations with SiO_2, while Fe_2O_3, FeO, MnO, P_2O_5 show somewhat less good correlations. However K_2O (and total alkalis) show an increase with differentiation, whereas Na_2O remains essentially constant. This observation for Na_2O is similar to that noted by Bickford et al (1981) for rocks from the Proterozoic plutonic complexes of southeast Missouri.

C.I.P.W. norms were calculated from the major element oxides using the computer programme written by G.J. Lees (based on the method of Kelsy, 1965) using the chemical composition of the granitic complex. The data obtained are given in tables (4-1-2a) to (4-1-2g). For comparison of norms with modal analyses see petrography chapter (table, 2-1-2a). The C.I.P.W. norms approximate to the modal analyses, quartz rich samples having relatively high quartz norms. The normative plagioclase values are largely comparable with modal analyses, with the exception of samples numbers 140, 213, 321, which give higher normative plagioclase values than indicated in the modes. Three

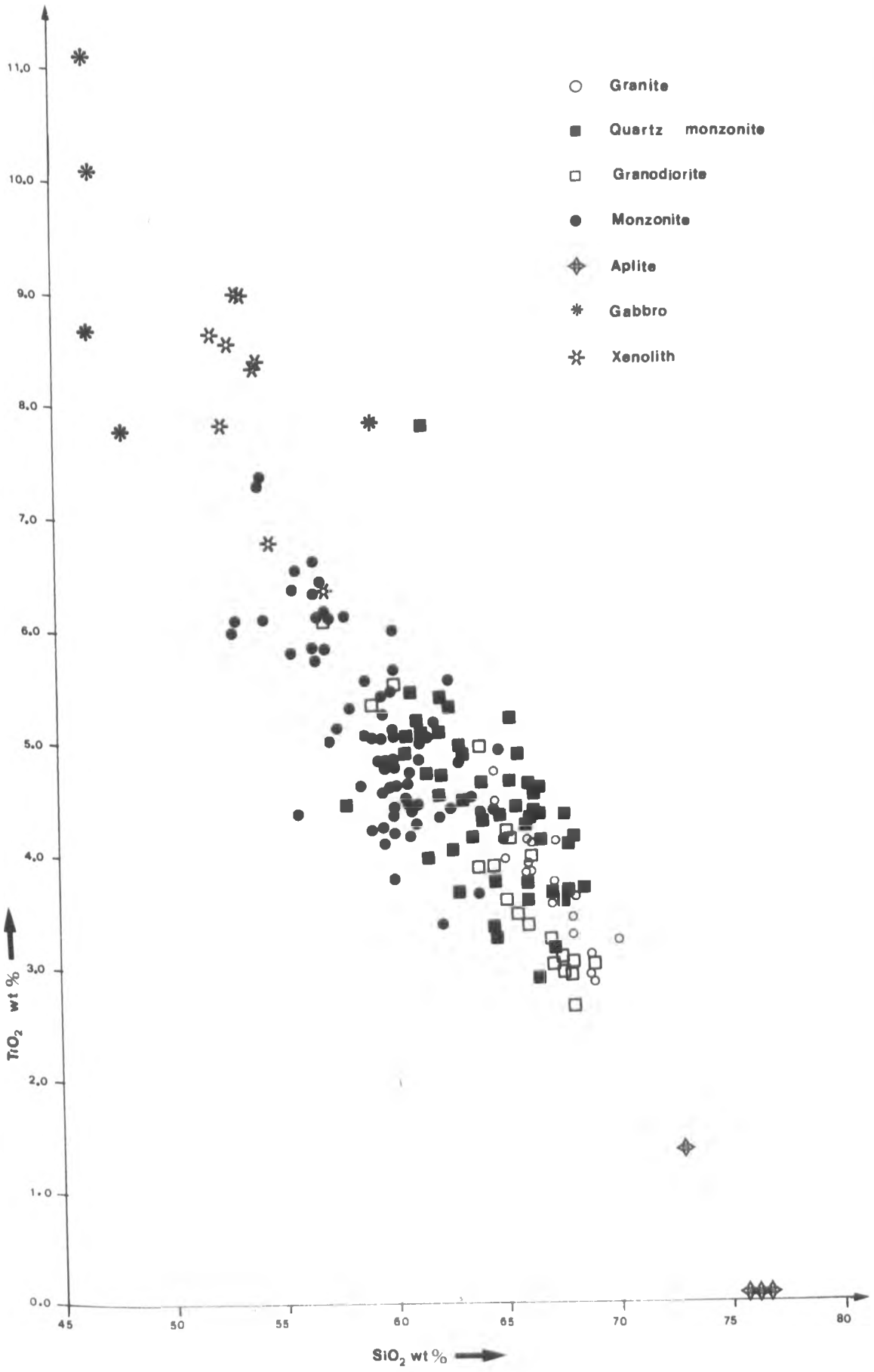
Granite
Quartz monzonite
Granodiorite
Monzonite
Aplite
Gabbro
Xenolith
11.0
10.0
9.0
8.0
7.0
6.0
5.0
4.0
3.0
2.0
1.0
0.0
TiO2 wt %
45
50
55
60
65
70
75
80
SiO2 wt %

Fig. (4-1-2a)

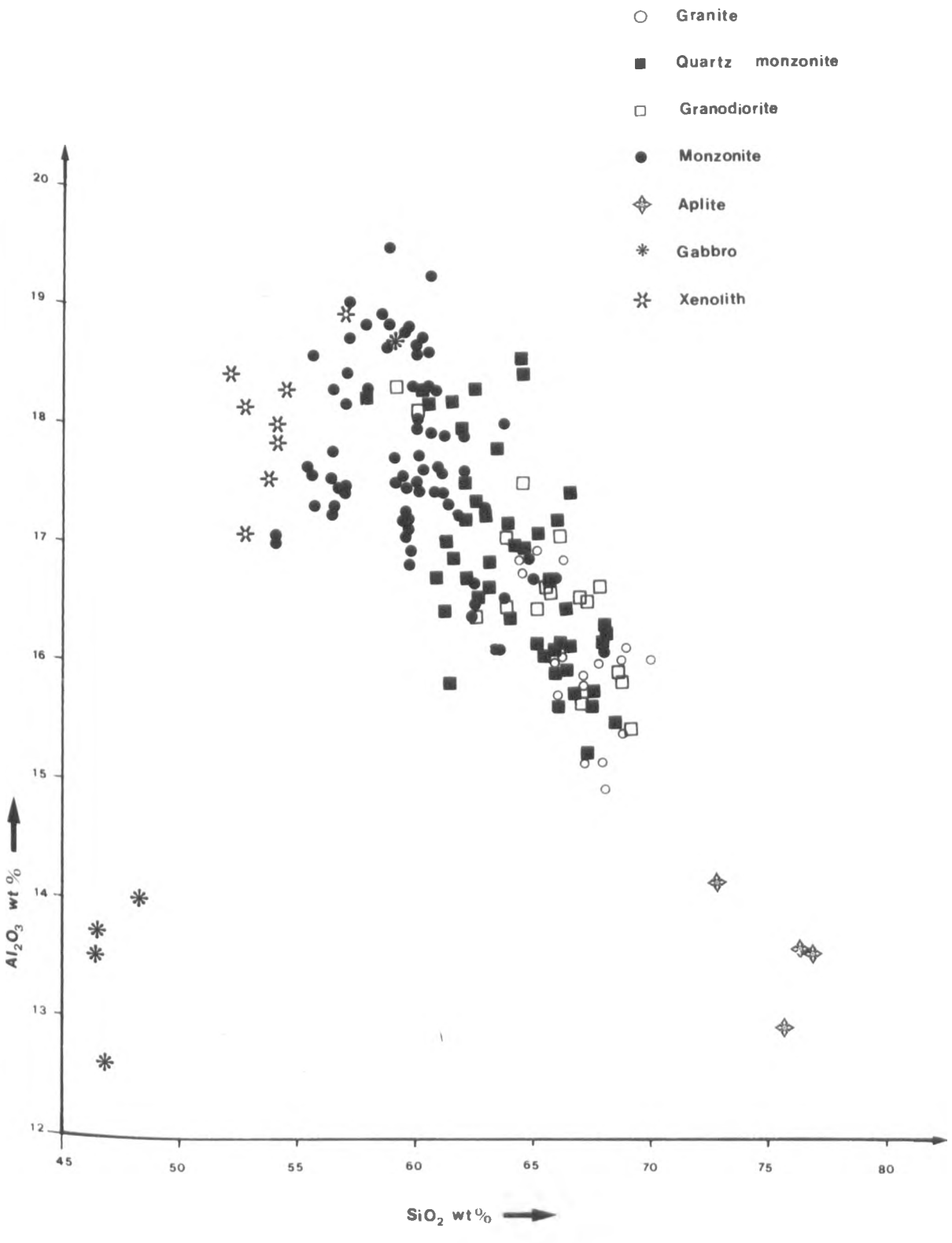
Granite
Quartz monzonite
Granodiorite
Monzonite
Aplite
Gabbro
Xenolith
20
19
18
17
16
15
14
13
12
Al_2O_3 wt %
45
50
55
60
65
70
75
80
SiO_2 wt%

Fig. (4-1-2b)

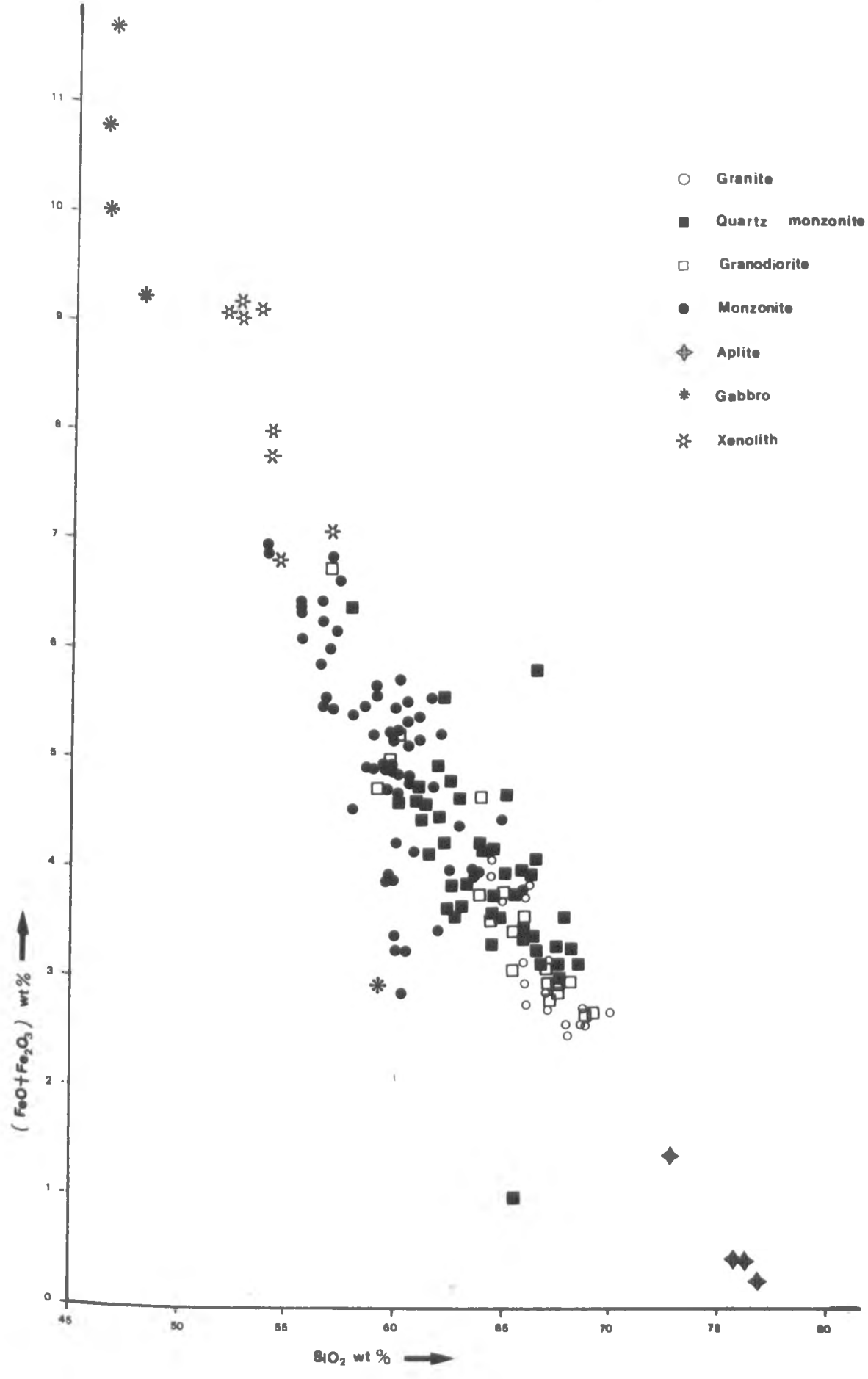
Granite
Quartz monzonite
Granodiorite
Monzonite
Aplite
Gabbro
Xenolith
(FeO+Fe2O3) wt %
SiO2 wt %
0
1
2
3
4
5
6
7
8
9
10
11
45
50
55
60
65
70
75
80

Fig. (4-1-2c)

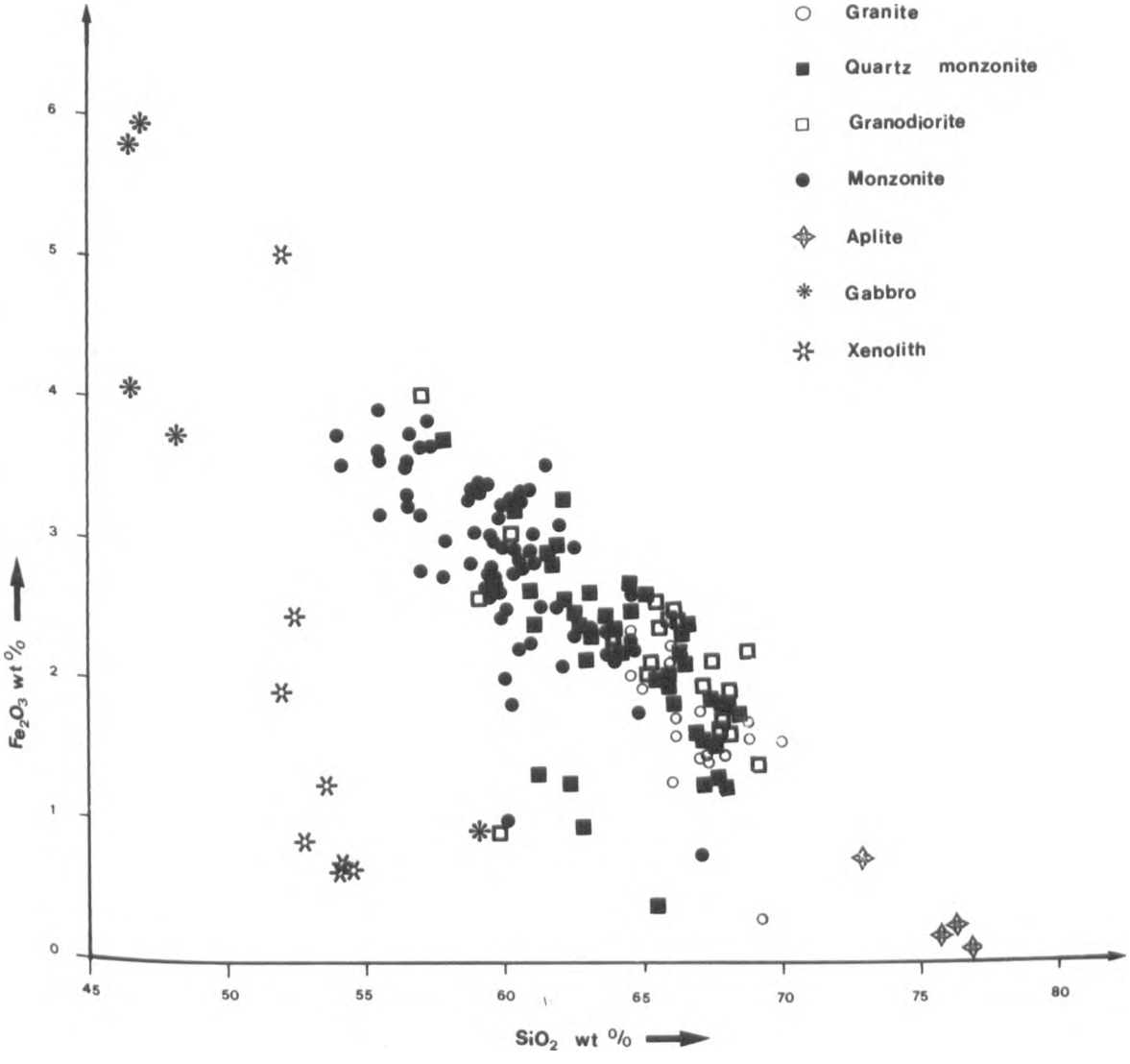
Granite
Quartz monzonite
Granodiorite
Monzonite
Aplite
Gabbro
Xenolith
Fe_2O_3 wt %
SiO_2 wt %
0
1
2
3
4
5
6
45
50
55
60
65
70
75
80

Fig. (4-1-2d)

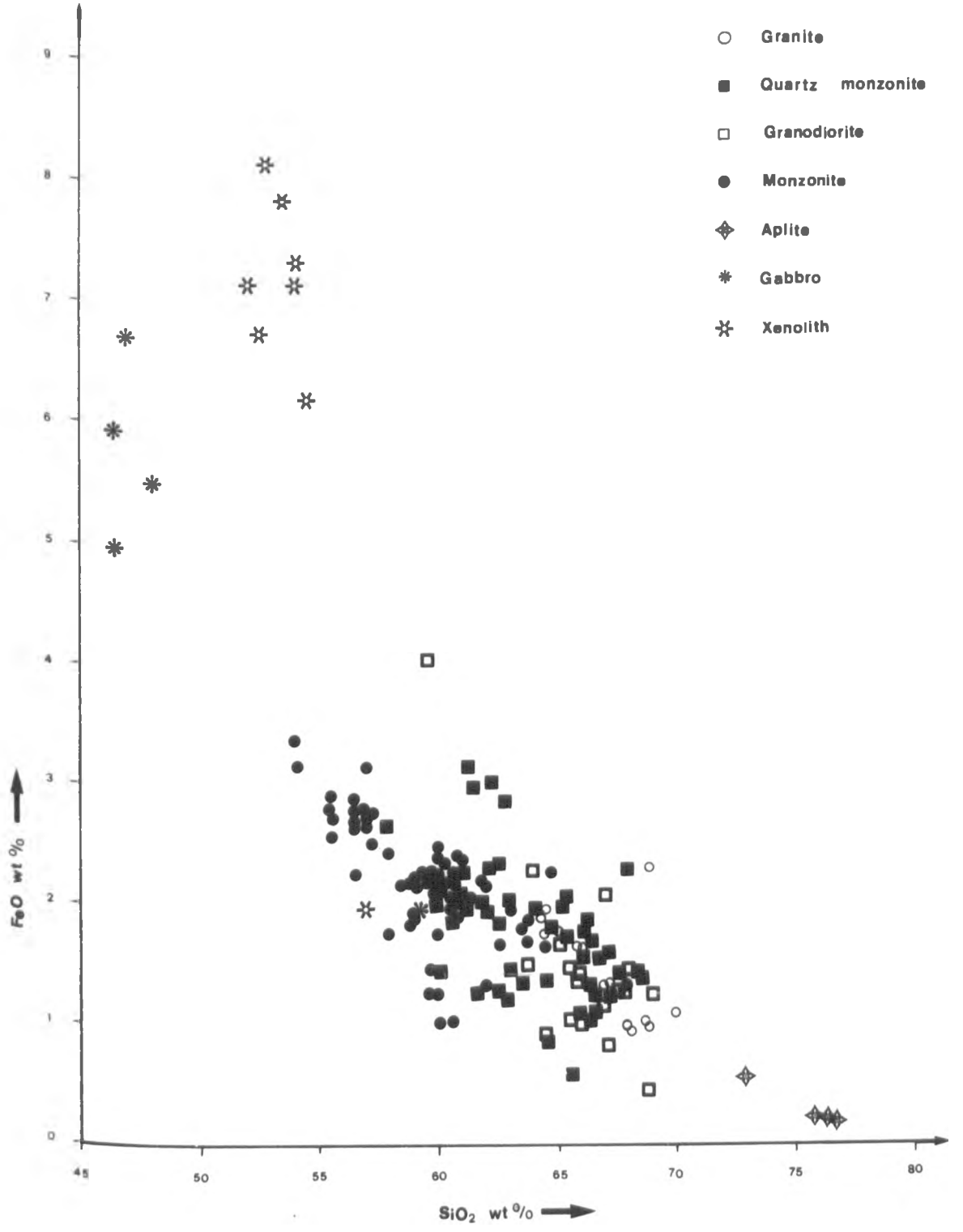
Granite
Quartz monzonite
Granodiorite
Monzonite
Aplite
Gabbro
Xenolith
FeO wt %
SiO2 wt %
0
1
2
3
4
5
6
7
8
9
45
50
55
60
65
70
75
80

Fig. (4 – 1 – 2e)

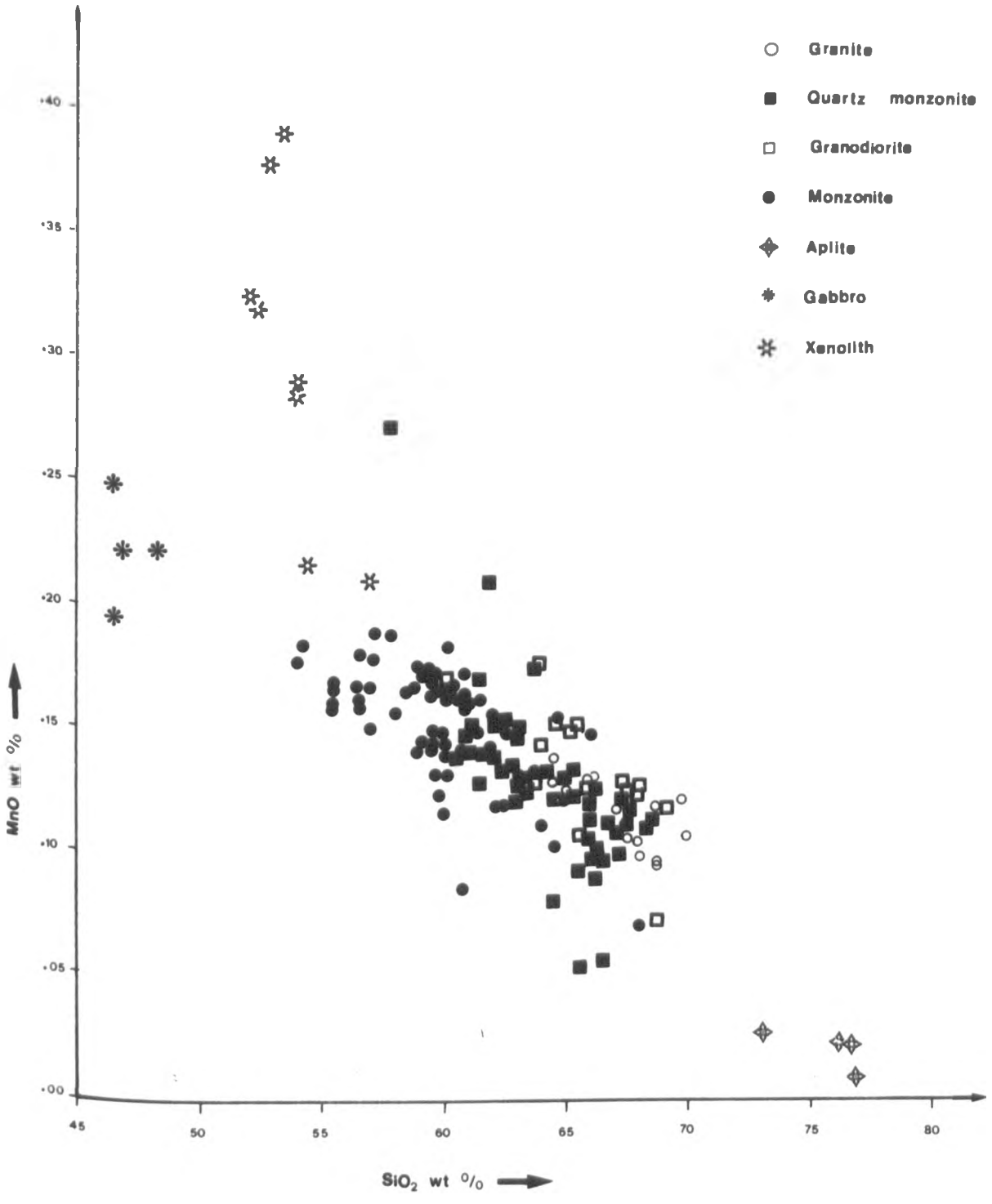
Granite
Quartz monzonite
Granodiorite
Monzonite
Aplite
Gabbro
Xenolith
MnO wt %
SiO2 wt %
·40
·35
·30
·25
·20
·15
·10
·05
·00
45
50
55
60
65
70
75
80

Fig. (4 – 1 – 2f)

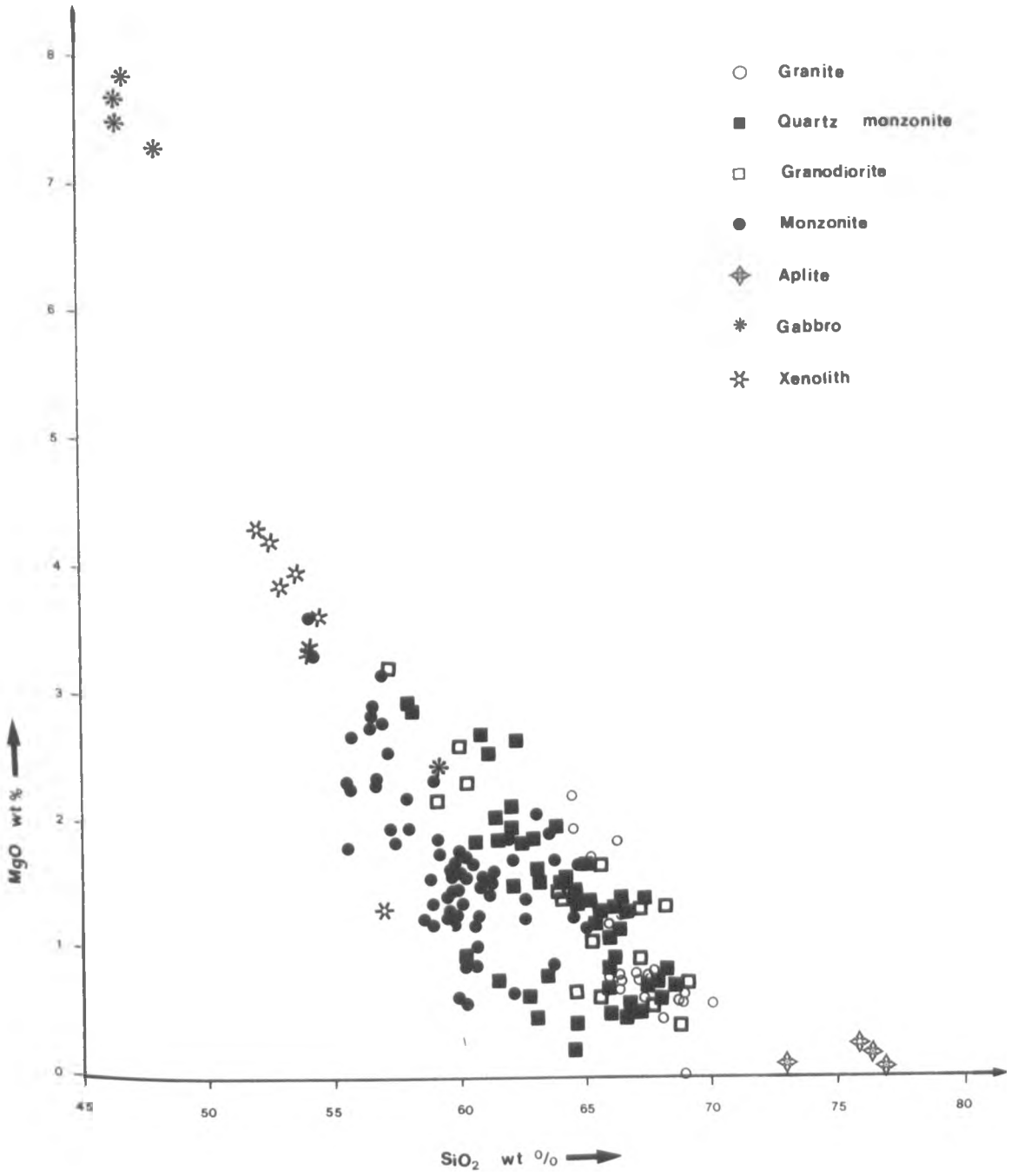
Granite
Quartz monzonite
Granodiorite
Monzonite
Aplite
Gabbro
Xenolith
MgO wt %
SiO2 wt %
0
1
2
3
4
5
6
7
8
45
50
55
60
65
70
75
80

Fig. (4-1-2g)

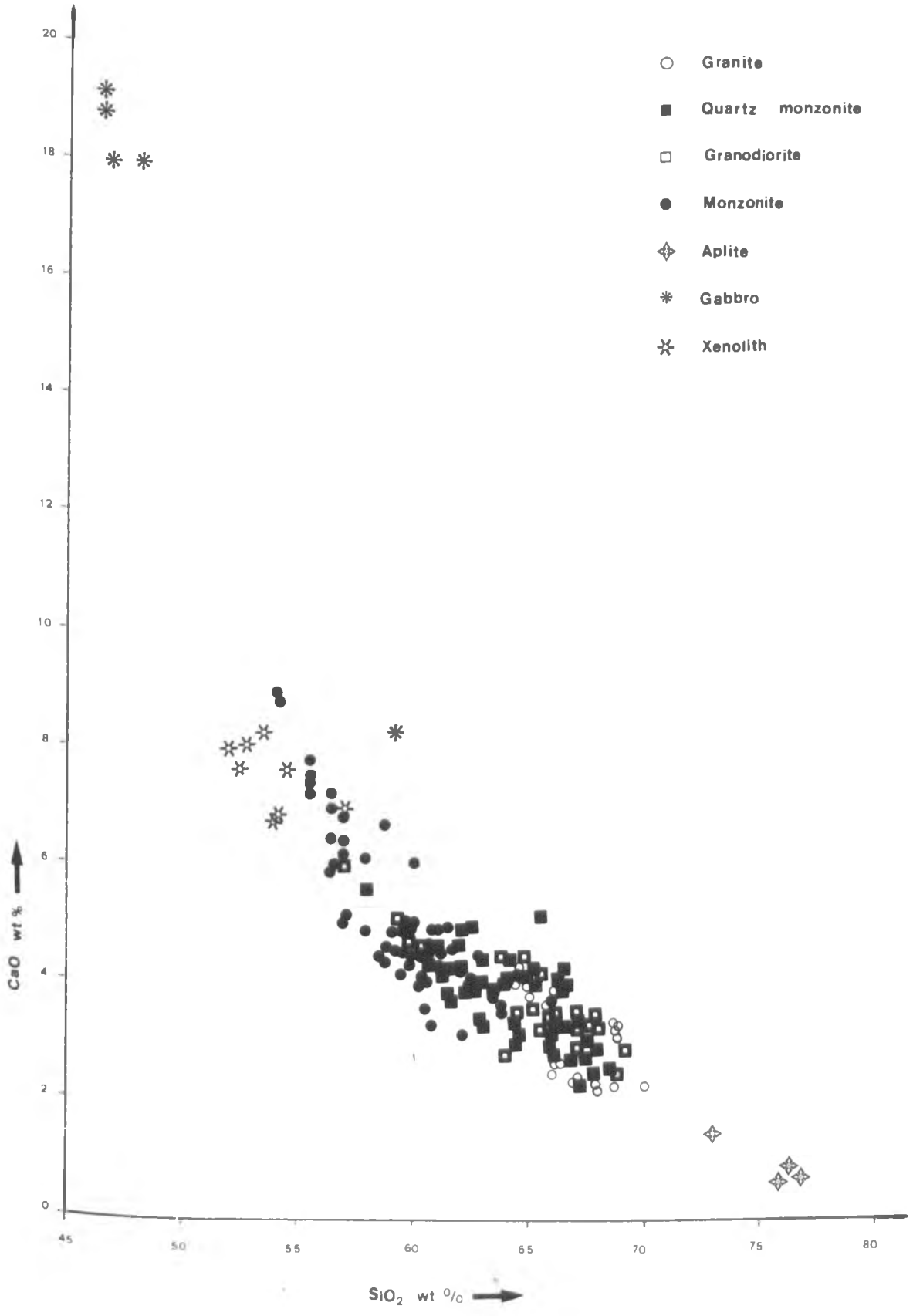
Granite
Quartz monzonite
Granodiorite
Monzonite
Aplite
Gabbro
Xenolith
CaO wt %
SiO2 wt %
0
2
4
6
8
10
12
14
16
18
20
45
50
55
60
65
70
75
80

Fig (4-1-2h)

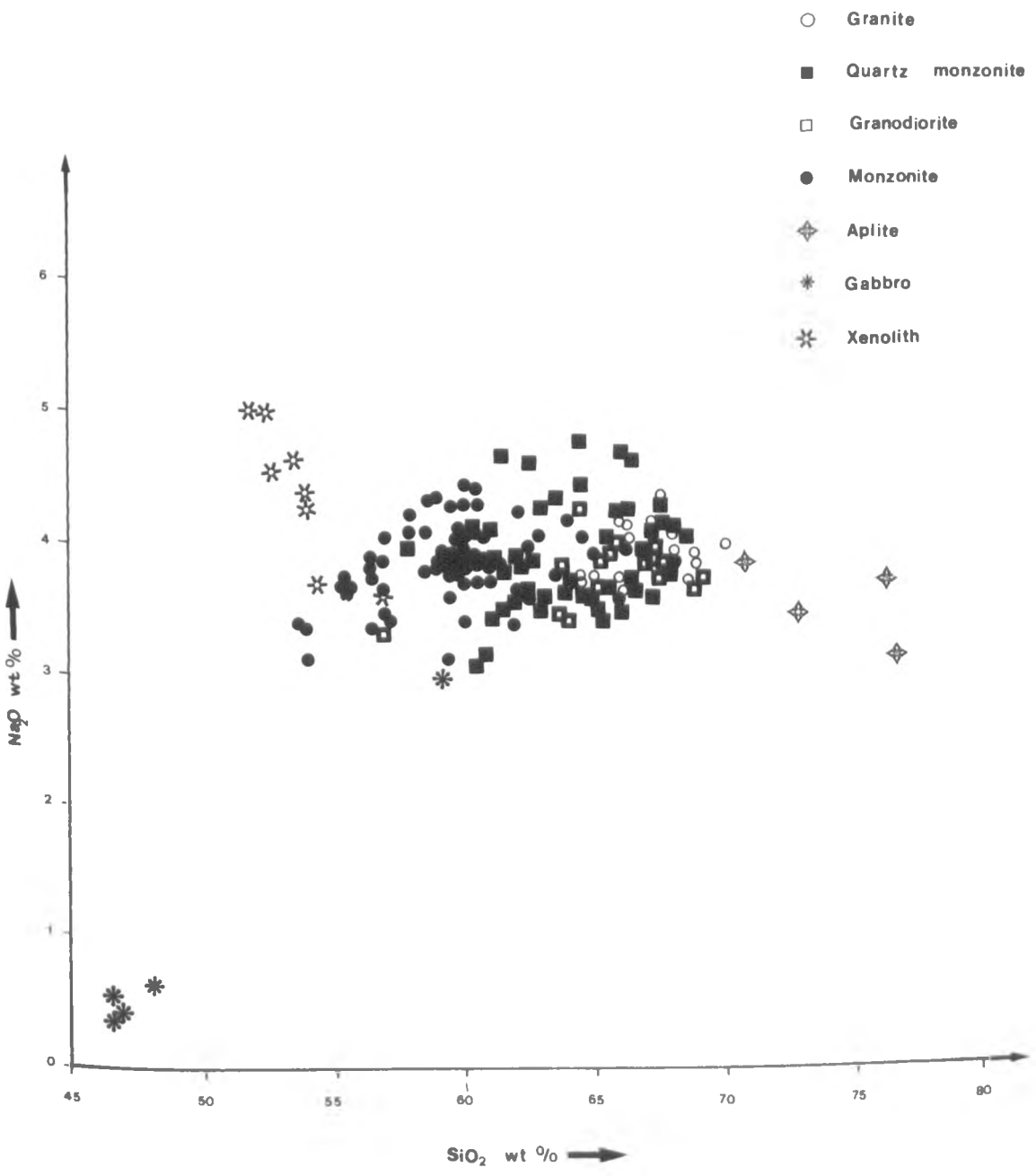
Granite
Quartz monzonite
Granodiorite
Monzonite
Aplite
Gabbro
Xenolith
Na2O wt %
SiO2 wt %
0
1
2
3
4
5
6
45
50
55
60
65
70
75
80

Fig. (4–1–2i)

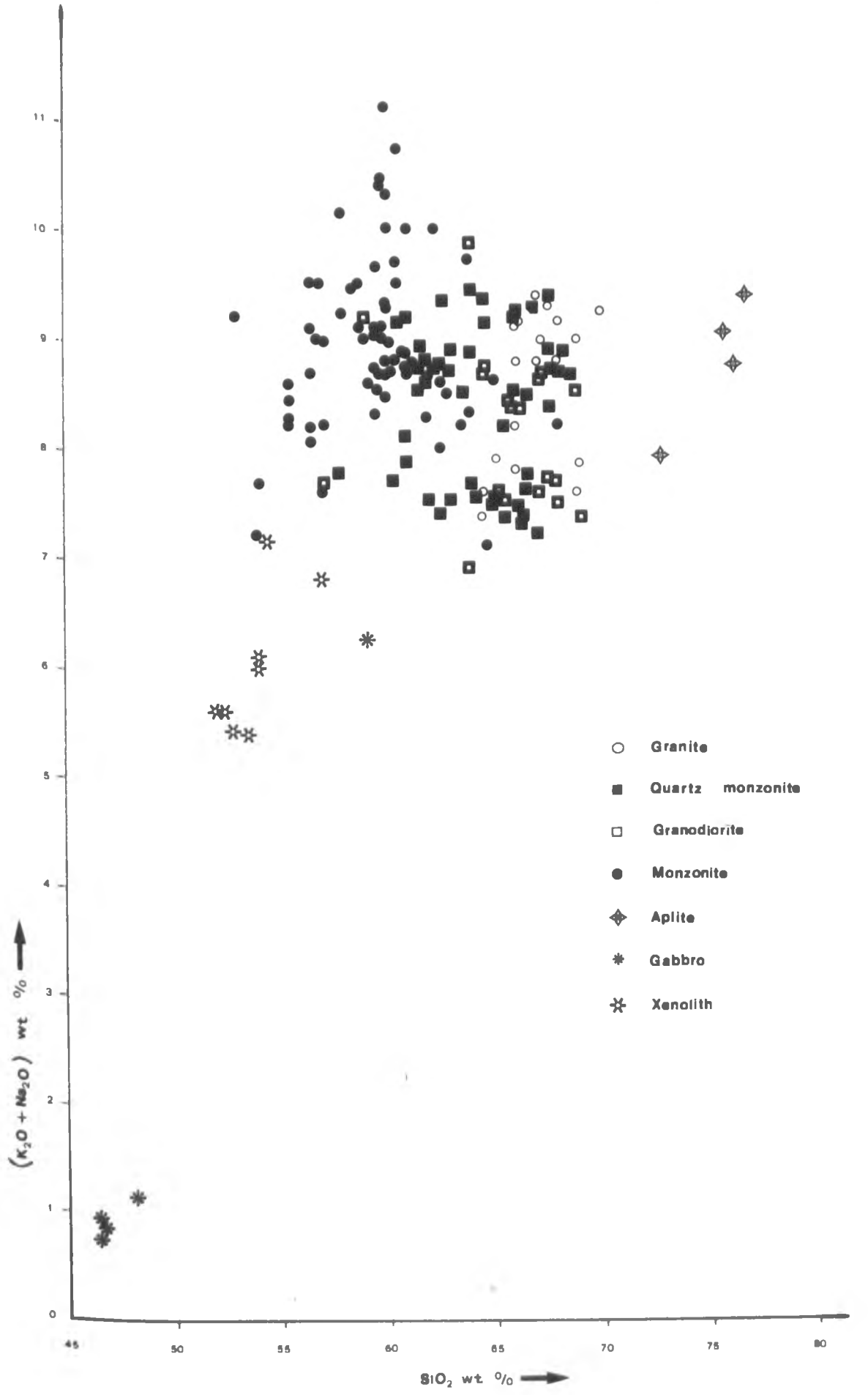
Granite
Quartz monzonite
Granodiorite
Monzonite
Aplite
Gabbro
Xenolith
$(K_2O + Na_2O)$ wt %
SiO_2 wt %
0
1
2
3
4
5
6
7
8
9
10
11
45
50
55
60
65
70
75
80

Fig. (4-1-2i)

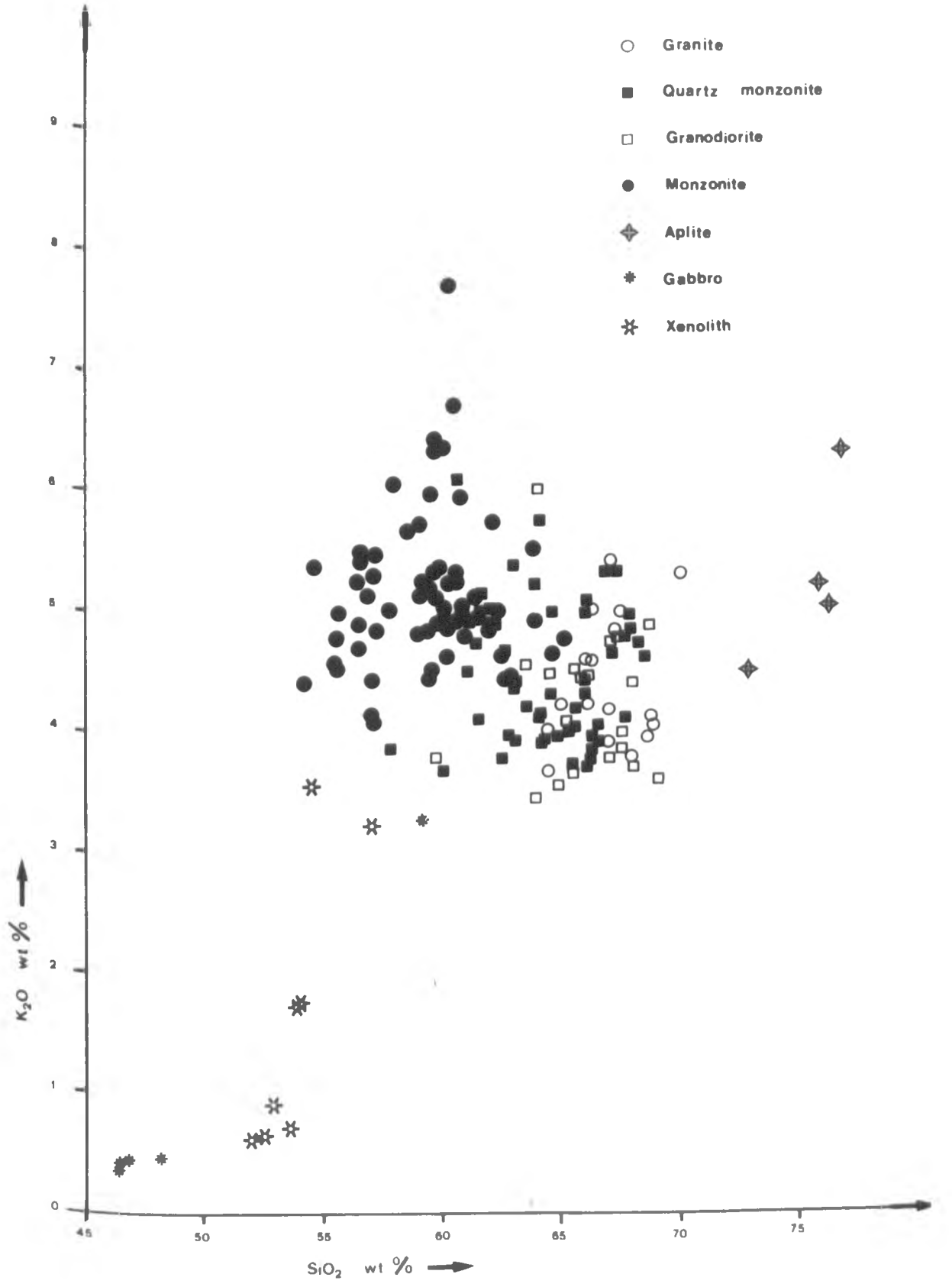
Granite
Quartz monzonite
Granodiorite
Monzonite
Aplite
Gabbro
Xenolith
K_2O wt %
SiO_2 wt %
0
1
2
3
4
5
6
7
8
9
45
50
55
60
65
70
75

Fig. (4-1-2k)

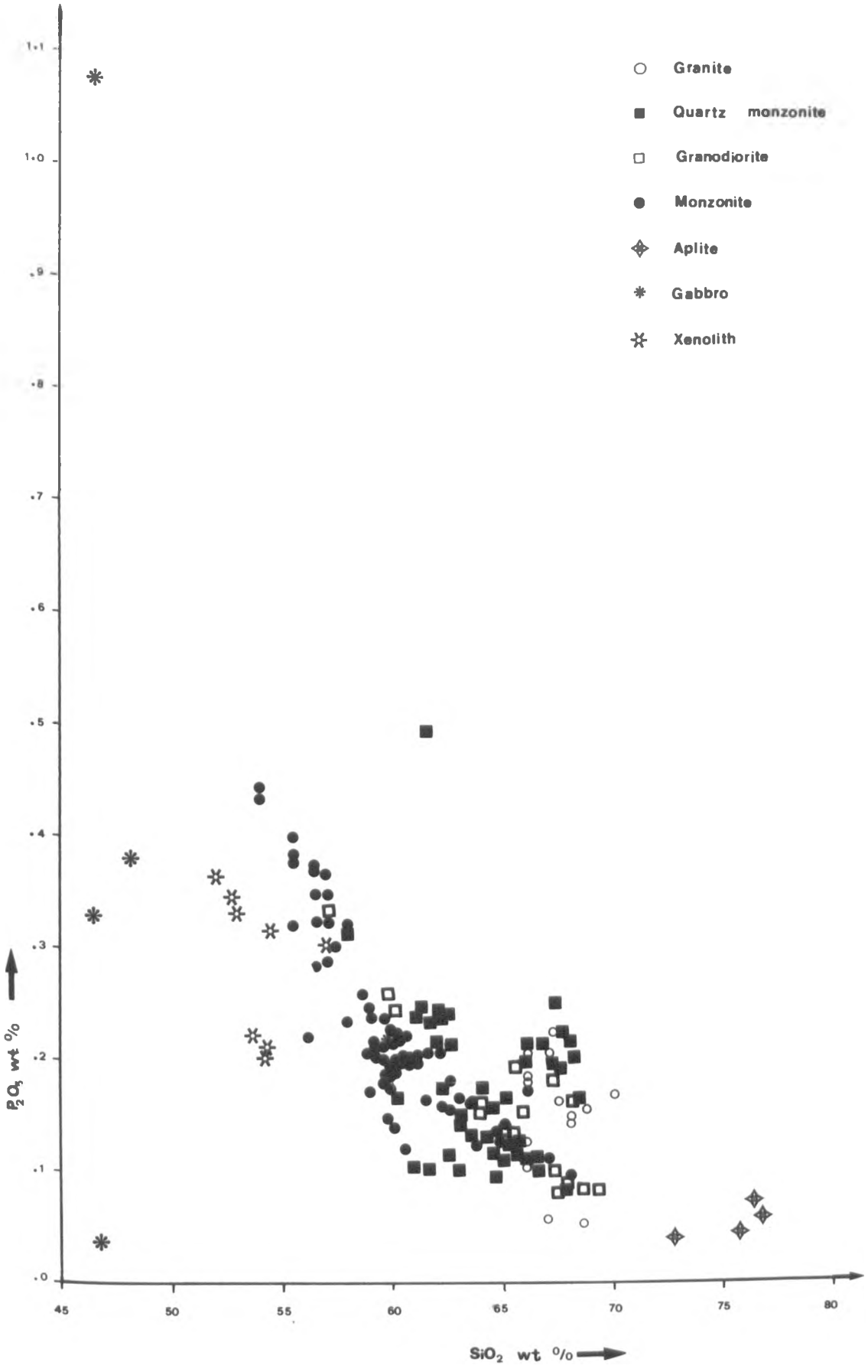
Granite
Quartz monzonite
Granodiorite
Monzonite
Aplite
Gabbro
Xenolith
1.1
1.0
.9
.8
.7
.6
.5
.4
.3
.2
.1
.0
P_2O_5 wt %
45
50
55
60
65
70
75
80
SiO_2 wt %

Fig. (4-1-21)

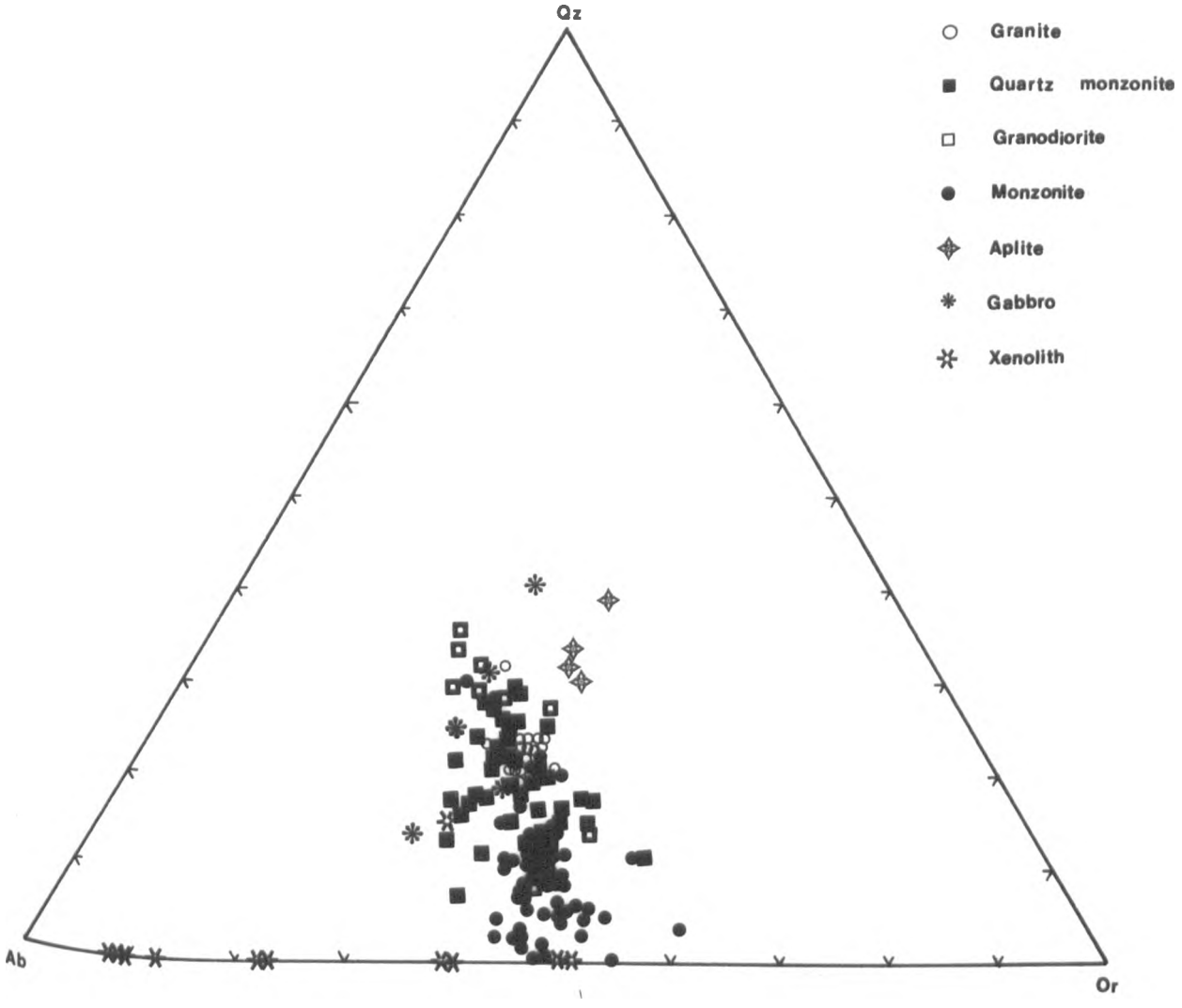
Qz
Ab
Or
Granite
Quartz monzonite
Granodiorite
Monzonite
Aplite
Gabbro
Xenolith

Fig. (4-1-2m)

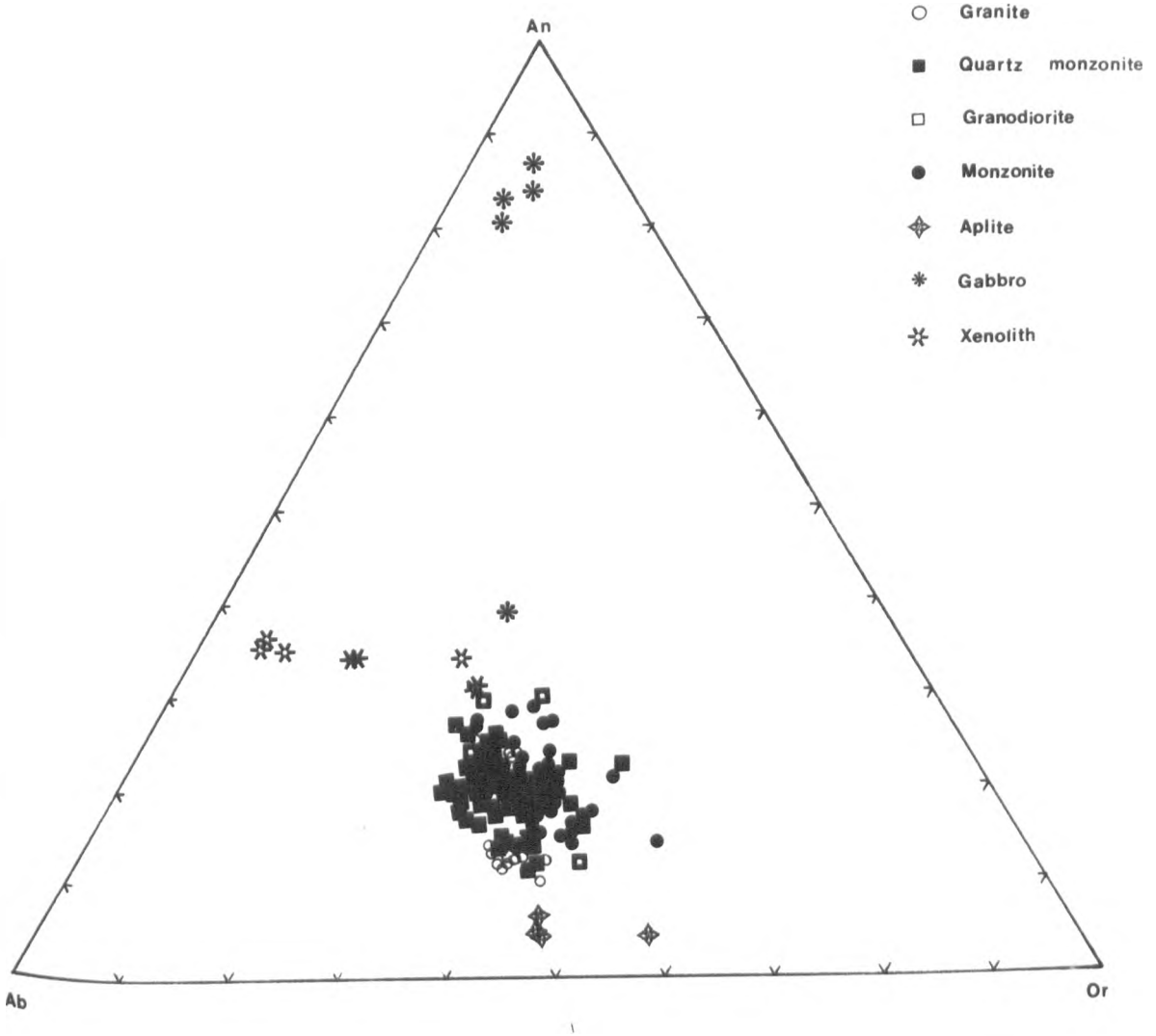
An
Ab
Or
Granite
Quartz monzonite
Granodiorite
Monzonite
Aplite
Gabbro
Xenolith

Fig. (4-1-2n)

possible explanations may account for this disparity: differences in orientation of the thin-sections may give different results; measurements of error in the counting method; and the sodium phase in K-feldspar is calculated as normative plagioclase.

All the samples are characterised by the presence of normative anorthite. Only sixteen samples (seven diorite xenoliths and nine monzonites) lack normative quartz. These monzonite samples are little different in composition from the others with this exception. These differences are so slight as to be of little or no petrographic significance but are purely a feature of the calculation method. Also twelve samples are characterised by small amounts of normative corundum. Among these samples, four are aplite, four quartz monzonite, three granodiorite and one granite.

The calculated normative data from the above mentioned tables are plotted in fig. (4-1-2m) and fig. 4-1-2n). The apices of fig. (4-1-2m) are normative quartz, albite and orthoclase and the apices of fig. (4-1-2n) are normative anorthite, albite and orthoclase. With reference to the above figures it can be seen that there is a trend with an approximately constant Or/Ab ratio with the exception of the xenoliths. These rocks are characterised by a lack of normative quartz and the individual results are quite scattered on the Qz-Ab-Or triangle.

Petro et al (1979), following the definitions of Shand (1927), reported that peraluminous rocks have Al_2O_3

greater than $CaO+Na_2O+K_2O$ (molecular proportions) and so are characterised by normative corundum. Metaluminous rocks have Al_2O_3 greater than Na_2O+K_2O but less than $CaO+Na_2O+K_2O$ and are characterised by normative anorthite. According to the above mentioned classification, one hundred and sixty-two samples are characterised as metaluminous rocks and twelve samples as peraluminous.

4-1-3 Discussion

The first thing which is apparent from the major element variation diagrams is the dispersion of points within each rock type group. This dispersion is much too large to be accounted for by analytical error (see table, C-3 in Appendix C, for values for each element), so must represent in large part a real variation between individual samples. Such dispersion is common in geochemical studies of calc-alkaline intrusive suites (Rapela and Shaw, 1979 ; Bateman et al, 1963; McCourt, 1981, etc.).

It is possible to identify two groups from the plotted data; one defined by the "intermediate rocks" and the other the "basic rocks" with a distinct compositional gap between gabbros and the dioritic xenoliths and monzonite. This compositonal gap can be seen in all the major element oxides and trace element diagrams (see below, trace elements) except total iron. In several plots the gabbros remain a completely discrete group, for example in Al_2O_3, MgO, CaO and Na_2O. In the TiO_2, total iron, Fe_2O_3, FeO,

MnO, total alkalis and K_2O the gabbros seem to indicate a close relationship between the gabbros and the other rock types. The Al_2O_3 contents of the gabbros are quite low reflecting the much higher proportion of ferromagnesian minerals and Na_2O appears to be roughly constant in all rock types. With P_2O_5 the separate analyses of the gabbros are so scattered as to make any conclusion of little value.

The dioritic xenoliths form a more satisfactory basic end to the general trend in the plots of TiO_2, Al_2O_3, total iron, MgO, CaO, total alkalis and possibly P_2O_5. This smooth trend is not present in the distribution of the following oxides: Fe_2O_3, FeO, MnO, Na_2O and K_2O.

In order to possibly explain some of this apparently anomalous behaviour in the dioritic xenoliths, two specimens (samples No.6a and No.6b) of quartz monzonite, both containing xenoliths, were separated and prepared for X-ray fluorescence analysis. Three analyses were taken from both samples. The samples were first cut into thin slices to reveal the xenolith. A sample was then taken from the centre of the xenolith (samples anal. No.$6a_1$ and No.$6b_1$), the periphery of the xenolith (samples anal. No. $6a_2$ and No. $6b_2$) and the surrounding quartz monzonite (samples anal. No. $6a_3$ and $6b_3$). These analyses were undertaken to study the relative movement of elements between the host rock and the xenolith, and within the xenolith.

From the comparison of the analytical data (tables, 4-1-2a and 4-1-2g, samples $6a_1$, $6a_2$, $6a_3$, $6b_1$, $6b_2$, $6b_3$) it

can be noted that TiO_2, Al_2O_3, total iron, MnO, MgO, CaO, Na_2O and P_2O_5 decrease from the centre of the xenolith through the periphery to the surrounding host quartz monzonite (the exception being sample No. $6a_2$ for Al_2O_3, P_2O_5 which could be analytical error).

Anomalous behaviour is seen in the analytical data presented for FeO, Fe_2O_3 and the ratio Fe_2O_3/FeO i.e. oxidation state of iron; for sample 6a the Fe_2O_3 and the ratio Fe_2O_3/FeO decreases from the centre of the xenolith to the periphery and then increases in the surrounding quartz monzonite. But for sample 6b the opposite is observed. From fig. (4-1-2e) it can be seen that FeO in the dioritic xenoliths is high but the total iron (see, fig. 4-1-2c) fits into the general trend of decreasing total iron with increasing differentiation, therefore it is possible to correlate this anomaly with a change in oxygen fugacity with increasing differentiation (i.e. low values in the diorites, higher values within the quartz monzonites).

The values of SiO_2 and K_2O increase from the centre of the xenoliths through the periphery to the surrounding host quartz monzonite. The very large increase of K_2O from the xenolith to the host can be explained by a very low content of alkali fledspar in the dioritic xenoliths.

Observation of the chemistry of host rock quartz monzonite and the analysed dioritic xenoliths indicate that there is no net transfer of major elements from the host rock to the xenolith. These observations can be correlated with the lack of K-feldspar megacrysts, either

grown within the xenolith or across the boundary between host and xenolith.

The rocks of the Serres-Drama granitic complex have been divided into two groups on the basis of field relations and petrography. These groups comprise a more "basic" one, consisting of the monzonite, the dioritic xenoliths and the gabbro, and a more "acid" one consisting of the quartz monzonite, granodiorite and granite. The two groups may be divided reasonably sharply on the basis of their SiO_2 contents with very little overlap at about 61-63% SiO_2.

It is possible to explain the distribution of chemical compositions of the rocks by reference to the changes in the mineralogy and the variation in the mineral chemistry, which can be summarised as follows:

Gabbro		Dioritic xenolith		Monzonite
Salitic pyroxene + anorthite + pargasitic/ tschermakitic hornblende + magnetite	→	magnesio hornblende + labradorite/ andesine + magnetite	→	magnesio hornblende + labradorite/ andesine + k-feldspar + magnetite

Intermediate group

magnesio hornblende + /̄biotite/̄ + andesine/oligoclase → actinolitic hornblende + magnetite + K-feldspar + quartz.

The presence of salitic pyroxene and large amounts of ferroan aluminous amphiboles can explain the high concentration of CaO, MgO, total iron, and TiO_2 and low amount

of alkalis in the gabbroic rocks. If one assumes that the magma is a closed system and all the rock types are related to each other, crystallisation of the above minerals will deplete the remaining liquids in these elements. The high proportion of mafic minerals in the gabbro compared to anorthitic plagioclase also accounts for the low concentration of Al_2O_3 in the gabbros.

If we consider that the amphibole is the commonest mafic mineral, then precipitation of large amounts of this mineral, which is undersaturated with respect to silica, will lead to a residual liquid which is richer in silica. The interpretation that the starting point for this sequence of fractional crystallisation is of gabbroic composition is based upon the more calcic and aluminous composition than would be expected if the starting point were diorite and the gabbros were of a cumulate origin.

The chemical composition of the dioritic xenoliths are lower in total iron, TiO_2, MgO, CaO and higher in alkalis and Al_2O_3 than the gabbros which reflects an increasing proportion of plagioclase feldspars compared to mafic minerals. The lower concentration of total iron is correlated with the presence of less iron-rich magnesiohornblende. The increase in the SiO_2 content of these dioritic xenoliths reflects the composition of the amphibole and the more albitic plagioclase feldspar.

The major difference in the mineralogy of the monzonite, compared to the dioritic xenoliths, is the presence of potassium fledspar. Most of the oxide concentrations

are lower in the monzonites than in the diorites, except for the alkalis and silica and this is related to the presence of potassium feldspar. The Na_2O content is approximately constant in both the diorites and monzonites, whereas there is a large increase in K_2O. The increase in silica is because potassium feldspar contains more silica than the labradorite-andesine-oligoclase plagioclase feldspars.

The major difference between the monzonite mineralogy and that of the 'intermediate' group is the increase in quartz content, which rises in quantity from the quartz monzonite to the aplite. This is well exemplified in fig. (4-1-2k) where the K_2O content, although individual points are widely dispersed, appears to decrease as the SiO_2 concentration increases.

In summary, the change in chemistry within the 'basic' group of rocks is closely correlated with changing composition of the major crystallising phases of amphibole and plagioclase feldspars which are joined by potassium feldspar in the crystallized monzonite. In the 'intermediate' group the dominant factor is the appearance and increase in the amount of quartz.

4-2-1 "Granite" type

There have been a large number of geochemical plots used to discriminate between various magma types. One of the more successful of these has been the AFM diagram used to distinguish between the iron enrichment trends of

tholeiitic and alkali basaltic rocks and the calc-alkaline rocks which show no evidence of iron enrichment, particularly in the early phase of fractionation.

On an A (Na_2O+K_2O), F ($FeO+Fe_2O_3+MnO$) and M(MgO) diagram, fig. (4-2-1a), aplite plots close to the A apex, gabbro near the F-M side and the quartz monzonite, granite, granodiorite and monzonite on a line from aplite towards the gabbro and the dioritic xenoliths plot between the end of the above mentioned line, and gabbro. The array of points indicates that the rocks tend towards alkali enrichment with a fairly constant Fe/Mg ratio and indicate no iron enrichment at all. This is suggestive of fractionation of ferromagnesian minerals. From the above diagram it can be seen that the granitic complex under study belongs to the calc-alkaline series.

The AFM plot of the present study has been reproduced (see fig. 4-2-1a) with the curves for the New Britain-Solomon Islands suite of rocks, which represents the most tholeiitic character of island arc calc-alkaline suites, and rocks from the New Guinea Continental arc, which plot on the iron-poor side of the normal calc-alkaline trend (data from Hine and Mason, 1978; Mason and McDonald, 1978).

Brown (1982) has also used the AFM diagram to discriminate between various calc-alkaline trends. He has used the word "maturity" to define the type of calc-alkaline trend i.e. a young island arc e.g. New Britain - Solomon Islands, where the intermediate rocks in the suite are tonalitic in character and are developed in the oceans

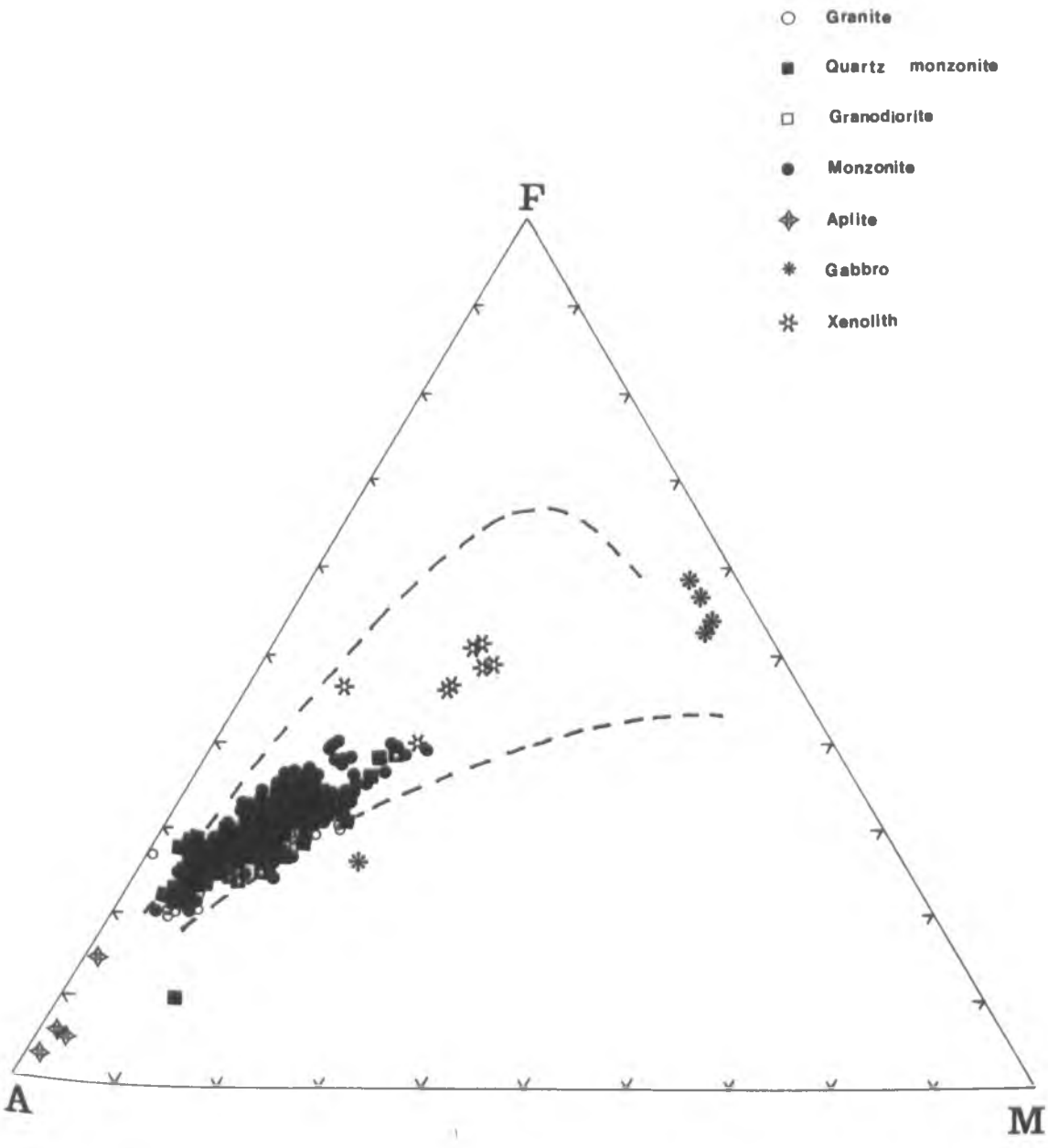
Granite
Quartz monzonite
Granodiorite
Monzonite
Aplite
Gabbro
Xenolith
F
A
M

Fig. (4-2-1a)

with little continental crust influence. Mature island arcs, e.g. New Guinea continental arc, are defined by the presence of monzonites in the intermediate suite of rocks and where there is a possibility of some continental crust influence.

Data calculated from tables (4-1-2a) to (4-1-2g) are used to plot the ratio CaO/K_2O+Na_2O versus SiO_2 in fig. (f-3-1c). From this diagram, the calc-alkali index (Peacock, 1931) can be determined from the value of SiO_2 at the intersection of the curve where $CaO/(K_2O+Na_2O)$ is equal to 1.00. From the above mentioned diagram the calc-alkali index for the Serres-Drama granitic complex is approximately 57.

Brown (1982) suggested that by using the calc-alkali index (Peacock, 1931; $CaO/(K_2O+Na_2O)$ vs SiO_2), suites of rocks can be classified as follows: if the calc-alkali index lies between 56-61 then the suite of rocks is classed as calc-alkaline; if the index is greater than 61 they are termed calcic; between 56-61 classed as alkali-calcic or less than 51 alkaline. The analysed samples from Serres-Drama granitic complex fall into the calc-alkaline series using the calc-alkali index classification.

Recent work on the mineralogy and geochemistry of "granitoids" found within continental crust has revealed several differences between two types of calc-alkaline plutonic complex which appear to relate to the ultimate origin of these granitoids. They are thought to be of either an igneous origin, or sedimentary origin and labelled "I-type" or "S-type" by Chappell and White (1974).

Alternatively the "I-type" have been called the "magnetite series" and the "S-type" the "ilmenite series", depending upon which iron oxide characterises the rocks (Ishihara, 1977, from Takahashi et al, 1980). Both types of complex are considered to have originated within the continental crust (Takahashi et al, 1980).

In distinguishing between I-type and S-type calc-alkaline granitoids or the magnetite and ilmenite series, emphasis has been placed on the whole-rock chemistry, mineral assemblages, field relations and isotopic composition.

Chappell and White (1974) developed chemical criteria to distinguish the two rock-types. I-type granitoids have a relatively high content of sodium (Na_2O normally more than 3.2% in the more felsic rocks and more than 2.2% in the more mafic rocks), Al_2O_3/Na_2O+K_2O+CaO (molar ratio) is low (less than 1.1), and the presence of normative diopside or a small amount of normative corundum (less than 1%). I-type granitoids also show a broad spectrum of compositions ranging from felsic to mafic and regular inter-element variation within plutons. Variation diagrams are linear or near linear.

They consider that petrographic features reflect the differences in chemical composition. In respect to the I-type granitoids hornblende is common in the more mafic I-type bodies and generally present in the felsic rocks. Hornblende is however absent in S-type granitoids, where muscovite is more common. Sphene tends to be a common

accessory mineral in I-type granites and apatite inclusions are common in the hornblende and biotite.

According to Chappell and White's (1974) chemical criteria, the majority of 174 samples from the Serres-Drama complex have Na_2O content greater than 3.2%, except three samples (aplite No.42, quartz monzonite No.121, monzonite No.195) which have Na_2O equal to 3.1% and the four samples of gabbro which have low Na_2O content. The molar ratio Al_2O_3/K_2O+Na_2O+CaO for all the samples is less than 1.1. From the calculated norms, one hundred and sixty-one samples have normative diopside and twelve samples normative corundum less than 1% (maximum corundum 0.88, sample No.148). There is a broad spectrum of chemical compositon from gabbro to aplite and the variation diagrams (as shown above) are approximately linear.

From the petrographic features, calcic amphibole is the main mafic mineral (see petrography and mineralogy chapters), sphene is a common accessory mineral and apatite inclusions occur in biotite and hornblende. Consequently it can be seen that the analysed samples from the Serres-Drama granitic complex fall within Chappell and White's (1974) classification of I-type calc-alkaline granitoids.

Ishihara's (1977, from Takaharshi et al, 1980) classification is essentially descriptive; the "magnetite-series" granitoids contain an easily recognizable amount of magnetite under the microscope, while the "ilmenite-series" is practically free of opaque oxide minerals and ilmenite is consistently present.

Takahashi et al (1980) conclude that the "magnetite-

series"/"ilmenite-series" classification is not exactly equivalent to the "I-type"/"S-type" classification. All the "magnetite-series" granitoids, as defined by Ishihara (1977, from Takahashi et al, 1980) are "I-types", but the "ilmenite-series" granitoids include both "S-type and I-type".

From the petrographic study (see petrography chapter) of the Serres-Drama granitic complex an amount of opaque minerals, usually more than 1% (modal analysis) can be seen. From the electron microprobe analysis (see mineralogy chapter) the opaque material is magnetite. Also the plot of amphibole $Mg/Mg+Fe^{+2}$ against host rock silica fig. (3-3-4e) is comparable to the data for the magnetite series quoted by Czamanske et al (1981). Consequently it can be seen that the Serres-Drama granitic complex falls within Ishihara's (1977) classification of "magnetite series". Therefore the criteria based upon petrography, mineral chemistry and bulk rock chemistry indicate that the Serres-Drama complex is of igneous origin and the process of fractional crystallisation has led to the variation in rock type.

4-3-1 Relationship between major element chemistry of the Serres-Drama complex and the tectonic environment of origin.

Petro et al (1979) have suggested criteria to distinguish between plutonic rock suites developed at compressional and extensional plate margins by major element

geochemistry as follows:

a) Frequency distributions of normative plagioclase and differentiation indices show that compressional suites are characterised by unimodal (intermediate) distributions, while the extensional suites are characterised by a bimodal (acidic-basic) distribution. The unimodal acidic distribution may be ambiguous.

b) The ternary AFM diagrams have for extensional suites more scatter along the FM-side than for compressional suites. The A-rich portion of extensional suites is characterised by dispersion parallel to the AF-side.

c) Calc/Alkali indices for compressional suites range from 60 to 64, while for extensional suites they range from 50 to 56. The intermediate range (56 to 60) may be ambiguous.

d) Peralkaline rocks are characteristic of extensional environments, while peraluminous rocks are characteristic of compressional environments. Metaluminous rocks are common in both suites.

Petro et al (1979) have stated that differentiation index and normative plagioclase show more clearly the differences between suites from contrasting environments than other types of index (e.g. SiO_2, modified Larsen index). Data from tables (5-1-2a) to (5-1-2j) have been used to plot the frequency distribution of the differentiation index. (Thornton and Tuttle, 1960 as normative Qz+Or+Ab) in fig. (4-3-1a). The resulting pattern is obviously a unimodal distribution with an intermediate mode. The frequency

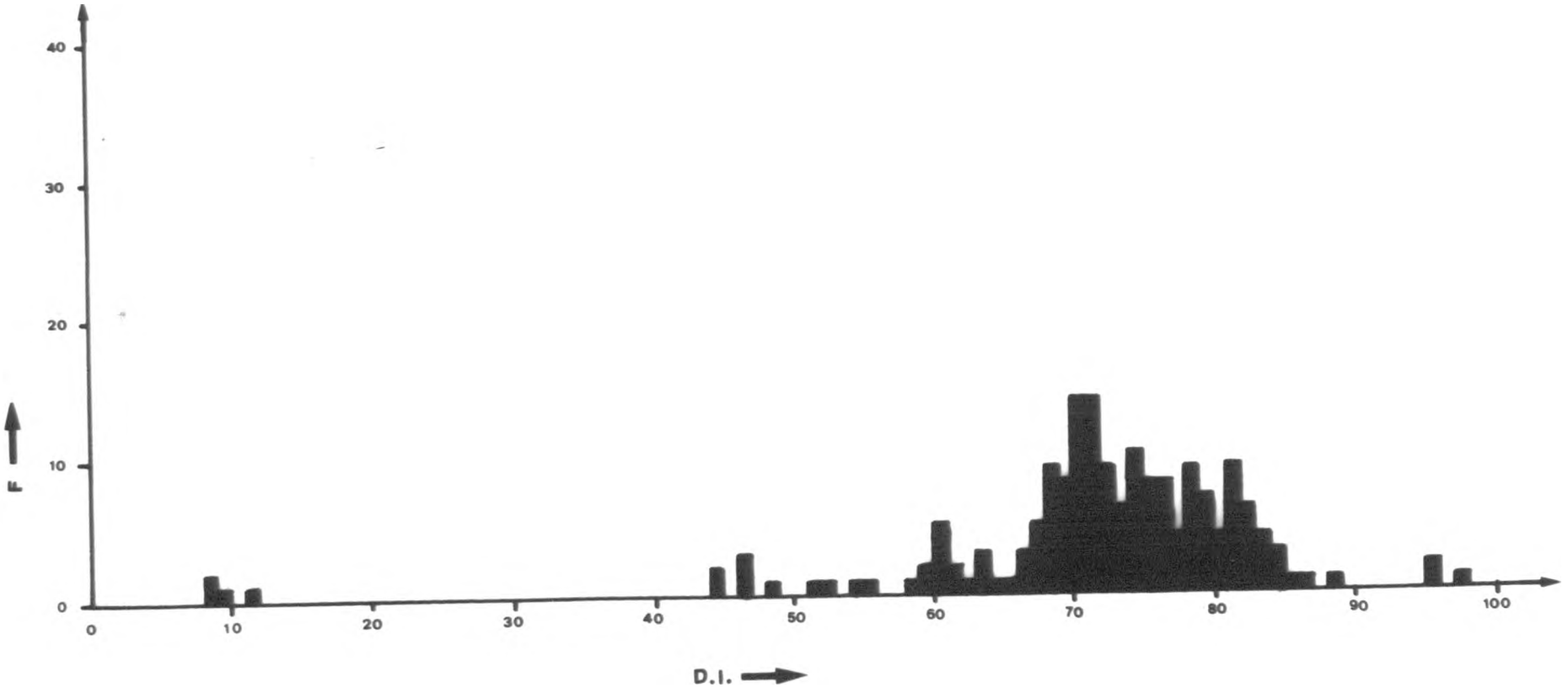

Fig. (4-3-1a)

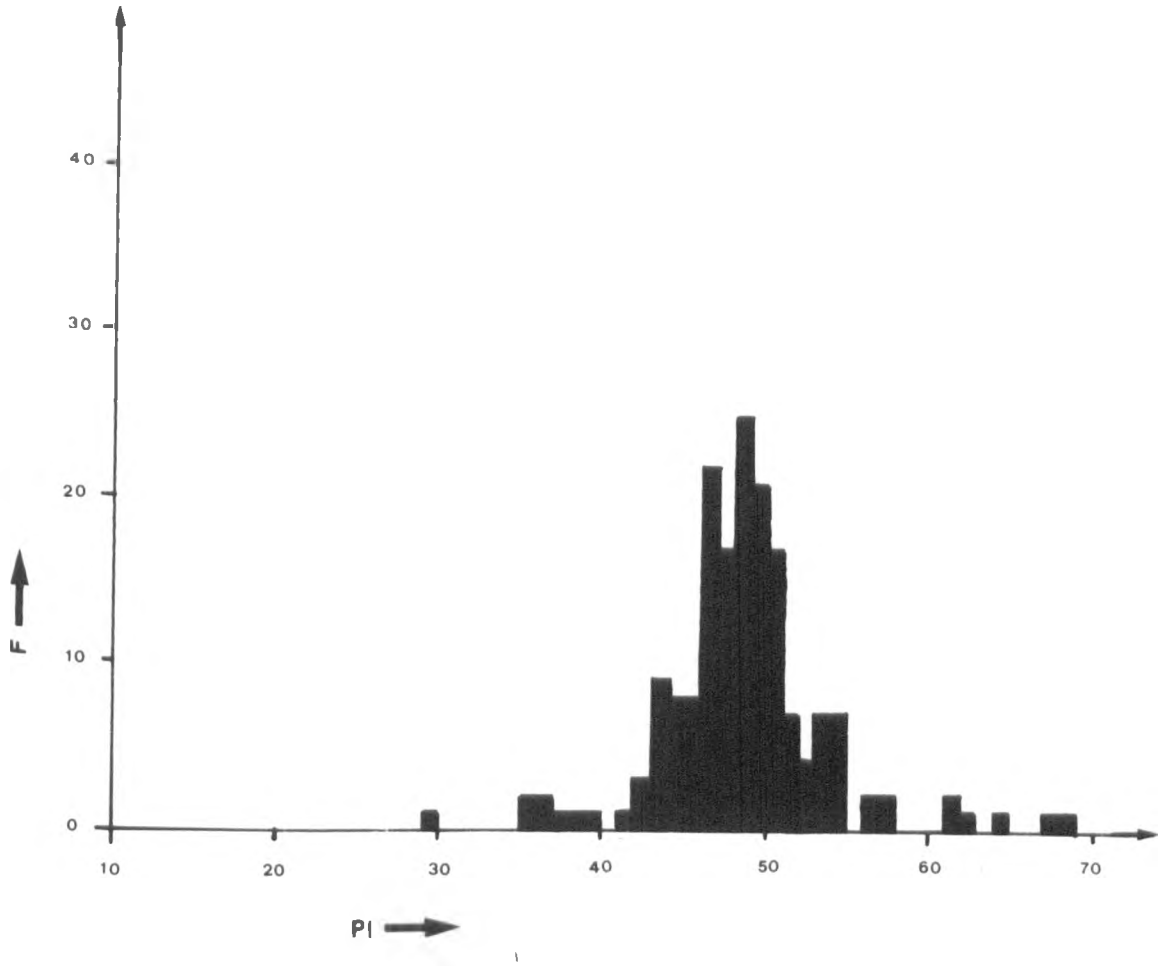

Fig. (4-3-1b)

distribution of normative plagioclase (calculated from tables (4-2-1a to 4-2-1j) has been plotted in fig. (4-3-1b). A unimodal distribution can again clearly be seen.

As mentioned before, twelve samples from the Serres-Drama complex are peraluminous, but only just so and this has been interpreted by Petro et al (op.cit) as being characteristic of compressional tectonics. The remaining one hundred and sixty-two are metaluminous, which are common in rock suites from both compressional and extensional tectonic environments. Data from the present study, plotted on a ternary AFM diagram, fig. (4-2-1a) are comparable to that of Petro et al (1979, fig. F,A,C) for compressional suites.

All the various parameters would tend to indicate that if these criteria (Petro et al, op.cit) linking geochemistry and tectonics are accepted then the rocks of the Serres-Drama granitic complex were formed within a compressional environment.

Brown (1982) suggests that calc-alkaline granitoids from "arcs" have geochemical and petrogenetic characteristic and time-dependent compositional trends which can be related to arc maturity (defined earlier) and the presence or absence of a sialic basement. The subcontinental lithosphere is considered as the main source of magma which eventually either consolidates at depth or erupts onto the surface.

The intra-continental 'arcs' such as the Alps, Himalayas and south-eastern Asia, are considered to be

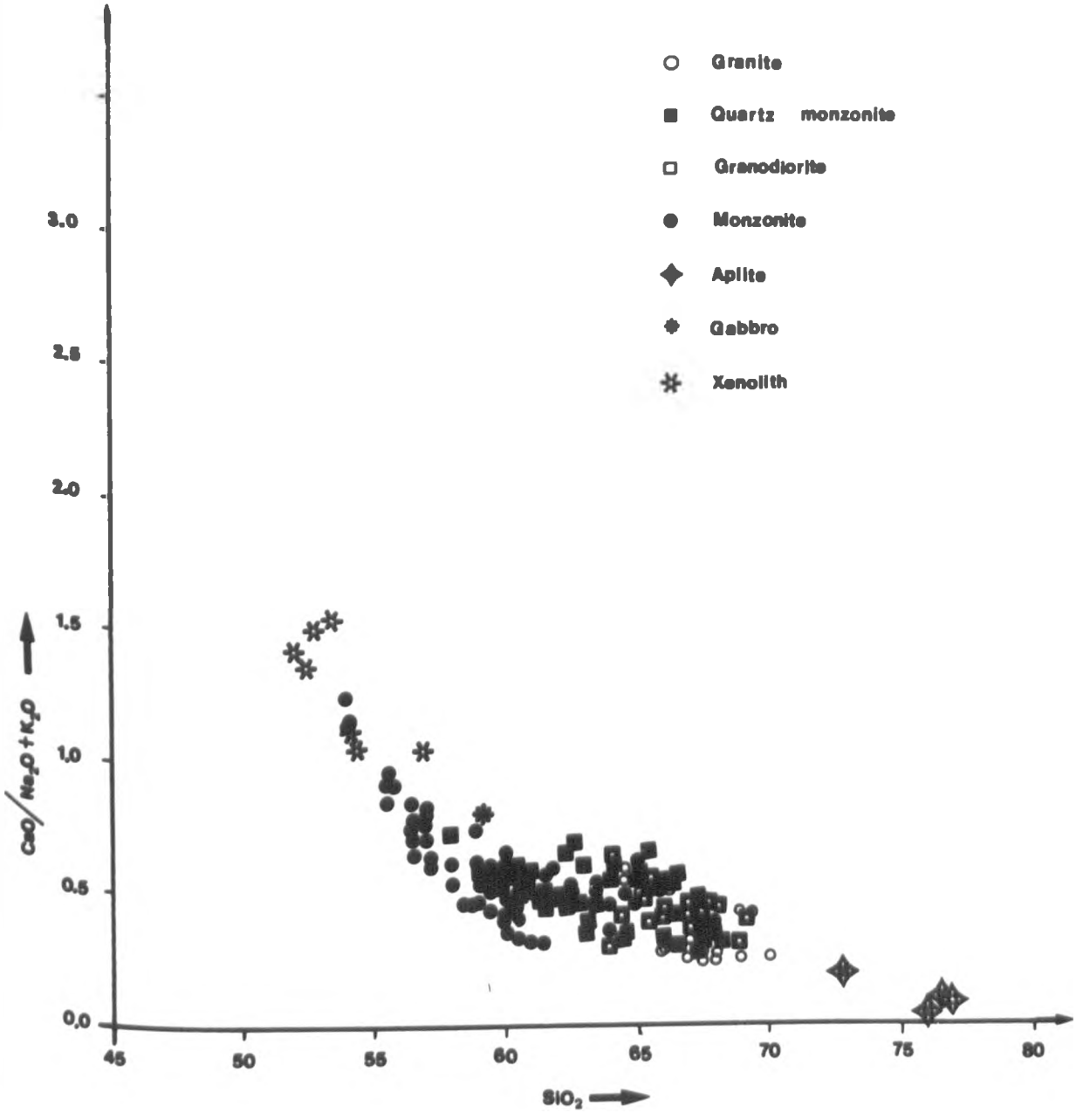
Granite
Quartz monzonite
Granodiorite
Monzonite
Aplite
Gabbro
Xenolith
3.0
2.5
2.0
1.5
1.0
0.5
0.0
CaO/Na2O+K2O
45
50
55
60
65
70
75
80
SiO2

Fig. (4 – 3 – 1c)

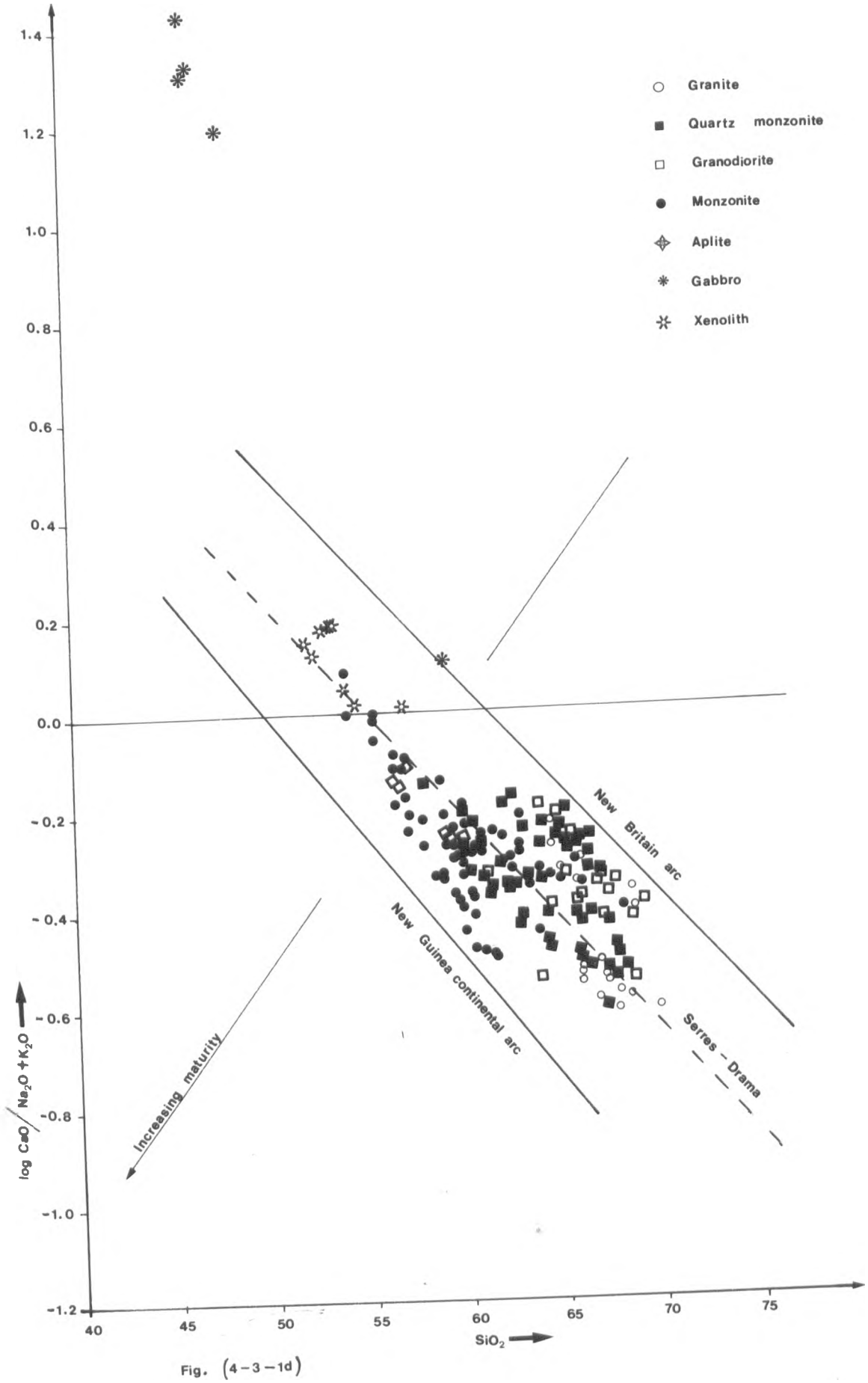
Granite
Quartz monzonite
Granodiorite
Monzonite
Aplite
Gabbro
Xenolith
New Britain arc
New Guinea continental arc
Serres - Drama
Increasing maturity
log CaO/ Na2O +K2O
SiO2
1.4
1.2
1.0
0.8
0.6
0.4
0.2
0.0
-0.2
-0.4
-0.6
-0.8
-1.0
-1.2
40
45
50
55
60
65
70
75

Fig. (4-3-1d)

the most mature convergent boundary zones of magma generation (Brown, op.cit.). The magmatic products are mostly intrusive granitoids, often with variable and generally smaller volumes of volcanic products.

Arcs resulting from continent-ocean and ocean-ocean convergence are characterised by calc-alkaline rocks (Baker, from Brown, 1982). AFM diagrams have become widely used as a discriminant diagram in contemporary petrogenetic studies since they present a "pictorial definition of arc maturity" (Brown, ibid). A group of curves exist for arc magmas which range from the island arc tholeiites to the more potassic calc-alkaline series of continental margins. The very large majority of Mesozoic-Cainozoic arc intrusives follow the established calc-alkaline trend (Larsen, 1948, from Brown, 1982).

The AFM diagram does not discriminate well between acid rocks of different calc-alkaline series as these usually cluster towards the alkali apex of the plot. Brown (1982) suggested the use of a second major element variation diagram ($\log_{10} CaO/_{Na_2O+K_2O}$), to illustrate clearly the increasing maturity of the suites of such rocks. As most of the plutonic rocks described in this study have intermediate and acid compositions, they have been plotted on this diagram in fig. (4-3-1d) together with the data for geochemically extreme suites of calc-alkaline rocks, fig. (4-2-1a).

The samples from the Serres-Drama granitic complex lie between these two extreme suites and occupy an

approximately median position. This also illustrates the increasing maturity (sensu Brown op.sic.) towards a normal calc-alkaline trend.

Mason and McDonald (1978) characterised the geochemical variation of potassium for calc-alkaline suites as low potassium (less than 0.7 per cent K_2O), normal potassium (K_2O lie between 0.7 to 2.5 per cent) and high potassium (K_2O greater than 2.5 per cent). The data for the high potassium suite (New Guinea continental arc) of Mason and McDonald (1978) is similar to the data presented for the present study. Therefore the Serres-Drama granitic complex is defined as being a high potassium suite using the above criterion.

Brown (1982) emphasised the extreme differences between immature intra-oceanic island arc and mature continental arc intrusives by using the plot of log. K_2O/Na_2O against silica. The difference between the alkali contents of silicic magmas from the two environments is shown up more sharply by this diagram than by the AFM triangle.

The calculated data of the present study are plotted in fig. (4-3-1e). The Serres-Drama rocks can be seen clearly to approach more closely the high maturity composition of rocks from the New Guinea continental suite.

Brown (op.cit.) concluded that major calc-alkaline gabbro-diorite-tonalite-granodiorite intrusives of mature continentalised arcs, with no ancient sialic basement, show increases in silica and potassium concentration with time

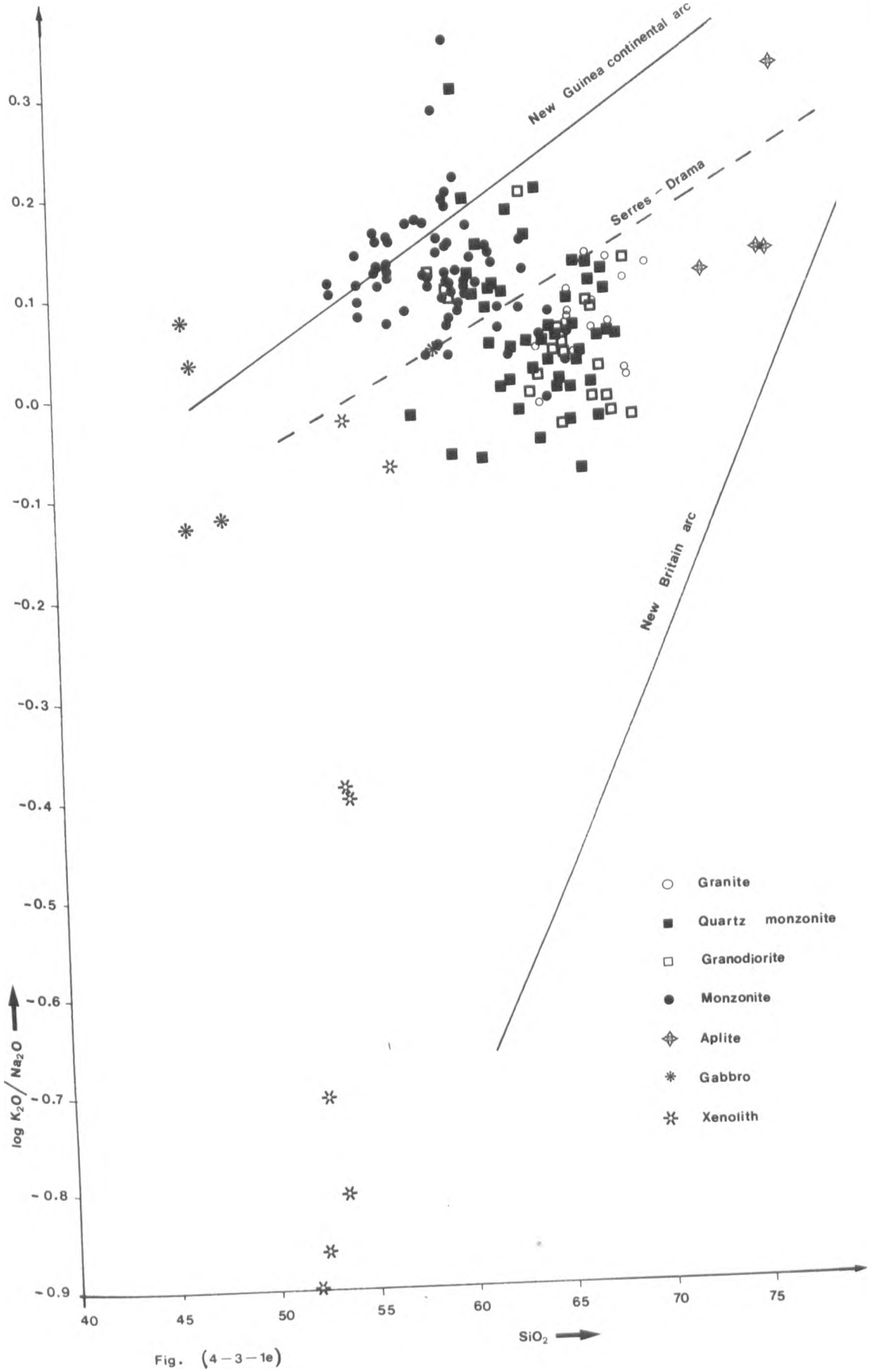
New Guinea continental arc
Serres – Drama
New Britain arc
Granite
Quartz monzonite
Granodiorite
Monzonite
Aplite
Gabbro
Xenolith
log K_2O/Na_2O
SiO_2
0.3
0.2
0.1
0.0
-0.1
-0.2
-0.3
-0.4
-0.5
-0.6
-0.7
-0.8
-0.9
40
45
50
55
60
65
70
75

Fig. (4-3-1e)

and distance from the site of subduction.

The character of the Serres-Drama complex groups it closely with normal calc-alkaline continental intrusives belonging to compressional zones of mature continental arcs.

4-4-1 Summary

As discussed above, the Serres-Drama granitic complex originated from a "I-type" calc-alkaline magma of the magnetite series which belongs to the compressional zone of mature continental arcs. From the analytical data it can be divided into two groups. The essential difference between the 'basic' group and the 'intermediate' group can be related to the mineralogy of the complex.

CHAPTER V : TRACE ELEMENT GEOCHEMISTRY

CHAPTER V : TRACE ELEMENT GEOCHEMISTRY

5-1-1 Introduction

Trace elements have been determined by X-ray fluorescence techniques on the same one hundred and seventy four samples as used for major element analysis, from the Serres-Drama granitic complex (details of analytical techniques and sample preparation can be found in Appendix C). The following fifteen trace elements were determined: Rb, Sr, Ba, Y, La, Ce, Nd, Zr, Nb, U, Th, Pb, Ga, Zn, Cu.

Twelve samples were also analysed by instrumental neutron activation for six low level trace elements: U, Th, Hf, Ta, Sc, Cs at the Universities Research Reactor, Risley.

As mentioned in the previous chapter on major element geochemistry, the samples were collected to include the full range of rock-types present in the Serres-Drama granitic complex.

The geochemistry of the trace elements of the Serres-Drama granitic complex was investigated to explore:

a) the variation in trace element geochemistry throughout the complex;

b) the compositional differences between individual rock-types; and

c) the compositional differences between the 'intermediate' and 'basic' groups.

5-1-2 Results of the trace element analyses

The data obtained by X-R-F analysis for trace elements for each rock-type and the calculated differentiation index of Thornton and Tuttle (as normative Qz + Ab + Or), the modified Larsen index (Nockolds and Allen, 1953), the K/Rb ratio are tabulated as follows: quartz monzonite in table (5-1-2a); granites in table (5-1-2b); granodiorites in table (5-1-2c); monzonites in table (5-1-2d); aplites in table (5-1-2e); gabbros in table (5-1-2f); and xenoliths in table (5-1-2g). The average values from the trace element analysis, the differentiation index and the modified Larsen index for each rock-type are tabulated in table (5-1-2h). The data from instrumental neutron activation analyses for twelve samples is tabulated in table (5-1-2i).

The range and the mean of each trace element content in the whole granitic complex is as follows:

element	range	mean
Rubidium	13 to 229 ppm	187
Strontium	50 to 1055 ppm	591
Barium	16 to 3032 ppm	940
Yttrium	4 to 36 ppm	20
Lanthanum	0 to 65 ppm	33
Cerium	0 to 111 ppm	42
Neodymium	0 to 37 ppm	18
Zirconium	17 to 548 ppm	179
Niobium	0 to 50 ppm	19
Uranium	0 to 27 ppm	9

TABLE: (5-1-3a). Trace element analyses, Differentiation Index (D.I.), Modified Larsen Index (M.L.I.) and the ratio K/Rb of quartz monzonite from the Serres-Drama granitic complex.

	6a3	6b3	8	64	66	67	68	69	118
Rb	226	224	235	270	275	263	233	217	172
Sr	504	492	458	443	428	426	460	520	550
Ba	721	686	612	935	652	612	703	767	1412
Y	30	24	20	17	23	36	25	23	22
La	42	38	42	29	36	44	40	33	33
Ce	73	68	66	43	49	71	63	52	35
Nd	28	20	26	19	18	23	25	27	19
Zr	262	238	252	278	228	229	302	206	190
Nb	26	24	21	28	21	39	24	18	15
U	16	15	21	13	16	20	16	11	7
Th	30	41	32	31	47	54	39	22	26
Pb	19	18	22	34	27	28	21	23	36
Ga	18	18	15	18	16	19	18	18	18
Zn	38	40	41	48	36	37	46	40	54
Cu	13	13	13	15	12	26	14	14	17
D.I.	70•7	71•4	71•6	75•2	78•3	74•9	71•4	71•6	67•0
M.L.I.	18•8	18•9	19•2	21•3	20•6	19•8	18•5	18•3	16•3
K/Rb	181•5	182•1	173•7	112•6	174•9	170•5	179•3	189•5	240•4

TABLE: (5-1-3a) Trace element analyses, Differentiation Index (D.I.), Modified Larsen Index (M.L.I.) and the ratio K/Rb of quartz monzonite from the Serres-Drama granitic complex (continued).

	119	120	121	129	130	132	181	190	205
Rb	153	175	223	136	184	204	142	149	155
Sr	544	551	738	573	564	609	527	412	421
Ba	954	1343	1845	919	1072	1410	795	829	875
Y	21	17	19	33	21	17	19	16	18
La	32	30	29	62	38	25	39	28	32
Ce	49	30	17	81	32	7	53	28	35
Nd	20	16	17	36	26	16	18	10	18
Zr	185	192	166	337	176	127	155	122	126
Nb	23	21	17	31	24	14	22	12	20
U	9	7	7	18	5	8	4	8	5
Th	22	15	17	39	22	20	14	20	19
Pb	34	31	27	31	33	22	27	22	27
Ga	19	20	22	24	21	19	19	19	16
Zn	55	61	48	52	46	40	65	41	43
Cu	17	25	14	15	13	12	35	14	9
D.I.	66·7	66·8	70·1	61·4	70·2	73·9	67·8	72·1	72·7
M.L.I	16·2	16·6	17·0	14·7	17·8	19·0	17·7	19·8	19·9
K/Rb	218·3	213·7	228·3	234·2	214·8	231·2	219·2	218·0	217·5

TABLE: (5-1-3a) *Trace element analyses, Differentiation Index(D.I.), Modified Larsen Index (M.L.I.) and the ratio K/Rb of quartz monzonite from the Serres-Drama granitic complex (continued).*

	206	207	209	212	214	215	216	217	218
Rb	137	145	150	132	159	180	197	162	173
Sr	447	433	419	469	578	562	580	525	655
Ba	893	913	924	933	960	1000	1035	958	1029
Y	18	17	17	15	23	23	20	19	22
La	29	31	28	31	35	41	42	49	28
Ce	37	36	31	28	37	40	38	46	37
Nd	17	12	14	15	12	16	12	17	16
Zr	153	140	127	138	202	217	206	195	160
Nb	18	13	12	17	16	17	16	18	18
U	7	5	6	5	6	5	8	3	-
Th	18	15	19	17	13	14	14	18	17
Pb	26	25	28	24	14	17	16	15	11
Ga	18	17	19	18	18	18	18	21	21
Zn	49	40	49	41	46	40	32	39	40
Cu	12	12	11	9	11	12	9	10	11
D.I.	69·4	71·4	71·5	70·8	75·0	76·3	79·9	80·8	76·3
M.L.I.	18·5	19·3	19·3	19·1	20·8	21·5	22·5	22·9	20·8
K/Rb	239·6	230·4	227·3	245·6	219·9	204·1	212·1	229·9	227·6

TABLE: (5-1-3a) *Trace element analyses, Differentiation Index (D.I.), Modified Larsen Index (M.L.I.) and the ratio K/Rb of quartz monzonite from the Serres-Drama granitic complex (continued).*

	219	221	222	223	226	228	235	236	237
Rb	132	132	155	146	129	140	140	143	144
Sr	667	490	420	557	397	447	384	398	401
Ba	867	712	656	890	759	893	681	854	785
Y	24	19	18	22	15	17	15	20	18
La	35	27	25	35	32	36	30	29	29
Ce	32	34	24	37	28	33	32	38	34
Nd	19	13	11	15	5	11	8	13	10
Zr	147	248	155	201	132	125	115	122	126
Nb	18	11	13	12	17	18	20	18	15
U	2	7	8	11	3	5	5	8	8
Th	27	17	18	32	26	24	17	14	18
Pb	14	16	14	21	23	33	26	26	25
Ga	20	20	19	22	17	16	15	15	17
Zn	41	36	40	46	30	22	30	40	41
Cu	7	8	8	11	9	9	10	12	14
D.I.	78·9	79·4	79·0	73·8	74·9	74·6	74·7	74·6	73·6
M.L.I.	22·7	23·0	22·3	20·7	20·3	19·5	20·7	20·5	20·4
K/Rb	274·0	245·8	230·7	232·1	260·1	248·6	224·0	232·0	215·2

TABLE: (5-1-3a) *Trace element analyses, Differentiation Index (D.I.), Modified Larsen Index (M.L.I.) and the ratio K/Rb of quartz monzonite from the Serres-Drama granitic complex (continued).*

	238	239	277	278	279	280	282	283	284
Rb	141	144	179	201	210	192	176	201	191
Sr	404	386	757	705	774	805	768	986	685
Ba	783	778	909	821	943	952	816	1042	813
Y	19	19	20	20	20	23	16	30	16
La	30	30	39	41	35	52	35	49	34
Ce	38	31	52	57	41	69	51	92	46
Nd	12	17	26	23	17	23	18	37	14
Zr	126	133	212	239	213	242	203	330	200
Nb	19	23	12	20	21	23	19	18	21
U	7	7	12	13	9	12	12	12	12
Th	17	18	39	46	42	48	34	33	42
Pb	20	23	43	36	43	37	39	36	41
Ga	17	14	22	18	18	20	19	21	19
Zn	37	34	54	50	45	50	44	69	46
Cu	11	11	16	12	16	18	10	24	11
D.I.	73•1	73•6	82•0	80•5	82•5	80•8	82•4	72•0	82•7
M.L.I.	20•3	20•3	23•1	23•1	22•9	22•3	23•3	17•9	23•6
K/Rb	219•4	222•3	232•3	201•5	212•8	221•0	224•4	213•7	201•7

TABLE: (5-1-3a) *Trace element analyses, Differentiation Index (D.I.), modified Larsen Index (M.L.I.) and the ratio K/Rb of quartz monzonite from the Serres-Drama granitic complex (continued).*

	286	287	289	290	312
Rb	197	208	166	213	133
Sr	712	723	836	774	686
Ba	814	895	709	872	1168
Y	18	16	21	19	23
La	34	34	42	39	15
Ce	43	49	65	58	48
Nd	14	18	22	18	31
Zr	207	192	255	221	230
Nb	24	25	17	16	14
U	12	13	10	8	3
Th	43	41	40	42	16
Pb	44	51	46	47	24
Ga	18	21	19	18	21
Zn	48	49	50	53	64
Cu	12	16	11	12	17
D.I.	82•2	84•2	80•5	81•0	68•1
M.L.I.	23•2	23•7	23•1	22•5	18•5
K/Rb	201•3	213•1	205•5	195•3	226•6

TABLE: (5-1-3b) Trace element analyses, Differentiation Index (D.I.), Modified Larsen Index (M.L.I.) and ratio K/Rb of granite from the Serres-Drama granitic complex.

	110	111	113	114	115	272	273	291	292
Rb	159	143	165	183	157	152	172	233	208
Sr	435	436	413	404	437	435	439	737	723
Ba	860	828	1045	1004	1052	766	822	847	786
Y	17	15	17	16	17	16	17	14	16
La	28	36	28	29	28	23	22	30	52
Ce	29	35	25	29	25	31	23	36	63
Md	12	17	15	14	15	15	14	13	20
Zr	118	141	119	123	121	127	114	180	229
Nb	13	14	20	14	13	10	8	16	18
U	5	5	6	9	5	7	8	9	9
Th	18	19	25	18	16	16	9	36	43
Pb	31	25	26	22	25	27	26	52	39
Ga	15	18	19	17	16	18	16	20	18
Zn	43	43	40	35	40	37	41	48	44
Cu	10	11	10	10	11	13	21	15	14
D.I.	70•9	69•9	73•0	76•4	73•8	80•0	78•6	82•9	82•3
M.L.I.	19•1	18•7	19•9	20•8	19•9	23•5	23•2	23•2	23•1
K/Rb	210•3	212•9	214•0	209•1	223•1	213•8	194•8	195•2	193•5

TABLE: (5-1-3b) Trace element analyses, Differentiation Index (D.I.), Modified Larsen Index (M.L.I.) and the ratio K/Rb of granite from the Serres-Drama granitic complex

	294	296	298	300	302	304	305	306	307
Rb	207	194	185	206	211	220	210	195	216
Sr	659	706	784	729	721	708	631	653	642
Ba	812	765	886	843	745	807	803	752	795
Y	13	13	18	18	16	14	13	13	13
La	35	38	40	37	43	38	10	13	12
Ce	36	41	47	44	54	50	33	37	34
Md	16	15	20	19	17	14	28	32	35
Zr	169	191-	215	191	209	194	150	166	152
Nb	20	19	18	17	19	20	24	23	25
U	11	10	10	8	11	14	7	10	9
Th	42	44	45	36	47	38	40	40	40
Pb	37	36	46	45	45	43	43	38	41
Ga	17	20	19	19	22	21	17	19	20
Zn	39	46	52	44	48	49	40	47	40
Cu	10	11	14	12	18	14	11	10	12
D.I.	86•2	83•6	81•6	81•3	80•6	82•3	85•1	83•4	84•4
M.L.I.	24•5	23•5	22•9	23•0	22•9	23•2	24•0	23•8	23•9
K/Rb	213•6	214•2	226•0	201•1	181•3	182•8	210•0	202•3	196•5

TABLE: (5-1-3c) Trace element analyses, Differentiaition Index (D.I.), Modified Larsen Index (M.L.I.) and ratio K/Rb of granodiorite from the Serres-Drama granitic complex

	4	34	37	46	47	48	50	51	57
Rb	213	148	146	164	130	195	130	192	182
Sr	501	466	449	742	457	481	497	756	518
Ba	639	878	780	1670	862	967	827	1116	874
Y	24	17	15	21	17	18	16	21	17
La	41	23	21	30	24	28	32	37	29
Ce	66	22	26	34	29	27	39	54	42
Md	23	8	8	19	11	13	16	24	14
Zr	271	103	99	163	102	116	123	169	147
Nb	24	15	15	16	15	15	13	11	13
U	13	4	6	5	2	6	5	6	7
Th	38	12	13	11	11	13	12	17	24
Pb	22	19	27	29	18	17	15	22	17
Ga	15	15	18	20	16	16	18	20	18
Zn	52	40	40	60	44	29	66	63	36
Cu	15	9	9	14	9	9	57	81	10
D.I.	64•7	79•7	75•9	68•1	76•8	79•2	72•8	58•9	77•6
M.L.I.	16•3	21•0	21•8	16•4	21•9	21•7	19•8	13•1	21•4
K/Rb	185•4	341•8	214•5	267•1	235•6	203•9	233•2	191•4	203•1

TABLE: (5-1-3c) Trace element analyses, Differentiation Index (D.I.), Modified Larsen Index (M.L.I.) and ratio K/rb of granodiorite from the Serres-Drams grantic complex

	63	163	164	165	166	167	168	169	170
Rb	217	134	173	204	218	189	198	170	151
Sr	577	453	434	438	369	485	490	489	469
Ba	821	825	713	853	585	802	832	932	780
Y	22	16	18	18	15	20	16	21	22
La	42	23	25	27	24	28	28	21	24
Ce	71	22	27	27	28	33	28	34	30
Nd	27	10	11	8	7	16	9	12	17
Zr	209	127	126	122	118	152	145	166	149
Nb	20	17	16	18	16	18	12	16	19
U	12	4	7	10	8	7	7	1	4
Th	30	19	18	39	19	17	19	17	21
Pb	20	25	26	25	20	21	24	30	31
Ga	19	15	16	14	15	18	18	18	16
Zn	49	37	35	34	28	38	36	48	52
Cu	22	13	17	15	9	17	10	7	11
D.I.	68•3	77•7	77•9	81•0	83•0	78•0	78•0	77•3	74•1
M.L.I.	16•9	22•3	22•5	22•9	23•7	21•9	21•9	21•6	20•8
K/Rb	186•0	247•8	184•8	194•5	187•4	199•6	185•2	219•2	221•0

TABLE: (5-1-3c) Trace element analyses, Differentiation Index (D.I.), Modified Larsen Index (M.L.I.) and ratio K/Rb of granodiorite from the Serres-Drama granitic complex

	171	213
Rb	126	156
Sr	563	411
Ba	776	686
Y	26	14
La	25	19
Ce	36	21
Nd	16	12
Zr	145	104
Nb	17	19
U	2	19
Th	9	5
Pb	26	15
Ga	18	24
Zn	62	39
Cu	14	5
D.I.	68•4	79•2
M.L.I.	18•9	23•2
K/Rb	228•7	191•2

TABLE: (5.1-3d) Trace element analyses, Differentiation Index (D.I.), Modified Larsen Index (M.L.I.) and ratio K/Rb of monzonite from the Serres-Drama granitic complex

	76	78	82	124	125	126	127	133	134
Rb	201	190	188	211	199	165	187	172	176
Sr	863	759	542	508	457	635	552	861	716
Ba	1113	839	1007	1051	772	1207	1020	1901	1378
Y	23	24	19	14	21	22	17	19	24
La	30	33	29	26	39	33	36	30	42
Ce	47	56	36	25	37	31	35	20	46
Nd	23	25	17	10	15	19	15	13	18
Zr	123	204	154	128	161	163	134	55	156
Nb	10	16	14	19	20	17	14	25	27
U	7	9	10	13	7	5	9	1	8
Th	20	28	22	29	31	27	25	11	21
Pb	27	24	25	26	26	31	25	43	27
Ga	23	24	20	16	19	21	20	20	19
Zn	55	56	35	46	44	55	44	54	51
Cu	60	69	9	13	16	23	17	18	11
D.I.	59•6	58•3	76•6	73•1	72•6	66•2	71•5	74•9	67•6
M.L.I.	13•3	13•1	20•8	19•4	19•0	16•3	18•5	18•5	16•6
K/Rb	196•7	181•5	197•6	193•3	189•3	222•6	198•2	309•8	239•4

TABLE: (5-1-3d) Trace element analyses, Differentiation Index (D.I.), Modified Larsen Index (M.L.I.) and ratio K/Rb of monzonite from Serres-Drama granitic complex

	135	137	139	140	141	142	143	144	145
Rb	247	267	186	147	142	250	218	243	247
Sr	825	1001	796	882	823	935	699	722	687
Ba	1708	2686	1619	1561	1630	1939	1215	1231	1082
Y	20	19	21	24	22	23	25	18	22
La	31	31	31	36	32	35	47	35	40
Ce	16	12	38	51	37	35	63	51	54
Nd	16	19	18	25	12	13	23	19	30
Zr	73	139	136	59	140	30	347	359	286
Nb	25	24	21	30	16	40	26	23	34
U	8	10	9	7	5	9	16	8	9
Th	17	9	12	14	14	18	39	47	45
Pb	34	21	32	43	26	38	32	33	31
Ga	19	19	19	19	18	18	20	22	23
Zn	36	48	46	62	45	44	66	50	52
Cu	11	20	16	32	14	29	48	52	49
D.I.	77•3	77•6	75•5	69•9	71•0	76•0	63•3	70•9	70•2
M.L.I.	19•9	18•9	18•7	16•7	17•9	16•7	15•4	17•9	17•7
K/Rb	225•7	240•3	283•8	275•6	294•2	211•9	185•6	195•6	191•9

TABLE: (5-1-3d) Trace element analyses, Differentiation Index (D.I.), Modified Larsen Index (M.L.I.) and ratio K/RB of monzonite from Serres-Drama granitic complax

	146	184	185	186	187	188	189	191	192
Rb	238	170	231	196	137	236	151	128	247
Sr	715	352	475	529	998	493	416	434	615
Ba	988	976	832	1052	1671	856	886	797	816
Y	21	15	16	20	23	15	16	19	24
La	41	37	32	33	33	38	31	32	39
Ce	55	34	33	33	36	35	31	42	50
Nd	19	12	13	15	20	15	12	19	20
Zr	395	156	130	150	60	145	122	137	259
Nb	24	17	28	26	28	20	17	17	23
U	9	10	5	7	2	11	9	8	17
Th	55	23	26	22	11	21	17	14	35
Pb	34	21	29	19	29	30	22	20	22
Ga	21	14	14	15	16	17	17	16	19
Zn	65	29	48	48	62	43	34	45	49
Cu	59	95	12	12	18	10	8	10	59
D.I.	65•6	79•9	76•2	73•5	66•9	75•7	74•3	69•7	69•1
M.L.I.	15•8	22•6	20•5	19•5	15•7	20•2	20•7	19•1	17•5
K/Rb	185•2	215•6	171•0	196•8	291•3	163•9	218•7	230•5	174•5

TABLE: (5-1-3d) Trace element analyses, Differentiation Index (D.I.), Modified Larsen Index (M.L.I.) and ratio K/Rb of monzonite from Serres-Drama granitic complex

	193	195	196	201	202	203	204	260	264
Rb	167	202	174	177	247	255	143	189	196
Sr	582	702	616	905	708	492	1015	711	504
Ba	1286	1581	1168	1467	1176	845	1557	2299	1015
Y	19	25	19	21	18	27	16	24	23
La	33	32	35	32	31	52	26	34	38
Ce	38	32	39	29	34	73	22	30	44
Nd	20	19	14	19	16	22	18	20	23
Zr	181	143	135	111	145	454	36	128	144
Nb	18	14	14	8	16	50	5	21	24
U	8	8	7	3	6	26	0	7	9
Th	20	16	23	20	17	93	4	16	20
Pb	32	30	19	40	56	53	40	38	28
Ga	16	15	18	20	20	18	21	16	19
Zn	56	43	47	75	69	52	72	55	53
Cu	17	30	7	59	46	40	42	38	16
D.I.	69•1	69•4	67•9	51•1	64•1	78•4	60•0	69•9	71•7
M.L.I.	17•5	17•0	17•1	8•5	13•8	21•2	13•1	17•5	19•0
K/Rb	241•7	246•1	214•5	192•5	184•5	181•1	263•4	225•8	183•0

TABLE: 5-1-3d) Trace element analyses, Differentiation Index (D.I.), Modified Larsen Index (M.L.I.) and ratio K/Rb of monzonite from Serres-Drama granitic complex

	269	320	321	323	324	325	329	330	334
Rb	187	299	239	288	287	225	202	191	188
Sr	605	578	752	668	662	808	862	856	912
Ba	1443	1000	1429	1108	1153	1406	1341	1327	1564
Y	25	18	28	21	21	22	23	21	20
La	38	39	48	38	40	27	25	35	32
Ce	41	54	55	50	42	28	40	31	28
Nd	19	16	26	18	20	22	19	19	22
Zr	149	447	402	143	257	107	136	129	98
Nb	22	37	26	20	19	8	9	14	10
U	10	21	14	10	12	5	6	4	5
Th	17	62	44	23	25	19	18	13	11
Pb	32	43	34	51	50	51	39	40	46
Ga	18	18	18	20	18	19	20	20	21
Zn	50	49	57	73	73	71	64	67	77
Cu	23	45	25	39	51	57	56	44	60
D.I.	71•3	78•0	71•9	66•5	68•7	60•2	60•0	58•8	54•1
M.L.I.	18•4	21•0	18•0	14•5	15•0	12•1	12•4	12•0	9•3
K/Rb	228•9	160•4	198•7	157•8	176•3	184•9	197•1	198•6	191•2

TABLE: (5-1-3d) Trace element analyses, Differentiation Index (D.I.), Modified Larsen Index (M.L.I.) and ratio K/Rb of monzonite from Serres-Drama granitic complex

	338	340	341	342	345	346	350	351	352
Rb	263	253	250	272	264	233	250	241	246
Sr	751	761	718	712	594	609	564	613	606
Ba	1166	1251	1169	1187	873	892	755	795	799
Y	17	20	21	22	26	31	25	27	26
La	29	34	33	35	51	50	40	39	37
Ce	38	31	35	40	78	84	51	49	54
Nd	20	16	19	18	27	29	19	16	20
Zr	171	125	167	173	534	542	223	258	211
Nb	16	17	15	14	36	38	25	26	23
U	9	11	9	13	26	25	8	11	9
Th	18	20	15	22	91	95	19	32	26
Pb	49	34	55	56	44	37	28	25	28
Ga	20	22	21	23	19	20	16	19	17
Zn	76	68	74	70	62	56	52	59	51
Cu	67	49	48	53	103	32	46	48	52
D.I.	63•2	61•1	63•3	65•7	73;9	72•3	71•5	68•3	68•6
M.L.I.	13•1	12•6	12•9	14•1	19•3	18•8	18•4	17•3	17•6
K/Rb	162•2	161•2	174•2	167•8	167•8	192•3	167•6	167•6	168•1

TABLE: (5-1-3d) Trace element analyses, Differentiation Index (D.I.), Modified Larsen Index (M.L.I.) and ratio K/Rb of monzonite from Serres-Drama granitic complex

	353	354	355	356	357	358	359	360	362
Rb	243	243	247	250	240	230	241	227	261
Sr	603	634	587	598	574	607	594	663	615
Ba	770	780	740	766	682	731	788	824	814
Y	26	24	26	24	28	27	21	25	22
La	43	40	44	39	37	47	40	40	35
Ce	52	55	62	53	58	61	48	46	41
Nd	17	23	17	18	19	20	22	24	26
Zr	215	198	267	236	223	197	188	162	253
Nb	25	21	32	24	30	26	19	24	22
U	12	13	12	13	15	22	14	10	15
Th	27	23	13	25	39	67	27	24	40
Pb	19	19	16	27	27	24	24	24	25
Ga	18	19	20	18	20	20	18	20	20
Zn	47	113	46	53	55	56	52	56	47
Cu	17	168	54	41	40	53	42	53	49
D.I.	70•3	70•1	70•0	70•8	68•8	70•8	69•8	68•1	71•6
M.L.I.	17•9	17•7	18•0	17•7	17•0	17•7	17•8	17•2	18•6
K/Rb	169•1	172•8	165•5	178•4	169•5	179•3	170•9	168 •5	167•7

TABLE: (5-1-3d) Trace element analyses, Differntiation Index (D.I.), Modified Larsen Index (M.L.I.) and ratio K/Rb of monzonite from Serres-Drama granitic complex.

	363	364	365	366	367	368
Rb	253	242	247	237	256	265
Sr	600	643	617	608	559	507
Ba	776	803	769	776	754	947
Y	25	27	24	24	29	29
La	36	44	38	50	56	59
Ce	55	57	59	70	87	85
Nd	19	21	24	24	29	29
Zr	227	198	234	224	548	500
Nb	24	25	24	27	46	44
U	15	19	15	9	27	16
Th	28	30	22	26	90	90
Pb	29	29	28	29	42	42
Ga	17	16	16	17	18	19
Zn	51	53	55	65	66	57
Cu	80	46	39	36	45	30
D.I.	69•9	68•9	70•5	70•4	73•7	75•9
M.L.I.	17•3	16•9	17•8	18•2	19•5	19•9
K/Rb	174•9	176•9	168•5	169•3	170•2	187•6

TABLE: (5-1-3e) Trace element analyses, Differentiation Index (D.I.), Modified Larsen Index (M.L.I.) and the ratio K/Rb of aplite from the Serres-Drama granitic complex.

	3	41	42	148
Rb	275	216	235	184
Sr	51	50	61	312
Ba	47	19	93	1027
Y	4	13	20	16
La	10	7	5	27
Ce	12	5	3	29
Nd	-	-	-	7
Zr	24	45	43	112
Nb	26	28	23	12
U	14	8	3	7
Th	23	22	15	16
Pb	29	33	27	30
Ga	12	16	13	13
Zn	13	15	14	17
Cu	9	6	5	6
D.I.	95•1	94•6	96•7	88•1
M.L.I.	28•2	28•1	27•9	26•2
K/Rb	158•5	194•9	225•1	203•2

TABLE: (5-1-3f) Trace element analyses, Differentiation Index (D.I.), Modified Larsen Index (M.L.I.) and the ratio K/Rb of gabbro from the Serres-Drama granitic complex.

	147	151	152	153	172
Rb	62	22	13	19	16
Sr	701	613	590	510	518
Ba	3034	155	48	131	41
Y	24	16	14	14	10
La	18	5	4	3	-
Ce	-	19	29	24	13
Nd	14	8	5	8	9
Zr	100	36	17	41	21
Nb	4	-	-	-	-
U	7	3	-	-	-
Th	5	1	3	1	-
Pb	17	14	7	7	9
Ga	16	14	16	19	16
Zn	45	72	61	84	66
Cu	11	91	33	128	280
D.I.	55•1	11•4	8•0	8•6	8•4
M.L.I.	12•2	-	-	-	-
K/Rb	441•3	183•6	257•7	172•6	230•6

TABLE: (5-1-3g) Trace element analyses, Differentiation Index (D.I.), Modified Larsen Index (M.L.I.) and ratio K/Rb of xenolith from Serres-Drama granitic complex.

	1	6a1	6a2	6b1	6b2	7b	7d	315
Rb	127	28	39	30	38	88	108	95
Sr	852	398	404	431	440	466	465	1055
Ba	1000	16	51	23	50	148	194	1177
Y	18	30	27	29	24	10	6	23
La	27	53	49	65	54	37	32	19
Ce	34	93	91	111	103	53	43	49
Nd	17	36	29	29	27	18	18	33
Zr	64	213	165	187	183	120	80	167
Nb	12	21	21	19	17	13	9	10
U	6	11	12	8	6	14	13	4
Th	13	10	12	8	7	9	5	19
Pb	33	13	10	14	17	11	15	21
Ga	21	21	22	24	23	20	20	22
Zn	86	95	96	93	90	76	79	79
Cu	64	19	16	17	14	31	38	49
D.I.	51•9	43•9	43•7	46•0	46•3	47•5	46•6	58•7
M.L.I.	10•6	10•3	10•1	10•0	10•6	12•1	12•1	14•3
K/Rb	229•6	218•2	192•1	175•0	150•3	166•4	136•1	275•8

TABLE: (5-1-2h) Average trace element composition of the whole complex, quartz monzonite (Qm) + granite (Gr) + granodiorite (Gd) and individual rock-suites from the Serres-Drama granitic complex.

	Whole comp. (sam. 174)	Qm+Gr +Gd (sam. 88)	Qm (sam. 50)	Gr (sam. 18)	Gd (sam. 20)	Monz. (sam. 69)	Aplit (sam. 4)	Gabb (sam. 5)	Xenol (sam. 8)
Rb	187 ±57	179 ±35	178 ±39	190 ±26	172 ±31	220 ±40	228 ±38	26 ±20	69 ±40
Sr	591 ±170	554 ±137	561 ±145	594 ±141	502 ±97	669 ±146	119 ±129	586 ±78	564 ±248
Ba	940 ±427	883 ±203	904 ±223	851 ±98	861 ±223	1139 ±397	296 ±488	682 ±1316	332 ±473
Y	20 ±5	19 ±4	20 ±4	15 ±2	19 ±3	22 ±4	13 ±7	16 ±5	21 ±9
La	33 ±11	32 ±9	35 ±8	30 ±11	28 ±6	37 ±7	12 ±10	6 ±7	42 ±17
Ce	42 ±19	41 ±15	44 ±17	37 ±11	35 ±14	45 ±16	12 ±12	17 ±11	72 ±30
Nd	18 ±7	17 ±7	18 ±7	18 ±7	14 ±6	19 ±4	2 ±4	9 ±3	26 ±7
Zr	179 ±92	176 ±55	195 ±57	162 ±37	143 ±41	203 ±120	56 ±39	43 ±33	147 ±54
Nb	19 ±8	18 ±5	19 ±5	17 ±5	16 ±3	23 ±9	22 ±7	1 ±2	15 ±5
U	9 ±5	8 ±4	9 ±5	9 ±2	6 ±3	11 ±6	8 ±5	2 ±3	9 ±4
Th	25 ±17	26 ±12	27 ±12	32 ±13	19 ±8	29 ±21	19 ±4	2 ±2	10 ±4
Pb	29 ±11	28 ±10	28 ±10	36 ±9	23 ±5	33 ±10	30 ±3	11 ±4	17 ±7
Ga	18 ±2	18 ±2	19 ±2	18 ±2	17 ±2	19 ±2	14 ±2	16 ±2	22 ±1
Zn	51 ±16	44 ±9	45 ±9	43 ±5	44 ±12	56 ±13	15 ±2	66 ±14	87 ±8
Cu	28 ±31	14 ±10	13 ±5	13 ±3	18 ±18	40 ±26	7 ±2	107 ±106	31 ±18
D.I.	71 ±13	76 ±6	75 ±5	80 ±5	75 ±6	69 ±6	94 ±4	18 ±21	48 ±5
M.L.I.	18 ±5	21 ±2	20 ±2	22 ±2	21 ±3	17 ±3	28 ±1	2 ±5	11 ±1

TABLE: (5-1-2i) Low level trace element concentration of Serres-Drama granitic complex (determined by I.N.A.A.).

	U ppm	Th ppm	Cs ppm	Sc ppm	Hf ppm	Ta ppm
			Diorite xenoliths			
6B1	9.10±0.10	11.20±0.10	1.64±0.07	11.90±0.20	6.0 ±0.10	0.76 ±0.04
315	4.01±0.08	14.40±0.20	1.10±0.03	3.00±0.20	5.1 ±0.09	0.8 ±0.09
			Gabbro			
152	0.61±0.02	2.16±0.06	0.52±0.02	24.90±0.20	1.63 ±0.08	7.5E-2±0.04
			Monzonite			
126	5.69±0.10	19.10±0.20	2.07±0.06	8.10±0.20	5.4 ±0.10	1.44 ±0.05
184	7.90±0.20	27.60±0.30	2.22±0.04	4.60±0.10	5.3 ±0.20	1.72 ±0.05
202	4.76±0.09	15.90±0.40	4.60±0.20	8.60±0.10	6.0 ±0.10	0.79 ±0.05
			Quartz monzonite			
6b3	17.70±0.20	62.50±0.60	2.97±0.07	4.90±0.30	8.0 ±0.20	2.2 ±0.08
119	6.15±0.10	22.70±0.20	3.04±0.07	9.40±0.20	6.7 ±0.10	1.44 ±0.07
215	3.64±0.09	18.80±0.40	1.44±0.09	2.90±0.10	6.3 ±0.10	0.86 ±0.09
277	10.90±0.20	47.70±0.50	1.40±0.04	6.20±0.20	8.5 ±0.10	0.99 ±0.07
			Granodiorite			
213	5.00±0.10	19.40±0.60	1.72±0.03	3.40±0.20	4.6 ±0.03	1.11 ±0.08
			Granite			
273	5.40±0.10	13.70±0.20	1.90±0.10	3.20±0.20	4.6 ±0.10	0.86 ±0.10

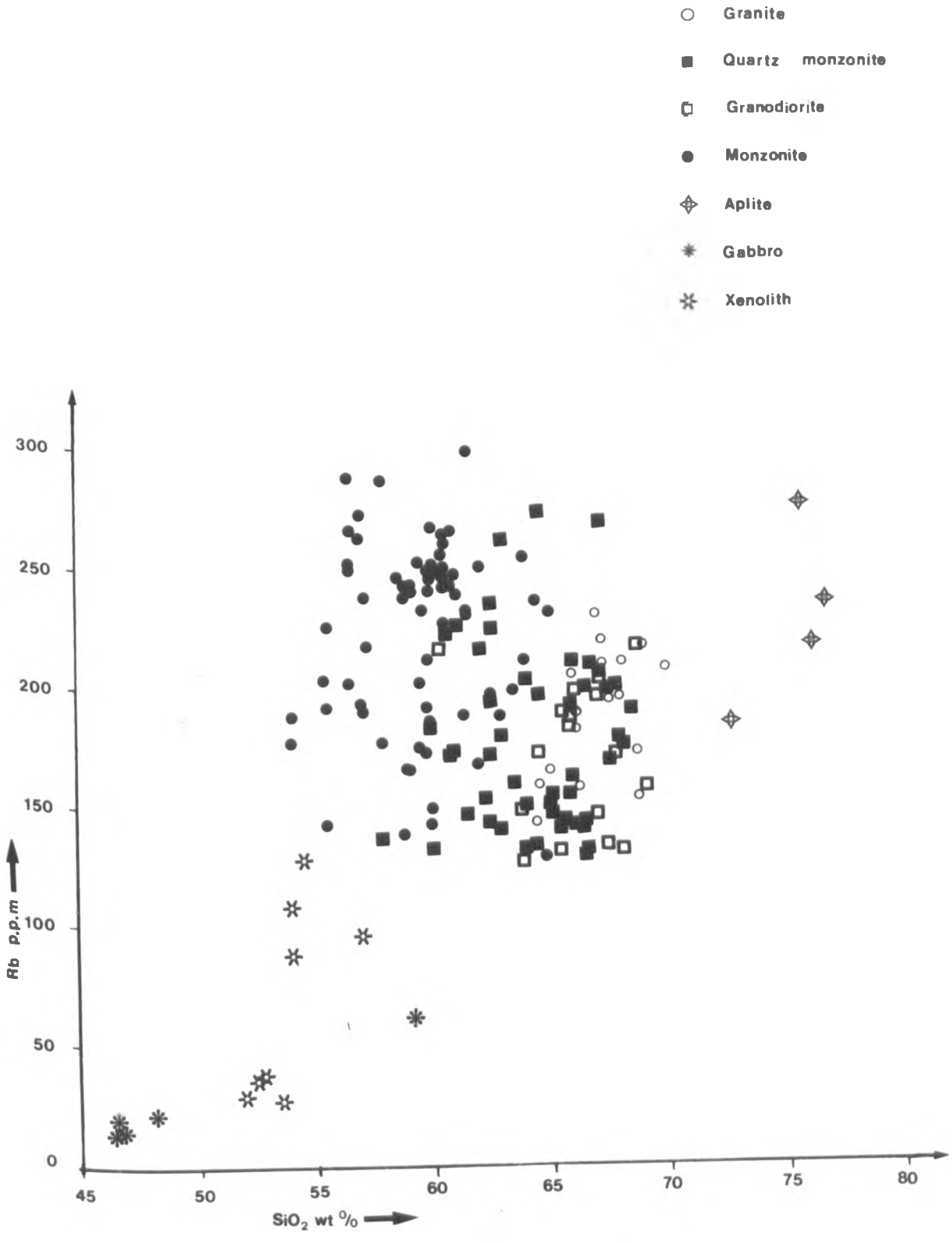
Granite
Quartz monzonite
Granodiorite
Monzonite
Aplite
Gabbro
Xenolith
300
250
200
150
100
50
0
Rb p.p.m
45
50
55
60
65
70
75
80
SiO2 wt %

Fig. (5-1-2a)

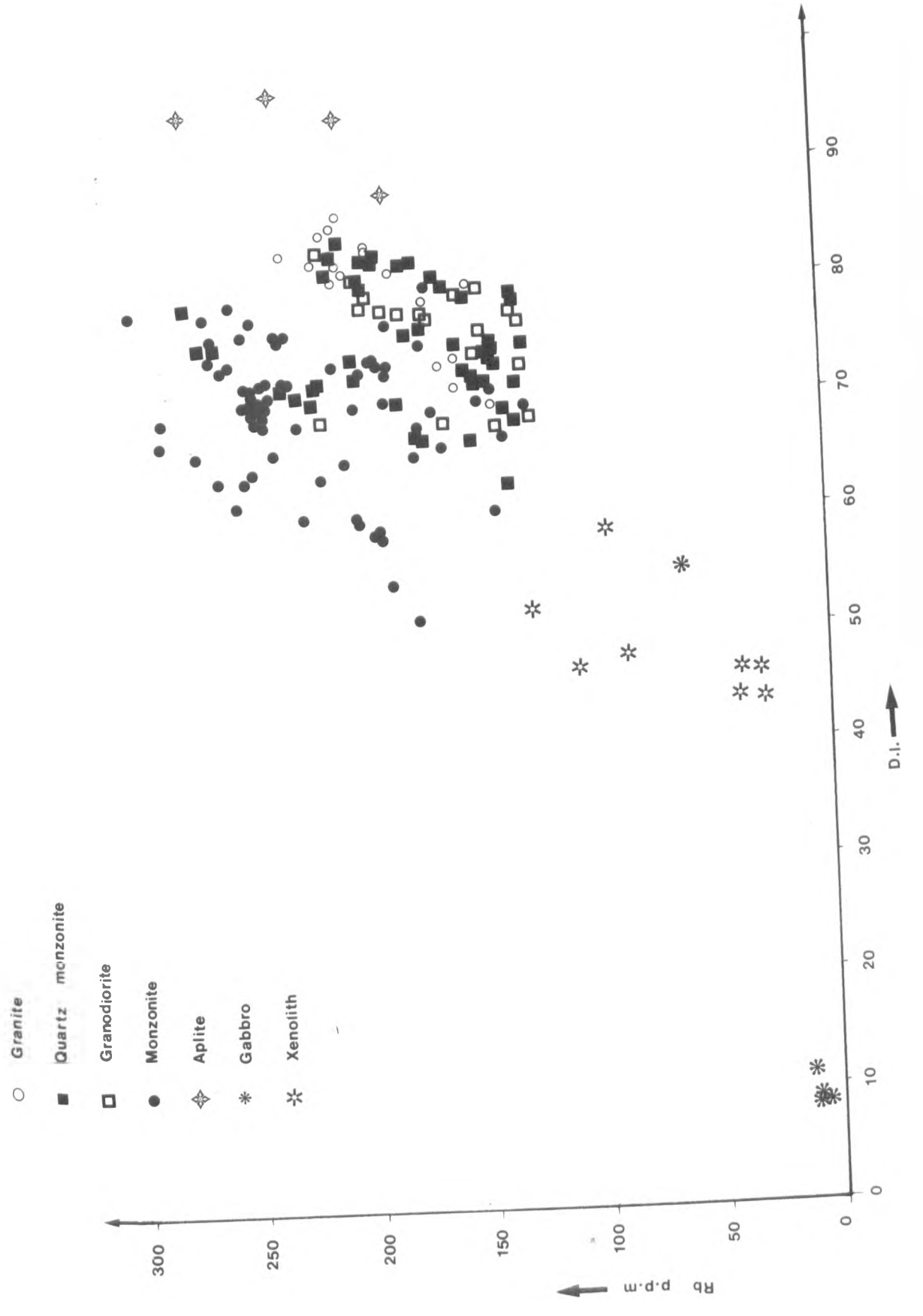
Granite
Quartz monzonite
Granodiorite
Monzonite
Aplite
Gabbro
Xenolith
Rb p.p.m
300
250
200
150
100
50
0
0
10
20
30
40
50
60
70
80
90
D.I.

Fig. (5-1-2b)

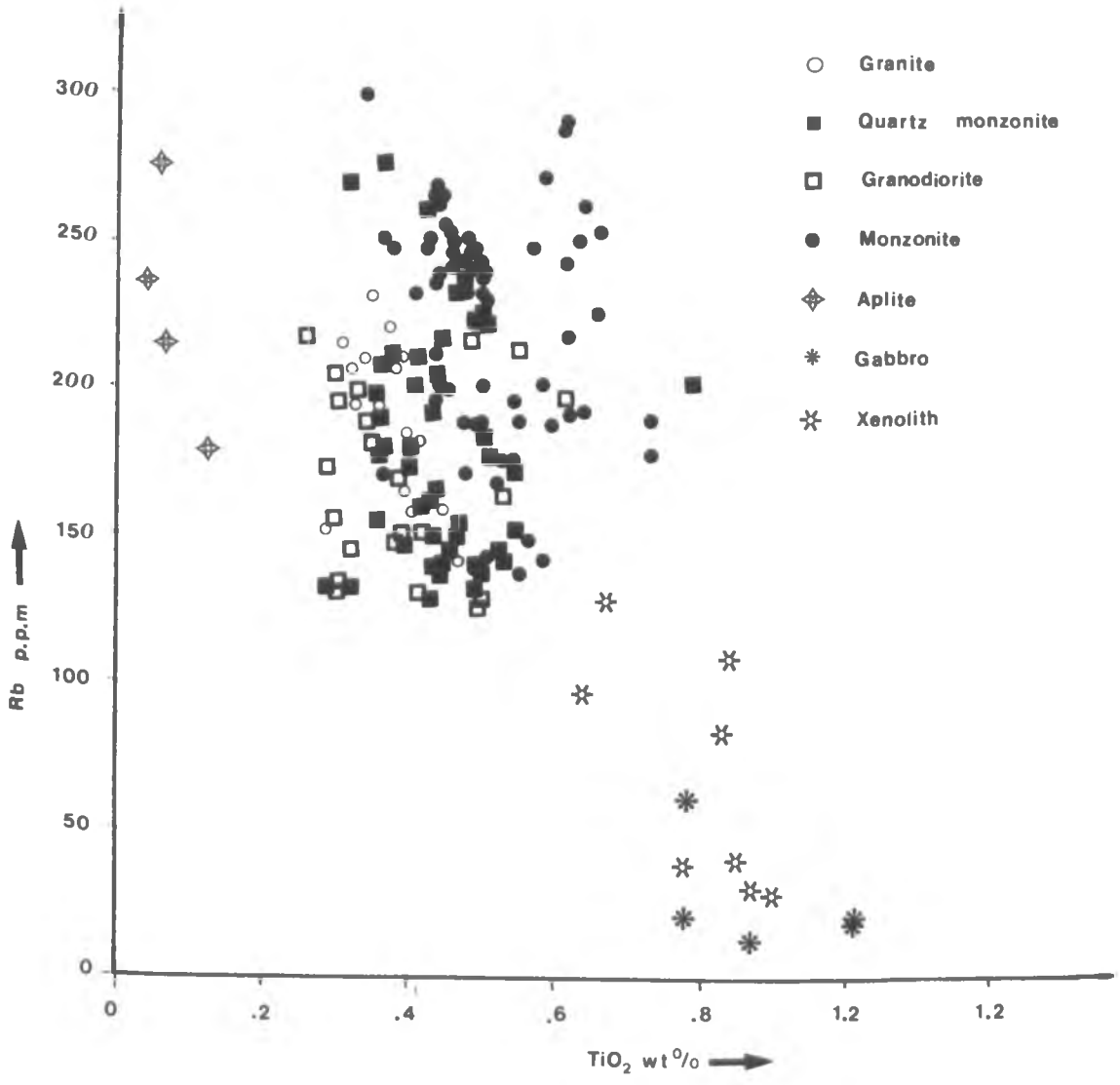
Granite
Quartz monzonite
Granodiorite
Monzonite
Aplite
Gabbro
Xenolith
300
250
200
150
100
50
0
Rb p.p.m
0
.2
.4
.6
.8
1.2
1.2
TiO2 wt %

Fig. (5-1-2c)

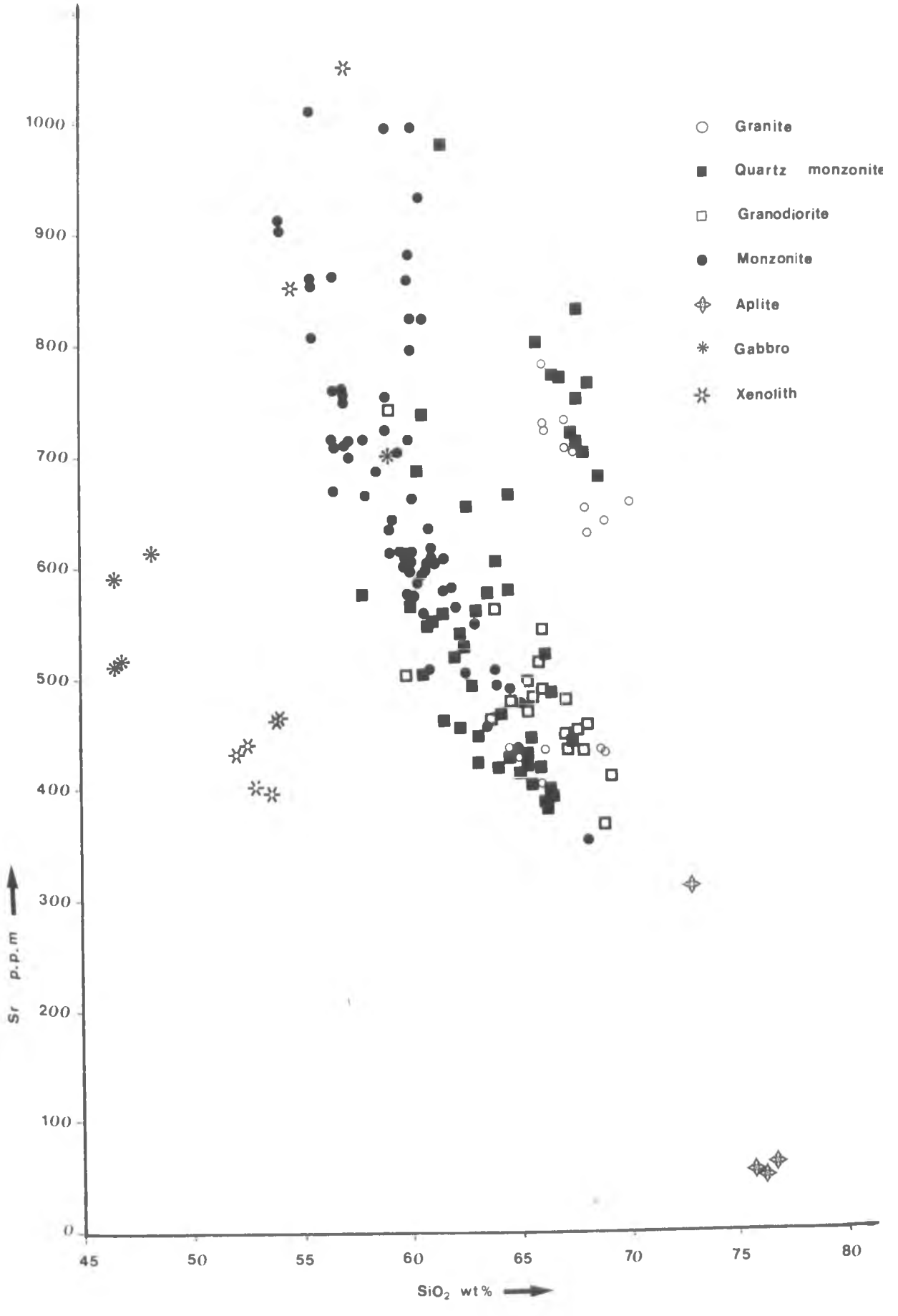
Granite
Quartz monzonite
Granodiorite
Monzonite
Aplite
Gabbro
Xenolith
1000
900
800
700
600
500
400
300
200
100
0
Sr p.p.m
45
50
55
60
65
70
75
80
SiO2 wt%

Fig. (5-1-2d)

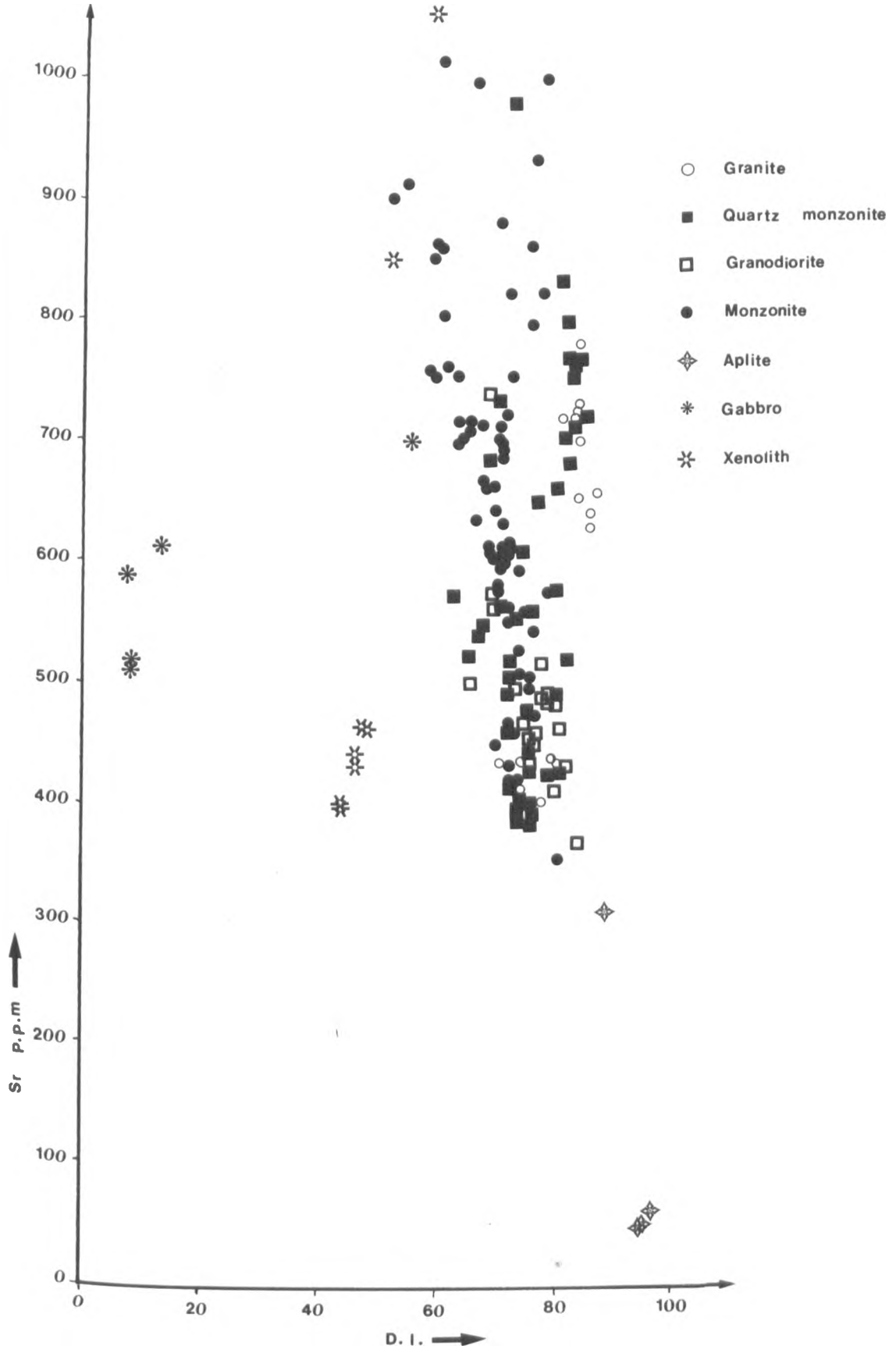
Granite
Quartz monzonite
Granodiorite
Monzonite
Aplite
Gabbro
Xenolith
Sr P.P.M
D. I.
0
100
200
300
400
500
600
700
800
900
1000
0
20
40
60
80
100

Fig. (5-1-2e)

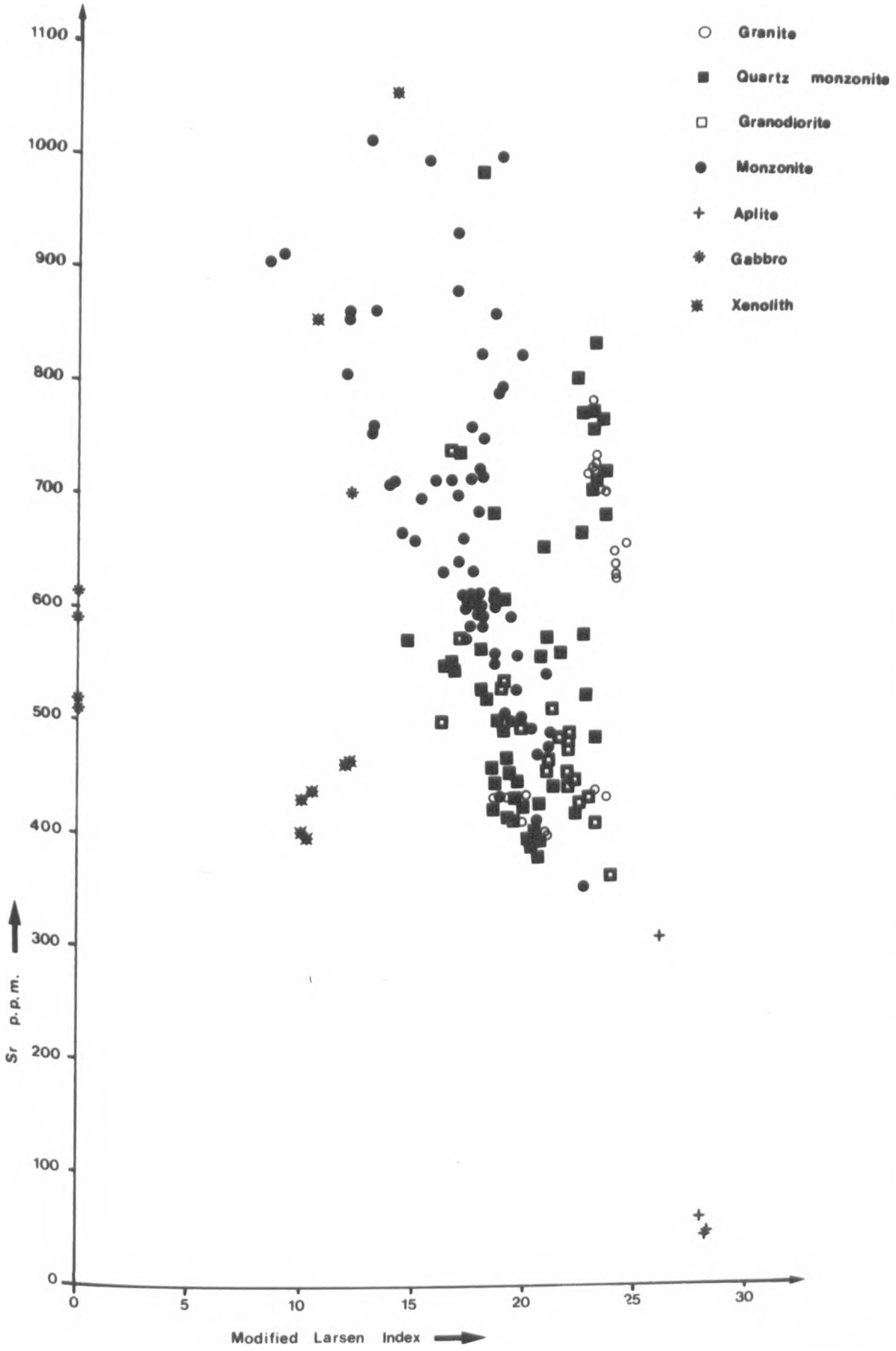
Granite
Quartz monzonite
Granodiorite
Monzonite
Aplite
Gabbro
Xenolith
1100
1000
900
800
700
600
500
400
300
200
100
0
Sr p.p.m.
0
5
10
15
20
25
30
Modified Larsen Index

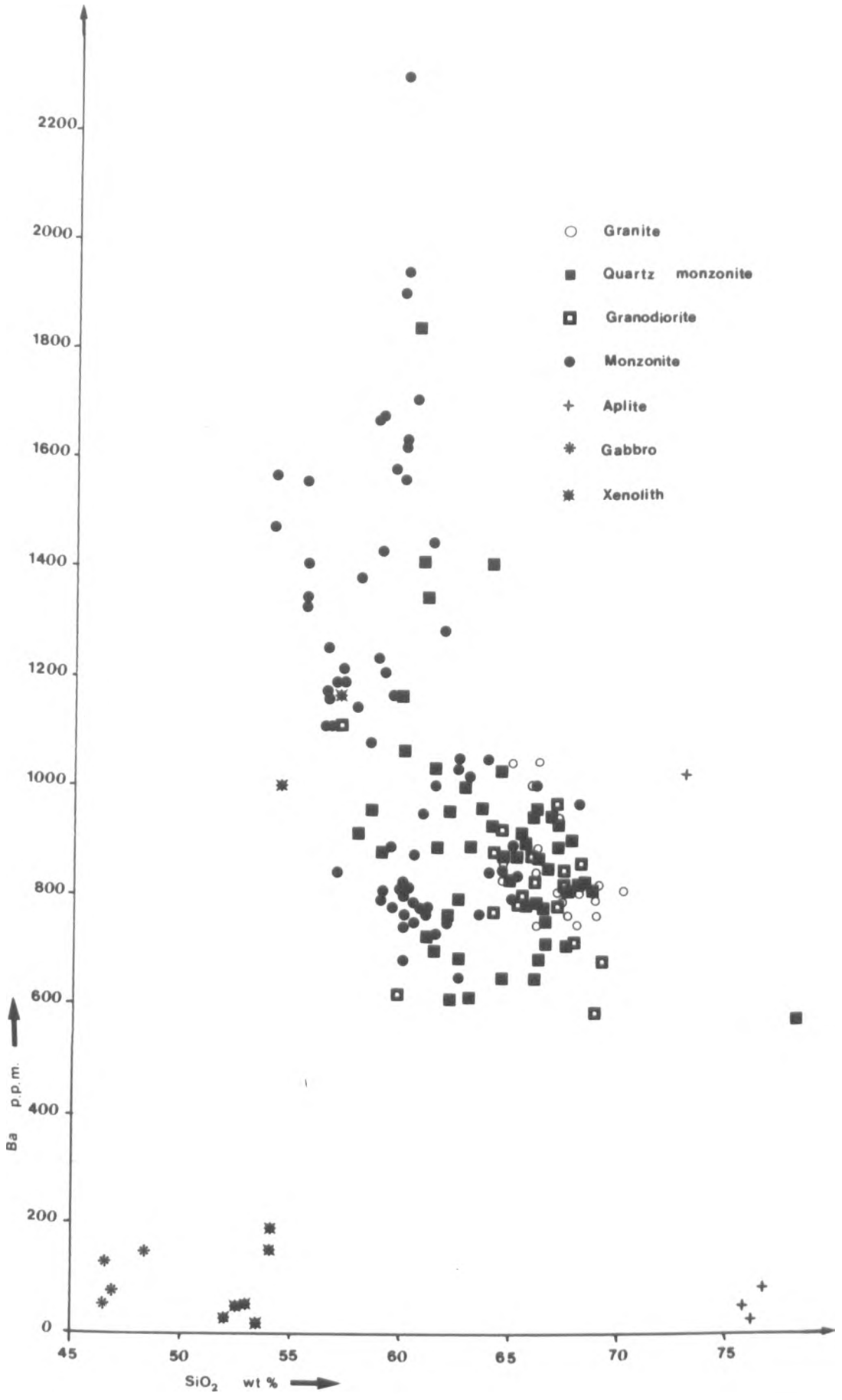
Granite
Quartz monzonite
Granodiorite
Monzonite
Aplite
Gabbro
Xenolith
2200
2000
1800
1600
1400
1200
1000
800
600
400
200
0
Ba p.p.m.
45
50
55
60
65
70
75
SiO2 wt %

Fig (5-1-2g)

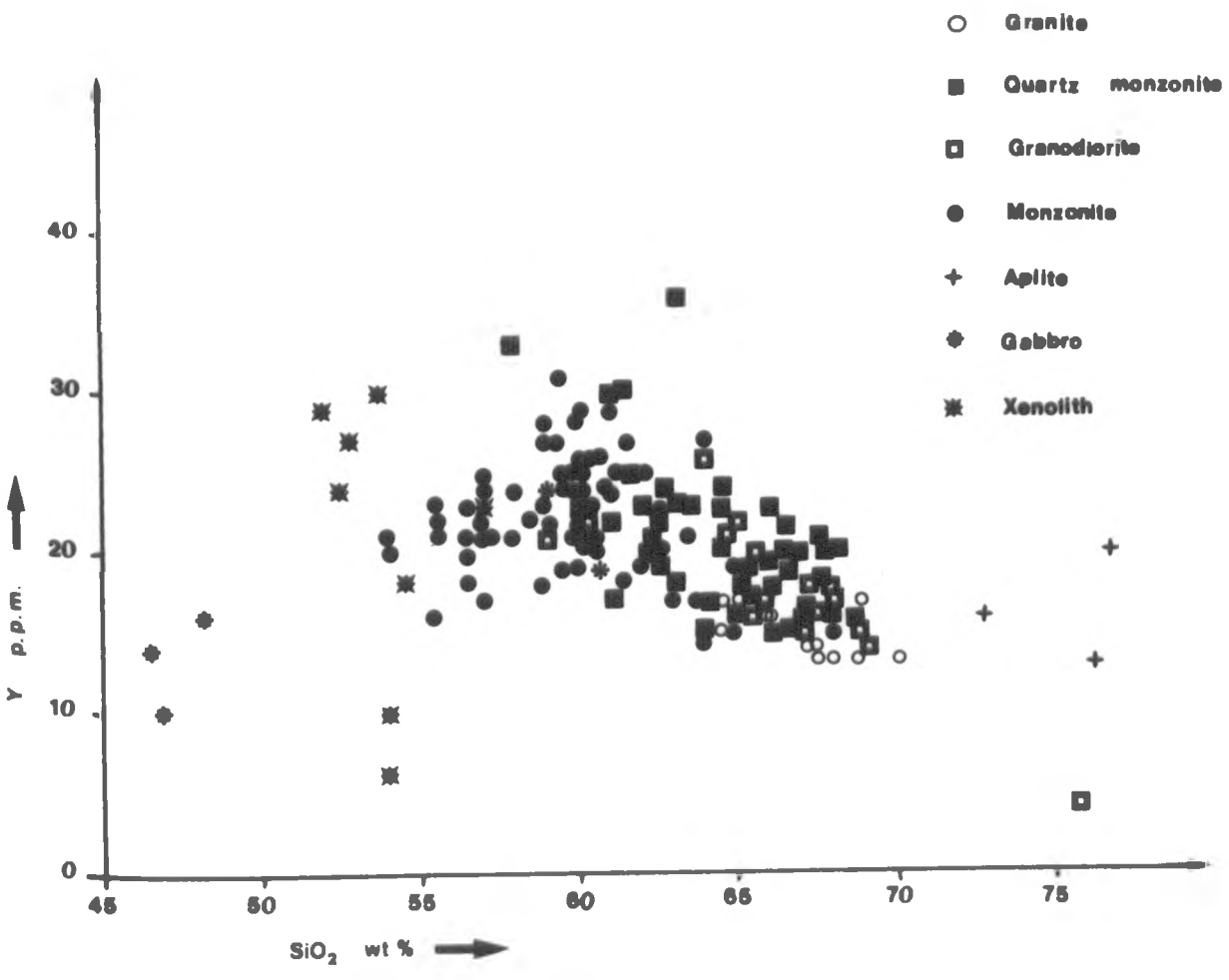
Granite
Quartz monzonite
Granodiorite
Monzonite
Aplite
Gabbro
Xenolith
Y p.p.m.
40
30
20
10
0
45
50
55
60
65
70
75
SiO2 wt %

Fig. (5-1-2h)

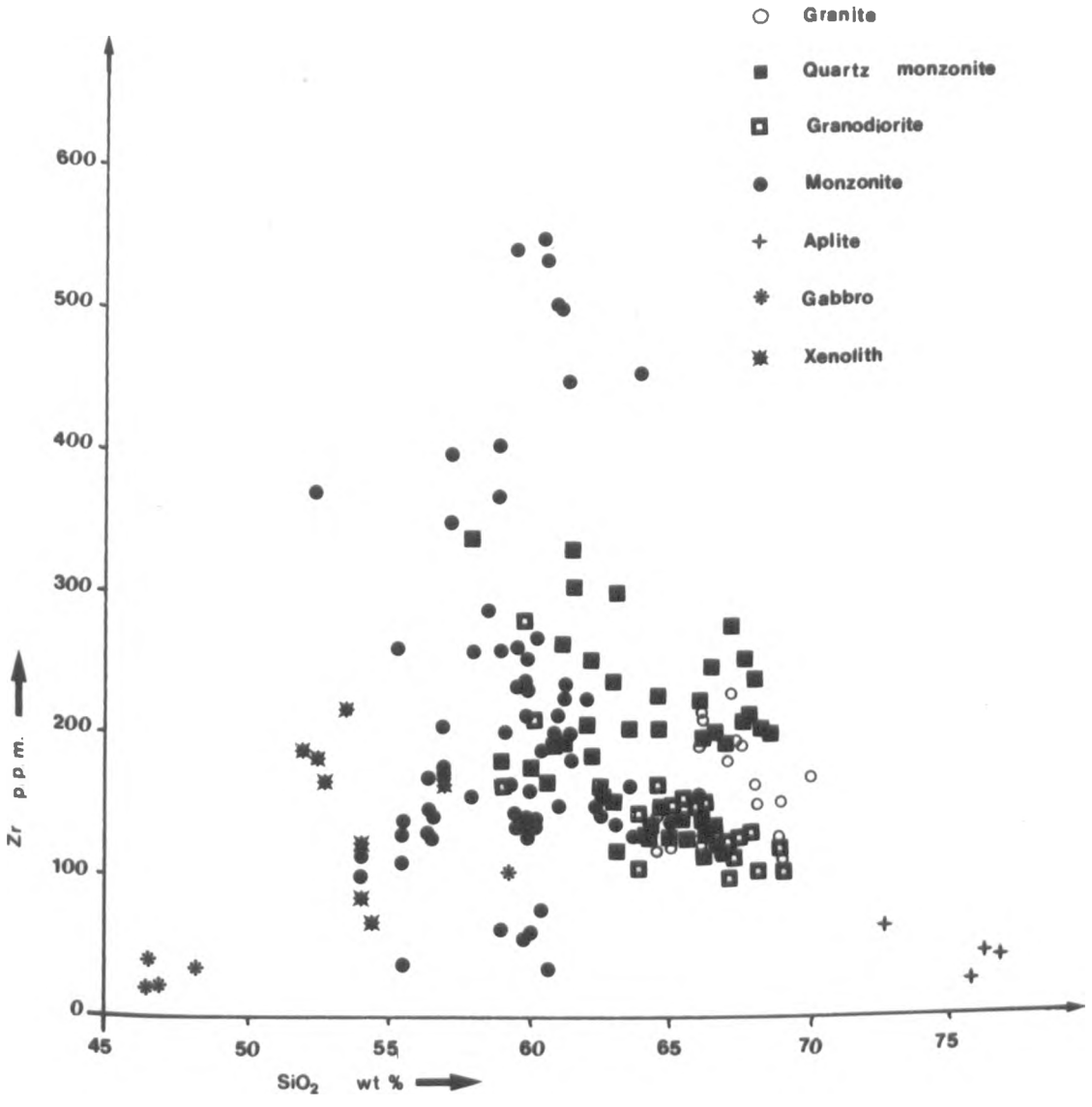
Granite
Quartz monzonite
Granodiorite
Monzonite
Aplite
Gabbro
Xenolith
600
500
400
300
200
100
0
Zr ppm.
45
50
55
60
65
70
75
SiO2 wt %

Fig. (5-1-2i)

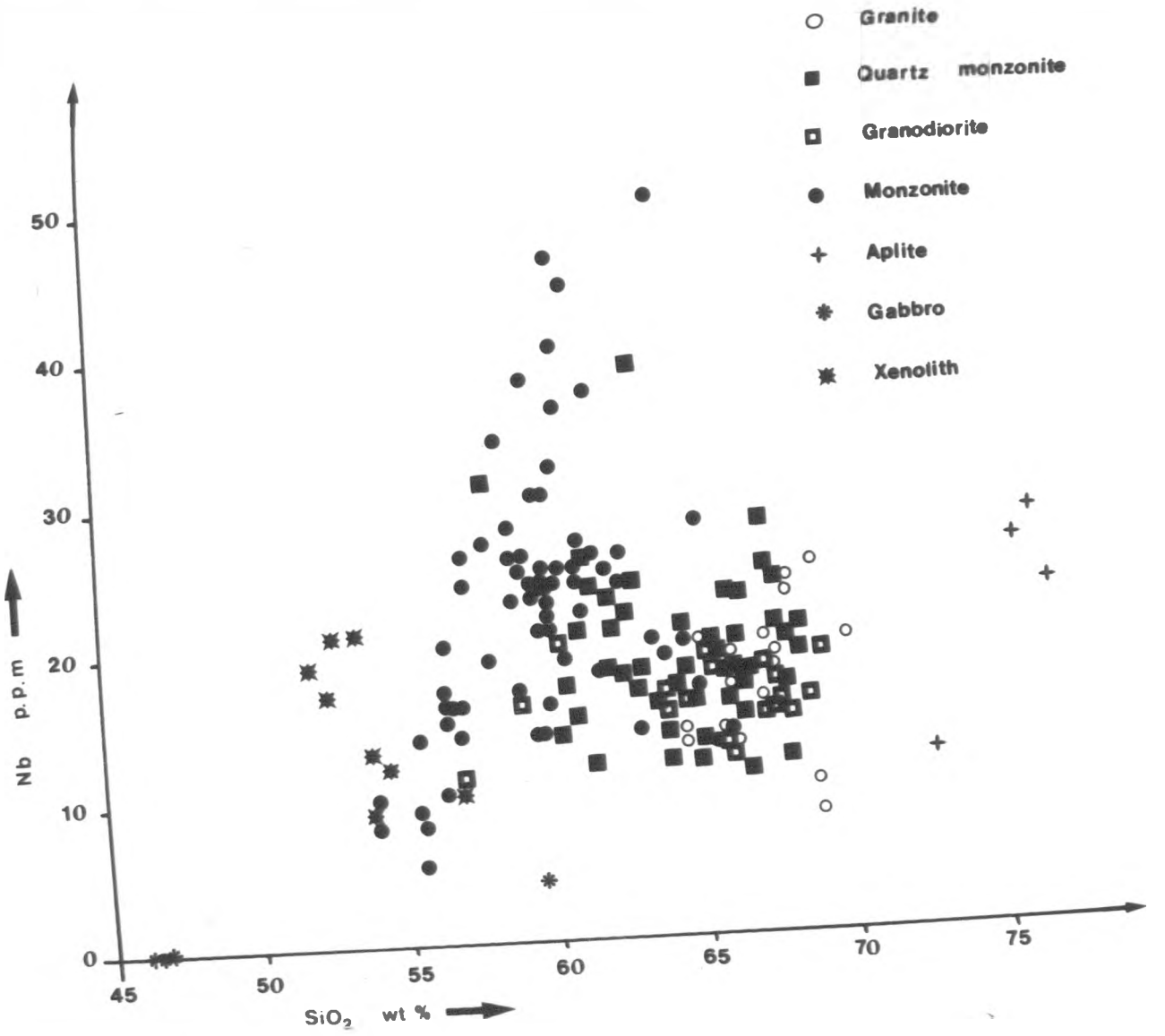
Granite
Quartz monzonite
Granodiorite
Monzonite
Aplite
Gabbro
Xenolith
Nb p.p.m
0
10
20
30
40
50
45
50
55
60
65
70
75
SiO2 wt %

Fig. (5-1-2j)

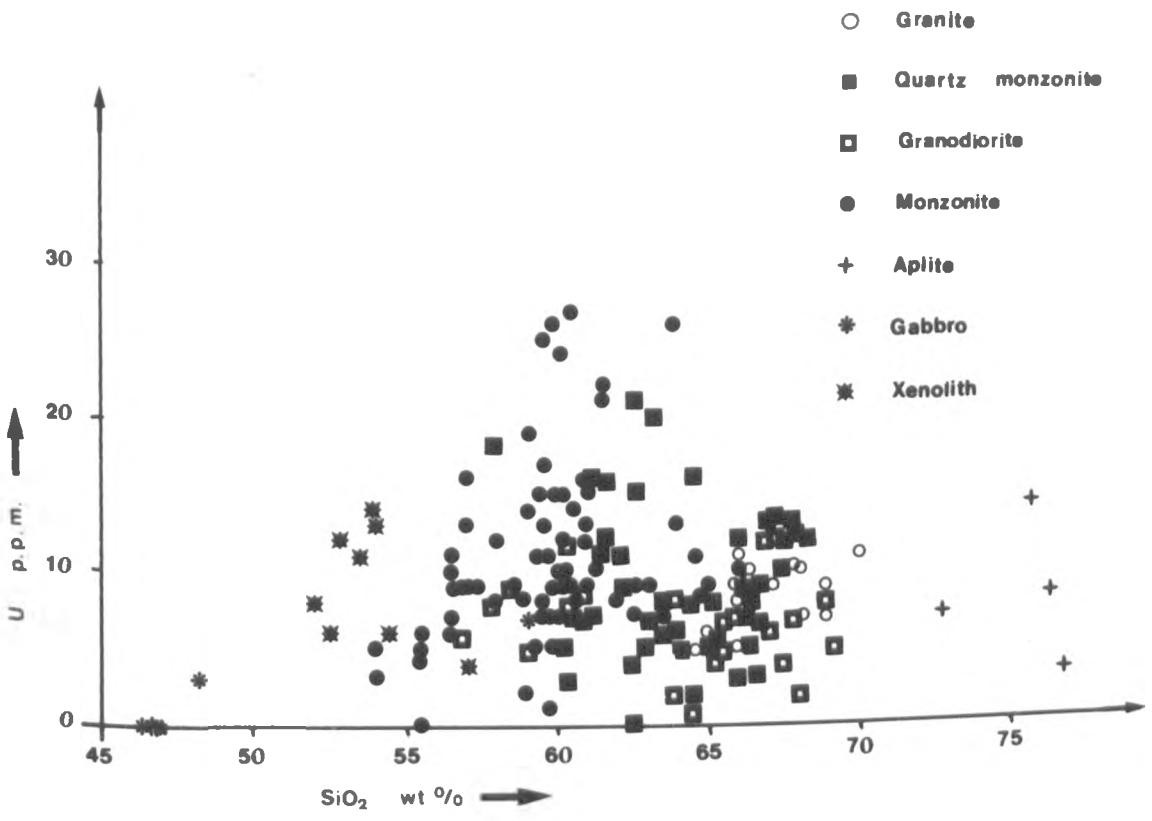
Granite
Quartz monzonite
Granodiorite
Monzonite
Aplite
Gabbro
Xenolith
30
20
10
0
U p.p.m.
45
50
55
60
65
70
75
SiO2 wt %

Fig (5-1-2k)

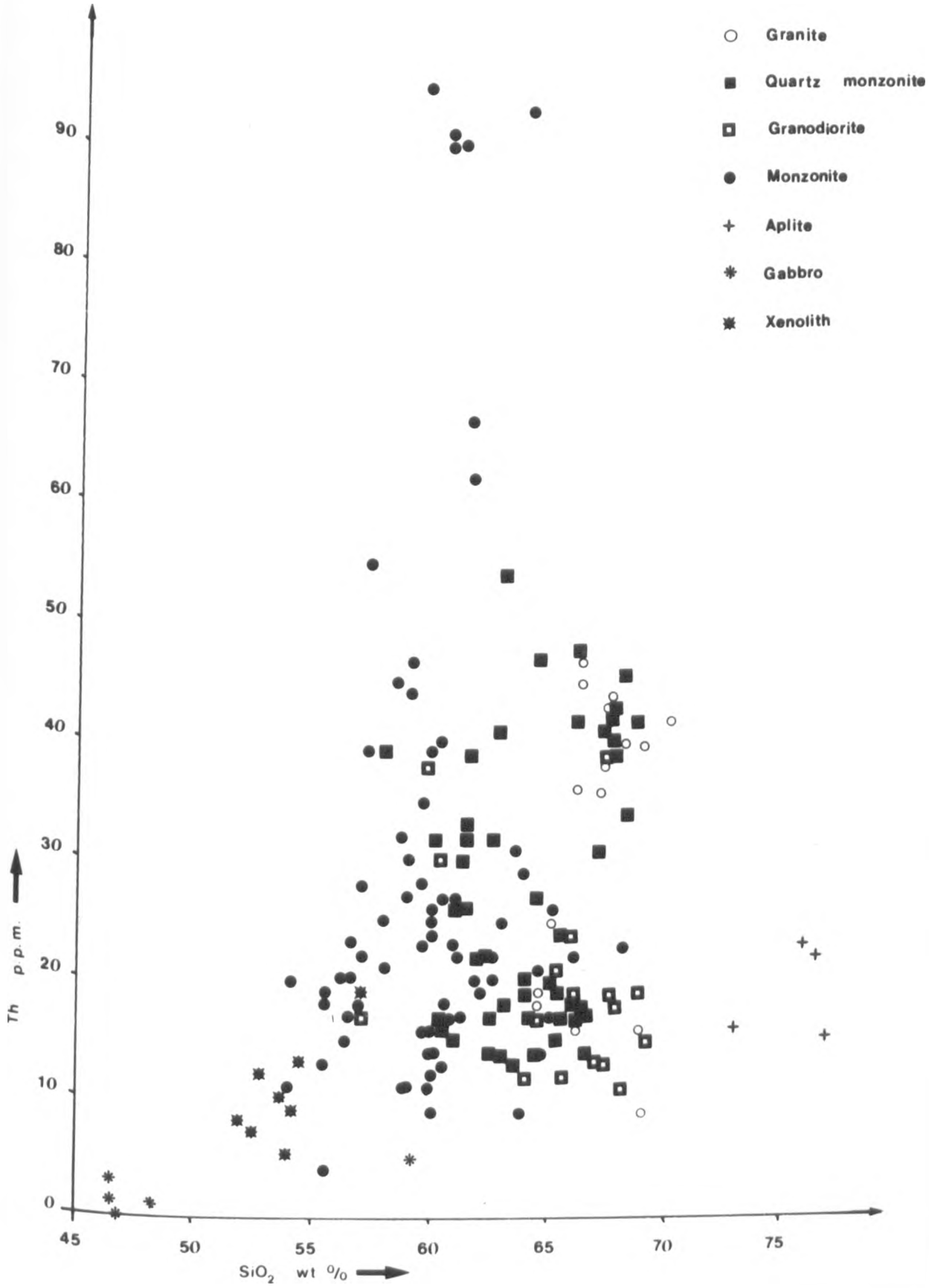
Granite
Quartz monzonite
Granodiorite
Monzonite
Aplite
Gabbro
Xenolith
90
80
70
60
50
40
30
20
10
0
Th p.p.m.
45
50
55
60
65
70
75
SiO2 wt %

Fig (5-1-21)

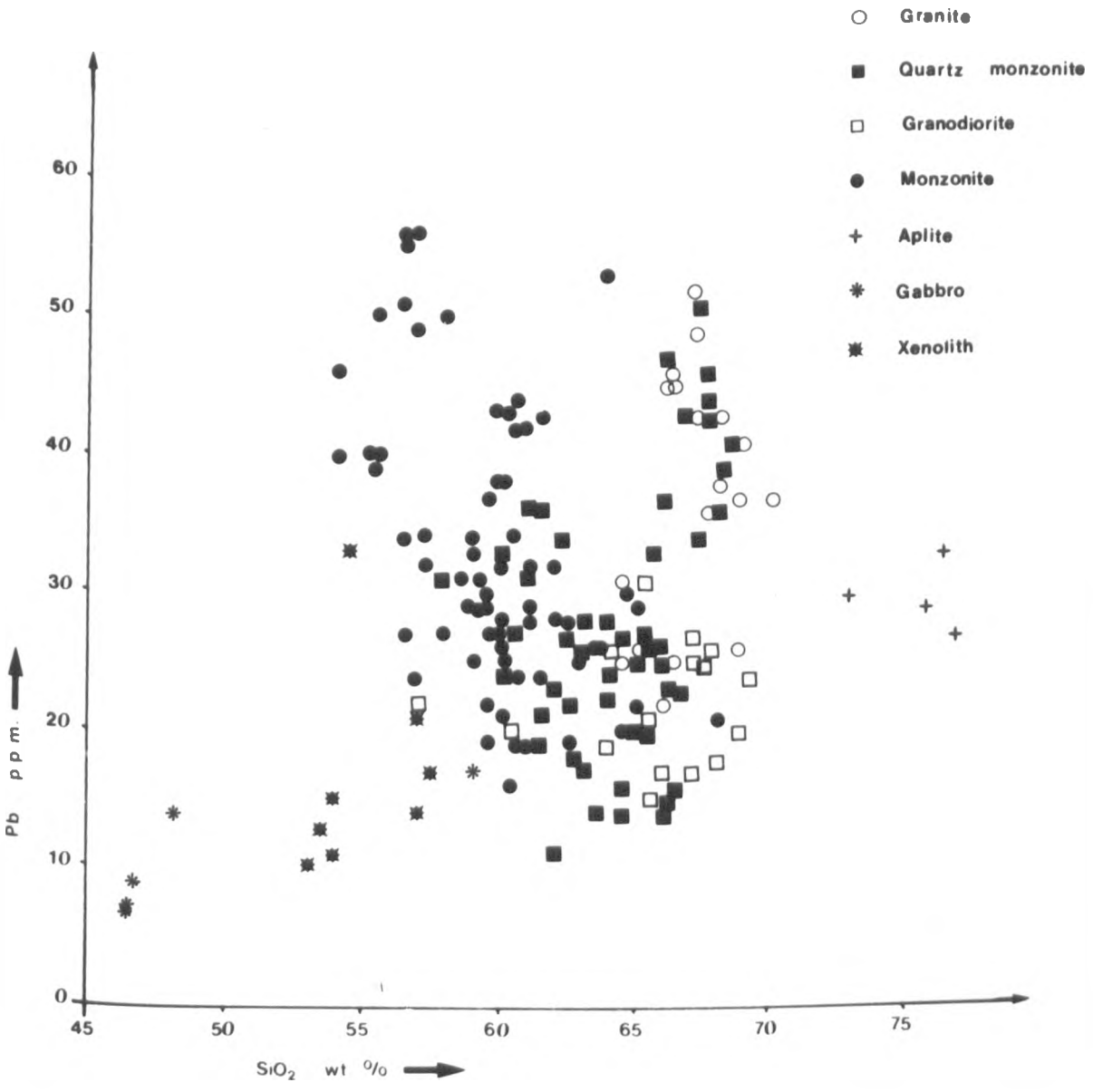
Granite
Quartz monzonite
Granodiorite
Monzonite
Aplite
Gabbro
Xenolith
Pb ppm.
60
50
40
30
20
10
0
45
50
55
60
65
70
75
SiO2 wt %

Fig (5-1-2m)

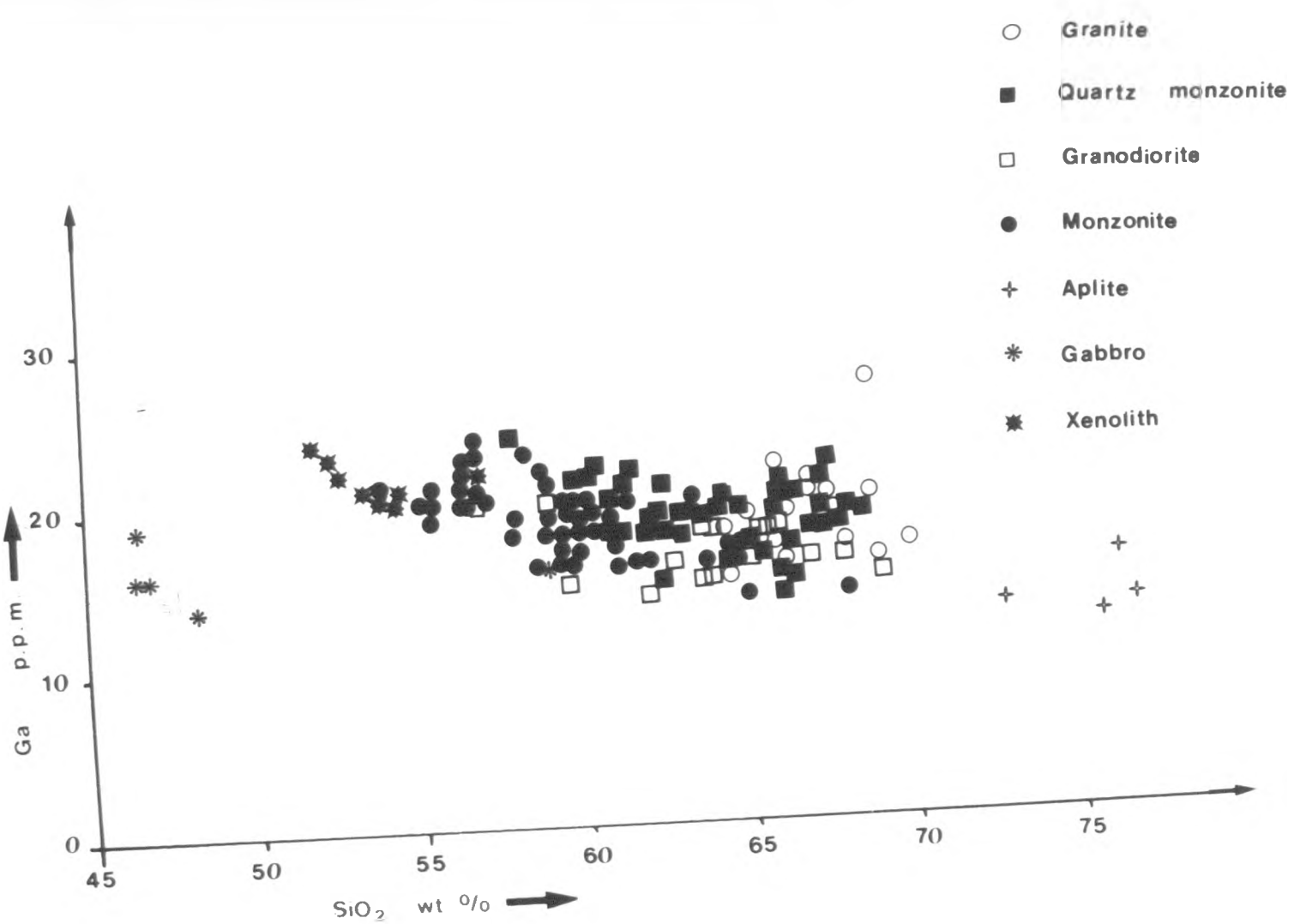
Granite
Quartz monzonite
Granodiorite
Monzonite
Aplite
Gabbro
Xenolith
30
20
10
0
Ga p.p.m
45
50
55
60
65
70
75
SiO2 wt %

Fig. (5-1-2n)

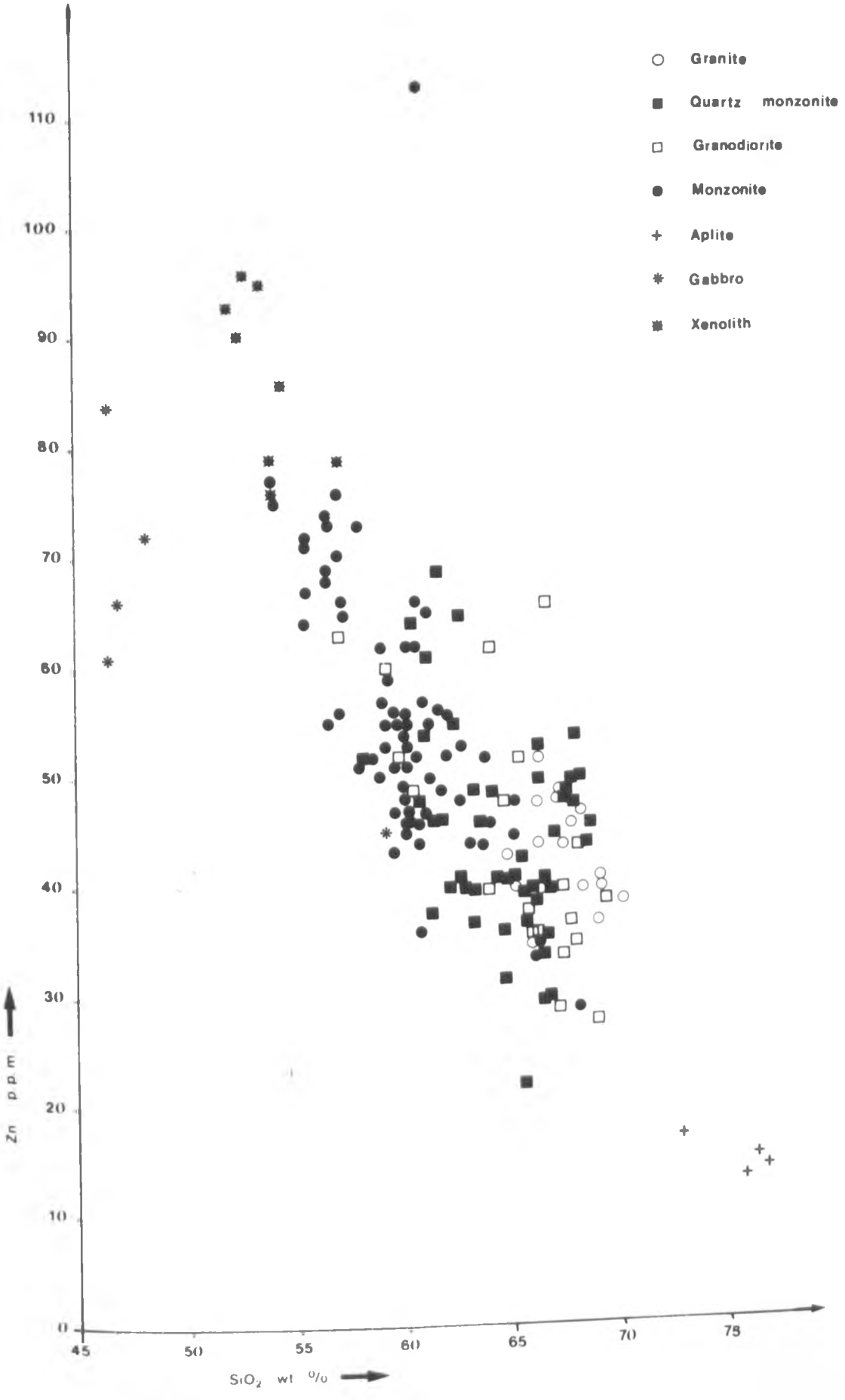
Granite
Quartz monzonite
Granodiorite
Monzonite
Aplite
Gabbro
Xenolith
110
100
90
80
70
60
50
40
30
20
10
0
Zn ppm
45
50
55
60
65
70
75
SiO2 wt %

Fig. (5-1-20)

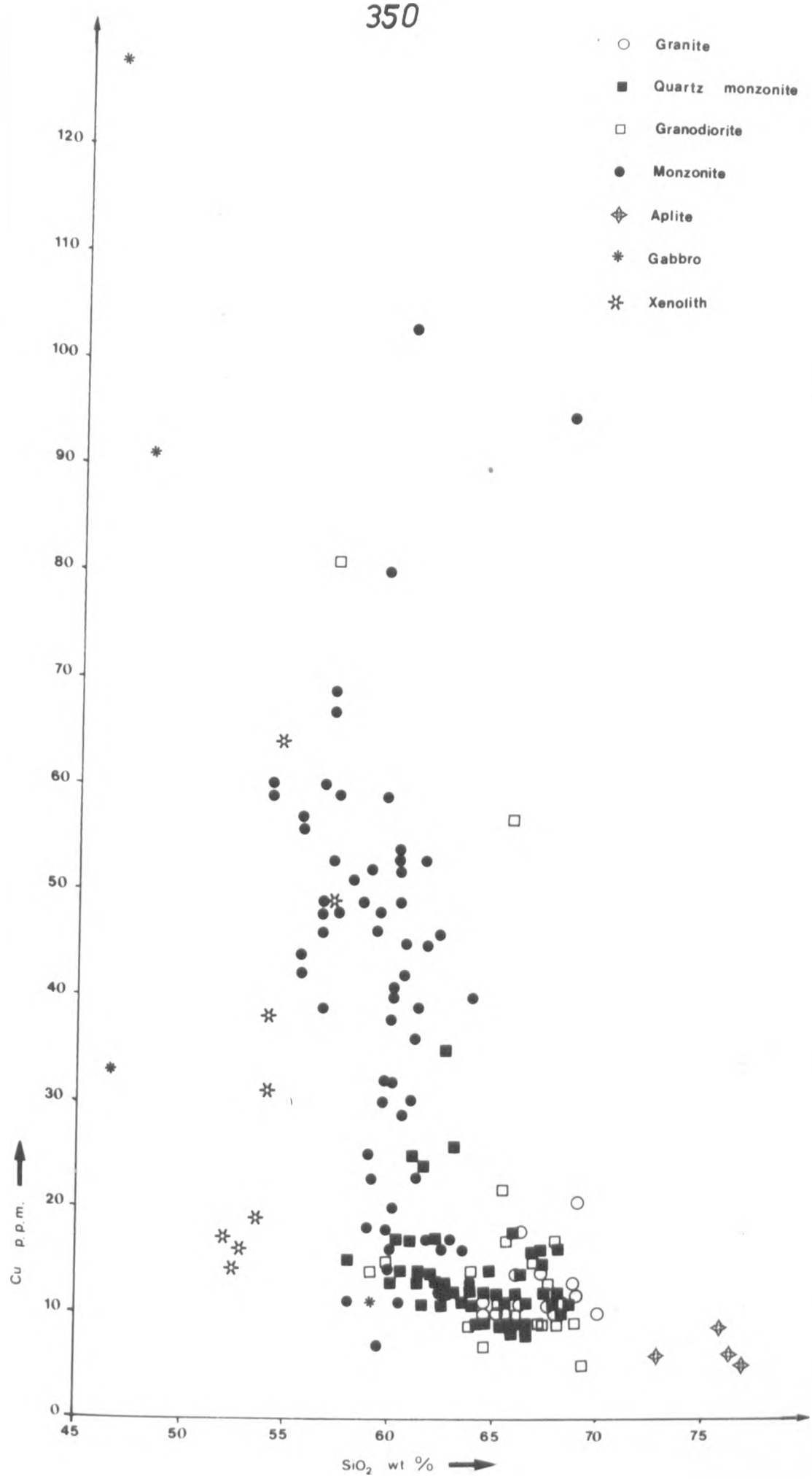
Granite
Quartz monzonite
Granodiorite
Monzonite
Aplite
Gabbro
Xenolith
120
110
100
90
80
70
60
50
40
30
20
10
0
Cu p.p.m.
45
50
55
60
65
70
75
SiO2 wt %

Fig (5-1-2p)

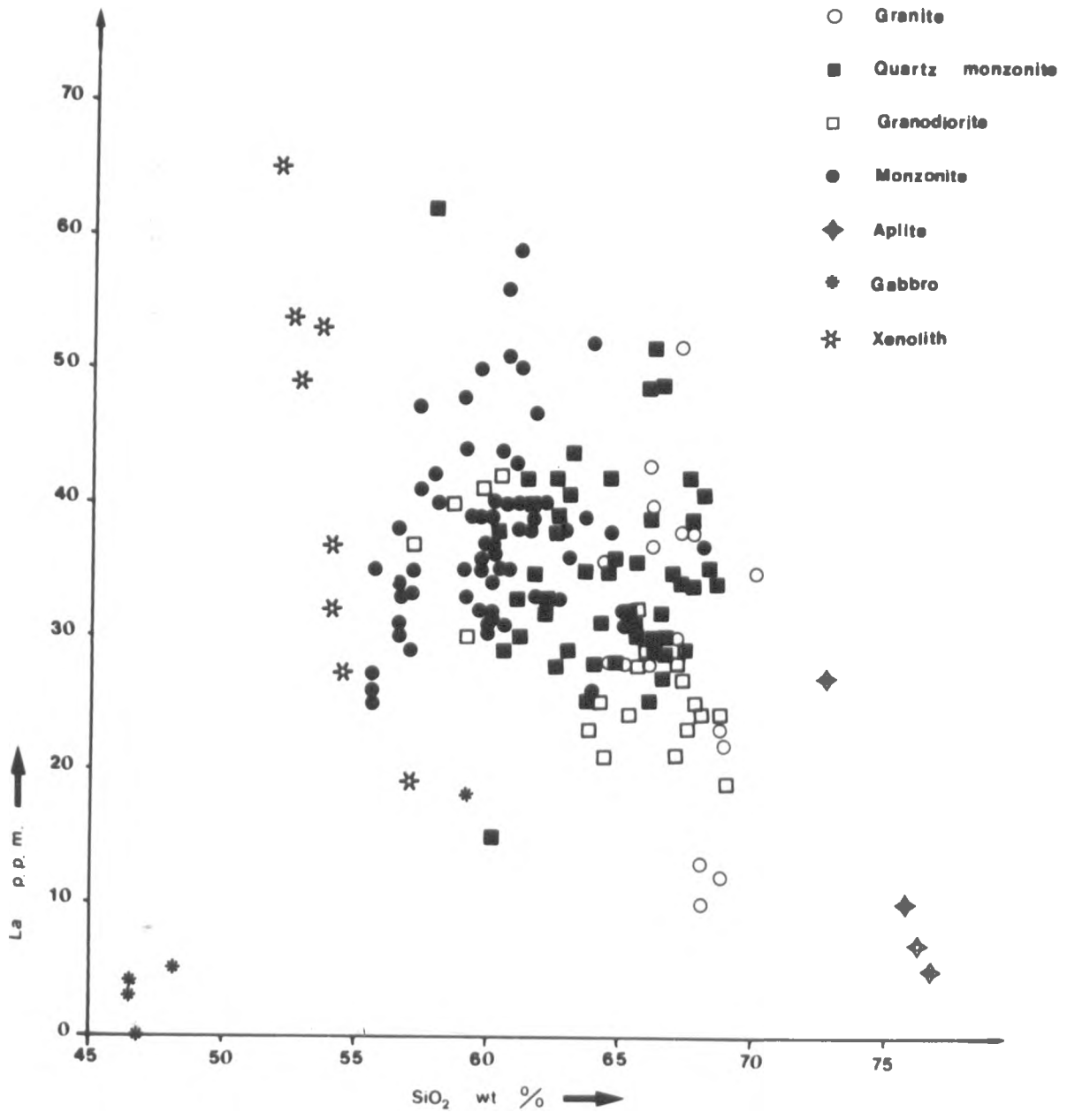
Granite
Quartz monzonite
Granodiorite
Monzonite
Aplite
Gabbro
Xenolith
70
60
50
40
30
20
10
0
La p.p.m.
45
50
55
60
65
70
75
SiO2 wt %

Fig. (5-1-2q)

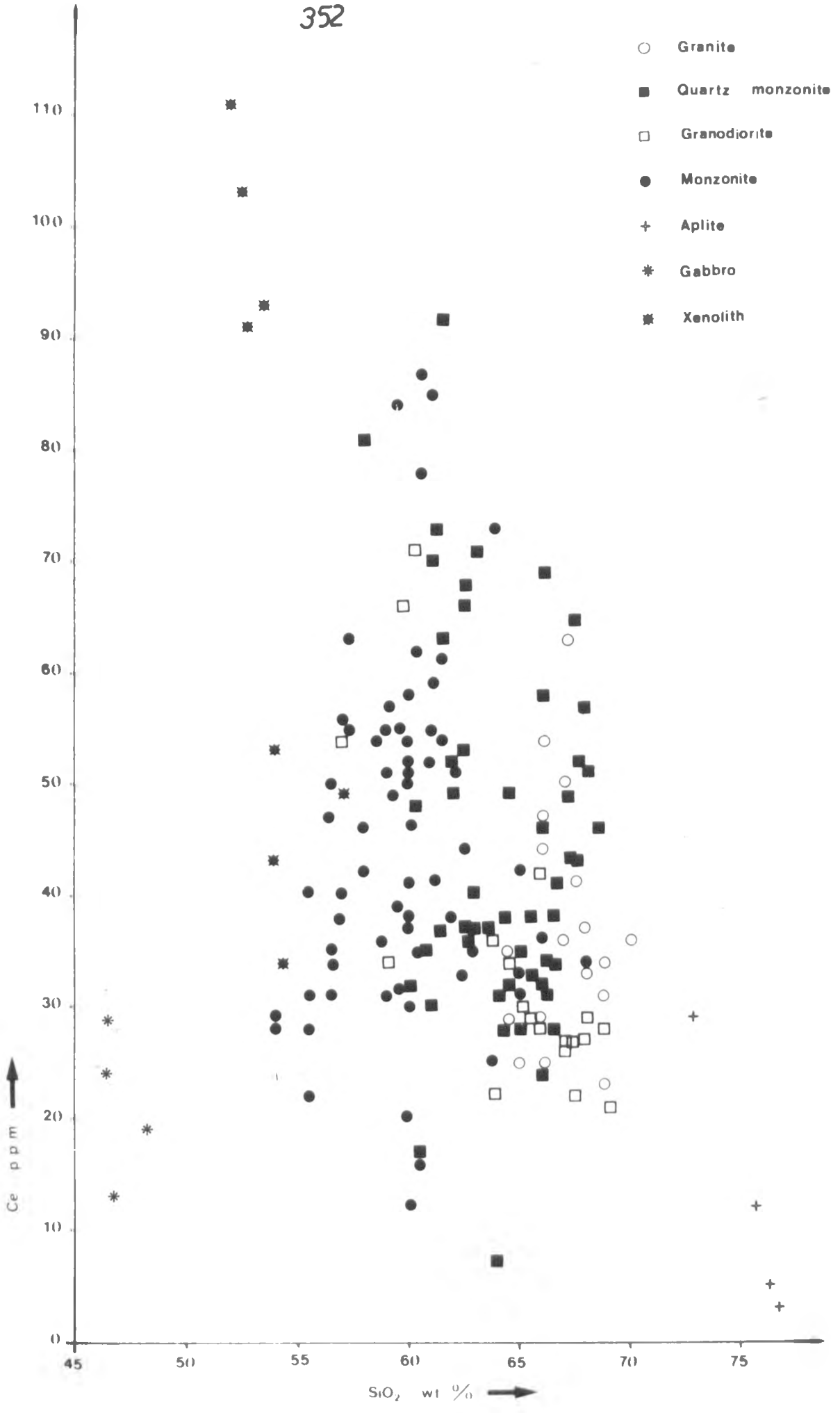
Granite
Quartz monzonite
Granodiorite
Monzonite
Aplite
Gabbro
Xenolith
110
100
90
80
70
60
50
40
30
20
10
0
Ce ppm
45
50
55
60
65
70
75
SiO2 wt %

Fig. (5-1-2r)

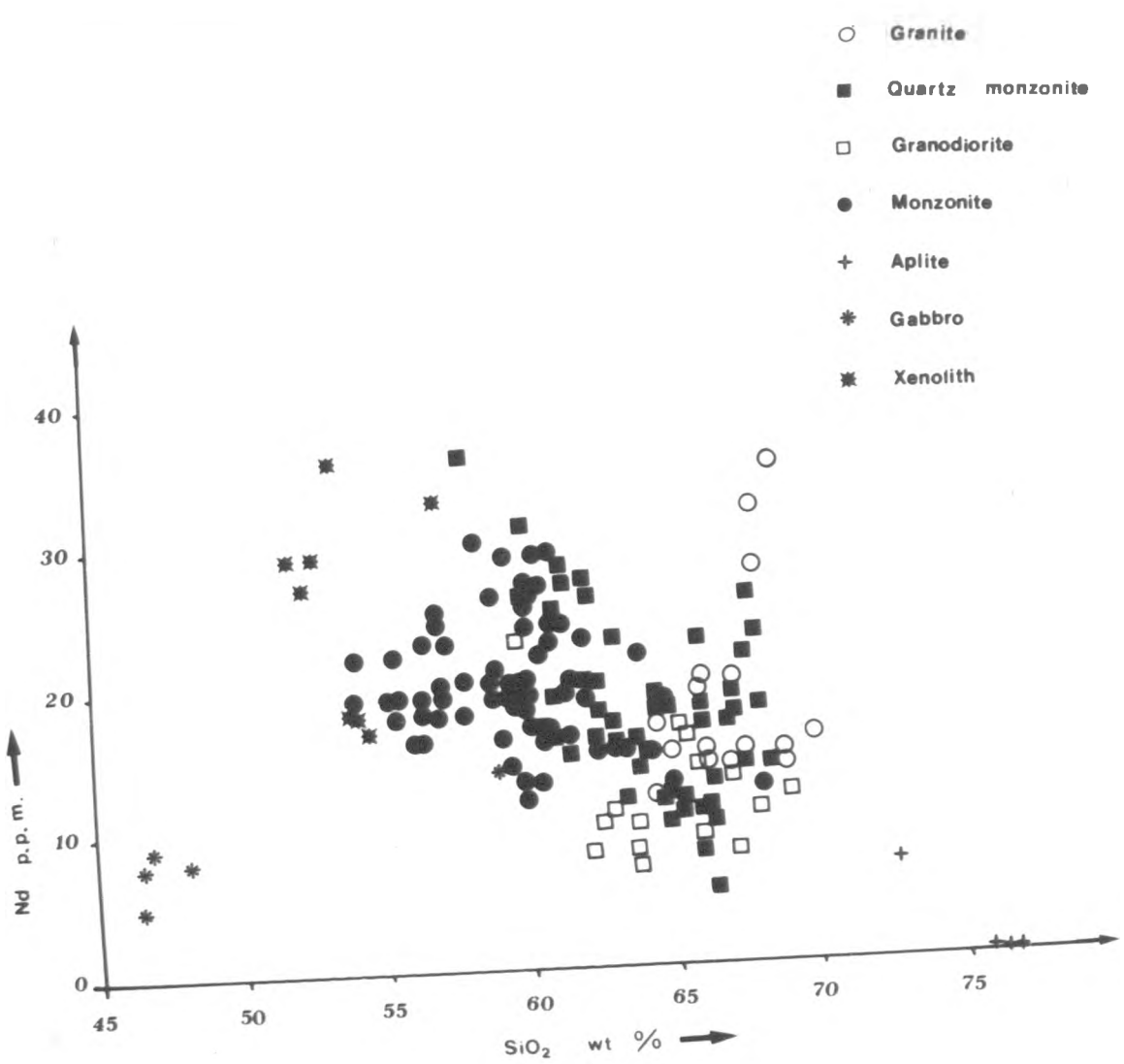
Granite
Quartz monzonite
Granodiorite
Monzonite
Aplite
Gabbro
Xenolith
40
30
20
10
0
Nd p.p.m.
45
50
55
60
65
70
75
SiO2 wt %

Fig. (5-1-2s)

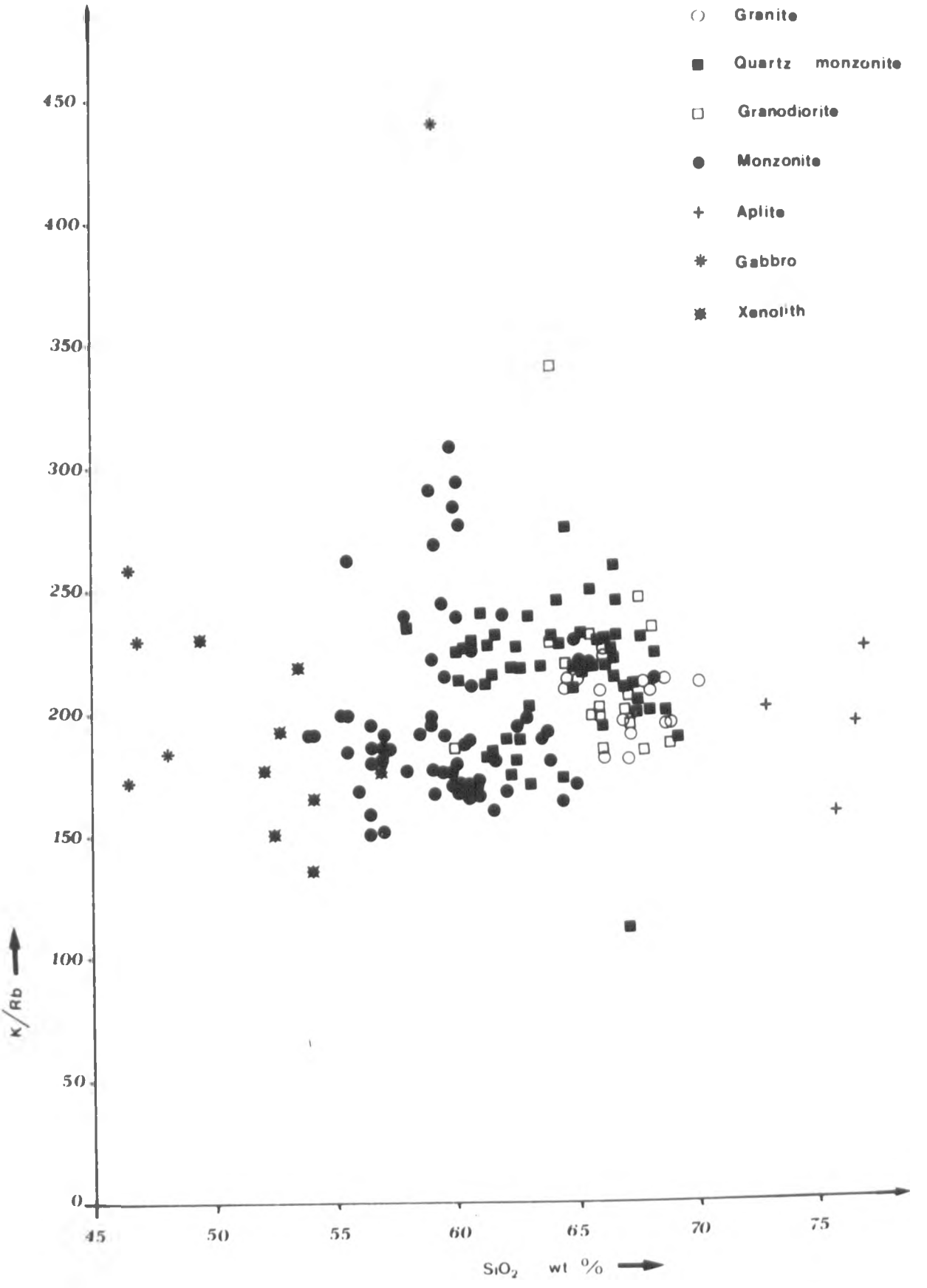
Granite
Quartz monzonite
Granodiorite
Monzonite
Aplite
Gabbro
Xenolith
450
400
350
300
250
200
150
100
50
0
K/Rb
45
50
55
60
65
70
75
SiO2 wt %

Fig. (5-1-21)

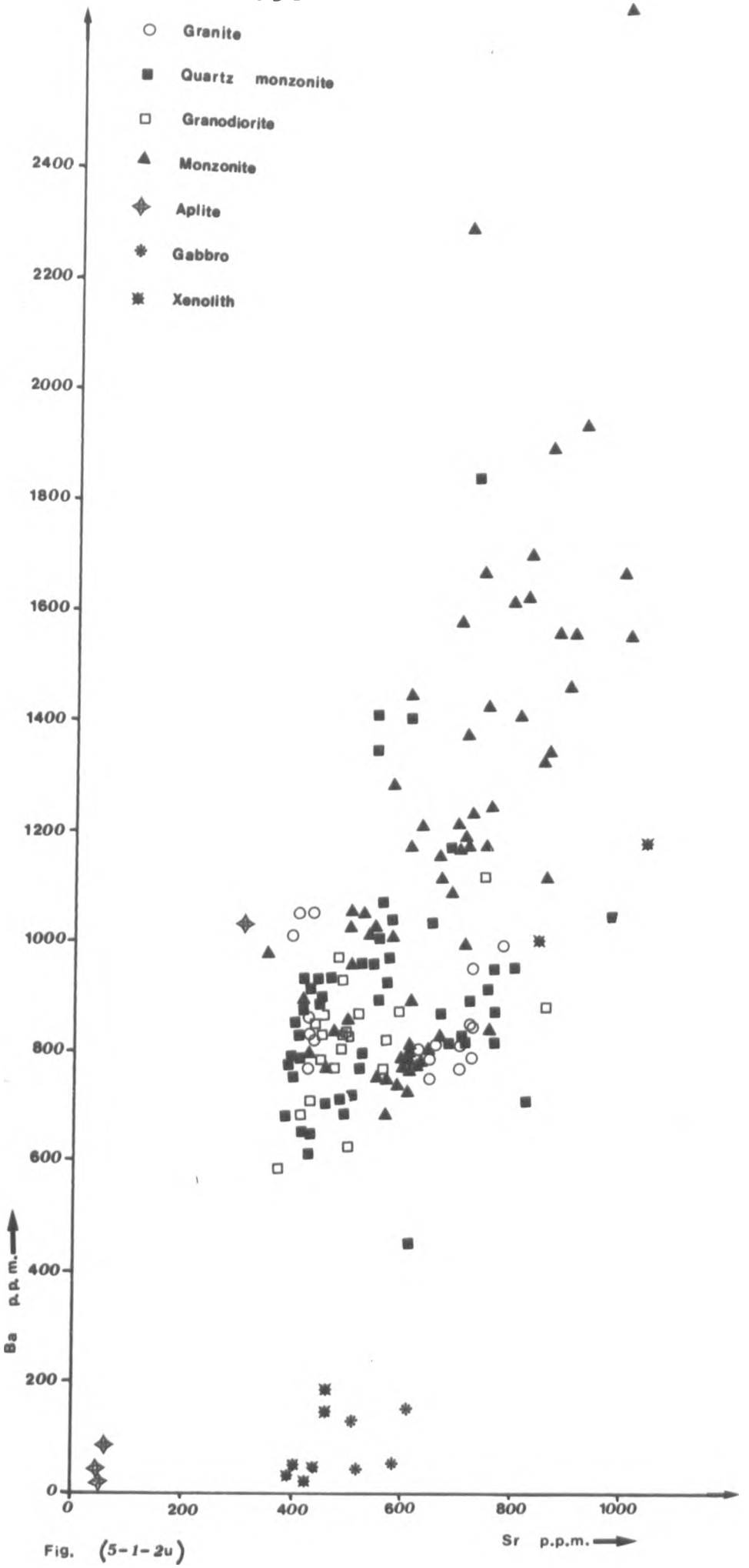
Granite
Quartz monzonite
Granodiorite
Monzonite
Aplite
Gabbro
Xenolith
2400
2200
2000
1800
1600
1400
1200
1000
800
600
400
200
0
Ba p.p.m.
0
200
400
600
800
1000
Sr p.p.m.

Fig. (5-1-2u)

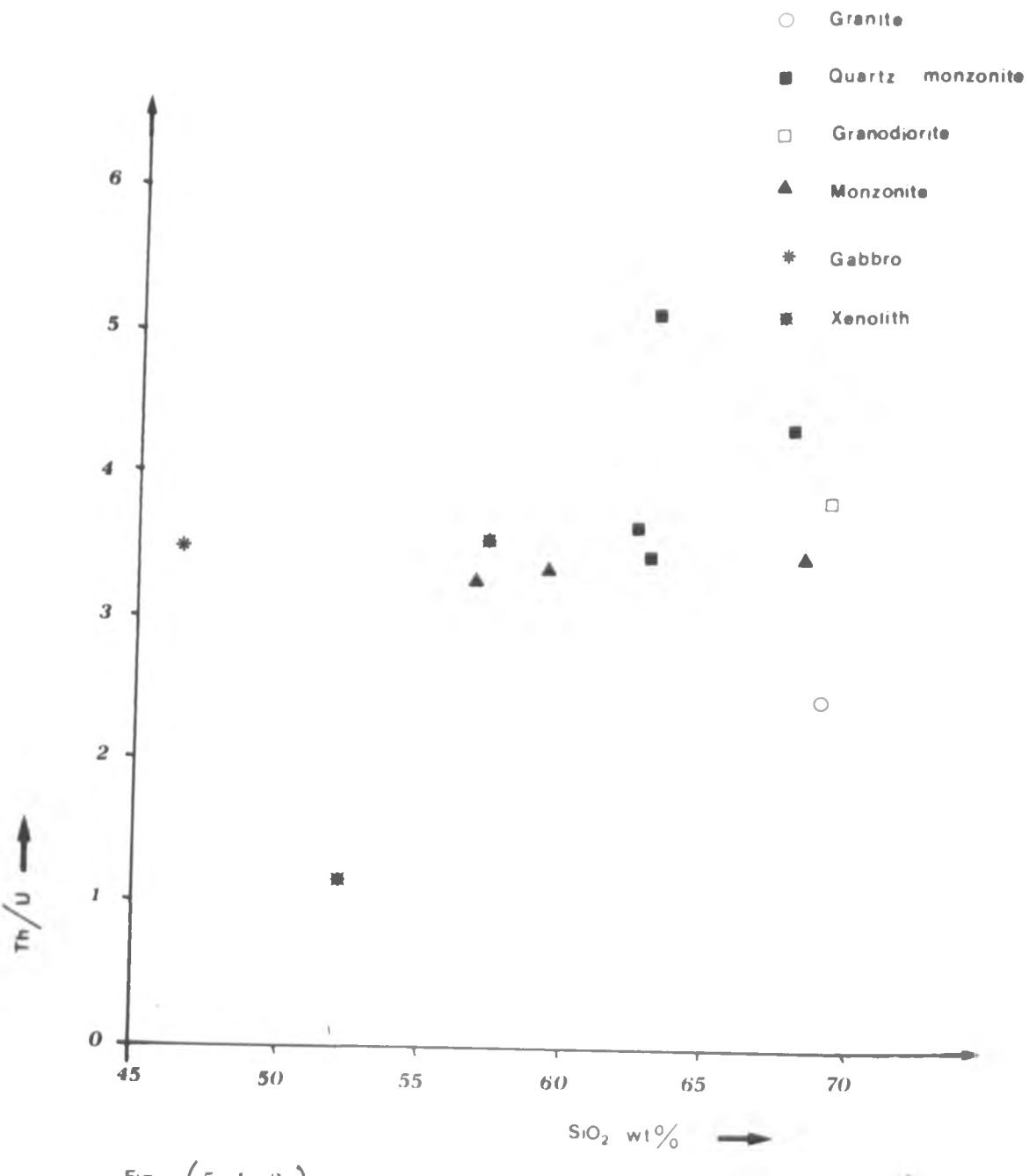
Granite
Quartz monzonite
Granodiorite
Monzonite
Gabbro
Xenolith
Th/U
SiO2 wt%
0
1
2
3
4
5
6
45
50
55
60
65
70

Fig. (5-1-2v)

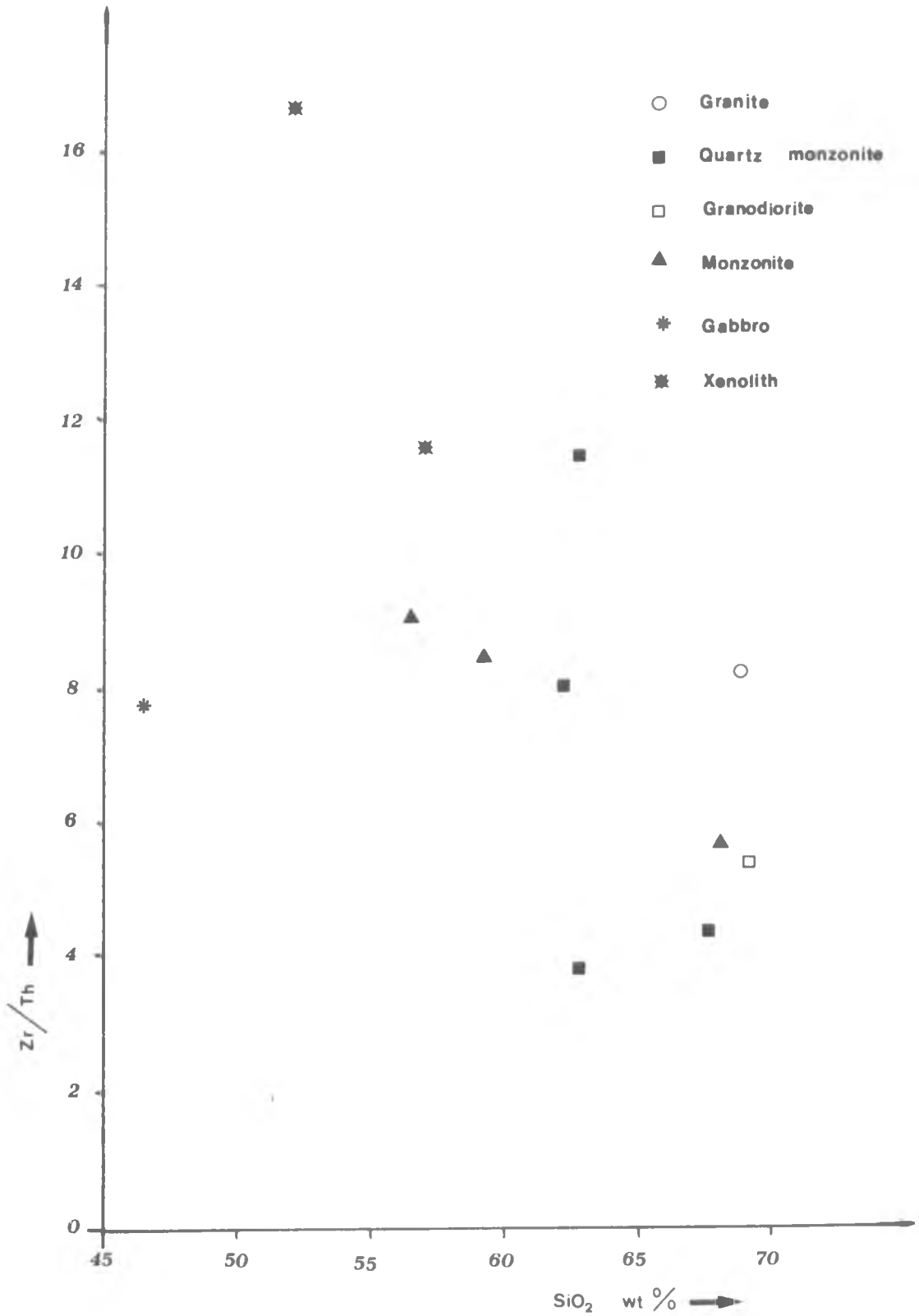
Granite
Quartz monzonite
Granodiorite
Monzonite
Gabbro
Xenolith
16
14
12
10
8
6
4
2
0
Zr/Th
45
50
55
60
65
70
SiO2 wt %

Fig. (5-1-2w)

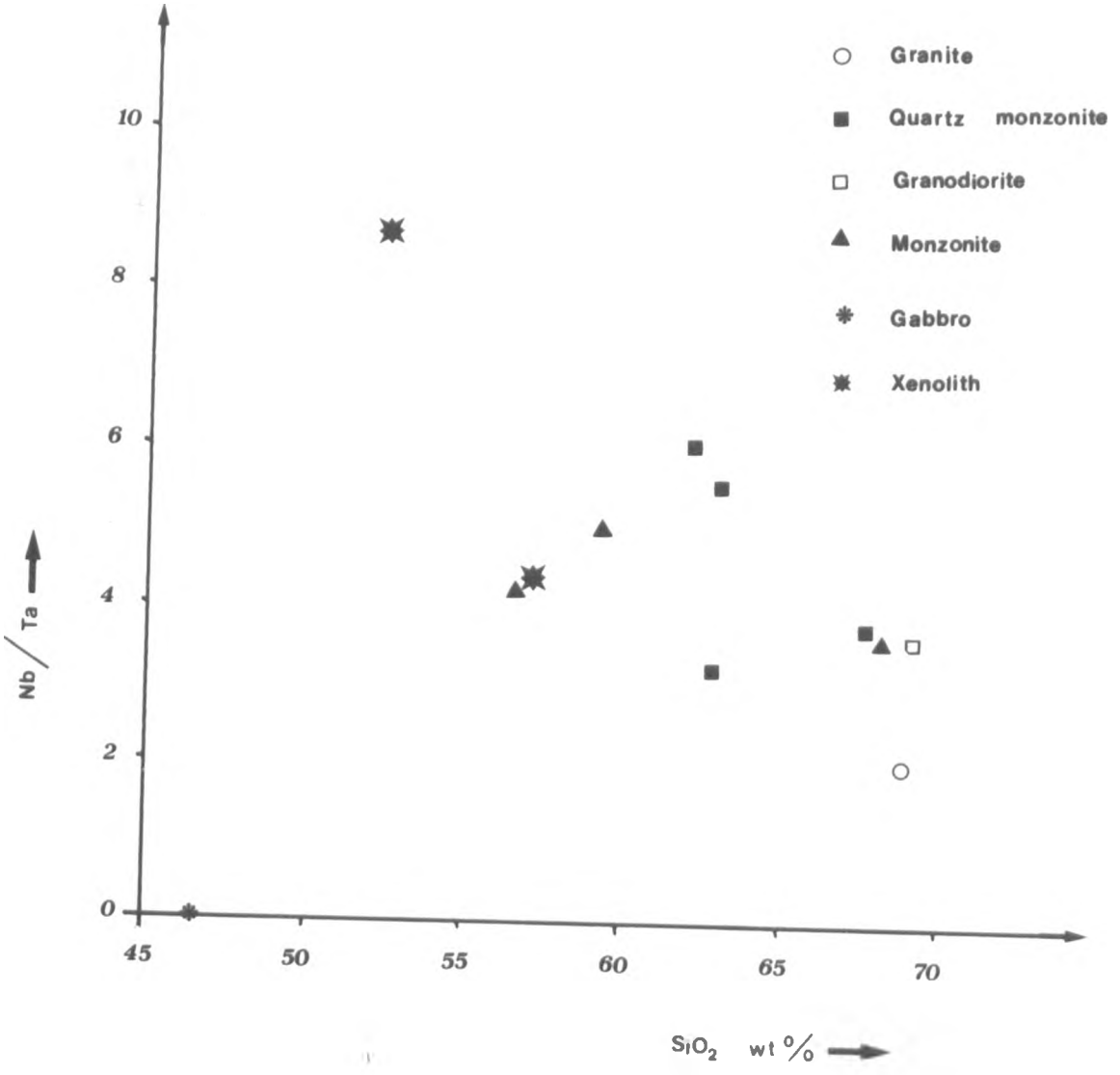
Granite
Quartz monzonite
Granodiorite
Monzonite
Gabbro
Xenolith
10
8
6
4
2
0
Nb / Ta
45
50
55
60
65
70
SiO2 wt %

Fig. (5 – 1 – 2x)

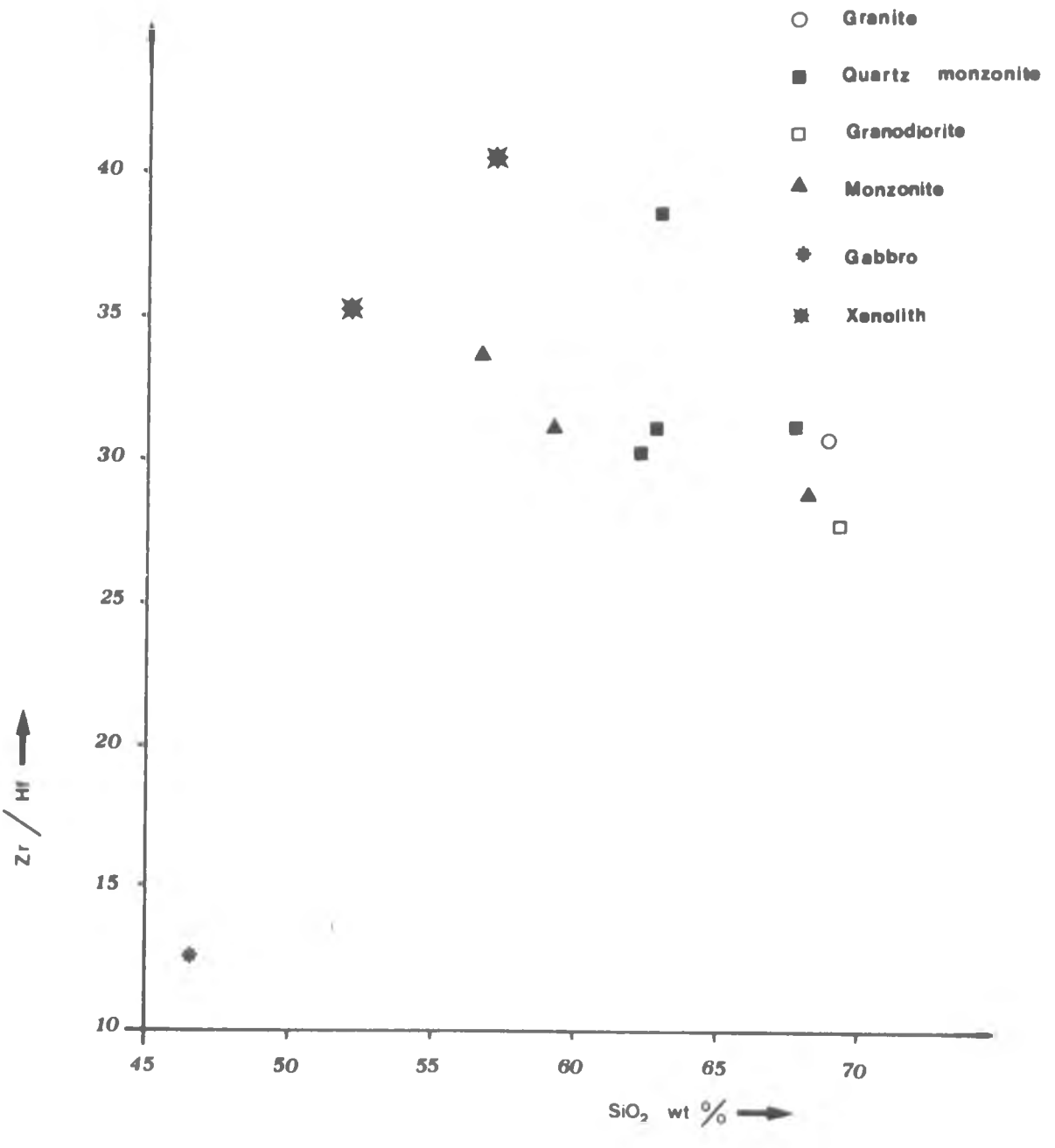
Granite
Quartz monzonite
Granodiorite
Monzonite
Gabbro
Xenolith
40
35
30
25
20
15
10
45
50
55
60
65
70
Zr / Hf
SiO2 wt %

Fig. (5-1-2y)

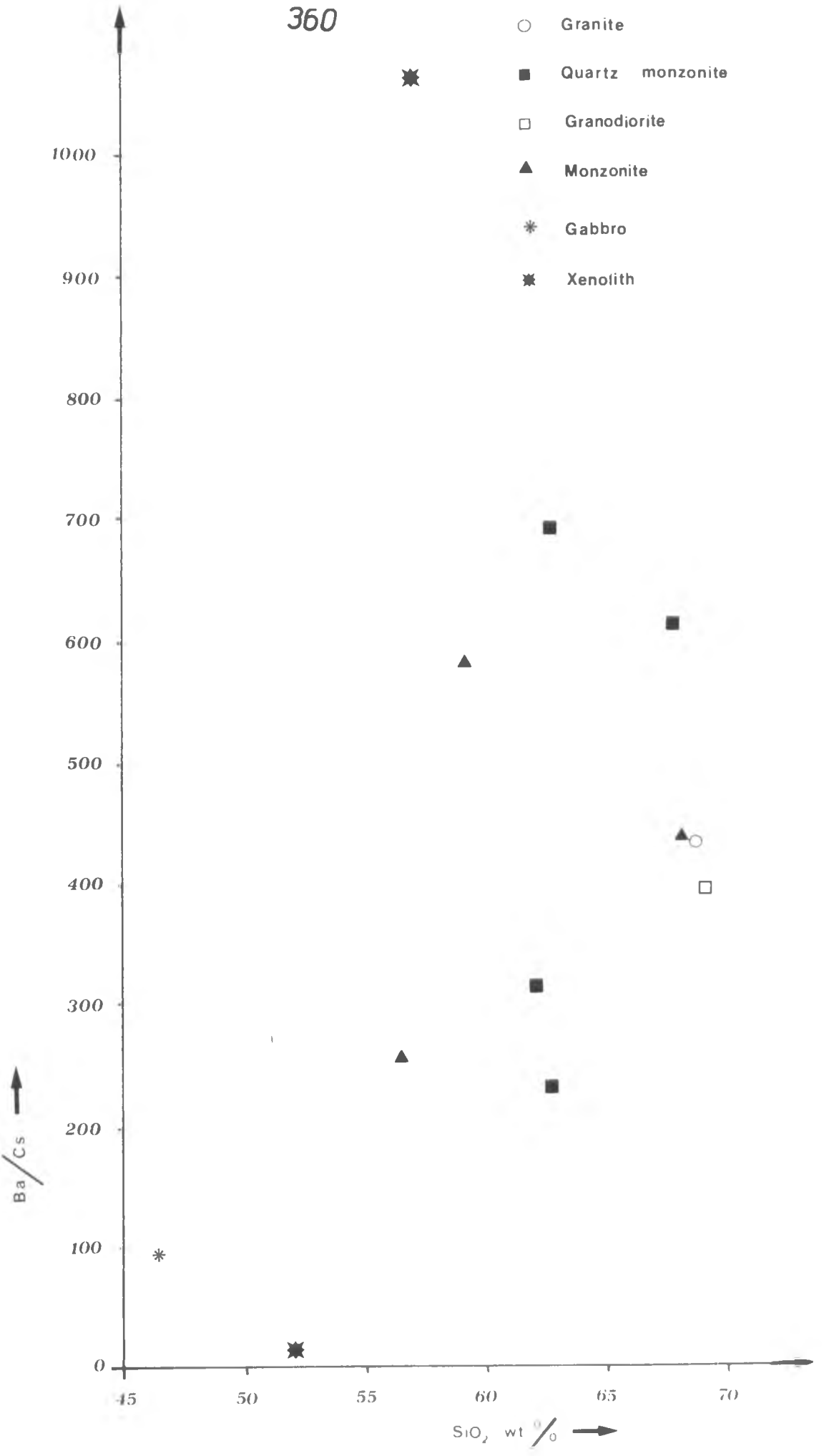
Granite
Quartz monzonite
Granodiorite
Monzonite
Gabbro
Xenolith
1000
900
800
700
600
500
400
300
200
100
0
Ba/Cs
45
50
55
60
65
70
SiO2 wt %

Fig. (5-1-22)

element	range	mean
Thorium	0 to 95 ppm	25
Lead	7 to 56 ppm	29
Gallium	12 to 24 ppm	18
Zinc	13 to 113 ppm	51
Copper	5 to 280 ppm	28

The analytical data from tables (5-1-2a) to (5-1-2g) have been plotted against parameters which are normally used to display variation in trace element concentration with increasing fractionation (weight per cent SiO_2, differentiation index of Thornton and Tuttle, and modified Larsen index). In addition to these diagrams, two additional plots were done: 1) rubidium is plotted against TiO_2 to reveal the effects of the early crystallising phases; 2) barium is plotted against strontium to ascertain whether these two elements behave coherently and enter the crystal lattice of one major crystallising phase (plagioclase feldspar) or several (both the plagioclase and alkali feldspar).

The data from table (5-1-2h) (except for Zr, Nb and Ba (which were tabulated in tables, 5-1-2a to 5-1-5g) are plotted in figures (5-1-2v) to (5-1-2z). In the above figures the ratios Th/U, Zr/Th, Nb/Ta, Zr/Hf, Ba/Cs are thought to behave coherently and they are plotted against weight per cent SiO_2.

It can be seen from the table (5-1-2h) that the average of all the trace elements of the 'intermediate' rock group are less than the corresponding average for

monzonite. The variation of trace elements in the individual rock groups are as follows: in the 'intermediate' group there is an increase in Rb, Sr, Nd, Th and Pb content from quartz monzonite and granodiorite to the granite, but Ba, Y, Zn and Cu decreases, while the behaviour of La, Ce, Zr, Nb, U and Ga indicate a decrease from the quartz monzonite through the granite to the granodiorite.

In the 'basic' rock group the La, Ce, Nd, Ga and Zn contents increase from the monzonite to the dioritic xenoliths and then decrease to the gabbro, but for Sr, Ba and Cu the opposite can be seen, while the Rb, Y, Zr, Nb, U, Th and Pb contents increase with increasing differentiation.

5-1-3 Discussion and conclusion.

The concentration of rubidium increases from a few parts per million to 300 ppm (fig. 5-1-2a). The highest values however are within the monzonite and the overall content does seem to decrease from these values in the monzonite through to the 'intermediate' rock types. If we consult the diagram showing the variation in K_2O within the complex (fig. 4-1-2k) it seems to be a mirror image of the rubidium values. The increase in K_2O was interpreted as being due to an increase in alkali feldspar content, therefore as a check, the K/Rb ratio was plotted (fig.5-1-2t) to determine whether rubidium was substituting for potassium in

alkali feldspar and biotite. This ratio remains constant at values between 200 and 250. It is therefore a reasonable conclusion to suggest that the distribution of rubidium within the complex is primarily a function of the amount of alkali feldspar present in the rock and secondarily biotite. There may also be a small increment to be added for amphibole, as this phase also contains potassium.

An attempt at correlating elements which are concentrated into the early crystallising phase against those concentrated into the late crystallising phases was made by plotting rubidium against weight per cent TiO_2 (fig. 5-1-2c). There is a strong negative correlation between these elements, indicating their different behaviour. Titanium is present in ferromagnesian minerals within the gabbros and in the accessory mineral, sphene, in the granitoids.

When rubidium is plotted against the differentiation index (Thornton and Tuttle, fig. 5-1-2b), there does seem to be some separation between the monzonite and the 'intermediate' group of rocks. Therefore there does seem to be some justification for two groups of compositions within the granitoids.

These various diagrams involving the behaviour of rubidium are a little different to those of Atherton et al (1979) for the Coastal Batholith of central Peru, where they note a decrease in K/Rb ratio with increasing fractionation. Close examination of their data for individual (complexes

e.g. S.R. Nepena does however show little difference in the K/Rb ratio within the granitoids.

The range of strontium concentration is from $\sim$50 up to $>$ 1000 ppm. When strontium is plotted against any of the parameters which indicate differentiation, several factors are brought out: 1) the gabbro and dioritic xenoliths plot in small fields as two discrete groups; 2) the granitoid rocks show a strong negative correlation of Sr against any of the differentiation indices; 3) no overlap exists between either the gabbro and the diorite or diorite and monzonite.

Strontium can either replace calcium in silicates by the nature of its size or be captured by potassium minerals because of its higher charge (Mason, 1966). Reference to figure (4-1-2h) (CaO vs SiO_2) shows that calcium has the highest concentration in the gabbroic rocks, followed by the diorites, where the calcium is present in basic plagioclase, clinopyroxene and amphibole. Therefore there is a lack of coherence between the behaviour of calcium and strontium. Indeed, strontium may enter all the calcium bearing minerals in variable amounts but obviously it must also be captured by alkali feldspar to explain the higher concentration in the monzonitic rocks. An alternative explanation may be that strontium more easily enters the structure of plagioclase feldspars of intermediate anorthite contents, rather than more basic compositions. There have been no reports of such behaviour therefore it appears more plausible to interpret the strontium data in terms of

substitution for both calcium and potassium in the rocks of granitoid composition. There is also a possibility of the small influence of sphene and apatite to be added to these conclusions.

The aplites appear to have very small concentrations of strontium, therefore this observation tends to support the suggestion that this element is captured by the earlier crystallising potassium feldspar and plagioclase in the monzonites thus depleting any remaining liquid in this element.

The behaviour of barium is very well demonstrated in rocks from the Serres-Drama complex. Both the gabbro and the diorites have concentrations which are below 200 ppm, whereas the monzonite has values up to $>$ 2500 ppm. This behaviour strongly suggests that barium, because of its greater size, does not replace calcium but substitutes for potassium in both potassium feldspar and biotite, particularly the former.

This factor is well brought out by sample No.137, a monzonite, which contains 2686 ppm barium. In addition to this large concentration of barium, this sample also has 267 ppm rubidium and 7.73% K_2O. Both these values are the highest in the complex. Therefore there is again coherent behaviour between a major element (potassium) and a trace element (barium).

All these trace elements discussed to date (Rb, Sr, and Ba) are very high compared to the Guadalcanal complex recently described by Chivas et al (1982), where the Rb

contents were $<$ 70 ppm, Sr $<$ 700 ppm and Ba $<$ 800 ppm. The Guadalcanal complex is calc-alkaline, and apart from aplite dykes the K_2O content $<$ 3.00%. These factors emphasise the difference between calc-alkaline plutonic complexes, where little or no sialic basement is present as in the oceanic island arcs and the ensialic calc-alkaline complexes, such as the Serres-Drama complex.

In order to reveal any differences or similarities between the behaviour of barium and strontium in the Serres-Drama complex, the two elements were plotted against each other (fig.5-1-2u). The diagram emphasises the comments made previously but in addition shows that both these elements did not enter the early crystallising phases but entered the feldspar minerals by admittance and capture. These elements were removed by the crystallising feldspars in the granitoids which left a residual liquid (aplite) depleted in both barium and strontium.

The light rare earth elements (L.R.E.E.) lanthanum, cerium and neodymium all show the same dispersions (figs. 5-1-2q , 5-1-2r, and 5-1-2s) in that concentrations of all three elements are lowest in the gabbros and highest in a group of dioritic xenoliths. From these diorites the concentration decreases through the granitoids to the aplites. These diagrams indicate that the L.R.E.E. have different behaviour compared to Rb, Sr and Ba in the Serres-Drama complex.

Little work has been done on the R.E.E. abundances in minerals from rocks of calc-alkaline affinity. Recently

Fourcade (in Hart and Allegre, 1980) has reported the R.E.E. concentration of minerals from a tonalite and monzo-granite from the Querigut massif, French Pyrenees. Fourcade noted that the abundance of R.E.E. in minerals from the tonalite decreased as follows: sphene > apatite > hornblende > plagioclase > biotites; and in the monzonite, apatite > biotite > plagioclase > potassium feldspar. Therefore the accessory minerals contain quite a proportion of the total R.E.E. content of the rocks.

It is obvious from the observations of Fourcade that the feldspars do not concentrate the R.E.E. but the accessory phases and hornblende are much more important. If we consider the modal analyses of rocks of the Serres-Drama complex (table 2-1-1a) the accessory phases are always below about 3% of the content of the rocks. They have, however, two orders, of magnitude greater concentration of R.E.E. than the feldspars, hence they must contribute quite a proportion to the total R.E.E. content of the rocks from the Serres-Drama complex. The other mineral which contains quite a proportion of R.E.E. is hornblende which is high in the dioritic rocks. Amphiboles from more alkaline rocks (Rowbotham, pers.comm.) have up to 104 ppm La, 165 ppm Ce, and 56 ppm Nd, therefore these minerals can take up quite large amounts of these elements.

It is possible to put forward a tentative conclusion that in the Serres-Drama complex the L.R.E.E. are concentrated in the accessory phases of apatite and sphene and also in the major phase hornblende.

It was concluded in the chapter on major element chemistry that there was no transfer of elements between host rock and the enclosed xenoliths. This conclusion is reinforced by the observation of the behaviour of the L.R.E.E. where the concentration of these elements are higher in the xenoliths (e.g. samples 6A1, 6A2, 6B1, 6B2) than in the host rocks (6A3, 6B3).

The concentration of zirconium varies between $<$ 50 to $>$ 500 ppm (fig. 5-1-2i) and is very low in the gabbros and the aplite. There is however a very wide dispersion within the granitoids, particularly the monzonite ($<$ 50 $>$ 500 ppm) which could presumably reflect the presence of the accessory phase zircon. The aplites have very small amounts of zircon present (Chapter Two) which accounts for the very low concentration of zirconium in the rock It is therefore concluded that zirconium is present primarily in the accessory phase zircon.

In contrast to the behaviour of zirconium the niobium (fig. 5-1-2j) rises from zero concentration in the gabbros to reach the highest values in the monzonites, although there is a very wide dispersion. The rest of the granitoids have some dispersion but there is no decrease in the aplites as for zirconium. Data for niobuim from calc-alkaline granitoid rocks in Wedepohl (1978) indicate the same concentration as those for the Serres-Drama complex. The dispersion of Nb values is again reminiscent of the behaviour of an accessory phase. Sphene is a likely host for Nb as it is possible to substitute for Ti in the crystal lattice of this mineral. Another

mineral which often acts on the host for Nb is ilmenite, again Nb replacing Ti, but there is no ilmenite present in the Serres-Drama complex. In contrast silicates have much smaller concentrations of this element, therefore it can be concluded that niobium is concentrated into the accessory phase sphene.

Yttrium varies between ~ 5 ppm and 35 ppm (fig. 5-1-2h) which is a normal range of values for calc-alkaline rocks. The behaviour of yttrium in magmatic rocks is similar to the R.E.E. (Mason, 1966) and therefore this element may be concentrated in the accessory mineral apatite where it replaces calcium in the crystal structure. Comparison of the distribution of yttrium (fig. 5-1-2h) with that of P_2O_5 (fig.4-1-21) shows that P_2O_5 concentrations decrease much more sharply than the Y therefore this element must also be held in another phase. Wedepohl (1978) and Rowbotham (pers. comm) show that yttrium can be substituted for calcium in amphiboles where Y replaces Ca in the M(4) sites. The data for Y is not so widely scattered as Zr which could be explained by this element being present both in a major and an accessory phase.

The two radiogenic elements uranium and thorium (fig. 5-1-2k and 5-1-21) show extremely wide scatter but the lowest concentrations are in the gabbroic rocks. It may at first sight appear to be difficult to interpret these data but several samples (203, 345, 346, 367 and 368) have both the highest contents of uranium and thorium. The scatter of the data is again suggestive of being

present in an accessory phase. Comparison of the data for zirconium shows that the samples with the highest U and Th also have the greatest amounts of Zr. In addition to this, a number of samples were cut and paper, sensitive to radiation, was placed on the surface and left for three months. When the paper had been developed it was noted that the radiation damage was concentrated in small grains, presumably zircon.

Both of these elements were determined by neutron activation techniques and apart from two results the Th/U ratio appears to be fairly constant (3.2 to 4.0) (figure 5-1-2v). There does, however, appear to be a decrease in the Zr/Th ratio from ~ 16 to 4 (fig. 5-1-2w) which may possibly indicate that thorium and zirconium do not behave in a totally coherent manner and if this observation is correct then thorium may enter a phase in addition to zircon.

Lead (fig. 4-1-2m) is another widely scattered element in the Serres-Drama complex and the dispersion is such that no conclusion can be made. Lead often replaces potassium in alkali feldspars but it is difficult to claim this in the present study.

One of the more consistent trace elements distributions is that of gallium (fig.4-1-2n) in which the concentration increases from the gabbro ~ 15 ppm to ~ 25 ppm in the dioritic xenoliths to ~ 10 ppm in the aplites. This smooth trend and little dispersion may indicate that gallium is present in a major phase. Indeed this element

substitutes for aluminium in silicates and the gallium distribution mimics that of aluminium. The Ga/Al ratio remains the same throughout the differentiation process, which agrees with the conclusion of Mason (1966) and Henderson (1982).

Zinc, with a ionic radius of 0.74 A^{o}, is a transition metal that substitutes for iron in the silicates. Zinc is highest in the gabbros and the dioritic xenoliths and decreases through the granitoid rocks to the aplites. This is the trend followed by iron (fig. 4-1-2c) in the Serres-Drama complex therefore it is possible to conclude that zinc follows iron with the ferromagnesian mineral. Rowbotham (1973) observed that amphiboles can carry up to 200 ppm zinc, whereas the other ferromagnesian minerals had much smaller values. It is reasonable therefore to conclude that zinc is present in the amphiboles within the Serres-Drama complex.

In contradistinction to zinc, copper (fig. 5-1-2p) does not enter silicate lattices to any degree and is a chalcophile element and so the distribution may reflect the amount of sulphide mineral throughout the complex.

In addition to the above elements, three others were determined on only 12 samples (Cs, Hf and Ta). Two of three elements, hafnium and tantalum are thought to be camouflaged in zirconium and niobium minerals respectively. Therefore to note what happens to these coherent elements, the ratios Zr/Hf (fig.5-1-2y) and Nb/Ta (fig. 5-1-2x) have been plotted against silica. In both cases there is

a negative correlation between the ratio and silica which indicates that both hafnium and tantalum are being excluded from the early crystallised accessory minerals. In conclusion, hafnium is found in zircon but greater amounts of this element are found in zircon from the more silica rich granitoids. Tantalum is concentrated into sphene but as with hafnium, higher concentrations are found in sphene from the more silica rich granitoids.

Taylor (1965) suggests that the Ba/Cs ratio would make a sensitive indicator of differentiation, Ba^{+2} being enriched in the earlier fractions of potassium-bearing minerals and Cs^{+} in the later. The Ba/Cs ratio has been plotted in fig. (5-1-2z) against SiO_2 as differentiation index we would expect the ratio to fall with differentiation. The scatter of points makes interpretation difficult as no consistent change in Ba/Cs ratios can be seen (i.e. using group means).

In summary, a study of the trace elements has shown that Rb, Sr, Ba, Ga and Zn distributions can be correlated with major phases which have crystallised in the complex. Rb and Ba are dominantly in the potassium feldspars; Sr in both potassium and plagioclase feldspars; Ga in all the aluminous phases; and Zn in the amphiboles. Elements such as Zr, Hf, U and Th are concentrated in the mineral zircon; Nb, Ta, L.R.E.E. in sphene; Y, L.R.E.E. in apatite; and Cu in a sulphide phase. Y, L.R.E.E. and Nb can also enter the amphibole structure.

CHAPTER VI : PETROGENESIS

CHAPTER VI

PETROGENESIS

6-1-1 Introduction

In the following account the petrogenesis of the Serres-Drama complex will be outlined. The approach is one of first discussing the general tectonic environment of the evolution of the northern Aegean during the Caenozoic. This will be followed by the description of a possible model to account for the spatial development of the rock types in the complex. Finally, phase equilibrium studies are discussed to explain how the magma crystallised and fractionated and the subsolidus reaction which took place.

The crystallisation of the Serres-Drama granitic complex can be traced by combining data from field study, petrography, mineralogy and geochemistry.

The magmatic origin of the complex is obvious from the field evidence (emplacement into the upper part of the oldest sequence of geneisses (E), and the overlying sequence of marbles (F)), petrography, mineralogy and geochemical data. Composite batholiths resulting from repeated intrusion of magma are known throughout the world, for example, those of Donegal (Pitcher and Berger, 1972), the coastal batholith of central Peru (Cobbing and Pitcher, 1972a), and the Sierra Nevada and Southern California batholiths (Larsen, 1948; Bateman et al, 1963). These

large batholiths may be separated into different intrusions with distinct geographical occurrences, and with different compositions, but with relationships between the younger units and the older ones.

Mason and Macdonald (1978), Chappell (1978) and Petro et al (1979) all accept that magmas of calc alkaline affinity have been produced either by partial melting of a down going oceanic slab or partial melting of the overlying 'wedge' of peridotite composition (Ringwood 1974). The melting process of the 'wedge' is caused either by rising temperatures due to subduction or the addition of water from a dehydrating oceanic slab or a combination of the two. Whichever process is involved it is very difficult to unravel because we are dealing with the end products of these processes. An additional problem has been cited by Petro et. al (op. cit.) and that is the effect of a mantle derived melt on the continental crust. Partial melting of continental crust is a likely possibility, thus compounding the difficulty in interpreting the various melting episodes.

These partial melts, whether they have been ultimately derived from the oceanic slab or the overlying peridotite wedge have ascended into continental crust in the Rhodope massif where partial melting of some of the continental crust may have occurred. Thus the early history of this pluton may have been very complicated prior to the lower pressure crystallisation which we can now see in the rocks of the Serres-Drama complex.

Papazochos and Papadopoulos (1977) and Papadopoulos (1982) suggest that there have been two phases of lithospheric subduction, distinct in time and space in the Aegean area during the Caenozoic. The evidence for this conclusion is based not only upon structural but also on magmatic evidence, where the age of both the plutonic and volcanic rocks decreased southwards. The older phase of subduction is associated with a lithospheric plate descending towards the north from where the present-day central Aegean is. This phase has largely ceased any activity but was at its acme during the Eocene, Oligocene and the Miocene in the northern Aegean.

Papazachos' and Papadopoulos' (ibid.) second phase is represented by a present-day subduction zone dipping to the north from the Mediterranean to the southern Aegean. This phase began during the Miocene and is presently very active but only affects the southern Aegean.

The Serres-Drama granitic complex is thought to fit the model developed by Papazachos and Papadopoulos (ibid.) (see fig. 6-1-1a). The above calc-alkaline suite is thought to have been produced in a subcontinental lithosphere. The Rhodope massif (Chapter I) was stabilized during the Palaezoic and the calc-alkaline magma was intruded into the these marbles, schists and gneisses during the Eocene-Oligocene.

This magma ascended into the upper continental crust where the parent magma differentiated into fractions with low silica and intermediate silica contents.

The whole rock analytical data suggests that the

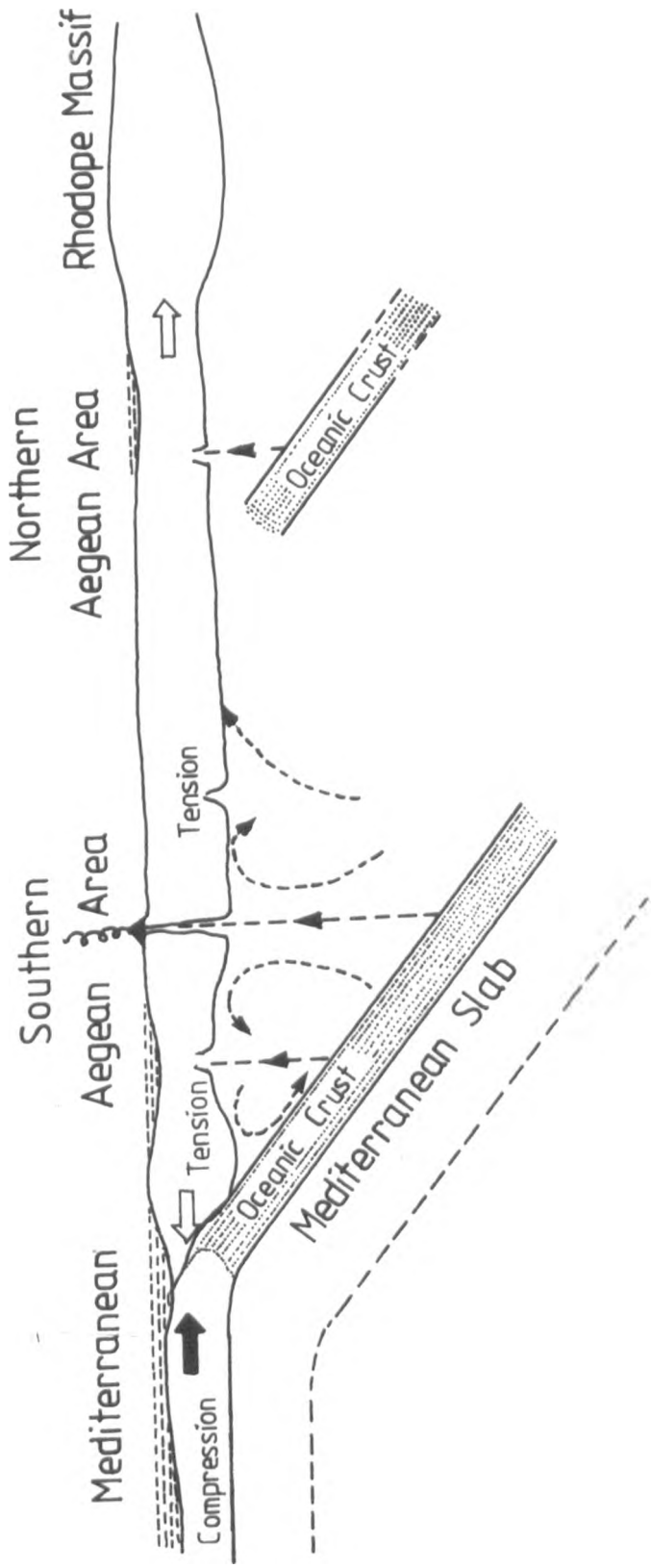

Fig. (4-1-1a) From Papadopoulos (1982)

Fig. (6-1-1b)

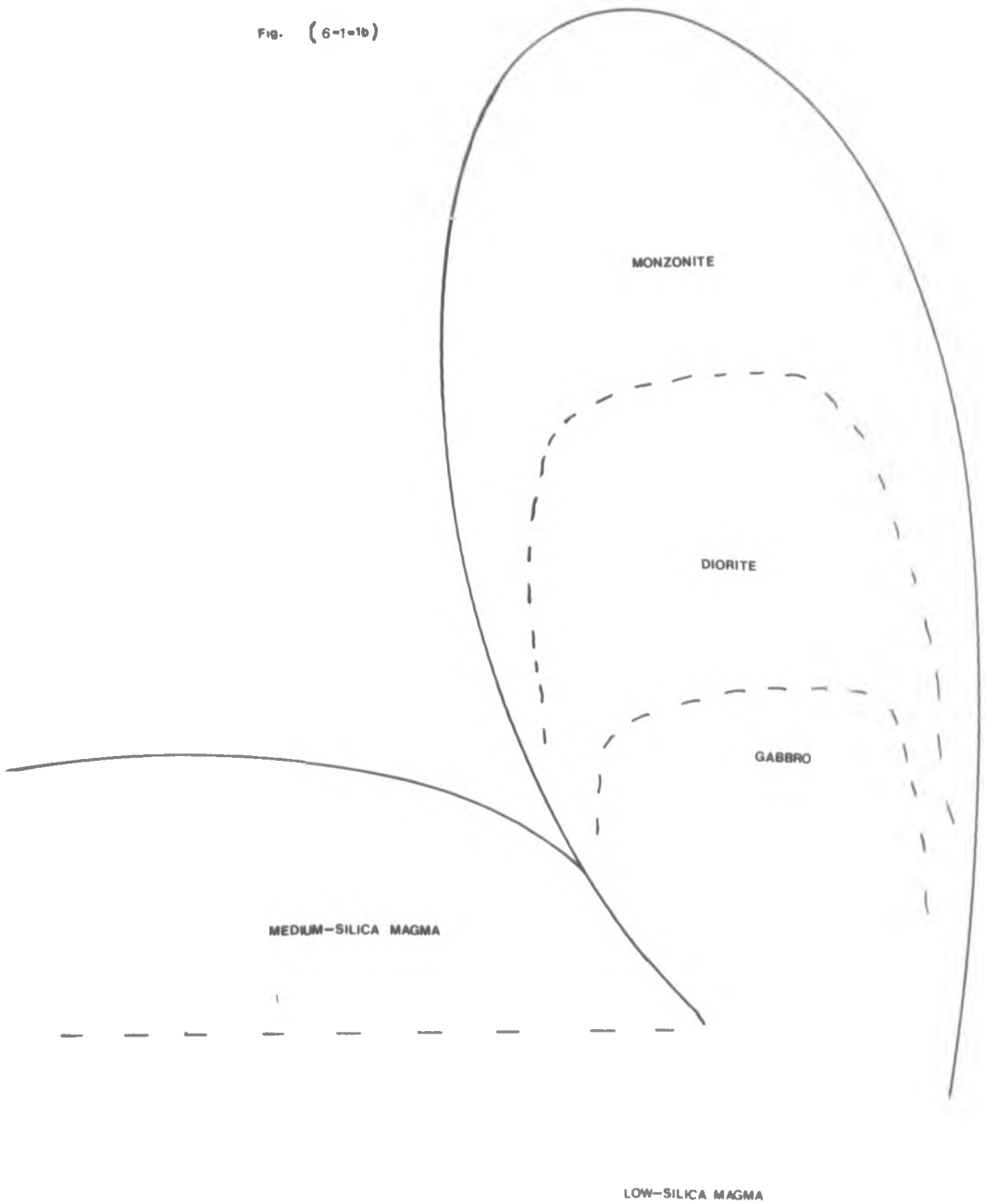
MONZONITE
DIORITE
GABBRO
MEDIUM-SILICA MAGMA
LOW-SILICA MAGMA

Fig. (6-1-1c)

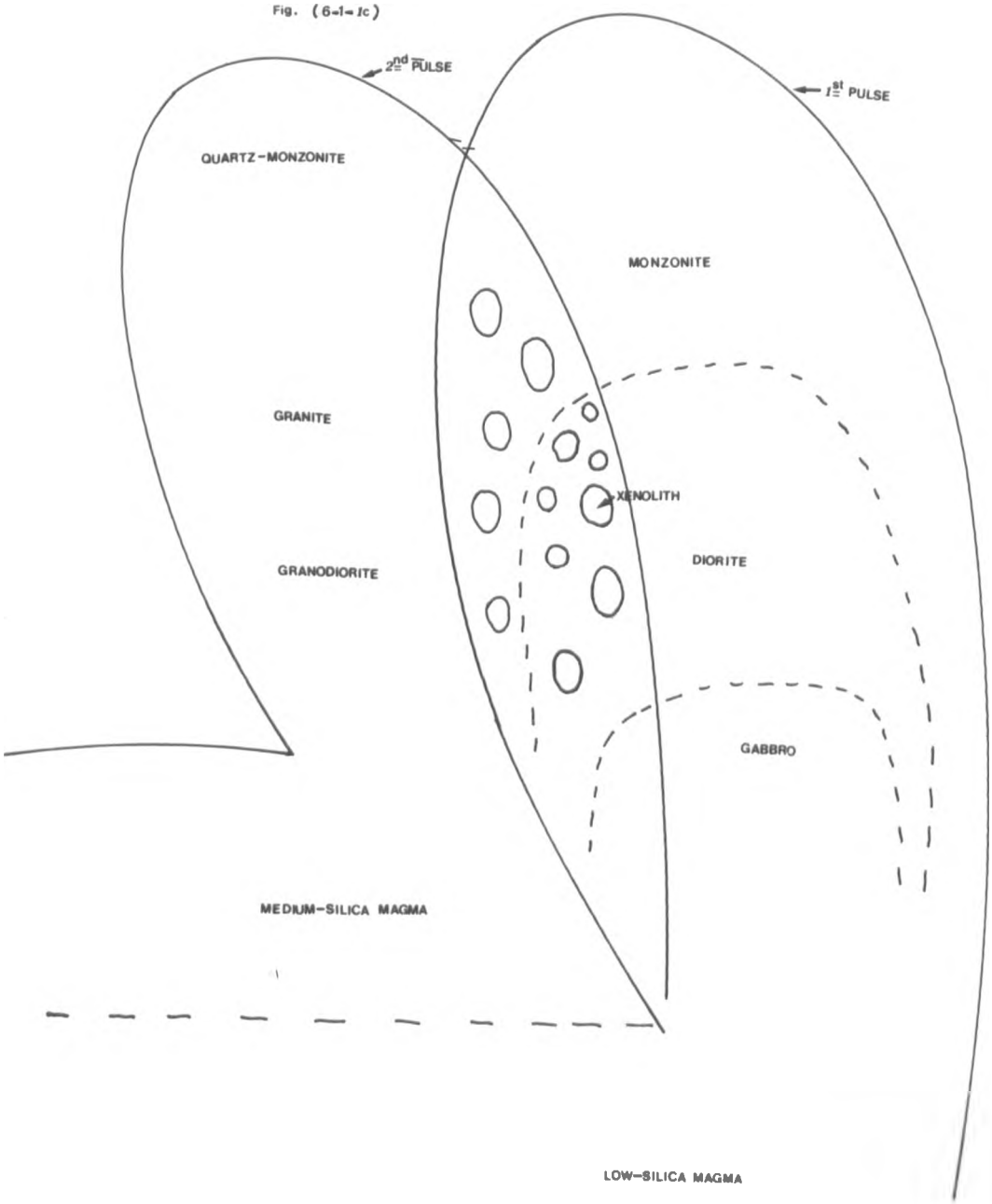
2nd PULSE
1st PULSE
QUARTZ-MONZONITE
MONZONITE
GRANITE
XENOLITH
GRANODIORITE
DIORITE
GABBRO
MEDIUM-SILICA MAGMA
LOW-SILICA MAGMA

complex has resulted from fractionation of early crystallising phases. This is particularly well demonstrated by the AFM diagrams (fig. 4-2-1a) where the trend of compositions is towards the alkali apex with a roughly constant Fe/Mg ratio. This behaviour suggest that a mafic mineral is controlling the liquid line of descent. The dominant mafic mineral in the Serres-Drama complex rocks is hornblende with an $Mg/Mg+Fe^2$ ratio which varies from 0.49-0.80. Although this ratio does vary the dominant substitutions in these amphiboles are "edenitic" and "tschermakitic" which are not affected by iron and magnesium occupancy. Therefore a possible conclusion is that amphibole fractionation is important in controlling the composition of later liquids.

Variation diagrams of the major element indicate that there are two groups of composition, one the "basic" group characterised by the presence of clinopyroxene and the "intermediate" group characterised by the presence of quartz. These two groups of rocks are interpreted as being the result of two pulses of magma from the same parent. The chemistry of the major elements indicate that the variation within each group is due to 'high-level' or crustal differentiation. Each trend plots on smooth curves of calc-alkaline affinity which is in agreement with the observations of Atherton et. al. (1979) and McCourt (1981).

From the low silica parent magma (see fig. 6-1-1b), the first pulse of magma separates and ascends. This pulse differentiates into monzonite, diorite and gabbro (see fig. 6-1-1b). The occurrence of gabbro in the Serres-Drama outcrop is very small (a few km^2) compared with the other

rock-types, this, in the opinion of the author, does not represent the main body of gabbro but only a small marginal area. The gabbro could be of a cumulative nature, although it does not show cumulate texture. But from microprobe analysis the clinopyroxenes (early crystallised mafic mineral) have similar compositions in gabbros, the dioritic xenoliths and the monzonites. Consequently they must have crystallised in a similar environment.

From the parent magma a liquid of intermediate silica content separates and intrudes the overlying rocks and partially assimilates all the diorite leaving only dioritic xenoliths. From the differentiation (as shown in the Harker plot) of the second pulse arise the quartz monzonite, granodiorite and granite which are fairly uniform with little variation in chemical composition and similar mineralogical compositions (see fig. 6-1-1c).

6-2-1 Crystallisation of the granites

Many workers (Winkler and Breitbart, 1977; McCourt, 1981; Brown, M. et al, 1981) have discussed the crystallisation of granites in terms of phase equilibria in the system Qz-Ab-Or-An-H_2O. Liquidus equilibria in this system at a 5 kilobar H_2O pressure as depicted by Winkler (1979) are shown in fig. (6-2-1).

The above tetrahedron is bounded by four triangles, each representing a four-component system as follows: a) Qz-Ab-Ar-H_2O system. Yoder (1968) has investigated this

system at 5 kb H_2O pressure. The main conclusions from this study are: a cotectic line connects the eutectic E_2 (determined by Stewart, 1957, 1967) with the eutectic E_1.

b) Qr-Or-An-H_2O system. There is a ternary eutectic E_5 (determined by Winkler and Lindeman, 1972; Winkler and Ghose, 1974, at various pressures). From E_5 three cotectic lines extend from E_5 to E_2, E_3 and E_4.

c) Ab-An-Or-H_2O system. Yoder et al (1957) have investigated this system at 5Kb H_2O pressure and they determined a cotectic curve from the eutectic E_4 towards the eutectic E_6.

d) Qz-Ab-Or-H_2O system. Three cotectic lines radiate from the eutectic P towards eutectic E_1, E_3 and E_6.

The space of the Or-Ab-Qz-An tetrahedron is divided by three cotectic surfaces. These cotectic surfaces separate each crystallising phase (quartz, plagioclase and alkali feldspar) from each other. These three cotectic surfaces intersect in a cotectic line, P-E_5 which indicates the compositions of melts coexisting with plagioclase and alkali feldspar and quartz and a gaseous phase. The cotectic line P-E_5 is located in the tetrahedron where the An content is low. Consequently a small change in An content has a pronounced effect on the composition of cotectic melts.

Whitney (1975) suggested that 'the anorthite content has a rather profound effect on the liquidus temperature. Even the small amount of anorthite in the synthetic granite composition raises its liquidus about 150° C above that noted by Tuttle and Bowen (1958) for anorthite-free

compositions at 2 kb'.

For petrogenetic considerations compositions within the tetrahedron Or-Ab-Qz-An are projected onto the plane Or-Ab-Qz from the An apex. The projection of the line P-E_5 is the P-E_5'. A perspective view of the system Or-Ab-Qz-An-H_2O with low temperature indicated by isotherms (fig. 6-2-2) and projection of the isobaric line P-E_5 with the isotherms as given in fig.(6-2-3). Numbers in the above isotherms give the percentage of the An and Qz component, respectively, of melt compositions situated on the cotectic surfaces and cotectic line.

Von Platen (1965) has investigated minimum melting temperatures and compositions for a group of planes at a fixed Ab/An ratio and at a fixed pressure of 2 kb (see fig. 6-2-4). He projected the boundary curves from the anorthite apex of the tetrahedron onto the orthoclase-albite-quartz base (see fig. 6-2-5). From his experimental data, increasing the ratio Ab/An decreases the minimum melt temperature and the compositional ratio quartz and orthoclase.

Two main effects arise from the addition of anorthite to the "granite" compositions: 1) the cotectic separating the quartz volume from the feldspar volume becomes closer to the quartz apex of the Qz-Ab-Or triangle and 2) the low temperature boundary curve between Ab and Or approaches more Or compositions. The salic components (Qz, Ab, Or) are plotted on figure 4-1-2n and the distribution of the compositions indicate that they cross the low temperature boundary curves rather than run parallel to them. The monzonites

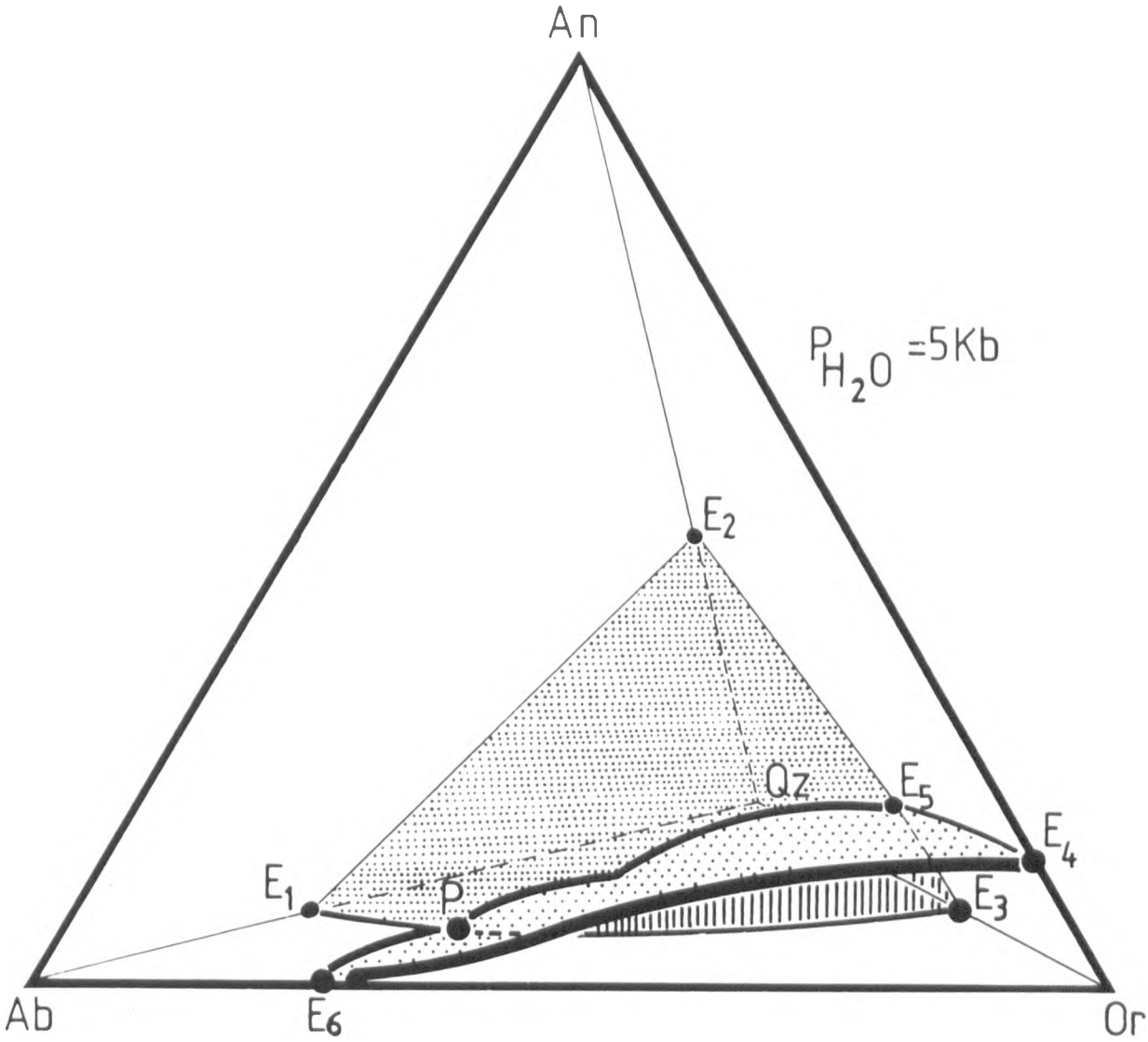

Fig.(6-2-1)

System Qz-Ab-Or-An. Diagrammatic phase relations at a given H_2O pressure. Above approximately 3kb point P is an eutectic point. (Winkler, 1979).

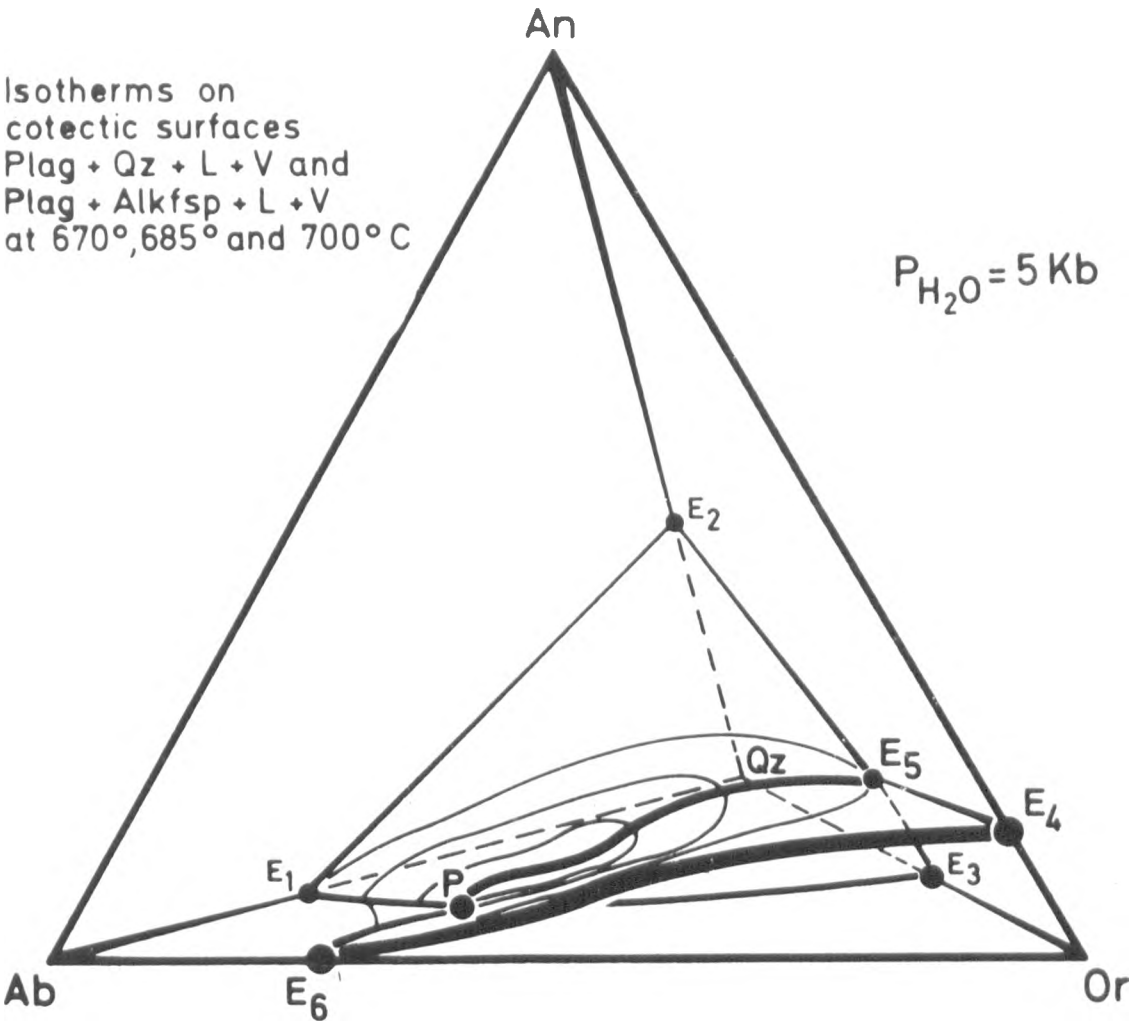

Perspective view of the system Qz-Ab-Or-An-H_2O with low temperature regions, indicated by isotherms, shown on the cotectic surfaces plag + qtz + L + V and plag + alk feldsp + L + V.

Fig. (6 – 2 – 2) (from Winkler, 1979)

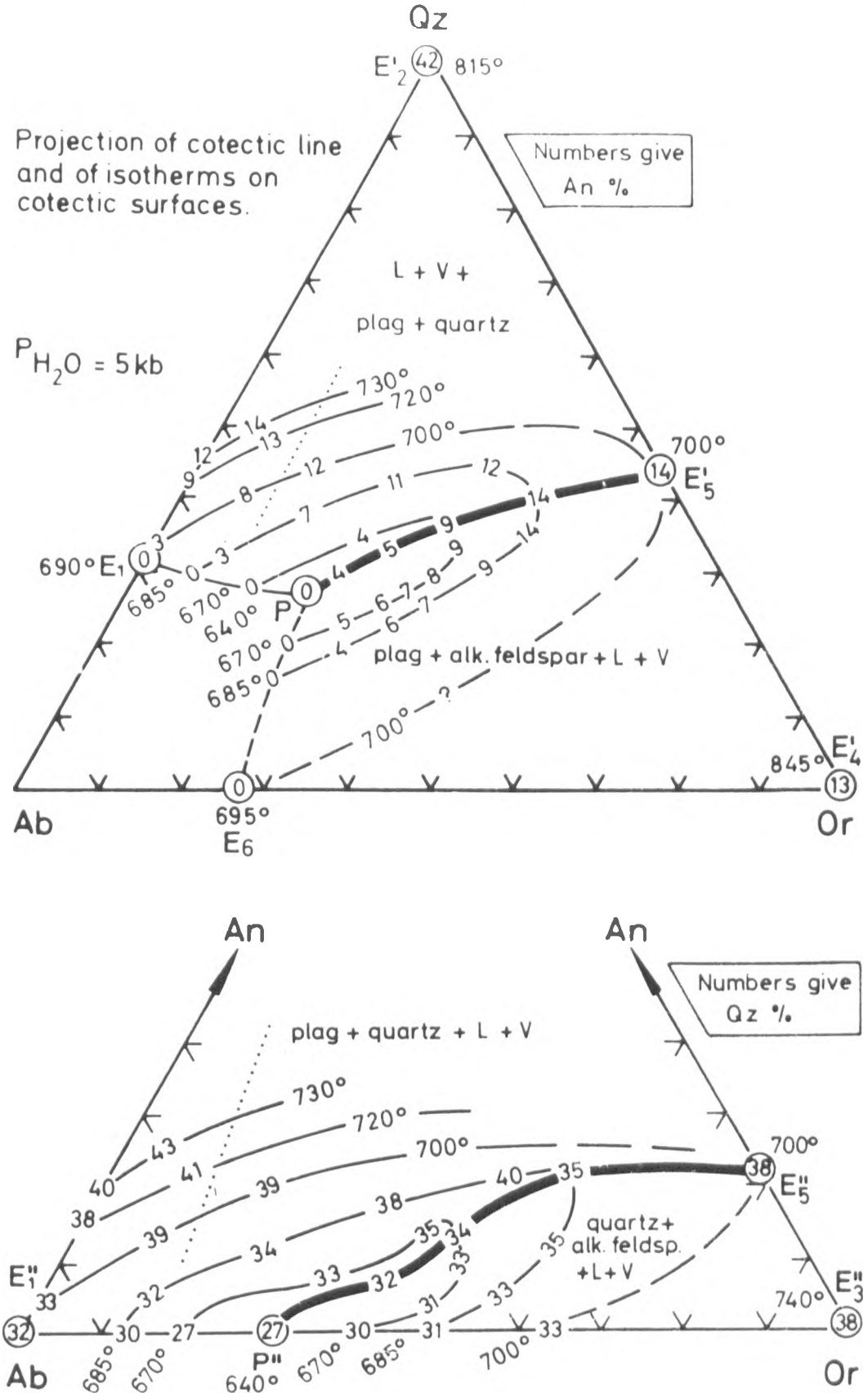

Projection of the isobaric cotectic line P-E_5 and of isotherms on the three cotectic surfaces of the system Qz-Ab-Or-An-H_2O. Data valid for 5 kb water pressure. Numbers give percent An (top) and Qz (bottom) component.

Fig. (6-2-3) (from Winkler, 1979)

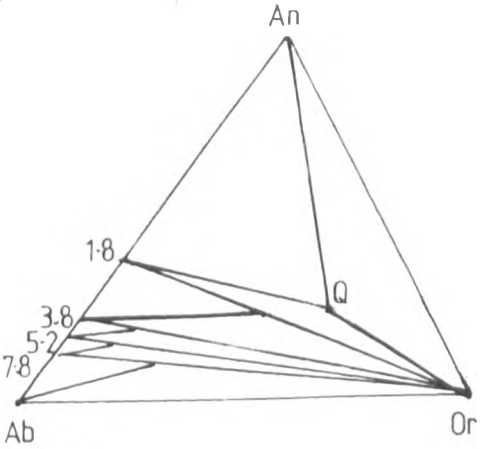

Fig. (6-2-4)

Compositional planes within the tetrahedron $NaAlSi_3O_8$–$KAlSi_3O_8$–$CaAl_2Si_2O_8$–SiO_2. The numbers represent albite-anorthite ratios (in weight percent) for each plane. [After von Platen, 1965; from Ehlers, 1972]

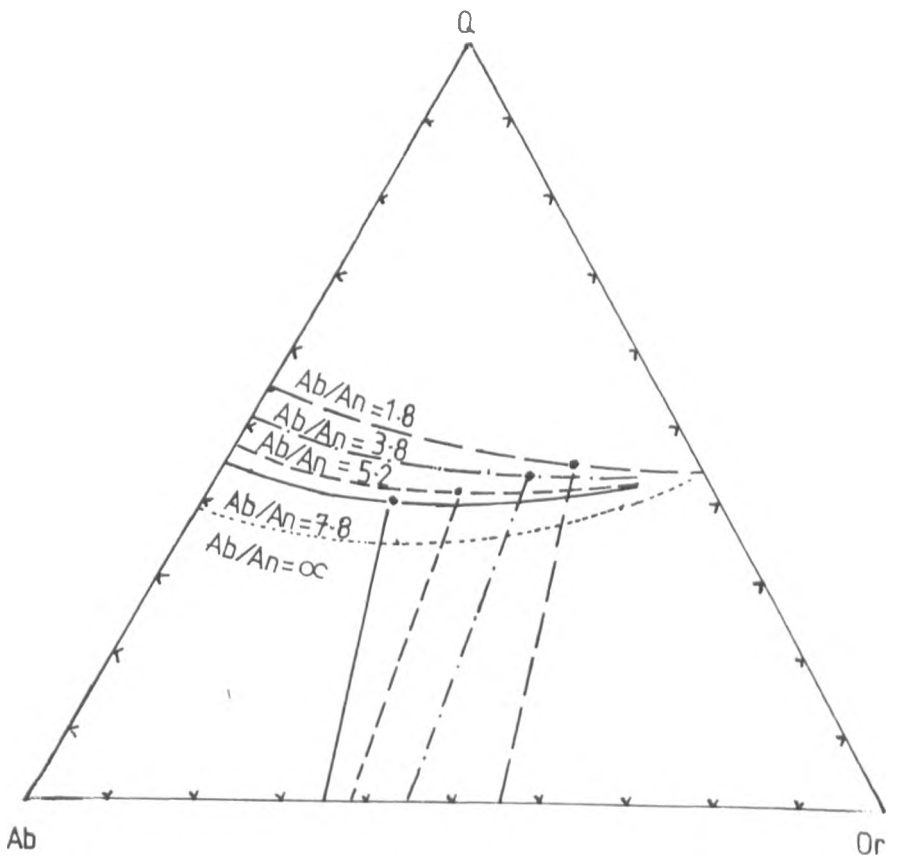

Fig. (6-2-5)

Minimum-temperature melts and boundary curves at a P_{H_2O} of 2kb, from the compositional planes of Fig. (6-2-4). All of the thermal data have been projected from the An apex to the base for easier comparison. [After von Platen, 1965 and Winkler, 1967; from Ehlers, 1972]

plot about 50 Ab: 50 Or indicating a Ab: An ratio of 3.8 (fig. 6-2-5), the quartz monzonites plot in an area where Ab: An is 5.2. Therefore these results appear to mark a response to lower An in successive melt fractions.

6-3-1 Crystallisation paths

The paths followed by liquids crystallising in the system Or-Ab-An-Qz can be estimated if assumptions are made about the feldspar composition changes that occur during crystallisation of the granitic complex.

Petrographic study showed that the plagioclase feldspars are zoned with a variety of anorthite contents. From microprobe analysis (Chapter III), the range of anorthite in the complex is between 18% and 94% (including the gabbro). The range of normative anorthite in the complex is between 2.63%. An (samples No.3, aplite) and 34.21% (sample No. 153, gabbro). This variation in composition reflects changes occuring during crystallisation. From the major element analysis, Ca decreases with increasing differentiation (except for plagioclase, Ca enter into clinopyroxenes and amphiboles), while Na remains roughly constant. From the above chemical data we can see that the albite content determined from normative compositions is possibly constant while the anorthite content decreases. Consequently the ratio Ab/An must increase with increasing differentiation (see fig. 6-2-5). Reference can be made to the normative data for the Serres-Drama complex where Qz-Ab-Or (fig.4-1-2m)

and An-Ab-Or (fig. 4-1-2n) are plotted and indicate that the Ab content is fairly constant in the granitoids (An-Ab-Or) and the Ab/Or ratio remains constant in the granitoids (Qz-Ab-Or).

6-4-1 Crystallisation of the granitic complex

The gabbros are interpreted as representing an early phase from which the other rocks are derived by fractional crystallisation. Phase equilibrium studies for plagioclase feldspar of high anorthite content were outlined earlier (Chapter 3) and it was shown that in order to generate plagioclose of $\sim An_{90}$, high water pressures were needed and it was concluded that if plagioclase of these compositions were crystallising from a "gabbroic" melt then clinopyroxene would not be stable but be replaced by amphibole.

Amphibole was shown to be replacing clinopyroxene as a liquidus phase early in the history of the Serres-Drama complex (Chapter 3) therefore liquids would be of a higher silica content after the fractionation of clinopyroxene, amphibole and anorthite.

Plagioclase will be the first felsic phase expected to crystallise from liquids with compositions corresponding to the Serres-Drama granitic complex, followed by alkali feldspar and finally quartz as an interstitial phase.

The C.I.P.W. normative salic components of the average of each rock type have been plotted on the two projections of the Qz-Ab-An-Or tetrahedron (Winkler, 1979)

(figs. 6-4-1 and 6-4-2) in an attempt to infer the order of crystallisation of the main mineral phases. It must be emphasised that the results can only be tentative indications because of the differences (particularly in An content) between the Serres-Drama rocks and those used in the Winkler study. The Serres-Drama rocks also have a high mafic mineral content. Winkler and Breitbart (1978, p.464) however state that biotite and hornblende have negligible effect on phase relations of major constituents.

The dioritic xenoliths plot in the plag + Qtz + L + V space in the An-Ab-Or projection.

Monzonite probably plots above (there are no An values on the 700° isotherm) the plag + alk felds + L + V cotectic surface in Qz-Ab-Or projection and below (-23% Qz) the plag + qtz + L + V cotectic surface in An-Ab-Or projection in the plagioclase field.

Quartz monzonite plots well above (+ 9% An) the plag + alk feldspar + L + V cotectic surface close to the cotectic line P-E'_5 in the Qz-Ab-Or projection and well below (-23% Qz) the plag + qtz + L + V cotectic surface in the Ab-An-Or projection in the plagioclase field.

Granodiorite plots above (+10% An) the plag + alk feldspar + L + V cotectic surface in the Qz-Ab-Or projection and below (probably, -21% Qz) the plag + qtz + L +V cotectic surface in An-Ab-Or projection in the plagioclase field.

Granite plots above (+11% An) the plag + alk feldspar + L + V cotectic surface in the Qz+Ab+Or projection and

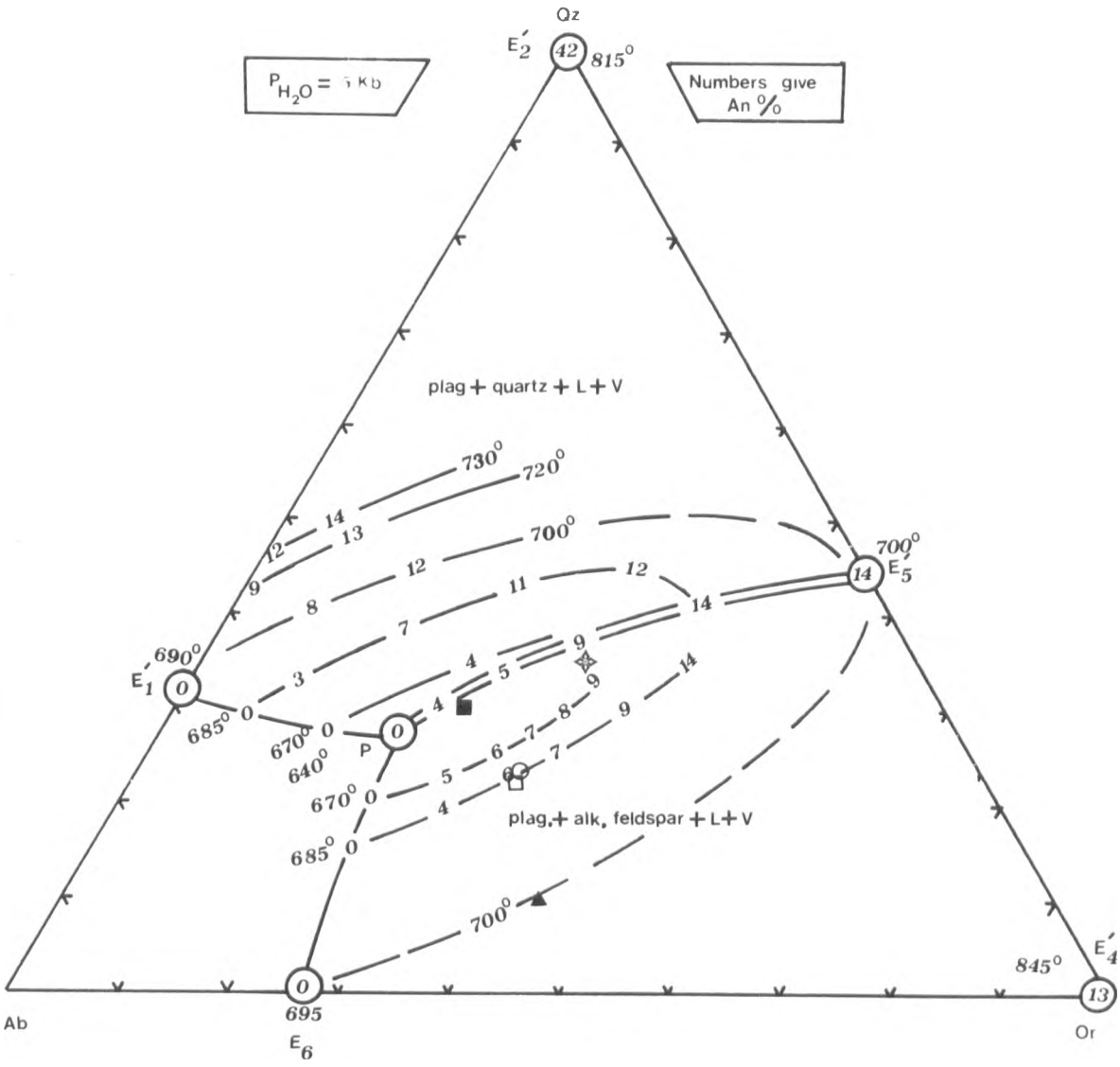

Fig. (6-4-1) (from Winkler et al, 1978)

○ Granite

■ Quartz monzonite

□ Granodiorite

▲ Monzonite

⌖ Aplite

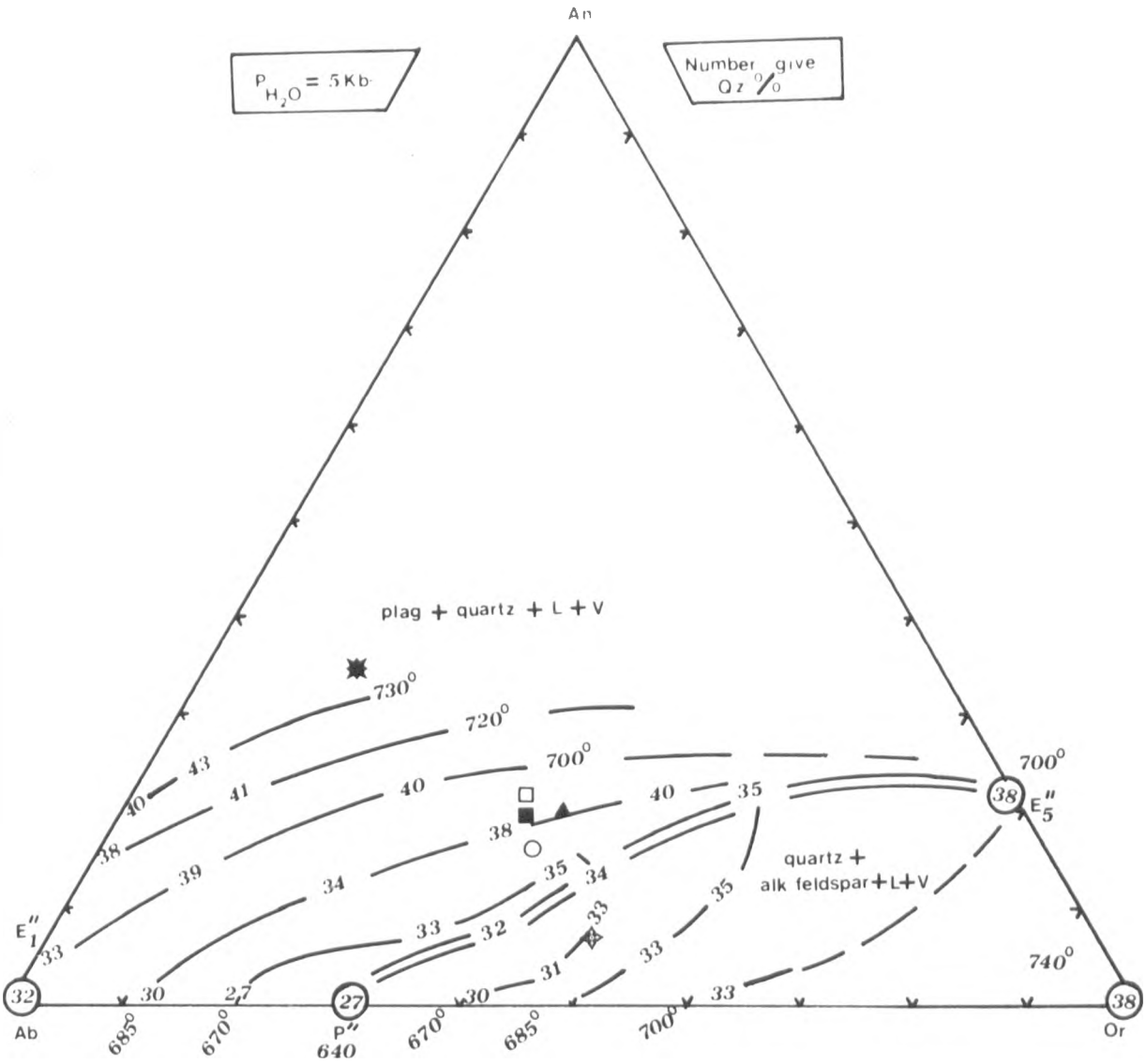

Fig. (6-4-2) (from Winkler et al., 1978)

- ○ Granite
- ■ Quartz monzonite
- □ Granodiorite
- ▲ Monzonite
- ✸ Xenolith
- ✧ Aplite

below (-c.17% Qz) the plag + Qtz + L + V cotectic surface in the An-Ab-Or projection, i.e. in the plagioclase field.

Aplite plots below (-5% An) the plag + alk feldspar + L + V cotectic surface in the Qz-Ab-Or projection and above (+8% Qz) the quartz + alk fledspar + L + V cotectic surface in the An-Ab-Or projection, i.e. in the quartz field.

From this it can be seen that all of the major rocks-types in the complex (excluding gabbro, xenoliths and aplite) plot in the plagioclase field of the An-Ab-Or-Qz tetrahedron. Consequently plagioclase is the expected liquidus phase, i.e. the first salic mineral to crystallise from the magma This agrees with petrographical observations. One important conclusion which could be advanced for the granitoid rocks is that the phase equilibria suggest that the temperatures of formation are above or close to 700° C.

Piwinskiii (1968) has shown (fig. 6-4-3) that for a calc-alkaline plutonic series similar in many ways to the Serres-Drama granitic complex (Sierra Nevada Batholith, the solidus temperature falls progressively with increasing differentiation index. At 2 kb pressure ($P_{H_2O} = P_{total}$) the solidus temperature for high alumina basalt (equivalent to gabbro D.I=25) is about 900° C. This falls to about 700° C for intermediate rocks over quite a wide range (DI ~ 55-70, tonalites and granodiorites) and finally falls to C.675° C for the granite (DI=93).

The phase equilibrium studies of Winkler and Breitbart

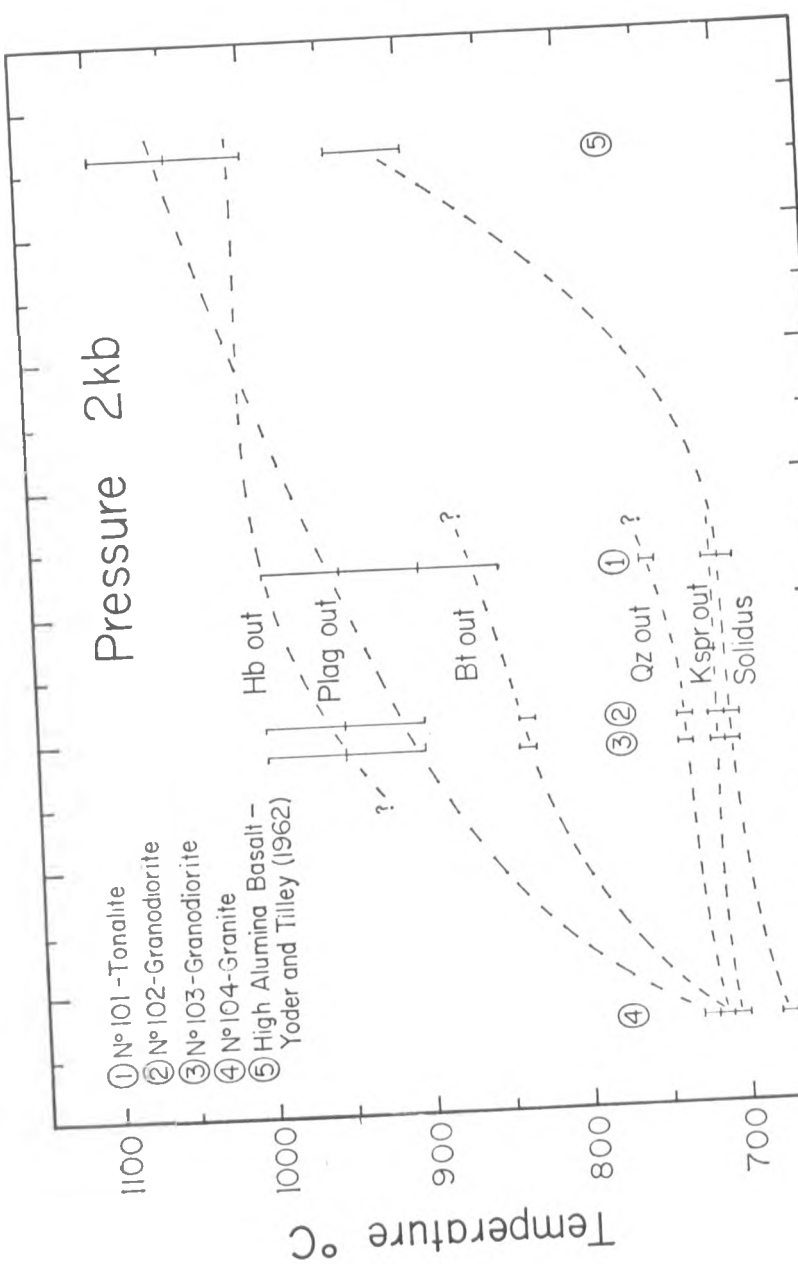

Temperature-Differentiation Index diagram for the "granitic" rocks of the Sierra Nevada Batholith at 2 kb. water pressure. Phase boundaries are connected with those determined for a high-alumina basalt by Yoder and Tilley (1962).

(op.cit.) and Piwinskii (op. cit.) one close to each other for the solidus temperatures (~ 700° C). If we discuss the Serres-Drama samples with reference to Piwinskii's work we can see that the gabbro (D.I.=18) has a solidus temperature in excess of 900° C with plagioclase feldspar as the liquidus phase (~ 1050° C) and is joined by hornblende at ~ 1000° C. The dioritic xenoliths (D.I.=48) have a solidus temperature in excess of 700° C but hornblende is now the liquidus phase. The granitoids - monzonite (D.I.=69) quartz monzonite (D.I.=75), granodiorite (D.I.=75), granite (D.I.=80) and aplite (D.I.=94) have similar solidus temperatures (~ 700° C) except the aplite (~ 670° C). The order of crystallisation fits very closely the petrography of the Serres-Drama complex i.e. hornblende, plagioclase, biotite, quartz and potassium feldspar in order of appearance from the liquid.

The maximum temperature determined on the alkali feldspar solvus is 650° C for othoclase. The sub-solvus reactions indicate that orthoclase is stable to temperatures down to 545° C when microcline seems to take over (540° C). The alkali feldspars seem to cease exsolution at 420° C and thereafter the whole system is closed (Chapter III).

From the phase equilibrium data it appears that the solidus surface (700° C minimum) is close to the solvus (650° C) for these compositions.

GENERAL CONCLUSIONS OF THE SERRES-DRAMA GRANITIC COMPLEX

In summary the Serres-Drama plutonic complex is a "granitic" intrusion of Tertiary age which has intruded a sequence of schists, gneisses and marbles of indeterminate age. The thermal metamorphism of the marbles produces an aureole which has reached the hornblende hornfels facies. The country rocks into which the intrusion has been emplaced area part of the Rhodope massif which is thought to be of both late Precambrian and lower Cambrian age.

Petrographically the rocks of the Serres-Drama complex are gabbros, diorites, monzonites, quartz monzonites, granodiorites and granites which have granite pegmatites and aplites cutting through them, particularly the "intermediate" rocks.

The mineralogy of the complex is closely related to each rock type. In the early formed gabbros anorthitic plagioclase feldspar is formed with clinopyroxene of salitic composition but more importantly hornblende of ferroan pargasite composition replaces the pyroxene in these rocks which are interpreted as being formed under high water vapour pressure.

After fractionation of these early formed minerals the rocks became dioritic in composition with basic plagioclase, salitic pyroxene and hornblende as the dominant minerals. These rocks are now found only as xenoliths

within the later rock types. There is no evidence of late growth of minerals, such as potassium feldspar within these diorites and little evidence of any addition of elements incorporated from the host rock.

The monzonitic rocks form an arcuate outcrop in the east of the intrusion and include the phase potassium feldspar both as a megacryst phase and as a part of the holocrystalline fabric of the rock. Potassium feldspar megacrysts are found in areas marginal to the monzonite outcrop and appear very late in the crystallisation sequence within these monzonites.

The gabbros, diorites and monzonites are thought to have developed from the same magma because of the presence of clinopyroxene of a similar composition in all three rock types. These rocks have been called the "basic" rocks.

The more evolved rocks of quartz monzonite, granodiorite and granite composition occupy the western portion of the intrusion. There do not appear to be any internal contacts between these rock types and their differences have been revealed by both petrographic techniques and geochemical analysis. These rocks have been called the "intermediate" rocks because of their chemical composition and the lack of clinopyroxene as a primary phase. It has been interpreted that these rocks belong to a more evolved pulse of magma than the 'basic' group of rocks. Marginal megacrystic developments of alkali feldspar again occurs within these rocks but appears to be the latest phase of crystallisation in the rocks.

Geochemical analysis of both major and trace elements of the Serres-Drama complex has been interpreted in terms of fractionation of a calc-alkaline "I-type" complex (Chappell and White, 1974) which is similar to the "magnetite" series of Ishihara (1977). This granitic complex has undergone "in-situ" fractionation to yield two pulses of magma now represented by the "basic" group of rocks and the "intermediate" group of rocks. The geochemical distribution of the major and trace elements have been interpreted in terms of both essential and accessory mineral phases.

This "I-type" complex is thought to be due to a subduction zone descending beneath the northern Aegean during the Eocene-Oligocene and the magma was produced either within the descending oceanic slab or the overlying peridotite wedge.

APPENDIX A

MINERAL STAINING TECHNIQUES

Uncovered thin-sections were etched and stained to distinguish the K-feldspar. The stain used was Sodium cobaltinitrite The method used was essentially that given in Hutchinson (1974, p.16). The cobaltinitrite causes the K-feldspar to be stained bright yellow, facilitating point-counting.

APPENDIX B

MICROPROBE ANALYSIS

Analyses of a number of minerals were performed by Dr G. Rowbotham on a Geoscan Mark II Microprobe at the University of Manchester. It was operated at an accelerating voltage of 15 kv and a current of 3.5×10^{-8} amps. An energy dispersive system was used for detection and measurement with calibration against metals, oxides and silicates.

APPENDIX C

C-3 ANALYTICAL TECHNIQUES

C-3-1 Preparation for analysis.

Specimens, usually larger than 1 kg, were collected. Sample locations are listed in table (4-1-1a).

Samples were split into rough cubes 1-2 cm across using a Denbigh hydraulic fly-press rock splitter, taking care to remove all weathered material and veins. The samples containing dioritic xenoliths (sample Nos. 6a and 6b) were sliced into 2 cm thick slabs before splitting with a hammer and bolster. The xenolithic material was separated from the host rock and then itself divided into fine grained and coarse-grained sections.

The split samples were then passed through a Sturtevant 2" x 5" jaw crusher, with Mn-steel jaws, which reduced them to chips between 5 mm and 1 cm in diameter. The samples were then homogenised by successive cone and quartering until two quarters were selected, each approximately 120 gms in weight. 50 gms of material from one of the quarters was crushed for 30 secs. (for X.R.F. analysis). After further homogenisation in a Turbula mixer/shaker for 15 minutes, approximately 20 gms of the X.R.F. fraction was milled for a final 30 minutes in a Glen-Creston M280 tungsten carbide ball mill.

Major element analyses were performed on fused

beads , produced by mixing 0.5 gms of ignited rock powder (ignited to 1000° c) with 2.5 gms of ignited lithium metaborate (Johnson-Matthey SP 100A). After fusing the mixture over a maker burner until a clear quiescent melt was produced, the bead was cast on a brass plate, maintained on a hot plate at a temperature of circa 230° c. The liquid was promptly pressed out with an aluminium plunger into a pre-formed copper wire binding ring. The beads were then annealed by leaving on ceramic tiles on the hot plate.

Trace elements and Na_2O analyses were determined on pressed powder pellets. These were prepared by mixing 8-10 drops of 2% Moviol (N90/98) binder solution with 6 gms of sample by hand in an agate mortar and pestle. This was then pressed at 25 tons P.S.L. for 4 minutes in a hydraulic press between two tungsten carbide plattens. The pellets were then dried in an oven overnight to cure the binder.

C-3-2 X-ray fluorescence analysis

Chemical analysis for ten major element oxides and fifteen trace elements was made by X-ray fluorescence spectometry.

The X-ray fluorescence analysis was performed in the Department of Geology at the University of Keele, using either a Phillips PW1212 fully automatic sequential or a Phillips PW1220 semi-automatic X-ray fluorescent

spectro meter. The methods used are similar to those given in Leake et al (1969).

Full operating conditions for the analyses are recorded in table (c-1) and (c-2). For the major elements, oxides (excepting MnO) a 2μ mylar window was used on the gas-flow proportional counter. Otherwise a 6μ mylar window was used.

The $LiBO_2$ fused beads are single sided, so that each bead was run three times and the mean of the three analyses recorded. The pressed powder pellets used for determining the trace elements and Na_2O are made thick enough for independent measurements to be made on either side of the disc (i.e. the thickness exceeds twice the critical thickness for the deepest penetrating X-ray measured (Zr Ka). Two cycles of measurement were made for each side of the pressed pellet, so each sample was in effect analysed in duplicate.

Counts in both peak and background angle positions were recorded and the net counts (P-B) were then used with or without corrections for interference effects.

Those elements determined on the fused beads were corrected for inter-element matrix effects, using a method essentially the same as that developed by Norrish and Hutton (1969). However, as lithium metaborate flux was used, a correction matrix for this flux was worked out, using binary mixtures of oxides by G.J. Lees. Calibration for major elements was made using international standard beads (mostly U.S.G.S. and N.I.M.). The apparent

fluorescence values of these standards were calculated from the correction matrix using the method outlined in Harvey et al (1973). The apparent fluorescence values of unknown samples obtained from the international standard calibration were then corrected using the programme MAJORC, developed by G.J. Lees. The precision and detection 1 units for the major elements are given in table (C-3).

Among the trace elements, Rb, Sr, Y, Zr, Cu, Ga, Zn, U, Th, Pb were all corrected for variations in mass-absorption coefficients, using the MoKα Compton scatter peak. The method is a modification of that described by Reynolds (1963). Corrections for inter-element interference had to be made on Y kα (Rb Kβ interference) and Zr Kα (Sr Kβ interference).

Of the trace elements, Nb, Ba, Ce, Nd, La, Ga, Zn, Cu were determined using an international standard calibration, while Rb, Sr, Y, Zr, U, Th, Pb were determined using the departmental addition-spiked matrix KUI-3 (Granodiorite from the Llanhelm granite, Dinan, Cotes-du-Nord, France). Loss on ignition was obtained by heating a known mass of pre-dried (at 110^{o} C) sample for thirty minutes at 1000^{o} C in a furnace in Pt crucibles. After removal and cooling in a dissicator, the sample mass was redetermined.

Ferrous oxide (FeO) was determined by titration with potassium dichromate. Sample digestion was performed in screw topped polythene bottles on a steam bath with a 1: 1

mixture of HF and H_2SO_3. After fifteen minutes the acid mixture was neutralised with 500ml saturated H_2BO_3. The solution was then titrated against standardised $K_2Cr_2O_7$ solution, using sodium diphenylamine sulphonate solution as indicator.

TABLE: (c-1): X.R.F. OPERATING CONDITIONS : MAJOR ELEMENTS

TUBE	Cr									W
Element	Na	Mg	Al	Si	P	K	Ca	Ti	Fe	Mn
Atomic No.	11	12	13	14	15	19	20	22	26	25
Peak	Ka	Ka	Ka	Ka	Ka	Ka	Ka	Ka	Ka	Ka
Tube Voltage (Kv)	40	40	60	40	60	40	40	40	60	60
Tube Control (mA)	32	32	24	16	24	8	8	8	8	28
Collimator	480	480	480	480	480	480	150	150	150	150
Crystal	TlAP	KAP	PE_t	PE_t	Ge	PE_t	LiF_{200}	LiF_{200}	LiF_{200}	LiF_{200}
Vacuum/Air path	VAC	VAC	VAC	VAC	VAC	VAC	VAC	VAC	VAC	VAC
Method	ABS	ABS	ABS	A.R	A.R	A.R	A.R	A.R	A.R	ABS
Counter	GFPC	GFPC	GFPC	GFPC	GFPC	GFPC	GFPC	GFPC	GFPC	GFPC
Theoretical Peak 2θ	54.75	43.59	145.07	109.21	141.01	50.69	113.07	86.12	57.51	95.19
Background 2θ	+4.00	+3.0	-6.50	-4.00	+4.00	+3.00	+2.50	+2.50	+1.80	+2.00
Time (sec)	40	100	FC	FC	40	FC	FC	FC	FC	40
Counts	FT	FT	10^4	10^4	FT	10^4	10^4	10^4	10^4	FT
No.of cycles	4	3	3	3	3	3	3	3	3	3
Disc/P.P.	PP	FD	FD	FD	FD	FD	FD	FD	FD	FD/PP

N.B. Collimator: 480 = 480μ blade spacing, 150 = 150μ blade spacing: FC = Fixed Count, FT = Fixed Time, FD = Fused Disc, PP = Pressed Power Pellet, GFPC = Gas Flow Proportional Counter.

TABLE: (c - 2): X.R.F. OPERATING CONDITONS : TRACE ELEMENTS

TUBE	Mo						
Element	Cu	Zn	Ga	Rb	Sr	Y	Zr
Atomic No	29	30	31	37	38	39	40
Peak	K_α	K_α	K_α	K_α	K_α	K_α	K_α
Tube Voltage (Kv)	60	60	60	60	60	60	60
Tube Current (mA)	30	30	30	28	28	28	28
Collimator	150	150	150	150	150	150	150
Counter	GFPC	GFPC	GFPC	SC	SC	SC	SC
Crystal	LiF_{220}	LiF_{220}	LiF_{220}	LiF_{220}	LiF_{220}	LiF_{220}	LiF_{220}
Method	ABS	ABS	ABS	ABS	ABS	ABS	ABS
Air/Vacuum path	VAC	VAC	VAC	VAC	VAC	VAC	VAC
Theoretical Peak 2θ	56.56	60.60	56.18	37.99	35.87	33.93	32.12
Background {	-1.01	+1.22	-1.04 +1.16	-1.10 +0.75	-1.02 +1.03	-0.85 +0.95	-0.44 +0.94
Time (sec)	40	40	40	40	40	40	40
Counts	FT	FT	FT	FT	FT	FT	FT
No. of cycles	4	4	4	4	4	4	4
Disc/P.P.	PP	PP	PP	PP	PP	PP	PP

TABLE: (c - 2): X.R.F. OPERATING CONDITIONS : TRACE ELEMENTS

TUBE	Mo			W				
Element	Pb	Th	U	Nb	Ba	La	Ce	Nd
Atomic No	82	90	92	41	56	57	58	60
Peak	$L_{1.4}$	L	L	K	L	L	$L_{1.4}$	$L_{1.4}$
Tube Voltage (Kv)	60	60	60	60	60	60	60	60
Tube Current (mA)	28	28	28	30	30	30	30	30
Collimator	150	150	150	150	480	480	480	480
Counter	SC	SC	SC	SC	GFPC	GFPC	GFPC	GFPC
Crystal	LiF_{220}	LiF_{220}	LiF_{220}	LiF_{220}	LiF_{220}	LiF_{220}	LiF_{220}	LiF_{220}
Method	ABS	ABS	ABS	ABS	ABS	ABS	ABS	ABS
Air/vacuum path	VAC	VAC	VAC	VAC	VAC	VAC	VAC	VAC
Theoretical Peak 2θ	40.34	39.23	37.31	30.45	115.25	138.70	111.63	99.02
Background	-0.40 +0.75	-0.55 +0.75	-0.47 +1.38	-0.45 +0.57	-1.25 +1.95	-2.98	+2.37	+1.32
Time (sec)	40	40	40	40	40	40	40	40
Counts	FT	FT	FT	FT	FT	FT	FT	FT
No of cycles	4	4	4	4	4	4	4	4
Disc/P.P.	PP	PP	PP	PP	PP	PP	PP	PP

TABLE (c-3) PRECISION AND DETECTION LIMITS

Precision has been determined by pooled variance on the results obtained from the multiplication measurements on individual samples. It is quoted as ± 2 X standard deviation.

Detection Limit is taken as:

$$2 \times \frac{\text{STD DEVIATION OF BACKGROUND}}{\text{SLOPE OF CALIBRATION}}$$

MAJOR ELEMENTS

ELEMENT	PRECISION	DETECTION LIMIT
SiO_2	± 2.1%	15.68%
TiO_2	± 0.015%	0.004%
Al_2O_3	± 0.80%	0.78%
Fe_2O_3±	± 0.20%	0.14%
FeO*	± 0.21%	0.004%
MnO	± 0.0010%	0.00006%
MgO	± 0.14%	0.86%
CaO	± 0.13%	0.012%
Na_2O	± 0.060%	0.025%
K_2O	± 0.15%	0.011%
P_2O_5	± 0.013%	0.04%
LOI*	± 0.03%	

TABLE: (c-3) PRECISION AND DETECTION LIMITS

Precision has been determined by pooled variance on the results obtained from the multiplication measurements on individual samples. It is quoted as ± 2 X standard deviation.

Detection Limit is taken as:

$$\frac{2 \times \text{STD DEVIATION OF BACKGROUND}}{\text{SLOPE OF CALIBRATION}}$$

TRACE ELEMENTS

ELEMENT	PRECISION	DETECTION LIMIT
Rb	± 17 ppm	6 ppm
Sr	± 20 ppm	6 ppm
Y	± 16 ppm	5 ppm
Zr	± 60 ppm	16 ppm
U	± 20 ppm	34 ppm
Th	± 23 ppm	14 ppm
Pb	± 28 ppm	5 ppm
Ga	± 8 ppm	14 ppm
Zn	± 4.6 ppm	5 ppm
Cu	± 0.7 ppm	16 ppm
Nb	± 3.6 ppm	5 ppm
Ba	± 42 ppm	72 ppm
La	± 7.7 ppm	0
Ce	± 8.6 ppm	0
Nd	± 12 ppm	24 ppm

Arculus, R.J., and Wills, K.J.A., (1980) The petrology of plutonic blocks and inclusions from the Lesser Antilles Island Arc. Journal of Petrology, Vol. 21, part 4, 743-799.

Bateman, P.C., Clark, L.D., Huber, N.J., Moore, J.G., and Rinehart, C.D. (1963). The Sierra Nevada Batholith. A synthesis of recent work across the central part. U.S.G.S., Prof. paper 414D., 49p.

Bateman, P.C., and Dodge, F.C.W., (1970). Variation of major chemical constituents across the Central Sierra Nevada Batholith. Geol. Soc. of Amer. Bulletin. Vol. 81., 409-420.

Bevins, R.E. (1979) The geology of the Strumble Head-Fishguard region, Dyfed, Wales. Unpub. Ph.D. thesis, Univ. of Keele, England. pp. 256.

Bickford, M.E., Sides, J.R., and Gullers, R.L. (1981) Chemical evolution of magma in the Proterozoic terrane of the St. Francois mountains, southeastern Missouri. 1. Field, Petrographic and major element data. Journ. of Geophysical Research, Vol. 86. 10365-10386.

Boccaleti, M., Manetti, P. and Peccerillo, A. (1974). The Balkanids as an instance of back-arc thrust belt. Possible relation with Hellenids, Geol. Soc. Amer. Bull. 85, 1077-1084.

Booth, B., (1966) Petrogenesis of the Land's End granites. Thesis, Ph.D. University of Keele, 389pp.

Boreadis, G. (1954). Geology of Thasos. Ann. Geol. des Pays Hell. III (In Greek).

Bottinga, Y., Kudo, A., Weill, D. (1966). Some observations on oscillatory zoning and crystallization of magmatic plagioclase. Amer. Mineral. 51., 792-806.

Bowen, N.L. (1913). The melting phenomena of the plagioclase feldspars. AJS 35, 577-599.

Bowen, N.L. (1928). Evolution of the igneous rocks 334pp. Princeton: Univ. Press (Reprinted Dover Publications Inc).

Breithaupt, A (1823). Charakterizik des Mineral-Systems. 2nd Edn. Dresden.

Breithaupt, A. (1830). Uber die Felsite und einige neue Specien Ihres Geschlechts. Schwiegger's J. Chem. Phys. 60, 324.

Brown, G.C. (1982). Calc-Alkaline intrusive rocks: their diversity, evolution and relation to volcanic arcs In Thorpe R.S., ed. Andesites, John Wiley & Sons.

Brown, M., Friend, C.R.L., McGregor, V.R., and Perkins, W.T. (1981). The late Archaean Quorqut complex of southern west Greenland. Journ. of Geophysical Research, Vol. 86, 10617-10632.

Chalmers, B. (1964). Principles of solidification: New York, John Wiley & Sons, 319p.

Chappell, B.W., and White, A.J.R. (1974) Two contrasting granite types. Pacific Geology, 8. 173-174.

Cherry, M.E., and Trembath, L.T., (1978) Structural state and composition of alkali feldspars in granites of the St. George Pluton, South-Western New Brunswick. Mineral. Mag. 38, 295-311.

Chivas, A.R. (1981). Geochemical evidence for magmatic fluids in porphyry copper igneous complex. Contrib. Mineral. Petrol. 78, 389-403.

Chivas, A.R., Andrews, A.S., Sinha, A.K., and O'Neil, J.R.(1982) Geochemistry of a Pliocene-Pleistocene oceanic-arc plutonic complex, Guadalcanal. Nature, Nov. 1982.

Christofides, G.T. (1977). The Xanthi plutonic complex Published Ph. D. thesis of University of Thessaloniki, Greece, 249p. (In Greek).

Cobbing, .E.J. and Pitcher, W.S., (1972). The coastal batholith of central Peru; Geol. Soc. London, J. Vol. 128, p. 421-460.

Czamanske, G.K. and Wones, D.R. (1973). Oxidation during magmatic differentiation, Finnmarka Complex, Oslo area, Norway: Part 2, the mafic silicates. Journal of Petrology, Vol. 14, pp. 349-380.

Davi, E. (1963). Geology of Samothaki, Ann. Geol. pays Hell. 14, 133-188.

De Boer, H. (1970). Geologisch-Petrographische Untersuchungen im Rhodope-Massif Griechisch-Ostmazedonien. Beih. Geol. Jb., 88. 43-79.

Deer, W.A., Howie, R.A. and Zussman, J. (1962, 1963, 1971, 1978). Rock-Forming Minerals, Vol. 1, 2, 3, 4, 5, Longman, London.

Dodge, F.C.W., Papike, J.J., and Mays, R.W. (1968). Hornblendes from granitic rocks of the central Sierra Nevada Batholoith, California. Journal of Petrology, Vol. 9. pp. 378-410.

Dodge, F.C.W., Smith, V.C., and Mays, R.E. (1969). Biotites from granitic rocks of the central Sierra Nevada Batholith, California. Journal of Petrology, Vol. 10, pp 250-271.

Edmondson, K.M. (1970). A study of alkali feldspars from some S.W. England granites. Thesis, M.Sc., Univ. of Keele.

Eggleton, R.A. (1979). The ordering path for igneous K-feldspar megacrysts. Amer. Mineral. 64, 906-911.

Ehlers, E.G. (1972). The interpretation of geological phase diagrams. Freeman and Company. Printed in the U.S.A.

Ernst, W.G., (1968). Amphiboles: Crystal chemistry, phase relations and occurrence. Springer-Verlag New York, Inc.

Evans, H.T., Jr D.E. Appleman, and D.S.Handwerker (1963). The least squares refinement of crystal unit cells with powder diffraction data by an automatic computer indexing method (abstr). Amer. Crystallog. Assoc. Cambridge, Mass. Ann. Meet., Program, p. 42-43.

Exley, R.A. (1980). Microprobe studies of REE-rich accessory minerals: implications for Skye granite petrogenesis and REE mobility in hydrothermal systems. Earth & Planet, Sci. Letters, 48. 97-110

Exley, C.S. and Stone, M. (1982). Petrology of the granites and minor intrusions. In: Sutherland edit. Igneous rocks of the British Isles: John Wiley & Sons, Chichester, New York, Brisbane, Toronto, Singapore pp. 293-302.

Exley, C.S., and Stone, M. (1982). Late-Stage phenomena. In: Sutherland Edit. Igneous rocks of the British Isles: John Wiley & Sons, Chichester, New York, Brisbane, Toronto, Singapore, pp. 303-309.

Exley, C.S. and Stone, M. (1982). Petrogensis. In Sutherland Edit. Igneous rocks of the British Isles: John Wiley & Sons, Chichester, New York, Brisbane, Toronto, Singapore pp. 311-320.

Fischer, G. (1964). Uber das granitmassiv des Symvolon-Gebirges bei Kavala. Geol. Rund., 53, 390 - 392.

Flemings, M.C., (1974). Solidification Processing: New York, McGraw Hill Book Co., 354p.

Foster, M.D. (1962). Interpretation of the composition and a classification of the chlorites. Geological Survey Professional Paper 414-A.

Fourcade, S (1979). in Hart, S.R., and Allegre, C.J.: Trace element constraints on magma genesis: in Hargraves R.B., edit. Physics of magmatic processes, 1980 Princeton University Press, Princeton, New Jersey.

Gokhale, N.W. (1968). Chemical composition of biotites as a guide to ascertain the origin of granites. Bull. Geol. Soc. Finland, 40, 107-111.

Goldsmith, J.R., and Laves, F. (1954). Potassium feldspars structurally intermediate between microcline and sanidine. Geoch. Cosmoch. Acta, 6, 100 - 118.

Harry, W.T. (1950) Aluminium replacing silicon in some silicate lattices. Min. Mag. 29, 142-149.

Harvey, P.K., Taylor, D.M., Hendry, R.D., and Bancroft, F. (1972). An accurate method for the analysis of rocks and chemically related materials by X-ray fluorescence spectrometry. X-ray Spectrometry Vol. 2, pp. 33-44

Helz, R.T. (1973). Phase relations of basalts in their melting range at P_{H_2O} = 5Kb as a function of oxygen fugacity. Part 1: Mafic phases: Jour. Petrology, vol. 14, p. 249-302.

Hills, E.S. (1936). Reverse and oscillatory zoning in plagioclase feldspars. Geol. Mag. 73, 49-56

Hine, R., and Mason, D.R. (1978). Intrusive rocks associated with porphyry copper mineralization, New Britain, Papua New Ginea. Econ. Geol. 73, p. 749-760.

Hutchison, C.S. (1974). Laboratory Handbook of petrographic techniques. John Wiley & Sons, New York, London, Sydney, Toronto. p. 525.

Iball, D.R., and Hubbard, F.H. (1982). Lattice structural variation in K-feldspar magacrysts of associated charnockite and alkali granite. Mineral. Magaz. vol. 46, pp. 247-251.

Johannes, W., (1978). Melting of plagioclase in the system

Ab-An-H_2O and Qz-Ab-An-H_2O at PH_2O = 5Kbs, an equilibrium problem. Cont. Miner. Petrol. 66, 295-303.

Kokkinakis, A. (1977). Das intrusivgebiet des Symvolon-Gebirges und von Kavala in Ostmakedonien Griechenland. Erlangung des Doktorades. Munchen.

Kopp, O. (1966). Geologie Thraziens III. Das Tertiar zwischen Rhodope und Evros. Ann. Geol. Pays. Hell. 15, 315-362.

Kronberg, P., Meyer, W., und Pilger, A. (1970). Geologie der Rila-Rhodope-Masse Zwischen Strimon und Nestos (Nordgriechenland). Beih. Geol. Jb., 88, 133-180.

Larsen, E.S. (1948). Batholith and associated rocks of Corona, Elsinoce and San Luis Rey quadrangles, southern California. Geol. Soc. Am. Mem. 29, 182p.

Laves, F. and Soldatos, K. (1962a). Plate perthite, a new perthitic inter-growth in microcline single crystals, a recrystallisation product. Z. Krist., 117, pp. 218-226.

Laves, F., und Soldatos, K. (1963). Die Albit/Mikroklin-Orientierungs-Beziehungen in Mikroklinperthiten. Z. Krist. 118, pp. 69-102.

Leake, B.E., (1965). The relationship between tetrahedral aluminium and the maximum possible octahedral aluminium in natural calciferous and sub-calciferous amphiboles. Amer. Min. 50, 843-851.

Leake, B.E., (1978). Nomenclature of amphiboles. Can. Mineral., 16, 501-520 (also Am. Mineral. 63, 1023-1052, 1978).

Leake, B.E., Hendry, G.L., Kemp, A., Plant, A.G., Harvey, P.K., Wilson, J.R., Coats, J.S., Aucott, J.W., and Lunel, T (1968). The chemical analysis of rock powders by automatic x-ray fluorescence. Chemical Geology - Elsevier Publishing Co., Amsterdam, Printed in the Netherlands.

Lewis, J.F., (1969). Composition, physical properties and origin of sodic anorthites from the ejected plutonic blocks of the Soufrière Volcano, St. Vincent, West Indies. Contr. Mineral and Petrol 21, 272-294.

Liatsikas, N., (1938). Beitrage zur Kenntnis der Jungteritaren, Eruptivgesteine in der Umgebung von Fere (West-Thrazien). Prakt. Akad. Ath. 13, 162-76, 314-29, 470-481.

Lofgren, G. (1974a). Temperature induced zoning in synthetic plagioclase feldspar. In Mackenzie, W.S., and Zussman, J. eds. The Feldspars: Manchester, England, Manchester Univ. Press. p. 362-376.

Marakis, G. (1968). Geochronology of some Macedonian granites (North Greece). (in Greek). Ann. Geol. des pays Hell, 21, 121-150.

Maratos, G.N., (1972). Geology of Greece. Athens. 189p. (in Greek).

Maratos, G.N., and Andronopoulos, B. (1964). Contribution to the age of the crystalline schist of the Rhodope massif (in Greek). Ann. Geol. des pays Hell, 6, 1964.

Maratos, G.N., and Andronopoulos, B. (1965). Chronostratigraphy of the Alikis Alexandroupolis area (in Greek). Ann. Geol. des pays. Hell. 6, 1965.

Mason, B., (1966). Principles of geochmistry. John Wiley & Inc., New York, London, Sydney.

Mason, D.R., and McDonald, J.A. (1978). Intrusive rocks and porphyry copper occurrences of the Papua New Guinea-Solomon Islands Region: A reconnaissance study. Economic Geology, vol. 73, pp. 857-877.

McCourt, W.J. (1981). The geochemistry and petrography of the coastal batholith of Peru, Lima segment. Geol. Soc. London, J. Vol. 138, pp. 407-420.

Megaw, H.D., (1962). Order and disorder in Feldspars. Norsk. Geol. Tidds. 42, No. 2. 104-137.

Melidonis, N. (1969a). Deposits of lignite and peat in Philippi area (in Greek). Ann. Geol des pays Hell, 13(3), 87-250.

Melidonis, N. (1969b). Uranium-bearing coal from the Aimoniou-Kotuli (in Greek). Ann. Geol. des pays Hell., 47. (1969).

Mountrakis, D. (1977). Geology of Greece (unpubl.) (in Greek).

Nockolds, S.R., and Allen, R. (1953). The geochemistry of some igneous rock series. Geochim. Cosmochim. Acta. Vol. 4, pp. 105-142.

Norrish, K., and Hutton, J.T. (1969). An accurate x-ray spectrographic method for the analysis of a wide range of geological samples. Geochim. Cosmochim. Acta. Vol. 33., No. 4., pp. 431-453.

Papadakis, A. (1972). Chemical composition of the plutonic rocks of the Greek Rhodope massif. (in Greek). Ann. Geol. des pays. Hell, 9. 129-143.

Papadakis, A.N. (1965). The Serres-Drama Pluton. Published Ph.D. thesis of University of Thessaloniki, Greece, 130 p. (in Greek).

Papadopoulos, G.A. (1982). Active deep tectonics of the Aegean and surrounding area. Published Ph.D. thesis of University of Thessaloniki, Greece, 176p. (in Greek).

Papazachos, B.C., and Papadopoulos, G.A. (1977). Deep tectonics and associated ore deposits in the Aegean area. Sixth Colloqium on the Geology of Aegean Region. Athens, September, 20-24, 1977.

Parsons, I. (1978a). Feldspars and fluids in cooling plutons. Mineral Mag. 42, (N° 321) p. 1-17.

Parsons, I. and Boyd, R (1971). Distribution of potassium feldspar polymorphs in intrusive sequences. Mineral Mag. 38., 295-311.

Peacock, M.A., (1931). Classification of igneous rock series, Journ. Geol. 39, 54-67.

Petro, W.L., Vogel, T.A., and Wilband, J.T. (1979). Major element chemistry of plutonic rock suites from compressional and extensional plate boundaries. Chemical Geology, 26, 217-235.

Petrov, P. (1977). Some features in the distribution of magmatic, hydrothermal and seismic activity in the area between the Balkanides and the Aegean Arc "Geologica Balcanica", 7, 99-116.

Pitcher, W.S., and Berger, A.R. (1972). The geology of Donegal: a study of granite emplacement and unroofing; Wiley-Interscience, 435p.

Piwinskii, A.J. (1968). Experimental studies of igneous rock series, central Sierra Nevada batholith, California. Journ. of Geology, Vol. 76, No. 5., p. 55-570.

Rapela, C.W., and Shaw, D.M., (1979). Trace and major element models of granitoid genesis in the Pampean Ranges, Argentina. Geoch. et. Cosmoch. Acta, Vol. 43, 1117-1129.

Renzeperis, P. (1956). The Tertiary vulcanites of the Evros area (west Thrace). Published Ph. D. thesis of University of Thessaloniki, Greece (in Greek).

Reynolds, R.C. (1963). Matrix corrections in trace element analysis by x-ray fluorescence: estimation of the mass absorption coefficient by Compton scatter Amer. Mineral. Vol. 48, pp. 1133-1143.

Robin, P.Y.G. (1974). Stress and strain in cryptoperthite lamellae and the coherent solvus of alkali feldspars. Amer. Mineral, 59, 1299-1318.

Rowbotham, G., (1973). Hydrothermal synthesis and mineralogy of the alkali amphiboles. Unpubl. Ph. D. thesis. University of Durham, England.

Rutter, J.W., and Chalmers, B., (1953). A prismatic substructure formed during the solidification of metal: Canadian Journ. Physics, 31, p.15 - 39.

Schenk, F. (1970). Geologie der westlichen Pangaion in Grieschisch. Ostma Kedonien. Beih. Geol. 16. 88, 81-132.

Shand, S.J. (1927). The Eruptive Rocks. Wiley, New York, N.Y.

Shaw, S.E., and Flood, R.H. (1981). The New England Batholith, eastern Australia: Geochemical variations in time and space. Journ. of Geophysical Research, Vol. 86, 10530-10544.

Sibley, D.F., Vogel, T.A., Walker, B.M., and Byerly, G. (1976). The origin of oscillatory zoning in plagioclase: A diffusion and growth controlled model. A.J.S., 276. 275-284.

Streckeisen, A. (1976). To each plutonic rock its proper name. Earth. Sci. Rev. 12, 1-33.

Sideris, C. (1973). Petrochemistry of some volcanic rocks from West Thrace. Tectonic and petrochemical relationships with volcanics at Greece. Chem. Erd, 3, 174.

Sklavounos, S.A. (1981). The Paranesti (Dipotamos) granite. Published Ph.D. thesis of University of Thessaloniki, Greece, 175p. (in Greek).

Smith, J.V. (1974). Feldspar Minerals. Crystal structure and Physical Properties. Vol. 1. Springer-Verlag Berlin, Heidelberg, New York.

Smith, J.V. (1974). Feldspar Minerals. Chemical and Textural Properties. Vol. 2. Springer-Verlag Berlin, Heidelberg, New York.

Soldatos, K. (1961). Die jungen Vulkanite der griechischen Rhodopen und ihre provinziellen Verhaltnisse. Volkanistitut Immanuel Friedlaender, Zurich.

Soldatos, K. and Papadakis, A. (1971). Beitrag zur kenntnis der ostlich von Xanthi vulkanishen gänge. Ann. Geol. Pays. Hell. 23, 308-322.

Spencer, A.M. (1974). Mesozoic-Cenozoic orogenic belts. Scottish Academic Press, Edinburgh.

Stewart, D.B., and Ribbe, P.H. (1969). Structural explanation for variation in cell parameters of alkali feldspar with Al/Si ordering. Amer. Journ. Sci. 267-A, 444-462.

Stewart, D.B., and Wright, T.L. (1974). Al/Si order and symmetry of natural alkali feldspars,and the relationship of strained cell parameters to bulk composition. Bull. Soc. Fr. Mineral. Cristallogr. 97, 356-377.

Takahashi, M., Aramaki, S., and Ishihara, S. (1980). Magnetite-series/ilmenite-series vs. I-type/ S-type granitoids. Min. Geol. Japan. Spec. Issue., 8, p. 13-28.

Taylor, S.R. (1965). The application of trace element data to problems in petrology. Phys. Chem. Earth Vol. 6. pp. 133-213.

Thompson, J.B., (1947). Role of aluminium in rock forming silicates. Bull. Geol. Soc. Am. 58, 1232.

Tiller, W.A., Jackson, K.A., Rutter, J.W., and Chalmers, B., (1953). The redistribution of solute atoms during the solidification of metals: Acta Metallurgica, V. 1., p 331-357.

Tilling, R.I. (1968). Zonal distribution of variations in structural state of alkali feldspar within the Rader Creek Pluton, Boulder Batholith, Montana. Journal of Petrology, 9, 331-357.

Tröger, E. (1955). Spezielle Petrographie der Eruptivgesteine. Nachtrag 1938 (Zweite Auft. Stuttgart 1955).

Tuttle, O.F., and Bowen, N.L. (1958). Origin of granite in the light of experimental studies etc. Geol. Soc. Amer. Memoir No. 74.

Vance, J.A., (1962). Zoning in igneous plagioclase: normal and oscillatory zoning. A.J.S. 260, 746-760.

Vance, J.A. (1965). Zoning in igneous plagioclase: patchy zoning. Journ. Geolg. 73, 636-651.

Von Platen, H. (1965). Experimental anatexis and genesis of migmatites. In W.S.Pitcher and Glenys W. Flinn (eds), Controls of metamorphism, Oliver and Boyd, Edinburgh, Scotland, pp. 202-218.

Vorma, A. (1971). Alkali feldspars of the Wiborg rapakivi massif. Bull. Comm. Geol. Finlande, 246.

Wedepohl, K.H. (1978). Handbook of Geochemistry, Vol. II/4 and Vol. II/5. Springer-Verlag Berlin, Heidelberg, New York.

Wills, K.J.A. (1974). The geological history of southern Dominica and plutonic nodules from the Lesser Antilles. Unpubl. Ph.D. thesis University of Durham, England.

Winkler, H.G.F. (1979). Petrogenesis of Metamorphic Rocks. Springer-Verlag, New York Inc.,

Winkler, H.G.F., and Brietbart, R. (1978). New aspects of granitic magmas. N. Jb. Miner. Mh., 1978 H. 10, 463-480 Stuttgart.

Winkler, H.G.F. and Lindemann, W. (1972). The system Qz-Or-An-H_2O within the granitic system Qz-Or-Ab-An-H_2O. Application to granitic magma formation. N. Jb. Miner. Mh., 49-61.

Winkler, H.G.F., and Ghose, N.C. (1974). Neues Jahrb. Mineral Monatsh 1947: 481-484.

Wright, T.L. (1968). X-ray and optical study of alkali feldspar: II an X-ray method of determining the composition and structural state from measurement of 2θ values for three reflections. Amer. Mineral 53, 88-104.

Wright, T.L. and Stewart, D.B. (1968). X-ray and optical study of alkali feldspar: I Determination of composition and structural state from refined unit cell parameters and 2V. Amer. Mineral, 53, 38-87.

Yoder, H.S. (1969). Calc-Alkaline andesites -experimental data bearing on the origin of their assumed characteristics. Bull. Ore. St. Dep. Geol. Miner. Ind. 65, 77-89.

Yoder, H.S. Stewart, D.B. and Smith, J.R. (1957). Feldspars. Yb. Carnegie Instn. Wash. 56, 206-216.

Addendum

Blanchet, R., and Mercier, J. (1978) in M. Lemoine (eds), Geological Atlas of Alpine Europe and Adjoining Alpine areas.

Czamanske, G.K., Ishihara, S., and Atkin, S.A. (1981). Chemistry of rock-forming minerals of the Cretaceous-Palaeocene Batholith in southwestern Japan and implications for magma genesis. Journ. of Geophysical Research, Vol. 86, pp. 10431-10469.

Harloff, C. (1927). Zonal structure in plagioclases. Leidsche Geol. Med. 2, 99-114.

Papike, J.J., Cameron, K.L. and Baldwin, C.K. (1974). Amphiboles and pyroxenes: Characterization of other than quadrilateral components and estimates of ferric iron from microprobe data. Geol. Soc. Am. Abstr. Programs, 6, 1053-1054.

Ringwood, A.E. (1974). The petrological evolution of island arc systems. Geol.Soc. London. J. 130, 183-204.

GEOLOGICAL MAP OF THE SERRES – DRAMA GRANITIC COMPLEX

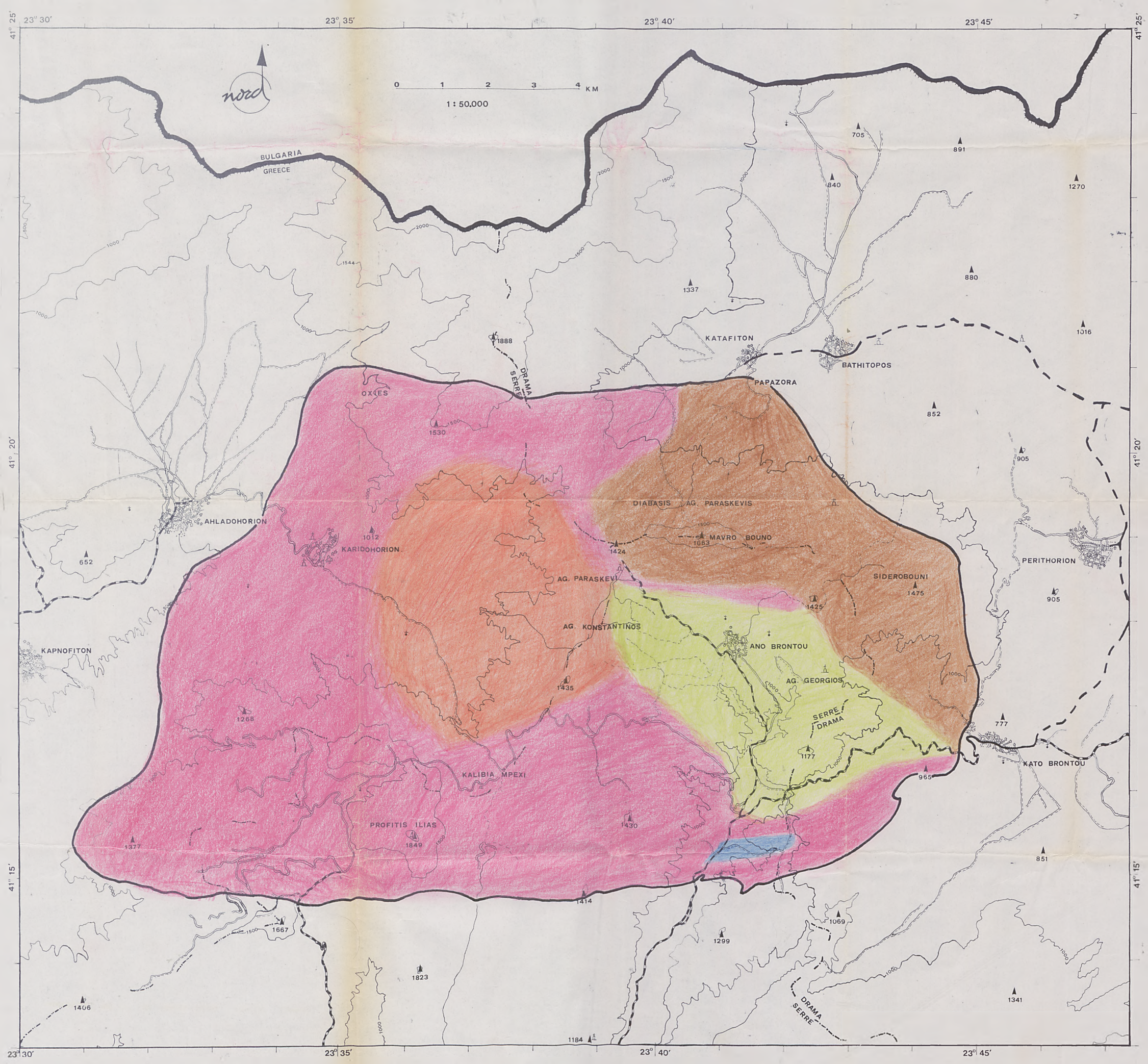

Granite | Granodiorite | Quartz monzonite | Monzonite | Gabbro

(after Papadakis, 1965, with modification)